frontiers | Research Topics

# Purinergic signalling in the central nervous system and its pharmacological importance in neurological and psychiatric illnesses

**Edited by**
Yong Tang, Patrizia Rubini, Beata Sperlagh and Henning Ulrich

**Published in**
Frontiers in Pharmacology

ISSN 1664-8714
ISBN 978-2-8325-4356-6
DOI 10.3389/978-2-8325-4356-6

## About Frontiers

Frontiers is more than just an open access publisher of scholarly articles: it is a pioneering approach to the world of academia, radically improving the way scholarly research is managed. The grand vision of Frontiers is a world where all people have an equal opportunity to seek, share and generate knowledge. Frontiers provides immediate and permanent online open access to all its publications, but this alone is not enough to realize our grand goals.

## Frontiers journal series

The Frontiers journal series is a multi-tier and interdisciplinary set of open-access, online journals, promising a paradigm shift from the current review, selection and dissemination processes in academic publishing. All Frontiers journals are driven by researchers for researchers; therefore, they constitute a service to the scholarly community. At the same time, the *Frontiers journal series* operates on a revolutionary invention, the tiered publishing system, initially addressing specific communities of scholars, and gradually climbing up to broader public understanding, thus serving the interests of the lay society, too.

## Dedication to quality

Each Frontiers article is a landmark of the highest quality, thanks to genuinely collaborative interactions between authors and review editors, who include some of the world's best academicians. Research must be certified by peers before entering a stream of knowledge that may eventually reach the public - and shape society; therefore, Frontiers only applies the most rigorous and unbiased reviews. Frontiers revolutionizes research publishing by freely delivering the most outstanding research, evaluated with no bias from both the academic and social point of view. By applying the most advanced information technologies, Frontiers is catapulting scholarly publishing into a new generation.

## What are Frontiers Research Topics?

Frontiers Research Topics are very popular trademarks of the *Frontiers journals series*: they are collections of at least ten articles, all centered on a particular subject. With their unique mix of varied contributions from Original Research to Review Articles, Frontiers Research Topics unify the most influential researchers, the latest key findings and historical advances in a hot research area.

Find out more on how to host your own Frontiers Research Topic or contribute to one as an author by contacting the Frontiers editorial office: frontiersin.org/about/contact

# Purinergic signalling in the central nervous system and its pharmacological importance in neurological and psychiatric illnesses

**Topic editors**

Yong Tang — Chengdu University of Traditional Chinese Medicine, China
Patrizia Rubini — Leipzig University, Germany
Beata Sperlagh — Institute of Experimental Medicine (MTA), Hungary
Henning Ulrich — University of São Paulo, Brazil

**Citation**

Tang, Y., Rubini, P., Sperlagh, B., Ulrich, H., eds. (2024). *Purinergic signalling in the central nervous system and its pharmacological importance in neurological and psychiatric illnesses*. Lausanne: Frontiers Media SA.
doi: 10.3389/978-2-8325-4356-6

# Table of contents

frontiers | Frontiers in Pharmacology

TYPE Editorial
PUBLISHED 12 January 2024
DOI 10.3389/fphar.2023.1355286



OPEN ACCESS

EDITED AND REVIEWED BY
Filippo Drago,
University of Catania, Italy

*CORRESPONDENCE
Yong Tang,
tangyong@cdutcm.edu.cn

RECEIVED 13 December 2023
ACCEPTED 31 December 2023
PUBLISHED 12 January 2024

CITATION
Tang Y, Rubini P, Sperlagh B and Ulrich H (2024), Editorial: Purinergic signalling in the central nervous system and its pharmacological importance in neurological and psychiatric illnesses.
*Front. Pharmacol.* 14:1355286.
doi: 10.3389/fphar.2023.1355286



# Editorial: Purinergic signalling in the central nervous system and its pharmacological importance in neurological and psychiatric illnesses

Yong Tang[1,2]*, Patrizia Rubini[1], Beata Sperlagh[3] and Henning Ulrich[1,4]

[1]International Joint Research Centre on Purinergic Signalling, Chengdu, China, [2]Acupuncture and Chronobiology Key Laboratory of Sichuan Province, School of Health and Rehabilitation, Chengdu University of Traditional Chinese Medicine, Chengdu, China, [3]Laboratory of Molecular Pharmacology, HUN-REN Institute of Experimental Medicine, Budapest, Hungary, [4]Department of Biochemistry, Institute of Chemistry, University of Sao Paulo, Sao Paulo, Brazil

KEYWORDS

**purinergic signalling, central nervous system, neurological and psychiatric illnesses, ATP, P1, P2, adenosine**

Editorial on the Research Topic
Purinergic signalling in the central nervous system and its pharmacological importance in neurological and psychiatric illnesses

This Research Topic aims to honour the 80th birthday of Professor Peter Illes, who is a member of the European Academy of Sciences, the founder/first president of the German Purine Club, and honorary president of the Chinese Purine Club. His connections with China explain that a number of Chinese scientists contributed with articles to this Research Topic. Peter Illes established a worldwide co-operation network on purinergic signalling and is an internationally recognized leader in the field of his discipline.

Adenosine Triphosphate (ATP) is an intracellular energy-storing molecule, but may also reach the extracellular space, where it participates in cell-to-cell signalling. For this purpose, ATP utilises a range of purinergic receptors activated either by ATP itself (P2X receptors; seven subtypes) or by ATP/ADP and UTP/UDP (P2Y receptors; eight subtypes) and finally via its enzymatic degradation product, adenosine (P1/A receptors; four subtypes). Purine nucleotides and nucleosides together with the whole plethora of receptors and degrading enzymes constitute the purinome. This fascinating and extensive network exists both in animals and humans and is essential in regulating important physiological functions. Disturbances in the network can lead to a variety of illnesses clinically associated with both neurological or psychiatric traits. In recent years, hope has arisen that pharmacology and medicinal chemistry together with various newly developed methods, will enable researchers to discover and design efficient drugs for treating these neurodegenerative and affective illnesses, based on disturbances of the purinergic system. Although this Research Topic clearly concentrates on brain diseases due to misbalance and inefficiency of the purinome, it has to be pointed out that a wide range of diseases arise because of the same reason in all parts of the human body, which is however no subject of the present discussions.

In this Research Topic, seven original articles, one mini-review, and two overviews were included. Of three review papers, one focuses on the potential application of P2Y12 receptor (R)-ligands in the diagnosis and treatment of epilepsy (Chen et al.), another two summarize the roles and neurobiological mechanisms of adenosine and its receptors in sleep-wake regulation, torpor and hibernation (Ma et al.), as well as the role of purinergic signalling in the modulation of blood-brain barrier (BBB) permeability (Wang et al.), respectively.

In the following we will enumerate in a one sentence synopsis the content of the individual articles included in our Research Topic. 1) The adenosine receptor-subtype A2A was identified to exert distinct control on the morphology of retinal ganglion cells (RGC), in order to cell-type specifically fine-tune the RGC dendritic morphological complexity during normal development and neonatal inflammation (Hu et al.). 2) P2X3 receptors in the dorsal root ganglion and spinal cord have been shown to mediate the analgesic effect of Polyphyllin VI (Luo et al.), known to be responsible for cell-cycle arrest and acupuncture efficiency. 3) Diclofenac was demonstrated, by the application of two-electrode voltage clamp electrophysiology, to be a strong antagonist of the human (h)P2X3 and hP2X2/3Rs, but a weaker blocker of hP2X1, hP2X4, and hP2X7Rs (Grohs et al.). 4) Morphotyping and single cell shape descriptor analysis demonstrated that in cultured microglia, treatment with the P2X7R agonist dibenzoyl-ATP (Bz-ATP), and the inflammatory activator lipopolysaccharide (LPS) in combination with Bz-ATP, increased round/ameboid microglia and decreased polarized ramified morphology of this cell type (von Mücke-Heim et al.). 5) Cytokines appear to play important roles in the antidepressant-like effect of zinc in male mice (Iring-Varga et al.). 6) A small nucleotide polymorphism (SNP) analysis performed in epileptic patients indicated that the TT genotype and T allele of rs4431401 in CD73 (ecto 5′-nucleotidase, generating adenosine from AMP) were genetic risk factors for epilepsy in male patients, whereas rs2267076, rs2298383, rs4822492, and rs4822489 polymorphisms of the A2AR were mainly associated with female subjects (Shi et al.). 7) Finally, eicosapentaenoic acid (EPA) was described to be an inhibitor of the vesicular nucleotide transporter (VNT), which actively transports nucleotides into secretory vesicles responsible for the storage of ATP. VNT certainly appears to plays an essential role in purinergic transmission, although it is still premature to conclude that EPA is a specific inhibitor of this enzyme (Moriyama et al.).

In this Research Topic, hP2X1, hP2X3, hP2X2/3, hP2X4, and hP2X7Rs, as well as the human SNPs of CD73 and A2ARs were investigated in diverse studies. It was an interesting finding that in male and female mice, different SNPs cause predisposition to epilepsy. However, only future studies will decide which of the reported data have major significance for clinical practice.

## Author contributions

YT: Conceptualization, Funding acquisition, Writing–original draft, Writing–review and editing. PR: Conceptualization, Funding acquisition, Writing–original draft, Writing–review and editing. BS: Conceptualization, Writing–original draft, Writing–review and editing. HU: Conceptualization, Funding acquisition, Writing–original draft, Writing–review and editing.

## Funding

The authors declare financial support was received for the research, authorship, and/or publication of this article. NSFC-RSF (82261138557), NSFC (82274668, 82230127), the Innovation Team and Talents Cultivation Program of the National Administration of Traditional Chinese Medicine (ZYYCXTD-D-202003), the Sichuan Science and Technology Program (2022YFH0006), Sichuan Provincial Administration of Traditional Chinese Medicine (2023zd024), the São Paulo Research Foundation (FAPESP 2018/07366-4), and National Council for Scientific and Technological Development (CNPq, Brasília) (406396/2021-3).

## Acknowledgments

We are mostly grateful to all authors for their highly valuable contribution. Also we really appreciate the work of reviewers whose constructive input contributed to improving the quality of the articles. Finally, we would like to acknowledge the support of NSFC-RSF (82261138557), NSFC (82274668, 82230127), the Innovation Team and Talents Cultivation Program of the National Administration of Traditional Chinese Medicine (ZYYCXTD-D-202003), the Sichuan Science and Technology Program (2022YFH0006), Sichuan Provincial Administration of Traditional Chinese Medicine (2023zd024), the São Paulo Research Foundation (FAPESP 2018/07366-4), and National Council for Scientific and Technological Development (CNPq, Brasília) (406396/2021-3).

## Conflict of interest

The authors declare that the research was conducted in the absence of any commercial or financial relationships that could be construed as a potential conflict of interest.

The authors declared that they were an editorial board member of Frontiers, at the time of submission. This had no impact on the peer review process and the final decision.

## Publisher's note

frontiers | Frontiers in Pharmacology

TYPE Original Research
PUBLISHED 07 December 2022
DOI 10.3389/fphar.2022.1080189



OPEN ACCESS

EDITED BY
Yong Tang,
Chengdu University of Traditional Chinese Medicine, China

REVIEWED BY
Felipe Ortega,
Complutense University of Madrid, Spain
Sergei V. Fedorovich,
Belarusian State University, Belarus

*CORRESPONDENCE
Yoshinori Moriyama,
moriyama_yoshinori@med.kurume-u.ac.jp

SPECIALTY SECTION
This article was submitted to Experimental Pharmacology and Drug Discovery, a section of the journal Frontiers in Pharmacology

RECEIVED 26 October 2022
ACCEPTED 21 November 2022
PUBLISHED 07 December 2022

CITATION
Moriyama Y, Hasuzawa N and Nomura M (2022), Is the vesicular nucleotide transporter a molecular target of eicosapentaenoic acid? *Front. Pharmacol.* 13:1080189. doi: 10.3389/fphar.2022.1080189



# Is the vesicular nucleotide transporter a molecular target of eicosapentaenoic acid?

Yoshinori Moriyama*, Nao Hasuzawa and Masatoshi Nomura

Division of Endocrinology and Metabolism, Department of Internal Medicine, Kurume University School of Medicine, Kurume, Japan

Vesicular nucleotide transporter (VNUT), an active transporter for nucleotides in secretory vesicles, is responsible for the vesicular storage of ATP and plays an essential role in purinergic chemical transmission. Inhibition of VNUT decreases the concentration of ATP in the luminal space of secretory vesicles, followed by decreased vesicular ATP release, resulting in the blockade of purinergic chemical transmission. Very recently, Miyaji and colleagues reported that eicosapentaenoic acid (EPA) is a potent VNUT inhibitor and effective in treating neuropathic and inflammatory pain and insulin resistance through inhibition of vesicular storage and release of ATP. However, our validation study indicated that, in bovine adrenal chromaffin granule membrane vesicles, EPA inhibited the formation of an electrochemical gradient of protons across the membrane with the concentration of 50% inhibition (IC50) being 1.0 μM without affecting concanamycin B-sensitive ATPase activity. Essentially, similar results were obtained with proteoliposomes containing purified vacuolar $H^+$-ATPase. Consistent with these observations, EPA inhibited the ATP-dependent uptakes of ATP and dopamine by chromaffin granule membrane vesicles, with ID50 being 1.2 and 1.0 μM, respectively. Furthermore, EPA inhibited ATP-dependent uptake of L-glutamate by mouse brain synaptic vesicles with ID50 being 0.35 μM. These results indicate that EPA at sub-μM acts as a proton conductor and increases proton permeability across the membrane, regardless of the presence or absence of VNUT, thereby inhibiting non-specifically the vesicular storage of neurotransmitters. Thus, EPA may affect a broader range of chemical transmission than proposed.

KEYWORDS

**chromaffin granules, eicosapentaenoic acid, purinergic chemical transmission, SLC17A9, synaptic vesicles, V-ATPase, VNUT**

**Abbreviations:** CCCP, carbonylcyanide m-chlorophenylhydrazone; con B, concanamycin B; EPA, eicosapentaenoic acid; ΔpH, transmembrane pH gradient; Δψ, transmembrane potential difference; IC50, the concentration of 50% inhibition; V-ATPase, vacuolar $H^+$-ATPase; VNUT, vesicular nucleotide transporter.

## Introduction

Purinergic chemical transduction is intercellular signal transduction that uses nucleotides such as ATP and adenosine as transmitters and regulates various higher-ordered vital activities such as pain perception and inflammation (Burnstock, 2007). To initiate the purinergic chemical transmission, cytoplasmic ATP appears in the extracellular space through three independent pathways, vesicular storage and release, permeation through ATP-permeable channels, and leakage from the cells (Lazarowski, 2012). Among them, vesicular storage and release of ATP occur through the exact mechanism of classical neurotransmitters such as acetylcholine and dopamine in the synaptic vesicles in neurons. First, the neurotransmitters are stored in the secretory vesicles through active transport by vesicular neurotransmitter transporters using an electrochemical gradient of protons across the membranes established by the V-ATPase. Then, the neurotransmitters are released extracellularly through exocytosis (Zimmermann, 2008; Omote & Moriyama, 2013; Moriyama et al., 2017).

Vesicular nucleotide transporter (VNUT), the ninth member of the SLC17-type organic anion transporter family, is a molecular device performing vesicular storage of nucleotides in ATP-secreting cells and plays an essential role in the purinergic chemical transduction (Sawada et al., 2008; Mutafova-Yambolieva & Durnin, 2014; Moriyama et al., 2017; Wightman et al., 2018; Miras-Portugal et al., 2019; Hasuzawa et al., 2020). Mice lacking the VNUT gene (*SLC17A9*) show depletion of ATP in secretory vesicles, followed by reduced or abolished vesicular ATP release, resulting in blockade of purinergic chemical transduction for suppression of pain perception and secretion of inflammatory cytokines (Sakamoto et al., 2014; Estevez-Herrera et al., 2016; Masuda et al., 2016; Moriyama et al., 2017; Kinoshita et al., 2018; Hasuzawa et al., 2020). In contrast, the cells harboring overexpressed VNUT secrete more ATP with increased pain perception and inflammation (Masuda et al., 2016; Hasuzawa et al., 2020). Agents that inhibit VNUT may reduce ATP concentration in the luminal space of the secretory vesicles, thereby reducing the amount of ATP released, concomitantly blocking purinergic chemical transmission (Miras-Portugal et al., 2019; Hasuzawa et al., 2021). Indeed, clodronate, the first-generation bisphosphonate, acts as a VNUT inhibitor and suppresses vesicular storage and release of ATP, providing therapeutic effects on intractable pain, chronic inflammation, hepatocyte fibrosis, and insulin resistance (Kato et al., 2017; Moriyama & Nomura, 2018; Hasuzawa et al., 2020; Tatsushima et al., 2021). Therefore, increased attention has been paid to developing VNUT inhibitors for treating intractable pain and intractable inflammatory diseases (Moriyama & Nomura, 2018; Miras-Portugal et al., 2019).

Eicosapentaenoic acid (EPA), an essential fatty acid belonging to ω3 fatty acids, exhibits a wide range of beneficial pharmacological actions, such as analgesic and anti-inflammatory effects, although its mechanism of action is far less understood (Simopoulos, 2002; Ko et al., 2010; Poudyal et al., 2011; Dyall, 2015; Liao et al., 2019). Very recently, Miyaji and colleagues reported that EPA is a potent VNUT inhibitor using proteoliposomes reconstituted with purified VNUT as an assay system and concluded that VNUT is a molecular target of EPA for treatment of neuropathic and inflammatory pain treatment (Kato et al., 2022). However, as mentioned above, vesicular storage and release of ATP require multiple factors besides VNUT. Impairment of each factor may arrest vesicular storage and release of ATP, providing similar effects to VNUT inhibitors. For example, proton conductors such as CCCP increase $H^+$ permeability across the vesicle membrane, thereby apparent inhibiting ATP uptake, followed by inhibition of vesicular storage and release of ATP (Omote & Moriyama, 2013; see Figure 1). V-ATPase inhibitors such as bafilomycins and concanamycins may have similar effects to proton conductors. Therefore, we suspected that Miyaji and colleagues needed to pay more attention to the possibility that EPA works on factors other than VNUT.

This study was conducted to validate that EPA is an inhibitor of VNUT. To rule out the possibility that EPA affects factors other than VNUT, we evaluated the effects of EPA on V-ATPase and vesicular uptake of neurotransmitters in chromaffin granule membrane vesicles and brain synaptic vesicles. Consequently, we obtained an unexpected result that EPA increased proton permeability across membranes, thereby non-specifically affecting the vesicular uptake of neurotransmitters. The novel role of the EPA on chemical transmission was also discussed.

## Materials and methods

### Materials

EPA obtained from Cayman Chemicals was suspended in ethanol to a concentration of 100 mg/ml. ATP-tris salt, CCCP, valinomycin, and oligomycin were obtained from Sigma-Aldrich. Bafilomycin $A_1$ was from Fuji film/Wako. Concanamycin B (con B), a V-ATPase inhibitor (Ito et al., 1995), was kindly supplied by Dr. Kouich Ito (Center for Cancer Research, MIT). [2,8-$^3$H] adenosine triphosphate tetrasodium salt (26.0 Ci/mmol), 3,4-[RING-2,5,6-$^3$H] dihydroxyphenylethylamine (dopamine) (30 Ci/mmol) were obtained from New England Nuclear. [3,4-$^3$H] L-glutamic acid (20 Ci/mmol) was from Moravek Inc.

### Preparations

Bovine adrenal glands were obtained from a local slaughterhouse and brought to the laboratory in an ice bath. Then chromaffin granule membrane vesicles were

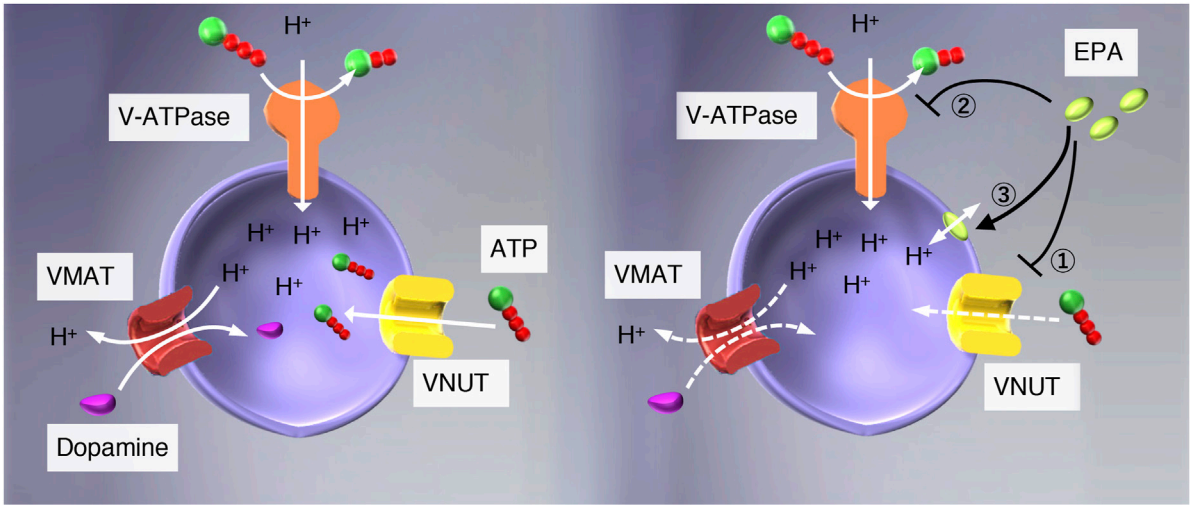


FIGURE 1
Possible modes of action of EPA in the vesicular storage of ATP. (*left*) V-ATPase pumps protons upon hydrolysis of ATP and establishes an electrochemical gradient of protons across the vesicular membranes, and drives storage of monoamine and ATP. (*right*) EPA may interact with 1) VNUT, 2) V-ATPase, or 3) vesicular membranes. If the interaction between EPA and VNUT is specific, EPA will not affect the ATP-dependent formation of ΔpH, Δψ, and ATP-dependent dopamine uptake in chromaffin granule membranes. ATP-dependent L-glutamate uptake in synaptic vesicles would be unaffected as well.

prepared as described previously (Moriyama & Nelson, 1987; Nelson et al., 1988). Synaptic vesicles [lysis pellet 2 (LP2)] were prepared from the mouse brain isolated from C57BL/6J male mice (25—30 weeks) as described previously (Huttner et al., 1983) with a slight modification (Moriyama & Futai, 1990). These membrane vesicles were frozen and kept at −80°C until use. All mouse procedures and protocols were conducted under the Guide for the Care and Use of Laboratory Animals and approved by the Ethics Committee on Animal Experimentation from Kurume University. Chromaffin granule V-ATPase was purified as described previously and stored at −80°C until use (Moriyama & Nelson, 1987). When necessary, the V-ATPase fraction (~0.5 ml) was diluted 50 folds into an appropriate buffer, centrifuged at 150,000 g for 1 h, and the resultant clear precipitate (the reconstituted proteoliposomes containing V-ATPase) was suspended in the buffer as specified, kept on ice and used within the day of preparation.

## Assays

ATP-dependent formation of ΔpH (acidic inside) of membrane vesicles or proteoliposomes was assayed using fluorescence quenching of acridine orange with excitation and emission wavelengths of 420 and 500 nm in 2 ml of the buffer consisting of 20 mM MOPS-tris, pH 7.0, 0.1 K KCl, 0.2 M sucrose, 5 mM Mg acetate, 0.2 μg valinomycin, 2 μM acridine orange and membranes (~20 μg for membrane vesicles or 2 μg for proteoliposomes (Moriyama et al., 1991). ATP-dependent formation of Δψ (inside positive) by membrane vesicles was measured using oxonol-V fluorescence quenching with excitation and emission wavelengths of 580 and 630 nm in the buffer consisting of 20 mM MOPS-tris, pH 7.0, 0.3 M sucrose, 5 mM KCl, 5 mM Mg-acetate, 5 μM oxonol-V and ~20 μg membrane vesicles (Moriyama et al., 1991). ATP-dependent ATP uptake by chromaffin granule membrane vesicles was assayed in the buffer 0.5 mM consisting of 20 mM MOPS-tris pH 7.0, 5 mM KCl, 5 m, 0.3 M sucrose, 5 mM Mg acetate, 1 mM radioactive ATP (15 KBq/one assay), 0.5 mM creatine phosphate, 10 unit creatine phosphate, and ~20 μg membrane vesicles as reported previously (Bankston & Guidotti, 1996). The assay mixture was incubated at 30°C, and aliquots (200 μl) were taken at the time intervals and filtrated through MF-MilliporeTM 0.45 μm MCE Membrane Filters. Then, the filters were washed with ice-cold 13 ml of 20 mM MOPS-tris pH 7.0, 0.3 M sucrose, 5 mM KCl, 5 mM Mg acetate, and solved in Clear-sol II (Nakalai Tesque). Then the radioactivity remaining on the filters was counted on a liquid scintillation counter. ATP-dependent uptake of L-glutamate was also assayed as described above, except that radio-labeled L-glutamate (0.1 mM, 8 KBq/one assay) was used, and both creatine phosphate and creatine kinase were omitted (Moriyama and Yamamoto, 1995). ATP-dependent dopamine uptake was also assayed as described

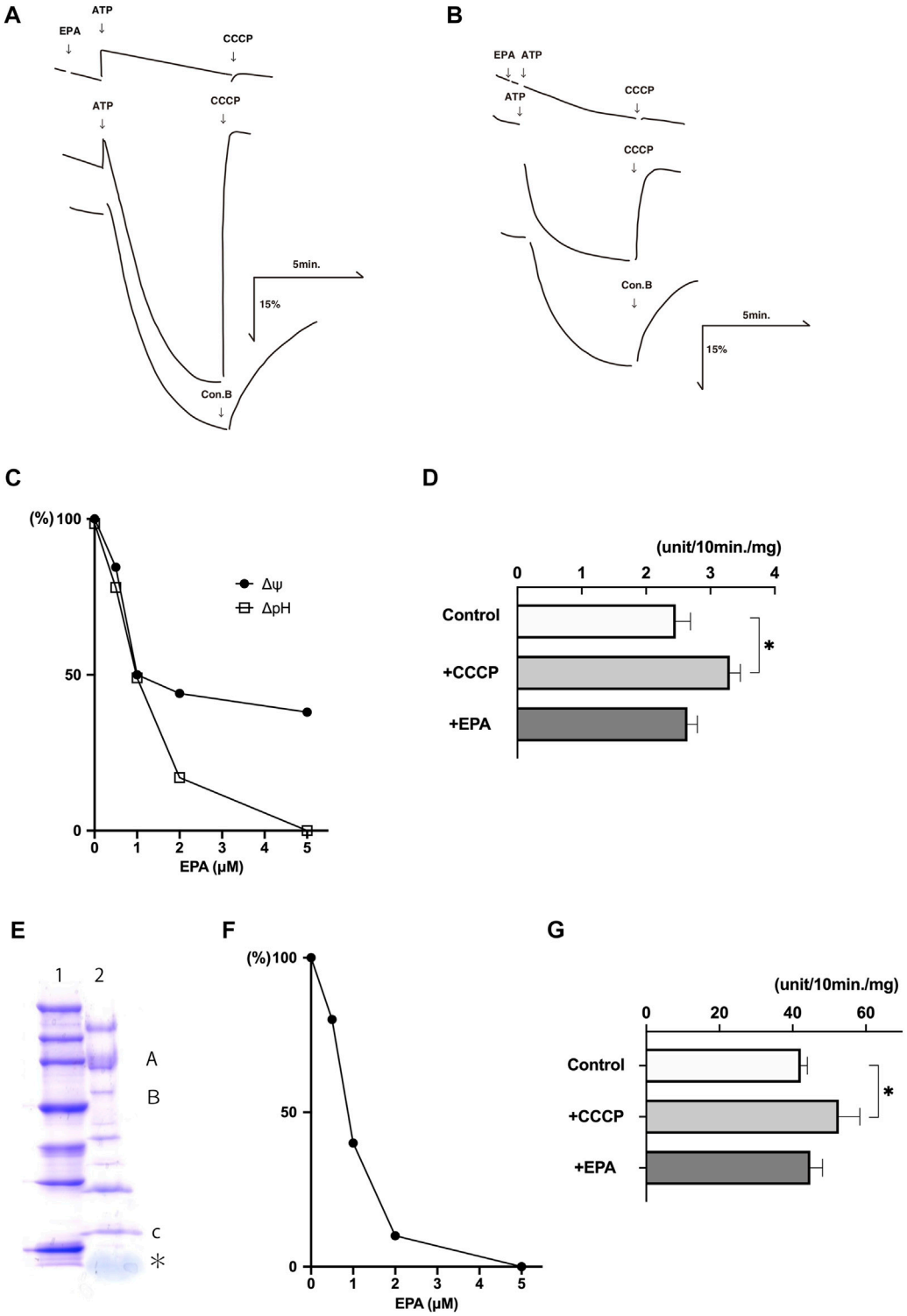


FIGURE 2
EPA uncouples ATP-dependent proton transport and ATPase activity in the chromaffin granule membrane vesicles and reconstituted proteoliposomes. Typical examples of the ATP-dependent formation of ΔpH (acridine orange fluorescence quenching) **(A)** and Δψ (oxonol-V fluorescence quenching) **(B)** in chromaffin granule membrane vesicles (20 μg protein) were shown. Additions, ATP at 2 mM; EPA 5 μM in (A) and 10 μM in (B); CCCP, 1 μM, con B 1 μM. **(C)**. Dose dependence on the effect of EPA. Acridine orange (□), oxonol-V (●). 100% corresponding to the fluorescence intensity before adding ATP. An average of duplicate determinations. **(D)** The effect of EPA at 5 μM and CCCP at 1 μM on the Mg-ATPase activity. About 60% of the total ATPase activity was sensitive to con B at 1 μM of the chromaffin granule membrane vesicles, corresponding to

(*Continued*)

FIGURE 2 (Continued)
0.25 units/mg protein. $n = 5$; $p < 0.005$. **(E)** Purified V-ATPase was dissociated with sample buffer containing 1% SDS, and protein (2 μg) was subjected to 5%—20% gradient polyacrylamide containing SDS (ePAGEL, Atto) and electrophoresed. After electrophoresis, the gel was stained with Coomassie Brilliant Blue. Lane 1, Molecular weight marker (Perfect Protein™ Markers, 15–150 kDa) (Novagen). Lane 2, Purified V-ATPase. The positions of subunits A, B, and c were also indicated. * corresponded to phospholipids. **(F)** Dose dependence of EPA on the ATP-dependent formation ΔpH (acridine orange fluorescence quenching). ATP-dependent acridine orange fluorescence quenching in the reconstituted proteoliposomes (4 μg protein) was measured as described in the Experimental procedures in the presence or absence of EPA at listed concentrations. Results were average of duplicate determinations and expressed as relative activities taking 100% as the maximum ATP-dependent quenching in the absence of EPA (25% fluorescence intensity). **(G)** ATP hydrolysis by the reconstituted proteoliposomes was measured in the 20 mM MOPS-tris, pH 7.0, 0.1 M NaCl, 5 mM Mg-acetate and the reconstituted proteoliposomes (4 μg protein) in the presence or absence of CCCP (1 μM) or EPA 5 μM. More than 95% of the ATPase activity was sensitive to con B at 1 μM. 100% corresponds to 4.0 units/mg protein. $n = 5$; $p < 0.01$.

above, except that the buffer consisting of 20 mM MOPS-tris pH 7.0, 0.1 M KCl, 0.1 M sucrose, 5 mM Mg-acetate, dopamine (10 μM, 15 KBq/one assay) and ~20 μg membrane vesicles used.

## Other procedures

ATPase activity was measured colorimetrically using 10 mM $KH_2PO_4$ solution as standard inorganic phosphate as described (Moriyama et al., 1991). One unit was defined as 1 μmol of Pi released/min/mg protein at 30°C. Polyacrylamide gel electrophoresis in the presence of SDS was performed as described (Moriyama et al., 1991). Protein concentrations were determined by the method by Bradford using bovine serum albumin as a standard according to the manufacturer's protocol (BIORAD).

## Data analysis

If otherwise specified, all numerical values are shown as means ± standard errors of the means (SEMs; $n$ = 3–5). Statistical significance was determined by Student's $t$-test.

# Results

## Effect of eicosapentaenoic acid on V-ATPase activities from chromaffin granules

As the first step of the study, we investigated the effect of EPA on the ATP-dependent proton transport of chromaffin granule membrane vesicles, which has been used as a model system for vesicular accumulation of neurotransmitters (Njus et al., 1986; Johnson, 1988; Nelson et al., 1988). Then, EPA in ethanol solution was included in the assay mixture to give the final concentrations according to the published procedure (Kato et al., 2022).

The addition of ATP to the buffer containing chromaffin granule membrane vesicles caused quenchings of the fluorescence of acridine orange, which restored upon the addition of CCCP, a proton conductor, or concanamycin B (con B), a V-ATPase inhibitor, indicating ATP-dependent formation of ΔpH (acidic inside) across the membranes (Figure 2A). EPA at 5 μM inhibited the ATP-dependent formation of ΔpH. Parallelly, we detected the ATP-dependent formation of Δψ (positive inside) across the chromaffin granule membrane vesicles by monitoring fluorescence quenching of oxonol-V (Figure 2B). EPA at 10 μM inhibited the ATP-dependent formation of Δψ. EPA-evoked inhibition on the ATP-dependent formation of ΔpH and Δψ exhibited in a dose-dependent fashion. The concentrations of EPA required 50% inhibition for ΔpH and Δψ were around 1 μM each (Figure 2C). Under the assay conditions, around 65% $Mg^{2+}$-ATPase activity was sensitive to con B at 1 μM. CCCP at 1 μM stimulated the con B-sensitive ATPase activity by ~ 140% (Figure 2D). EPA at 5 μM slightly stimulated the con B-sensitive ATPase activity (Figure 2D).

Essentially similar effects were obtained with the proteoliposomes containing purified V-ATPase. We purified chromaffin granule V-ATPase according to the established procedure (Moriyama & Nelson, 1987; Nelson et al., 1988). Figure 2E indicated a Coomassie Brilliant Blue (CBB)-stained image of purified V-ATPase after SDS gel electrophoresis, showing the same subunit structure of chromaffin granule V-ATPase as reported previously (Moriyama & Nelson, 1987). Because purified ATPase fraction also contains endogenous phospholipids, the proteoliposomes containing V-ATPase can form upon dilution of V-ATPase fraction with an appropriate buffer. As shown in Figure 2F, EPA inhibited ATP-dependent quenching of acridine orange with ID50 being 1 μM. Under the conditions, EPA at 5 μM did not inhibit the $Mg^{2+}$-ATPase activity, and CCCP at 1 μM stimulated it (Figure 2G). Together, these results indicated that EPA does not affect the V-ATPase but increases proton permeability across the membrane in the chromaffin granule membrane and proteoliposomes. Thus, EPA

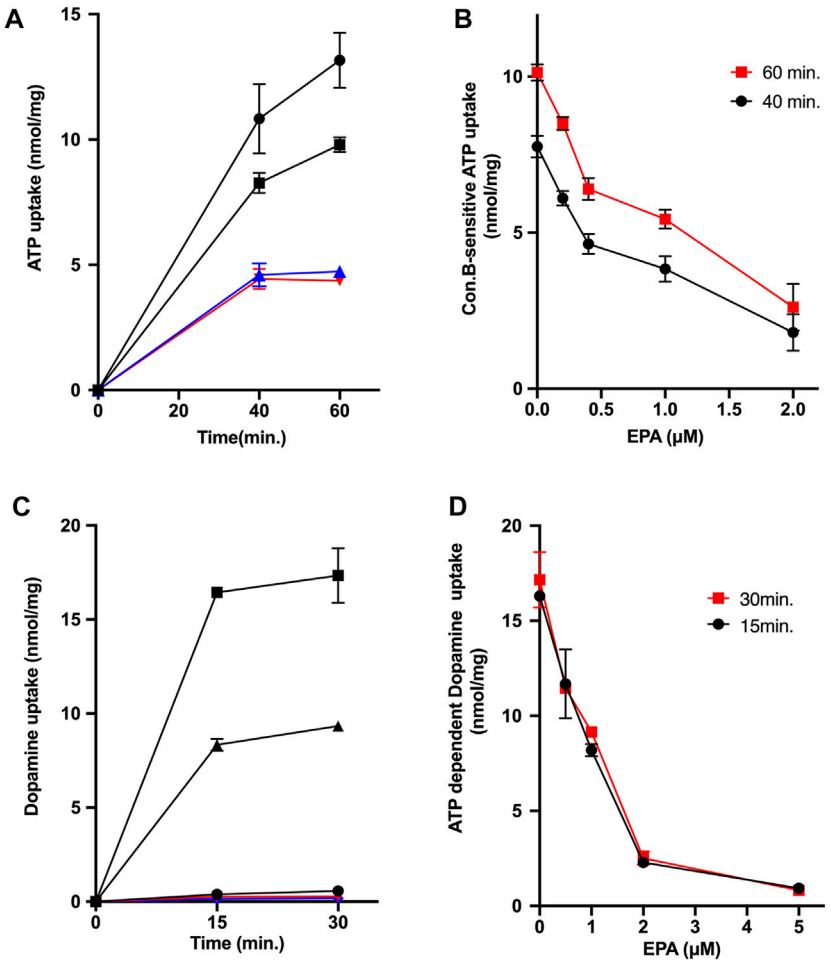


FIGURE 3
EPA inhibits uptakes of ATP and dopamine in chromaffin granule membrane vesicles. **(A,B)** Effect of EPA on the ATP-dependent ATP uptake by chromaffin granule membrane vesicles. **(A)** indicates the time course of ATP uptake. Assays were performed in the absence (●) or presence of EPA, 1 μM (■), con B, 1 μM (▼), or CCCP 1 μM (▲). **(B)** indicates the EPA dose dependence. ATP uptake was assayed as in Figure 3 in the presence or absence of the listed concentration of EPA. The amount of ATP uptake in the presence of con B at 1 μM at either 40 min or 60 min was subtracted from the total amount of ATP uptake to obtain V-ATPase coupled ATP uptake. Note that con B-resistant ATP uptake was insensitive to EPA. **(C,D)** Effect of EPA on the ATP-dependent dopamine uptake by chromaffin granule membrane vesicles. **(C)** indicates the time course of dopamine uptake. Assays were performed in the absence (●) or presence (■, ▲, ▼, ■). Additions; EPA at 1 μM (▲); CCCP at 1 μM (▼); con B at 1 μM (■). **(D)** indicates the dose dependence on the effect of EPA. The ATP-dependent dopamine uptake at the listed EPA concentrations at 15 min (●) or 30 min (■) was shown.

uncouples ATP-dependent proton transport and ATP hydrolysis by V-ATPase.

## Effect of eicosapentaenoic acid on ATP-dependent uptakes of ATP and dopamine by chromaffin granule membrane vesicles

Subsequently, we investigated the effects of EPA on ATP-dependent uptakes of ATP and dopamine by chromaffin granule membrane vesicles: Both activities are regarded to reflect the transport activity by VNUT and the combinations of VMAT1 and VMAT2, respectively (Henry et al., 1994; Bankston & Guidotti, 1996; Moriyama et al., 2017). As shown in Figure 3A, ATP-dependent ATP uptake by chromaffin granule membrane vesicles was observed in the presence of 5 mM KCl, which was inhibited by the addition of CCCP or con B. EPA also inhibited the ATP uptake at 60 min with ID50 being around 1.2 μM (Figure 3B). We further measured ATP-dependent dopamine uptake by chromaffin granule membrane vesicles. The dopamine uptake was driven by the addition of ATP (Figure 3C). The ATP-dependent dopamine uptake was inhibited by the addition of either CCCP or con B (Figure 3C). EPA also inhibited ATP-

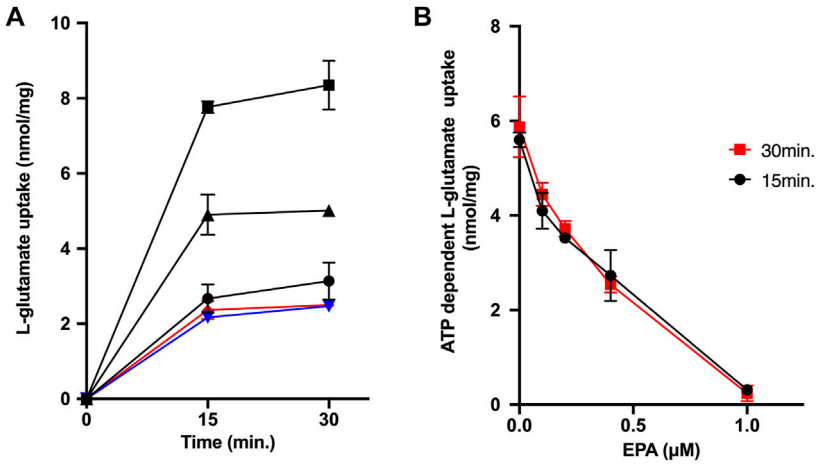


FIGURE 4
EPA inhibits ATP-dependent L-glutamate uptake by synaptic vesicles. **(A)** Time course. Additions, no additions (●); ATP (■); ATP + EPA at 0.4 μM (▲); ATP + con B at 1 μM (▼); ATP + CCCP at 1 μM (▲). **(B)** EPA Dose dependence. ATP-dependent L-glutamate uptake at the listed EPA concentrations at 15 min (●) or 30 min (■) were measured.

dependent dopamine uptake with the ID50 values being 1 μM (Figures 3C,D).

## Effect of eicosapentaenoic acid on ATP-dependent uptake of L-glutamate by synaptic vesicles

Finally, we measured ATP-dependent glutamate uptake by synaptic vesicles as an index of transport activities by VGLUT1 and VGLUT2 (Pietrancosta et al., 2020). As shown in Figure 4A, synaptic vesicles took up L-glutamate upon adding ATP. Conversely, either CCCP or con B inhibited the ATP-dependent L-glutamate uptake. EPA strongly inhibited the ATP-dependent L-glutamate uptake, with ID50 values being 0.35 μM (Figures 4A,B).

# Discussion

In the present study, we investigated the validity of EPA as a VNUT inhibitor. Miyaji and colleagues have evaluated the action of EPA using soybean phospholipid liposomes in which purified VNUT was incorporated (Kato et al., 2022). Because the transporter function, and the action of hydrophobic compounds, are occasionally affected by the phospholipid composition, we investigated the effect of EPA on the functions of V-ATPase and vesicular transporters in the chromaffin granule membrane vesicles and synaptic vesicles as examples of native secretory vesicles.

We found that EPA increased the proton permeability of chromaffin granule membranes. The ID50 values on the effects on ΔpH (acridine orange fluorescence quenching) and Δψ (oxonol-V fluorescence quenching) were almost equal, around 1 μM. Under these conditions, EPA did not inhibit the con B-sensitive ATPase activity, which corresponded to V-ATPase activity in the chromaffin granule membrane and proteoliposomes. Furthermore, a proton conductor, CCCP, exhibited a similar but more pronounced effect to that of EPA, a well-known phenomenon observed when a proton conductor is applied to vesicles containing electrogenic proton ATPase. Thus, it is evident that EPA increases proton permeability across the membranes and acts as an uncoupler in chromaffin granule membranes.

The property of EPA as an uncoupler in secretory vesicles raised the possibility that EPA inhibits the uptake of neurotransmitters by secretory vesicles because vesicular neurotransmitter transporters are energetically coupled with V-ATPase. Indeed, EPA inhibited ATP-dependent ATP and dopamine uptake in chromaffin granule membrane vesicles, with ID50 values being 1.2 and 1.0 μM, respectively. ATP-dependent ATP uptake means ATP uptake driven by V-ATPase, defined as the difference in ATP uptake when V-ATPase is inhibited by con B (con B-sensitive ATP uptake). Notably, the inhibitory effect of EPA on ATP uptake is approximately equal to that of dopamine uptake, not more potent than dopamine uptake. Moreover, according to Miyaji and colleagues, the ID50 of EPA on the ATP uptake in the reconstituted proteoliposomes is 67 nM, and about 20% ATP uptake activity remains even at 1 μM (Kato et al., 2022). However, this degree of inhibition is not particularly strong

compared to the effect of EPA on the ATP uptake by the chromaffin granule membrane vesicles shown in this paper. Moreover, we found that EPA inhibited ATP-dependent L-glutamate uptake in synaptic vesicles with ID50 values of 0.35 μM, whose inhibitory potency is comparable to that of VNUT reported by Miyaji and colleagues (Kato et al., 2022). Therefore, we concluded that, in chromaffin granules and synaptic vesicles, EPA acts as a proton conductor rather than a specific inhibitor of VNUT and non-specifically inhibits the vesicular storage of neurotransmitters. It should be stressed that the present results do not deny the existence of any direct interaction between VNUT and EPA. However, such hypothetical interactions, if any, may not be VNUT-specific, but may have broader coverage.

The proposal by Miyaji and colleagues that EPA, as a VNUT inhibitor, can block purinergic chemical transmission might lose the point. However, it could be significant because it focuses on vesicular neurotransmitter storage. The present results expanded their idea and suggested that EPA may act non-specifically on the vesicular storage of neurotransmitters and inhibit a broader range of chemical transmission, including purinergic chemical transmission. Furthermore, since the primary reaction site for uncouplers is mitochondria, the results presented in this study speculate that EPA also likely influences mitochondrial bioenergetics, including oxidative phosphorylation. Overall, these actions may explain, at least in part, EPA-evoked beneficial therapeutic effects.

Currently, the mechanism by which EPA increases $H^+$ permeability across secretory vesicle membranes is unknown. However, hydrophobic acids, such as various fatty acids, generally have an uncoupling action (Paola & Lorusso, 2006). Furthermore, a certain level $\Delta\psi$ remains even with adding 2—5 μM EPA. At the same time, the uptake of neurotransmitters by secretory vesicles is inhibited (Figures 3B,D), suggesting that EPA may possess the ability as a decoupler that inhibits oxidative phosphorylation without increasing proton permeability (Shinohara & Terada, 2000).

In conclusion, given the current results, it is difficult to conclude that EPA is a VNUT-specific inhibitor because of its nonspecific effectiveness in the vesicular uptake of neurotransmitters.

## Data availability statement

The original contributions presented in the study are included in the article/Supplementary Material, further inquiries can be directed to the corresponding author.

## Ethics statement

The animal study was reviewed and approved by the Ethics Committee on Animal Experimentation from Kurume University.

## Author contributions

YM, NH, and MN designed the research, performed all experiments, analyzed the data, wrote and approved the manuscripts, and agreed to be announced for all aspects of the work.

## Funding

The Japanese Society for the Promotion of Science (JSPS) KAKENHI (MN, Grant Number 26461383; NH, Grant Number 21K17653; YM, Grant Number 25253008) supported the work.

## Conflict of interest

The authors declare that the research was conducted in the absence of any commercial or financial relationships that could be construed as a potential conflict of interest.

## Publisher's note



## References

Bankston, L. A., and Guidotti, G. (1996). Characterization of ATP transport into chromaffin granule ghosts. Synergy of ATP and serotonin accumulation in chromaffin granule ghosts. *J. Biol. Chem.* 271, 17132–17138. doi:10.1074/jbc.271.29.17132

Burnstock, G. (2007). Physiology and pathophysiology of purinergic neurotransmission. *Physiol. Rev.* 87, 659–797. doi:10.1152/physrev.00043.2006

Dyall, S. C. (2015). Long-chain omega-3 fatty acids and the brain: A review of the independent and shared effects of EPA, DPA and DHA. *Front. Aging Neurosci.* 7, 52. doi:10.3389/fnagi.2015.00052

Esteves-Herrera, J., Dominguez, N., Pardo, M. T., Gonzalez-Santana, A., Westhead, E. W., Borges, R., et al. (2016). Atp: The crucial component of secretory vesicles. *Proc. Natl. Acad. Sci. U. S. A.* 113, E4098–E4106. doi:10.1073/pnas.1600690113

Ghoreishi, Z., Esfahani, A., Djazayeri, A., Djalali, M., Goldstein, B., Ayromlou, H., et al. (2012). Omega-3 fatty acids are protective against paclitaxel-induced peripheral neuropathy: A randomized double-blind placebo-controlled trial. *BMC Cancer* 12, 355. doi:10.1186/1471-2407-12-355

Hasuzawa, N., Matsushima, K., Wang, L., Kabashima, M., Tokubuchi, R., Nagayama, A., et al. (2021). Clodronate, an inhibitor of the vesicular nucleotide

transporter, ameliorates steatohepatitis and acute liver injury. *Sci. Rep.* 11, 5192. doi:10.1038/s41598-021-83144-w

Hasuzawa, N., Moriyama, S., Moriyama, Y., and Nomura, M. (2020). Physiopathological roles of vesicular nucleotide transporter (VNUT), an essential component for vesicular ATP release. *Biochim. Biophys. Acta. Biomembr.* 1862, 183408. doi:10.1016/j.bbamem.2020.183408

Henry, J-P., Botton, D., Sagne, C., Isambert, M-F., Desmos, C., Blanchard, V., et al. (1994). Biochemistry and molecular biology of the vesicular monoamine transporter from chromaffin granules. *J. Exp. Biol.* 196, 251–262. doi:10.1242/jeb.196.1.251

Huttner, W. B., Schiebler, W., Greengard, P., and De Camilli, P. (1983). Synapsin I (protein I), a nerve terminal-specific phosphoprotein. III. Its association with synaptic vesicles studied in a highly purified synaptic vesicle preparation. *J. Cell Biol.* 96, 1374–1388. doi:10.1083/jcb.96.5.1374

Ito, K., Kobayashi, T., Moriyama, Y., Toshima, K., Tatsuta, K., Kakiuchi, T., et al. (1995). Concanamycin B inhibits the expression of newly-synthesized MHC class II molecules on the cell surface. *J. Antibiot.* 48, 488–494. doi:10.7164/antibiotics.48.488

Johnson, R. G. (1988). Accumulation of biological amines into chromaffin granules: A model for hormone and neurotransmitter transport. *Physiol. Rev.* 68, 232–307. doi:10.1152/physrev.1988.68.1.232

Kato, Y., Hiasa, M., Ichikawa, R., Hasuzawa, N., Kadowaki, A., Iwatsuki, K., et al. (2017). Identification of a vesicular ATP release inhibitor for the treatment of neuropathic and inflammatory pain. *Proc. Natl. Acad. Sci. U. S. A.* 114, E6297–E6305. doi:10.1073/pnas.1704847114

Kato, Y., Ohsugi, K., Fukuno, Y., Iwatsuki, K., Harada, Y., and Miyaji, T. (2022). Vesicular nucleotide transporter is a molecular target of eicosapentaenoic acid for neuropathic and inflammatory pain treatment. *Proc. Natl. Acad. Sci. U. S. A.* 119, e2122158119. doi:10.1073/pnas.2122158119

Kinoshita, M., Hirayama, Y., Fujishita, K., Shibata, K., Shinozaki, Y., Shigetomi, E., et al. (2018). Anti-depressant fluoxetine reveals its therapeutic effect via astrocytes. *EBioMedicine* 32, 72–83. doi:10.1016/j.ebiom.2018.05.036

Ko, G. D., Nowacki, N. B., Arseneau, L., and Hum, A. (2010). Omega-3 fatty acids for neuropathic pain: Case series. *Clin. J. Pain* 26, 168–172. doi:10.1097/AJP.0b013e3181bb8533

Lazarowski, E. R. (2012). Vesicular and conductive mechanisms of nucleotide release. *Purinergic Signal.* 8, 359–373. doi:10.1007/s11302-012-9304-9

Liao, Y., Xie, B., Zhang, H., He, Q., Guo, L., Subramanieapillai, M., et al. (2019). Efficacy of omega-3 PUAs in depression: a meta-analysis. *Transl Psychiatry* 9, 190

Masuda, T., Ozono, Y., Mukuriya, S., Kohno, Y., Tozaki-Saitoh, H., Iwatsuki, K., et al. (2016). Dorsal horn neurons release extracellular ATP in a VNUT-dependent manner that underlies neuropathic pain. *Nat. Commun.* 12529, 12529. doi:10.1038/ncomms12529

Miras-Portugal, M. T., Menéndez-Méndez, A., Gómez-Villafuertes, R., Ortega, F., Delicado, E. G., Pérez-Sen, R., et al. (2019). Physiopathological role of the vesicular nucleotide transporter (VNUT) in the central nervous system: Relevance of the vesicular nucleotide release as a potential therapeutic target. *Front. Cell. Neurosci.* 13, 224. doi:10.3389/fncel.2019.00224

Moriyama, Y., and Futai, M. (1990). $H^+$-ATPase, a primary $H^+$ pump for the accumulation of neurotransmitters, is a major constituent of brain synaptic vesicles. *Biochem. Biophys. Res. Commun.* 173, 443–448. doi:10.1016/s0006-291x(05)81078-2

Moriyama, Y., Hiasa, M., Sakamoto, S., Omote, H., and Nomura, M. (2017). Vesicular nucleotide transporter (VNUT): Appearance of an actress on the stage of purinergic signaling. *Purinergic Signal.* 13, 387–404. doi:10.1007/s11302-017-9568-1

Moriyama, Y., Iwamoto, A., Hanada, H., Maeda, M., and Futai, M. (1991). One-step purification of *Escherichia coli* $H^+$-ATPase ($F_0F_1$) and its reconstitution into liposomes with neurotransmitter transporters. *J. Biol. Chem.* 266, 22141–22146. doi:10.1016/s0021-9258(18)54545-2

Moriyama, Y., and Nelson, N. (1987). The purified ATPase from chromaffin granule membranes is an anion-dependent proton pump. *J. Biol. Chem.* 262, 9175–9180. doi:10.1016/s0021-9258(18)48064-7

Moriyama, Y., and Nomura, M. (2018). Clodronate: A vesicular ATP release blocker. *Trends Pharmacol. Sci.* 39, 13–23. doi:10.1016/j.tips.2017.10.007

Moriyama, Y., and Yamamoto, A. (1995). Vesicular L-glutamate transporter in microvesicles from bovine pineal glands. Driving force, mechanism of chloride anion activation, and substrate specificity. *J. Biol. Chem.* 270, 22314–22320. doi:10.1074/jbc.270.38.22314

Mutafova-Yambolieva, V. N., and Durnin, L. (2014). The purinergic neurotransmitter revisited: A single substance or multiple players? *Pharmacol. Ther.* 144, 162–191. doi:10.1016/j.pharmthera.2014.05.012

Nelson, N., Cidon, S., and Moriyama, Y. (1988). Chromaffin granule proton pump. *Methods Enzymol.* 157, 619–633. doi:10.1016/0076-6879(88)57110-0

Njus, D., Kelley, P. M., and Harnadek, G. J. (1986). Bioenergetics of secretory vesicles. *Biochim Biophys Acta* 853, 237–265.

Omote, H., and Moriyama, Y. (2013). Vesicular neurotransmitter transporters: An approach for studying transporters with purified proteins. *Physiology* 28, 39–50. doi:10.1152/physiol.00033.2012

Paola, M. D., and Lorusso, M. (2006). Interaction of free fatty acids with mitochondria: Coupling, uncoupling, and permeability transition. *Biochim. Biophys. Acta* 1757, 1330–1337. doi:10.1016/j.bbabio.2006.03.024

Pietrancosta, N., Djibo, M., Daumas, S., Mestikawy, S. E., and Erickson, J. D. (2020). Molecular, structural, functional, and pharmacological sites for vesicular glutamate transporter regulation. *Mol. Neurobiol.* 57, 3118–3142. doi:10.1007/s12035-020-01912-7

Poudyal, H., Panchal, S. K., Diwan, V., and Brown, L. (2011). Omega-3 fatty acids and metabolic syndrome: Effects and emerging mechanisms of action. *Prog. Lipid Res.* 50, 372–387. doi:10.1016/j.plipres.2011.06.003

Sakamoto, S., Miyaji, T., Hiasa, M., Ichikawa, R., Uematsu, A., Iwatsuki, K., et al. (2014). Impairment of vesicular ATP release affects glucose metabolism and increases insulin sensitivity. *Sci. Rep.* 4, 6689. doi:10.1038/srep06689

Sawada, K., Echigo, N., Juge, N., Otsuka, M., Omote, H., Yamamoto, A., et al. (2008). Identification of a vesicular nucleotide transporter. *Proc. Natl. Acad. Sci. U. S. A.* 105, 5683–5686. doi:10.1073/pnas.0800141105

Shinohara, Y., and Terada, H. (2000). "Uncouplers and oxidative phosphorylation: Activities and physiological significance," in *Membrane structure in disease and Drug therapy*. Editor G. D. Zimmer (New York: Marcel Dekker), 107–126.

Simopoulos, A. P. (2002). Omega-3 fatty acids in inflammation and autoimmune diseases. *J. Am. Coll. Nutr.* 21, 495–505. doi:10.1080/07315724.2002.10719248

Tatsushima, K., Hasuzawa, N., Wang, L., Hiasa, M., Sakamoto, S., Ashida, K., et al. (2021). Vesicular ATP release from hepatocytes plays a role in the progression of nonalcoholic steatohepatitis. *Biochim. Biophys. Acta. Mol. Basis Dis.* 1876, e166013. doi:10.1016/j.bbadis.2020.166013

Wightman, R. M., Dominguez, N., and Borges, R. (2018). How intravesicular composition affects exocytosis. *Pflugers Arch.* 470, 135–141. doi:10.1007/s00424-017-2035-6

Zimmermann, H. (2008). ATP and acetylcholine, equal brethren. *Neurochem. Int.* 52, 634–648. doi:10.1016/j.neuint.2007.09.004

frontiers | Frontiers in Pharmacology

TYPE Original Research
PUBLISHED 16 December 2022
DOI 10.3389/fphar.2022.1082997



OPEN ACCESS

EDITED BY
Yong Tang,
Chengdu University of Traditional Chinese Medicine, China

REVIEWED BY
Ana Raquel Santiago,
University of Coimbra, Portugal
Paulo Fernando Santos,
University of Coimbra, Portugal

*CORRESPONDENCE
Ying Gao,
gaoying105@163.com
Jia Qu,
jia.qu@163.com

†These authors have contributed equally to this work and share first authorship

SPECIALTY SECTION
This article was submitted to Experimental Pharmacology and Drug Discovery, a section of the journal Frontiers in Pharmacology

RECEIVED 28 October 2022
ACCEPTED 05 December 2022
PUBLISHED 16 December 2022

CITATION
Hu S, Li Y, Zhang Y, Shi R, Tang P, Zhang D, Kuang X, Chen J, Qu J and Gao Y (2022), The adenosine $A_{2A}$ receptor antagonist KW6002 distinctly regulates retinal ganglion cell morphology during postnatal development and neonatal inflammation.
*Front. Pharmacol.* 13:1082997.
doi: 10.3389/fphar.2022.1082997



# The adenosine $A_{2A}$ receptor antagonist KW6002 distinctly regulates retinal ganglion cell morphology during postnatal development and neonatal inflammation

Shisi Hu[1,2,3,4†], Yaoyao Li[1,2,3†], Yuanjie Zhang[1,2,3], Ruyi Shi[1,2,3], Ping Tang[1,2,3], Di Zhang[1,2,3], Xiuli Kuang[1,2,3], Jiangfan Chen[1,2,3], Jia Qu[2,3*] and Ying Gao[1,2,3*]

[1]The Molecular Neuropharmacology Laboratory and the Eye-Brain Research Center, State Key Laboratory of Ophthalmology, Optometry and Visual Science, Wenzhou Medical University, Wenzhou, China, [2]State Key Laboratory of Ophthalmology, Optometry and Visual Science, Wenzhou Medical University, Wenzhou, China, [3]School of Ophthalmology and Optometry and Eye Hospital, Wenzhou Medical University, Wenzhou, China, [4]Hainan Eye Hospital and Key Laboratory of Ophthalmology, Zhongshan Ophthalmic Center, Sun Yat-sen University, Haikou, China

Adenosine $A_{2A}$ receptors ($A_{2A}$Rs) appear early in the retina during postnatal development, but the roles of the $A_{2A}$Rs in the morphogenesis of distinct types of retinal ganglion cells (RGCs) during postnatal development and neonatal inflammatory response remain undetermined. As the RGCs are rather heterogeneous in morphology and functions in the retina, here we resorted to the Thy1-YFPH transgenic mice and three-dimensional (3D) neuron reconstruction to investigate how $A_{2A}$Rs regulate the morphogenesis of three morphologically distinct types of RGCs (namely Type I, II, III) during postnatal development and neonatal inflammation. We found that the $A_{2A}$R antagonist KW6002 did not change the proportion of the three RGC types during retinal development, but exerted a bidirectional effect on dendritic complexity of Type I and III RGCs and cell type-specifically altered their morphologies with decreased dendrite density of Type I, decreased the dendritic field area of Type II and III, increased dendrite density of Type III RGCs. Moreover, under neonatal inflammation condition, KW6002 specifically increased the proportion of Type I RGCs with enhanced the dendrite surface area and volume and the proportion of Type II RGCs with enlarged the soma area and perimeter. Thus, $A_{2A}$Rs exert distinct control of RGC morphologies to cell type-specifically fine-tune the RGC dendrites during normal development but to mainly suppress RGC soma and dendrite volume under neonatal inflammation.

KEYWORDS

**adenosine $A_{2A}$ receptor, retinal ganglion cell, morphology, 3D reconstruction, development, neonatal inflammation**

## 1 Introduction

Adenosine, an endogenous nucleoside, is a neuromodulator and intracellular messenger, which is widely present in the central nervous system, including the retina. Adenosine can modulate neuronal excitability, neurotransmitter release and synaptic activity by acting at four subtypes of adenosine receptors, namely A1, $A_{2A}$, $A_{2B}$, and A3 receptors (Chen et al., 2013). Among them, adenosine $A_{2A}$ receptor ($A_{2A}R$) appears early in the retina during development, which is detected at embryonic day 6 in chick embryo retina (Brito et al., 2012) and is also expressed widely in the retina, such as photoreceptors, inner nuclear layer neurons, starburst amacrine cells and retinal ganglion cells (RGCs). Previous studies have shown that the retinal $A_{2A}Rs$ exert control of dark-adaption in regulating photoreceptor coupling (Li et al., 2013), expression of rod opsin mRNA in tiger salamander (Alfinito et al., 2002), the release of glutamate from rod photoreceptors (Stella et al., 2003), the generation of the electroretinogram a- and b-waves and oscillatory potentials (OPs) (Jonsson and Eysteinsson, 2017) and the generation and modulation of retinal waves (Huang et al., 2014).

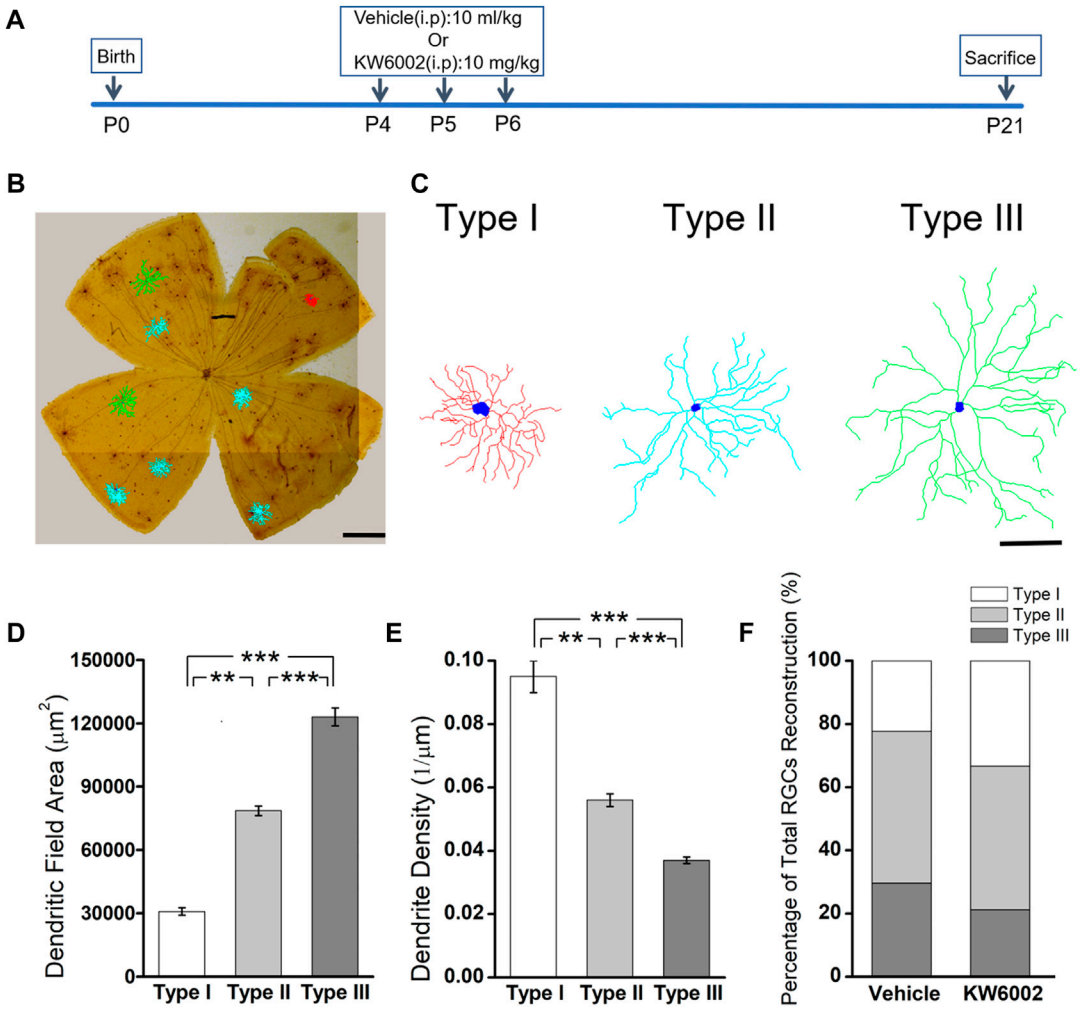


FIGURE 1
The effect of $A_{2A}R$ antagonist KW6002 on the proportion of different morphological types of RGCs during the development. **(A)** Timeline of KW6002 (or vehicle) administration in transgenic Thy-1 YFPH mice. **(B)** Representative flat-mounted whole retina showing three different morphological types of RGCs in different colors from transgenic Thy-1 YFPH mice (red, Type I; blue, Type II; green, Type III). The morphology of an individual RGC was revealed by immunohistochemistry and reconstructed by the Neurolucida system. Scale bar, 500 μm. **(C)** Representative 3D reconstructions of the three morphological types of RGCs as shown in B. Scale bar, 100 μm.**(D,E)** Quantitative evaluation of dendritic field area **(D)** and dendrite density **(E)** among different morphological types of RGCs. **(F)** The proportion of different morphological types of RGCs from the control and KW6002-treated mice during the development. Values are mean ± SEM; $^{**}p < 0.01$, $^{***}p < 0.001$. 54 RGCs from six retinas (3 vehicle-treated mice) and 66 RGCs from eight retinas (4 KW6002-treated mice) were analyzed in the control and KW6002-treated group, respectively. On average, nine RGCs were analyzed in each eye in the control group, while 8.25 RGCs per eye were analyzed in KW6002-treated group.

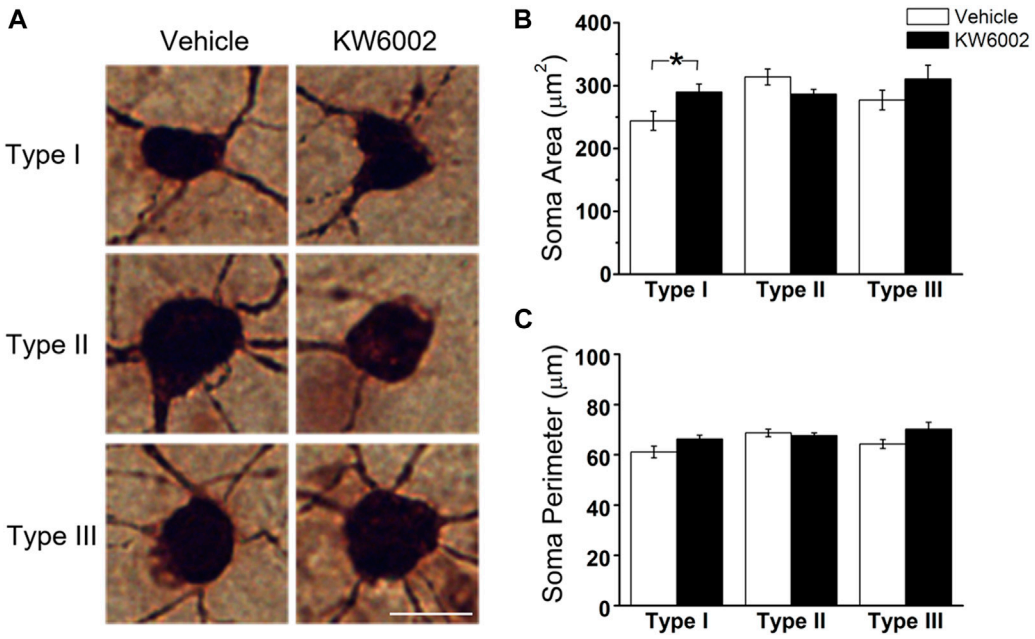


FIGURE 2
The effect of KW6002 on the somatic morphology of the three RGC types during the development. **(A)** Representative pictures of somata in each RGC type examined from vehicle -treated and KW6002-treated group. Scale bar, 20 μm. **(B,C)** Comparative analysis of soma area **(B)** and perimeter **(C)** of different RGC types between vehicle-treated and KW6002-treated mice. Data represent mean ± SEM. *$p < 0.05$.

Both *in vitro* and *in vivo* studies have revealed that $A_{2A}$Rs play important roles in brain development (Silva et al., 2013; Ribeiro et al., 2016; Alcada-Morais et al., 2021). Our previous study has found that $A_{2A}$Rs modulate microglia-mediated synaptic pruning of the retinogeniculate pathway in the dorsal lateral geniculate during postnatal development (Miao et al., 2021). However, the exact role of the $A_{2A}$Rs on the development of retinal neurons including different RGC types is still not known. The RGCs are rather heterogeneous and have been classified into over 30 different types, based on their dendritic anatomies, functional characteristics or transcriptomic features (Baden et al., 2016; Bae et al., 2018; Goetz et al., 2022; Huang et al., 2022). Furthermore, retinal $A_{2A}$Rs also participate in not only the normal retinal development but also the development under pathological processes in the retina, such as neuroinflammation and inflammation-associated retinal degeneration. While the involvement of adenosine and $A_{2A}$R in the regulation of brain microglia in two neonatal rat models of neuroinflammation (Colella et al., 2018) has been studied, much less attention has been paid to the effects of $A_{2A}$Rs on the development of RGCs after neonatal inflammation.

In the present study, we investigated how $A_{2A}$Rs regulate the morphology of RGCs during retinal development and neonatal inflammation, using the Thy1-YFPH transgenic mice coupled with three-dimensional (3D) neuron reconstruction method. We demonstrated that during normal development, the $A_{2A}$R antagonist KW6002 mainly decreased RGC morphogenesis as evident by the reduced dendritic field area of Type II and III RGCs, and the reduced dendrite density of Type I but with the increased the dendrite density of Type III RGCs. Moreover, under neonatal inflammation, KW6002 specifically increased the proportion of Type I RGCs with enhanced the dendrite surface area and volume and the proportion of Type II RGCs with enlarged the soma area and perimeter. Thus, $A_{2A}$Rs distinctly regulate RGC morphologies by fine-tuning the RGC dendrites in a cell type-specific manner during normal development, but mainly suppressing RGC soma and dendrite volume under neonatal inflammation.

# 2 Materials and methods

## 2.1 Animals

All animal protocols were approved by the Animal Care Committee of Wenzhou Medical University. The YFPH line of transgenic mice was obtained from the Jackson Laboratory (strain: B6. Cg-Tg (Thy1-YFPH) 2Jrs/J; Bar Harbor, Maine). All mice were given *ad libitum* access to food and water under a 12 h light/dark cycle with 50–60% humidity. The day of birth was counted as postnatal day 0 (P0).

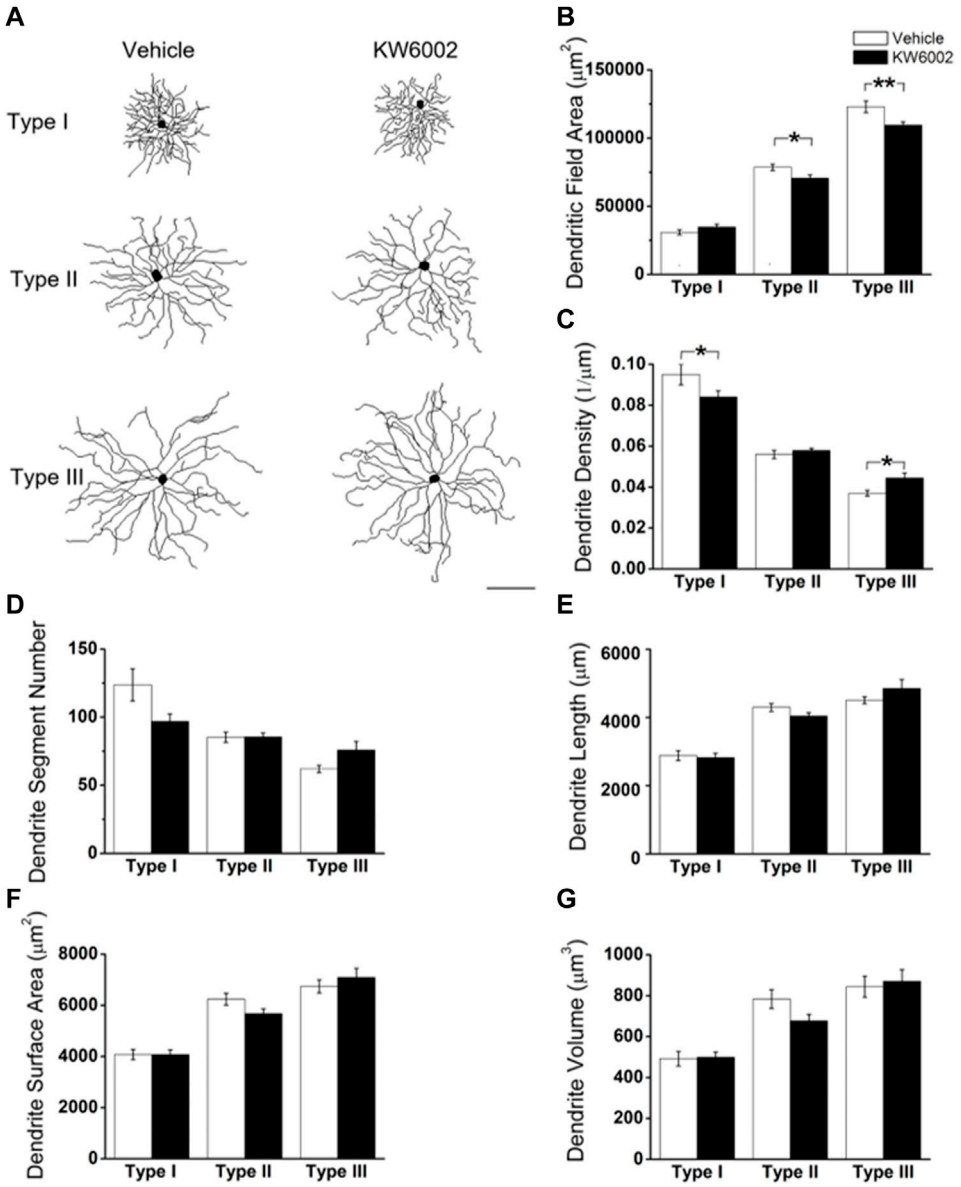


FIGURE 3
KW6002 differentially affected the dendritic morphology of RGCs during the development. **(A)** Representative 3D reconstructions of the three RGC types from the vehicle-treated and KW6002-treated mice. **(B–G)** Comparative analysis of dendritic field area **(B)**, dendrite density **(C)**, dendrite segment number **(D)**, dendrite length **(E)**, dendrite surface area **(F)** and dendrite volume **(G)** in each RGC type between the vehicle-treated and KW6002-treated group. Data represent mean ± SEM. *$p < 0.05$; **$p < 0.01$. Scale bar, 100 μm.

The littermates of the Thy1-YFPH mice were randomly divided into two groups. Pups received intraperitoneal (IP) injections of the $A_{2A}R$ antagonist KW6002 (10 mg/kg body weight, freshly prepared in dimethyl sulfoxide (DMSO, Sigma), ethoxylated castor oil (Sigma), and phosphate-buffered saline (PBS) with a proportion of 15%:15%:70% (Miao et al., 2021)) every day from P4 to P6. The control group was administered the corresponding vehicle in the same volume. The neonatal inflammation was induced in Thy1-YFPH mice by an intraperitoneal injection of lipopolysaccharide (LPS, 1 mg/kg, *E. coli* 055: B5; Sigma) 4 min after KW6002 treatment at P4.

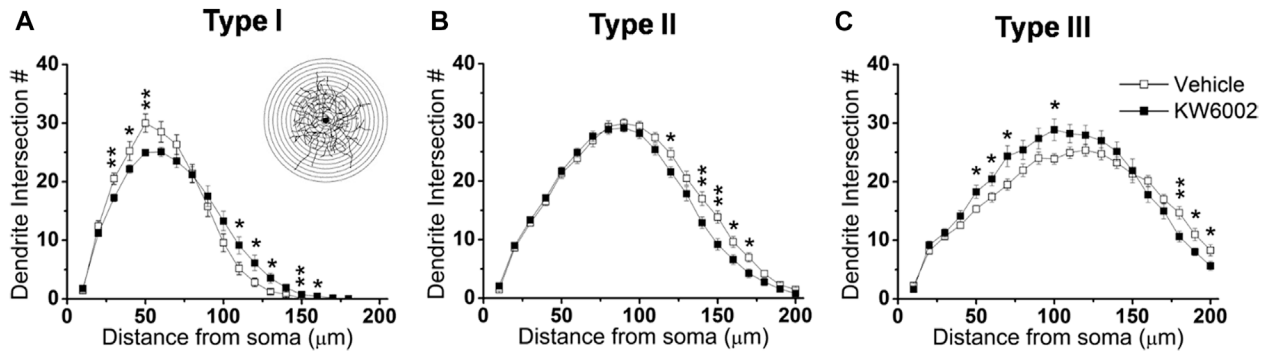


FIGURE 4
The dendritic complexity of RGCs was differentially altered by KW6002 during the development.**(A–C)** Quantitative Sholl analysis of dendrite intersection numbers in each RGC type from the vehicle-treated and KW6002-treated group during the development. Inset, a series of concentric circles with increasing radius at a 10 μm step were superimposed on the RGC. Data represent mean ± SEM. *$p < 0.05$; **$p < 0.01$.

## 2.2 Immunohistochemistry of retinal whole-mounts

Immunohistochemistry experiments were carried out as previously described (Gao et al., 2018). Briefly, after the Thy1-YFPH mice were anesthetized, the eyes were enucleated on P21 and fixed in 4% paraformaldehyde (PFA) for 30 min. The retinas were isolated from eyeballs, fixed in 4% PFA for additional 10 min, and incubated with 3% $H_2O_2$ for 20 min. After being blocked in a blocking solution (5% normal donkey serum plus 1% BSA, 0.2% glycine, 0.2% lysine, and 0.3% Triton X-100) for 2 h at room temperature, retinas were incubated with goat polyclonal antibodies against GFP (1:500, NB100-1770, Novus Biologicals) for 2 days at 4°C. Then the retinas were sequentially incubated with the biotinylated donkey anti-goat antibodies, the avidin-biotin complex (Vectastain ABC Elite Kit; Vector Laboratories, USA), the 3,3′-diaminobenzidine (DAB tablets, Sigma), and finally flat-mounted on glass slides with aqueous mounting medium (IMMCO Diagnostics, Inc).

## 2.3 3D reconstruction and quantitative morphometry

The fully and strongly stained YFP-positive RGCs (that achieve the standard for the detailed morphological analyses) were randomly selected and reconstructed, while those with faint staining and uncompleted structure were discarded. The morphology of RGCs was reconstructed by using Neurolucida system (MicroBrightField Inc., USA) and a bright-field light microscope (Zeiss, Germany) at a magnification of ×63, as previously described (Gao et al., 2018). A battery of morphological parameters were extracted from 251 fully reconstructed RGCs by the NeuroExplorer (MicroBrightField Inc., USA). Sholl analysis on dendrites of RGCs was also performed using "Sholl Analysis" in Neuroexplorer (Sholl, 1953). The spatial distributions of dendritic intersection with the concentric circles were quantified in terms of stepped distance circle regions (10 μm) from the soma.

## 2.4 Statistical analysis

Results were expressed as mean ± standard error of mean (SEM). Kruskal-Wallis one-way ANOVA (k samples), independent Student's *t*-test and chi-square test were performed by SPSS 26. The significant level was set at $p < 0.05$ for all comparisons.

# 3 Results

## 3.1 The $A_{2A}R$ antagonist KW6002 did not alter the proportion of RGC morphological types during the development

Since the RGCs are rather heterogeneous in the retina, we take advantage of the Thy-1 YFPH transgenic line, which expresses the yellow fluorescent protein (YFP) only in a fraction of RGCs (Barnstable and Dräger, 1984; Feng et al., 2000), to study the effect of $A_{2A}R$ on the development of RGCs. During retinal development, Thy-1 YFPH neonates received intraperitoneal injections of the $A_{2A}R$ antagonist KW6002 from P4 to P6 and were sacrificed at P21 (Figure 1A). 3D reconstruction of well-stained $YFP^+$ cells (n = 120 cells) for detailed morphometric analyses was performed in the retina at P21 (Figure 1B). As described previously, we classified these Thy1-positive RGCs labeled with YFP into three major morphological classes (Type I, II

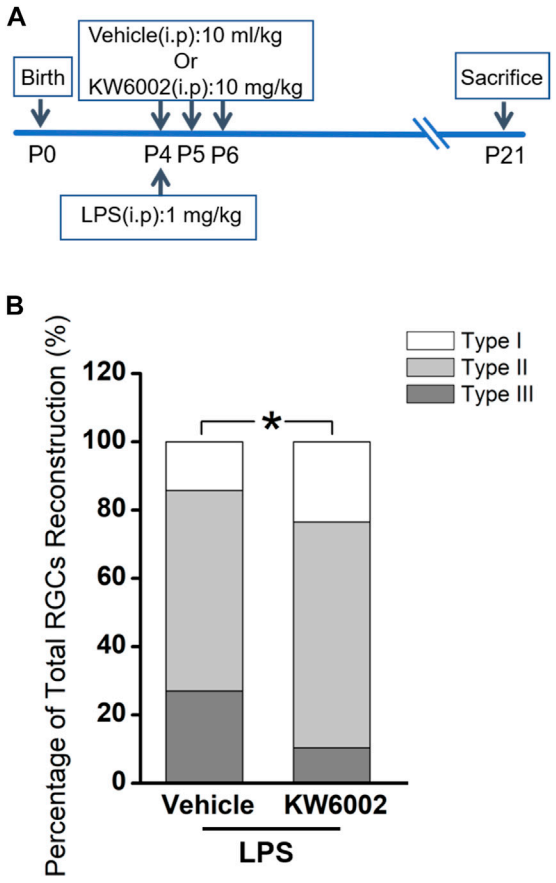


FIGURE 5
KW6002 changed the proportion of RGC morphological types after neonatal inflammation. **(A)** Timeline of KW6002 (or vehicle) administration with an intraperitoneal injection of LPS in transgenic Thy-1 YFPH mice. **(B)** The proportion of different morphological types of RGCs from the control and KW6002-treated mice after neonatal LPS exposure. *$p < 0.05$. 63 RGCs from 14 retinas (7 vehicle-treated mice) and 68 RGCs from 12 retinas (6 KW6002-treated mice) in the control and KW6002-treated group after neonatal LPS exposure, respectively. On average, 4.5 and 5.67 RGCs per eye were analyzed in each group.

and III), based on the morphological features of the dendritic field and dendrite density (Gao et al., 2018). Type I had a small dendritic field area and high dendrite density, whereas Type III had a large dendritic field area but low dendrite density. Type II was just between Type I and III (Figure 1C). The quantitative analysis further confirmed the significant differences among the three RGC types (**$p < 0.01$, ***$p < 0.001$, Figures 1D,E). Compositions of the three RGC types were similar between the KW6002-treated and control groups (Type I: control, n = 12, 22.22% vs. KW6002, n = 22, 33.33%; Type II: control, n = 26, 48.15% vs. KW6002, n = 30, 45.45%; Type III: control, n = 16, 29.63% vs. KW6002, n = 14, 21.21%; $p > 0.05$; Figure 1F). Therefore, KW6002 had no effect on the proportion of these RGC morphological types during retinal development.

## 3.2 KW6002 mainly decreased RGC morphogenesis by the reduced dendritic field area of Type II and III RGCs, and the reduced dendrite density of Type I but with the increased dendrite density of Type III RGCs

The RGC somata have different shapes, such as triangular, round, and oval. RGCs with different morphological shapes are used to the different parameters. We firstly studied the somatic development of RGCs and found that KW6002 significantly increased the soma area by 18.69% in Type I (control, 244.04 ± 15.10 μm$^2$ vs. KW6002, 289.66 ± 13.04 μm$^2$; *$p <$ 0.05; Figures 2A,B and Supplementary Table S1), while no significant effect was found on Type II and III ($p > 0.05$; Figures 2A,B). Meanwhile, no significant difference was found in the soma perimeter of the three morphological types of RGCs by KW6002 ($p > 0.05$; Figures 2A,C). These results indicate that $A_{2A}$Rs can differentially modulate the somatic development of RGCs during retinal development.

We further compared the morphological features of dendrites, such as dendritic field area, dendrite density, segment number, length, surface area and volume etc, between the two groups (Figure 3). The dendritic field area was diminished by 10.13% and 10.99%, respectively, in Type II (control, 78,610.04 ± 2295.94 μm$^2$ vs. KW6002, 70,646.83 ± 2472.02 μm$^2$; *$p < 0.05$; Figures 3A,B) and Type III RGCs (control, 123,035.42 ± 4269.09 μm$^2$ vs. KW6002, 109,513.94 ± 2438.7 μm$^2$; **$p < 0.01$; Figures 3A,B) after KW6002 treatment, whereas no significant effect was found in Type I ($p > 0.05$; Figure 3B). Compared to the control group, KW6002 attenuated the dendrite density by 12.00% (control, 9.50 ± 0.48 (×10$^{-2}$, 1/μm) vs. KW6002, 8.36 ± 0.28 (×10$^{-2}$, 1/μm); *$p < 0.05$; Figure 3C) in Type I RGCs, but induced 19.62% enhancement of the dendrite density (control, 3.72 ± 0.14 (×10$^{-2}$, 1/μm) vs. KW6002, 4.45 ± 0.24 (×10$^{-2}$, 1/μm); *$p < 0.05$; Figure 3C) in Type III RGCs. KW6002 didn't change the dendrite segment number and total dendrite length of all three RGC types during normal development ($p > 0.05$; Figures 3D,E). As to the dendrite surface area and volume, no significant effect was found in each RGC type after KW6002 treatment during normal development ($p > 0.05$; Figures 3F,G). These results implied that $A_{2A}$Rs can reorganize the dendritic architecture of RGCs in the retina, which is dependent on the RGC types.

To further investigate the effect of KW6002 on the spatial distribution of dendritic morphology, Sholl analyses were performed on quantifications of the distribution of dendritic intersections and revealed that KW6002 had a dual effect on Type I and III RGCs. KW6002 significantly decreased the dendritic intersection of Type I RGCs at 30–50 μm, but increased them at 110–160 μm from the soma (*$p < 0.05$ or **$p < 0.01$; Figure 4A) On the contrary, as to the Type III RGCs, the dendritic intersections were significantly increased at

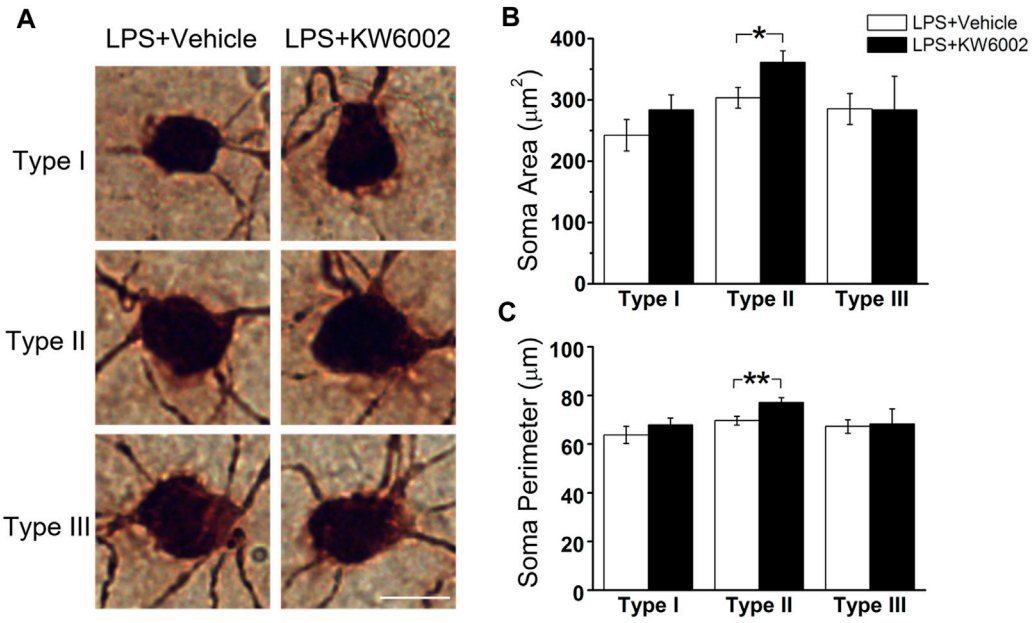


FIGURE 6
KW6002 enlarged the soma of Type II RGCs after neonatal LPS exposure. **(A)** Representative pictures of somata in each RGC type examined from vehicle -treated and KW6002-treated group after neonatal LPS exposure. Scale bar, 20 μm. **(B,C)** Comparative analysis of soma area **(B)** and perimeter **(C)** of different RGC types between vehicle-treated and KW6002-treated mice after neonatal LPS exposure. Data represent mean ± SEM. $^{*}p < 0.05$; $^{**}p < 0.01$.

50–70 μm and 100 μm but decreased at 180–200 μm from the soma ($^{*}p < 0.05$ or $^{**}p < 0.01$; Figure 4C) after KW6002 treatment. Meanwhile, KW6002 significantly decreased the dendritic intersection of Type II RGCs mainly at 120–170 μm, which is far from the soma ($^{*}p < 0.05$ or $^{**}p < 0.01$; Figure 4B). These results indicate the fine-tune effect of $A_{2A}$Rs on the dendritic development of RGCs during the retinal development.

## 3.3 KW6002 changed the proportion of RGC morphological types after neonatal inflammation

Apart from its physiological role, we further studied the effects of $A_{2A}$R on the development of RGCs after the neonatal inflammation. To induce the neonatal inflammation, neonates received a single intraperitoneal injection of LPS immediately after KW6002 treatment at P4. Then they were administrated with KW6002 in the same manner as that in the normal condition and were sacrificed at P21 (Figure 5A). The well-stained $YFP^{+}$ cells (n = 131 cells) in the retina were 3D reconstructed for detailed morphometric analyses at P21. We found that after neonatal LPS exposure, the compositions of Type I and Type II RGCs significantly increased, but Type III decreased in the KW6002-treated groups, compared to the control groups (Type I: control, n = 9, 14.29% vs. KW6002, n = 16, 23.53%; Type II: control, n = 37, 58.73% vs. KW6002, n = 45, 66.18%; Type III: control, n = 17, 26.98% vs. KW6002, n = 7, 10.29%; $^{*}p < 0.05$; Figure 5B). These results indicate that $A_{2A}$Rs altered the compositions of the three RGC types after neonatal inflammation.

## 3.4 KW6002 increased the proportion of Type I RGCs with enhanced the dendrite surface area and volume and Type II RGCs with enlarged soma after neonatal inflammation

After LPS treatment, KW6002 significantly enlarged the soma area by 19.10% (control, 303.54 ± 16.96 $\mu m^2$ vs. KW6002, 361.51 ± 18.69 $\mu m^2$; $^{*}p < 0.05$; Figures 6A,B and Supplementary Table S2) and the soma perimeter by 10.73% (control, 69.64 ± 1.79 μm vs. KW6002, 77.11 ± 2.01 μm; $^{**}p < 0.01$; Figure 6C) in Type II. However, KW6002 had no significant effect on the soma area and perimeter of Type I and III after neonatal LPS exposure($p > 0.05$; Figures 6B,C). Beside the soma, we also examined the dendritic morphology and found that the dendritic field area and total dendrite length of the three morphological types of RGCs were not affected by KW6002 after neonatal LPS exposure ($p > 0.05$; Figures 7A,

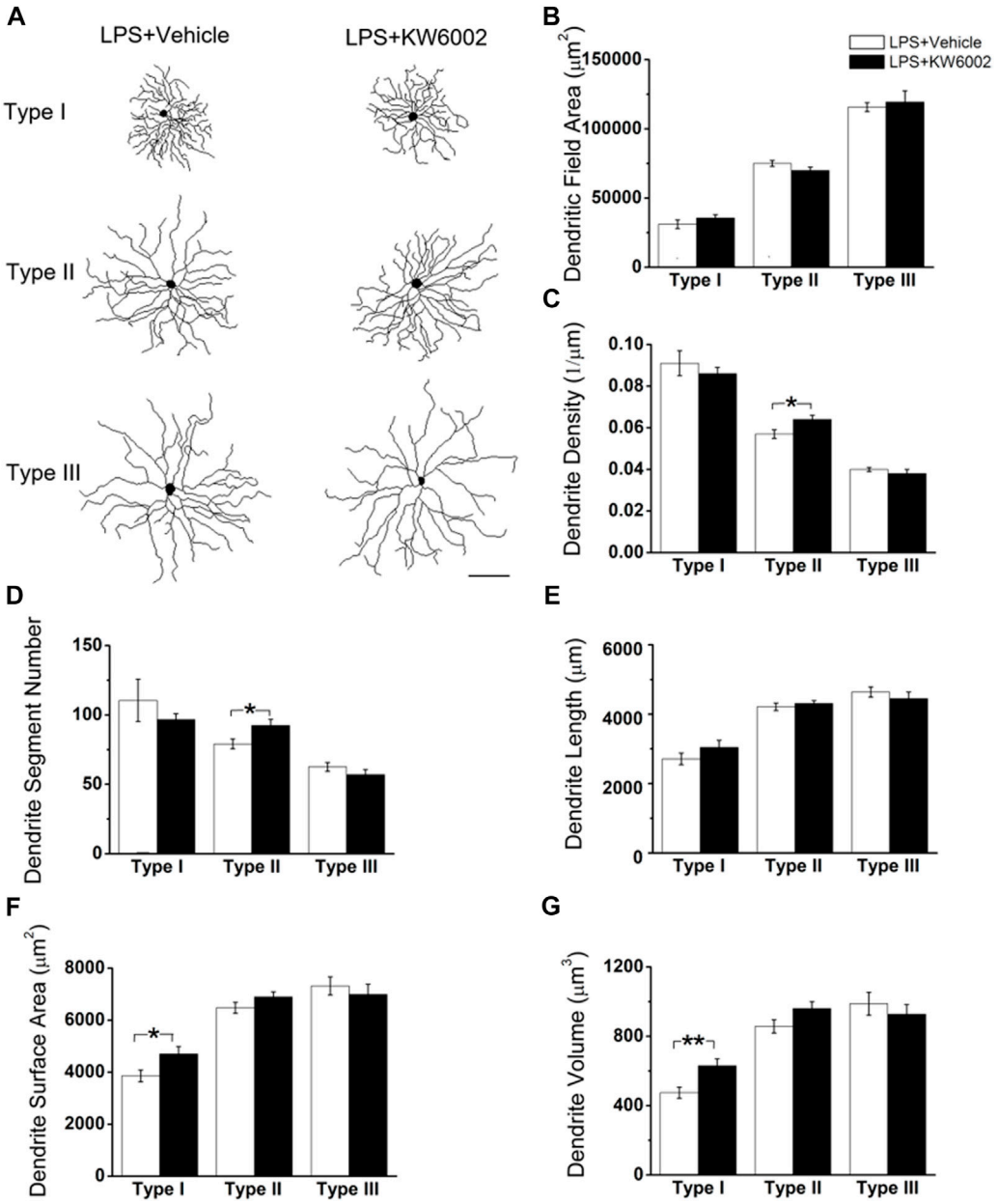


FIGURE 7
The effect of KW6002 on the dendritic morphology of RGCs after neonatal LPS exposure. **(A)** Representative 3D reconstructions of the three RGC types from the vehicle-treated and KW6002-treated mice after neonatal LPS exposure. **(B–G)** Comparative analysis of dendritic field area **(B)**, dendrite density **(C)**, dendrite segment number **(D)**, dendrite length **(E)**, dendrite surface area **(F)** and dendrite volume **(G)** in each RGC type between the vehicle-treated and KW6002-treated group after neonatal LPS exposure. Data represent mean ± SEM. $*p < 0.05$; $**p < 0.01$. Scale bar, 100 μm.

B,E). Interestingly, KW6002 significantly augmented the dendrite density (control, 5.73 ± 0.17 ($\times 10^{-2}$, 1/μm) vs. KW6002, 6.32 ± 0.19 ($\times 10^{-2}$, 1/μm); $*p < 0.05$; Figure 7C) and segment number (control, 79.16 ± 3.50 vs. KW6002, 92.29 ± 4.03; $*p < 0.05$; Figure 7D) of Type II RGCs, but didn't affect those of Type I and Type III RGCs after neonatal LPS exposure. Moreover, KW6002 significantly enhanced the dendrite surface area and volume of Type I RGCs (control, 3861.30 ± 227.05 μm$^2$ vs. KW6002, 4700.80 ± 283.86 μm$^2$; $*p < 0.05$; Figure 7F; control, 474.82 ± 31.88 μm$^3$ vs. KW6002, 629.75 ±

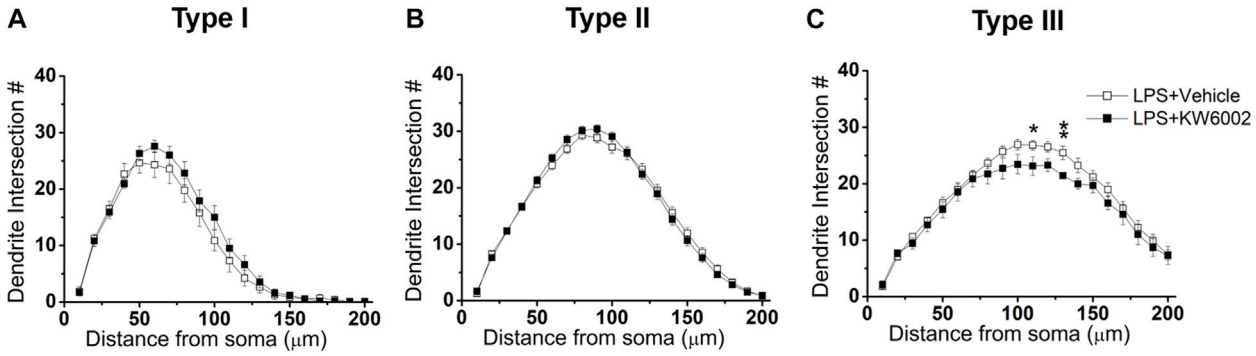


FIGURE 8
KW6002 decreased the dendritic complexity of Type III RGCs after neonatal LPS exposure. **(A–C)** Quantitative Sholl analysis of dendrite intersection numbers in each RGC type from the vehicle-treated and KW6002-treated group after neonatal LPS exposure. Data represent mean ± SEM. *$p < 0.05$; **$p < 0.01$.

40.26 μm$^3$; **$p < 0.01$; Figure 7G) after neonatal exposure to LPS, while no significant change was found in the other two RGC types. These results suggest that $A_{2A}$Rs induced differential alterations in the soma and dendritic architecture of RGCs after neonatal inflammation.

We further performed Sholl analyses to study the effect of KW6002 on the spatial distribution of dendritic morphology after neonatal LPS exposure. We found that KW6002 only significantly decline dendritic intersections at 110 and 130 μm from the soma in Type III RGCs (*$p < 0.05$ or **$p < 0.01$; Figure 8C), while no significant difference was found either in Type I or Type II RGCs ($p > 0.05$; Figures 8A,B). These results suggest that $A_{2A}$Rs only had slight effect on dendritic complexity after neonatal LPS exposure.

## 4 Discussion

The $A_{2A}$R is recently proposed as a potential therapeutic target for retinal diseases (Santiago et al., 2020). However, what exact role of $A_{2A}$R plays in retinal development, especially RGC morphogenesis, is still not be fully elucidated. To simplify the framework for analysis of rather heterogenous RGC types in the retina, here we classified the Thy1-positive RGCs from Thy-1 YFPH transgenic mouse strain into three major morphological types (Type I, II and III) as our previous study (Gao et al., 2018). We found that $A_{2A}$R antagonist KW6002 produced mainly decreased RGC morphogenesis as evident by the reduced dendritic field area of Type II and III, and the reduced dendrite density of Type I but with the increased dendrite density of Type III (Figure 9). The dendritic field represents the input receptive area, while dendrite density represents the intensity of bipolar and amacrine axonal input that RGCs receive within their covered region. Thus $A_{2A}$Rs may modulate the RGC input receptive area and input from bipolar and amacrine in a cell-type specific manner during development. Furthermore, KW6002 had a bidirectional effect on dendritic complexity of Type I and Type III RGCs, suggesting that the fine-tune ability of the $A_{2A}$Rs on the dendritic development of RGCs. Due to lack of an appropriate $A_{2A}$R antibody that reliably and specifically detects $A_{2A}$R in RGCs, whether the different density of $A_{2A}$Rs in the three types of RGCs leads to the distinct effects of KW6002 on the morphology of RGCs remains to be studied in the future. Given the morphology similarity of Type I cells with W3B-RGC (Kim et al., 2010), which is postulated as a selective feature detector (Zhang et al., 2012), Type II cells with ON-sustained alpha RGCs (Bleckert et al., 2014; Krieger et al., 2017; Smeds et al., 2019), and Type III cells with melanopsin M2 cell (Sanes and Masland, 2015), we speculate that $A_{2A}$R activity may potentially modulate local edge detecting (Type I RGC), single-photon visual signal transmission to the brain (Type II RGC) and the function of intrinsically photosensitive melanopsin-containing RGC (Type III RGC). The exact function of three RGCs affected by $A_{2A}$R needs to be characterized by further functional studies.

We further studied the effect of $A_{2A}$R on RGC morphology after neonatal LPS exposure and found that antagonism of $A_{2A}$R changed the compositions of the three RGC types, while no composition change was found in normal development or after neonatal inflammation (Supplementary Figure S1) (Gao et al., 2018). Previous studies have reported that the $A_{2A}$R antagonist prevents RGC loss in retinal organotypic cultures upon exposure to LPS (Madeira et al., 2015) and in several models of retinal neurodegeneration (Madeira et al., 2016; Boia et al., 2017; Aires et al., 2019a; Aires et al., 2019b). It may be possible that $A_{2A}$R antagonists preferentially protect Type I and II RGCs from death after neonatal inflammation, thus upregulating the proportion of the two types. Notably, after neonatal

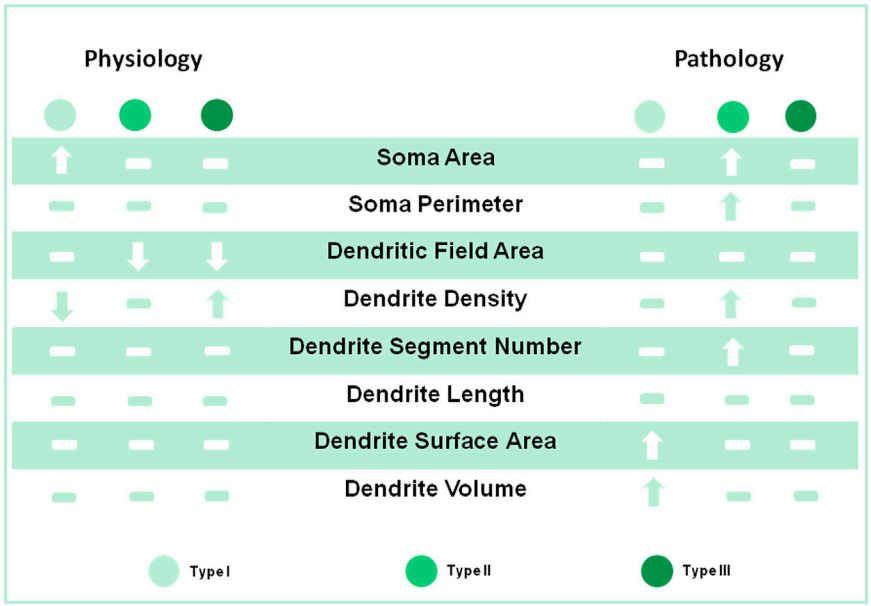


FIGURE 9
Summary of RGC morphological changes by KW6002 under physiological and pathological conditions The $A_{2A}R$ antagonist KW6002 differentially altered these morphological parameters of different RGC types during normal and neonatal inflammation. The arrow means significant up or down-regulation by KW6002, while horizontal line means no significant difference.

inflammation, $A_{2A}R$ antagonist KW6002 specifically increased the proportion of Type I RGCs with enhanced the dendrite surface area and volume and the proportion of Type II RGCs with enlarged the soma area and perimeter, indicating that the $A_{2A}R$ activation exerts mainly suppression on RGC soma and dendrite volume under neonatal inflammation. The increased RGC size of Type I and II by KW6002 may be associated with the upregulation of cell processes such as mitochondrial dynamics to resist cell loss (Miettinen and Bjorklund, 2016). Furthermore, the modulation pattern of $A_{2A}R$ antagonist on RGC morphology is quite different from that during normal development (Figure 9), which indicating that $A_{2A}Rs$ have distinct effects on RGC morphological development under physiological and pathological conditions. These distinct effects on RGC morphology by KW6002 treatment may attribute to the different local environmental changes. Indeed, different glutamate concentration has been shown to switch the effect of $A_{2A}R$ from anti-inflammatory to proinflammatory (Dai et al., 2010). In addition, these distinct effects of $A_{2A}Rs$ on RGC morphology may be attributed to different cell types targeted by KW6002. During the normal retinal development, KW6002 may mainly block the $A_{2A}R$ on the RGCs, thus affecting the morphological development of RGCs. However, after neonatal inflammation KW6002 may act on the $A_{2A}R$ on microglia or both on microglia and RGCs to modulate the morphology of RGCs, since previous studies have found that inflammation can cause a marked increase in microglial $A_{2A}R$ (Canas et al., 2004; Wittendorp et al., 2004). Whether the direct effect of KW6002 on microglia or not remains to be determined by future experiment with genetic deleption of the microglial $A_{2A}R$. Our results are in notably agreement with previous studies showing that the complex and differential roles of $A_{2A}R$ play under physiological and pathological conditions. For example, we recently found that genetic inactivation of $A_{2A}R$ attenuates pathologic angiogenesis in the development of retinopathy of prematurity, but it does not affect developmental angiogenesis in the mouse retina (Liu et al., 2010; Zhang et al., 2017; Zhang et al., 2022). The effect of $A_{2A}R$ on the control of peripheral inflammation and chronic neuroinflammation is also opposite (Cunha, 2005). Therefore, $A_{2A}R$ signaling may distinctly regulate RGC development under normal and pathological conditions in the retina and the underlying mechanisms need to be further investigated in the future.

Collectively, during development $A_{2A}R$ activation can modulate the RGC morphology in a cell type-specific manner and fine-tune the dendritic development by bidirectionally regulating the dendritic complexity of Type I and III RGCs. After neonatal inflammation, $A_{2A}R$ activation mainly reduces the soma and dendrites of Type I and II RGCs and diminishes their proportions, which is totally different from the roles it plays during the development. These findings may provide an integrated view of the multi-faced effects of $A_{2A}R$ signaling on the morphology of RGCs, which is depending on the cell-types and conditions.

## Data availability statement

The original contributions presented in the study are included in the article/Supplementary Material, further inquiries can be directed to the corresponding authors.

## Ethics statement

The animal study was reviewed and approved by Animal Care Committee of Wenzhou Medical University.

## Author contributions

YG and JQ designed the study and coordinated the experiments. SH and YL conducted the experiments and analyzed the data. YZ, RS, PT, and DZ contributed to acquire the 3D reconstruction dataset. XK made constructive suggestions for imaging. YG wrote the manuscript. JQ modified the manuscript. JC helped with editing the manuscript and assisted with funding acquisition. All authors commented on the manuscript.

## Funding

This work was supported by the Natural Science Foundation of Zhejiang Province of China (Grant Number LY21H090014), the National Natural Science Foundation of China (Grant Numbers 81600991 and 82151308), the Research Fund for International Senior Scientists (Grant Number 82150710558), and Funds from Wenzhou Medical University (Grant Number KYYW202106) and Hainan Province Clinical Medical Center.

## Conflict of interest

The authors declare that the research was conducted in the absence of any commercial or financial relationships that could be construed as a potential conflict of interest.

## Publisher's note

All claims expressed in this article are solely those of the authors and do not necessarily represent those of their affiliated organizations, or those of the publisher, the editors and the reviewers. Any product that may be evaluated in this article, or claim that may be made by its manufacturer, is not guaranteed or endorsed by the publisher.

## Supplementary material

The Supplementary Material for this article can be found online at: https://www.frontiersin.org/articles/10.3389/fphar.2022.1082997/full#supplementary-material

## References

Aires, I. D., Boia, R., Rodrigues-Neves, A. C., Madeira, M. H., Marques, C., Ambrosio, A. F., et al. (2019a). Blockade of microglial adenosine A2A receptor suppresses elevated pressure-induced inflammation, oxidative stress, and cell death in retinal cells. *Glia* 67 (5), 896–914. doi:10.1002/glia.23579

Aires, I. D., Madeira, M. H., Boia, R., Rodrigues-Neves, A. C., Martins, J. M., Ambrosio, A. F., et al. (2019b). Intravitreal injection of adenosine A(2A) receptor antagonist reduces neuroinflammation, vascular leakage and cell death in the retina of diabetic mice. *Sci. Rep.* 9, 17207. doi:10.1038/s41598-019-53627-y

Alcada-Morais, S., Goncalves, N., Moreno-Juan, V., Andres, B., Ferreira, S., Marques, J. M., et al. (2021). Adenosine A2A receptors contribute to the radial migration of cortical projection neurons through the regulation of neuronal polarization and axon formation. *Cereb. Cortex* 31 (12), 5652–5663. doi:10.1093/cercor/bhab188

Alfinito, P. D., Alli, R., and Townes-Anderson, E. (2002). Adenosine A(2a) receptor-mediated inhibition of rod opsin mRNA expression in tiger salamander. *J. Neurochem.* 83 (3), 665–672. doi:10.1046/j.1471-4159.2002.01162.x

Baden, T., Berens, P., Franke, K., Roman Roson, M., Bethge, M., and Euler, T. (2016). The functional diversity of retinal ganglion cells in the mouse. *Nature* 529 (7586), 345–350. doi:10.1038/nature16468

Bae, J. A., Mu, S., Kim, J. S., Turner, N. L., Tartavull, I., Kemnitz, N., et al. (2018). Digital museum of retinal ganglion cells with dense anatomy and physiology. *Cell.* 173 (5), 1293–1306. doi:10.1016/j.cell.2018.04.040

Barnstable, C. J., and Dräger, U. C. (1984). Thy-1 antigen: A ganglion cell specific marker in rodent retina. *Neuroscience* 11 (4), 847–855. doi:10.1016/0306-4522(84)90195-7

Bleckert, A., Schwartz, G. W., Turner, M. H., Rieke, F., and Wong, R. O. (2014). Visual space is represented by nonmatching topographies of distinct mouse retinal ganglion cell types. *Curr. Biol.* 24 (3), 310–315. doi:10.1016/j.cub.2013.12.020

Boia, R., Elvas, F., Madeira, M. H., Aires, I. D., Rodrigues-Neves, A. C., Tralhao, P., et al. (2017). Treatment with A2A receptor antagonist KW6002 and caffeine intake regulate microglia reactivity and protect retina against transient ischemic damage. *Cell. Death Dis.* 8 (10), e3065. doi:10.1038/cddis.2017.451

Brito, R., Pereira, M. R., Paes-de-Carvalho, R., and Calaza, K. D. (2012). Expression of A1 adenosine receptors in the developing avian retina: *In vivo* modulation by A2A receptors and endogenous adenosine. *J. Neurochem.* 123 (2), 239–249. doi:10.1111/j.1471-4159.2012.07909.x

Canas, P., Rebola, N., Rodrigues, R. J., Oliveira, C. R., and Cunha, R. A. (2004). Increased adenosine A2A immunoreactivity in activated rat microglia in culture. *FENS Abstr.* 2, A223–A229.

Chen, J. F., Eltzschig, H. K., and Fredholm, B. B. (2013). Adenosine receptors as drug targets-what are the challenges? *Nat. Rev. Drug Discov.* 12 (4), 265–286. doi:10.1038/nrd3955

Colella, M., Zinni, M., Pansiot, J., Cassanello, M., Mairesse, J., Ramenghi, L., et al. (2018). Modulation of microglial activation by adenosine A2a receptor in animal models of perinatal brain injury. *Front. Neurol.* 9, 605. doi:10.3389/fneur.2018.00605

Cunha, R. A. (2005). Neuroprotection by adenosine in the brain: From A(1) receptor activation to A (2A) receptor blockade. *Purinergic Signal.* 1 (2), 111–134. doi:10.1007/s11302-005-0649-1

Dai, S. S., Zhou, Y. G., Li, W., An, J. H., Li, P., Yang, N., et al. (2010). Local glutamate level dictates adenosine A2A receptor regulation of neuroinflammation and traumatic brain injury. *J. Neurosci.* 30 (16), 5802–5810. doi:10.1523/JNEUROSCI.0268-10.2010

Feng, G., Mellor, R. H., Bernstein, M., Keller-Peck, C., Nguyen, Q. T., Wallace, M., et al. (2000). Imaging neuronal subsets in transgenic mice expressing multiple spectral variants of GFP. *Neuron* 28 (1), 41–51. doi:10.1016/s0896-6273(00)00084-2

Gao, Y., Hu, S., Li, Q., Wang, M., Zhi, Z., Kuang, X., et al. (2018). Neonatal inflammation induces reorganization in dendritic morphology of retinal ganglion cells but not their retinogeniculate projection in mice. *Neurosci. Lett.* 676, 34–40. doi:10.1016/j.neulet.2018.04.012

Goetz, J., Jessen, Z. F., Jacobi, A., Mani, A., Cooler, S., Greer, D., et al. (2022). Unified classification of mouse retinal ganglion cells using function, morphology, and gene expression. *Cell. Rep.* 40 (2), 111040. doi:10.1016/j.celrep.2022.111040

Huang, P. C., Hsiao, Y. T., Kao, S. Y., Chen, C. F., Chen, Y. C., Chiang, C. W., et al. (2014). Adenosine A(2A) receptor up-regulates retinal wave frequency via starburst amacrine cells in the developing rat retina. *PLoS One* 9 (4), e95090. doi:10.1371/journal.pone.0095090

Huang, W., Xu, Q., Su, J., Tang, L., Hao, Z. Z., Xu, C., et al. (2022). Linking transcriptomes with morphological and functional phenotypes in mammalian retinal ganglion cells. *Cell. Rep.* 40 (11), 111322. doi:10.1016/j.celrep.2022.111322

Jonsson, G., and Eysteinsson, T. (2017). Retinal A2A and A3 adenosine receptors modulate the components of the rat electroretinogram. *Vis. Neurosci.* 34, E001. doi:10.1017/S0952523816000171

Kim, I. J., Zhang, Y., Meister, M., and Sanes, J. R. (2010). Laminar restriction of retinal ganglion cell dendrites and axons: Subtype-specific developmental patterns revealed with transgenic markers. *J. Neurosci.* 30 (4), 1452–1462. doi:10.1523/JNEUROSCI.4779-09.2010

Krieger, B., Qiao, M., Rousso, D. L., Sanes, J. R., and Meister, M. (2017). Four alpha ganglion cell types in mouse retina: Function, structure, and molecular signatures. *PLoS One* 12 (7), e0180091. doi:10.1371/journal.pone.0180091

Li, H., Zhang, Z., Blackburn, M. R., Wang, S. W., Ribelayga, C. P., and O'Brien, J. (2013). Adenosine and dopamine receptors coregulate photoreceptor coupling via gap junction phosphorylation in mouse retina. *J. Neurosci.* 33 (7), 3135–3150. doi:10.1523/JNEUROSCI.2807-12.2013

Liu, X. L., Zhou, R., Pan, Q. Q., Jia, X. L., Gao, W. N., Wu, J., et al. (2010). Genetic inactivation of the adenosine A2A receptor attenuates pathologic but not developmental angiogenesis in the mouse retina. *Invest. Ophthalmol. Vis. Sci.* 51 (12), 6625–6632. doi:10.1167/iovs.09-4900

Madeira, M. H., Boia, R., Elvas, F., Martins, T., Cunha, R. A., Ambrosio, A. F., et al. (2016). Selective A2A receptor antagonist prevents microglia-mediated neuroinflammation and protects retinal ganglion cells from high intraocular pressure-induced transient ischemic injury. *Transl. Res.* 169, 112–128. doi:10.1016/j.trsl.2015.11.005

Madeira, M. H., Elvas, F., Boia, R., Goncalves, F. Q., Cunha, R. A., Ambrosio, A. F., et al. (2015). Adenosine A2AR blockade prevents neuroinflammation-induced death of retinal ganglion cells caused by elevated pressure. *J. Neuroinflammation* 12, 115. doi:10.1186/s12974-015-0333-5

Miao, Y., Chen, X., You, F., Jia, M., Li, T., Tang, P., et al. (2021). Adenosine A2A receptor modulates microglia-mediated synaptic pruning of the retinogeniculate pathway during postnatal development. *Neuropharmacology* 200, 108806. doi:10.1016/j.neuropharm.2021.108806

Miettinen, T. P., and Bjorklund, M. (2016). Cellular allometry of mitochondrial functionality establishes the optimal cell size. *Dev. Cell.* 39 (3), 370–382. doi:10.1016/j.devcel.2016.09.004

Ribeiro, F. F., Neves-Tome, R., Assaife-Lopes, N., Santos, T. E., Silva, R. F., Brites, D., et al. (2016). Axonal elongation and dendritic branching is enhanced by adenosine A2A receptors activation in cerebral cortical neurons. *Brain Struct. Funct.* 221 (5), 2777–2799. doi:10.1007/s00429-015-1072-1

Sanes, J. R., and Masland, R. H. (2015). The types of retinal ganglion cells: Current status and implications for neuronal classification. *Annu. Rev. Neurosci.* 38, 221–246. doi:10.1146/annurev-neuro-071714-034120

Santiago, A. R., Madeira, M. H., Boia, R., Aires, I. D., Rodrigues-Neves, A. C., Santos, P. F., et al. (2020). Keep an eye on adenosine: Its role in retinal inflammation. *Pharmacol. Ther.* 210, 107513. doi:10.1016/j.pharmthera.2020.107513

Sholl, D. A. (1953). Dendritic organization in the neurons of the visual and motor cortices of the cat. *J. Anat.* 87 (4), 387–406.

Silva, C. G., Metin, C., Fazeli, W., Machado, N. J., Darmopil, S., Launay, P. S., et al. (2013). Adenosine receptor antagonists including caffeine alter fetal brain development in mice. *Sci. Transl. Med.* 5 (197), 197ra104. doi:10.1126/scitranslmed.3006258

Smeds, L., Takeshita, D., Turunen, T., Tiihonen, J., Westo, J., Martyniuk, N., et al. (2019). Paradoxical rules of spike train decoding revealed at the sensitivity limit of vision. *Neuron* 104 (3), 576–587. doi:10.1016/j.neuron.2019.08.005

Stella, S. L., Jr., Bryson, E. J., Cadetti, L., and Thoreson, W. B. (2003). Endogenous adenosine reduces glutamatergic output from rods through activation of A2-like adenosine receptors. *J. Neurophysiol.* 90 (1), 165–174. doi:10.1152/jn.00671.2002

Wittendorp, M. C., Boddeke, H. W., and Biber, K. (2004). Adenosine A3 receptor-induced CCL2 synthesis in cultured mouse astrocytes. *Glia* 46 (4), 410–418. doi:10.1002/glia.20016

Zhang, S., Li, B., Tang, L., Tong, M., Jiang, N., Gu, X., et al. (2022). Disruption of CD73-derived and equilibrative nucleoside transporter 1-mediated adenosine signaling exacerbates oxygen-induced retinopathy. *Am. J. Pathol.* 192, 1633–1646. doi:10.1016/j.ajpath.2022.07.014

Zhang, S., Zhou, R., Li, B., Li, H., Wang, Y., Gu, X., et al. (2017). Caffeine preferentially protects against oxygen-induced retinopathy. *FASEB J.* 31 (8), 3334–3348. doi:10.1096/fj.201601285R

Zhang, Y., Kim, I. J., Sanes, J. R., and Meister, M. (2012). The most numerous ganglion cell type of the mouse retina is a selective feature detector. *Proc. Natl. Acad. Sci. U. S. A.* 109 (36), E2391–E2398. doi:10.1073/pnas.1211547109

frontiers | Frontiers in Pharmacology

TYPE Review
PUBLISHED 07 February 2023
DOI 10.3389/fphar.2023.1112758



OPEN ACCESS

EDITED BY
Henning Ulrich,
University of São Paulo, Brazil

REVIEWED BY
Mariachiara Zuccarini,
University of Studies G. d'Annunzio Chieti and Pescara, Italy
Ivana Grković,
University of Belgrade, Serbia

*CORRESPONDENCE
Qiaofeng Wu,
wuqiaofeng@cdutcm.edu.cn

†These authors have contributed equally to this work

SPECIALTY SECTION
This article was submitted to Experimental Pharmacology and Drug Discovery, a section of the journal Frontiers in Pharmacology

RECEIVED 30 November 2022
ACCEPTED 27 January 2023
PUBLISHED 07 February 2023

CITATION
Wang Y, Zhu Y, Wang J, Dong L, Liu S, Li S and Wu Q (2023), Purinergic signaling: A gatekeeper of blood-brain barrier permeation.
*Front. Pharmacol.* 14:1112758.
doi: 10.3389/fphar.2023.1112758



# Purinergic signaling: A gatekeeper of blood-brain barrier permeation

Yuemei Wang†, Yuanbing Zhu†, Junmeng Wang, Longcong Dong, Shuqing Liu, Sihui Li and Qiaofeng Wu*

Acupuncture and Moxibustion College, Chengdu University of Traditional Chinese Medicine, Chengdu, Sichuan, China

This review outlined evidence that purinergic signaling is involved in the modulation of blood-brain barrier (BBB) permeability. The functional and structural integrity of the BBB is critical for maintaining the homeostasis of the brain microenvironment. BBB integrity is maintained primarily by endothelial cells and basement membrane but also be regulated by pericytes, neurons, astrocytes, microglia and oligodendrocytes. In this review, we summarized the purinergic receptors and nucleotidases expressed on BBB cells and focused on the regulation of BBB permeability by purinergic signaling. The permeability of BBB is regulated by a series of purinergic receptors classified as $P2Y_1$, $P2Y_4$, $P2Y_{12}$, P2X4, P2X7, $A_1$, $A_{2A}$, $A_{2B}$, and $A_3$, which serve as targets for endogenous ATP, ADP, or adenosine. $P2Y_1$ and $P2Y_4$ antagonists could attenuate BBB damage. In contrast, $P2Y_{12}$-mediated chemotaxis of microglial cell processes is necessary for rapid closure of the BBB after BBB breakdown. Antagonists of P2X4 and P2X7 inhibit the activation of these receptors, reduce the release of interleukin-1 beta (IL-1β), and promote the function of BBB closure. In addition, the CD39/CD73 nucleotidase axis participates in extracellular adenosine metabolism and promotes BBB permeability through $A_1$ and $A_{2A}$ on BBB cells. Furthermore, $A_{2B}$ and $A_3$ receptor agonists protect BBB integrity. Thus, the regulation of the BBB by purinergic signaling is complex and affects the opening and closing of the BBB through different pathways. Appropriate selective agonists/antagonists of purinergic receptors and corresponding enzyme inhibitors could modulate the permeability of the BBB, effectively delivering therapeutic drugs/cells to the central nervous system (CNS) or limiting the entry of inflammatory immune cells into the brain and re-establishing CNS homeostasis.

KEYWORDS

**purinergic signaling, blood-brain barrier, endothelial cells, P2Y receptors, P2X receptors, P1 receptors, CD39, CD73**

## 1 Introduction

A well-developed central nervous system (CNS) barrier is very important for maintaining the homeostasis of the neural microenvironment. The blood-brain barrier (BBB) is a critical component of the CNS barrier and is composed of continuous endothelial cells within brain microvessels, which outline the physical structure of the BBB along with the end-feet of astrocytic glial cells, pericytes, and microglia (Kadry et al., 2020) (Figure 1). The BBB is the major site of blood-CNS exchange, controlling substances that can enter or leave the nervous tissue in a precise and tight manner. It also prevents harmful substances such as pathogens and toxins from entering the brain while allowing circulating nutrient substances from the blood to enter. BBB provides strong support for synaptic function, information processing, and neural communication, which explains why BBB is essential for maintaining the homeostasis of the intracerebral environment and peripheral blood.

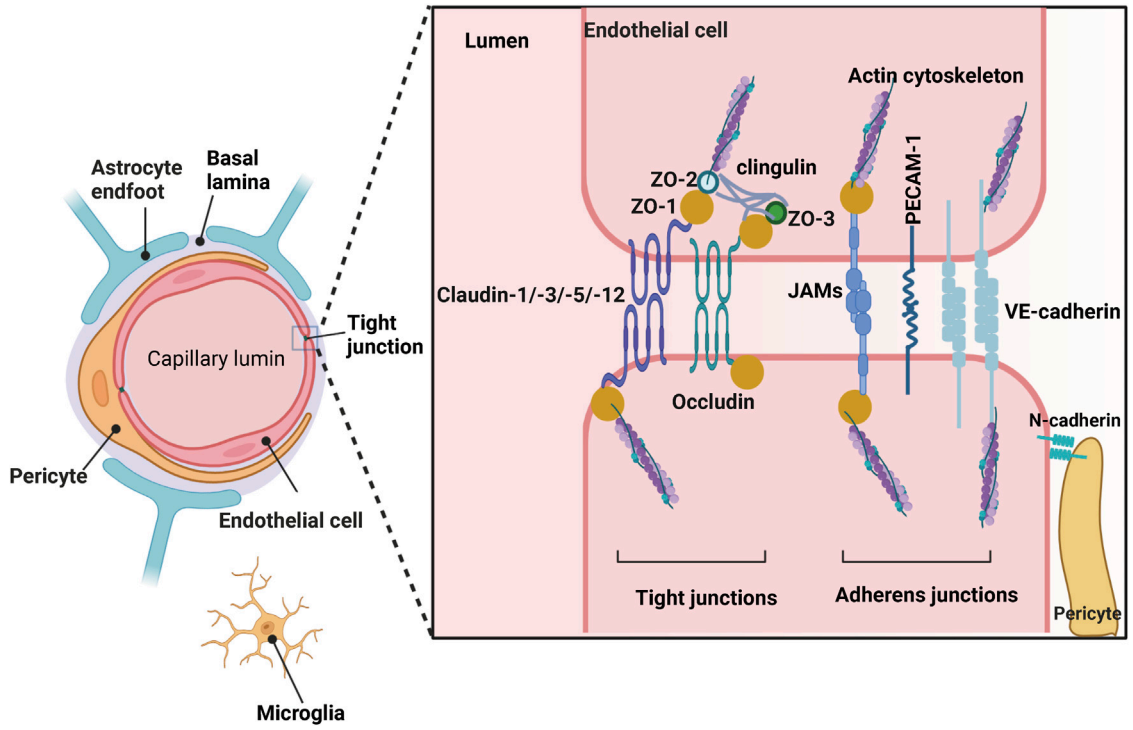


FIGURE 1
Structure of the blood-brain barrier (BBB) depicted graphically. Created with BioRender.com.

BBB is highly selective for substances to cross; these distinct properties tightly control the delivery of ions, molecules, and cells between the blood and the neural microenvironment. BBB endothelial cells are connected by various molecular junctional complexes, including tight junctions and adherens junctions. Tight junctions (TJ) involve occludin and claudin-1, claudin-3, claudin-5, and claudin-12, ZO-1, ZO-2, and ZO-3, and adherens junctions involve cadherins, the platelet endothelial cell adhesion molecule (PECAM-1), and the junctional adhesion molecules (JAMs): JAMA, JAMB, and JAMC (Sweeney et al., 2019) (Figure 1). Oxygen, carbon dioxide, and small lipid-soluble molecules (weight <400 Da) or containing <8 hydrogen bonds (such as ethanol) could cross the BBB in transmembrane diffusion manner (Sweeney et al., 2019). Additionally, the BBB also provides a combination of specific ion channels and transporters on the abluminal membrane of the BBB to regulate the balance of ions in the brain, such as the sodium pump ($Na^+$, $K^+$-ATPase), regulating sodium influx into and exchange for potassium efflux out. In addition, ATP-binding cassette (ABC) transporters are concentrated on the luminal side of the BBB, mediating the movement of molecules such as drugs and xenobiotic agents (Dean et al., 2022). The existence of solute carrier-mediated transport (CMT) and receptor-mediated transcytosis (RMT) ensures the entry of macromolecules into the brain. CMT improves the transport of macromolecules like carbohydrates, amino acids, fatty acids, hormones, vitamins, et al., while RMT ensures the exchange of proteins and peptides between the blood and brain (Zhao et al., 2015; Sweeney et al., 2019).

Although the presence of the BBB protects the CNS from neurotoxic substances circulating in the blood, the BBB also prevents the transfer of most macromolecules (e.g., peptides, proteins, and nucleic acids), severely limiting the treatment of CNS diseases (e.g., neurodegenerative diseases, brain tumors, brain infections, and strokes). BBB breakdown has been identified as a critical component in several neurological conditions. It is reported that in clinical trials and animal experiments, BBB dysfunction promoted the progression of various CNS disorders such as Alzheimer's disease (AD) (Cai et al., 2018; Zhao et al., 2021), multiple sclerosis (MS) (Niu et al., 2019), hypoxia and ischemia (Yang et al., 2018), and traumatic brain injury (TBI) (Dinet et al., 2019; van Vliet et al., 2020). Therefore, an in-depth dissection of the mechanisms to understand the basic properties of BBB is necessary to elucidate the development of the physiology and pathology of the CNS.

Purinergic signaling is essential in the CNS for maintaining the function of neurons, astrocytes, and microglia and controlling their homeostasis, consequently influencing synaptic transmission and higher cognitive processes (Burnstock, 2017; Burnstock, 2020; Illes et al., 2020). It has been demonstrated that several purinergic receptors are broadly dispersed throughout the CNS, being present in neurons, glial cells, and endothelial cells (Burnstock, 2007; Muhleder et al., 2020). The integrity of the endothelial barrier is affected by the action of extracellular adenosine triphosphate (ATP) and its metabolites adenosine diphosphate (ADP) and adenosine (ADO) on the purinoceptors of endothelial cells (Communi et al., 2000). Endothelial cells are capable of releasing nucleotides in response to a variety of physiological or pathological stimuli. Endothelial cells produce nucleotides in reaction to pathological stimuli including inflammation, hypoxia, blood flow fluctuations, shear stress, and changes in osmotic pressure (Gunduz et al., 2006; Hartel et al., 2007). Meanwhile, a growing number of studies have shown

significant modulation of the endothelial barrier by purinergic substances or purinergic receptors, including modulation of BBB permeability (Wang et al., 2015; Chen et al., 2020; Wu et al., 2022). Here, we present current *in vivo* and *in vitro* investigations that implicate purinergic receptors and major metabolic enzymes as crucial regulatory routes for BBB permeability. Modulation of purinergic signaling, on the one hand, has effects on promoting its integrity and protecting the CNS from damage by peripheral harmful substances and, on the other hand, is expected to allow therapeutic drugs to cross the BBB effectively to reach the brain parenchyma and optimize the treatment of CNS diseases.

## 2 Purinergic system

Purinergic signaling was proposed by Geoffrey Burnstock in 1972, with the theory indicating that virtually all extracellular purines were involved in cell communication in all animals and humans (Burnstock, 1972). The four major purines, as important components of the purine system, are ATP, ADP, adenosine monophosphate (AMP), and adenosine. ATP supports intracellular energy storage and also serves as a neurotransmitter and signaling molecule for intercellular communication (Burnstock, 1972). The purinergic system also includes three key enzymes, named the ectonucleoside triphosphate diphosphohydrolases (E-NTPDases: NTPDase1/CD39), ectonucleotide pyrophosphatase/phosphodiesterases (E-NPP), and ecto-5′-nucleotidase (E-5′-nucleotidase/CD73). Extracellular ATP is broken down by metabolic enzymes to produce ADP, AMP, and adenosine, which may stimulate a series of purinergic receptors expressed on the cell surface (Abbracchio and Burnstock, 1994). Purinergic receptors are divided into two main categories, P1 and P2 receptors. The P1 receptor is composed of four adenosine-selective receptor subtypes: $A_1$, $A_{2A}$, $A_{2B}$, and $A_3$ receptors. P2 receptors mainly include P2X receptors and P2Y receptors. In detail, P2X receptors include P2X1-7, seven ligand-gated cation channel subtypes, and P2Y receptors contain $P2Y_{1,\ 2,\ 4,\ 6}$ and $_{11-14}$, eight metabolic G-protein-coupled receptor (GPCR) subtypes. Notably, P2X receptors respond only to ATP, whereas P2Y receptors respond to multiple nucleotides, including ATP/ADP, UTP/UDP, or UDP-glucose. Adenine-based nucleotides such as ATP are actively released by cells in the neurovascular unit, particularly astrocytes, microglia, and endothelial cells, which activate a variety of nearby purinergic receptors and induce changes in BBB barrier function (Burnstock and Knight, 2017; Lee et al., 2021).

The focus of purinergic research has been on adenine-based nucleotides and adenosine, while guanine-based components of this system have received comparatively less attention. Until now, there has been growing evidence of the extracellular effects of guanine-based purines. The nucleotides guanosine 5′-triphosphate (GTP), guanosine 5′-diphosphate (GDP), and guanosine 5′-monophosphate (GMP) constitute the guanine-based purines (GBPs). These purines are metabolized to guanosine by extracellular nucleotidases, and conversely, guanosine is converted to guanine by purine nucleoside phosphorylases (Rathbone et al., 2008).

Guanosine has been demonstrated to be neuroprotective in numerous *in vitro* and *in vivo* models of CNS illnesses, such as ischemic stroke, AD, Parkinson's disease (PD), etc. (Su et al., 2009; Hansel et al., 2015; Lanznaster et al., 2017). The neuroprotective mechanisms of guanosine may involve the decrease of glutamatergic excitotoxicity to influence astrocyte function (Schmidt et al., 2007; Schmidt et al., 2008); modulation of the adenosinergic system (Almeida et al., 2017); as well as impacts on the inflammatory cascade response and oxidative stress (Paniz et al., 2014; Kovacs et al., 2015). However, there are few reports of guanosine-related purines directly regulating the integrity of the blood-brain barrier. In a rat model of cerebral ischemia, intranasal guanosine was delivered 3 h after stroke to prevent ischemia-induced motor impairment, brain cell death, and blood-brain barrier permeability (Muller et al., 2021).

Notably, it has been demonstrated that 3′-5′-cyclic guanosine monophosphate (cGMP), produced by GTP catalyzed by guanylate cyclase, disrupts the integrity of the BBB (Choi et al., 2018; Janigro et al., 1994; Chi et al., 1999). Although guanosine effects could open a new window in therapeutic approaches toward purinergic signaling in the CNS (Massari et al., 2021), due to the limited data on the effects of guanosine on the blood-brain barrier, this review focuses primarily on determining the association between adenine-based nucleotides, their receptors, and BBB permeability.

## 3 P2X receptors and signaling

P2X receptors belong to the family of ligand-gated ion channels, and seven subunits have been identified, namely P2XR (1–7). P2X receptors direct the inward flow of $Ca^{2+}$, $Na^{+}$, and $K^{+}$ cations upon activation by extracellular nucleotides such as ATP (Shieh et al., 2006; Bernier et al., 2018). P2X receptors are widely distributed in tissues. P2X receptors in smooth muscle cells mediate fast excitatory junctional potentials, while in the central nervous system, activation of P2X receptors causes calcium ions to enter neurons and elicit neuromodulatory responses. Although the ATP-binding sites of P2X receptors are highly conserved, there are differences in ATP potency among the different isoforms (Illes et al., 2021). P2XR (1–6) receptors are active at low micromolar to submicromolar concentrations of ATP, whereas P2X7 receptors require hundreds of micromolar concentrations of ATP to activate.

### 3.1 P2X receptors in neurovascular unit (NVU)

Neuronal and perivascular microglia are in touch with endothelial cells, pericytes, and astrocytes, which form the neurovascular unit. All P2X receptor mRNAs and proteins have been detected in the endothelium of multiple vessels (Loesch and Burnstock, 2000; Glass et al., 2002; Ramirez and Kunze, 2002; Wilson et al., 2007), but the expression of these receptors is not completely uniform in the neurovascular units of the brain. Using immunocytochemistry and transmission electron microscopy, Andrzej Loesch found that P2X1 was predominantly expressed in the astrocyte end-foot of the rat cerebellar vascular neural unit, with no significant expression in cerebellar endothelial cells and pericytes (Loesch, 2021). Similarly, the perivascular component of glial cells in the cerebellum showed P2X4 receptor immunoreactivity, while it was unlabeled in endothelial and pericytes (Loesch, 2021). However, both microvascular endothelial and perivascular astrocytes in the hypothalamus were immunoreactive for P2X4 receptors, but positive expression of P2X4 receptors in pericytes was not observed (Loesch, 2021). In addition, P2X6 receptors were expressed mainly in rat paraventricular

**TABLE 1 Effect of P2 receptors agonist/antagonist on blood-brain barrier permeability.**

| Receptor/Agonist/Antagonists | Drug name | Model | Observation | Reference(s) |
|---|---|---|---|---|
| P2X4 antagonists | 5-BDBD | Mouse ICH | Cerebral edema↓; Infiltrating leukocytes and microglia↓; Claudin-5↑; Extravasation of Evans Blue↓ | Wu et al. (2022) |
| P2X4 antagonists | 5-BDBD | Mouse<br>MCAO | Neurological deficit scores↓; IL-1β↓; Infiltrating leukocytes↓; Microglia/monocyte activation↓; Extravasation of Evans Blue↓ | Srivastava et al. (2020) |
| P2X7 antagonist | A-804598 | E-cigarette-induced BBB damage *in vitro* | Prevent BBB damage by improving mitochondrial dysfunction in endothelial cells | Mekala et al. (2022) |
| P2X7 antagonist | A-804598 | LPS-induced BBB injury mouse | Hippocampal Occludin and ZO-1↑; Prevent BBB damage | Wang et al. (2022) |
| P2X7 agonist | BzATP | Human astrocytes and hCMEC/D3 coculture | ZO-1 and Occludin↓; IL-1β and MMP-9↑; 10 KDa dextran extravasation↑; Increased BBB permeability | Yang et al. (2016) |
| P2X7 antagonist | A-438079 | Human astrocytes and hCMEC/D3 coculture | ZO-1 and Occludin↑; IL-1β and MMP-9↓; 10 KDa dextran extravasation↓; Prevent BBB damage | Yang et al. (2016) |
| P2X7 KO | | Cecal ligation and puncture (CLP) mouse | Caspase-1 and MMP-9↓; breakdown product of ZO-1 and spectrin↓ | Wang et al. (2015) |
| P2X7 antagonist | A-438079 | Rat intracerebral hemorrhage (ICH) | Neurobehavioral deficits↓; brain water content↓; Evans blue extravasation↓; activated RhoA↓; Occludin, VE-Cadherin, ZO-1↑ | Zhao et al. (2016) |
| P2X7 antagonists | Bright Blue G (BBG) and A-438079 | MDMA-induced neuroinflammation in rats | MMP-9, MMP-3 activity↓, basal lamina degradation↓; IgG extravasation↓; microglial activation↓; Reduces BBB breakdown | Rubio-Araiz et al. (2014) |
| P2X7 antagonists | BBG | Rat model EAE | Clinical signs of EAE↓; claudin-5 and PDGFβR↑; Decreased BBB permeability | Grygorowicz et al. (2018) |
| $P2Y_1$ antagonist | MRS2500 | Hypoxic damage stimulated mouse primary brain microvascular endothelial cells *in vitro* | ZO-1 and VE-cadherin↑; Enhanced endothelial barrier integrity | Raghavan et al. (2022) |
| $P2Y_4$ antagonist | Reactive Blue 2(RB-2) | Kainic acid-induced epileptic rat model | P2Y4/TSP-1/TGF-beta1/pSmad2/3 pathway↓, Evans Blue contents↓; Outflow of Alexa Fluor 488 from capillaries↓ | Zhang et al. (2019) |
| $P2Y_{12}$ antagonist/$P2Y_{12}$ KO | $P2Y_{12}$ antagonist clopidogrel | Laser-induced BBB opening in mice | Exhibited significantly diminished movement of juxtavascular microglial processes; outflow of Alexa Fluor 488 from capillaries↑; Aggravated BBB defects | Lou et al. (2016) |

nucleus microvascular endothelial cells and perivascular astrocytes end-foot (Loesch, 2021). Human brain microvascular endothelial cells (HBMECs) express P2X7 receptors (Wang et al., 2022). After stimulation by LPS, intracellular mitochondria produced a large amount of ATP and activated P2X7R, which further mediated the activation of the intracellular Omi/HtrA2 apoptosis signaling pathway and promoted cell apoptosis (Wang et al., 2022). Although the expression of these receptors in neurovascular units is partially understood, how P2X receptors regulate BBB permeability is less well studied, and the regulation of BBB by receptors other than P2X4 and P2X7 is unclear. Table 1 shows the effects of P2X receptor agonists and antagonists on the BBB.

## 3.2 P2X receptors and blood-brain barrier

### 3.2.1 P2X4

P2X4 is a typical P2X receptor, which can bind to P2X2, P2X5, and/or P2X6 to form heterotrimers (Antonio et al., 2014). It is expressed on the plasma membrane and in intracellular compartments. Meanwhile, P2X4 is a highly sensitive purinergic receptor that recognizes extracellular free ATP produced by dying cells following tissue injury, and is located in central and peripheral neurons, microglia, astrocytes, endothelial cells, and epithelial tissues (Montilla et al., 2020). The function of the P2X4 receptor in microglia has received extensive attention because of the relatively high level of expression of this receptor in these cells (Stokes et al., 2017). Microglia rely on migration and motility for active surveillance of the brain. P2X4 receptor activation drives microglia movement mainly through the phosphatidylinositol 3-kinase (PI3K)/Akt pathway (Ohsawa et al., 2007). Thus, microglia that move to the injured brain area express high levels of the P2X4 receptor (Domercq et al., 2013). P2X4 also contributes to the immune response of microglia, which affects BBB permeability in neuroinflammatory and degenerative diseases (Vazquez-Villoldo et al., 2014). After intracerebral hemorrhage (ICH), microglia activation and immune cell infiltration exacerbate cell death and BBB damage. P2X4R was shown to be overexpressed in the brains

of ICH patients as well as in ICH animals. Its activation inhibited the secretion of anti-inflammatory cytokines from microglia after cerebral hemorrhage, which exacerbated inflammatory brain injury. Concomitantly, P2X4R inhibition with the selective inhibitor (5-(3-bromophenyl)-1,3-dihydro-2H-benzofuro[3,2-e]-1,4-diazepin-2-one (5-BDBD)) dramatically reduced cerebral edema, blood-brain barrier leakage in ICH animals by decreasing pro-inflammatory activity of microglia (Wu et al., 2022). In addition, 5-BDBD treatment significantly inhibited P2X4R expression in monocytes and microglia after ischemic stroke, while reducing neurological deficit scores, interleukin-1 beta (IL-1β) levels, and BBB permeability (Srivastava et al., 2020). Furthermore, P2X4R knockout reduced leukocyte infiltration into brain tissue and improved neurological function in an ischemic stroke model (Verma et al., 2017). Thus, P2X4 receptor regulation of microglia activity may be partially involved in the regulation of BBB permeability, but the in-depth mechanisms need further investigation.

### 3.2.2 P2X7

ATP-induced proinflammatory effects of the P2X7 receptor have been extensively studied. The P2X7 receptor is best known for its effects on proliferation, apoptosis, and inflammation (Gu and Wiley, 2018). In addition, the P2X7 receptor (P2X7R) is of particular interest because of its association with BBB disruption (Andrejew et al., 2019). Recently, P2X7R has been implicated in alcohol and nicotine-induced BBB damage (Le Dare et al., 2019; Le Dare et al., 2021). Electronic-cigarette (E-Cig) vape (0% or 1.8% nicotine) decreased occludin and glucose transporter 1 (Glut1) protein expression in brain tissue and increased BBB permeability *in vivo* (Heldt et al., 2020). *In vitro* (Mekala et al., 2022), treatment of brain microvascular endothelial cells with ethanol (ETH), acetaldehyde (ALD), or 1.8% e-Cig elevated P2X7R and TRPV1 channel gene expression. Meanwhile, the P2X7R antagonist A804598 (10 μM) restored mitochondrial oxidative phosphorylation levels and played a protective role in preventing extracellular ATP release. BBB functional assays using trans-endothelial electrical resistance showed that blocking P2X7R channels enhanced barrier function. P2X7R antagonist may prevent alcohol or e-cigarette-induced BBB damage by improving mitochondrial dysfunction in endothelial cells. In addition, P2X7R plays a key role in LPS-induced BBB injury in mice. LPS significantly upregulated hippocampus P2X7R expression, whereas treatment with the P2X7R inhibitor A-438079 prevented the LPS-induced decrease in hippocampal Occludin and ZO-1 expression in mice (Wang et al., 2022).

Microglia also contribute to the structural and functional integrity of the BBB. Although P2X7 receptors are expressed in a variety of cells in the brain, such as oligodendrocytes and astrocytes, their expression is highest in microglia (Illes et al., 2012; Illes, 2020). P2X7 is a receptor involved in microglial activation, which is significantly upregulated in the postmortem brain of Alzheimer's patients and in animal models of various neurodegenerative diseases, promoting central neuroimmune and inflammatory responses that exacerbate disease progression (Takenouchi et al., 2010). Stimulation of P2X7Rs on the surface of microglia by high concentrations of ATP molecules activates NLRP3, which initiates the cleavage of pro-caspase-1 to caspase-1, followed by caspase-1-induced protein hydrolysis to convert pro-IL-1β to mature IL-1β. Studies have shown that P2X7 receptor activation of microglia leads to the release of the pro-inflammatory cytokine IL-1β (Ferrari et al., 2006; Takenouchi et al., 2009), which promotes the production of matrix metalloproteinase-9 (MMP-9) (Gu and Wiley, 2006) and decreases the expression of the tight junction protein ZO-1, thereby disrupting the blood-brain barrier *in vivo* and vitro (Harkness et al., 2000; Mori et al., 2002; Oliveira-Giacomelli et al., 2021). A breakdown in the blood-brain barrier resulted in neuroinflammation, ion dysregulation, and cerebral edema, leading to increased intracranial pressure, neuronal malfunction, and neurodegeneration (Profaci et al., 2020). For instance, extracellular aggregation of amyloid (Aβ) peptides is a key characteristic of AD, serving as an important trigger for glial cell activation and ATP release, thereby activating P2X7 receptors. Under AD pathology, high concentrations of ATP or Aβ peptides promoted the activation of P2X7 in microglia, which in turn induced increased release of chemokines such as CCL3 and the recruitment of $CD8^+$ T cells into the hippocampus and choroid plexus and exacerbated the development of central inflammation (Martin et al., 2019) (Figure 2).

In addition, postmortem patients with PD have more phagocytically active reactive microglia in the brain (Toulorge et al., 2016), as well as increased microglia activation in the striatum and substantia nigra in a rat model (Carmo et al., 2014), accompanied by elevated P2X7 receptor gene expression (Oliveira-Giacomelli et al., 2021). α-synuclein protein is a crucial component of PD pathogenesis, and its aggregation is believed to be connected with disruption of the blood-brain barrier. Administration of α-synuclein dramatically increased the permeability of endothelium co-cultured with rat brain pericyte cells, while inducing the release of IL-1β, IL-6, TNF-α, MCP-1, and MMP-9 (Dohgu et al., 2019). Furthermore, α-synuclein protein activates microglia, causes the release of excitotoxic glutamate from microglia, and releases reactive oxygen species (ROS) to damage dopaminergic neurons (Dos-Santos-Pereira et al., 2018), as well as also binding to and stimulating transcription of P2X7 receptors in microglia (Jiang et al., 2015). Interestingly, P2X7 receptor activation increases IL-1β release, which in turn promotes MMP-9 secretion and disrupts the blood-brain barrier's tight junctions (Yang et al., 2016). In PD disease, breakdown of the BBB causes extravasation of erythrocytes (Pienaar et al., 2015), which leads to cerebral microhemorrhages, as well as causing brain infiltration of peripheral immune cells and exacerbating the PD pathological process (Sweeney et al., 2018) (Figure 2).

P2X7 signaling in endothelial cells also plays a key role in BBB permeability regulation. Increased P2X7 receptor signaling in brain microvascular endothelial cells of septic encephalopathy (SE) mice induced by cecal ligation and puncture (CLP) enhanced the adhesion of Mac-1-expressing leukocytes to endothelial cells via intercellular cell adhesion molecule-1 (ICAM-1) and upregulated endothelial cell chemokine (C-X3-C motif) ligand 1 (CX3CL1), which triggered microglia activation. In addition, activation of NLRP3/caspase-1/IL-1β signaling *via* P2X7 receptor signaling in endothelial cells also accelerates BBB breakdown and neurovascular damage during SE (Wang et al., 2015) (Figure 3).

It has been determined that astrocytes participate in BBB function and can affect the permeability of the BBB (Bang et al., 2017; Heithoff et al., 2021). Formation and maintenance of the blood-brain barrier require astrocyte endfeet on the abluminal side of endothelial cells. In primary astrocytes, BzATP activates the P2X7 receptor and generates a 2.5-fold increase in RhoA activity, which is reduced by the P2X7 antagonist BBG, demonstrating that RhoA is activated in the signaling pathway downstream of the P2X7 receptor (Henriquez et al., 2011; Beckel et al., 2014). *In vivo*,

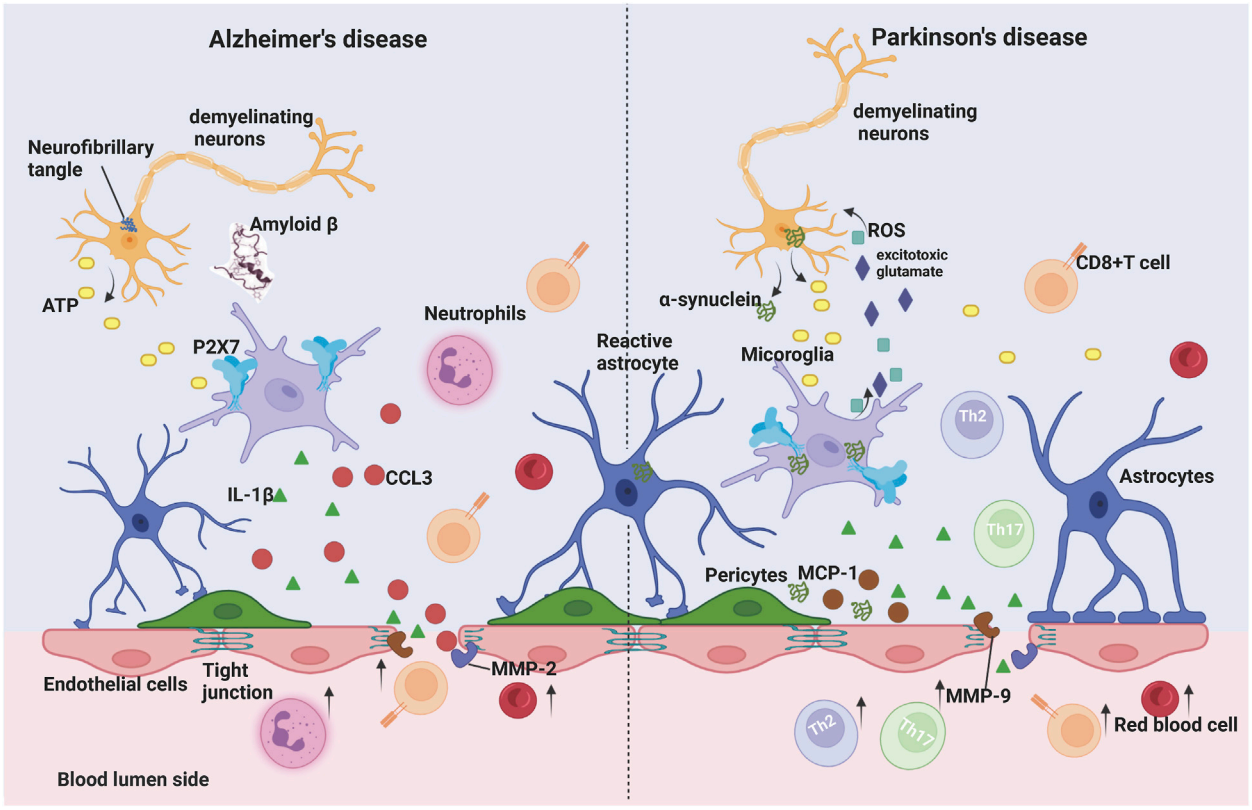


FIGURE 2
Microglia P2X7 receptor signaling on blood-brain barrier permeability in Alzheimer's disease (AD) and Parkinson's disease (PD). In AD, the process of neuronal death induces high levels of ATP release into the extracellular space, which activates microglia P2X7 receptors and leads to the release of IL-1β. In addition, the ATP/P2X7 receptor pathway enhances metalloproteinase (MMP) activity, leading to degradation of tight junction (TJ) protein, which results in increased blood-brain barrier permeability. Aβ peptide synergistically promotes P2X7 activation in microglia, which further induces increased release of chemokines such as CCL3 and recruitment of neutrophils and $CD8^+$ T cells into the central nervous system (CNS) in the presence of BBB injury, promoting disease progression. In PD, α-synuclein aggregation leads to dopaminergic neuron death, increased ATP levels and P2X7 hyperactivation. On the other hand, α-synuclein activates microglia, leading to the release of excitatory glutamate and reactive oxygen species (ROS) from microglia to damage dopaminergic neurons, while α-synuclein binds to and stimulates the transcription of P2X7 receptors in microglia. α-synuclein and P2X7 receptors both increase the release of IL-1β and chemokines, increase MMP activity, disrupt the BBB, and lead to extravasation of red blood cells, which leads to cerebral microhemorrhage, as well as causing parenchymal infiltration of peripheral immune cells and exacerbating the pathological process of PD. Created with BioRender.com.

increased expression of P2X7 receptors was observed in astrocytes and endothelial cells surrounding the hematoma 24 h after ICH in rats (Zhao et al., 2016). Disruption of the blood-brain barrier is one of the most significant pathophysiological alterations early in the course of ICH, leading to the production of vasogenic brain edema, which can result in a poor prognosis for the disease (Zhou et al., 2014). By suppressing RhoA activation, A438079, and P2X7R siRNA alleviated neurological impairments, brain edema, and minimized BBB degradation (Zhao et al., 2016). Numerous studies have identified RhoA, a small guanosine triphosphatase (GTPase), as a key regulator of barrier formation and disruption. RhoA governs endothelium actin cytoskeleton dynamics and contraction, affecting intercellular junctional complexes, vascular permeability, and signal transduction (Amado-Azevedo et al., 2014; Ramos and Antonetti, 2017). Activation of RhoA in endothelial cells promotes the onset of BBB barrier disruption, as evidenced by the fact that its activation leads to stress fiber formation associated with disruption of interendothelial junctions, thereby increasing paracellular flux (Beckers et al., 2010; Ramos and Antonetti, 2017).

The basement membrane (BM) is the extracellular matrix (ECM) that provides structural support for the BBB and also serves as a link between NVU intercellular communication and signaling pathways. It consists of structural proteins including type IV collagen, fibronectin, laminin, and other glycoproteins (Langen et al., 2019). P2X7 receptors are involved in the degradation of laminin and type IV collagen by the neurotoxic compound 3,4-methyldioxymethamphetamine (MDMA) (Rubio-Araiz et al., 2014). The intervention with MDMA activated microglia in the hippocampus and increased microglial P2X7 receptor expression. MDMA increased matrix metalloproteinase-3 (MMP-3) and MMP-9 activity in the hippocampus, which was accompanied by a decrease in laminin and collagen IV expression, an increase in IgG extravasation into the brain parenchyma, and finally lead to higher BBB permeability. Following treatment with P2X7 antagonists (Bright Blue G (BBG) and A-438079), BBB damage was minimized and its integrity was maintained (Rubio-Araiz et al., 2014; Perez-Hernandez et al., 2017).

Pericytes are in close contact with endothelial cells *via* "peg and socket" junctions in the common basal lamina, which are necessary for the formation and maintenance of the BBB (Cheslow and Alvarez,

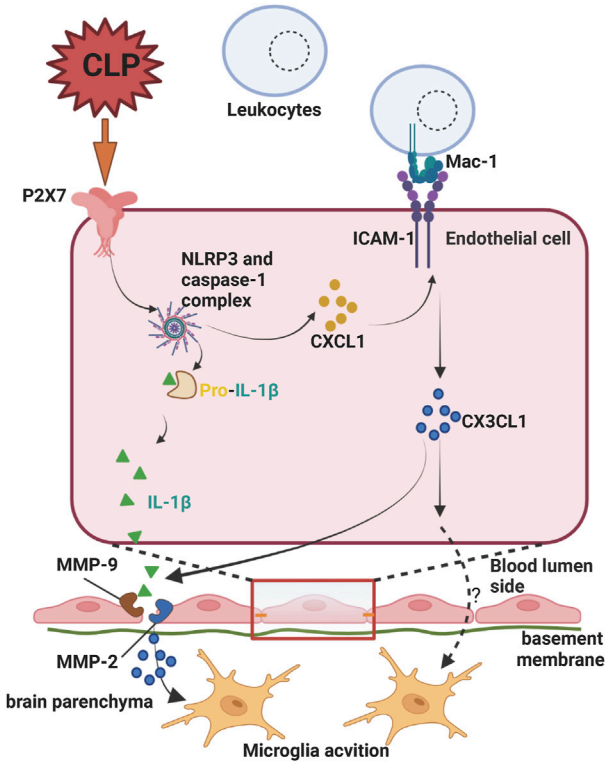


FIGURE 3
Endothelial P2X7 signaling on the permeability of the blood-brain barrier in septic encephalopathy (SE). Increased P2X7 receptor signaling in brain microvascular endothelial cells of SE mice generated by cecal ligation and puncture (CLP) increased adherence of Mac-1 expressing leukocytes to endothelial cells intercellular cell adhesion molecule-1(ICAM-1) and upregulated endothelial cell chemokine (C-X3-C motif) ligand 1 (CX3CL1), which activated microglia. The uncertainty exists as to whether CX3CL1 directly alters blood-brain barrier integrity during this process. P2X7 receptor signaling also promoted BBB breakdown and neurovascular injury during SE by activating NLRP3/caspase-1/IL-1β signaling. Created with BioRender.com.

2016; Liebner et al., 2018). One study has shown that P2X7R is co-expressed with PDGFβR, a pericyte marker localized to microvascular units (Grygorowicz et al., 2018). In a rat model of experimental autoimmune encephalomyelitis (EAE), P2X7 receptor expression was increased in capillaries, which correlated with low levels of expression of PDGFβR protein and Claudin-5. Treatment of P2X7R antagonists with immunized rats significantly reduced the clinical signs of EAE and enhanced the expression of claudin-5 and PDGFβR. These results suggest that P2X7 receptors located on pericytes may be involved in pathological mechanisms in brain microvessels that affect BBB integrity during EAE (Grygorowicz et al., 2018).

# 4 P2Y receptors and signaling

P2Y receptors are GPCRs with eight isoforms that respond to extracellular adenine and uracil nucleotides. P2Y receptors contain two subfamilies, the $G_q$ protein-coupled $P2Y_1$-like receptors $P2Y_{1, 2, 4, 6, 11}$, and the $G_i$ protein-coupled $P2Y_{12}$-like receptors $P2Y_{12-14}$. Almost all cells contain P2Y receptors, which are implicated in pathophysiological reactions like pain, inflammation, platelet aggregation, and neuroprotective effects (von Kugelgen, 2021). P2Y receptors are one of the most extensively researched therapeutic targets in the treatment of clinical diseases; e.g., clopidogrel, an antagonist targeting platelet $P2Y_{12}$, is an anti-thrombogenic drug, and diclofosfamide, a nucleotide agonist targeting $P2Y_2$ receptor, is used to treat dry eye disease (Guo et al., 2021).

## 4.1 P2Y receptors in NVU

P2Y receptors are mostly expressed in neurons, glial cells, and microvasculature in the brain, where they co-mediate neurotransmission, neuroprotection, neuron-glia interactions, and cerebral blood flow regulation alongside P2X receptors (Weisman et al., 2012; Toth et al., 2015; Burnstock, 2017). $P2Y_1$ and $P2Y_2$ receptors are present in brain pericapillary cells, and extracellular ATP causes pericyte contraction by stimulating these two receptors and causing intracellular $Ca2^+$ concentrations to rise (Horlyck et al., 2021). $P2Y_1$, $P2Y_2$, and $P2Y_{13}$ receptors, which are present in neurons, are involved in the regulation of neuronal differentiation and neuroprotection (Perez-Sen et al., 2015; Miras-Portugal et al., 2019). Notably, $P2Y_1$, $P2Y_2$, $P2Y_4$, and $P2Y_6$ receptors in endothelial cells have an induced vasodilation effect (Jacobson et al., 2020). Astrocytes in the hippocampus, cortex, striatum, cerebellum, and spinal cord express multiple P2Y receptors, such as $P2Y_{1, 4, 6, 13}$ (Franke et al., 2012). Indeed, $P2Y_{12}$ is relatively restricted in distribution, is mainly expressed in microglia, and has an important role in inflammation and neuropathic pain (Tozaki-Saitoh et al., 2008). The effects of P2Y receptors agonists or antagonists on BBB are shown in Table 1.

## 4.2 P2Y receptors and blood-brain barrier

Multiple P2Y receptor subtypes are expressed by endothelial cells throughout the vascular system. P2Y receptors in endothelial cells have been studied mainly in the context of their NO-mediated vasodilatory properties. Therefore, there are fewer findings on the role of P2Y receptors in maintaining the BBB. Bowden and Patel have identified the importance of the tyrosine kinase/mitogen-activated protein kinase (MAPK) cascades in P2Y receptor regulation of prostacyclin production in major vascular endothelial cells (Bowden et al., 1995; Patel et al., 1996). MAPK cascades are essential for cell adhesion, and there is substantial evidence that tyrosine-phosphorylated proteins are involved in maintaining the BBB integrity. Coexisting P2Y receptors in brain endothelial cells may variably control phosphoinositide hydrolysis, cyclic AMP, and MAPK, resulting in various effects on the BBB (Albert et al., 1997). The $P2Y_1$ receptor exacerbates leukocyte recruitment and induces inflammation, and the $P2Y_1$ inhibitor MRS2500 is able to reduce vascular inflammation. Meanwhile, in $P2Y_1$-deficient mouse, monocyte adherence to inflammatory factor-stimulated mouse endothelial cell monolayers was drastically reduced *in vitro* (Zerr et al., 2011). Additionally, it has been discovered that primary cultured brain microvascular endothelial cells have minimal $P2Y_1$ receptor expression and that hypoxic damage stimulated elevation of this receptor expression, which resulted in degradation of endothelial

cell junctional proteins and increased endothelial permeability (Raghavan et al., 2022). Similarly, the $P2Y_1$ receptor antagonist MRS2500 enhanced endothelial barrier integrity.

The development of epilepsy is accompanied by a disruption of BBB (Sweeney et al., 2019). The kainic acid-induced epileptic rat model presented angiogenesis and disruption of BBB integrity, along with a significant increase in the expression of TSP-1, TGF-β1, and pSmad2/3. Treatment with pyridoxal phosphate-6-azophenyl-2′, 4′-disulfonic acid (a broad P2 receptor antagonist) or Reactive Blue 2 (a $P2Y_4$ receptor antagonist) inhibited TSP-1 expression and Smad2/3 phosphorylation level, while significantly reducing acute seizure severity, decreasing Evans Blue contents, and attenuating BBB damage (Zhang et al., 2019).

The $P2Y_{12}$ receptor is a unique purinergic receptor expressed only by microglia in the central nervous system (CNS) (Gu et al., 2016). As a chemotactic receptor, it is highly expressed in microglia (Sasaki et al., 2003) and drives microglial migration to areas of CNS damage (Ransohoff and Cardona, 2010; Sipe et al., 2016). Following central capillary injury, perivascular microglia, a component of the neurovascular unit, rapidly generate dense aggregates of microglial protrusions at the site of injury. In addition, $P2Y_{12}$ receptor-mediated chemotaxis of microglia processes is necessary for the rapid closure of the BBB after its rupture (Lou et al., 2016). Movement of paravalvular microglial protrusions was significantly reduced and failed to close the opening of the laser-induced BBB in mice intervened with the $P2Y_{12}$ receptor inhibitor clopidogrel and in mice knocked out with the $P2RY_{12}$ gene (Lou et al., 2016). Given that $P2Y_{12}$ receptor antagonists are commonly used as platelet inhibitors in patients with coronary heart disease and cerebrovascular disease, who are at increased risk for stroke with impaired BBB destruction, these findings may have clinical implications.

# 5 Adenosine and adenosine (P1) receptors

Adenosine is a bioactive compound that has been shown to possess strong neuromodulatory effects. It is able to function as a signaling molecule between the body's periphery and the brain since it can easily penetrate the BBB (Chiu and Freund, 2014). AMP is a major source of intracellular and extracellular adenosine. Intracellular adenosine is a synergistic intermediary between nucleic acids and ATP, which is generated by AMP metabolism via 5′-nucleotidase and synthesized by adenosine kinase. Adenosine can also be produced outside of the cells by the breakdown of ATP or ADP that has been released by the cell. In this pathway, CD39 or E-NTPDase converts ATP/ADP to AMP, while CD73 or 5′nucleotidase converts AMP to adenosine (Yegutkin, 2008). Adenosine exerts its effect by acting on four expressed G-protein-coupled adenosine receptors ($A_1$, $A_{2A}$, $A_{2B}$, and $A_3$) on cell surfaces, and these receptors are expressed in some combination on almost all CNS cells. Under physiological conditions, extracellular adenosine levels range between 20 and 300 nM (Newby, 1985; Newby et al., 1985); however, local adenosine concentrations in the brain increase nearly 1000-fold under stress and inflammatory conditions (Hagberg et al., 1987). $A_1$ and $A_{2A}$ receptors have a higher affinity for adenosine, in contrast to $A_{2B}$ and $A_3$ receptors, which have a lower affinity for adenosine, indicating that $A_1$ and $A_{2A}$ receptors in the CNS could be activated by reasonable levels of extracellular adenosine (Carman et al., 2011).

## 5.1 Adenosine receptors in NVU

The human brain endothelial cell line hCMEC/D3 exhibited $A_1$, $A_{2A}$, and $A_{2B}$ receptors (Mills et al., 2011). $A_1$ and $A_{2A}$ receptors were also expressed in primary human brain endothelial cells and in Bend.3 mouse brain endothelial cells (Carman et al., 2011). In addition, *in vivo* immunofluorescence reveals that $A_1$ and $A_{2A}$ receptor proteins are expressed in mouse cortical brain endothelial cells, while *in vitro*, the two receptor proteins are present in primary mouse brain endothelial cells (Carman et al., 2011). Four P1 receptors ($A_1$, $A_{2A}$, $A_{2B}$, and $A_3$) have been identified in astrocytes (Dare et al., 2007). In astrocytes, cyclic adenosine monophosphate (cAMP) synthesis is inhibited by $A_1$ receptors, while $A_2$ receptors enhance cAMP synthesis, and $A_{2B}$ receptors are able to lead to a dose-dependent accumulation of cAMP (Peakman and Hill, 1994). Adenosine receptors govern various features of astrocytes, including $A_{2A}$ receptors that regulate glutamate uptake (Matos et al., 2012), but also $A_1$ receptors that preserve cell integrity (Ciccarelli et al., 2001; D'Alimonte et al., 2007), and $A_3$ receptors that protect against hypoxia-induced cell death and regulate CCL2 chemokine production (Wittendorp et al., 2004; Bjorklund et al., 2008). In physiological conditions, $A_1$, $A_{2A}$, $A_{2B}$ and $A_3$ receptors are moderately expressed in glial cells, but their levels are upregulated in a central inflammatory environment (Hasko et al., 2005). The blood-brain barrier could be altered with disruptive changes in endothelial cells and tight junctions during central chronic inflammation, mediated mainly by adenosine receptors and CD39/CD73 expression (Selmi et al., 2016). The effects of adenosine receptors agonists or antagonists on BBB are shown in Table 2.

## 5.2 Adenosine receptors and blood-brain barrier

### 5.2.1 $A_1$ and $A_{2A}$ receptors

Adenosine $A_1$ and $A_{2A}$ receptors are expressed on both human and murine brain microvascular endothelial cells (Kalaria and Harik, 1988; Carman et al., 2011; Mills et al., 2011). Two studies have shown that Ginkgo biloba extract increases BBB permeability by activating the $A_1$ adenosine receptor signaling pathway (Guo et al., 2020; Liang et al., 2020). In these studies, BBB models were constructed by co-culture with human cerebral microvascular endothelial cells (hCMEC/D3) and human normal glial cells (HEB) *in vitro*. The hCMEC/D3 cell line is the first stable, well-differentiated human brain endothelial cell line that expresses CD73, a cell surface enzyme that converts extracellular AMP to adenosine, as well as adenosine receptor subtypes $A_1$, $A_{2A}$, and $A_{2B}$ (Mills et al., 2011). Intervention with Ginkgo biloba extract increased BBB permeability, as evidenced by an increased fluorescein sodium (Na-F) penetration rate, disruption of tight junction structures, and increased actin-binding proteins ezrin, radixin and moesin (ERM) and myosin light chain (MLC) phosphorylation levels *in vitro* (Guo et al., 2020; Liang et al., 2020). ERM (ezrin/radixin/moesin) has been shown to be an important actin-binding molecule and the target of threonine phosphorylation in a variety of signaling pathways (Garcia-Ponce et al., 2015). Increased phosphorylation of ERM can induce actin remodeling and increase vascular permeability. Meanwhile, the phosphorylation of myosin light chain kinase (MLCK) to MLC causes actin filaments at the tight junction of endothelial cells to contract, leading to the

**TABLE 2 Effect of P1 receptors agonist/antagonist on blood-brain barrier permeability.**

| Receptor/Agonist/ Antagonists | Drug name | Model | Observation | Reference(s) |
|---|---|---|---|---|
| $A_1$ antagonist | DPCPX | *In vitro* BBB model:Co-culture of hCMEC/D3 and HEB | ERM and MLC phosphorylation↓; TEER↑; Na-F permeability↓; Improved BBB integrity | Liang et al. (2020) |
| $A_1$ and $A_{2A}$ agonists; $A_1$ KO; $A_{2A}$ KO | $A_1$ agonists: CCPA; $A_{2A}$ agonists: CGS 21680 or Lexiscan | Mouse model of brain drug delivery; mouse brain endothelial cells *in vitro* | *In vivo*:the permeability of the BBB to low molecule dextran↑; *In vitro*: TEER↓; Tight junction molecules↓; Actinomyosinstress fiber formation↑; $A_1/A_{2A}$ agonists induced BBB permeability, effects lost in KO mice | Carman et al. (2011) |
| Broad-spectrum adenosine receptors(AR) antagonist | Caffeine | MPTP-induced PD mouse model | Leakage of Evan's blue dye and FITC-albumin ↓; ZO-1and occludin↑; Reactive gliosis↓ | Chen et al. (2008a) |
| Broad-spectrum AR antagonist | Caffeine | Cholesterol-induced AD model in rabbits | Extravasation of IgG and fibrinogen↓; Leakage of Evan's blue dye↓, Occludin and ZO-1↑; astrocytes activation and microglia density↓ | Chen et al. (2008b) |
| $A_{2A}$ antagonist | SCH58261 | Sleep-restricted rats model | ZO-1 and claudin-5↑; 10 and 70 kDa FITC-dextran permeability↓; Evans blue permeability; GFAP and Iba-1 overexpression↓ | Hurtado-Alvarado et al. (2016) |
| Adora2a $^{\Delta VEC}$ mice | | Thromboembolic stroke mice | Evans blue leakage↓; Leukocyte infiltration, brain edema, and neuroinflammation↓; NLRP3, caspase 1,IL-1β↓; Improved BBB integrity | Zhou et al. (2019) |
| A2A antagonist; Adora2a$^{\Delta VEC}$ mice | SCH58261 | Diet-induced insulin-resistant mice | Evans blue and NaFl leakage↓; claudin-5 and Occludin↑ | Yamamoto et al. (2019) |
| FDA-approved $A_{2A}$ agonist | Lexiscan | Human brain endothelial barrier (hBBB) model *in vitro* | Phosphorylation of ERM and FAK↑; Claudin-5 and VE-Cadherin↓ | Kim and Bynoe (2015) |
| $A_{2A}$ agonist | CGS21680 | Brain metastasis of lung cancer | Proliferation and migration ability of PC-9 cells↓; Claudin-5, Occludin, and ZO-1↑, MMP2 and MMP9↓ Improved BBB integrity | Chen et al. (2020) |
| $A_{2A}$ agonist | CGS21680 | *In vivo*: EAE model mice; *In vitro*: Th1 cytokine stimulation in mouse brain endothelial cells | MLC phosphorylation↓; ZO-1 and Claudin-5↑; Formation of stress fibers↓; Safeguard BBB function | Liu et al. (2018) |
| $A_{2B}$ agonist | BAY 60–6583 | Rats with (tMCAO) | Volume of tissue lesions↓; Brain swelling↓; leakage of albumin↓; MMP-9↓; ZO-1 degradation↓; Protects the blood-brain barrier | Li et al. (2017) |
| $A_3$ agonist | AST-004 | Mouse Model of Traumatic Brain Injury | Leakage of Evans Blue↓; ATP production in astrocytes↑ | Bozdemir et al. (2021) |

opening of the barrier. Indeed, administration of the $A_1$ receptor antagonist DPCPX or adenosine $A_1$ receptor siRNA inhibited ERM and MLC phosphorylation levels, altered TJ ultrastructure, and improved BBB integrity (Guo et al., 2020; Liang et al., 2020) (Figure 4).

$A_{2A}$ receptors are expressed at increased levels in brain tissue in multiple animal models, such as sleep restriction and thromboembolic stroke, accompanied by BBB damage (Hurtado-Alvarado et al., 2018; Zhou et al., 2019; Medina-Flores et al., 2020). Lack of sleep produces a low-grade inflammatory state that increases pro-inflammatory mediators, which regulate BBB function in a subtle but sustained manner (Hurtado-Alvarado et al., 2018). Sleep restriction increased the expression of $A_{2A}$ adenosine receptors in the hippocampus and basal nucleus. Blockade of $A_{2A}$ receptors by SCH58261 reversed sleep restriction-induced BBB dysfunction, including increased dextrans coupled to fluorescein (FITC-dextrans) and Evans blue permeability, degraded tight junction protein expression, and increased expression of neuroinflammatory markers Iba-1 and GFAP (Hurtado-Alvarado et al., 2016).

Besides, the human striatum contains high levels of $A_{2A}$ receptors, while the cerebral cortex, hippocampus, and immune cells contain lower levels (van Waarde et al., 2018). It was demonstrated that the broad AR agonist NECA [activates all ARs ($A_1$, $A_{2A}$, $A_{2B}$, $A_3$)], the selective $A_1$ agonist CCPA and the $A_{2A}$ receptor agonists CGS 21680 or Lexiscan increased the permeability of the BBB to 10 kDa dextran, while the effect of these ARs on BBB permeability was attenuated in mice knocked out of $A_1$ or $A_{2A}$ receptors (Carman et al., 2011). Notably, *in vitro*, NECA and Lexiscan intervention in mouse brain endothelial cells inhibited the expression of intercellular tight junctions ZO-1, claudin-5, and Occludin and reduced transendothelial electrical resistance (TEER) (Carman et al., 2011).

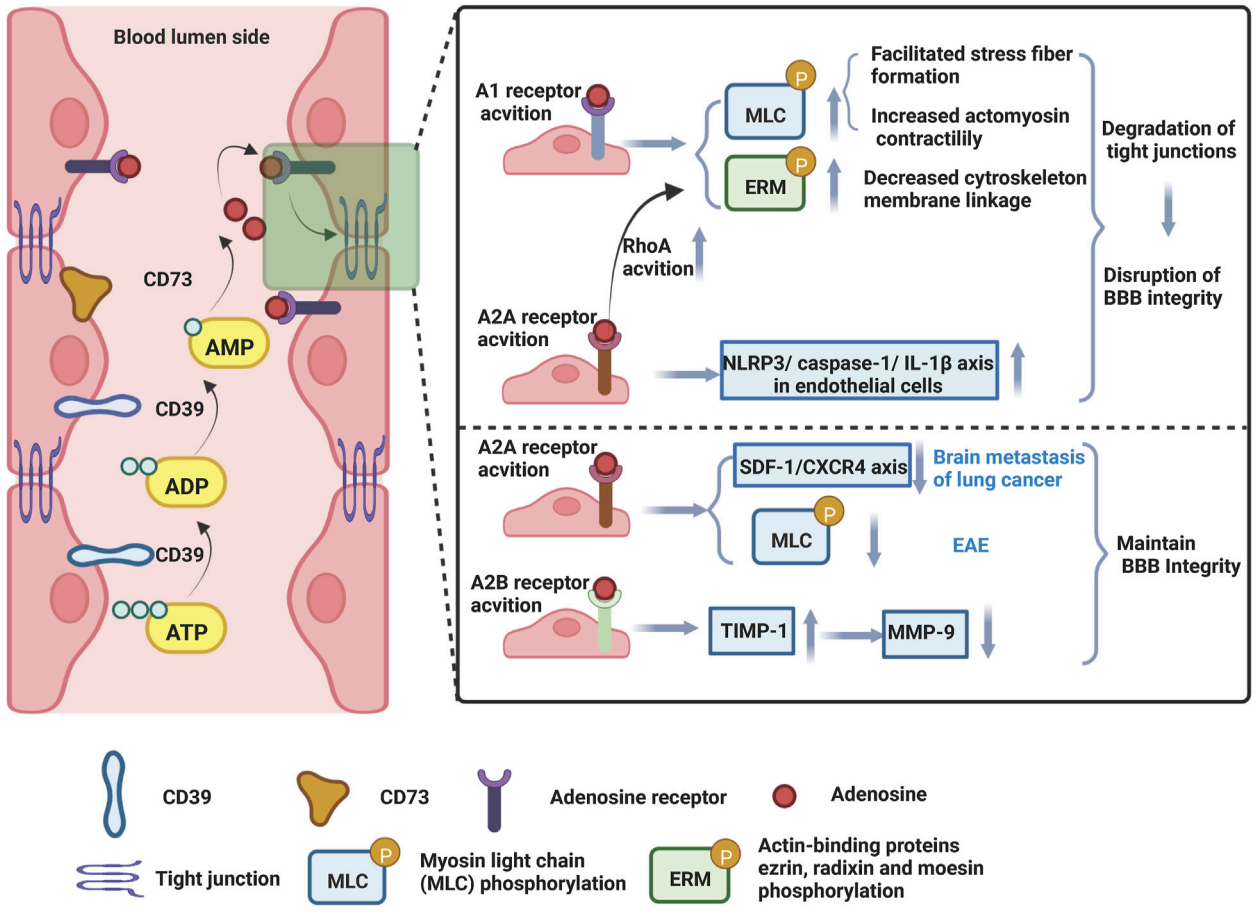


FIGURE 4
Adenosine receptors (ARs) modulate the permeability of blood-brain barrier. Endothelial cells of the microvasculature of the brain express adenosine receptors, CD39, and CD73. Under conditions of tissue damage, stress, and inflammation, ATP is released and converted by CD39 into ADP and AMP, which are then converted to adenosine by CD73. Adenosine binds to adenosine receptors on endothelial cells and operates to restructure the actin cytoskeleton, thereby disrupting tight junctions and adherens junctions and affecting BBB integrity. Created with BioRender.com.

Consistent with these results, in animal models of neurodegenerative disease, investigators observed that caffeine, a broad-spectrum AR antagonist, attenuated Parkinson and Alzheimer animal models-induced leakage of Evans blue dye, degradation of occludin and ZO-1, and ameliorated BBB dysfunction (Chen et al., 2008a; Chen et al., 2008b). Likewise, the FDA-approved $A_{2A}$ AR agonist Lexiscan, a selective $A_{2A}$ receptor agonist, increased the permeability of the human brain endothelial barrier (hBBB) model *in vitro* (Kim and Bynoe, 2015). $A_{2A}$ receptor activation mediated increase in cAMP and RhoA signaling activation, which in turn stimulated instability of the actin-cytoskeleton, decreased phosphorylation of factors involved in focal adhesion ERM and focal adhesion kinase (FAK) and degradation of Claudin-5 and VE-Cadherin, hence increasing the permeability of the hBBB (Figure 4). Notably, the high permeability of hBBB induced by $A_{2A}$ agonists is rapid, time-dependent and reversible.

Accordingly, expression of $A_{2A}$ receptors in endothelial cells was increased after thromboembolic stroke (Zhou et al., 2019). In mice specifically lacking endothelial Adora2a (Adora2a $^{\Delta VEC}$), Evans blue leakage, leukocyte infiltration, brain edema, and neuroinflammation were attenuated. *In vitro* silencing of the Adora2a gene using siRNA in cultured brain microvascular endothelial cells also attenuated endothelial inflammation by inhibiting the NLRP3 inflammasome and downregulating expression of cleaved caspase 1 and IL-1β (Zhou et al., 2019). These results suggest that $A_{2A}$ receptor-mediated NLRP3 activation may have a role in brain endothelial inflammation and need to be investigated in depth. It has also been shown that obesity and insulin resistance disrupt the BBB in both humans and animals (Banks, 2019; Banks and Rhea, 2021). The activation of $A_{2A}$ receptors in endothelial cells is also closely associated with cognitive impairment caused by obesity. In this study, diet-induced insulin-resistant mice exhibited elevated BBB permeability to low molecular weight sodium fluorescein (NaFl) and Evans blue; however, administration of the $A_{2A}$ antagonist SCH58261 restored the BBB barrier integrity (Yamamoto et al., 2019). SCH58261 is a selective adenosine $A_{2A}$ receptor antagonist that crosses the BBB (Mohamed et al., 2012). Further study showed that Adora2a activation in endothelial cells exacerbated BBB damage and cognitive dysfunction in diet-induced insulin-resistant mice, while mice specifically knockout of endothelial Adora2a protected BBB integrity after suffering from diet-induced insulin resistance (Yamamoto et al., 2019). These results indicate that Adora2a-mediated signaling in vascular endothelial cells, which resulted in BBB failure, may be a potential mechanism for cognitive deficiencies caused by obesity and insulin resistance.

Certain viruses and bacteria infiltrated the CNS through boosting the local expression of adenosine, which promoted the BBB permeability and quickly opened the BBB (Zhao et al., 2020). For instance, *Haemophilus influenzae type a* (Hia) infection stimulated $A_{2A}$ and $A_{2B}$ adenosine receptors in a model of BBB co-cultured with human brain microvascular endothelial cells (BMEC) and pericytes (BMPC) *in vitro*, which induced the release of large amounts of VEGF from pericytes. VEGF caused pericyte shedding and endothelial cell proliferation, which triggered the BBB disorder (Caporarello et al., 2018). In addition, adenosine produced by a surface enzyme (Ssads) of *Streptococcus suis* promotes its pathogen's entrance into the brains of mice, hence causing meningitis. A1 AR activation increases *S. suis* BBB penetration, and $A_1$ AR signaling exploitation may represent a generic virulence mechanism (Zhao et al., 2020).

Conversely, some studies have shown that $A_{2A}$ receptor activation also protects the integrity of BBB barrier. Brain metastases is the most common and lethal malignancy of the CNS, (Lowery and Yu, 2017; Singh et al., 2018), yet it is unknown how primary cancer cells traverse the BBB and metastasis to physiological regions of brain tissue. The $A_{2A}$ receptor agonist CGS21680 inhibited the proliferation and migration ability of PC-9 cells, a type of lung cancer cell, and suppressed brain metastasis (Chen et al., 2020). Notably, activation of $A_{2A}$ receptors *in vitro* increased the expression levels of Claudin-5, Occludin, and ZO-1, reduced the expression of MMP-2 and MMP-9, and increased the BBB integrity, whereas the opposite effect was obtained with the $A_{2A}$ receptor antagonist SCH58261 (Chen et al., 2020). Stromal cell-derived factor-1 (SDF-1) is an important chemokine in homeostasis that interacts with C-X-C motif chemokine receptor 4 (CXCR4), which is commonly classified as a GPCR (Janssens et al., 2018). The interaction between SDF-1 and CXCR4 has been identified to regulate several cellular physiological processes, such as transcription, energy metabolism, cell adhesion, and chemotaxis (Mao et al., 2017). Their findings also showed that $A_{2A}$ receptor stimulation inhibited CXCR4 expression and that $A_{2A}$ receptor agonists and CXCR4 antagonists protected nude mice from the metastasis of malignant tumor cells *in vivo* and prolonged their survival time (Chen et al., 2020). Mechanistically, $A_{2A}$ receptor activation maintained BBB integrity by regulating the SDF-1/CXCR4 axis, which in turn inhibited brain metastasis (Figure 4). Besides, specific $A_{2A}$ receptor agonist CGS-21680 improved pathological and clinical manifestations of EAE by decreasing BBB permeability, inhibiting neuroinflammation (Liu et al., 2018). Th1 cytokines are known to activate MLCK, which promotes phosphorylation of MLC (p-MLC) and disrupts actin-myosin interactions, thereby regulating endothelial cell morphology (Capaldo and Nusrat, 2009). Thus, activation of MLCK also leads to TJ injury (Rissanen et al., 2013). *In vitro*, brain endothelial cells treated with the Th1 cytokines IL-1β, TNF-α, and IFN-γ exhibited barrier failure. By inhibiting MLC phosphorylation and promoting ZO-1 and Claudin-5 expression, the $A_{2A}$ receptor-specific agonist CGS-21680 provided direct BBB protection (Liu et al., 2018). In addition, CGS-21680 helps maintain the shape of endothelial cells by reducing the formation of stress fibers in cells caused by Th1 cytokines (Liu et al., 2018). Activation of the $A_{2A}$ receptor may safeguard BBB function by suppressing MLCK-mediated MLC phosphorylation in EAE (Figure 4). According to tissue injury and associated pathological conditions, activating $A_{2A}$ receptors has both beneficial and detrimental effects in different diseases (Chen et al., 2013). It was shown that $A_{2A}$ inhibited specific lymphocyte proliferation, reduced infiltration of $CD4^+$ T lymphocytes, and suppressed inflammatory cytokine production, thus inhibiting EAE progression. Additionally, Lexiscan, an $A_{2A}$ receptor-specific agonist, is an FDA-approved drug with proven therapeutic effects in inflammatory bowel disease, lung injury, and hepatic ischemia-reperfusion (Liu et al., 2016). Based on the complexity of the brain microenvironment, the activation of $A_{2A}$ receptors may also have a dual effect on the function of the BBB.

### 5.2.2 $A_{2B}$ and $A_3$ receptors

The interaction of $A_{2B}$ receptors and $A_3$ receptors with the BBB has been less reported. The $A_{2B}$ receptor agonist BAY 60-6583 reduced the volume of tissue plasminogen activator (tPA)-induced lesions and attenuated brain swelling and BBB disruption in rats with ischemic stroke (Li et al., 2017). BAY 60-6583 inhibited tPA-enhanced MMP-9 activation, possibly by increasing the tissue inhibitor matrix metalloproteinase 1 (TIMP-1), thereby reducing TJ protein degradation and protecting the blood-brain barrier (Li et al., 2017) (Figure 4).

In a mouse model of traumatic brain injury, the adenosine $A_3$ receptor agonist AST-004 decreased the permeability of BBB and neuroinflammation, and enhanced spatial memory (Bozdemir et al., 2021). Intervention with AST-004 boosted ATP production in astrocytes and enhanced neuroprotective efficacy after brain injury; however, the precise mechanism of enhancing BBB function requires additional investigation.

### 5.2.3 CD39 and CD73

Ecto-5′-nucleotidase CD73 is an enzyme present on the cell surface that participates in the purine catabolism process and is capable of catalyzing the breakdown of AMP to adenosine. In the central nervous system, neurons, astrocytes, endothelium, and other cells release ATP, then CD39 catalyzes the conversion of ATP/ADP to AMP, and CD73 metabolizes AMP to adenosine (Burnstock and Boeynaems, 2014; Fuentes and Palomo, 2015). Multiple types of endothelial cells express CD39 and CD73 (Koszalka et al., 2004; Dudzinska et al., 2014), and expression of CD39/CD73 at the cellular level regulates tissue barrier function via modulating ATP levels (Colgan et al., 2006). CD73 is expressed in mouse (Bend.3) and hCMEC/D3 brain endothelial cell lines *in vitro* (Carman et al., 2011; Mills et al., 2011). Compared to human brain endothelial cells, mouse brain endothelial cell CD73 expression is extremely low *in vivo* (Mills et al., 2008). CD73 is highly expressed on choroid plexus epithelial cells that form the blood-cerebrospinal fluid barrier, but its expression is lower on brain endothelial barrier cells under steady-state conditions (Mills et al., 2008). However, CD73 was increased in the presence of cellular stress, local inflammation, or tissue injury that produced adenosine. Meanwhile, CD39 is widely expressed in brain endothelial cells (Wang and Guidotti, 1998), and CD39 on endothelial cells is conducive to reducing inflammatory cell transport and platelet reactivity, thereby reducing tissue damage after cerebral ischemia (Hyman et al., 2009). Extracellular adenosine is generated by ATP via metabolism of the CD39/CD73 extracellular nucleotidase axis and subsequently could regulate BBB permeability via adenosine receptor signaling expressed on BBB cells (Bynoe et al., 2015).

In BBB, CD73 expression is at a low level but is sensitive to cAMP through its promoter (Narravula et al., 2000). The released adenosine activates cell surface adenosine $A_{2B}$ receptors, leading to reorganization of endothelial junctions and promoting barrier

**TABLE 3 BBB-permeable $A_{2A}$-related compounds under clinical trials in neurodegenerative diseases.**

| Compound | Company or sponsor (country) | Disease | Dose | Clinicaltrials.Gov number (phase) |
|---|---|---|---|---|
| Caffeine | University Hospital, Lille (France) | AD | 200 mg | NCT04570085 (3) |
| | | | BID | |
| Istradefylline | Kyowa Hakko Bio (Japan) | PD | 20 or 40 mg | NCT00250393 (2) |
| | | | BID | NCT00955526 (3) |
| | | | | NCT01968031 (3) |
| Tozadenant | Hoffmann-La Roche (The Switzerland); Biotie Therapies (Finland) | PD | 120 or 180 mg BID | NCT01283594(2) |
| | | | | NCT03051607 (3) |
| Vipadenant | Vernalis (United Kingdom); Biogen Idec, RedoxTherapies (Juno Therapeutics) (US) | PD | 30 or 100 mg | NCT00438607(2) |
| | | | QD | NCT00442780 (2) |

function (Narravula et al., 2000). In addition, interferon (IFN)-β treatment increased CD73 expression in human blood-brain barrier endothelial cells (BBB-EC) and human astrocytes, and upregulation of CD73 and increased adenosine production may contribute to the beneficial effects of IFN-β on multiple sclerosis(MS) by enhancing endothelial barrier function (Niemela et al., 2008). Grunewald et al. also demonstrated that *in vitro*, CD73 increased adenosine production and maintained cell shape and actin cytoskeleton stability, thereby reducing endothelial barrier permeability (Grunewald and Ridley, 2010).

## 6 BBB-permeable $A_{2A}$-related compounds under clinical trials in neurodegenerative diseases

BBB-permeable purine-related compounds are primarily associated with $A_{2A}$ receptors in clinical trials of neurodegenerative diseases. Caffeine is the most commonly consumed $A_{2A}$ receptor antagonist that penetrates the blood-brain barrier. Caffeine enhances cognitive performance by decreasing hippocampus tau hyperphosphorylation, attenuating neuroinflammation, and reversing memory loss (Laurent et al., 2014; Carvalho et al., 2019; Jacobson et al., 2022), offering evidence for targeting $A_{2A}$ receptors in the therapy of AD. The effect of caffeine on cognitive function in AD is being investigated in the Phase 3 clinical trial NCT04570085. Istradefylline is a potent selective $A_{2A}$ antagonist that crosses the blood-brain barrier and has a high affinity for human $A_{2A}$ receptors, improving dyskinesia in PD patients (Muller, 2015; Torti et al., 2018). Indeed, it has been used as a combination therapy with Levodopa (L-DOPA) in PD treatment. It was approved early in Japan and Korea and passed various clinical safety and efficacy tests in the United States in August 2019. In addition, Tozadenant (SYN115) was originally developed for the treatment of PD and has been studied as a monotherapy for PD and as a combination therapy with L-DOPA or dopamine agonists (Pourcher and Huot, 2015; Shang et al., 2021). In the initial clinical studies for the therapeutic efficacy of the decreased closure time, no major adverse effects were observed; however, seven cases of sepsis and six deaths occurred in 890 patients in phase 3 clinical trial (Lewitt et al., 2020). As a result, clinical development of this drug was terminated in 2018. Noteblely, Tozadenant analogues, including $^{18}$F-labeled radiotracers for prospective positron emission tomography (PET) imaging, have recently been identified as $A_{2A}$ antagonists (Renk et al., 2021). Besides, vipadenant also belongs to a group of potent $A_{2A}$ antagonists, which was used for the treatment of PD (Pourcher and Huot, 2015), but its development was stopped due to safety concerns and later switched to cancer immunotherapy (Yu et al., 2020). Table 3 summarized the BBB-permeable $A_{2A}$-related compounds under clinical trials in neurodegenerative diseases, and some of these clinical trials have been completed while others are still ongoing.

## 7 Prospects for improving drug delivery within the CNS

The BBB strictly regulates the movement of ions, molecules and cells between the blood and brain cells and is essential for neurological function and protection. Despite the BBB's protective function, it restricts the availability of therapeutic compounds to the brain, making it more difficult to treat illnesses of the central nervous system (Profaci et al., 2020). The emergence of drug modification modalities based on receptor-mediated transcytosis, neurotropic virus-mediated transport, nanoparticles and exosomes all provide solutions for crossing the BBB, and drugs supported by these technologies are currently being evaluated in multiple clinical trials (Zhou et al., 2018; Liu et al., 2021; Terstappen et al., 2021). Our literature review demonstrates that antagonists of P2X7 and $A_{2A}$ receptors have beneficial therapeutic effects on brain damage, central inflammation, neurodegeneration etc., and attenuate the concurrent deterioration of the BBB barrier function. Up to now, a number of P2X7R antagonists that can cross the BBB have been developed (Bhattacharya, 2018; Wei et al., 2018). The compounds JNJ-47965567 and JNJ-42253432 demonstrated significant activity against P2X7R in rodents and humans, as well as effective BBB penetration. Likewise, novel blood-brain barrier permeable derivatives have been designed and synthesized as potential P2X7 antagonists known as compound 6 (2-(6-chloro-9h-purin-9-YL)-1-(2,4-dichlorophenyl) ethan 1-one), named ITH15004 (Calzaferri et al., 2021). It is a most potent, selective and highly BBB permeable antagonist and is considered to be the first non-nucleotide purine proposition for future drug optimization (Calzaferri et al., 2021). In addition, overexpression

of $A_{2A}$ receptor leads to progressive neurodegeneration, and $A_{2A}$ antagonists have broad prospects for the treatment of CNS diseases. In the latest literature review, Merighi et al. used standard commercial software to calculate multi-parameter optimization (MPO) scores of CNS drugs for $A_{2A}$ antagonists in clinical trials to predict the likelihood of the compound crossing the blood-brain barrier with appropriate metabolic stability (Merighi et al., 2022). Meanwhile, their analysis suggested that alkylxanthines caffeine and DMPX have good ability to cross the blood-brain barrier and are expected to be potential drugs for the treatment of CNS diseases (Merighi et al., 2022).

In addition, researchers concentrated on developing strategies to control the BBB in order to facilitate access to the CNS (Rajadhyaksha et al., 2011). Determining how to accomplish this in a safe and effective manner has a profound impact on the treatment of a variety of neurological conditions. Current interventions include the use of drugs such as mannitol or bradykinin analog (Cereport/RMP7) to induce disruption of barrier function. Hypertonic mannitol, reduces tight junction integrity through endothelial cell contraction (Dabrowski et al., 2021), but its limitation is that it may cause seizures (Marchi et al., 2007). Cereport/RMP-7 has shown some potential to transiently increase BBB permeability (Borlongan and Emerich, 2003) and has shown some efficacy in animal models for the treatment of CNS pathology, but has not yielded satisfactory results in clinical trials (Prados et al., 2003).

Agonists of some receptors are able to open the BBB to allow large molecules or cells to enter. The observation of transiently increased BBB permeability upon $A_{2A}$ receptor activation suggests that exploiting this pharmacological effect holds the promise of facilitating drug delivery within the CNS (Carman et al., 2011; Kim and Bynoe, 2015). By labeling several copies of $A_{2A}$ receptor-activating ligands on dendrimers, a sequence of nanoagonists (NAs) was produced. NAs tagged with varying amounts of AR-activating ligands can adjust the BBB opening time-window within a range of 0.5–2.0 h (Gao et al., 2014). The FDA-approved $A_{2A}$ receptor agonist Lexiscan or the broad-spectrum agonist NECA increases BBB permeability and allows delivery of macromolecules to the CNS (Carman et al., 2011). Notably, there was a correlation between the duration of induced permeability and the half-life of the agonist. The half-life of BBB permeation induced by NECA intervention was 4 h. Its duration is substantially longer than that of Lexican, which induces BBB permeation with a half-life of 2.5 min (Carman et al., 2011). These findings suggest that the use of this agonist to briefly open the BBB may facilitate the delivery of therapeutic antibodies to the central nervous system. Since NECA is a broad-spectrum adenosine receptor agonist, additional research is necessary to better comprehend the mechanisms by which $A_1/A_{2A}/A_{2B}$ receptors specifically mediate signaling involved in BBB permeability regulation and to optimize the parameters for drug design.

## 8 Conclusion

Extracellular nucleotides acting on purinergic receptors of BBB cells modulate the permeability of the blood-brain barrier, with different types of receptors and concentrations of nucleotides affecting the specific modulatory effects. Inhibition or knockdown of P2X4, P2X7, $P2Y_1$, or $P2Y_4$ receptors protect BBB barrier integrity, limiting the entry of toxic substances, inflammatory immune cells, etc. into the brain and conversely, inhibition of $P2Y_{12}$ receptor further exacerbates BBB permeability. The P2X7 receptor is highly investigated in the regulation of BBB integrity, although the distribution of other P2 receptors in the NVU and the pharmacological effects of inhibitors of these receptors are comparatively less explored. Additionally, specific subtypes of P1 receptors also variably influence BBB permeability, with $A_1$ and $A_{2A}$ receptor activation boosting BBB permeability and $A_{2B}$ and $A_3$ receptor agonists protecting BBB integrity. Although a small number of studies have demonstrated a protective effect of $A_{2A}$ agonists on BBB integrity, it cannot be overlooked that $A_1$ and $A_{2A}$ agonists transiently open the BBB to facilitate the passage of large or small molecules and that this process is reversible, with the BBB closing as the drug's half-life passes, offering great promise for drug delivery to the CNS. Therefore, purinergic signaling, as the gatekeeper of the BBB, has a switching regulatory function on the BBB, and the intervention of appropriate agonist/antagonist of purinergic receptors is beneficial to restore CNS homeostasis under pathological conditions. Furthermore, purinergic receptors are widely distributed in NVU, and their regulation of the blood-brain barrier is intricate. However, studies on the regulatory effects of purinergic receptors on the BBB have primarily focused on endothelial cells, and the targeting of these receptors on other BBB cells such as pericytes is not well understood. For validation purposes, more *in vitro* BBB models and *in vivo* research targeting purinergic receptors on cells other than endothelial cells are required.

## Author contributions

YW retrieved the literature and drafted the manuscript. YZ drafted part of the manuscript. JW, LD, SHL, SIL, made the figures; QW proposed and revised the manuscript. All the authors reviewed the manuscript. Each of the authors agrees to be accountable for the content of the work.

## Funding

This research was funded by the National Natural Science Foundation of China (No. 82174512), the National Key R&D Program of China (No. 2022YFC3500703), the Innovation Team and Talents Cultivation Program of National Administration of Traditional Chinese Medicine (No. ZYYCXTD-D-202003) and the Fund of Science and Technology Department of Sichuan Province, China (No. 2021ZYD0081, 2022ZDZX0033).

## Conflict of interest

The authors declare that the research was conducted in the absence of any commercial or financial relationships that could be construed as a potential conflict of interest.

## Publisher's note

# References


Abbracchio, M. P., and Burnstock, G. (1994). Purinoceptors: Are there families of P2X and P2Y purinoceptors? *Pharmacol. Ther.* 64 (3), 445–475. doi:10.1016/0163-7258(94)00048-4

Albert, J. L., Boyle, J. P., Roberts, J. A., Challiss, R. A., Gubby, S. E., and Boarder, M. R. (1997). Regulation of brain capillary endothelial cells by P2Y receptors coupled to Ca2+, phospholipase C and mitogen-activated protein kinase. *Br. J. Pharmacol.* 122 (5), 935–941. doi:10.1038/sj.bjp.0701453

Almeida, R. F., Comasseto, D. D., Ramos, D. B., Hansel, G., Zimmer, E. R., Loureiro, S. O., et al. (2017). Guanosine anxiolytic-like effect involves adenosinergic and glutamatergic neurotransmitter systems. *Mol. Neurobiol.* 54 (1), 423–436. doi:10.1007/s12035-015-9660-x

Amado-Azevedo, J., Valent, E. T., and Van Nieuw, A. G. (2014). Regulation of the endothelial barrier function: A filum granum of cellular forces, rho-GTPase signaling and microenvironment. *Cell Tissue Res.* 355 (3), 557–576. doi:10.1007/s00441-014-1828-6

Andrejew, R., Glaser, T., Oliveira-Giacomelli, A., Ribeiro, D., Godoy, M., Granato, A., et al. (2019). Targeting purinergic signaling and cell therapy in cardiovascular and neurodegenerative diseases. *Adv. Exp. Med. Biol.* 1201, 275–353. doi:10.1007/978-3-030-31206-0_14

Antonio, L. S., Stewart, A. P., Varanda, W. A., and Edwardson, J. M. (2014). Identification of P2X2/P2X4/P2X6 heterotrimeric receptors using atomic force microscopy (AFM) imaging. *FEBS Lett.* 588 (12), 2125–2128. doi:10.1016/j.febslet.2014.04.048

Bang, S., Lee, S. R., Ko, J., Son, K., Tahk, D., Ahn, J., et al. (2017). A low permeability microfluidic blood-brain barrier platform with direct contact between perfusable vascular network and astrocytes. *Sci. Rep.* 7 (1), 8083. doi:10.1038/s41598-017-07416-0

Banks, W. A., and Rhea, E. M. (2021). The blood-brain barrier, oxidative stress, and insulin resistance. *Antioxidants (Basel)* 10 (11), 1695. doi:10.3390/antiox10111695

Banks, W. A. (2019). The blood-brain barrier as an endocrine tissue. *Nat. Rev. Endocrinol.* 15 (8), 444–455. doi:10.1038/s41574-019-0213-7

Beckel, J. M., Argall, A. J., Lim, J. C., Xia, J., Lu, W., Coffey, E. E., et al. (2014). Mechanosensitive release of adenosine 5'-triphosphate through pannexin channels and mechanosensitive upregulation of pannexin channels in optic nerve head astrocytes: A mechanism for purinergic involvement in chronic strain. *Glia* 62 (9), 1486–1501. doi:10.1002/glia.22695

Beckers, C. M., van Hinsbergh, V. W., and van Nieuw, A. G. (2010). Driving Rho GTPase activity in endothelial cells regulates barrier integrity. *Thromb. Haemost.* 103 (1), 40–55. doi:10.1160/TH09-06-0403

Bernier, L. P., Ase, A. R., and Seguela, P. (2018). P2X receptor channels in chronic pain pathways. *Br. J. Pharmacol.* 175 (12), 2219–2230. doi:10.1111/bph.13957

Bhattacharya, A. (2018). Recent advances in CNS P2X7 physiology and pharmacology: Focus on neuropsychiatric disorders. *Front. Pharmacol.* 9, 30. doi:10.3389/fphar.2018.00030

Bjorklund, O., Shang, M., Tonazzini, I., Dare, E., and Fredholm, B. B. (2008). Adenosine A1 and A3 receptors protect astrocytes from hypoxic damage. *Eur. J. Pharmacol.* 596 (1-3), 6–13. doi:10.1016/j.ejphar.2008.08.002

Borlongan, C. V., and Emerich, D. F. (2003). Facilitation of drug entry into the CNS via transient permeation of blood brain barrier: Laboratory and preliminary clinical evidence from bradykinin receptor agonist, cereport. *Cereport. Brain Res. Bull.* 60 (3), 297–306. doi:10.1016/s0361-9230(03)00043-1

Bowden, A., Patel, V., Brown, C., and Boarder, M. R. (1995). Evidence for requirement of tyrosine phosphorylation in endothelial P2Y- and P2U- purinoceptor stimulation of prostacyclin release. *Br. J. Pharmacol.* 116 (6), 2563–2568. doi:10.1111/j.1476-5381.1995.tb17208.x

Bozdemir, E., Vigil, F. A., Chun, S. H., Espinoza, L., Bugay, V., Khoury, S. M., et al. (2021). Neuroprotective roles of the adenosine A(3) receptor agonist AST-004 in mouse model of traumatic brain injury. *Neurotherapeutics* 18 (4), 2707–2721. doi:10.1007/s13311-021-01113-7

Burnstock, G., and Boeynaems, J. M. (2014). Purinergic signalling and immune cells. *Purinergic Signal* 10 (4), 529–564. doi:10.1007/s11302-014-9427-2

Burnstock, G. (2020). Introduction to purinergic signalling in the brain. *Adv. Exp. Med. Biol.* 1202, 1–12. doi:10.1007/978-3-030-30651-9_1

Burnstock, G., and Knight, G. E. (2017). Cell culture: Complications due to mechanical release of ATP and activation of purinoceptors. *Cell Tissue Res.* 370 (1), 1–11. doi:10.1007/s00441-017-2618-8

Burnstock, G. (2007). Physiology and pathophysiology of purinergic neurotransmission. *Physiol. Rev.* 87 (2), 659–797. doi:10.1152/physrev.00043.2006

Burnstock, G. (1972). Purinergic nerves. *Pharmacol. Rev.* 24 (3), 509–581.

Burnstock, G. (2017). Purinergic signalling and neurological diseases: An update. *CNS Neurol. Disord. Drug Targets* 16 (3), 257–265. doi:10.2174/1871527315666160922104848

Bynoe, M. S., Viret, C., Yan, A., and Kim, D. G. (2015). Adenosine receptor signaling: A key to opening the blood-brain door. *Fluids Barriers CNS* 12, 20. doi:10.1186/s12987-015-0017-7

Cai, Z., Qiao, P. F., Wan, C. Q., Cai, M., Zhou, N. K., and Li, Q. (2018). Role of blood-brain barrier in Alzheimer's disease. *J. Alzheimers Dis.* 63 (4), 1223–1234. doi:10.3233/JAD-180098

Calzaferri, F., Narros-Fernandez, P., de Pascual, R., de Diego, A., Nicke, A., Egea, J., et al. (2021). Synthesis and pharmacological evaluation of novel non-nucleotide purine derivatives as P2X7 antagonists for the treatment of neuroinflammation. *J. Med. Chem.* 64 (4), 2272–2290. doi:10.1021/acs.jmedchem.0c02145

Capaldo, C. T., and Nusrat, A. (2009). Cytokine regulation of tight junctions. *Biochim. Biophys. Acta* 1788 (4), 864–871. doi:10.1016/j.bbamem.2008.08.027

Caporarello, N., Olivieri, M., Cristaldi, M., Scalia, M., Toscano, M. A., Genovese, C., et al. (2018). Blood-brain barrier in a Haemophilus influenzae type a *in vitro* infection: Role of adenosine receptors A2A and A2B. *Mol. Neurobiol.* 55 (6), 5321–5336. doi:10.1007/s12035-017-0769-y

Carman, A. J., Mills, J. H., Krenz, A., Kim, D. G., and Bynoe, M. S. (2011). Adenosine receptor signaling modulates permeability of the blood-brain barrier. *J. Neurosci.* 31 (37), 13272–13280. doi:10.1523/JNEUROSCI.3337-11.2011

Carmo, M. R., Menezes, A. P., Nunes, A. C., Pliassova, A., Rolo, A. P., Palmeira, C. M., et al. (2014). The P2X7 receptor antagonist Brilliant Blue G attenuates contralateral rotations in a rat model of Parkinsonism through a combined control of synaptotoxicity, neurotoxicity and gliosis. *Neuropharmacology* 81, 142–152. doi:10.1016/j.neuropharm.2014.01.045

Carvalho, K., Faivre, E., Pietrowski, M. J., Marques, X., Gomez-Murcia, V., Deleau, A., et al. (2019). Exacerbation of C1q dysregulation, synaptic loss and memory deficits in tau pathology linked to neuronal adenosine A2A receptor. *Brain* 142 (11), 3636–3654. doi:10.1093/brain/awz288

Chen, J. F., Eltzschig, H. K., and Fredholm, B. B. (2013). Adenosine receptors as drug targets--what are the challenges? *Nat. Rev. Drug Discov.* 12 (4), 265–286. doi:10.1038/nrd3955

Chen, L., Li, L., Zhou, C., Chen, X., and Cao, Y. (2020). Adenosine A2A receptor activation reduces brain metastasis via SDF-1/CXCR4 axis and protecting blood-brain barrier. *Mol. Carcinog.* 59 (4), 390–398. doi:10.1002/mc.23161

Chen, X., Gawryluk, J. W., Wagener, J. F., Ghribi, O., and Geiger, J. D. (2008a). Caffeine blocks disruption of blood brain barrier in a rabbit model of Alzheimer's disease. *J. Neuroinflammation* 5, 12. doi:10.1186/1742-2094-5-12

Chen, X., Lan, X., Roche, I., Liu, R., and Geiger, J. D. (2008b). Caffeine protects against MPTP-induced blood-brain barrier dysfunction in mouse striatum. *J. Neurochem.* 107 (4), 1147–1157. doi:10.1111/j.1471-4159.2008.05697.x

Cheslow, L., and Alvarez, J. I. (2016). Glial-endothelial crosstalk regulates blood-brain barrier function. *Curr. Opin. Pharmacol.* 26, 39–46. doi:10.1016/j.coph.2015.09.010

Chi, O. Z., Liu, X., and Weiss, H. R. (1999). Effects of cyclic GMP on microvascular permeability of the cerebral cortex. *Microvasc. Res.* 58 (1), 35–40. doi:10.1006/mvre.1999.2152

Chiu, G. S., and Freund, G. G. (2014). Modulation of neuroimmunity by adenosine and its receptors: Metabolism to mental illness. *Metabolism* 63 (12), 1491–1498. doi:10.1016/j.metabol.2014.09.003

Choi, H. J., Kim, N. E., Kim, J., An, S., Yang, S. H., Ha, J., et al. (2018). Dabigatran reduces endothelial permeability through inhibition of thrombin-induced cytoskeleton reorganization. *Thromb. Res.* 167, 165–171. doi:10.1016/j.thromres.2018.04.019

Ciccarelli, R., Ballerini, P., Sabatino, G., Rathbone, M. P., D'Onofrio, M., Caciagli, F., et al. (2001). Involvement of astrocytes in purine-mediated reparative processes in the brain. *Int. J. Dev. Neurosci.* 19 (4), 395–414. doi:10.1016/s0736-5748(00)00084-8

Colgan, S. P., Eltzschig, H. K., Eckle, T., and Thompson, L. F. (2006). Physiological roles for ecto-5'-nucleotidase (CD73). *Purinergic Signal* 2 (2), 351–360. doi:10.1007/s11302-005-5302-5

Communi, D., Janssens, R., Suarez-Huerta, N., Robaye, B., and Boeynaems, J. M. (2000). Advances in signalling by extracellular nucleotides. the role and transduction mechanisms of P2Y receptors. *Cell. Signal.* 12 (6), 351–360. doi:10.1016/s0898-6568(00)00083-8

D'Alimonte, I., Ballerini, P., Nargi, E., Buccella, S., Giuliani, P., Di Iorio, P., et al. (2007). Staurosporine-induced apoptosis in astrocytes is prevented by A1 adenosine receptor activation. *Neurosci. Lett.* 418 (1), 66–71. doi:10.1016/j.neulet.2007.02.061

Dabrowski, W., Siwicka-Gieroba, D., Robba, C., Bielacz, M., Solek-Pastuszka, J., Kotfis, K., et al. (2021). Potentially detrimental effects of hyperosmolality in patients treated for traumatic brain injury. *J. Clin. Med.* 10 (18), 4141. doi:10.3390/jcm10184141

Dare, E., Schulte, G., Karovic, O., Hammarberg, C., and Fredholm, B. B. (2007). Modulation of glial cell functions by adenosine receptors. *Physiol. Behav.* 92 (1-2), 15–20. doi:10.1016/j.physbeh.2007.05.031

Dean, M., Moitra, K., and Allikmets, R. (2022). The human ATP-binding cassette (ABC) transporter superfamily. *Hum. Mutat.* 43 (9), 1162–1182. doi:10.1002/humu.24418

Dinet, V., Petry, K. G., and Badaut, J. (2019). Brain-immune interactions and neuroinflammation after traumatic brain injury. *Front. Neurosci.* 13, 1178. doi:10.3389/fnins.2019.01178

Dohgu, S., Takata, F., Matsumoto, J., Kimura, I., Yamauchi, A., and Kataoka, Y. (2019). Monomeric alpha-synuclein induces blood-brain barrier dysfunction through activated brain pericytes releasing inflammatory mediators *in vitro*. *Microvasc. Res.* 124, 61–66. doi:10.1016/j.mvr.2019.03.005

Domercq, M., Vazquez-Villoldo, N., and Matute, C. (2013). Neurotransmitter signaling in the pathophysiology of microglia. *Front. Cell. Neurosci.* 7, 49. doi:10.3389/fncel.2013.00049

Dos-Santos-Pereira, M., Acuna, L., Hamadat, S., Rocca, J., Gonzalez-Lizarraga, F., Chehin, R., et al. (2018). Microglial glutamate release evoked by alpha-synuclein aggregates is prevented by dopamine. *Glia* 66 (11), 2353–2365. doi:10.1002/glia.23472

Dudzinska, D., Luzak, B., Boncler, M., Rywaniak, J., Sosnowska, D., Podsedek, A., et al. (2014). CD39/NTPDase-1 expression and activity in human umbilical vein endothelial cells are differentially regulated by leaf extracts from Rubus caesius and Rubus idaeus. *Cell. Mol. Biol. Lett.* 19 (3), 361–380. doi:10.2478/s11658-014-0202-8

Ferrari, D., Pizzirani, C., Adinolfi, E., Lemoli, R. M., Curti, A., Idzko, M., et al. (2006). The P2X7 receptor: A key player in IL-1 processing and release. *J. Immunol.* 176 (7), 3877–3883. doi:10.4049/jimmunol.176.7.3877

Franke, H., Verkhratsky, A., Burnstock, G., and Illes, P. (2012). Pathophysiology of astroglial purinergic signalling. *Purinergic Signal* 8 (3), 629–657. doi:10.1007/s11302-012-9300-0

Fuentes, E., and Palomo, I. (2015). Extracellular ATP metabolism on vascular endothelial cells: A pathway with pro-thrombotic and anti-thrombotic molecules. *Vasc. Pharmacol.* 75, 1–6. doi:10.1016/j.vph.2015.05.002

Gao, X., Qian, J., Zheng, S., Changyi, Y., Zhang, J., Ju, S., et al. (2014). Overcoming the blood-brain barrier for delivering drugs into the brain by using adenosine receptor nanoagonist. *ACS Nano* 8 (4), 3678–3689. doi:10.1021/nn5003375

Garcia-Ponce, A., Citalan-Madrid, A. F., Velazquez-Avila, M., Vargas-Robles, H., and Schnoor, M. (2015). The role of actin-binding proteins in the control of endothelial barrier integrity. *Thromb. Haemost.* 113 (1), 20–36. doi:10.1160/TH14-04-0298

Glass, R., Loesch, A., Bodin, P., and Burnstock, G. (2002). P2X4 and P2X6 receptors associate with VE-cadherin in human endothelial cells. *Cell. Mol. Life Sci.* 59 (5), 870–881. doi:10.1007/s00018-002-8474-y

Grunewald, J. K., and Ridley, A. J. (2010). CD73 represses pro-inflammatory responses in human endothelial cells. . 7 (1), 10. doi:10.1186/1476-9255-7-10

Grygorowicz, T., Dabrowska-Bouta, B., and Struzynska, L. (2018). Administration of an antagonist of P2X7 receptor to EAE rats prevents a decrease of expression of claudin-5 in cerebral capillaries. *Purinergic Signal* 14 (4), 385–393. doi:10.1007/s11302-018-9620-9

Gu, B. J., and Wiley, J. S. (2018). P2X7 as a scavenger receptor for innate phagocytosis in the brain. *Br. J. Pharmacol.* 175 (22), 4195–4208. doi:10.1111/bph.14470

Gu, B. J., and Wiley, J. S. (2006). Rapid ATP-induced release of matrix metalloproteinase 9 is mediated by the P2X7 receptor. *Blood* 107 (12), 4946–4953. doi:10.1182/blood-2005-07-2994

Gu, N., Eyo, U. B., Murugan, M., Peng, J., Matta, S., Dong, H., et al. (2016). Microglial P2Y12 receptors regulate microglial activation and surveillance during neuropathic pain. *Brain Behav. Immun.* 55, 82–92. doi:10.1016/j.bbi.2015.11.007

Gunduz, D., Kasseckert, S. A., Hartel, F. V., Aslam, M., Abdallah, Y., Schafer, M., et al. (2006). Accumulation of extracellular ATP protects against acute reperfusion injury in rat heart endothelial cells. *Cardiovasc. Res.* 71 (4), 764–773. doi:10.1016/j.cardiores.2006.06.011

Guo, C., Wang, H., Liang, W., Xu, W., Li, Y., Song, L., et al. (2020). Bilobalide reversibly modulates blood-brain barrier permeability through promoting adenosine A1 receptor-mediated phosphorylation of actin-binding proteins. *Biochem. Biophys. Res. Commun.* 526 (4), 1077–1084. doi:10.1016/j.bbrc.2020.03.186

Guo, X., Li, Q., Pi, S., Xia, Y., and Mao, L. (2021). G protein-coupled purinergic P2Y receptor oligomerization: Pharmacological changes and dynamic regulation. *Biochem. Pharmacol.* 192, 114689. doi:10.1016/j.bcp.2021.114689

Hagberg, H., Andersson, P., Lacarewicz, J., Jacobson, I., Butcher, S., and Sandberg, M. (1987). Extracellular adenosine, inosine, hypoxanthine, and xanthine in relation to tissue nucleotides and purines in rat striatum during transient ischemia. *J. Neurochem.* 49 (1), 227–231. doi:10.1111/j.1471-4159.1987.tb03419.x

Hansel, G., Tonon, A. C., Guella, F. L., Pettenuzzo, L. F., Duarte, T., Duarte, M., et al. (2015). Guanosine protects against cortical focal ischemia. Involvement of inflammatory response. *Mol. Neurobiol.* 52 (3), 1791–1803. doi:10.1007/s12035-014-8978-0

Harkness, K. A., Adamson, P., Sussman, J. D., Davies-Jones, G. A., Greenwood, J., and Woodroofe, M. N. (2000). Dexamethasone regulation of matrix metalloproteinase expression in CNS vascular endothelium. *Brain* 123, 698–709. doi:10.1093/brain/123.4.698

Hartel, F. V., Rodewald, C. W., Aslam, M., Gunduz, D., Hafer, L., Neumann, J., et al. (2007). Extracellular ATP induces assembly and activation of the myosin light chain phosphatase complex in endothelial cells. *Cardiovasc. Res.* 74 (3), 487–496. doi:10.1016/j.cardiores.2007.02.013

Hasko, G., Pacher, P., Vizi, E. S., and Illes, P. (2005). Adenosine receptor signaling in the brain immune system. *Trends Pharmacol. Sci.* 26 (10), 511–516. doi:10.1016/j.tips.2005.08.004

Heithoff, B. P., George, K. K., Phares, A. N., Zuidhoek, I. A., Munoz-Ballester, C., and Robel, S. (2021). Astrocytes are necessary for blood-brain barrier maintenance in the adult mouse brain. *Glia* 69 (2), 436–472. doi:10.1002/glia.23908

Heldt, N. A., Seliga, A., Winfield, M., Gajghate, S., Reichenbach, N., Yu, X., et al. (2020). Electronic cigarette exposure disrupts blood-brain barrier integrity and promotes neuroinflammation. *Brain Behav. Immun.* 88, 363–380. doi:10.1016/j.bbi.2020.03.034

Henriquez, M., Herrera-Molina, R., Valdivia, A., Alvarez, A., Kong, M., Munoz, N., et al. (2011). ATP release due to Thy-1-integrin binding induces P2X7-mediated calcium entry required for focal adhesion formation. *J. Cell Sci.* 124, 1581–1588. doi:10.1242/jcs.073171

Horlyck, S., Cai, C., Helms, H., Lauritzen, M., and Brodin, B. (2021). ATP induces contraction of cultured brain capillary pericytes via activation of P2Y-type purinergic receptors. *Am. J. Physiol. Heart Circ. Physiol.* 320 (2), H699–H712. doi:10.1152/ajpheart.00560.2020

Hurtado-Alvarado, G., Becerril-Villanueva, E., Contis-Montes, D. O. A., Dominguez-Salazar, E., Salinas-Jazmin, N., Perez-Tapia, S. M., et al. (2018). The yin/yang of inflammatory status: Blood-brain barrier regulation during sleep. *Brain Behav. Immun.* 69, 154–166. doi:10.1016/j.bbi.2017.11.009

Hurtado-Alvarado, G., Dominguez-Salazar, E., Velazquez-Moctezuma, J., and Gomez-Gonzalez, B. (2016). A2A adenosine receptor antagonism reverts the blood-brain barrier dysfunction induced by sleep restriction. *PLoS One* 11 (11), e0167236. doi:10.1371/journal.pone.0167236

Hyman, M. C., Petrovic-Djergovic, D., Visovatti, S. H., Liao, H., Yanamadala, S., Bouis, D., et al. (2009). Self-regulation of inflammatory cell trafficking in mice by the leukocyte surface apyrase CD39. *J. Clin. Invest.* 119 (5), 1136–1149. doi:10.1172/JCI36433

Illes, P., Muller, C. E., Jacobson, K. A., Grutter, T., Nicke, A., Fountain, S. J., et al. (2021). Update of P2X receptor properties and their pharmacology: IUPHAR review 30. *Br. J. Pharmacol.* 178 (3), 489–514. doi:10.1111/bph.15299

Illes, P. (2020). P2X7 receptors amplify CNS damage in neurodegenerative diseases. *Int. J. Mol. Sci.* 21 (17), 5996. doi:10.3390/ijms21175996

Illes, P., Verkhratsky, A., Burnstock, G., and Franke, H. (2012). P2X receptors and their roles in astroglia in the central and peripheral nervous system. *Neuroscientist* 18 (5), 422–438. doi:10.1177/1073858411418524

Illes, P., Xu, G. Y., and Tang, Y. (2020). Purinergic signaling in the central nervous system in health and disease. *Neurosci. Bull.* 36 (11), 1239–1241. doi:10.1007/s12264-020-00602-7

Jacobson, K. A., Delicado, E. G., Gachet, C., Kennedy, C., von Kugelgen, I., Li, B., et al. (2020). Update of P2Y receptor pharmacology: IUPHAR review 27. *Br. J. Pharmacol.* 177 (11), 2413–2433. doi:10.1111/bph.15005

Jacobson, K. A., Gao, Z. G., Matricon, P., Eddy, M. T., and Carlsson, J. (2022). Adenosine A(2A) receptor antagonists: From caffeine to selective non-xanthines. *Br. J. Pharmacol.* 179 (14), 3496–3511. doi:10.1111/bph.15103

Janigro, D., West, G. A., Nguyen, T. S., and Winn, H. R. (1994). Regulation of blood-brain barrier endothelial cells by nitric oxide. *Circ. Res.* 75 (3), 528–538. doi:10.1161/01.res.75.3.528

Janssens, R., Struyf, S., and Proost, P. (2018). The unique structural and functional features of CXCL12. *Cell. Mol. Immunol.* 15 (4), 299–311. doi:10.1038/cmi.2017.107

Jiang, T., Hoekstra, J., Heng, X., Kang, W., Ding, J., Liu, J., et al. (2015). P2X7 receptor is critical in alpha-synuclein--mediated microglial NADPH oxidase activation. *Neurobiol. Aging.* 36 (7), 2304–2318. doi:10.1016/j.neurobiolaging.2015.03.015

Kadry, H., Noorani, B., and Cucullo, L. (2020). A blood-brain barrier overview on structure, function, impairment, and biomarkers of integrity. *Fluids Barriers CNS* 17 (1), 69. doi:10.1186/s12987-020-00230-3

Kalaria, R. N., and Harik, S. I. (1988). Adenosine receptors and the nucleoside transporter in human brain vasculature. *J. Cereb. Blood Flow. Metab.* 8 (1), 32–39. doi:10.1038/jcbfm.1988.5

Kim, D. G., and Bynoe, M. S. (2015). A2A adenosine receptor regulates the human blood-brain barrier permeability. *Mol. Neurobiol.* 52 (1), 664–678. doi:10.1007/s12035-014-8879-2

Koszalka, P., Ozuyaman, B., Huo, Y., Zernecke, A., Flogel, U., Braun, N., et al. (2004). Targeted disruption of cd73/ecto-5'-nucleotidase alters thromboregulation and augments vascular inflammatory response. *Circ. Res.* 95 (8), 814–821. doi:10.1161/01.RES.0000144796.82787.6f

Kovacs, Z., Kekesi, K. A., Dobolyi, A., Lakatos, R., and Juhasz, G. (2015). Absence epileptic activity changing effects of non-adenosine nucleoside inosine, guanosine and uridine in Wistar Albino Glaxo Rijswijk rats. *Neuroscience* 300, 593–608. doi:10.1016/j.neuroscience.2015.05.054

Langen, U. H., Ayloo, S., and Gu, C. (2019). Development and cell biology of the blood-brain barrier. *Annu. Rev. Cell Dev. Biol.* 35, 591–613. doi:10.1146/annurev-cellbio-100617-062608

Lanznaster, D., Mack, J. M., Coelho, V., Ganzella, M., Almeida, R. F., Dal-Cim, T., et al. (2017). Guanosine prevents anhedonic-like behavior and impairment in hippocampal glutamate transport following amyloid-β1-40 administration in mice. *Mol. Neurobiol.* 54 (7), 5482–5496. doi:10.1007/s12035-016-0082-1

Laurent, C., Eddarkaoui, S., Derisbourg, M., Leboucher, A., Demeyer, D., Carrier, S., et al. (2014). Beneficial effects of caffeine in a transgenic model of Alzheimer's disease-like tau pathology. *Neurobiol. Aging.* 35 (9), 2079–2090. doi:10.1016/j.neurobiolaging.2014.03.027

Le Dare, B., Ferron, P. J., and Gicquel, T. (2021). The purinergic P2X7 receptor-NLRP3 inflammasome pathway: A new target in alcoholic liver disease? *Int. J. Mol. Sci.* 22 (4), 2139. doi:10.3390/ijms22042139

Le Dare, B., Victoni, T., Bodin, A., Vlach, M., Vene, E., Loyer, P., et al. (2019). Ethanol upregulates the P2X7 purinergic receptor in human macrophages. *Fundam. Clin. Pharmacol.* 33 (1), 63–74. doi:10.1111/fcp.12433

Lee, N. T., Ong, L. K., Gyawali, P., Nassir, C., Mustapha, M., Nandurkar, H. H., et al. (2021). Role of purinergic signalling in endothelial dysfunction and thrombo-

inflammation in ischaemic stroke and cerebral small vessel disease. *Biomolecules* 11 (7), 994. doi:10.3390/biom11070994

Lewitt, P. A., Aradi, S. D., Hauser, R. A., and Rascol, O. (2020). The challenge of developing adenosine A(2A) antagonists for Parkinson disease: Istradefylline, preladenant, and tozadenant. *Park. Relat. Disord.* 80, S54–S63. doi:10.1016/j.parkreldis.2020.10.027

Li, Q., Han, X., Lan, X., Hong, X., Li, Q., Gao, Y., et al. (2017). Inhibition of tPA-induced hemorrhagic transformation involves adenosine A2b receptor activation after cerebral ischemia. *Neurobiol. Dis.* 108, 173–182. doi:10.1016/j.nbd.2017.08.011

Liang, W., Xu, W., Zhu, J., Zhu, Y., Gu, Q., Li, Y., et al. (2020). Ginkgo biloba extract improves brain uptake of ginsenosides by increasing blood-brain barrier permeability via activating A1 adenosine receptor signaling pathway. *J. Ethnopharmacol.* 246, 112243. doi:10.1016/j.jep.2019.112243

Liebner, S., Dijkhuizen, R. M., Reiss, Y., Plate, K. H., Agalliu, D., and Constantin, G. (2018). Functional morphology of the blood-brain barrier in health and disease. *Acta Neuropathol.* 135 (3), 311–336. doi:10.1007/s00401-018-1815-1

Liu, D., Zhu, M., Zhang, Y., and Diao, Y. (2021). Crossing the blood-brain barrier with AAV vectors. *Metab. Brain Dis.* 36 (1), 45–52. doi:10.1007/s11011-020-00630-2

Liu, Y., Alahiri, M., Ulloa, B., Xie, B., and Sadiq, S. A. (2018). Adenosine A2A receptor agonist ameliorates EAE and correlates with Th1 cytokine-induced blood brain barrier dysfunction via suppression of MLCK signaling pathway. *Immun. Inflamm. Dis.* 6 (1), 72–80. doi:10.1002/iid3.187

Liu, Y., Zou, H., Zhao, P., Sun, B., Wang, J., Kong, Q., et al. (2016). Activation of the adenosine A2A receptor attenuates experimental autoimmune encephalomyelitis and is associated with increased intracellular calcium levels. *Neuroscience* 330, 150–161. doi:10.1016/j.neuroscience.2016.05.028

Loesch, A., and Burnstock, G. (2000). Ultrastructural localisation of ATP-gated P2X2 receptor immunoreactivity in vascular endothelial cells in rat brain. *Endothelium* 7 (2), 93–98. doi:10.3109/10623320009072204

Loesch, A. (2021). On P2X receptors in the brain: Microvessels. Dedicated to the memory of the late professor Geoffrey Burnstock (1929-2020). *Cell Tissue Res.* 384 (3), 577–588. doi:10.1007/s00441-021-03411-0

Lou, N., Takano, T., Pei, Y., Xavier, A. L., Goldman, S. A., and Nedergaard, M. (2016). Purinergic receptor P2RY12-dependent microglial closure of the injured blood-brain barrier. *Proc. Natl. Acad. Sci. U. S. A.* 113 (4), 1074–1079. doi:10.1073/pnas.1520398113

Lowery, F. J., and Yu, D. (2017). Brain metastasis: Unique challenges and open opportunities. *Biochim. Biophys. Acta Rev. Cancer* 1867 (1), 49–57. doi:10.1016/j.bbcan.2016.12.001

Mao, T. L., Fan, K. F., and Liu, C. L. (2017). Targeting the CXCR4/CXCL12 axis in treating epithelial ovarian cancer. *Gene Ther.* 24 (10), 621–629. doi:10.1038/gt.2017.69

Marchi, N., Angelov, L., Masaryk, T., Fazio, V., Granata, T., Hernandez, N., et al. (2007). Seizure-promoting effect of blood-brain barrier disruption. *Epilepsia* 48 (4), 732–742. doi:10.1111/j.1528-1167.2007.00988.x

Martin, E., Amar, M., Dalle, C., Youssef, I., Boucher, C., Le Duigou, C., et al. (2019). New role of P2X7 receptor in an Alzheimer's disease mouse model. *Mol. Psychiatr.* 24 (1), 108–125. doi:10.1038/s41380-018-0108-3

Massari, C. M., Zuccarini, M., Di Iorio, P., and Tasca, C. I. (2021). Guanosine mechanisms of action: Toward molecular targets. *Front. Pharmacol.* 12, 653146. doi:10.3389/fphar.2021.653146

Matos, M., Augusto, E., Santos-Rodrigues, A. D., Schwarzschild, M. A., Chen, J. F., Cunha, R. A., et al. (2012). Adenosine A2A receptors modulate glutamate uptake in cultured astrocytes and gliosomes. *Glia* 60 (5), 702–716. doi:10.1002/glia.22290

Medina-Flores, F., Hurtado-Alvarado, G., Contis-Montes, D. O. A., Lopez-Cervantes, S. P., Konigsberg, M., Deli, M. A., et al. (2020). Sleep loss disrupts pericyte-brain endothelial cell interactions impairing blood-brain barrier function. *Brain Behav. Immun.* 89, 118–132. doi:10.1016/j.bbi.2020.05.077

Mekala, N., Gheewala, N., Rom, S., Sriram, U., and Persidsky, Y. (2022). Blocking of P2X7r reduces mitochondrial stress induced by alcohol and electronic cigarette exposure in brain microvascular endothelial cells. *Antioxidants (Basel)* 11 (7), 1328. doi:10.3390/antiox11071328

Merighi, S., Borea, P. A., Varani, K., Vincenzi, F., Travagli, A., Nigro, M., et al. (2022). Pathophysiological role and medicinal chemistry of A2A adenosine receptor antagonists in Alzheimer's disease. *Molecules* 27 (9), 2680. doi:10.3390/molecules27092680

Mills, J. H., Alabanza, L., Weksler, B. B., Couraud, P. O., Romero, I. A., and Bynoe, M. S. (2011). Human brain endothelial cells are responsive to adenosine receptor activation. *Purinergic Signal* 7 (2), 265–273. doi:10.1007/s11302-011-9222-2

Mills, J. H., Thompson, L. F., Mueller, C., Waickman, A. T., Jalkanen, S., Niemela, J., et al. (2008). CD73 is required for efficient entry of lymphocytes into the central nervous system during experimental autoimmune encephalomyelitis. *Proc. Natl. Acad. Sci. U. S. A.* 105 (27), 9325–9330. doi:10.1073/pnas.0711175105

Miras-Portugal, M. T., Queipo, M. J., Gil-Redondo, J. C., Ortega, F., Gomez-Villafuertes, R., Gualix, J., et al. (2019). P2 receptor interaction and signalling cascades in neuroprotection. *Brain Res. Bull.* 151, 74–83. doi:10.1016/j.brainresbull.2018.12.012

Mohamed, R. A., Agha, A. M., and Nassar, N. N. (2012). SCH58261 the selective adenosine A(2A) receptor blocker modulates ischemia reperfusion injury following bilateral carotid occlusion: Role of inflammatory mediators. *Neurochem. Res.* 37 (3), 538–547. doi:10.1007/s11064-011-0640-x

Montilla, A., Mata, G. P., Matute, C., and Domercq, M. (2020). Contribution of P2X4 receptors to CNS function and pathophysiology. *Int. J. Mol. Sci.* 21 (15), 5562. doi:10.3390/ijms21155562

Mori, T., Wang, X., Aoki, T., and Lo, E. H. (2002). Downregulation of matrix metalloproteinase-9 and attenuation of edema via inhibition of ERK mitogen activated protein kinase in traumatic brain injury. *J. Neurotrauma* 19 (11), 1411–1419. doi:10.1089/089771502320914642

Muhleder, S., Fuchs, C., Basilio, J., Szwarc, D., Pill, K., Labuda, K., et al. (2020). Purinergic P2Y2 receptors modulate endothelial sprouting. *Cell. Mol. Life Sci.* 77 (5), 885–901. doi:10.1007/s00018-019-03213-2

Muller, G. C., Loureiro, S. O., Pettenuzzo, L. F., Almeida, R. F., Ynumaru, E. Y., Guazzelli, P. A., et al. (2021). Effects of intranasal guanosine administration on brain function in a rat model of ischemic stroke. *Purinergic Signal* 17 (2), 255–271. doi:10.1007/s11302-021-09766-x

Muller, T. (2015). The safety of istradefylline for the treatment of Parkinson's disease. *Expert Opin. Drug Saf.* 14 (5), 769–775. doi:10.1517/14740338.2015.1014798

Narravula, S., Lennon, P. F., Mueller, B. U., and Colgan, S. P. (2000). Regulation of endothelial CD73 by adenosine: Paracrine pathway for enhanced endothelial barrier function. *J. Immunol.* 165 (9), 5262–5268. doi:10.4049/jimmunol.165.9.5262

Newby, A. C. (1985). The role of adenosine kinase in regulating adenosine concentration. *Biochem. J.* 226 (1), 343–344. doi:10.1042/bj2260343

Newby, A. C., Worku, Y., and Holmquist, C. A. (1985). Adenosine formation Evidence for a direct biochemical link with energy metabolism. *Adv. Myocardiol.* 6, 273–284.

Niemela, J., Ifergan, I., Yegutkin, G. G., Jalkanen, S., Prat, A., and Airas, L. (2008). IFN-beta regulates CD73 and adenosine expression at the blood-brain barrier. *Eur. J. Immunol.* 38 (10), 2718–2726. doi:10.1002/eji.200838437

Niu, J., Tsai, H. H., Hoi, K. K., Huang, N., Yu, G., Kim, K., et al. (2019). Aberrant oligodendroglial-vascular interactions disrupt the blood-brain barrier, triggering CNS inflammation. *Nat. Neurosci.* 22 (5), 709–718. doi:10.1038/s41593-019-0369-4

Ohsawa, K., Irino, Y., Nakamura, Y., Akazawa, C., Inoue, K., and Kohsaka, S. (2007). Involvement of P2X4 and P2Y12 receptors in ATP-induced microglial chemotaxis. *Glia* 55 (6), 604–616. doi:10.1002/glia.20489

Oliveira-Giacomelli, A., Petiz, L. L., Andrejew, R., Turrini, N., Silva, J. B., Sack, U., et al. (2021). Role of P2X7 receptors in immune responses during neurodegeneration. *Front. Cell. Neurosci.* 15, 662935. doi:10.3389/fncel.2021.662935

Paniz, L. G., Calcagnotto, M. E., Pandolfo, P., Machado, D. G., Santos, G. F., Hansel, G., et al. (2014). Neuroprotective effects of guanosine administration on behavioral, brain activity, neurochemical and redox parameters in a rat model of chronic hepatic encephalopathy. *Metab. Brain Dis.* 29 (3), 645–654. doi:10.1007/s11011-014-9548-x

Patel, V., Brown, C., Goodwin, A., Wilkie, N., and Boarder, M. R. (1996). Phosphorylation and activation of p42 and p44 mitogen-activated protein kinase are required for the P2 purinoceptor stimulation of endothelial prostacyclin production. *Biochem. J.* 320, 221–226. doi:10.1042/bj3200221

Peakman, M. C., and Hill, S. J. (1994). Adenosine A2B-receptor-mediated cyclic AMP accumulation in primary rat astrocytes. *Br. J. Pharmacol.* 111 (1), 191–198. doi:10.1111/j.1476-5381.1994.tb14043.x

Perez-Hernandez, M., Fernandez-Valle, M. E., Rubio-Araiz, A., Vidal, R., Gutierrez-Lopez, M. D., O'Shea, E., et al. (2017). 3,4-Methylenedioxymethamphetamine (MDMA, ecstasy) produces edema due to BBB disruption induced by MMP-9 activation in rat hippocampus. *Neuropharmacology* 118, 157–166. doi:10.1016/j.neuropharm.2017.03.019

Perez-Sen, R., Queipo, M. J., Morente, V., Ortega, F., Delicado, E. G., and Miras-Portugal, M. T. (2015). Neuroprotection mediated by P2Y13 nucleotide receptors in neurons. *Comput. Struct. Biotechnol. J.* 13, 160–168. doi:10.1016/j.csbj.2015.02.002

Pienaar, I. S., Lee, C. H., Elson, J. L., Mcguinness, L., Gentleman, S. M., Kalaria, R. N., et al. (2015). Deep-brain stimulation associates with improved microvascular integrity in the subthalamic nucleus in Parkinson's disease. *Neurobiol. Dis.* 74, 392–405. doi:10.1016/j.nbd.2014.12.006

Pourcher, E., and Huot, P. (2015). Adenosine 2A receptor antagonists for the treatment of motor symptoms in Parkinson's disease. *Mov. Disord. Clin. Pract.* 2 (4), 331–340. doi:10.1002/mdc3.12187

Prados, M. D., Schold, S. J., Fine, H. A., Jaeckle, K., Hochberg, F., Mechtler, L., et al. (2003). A randomized, double-blind, placebo-controlled, phase 2 study of RMP-7 in combination with carboplatin administered intravenously for the treatment of recurrent malignant glioma. *Neuro Oncol.* 5 (2), 96–103. doi:10.1093/neuonc/5.2.96

Profaci, C. P., Munji, R. N., Pulido, R. S., and Daneman, R. (2020). The blood-brain barrier in health and disease: Important unanswered questions. *J. Exp. Med.* 217 (4), e20190062. doi:10.1084/jem.20190062

Raghavan, S., Brishti, M. A., Collier, D. M., and Leo, M. D. (2022). Hypoxia induces purinergic receptor signaling to disrupt endothelial barrier function. *Front. Physiology* 13, 1049698. doi:10.3389/fphys.2022.1049698

Rajadhyaksha, M., Boyden, T., Liras, J., El-Kattan, A., and Brodfuehrer, J. (2011). Current advances in delivery of biotherapeutics across the blood-brain barrier. *Curr. Drug Discov. Technol.* 8 (2), 87–101. doi:10.2174/157016311795563866

Ramirez, A. N., and Kunze, D. L. (2002). P2X purinergic receptor channel expression and function in bovine aortic endothelium. *Am. J. Physiol. Heart Circ. Physiol.* 282 (6), H2106–H2116. doi:10.1152/ajpheart.00892.2001

Ramos, C. J., and Antonetti, D. A. (2017). The role of small GTPases and EPAC-Rap signaling in the regulation of the blood-brain and blood-retinal barriers. *Tissue Barriers* 5 (3), e1339768. doi:10.1080/21688370.2017.1339768

Ransohoff, R. M., and Cardona, A. E. (2010). The myeloid cells of the central nervous system parenchyma. *Nature* 468 (7321), 253–262. doi:10.1038/nature09615

Rathbone, M., Pilutti, L., Caciagli, F., and Jiang, S. (2008). Neurotrophic effects of extracellular guanosine. *Nucleosides Nucleotides Nucleic Acids* 27 (6), 666–672. doi:10.1080/15257770802143913

Renk, D. R., Skraban, M., Bier, D., Schulze, A., Wabbals, E., Wedekind, F., et al. (2021). Design, synthesis and biological evaluation of Tozadenant analogues as adenosine A(2A) receptor ligands. *Eur. J. Med. Chem.* 214, 113214. doi:10.1016/j.ejmech.2021.113214

Rissanen, E., Virta, J. R., Paavilainen, T., Tuisku, J., Helin, S., Luoto, P., et al. (2013). Adenosine A2A receptors in secondary progressive multiple sclerosis: A [(11)C]TMSX brain PET study. *J. Cereb. Blood Flow. Metab.* 33 (9), 1394–1401. doi:10.1038/jcbfm.2013.85

Rubio-Araiz, A., Perez-Hernandez, M., Urrutia, A., Porcu, F., Borcel, E., Gutierrez-Lopez, M. D., et al. (2014). 3,4-Methylenedioxymethamphetamine (MDMA, ecstasy) disrupts blood-brain barrier integrity through a mechanism involving P2X7 receptors. *Int. J. Neuropsychopharmacol.* 17 (8), 1243–1255. doi:10.1017/S1461145714000145

Sasaki, Y., Hoshi, M., Akazawa, C., Nakamura, Y., Tsuzuki, H., Inoue, K., et al. (2003). Selective expression of Gi/o-coupled ATP receptor P2Y12 in microglia in rat brain. *Glia* 44 (3), 242–250. doi:10.1002/glia.10293

Schmidt, A. P., Lara, D. R., and Souza, D. O. (2007). Proposal of a guanine-based purinergic system in the mammalian central nervous system. *Pharmacol. Ther.* 116 (3), 401–416. doi:10.1016/j.pharmthera.2007.07.004

Schmidt, A. P., Tort, A. B., Souza, D. O., and Lara, D. R. (2008). Guanosine and its modulatory effects on the glutamatergic system. *Eur. Neuropsychopharmacol.* 18 (8), 620–622. doi:10.1016/j.euroneuro.2008.01.007

Selmi, C., Barin, J. G., and Rose, N. R. (2016). Current trends in autoimmunity and the nervous system. *J. Autoimmun.* 75, 20–29. doi:10.1016/j.jaut.2016.08.005

Shang, P., Baker, M., Banks, S., Hong, S. I., and Choi, D. S. (2021). Emerging nondopaminergic medications for Parkinson's disease: Focusing on A2A receptor antagonists and GLP1 receptor agonists. *J. Mov. Disord.* 14 (3), 193–203. doi:10.14802/jmd.21035

Shieh, C. C., Jarvis, M. F., Lee, C. H., and Perner, R. J. (2006). P2X receptor ligands and pain. *Expert Opin. Ther. Pat.* 16 (8), 1113–1127. doi:10.1517/13543776.16.8.1113

Singh, M., Venugopal, C., Tokar, T., Mcfarlane, N., Subapanditha, M. K., Qazi, M., et al. (2018). Therapeutic targeting of the premetastatic stage in human lung-to-brain metastasis. *Cancer Res.* 78 (17), 5124–5134. doi:10.1158/0008-5472.CAN-18-1022

Sipe, G. O., Lowery, R. L., Tremblay, M. E., Kelly, E. A., Lamantia, C. E., and Majewska, A. K. (2016). Microglial P2Y12 is necessary for synaptic plasticity in mouse visual cortex. *Nat. Commun.* 7, 10905. doi:10.1038/ncomms10905

Srivastava, P., Cronin, C. G., Scranton, V. L., Jacobson, K. A., Liang, B. T., and Verma, R. (2020). Neuroprotective and neuro-rehabilitative effects of acute purinergic receptor P2X4 (P2X4R) blockade after ischemic stroke. *Exp. Neurol.* 329, 113308. doi:10.1016/j.expneurol.2020.113308

Stokes, L., Layhadi, J. A., Bibic, L., Dhuna, K., and Fountain, S. J. (2017). P2X4 receptor function in the nervous system and current breakthroughs in pharmacology. *Front. Pharmacol.* 8, 291. doi:10.3389/fphar.2017.00291

Su, C., Elfeki, N., Ballerini, P., D'Alimonte, I., Bau, C., Ciccarelli, R., et al. (2009). Guanosine improves motor behavior, reduces apoptosis, and stimulates neurogenesis in rats with parkinsonism. *J. Neurosci. Res.* 87 (3), 617–625. doi:10.1002/jnr.21883

Sweeney, M. D., Sagare, A. P., and Zlokovic, B. V. (2018). Blood-brain barrier breakdown in Alzheimer disease and other neurodegenerative disorders. *Nat. Rev. Neurol.* 14 (3), 133–150. doi:10.1038/nrneurol.2017.188

Sweeney, M. D., Zhao, Z., Montagne, A., Nelson, A. R., and Zlokovic, B. V. (2019). Blood-brain barrier: From physiology to disease and back. *Physiol. Rev.* 99 (1), 21–78. doi:10.1152/physrev.00050.2017

Takenouchi, T., Sekiyama, K., Sekigawa, A., Fujita, M., Waragai, M., Sugama, S., et al. (2010). P2X7 receptor signaling pathway as a therapeutic target for neurodegenerative diseases. . 58 (2), 91–96. doi:10.1007/s00005-010-0069-y

Takenouchi, T., Sugama, S., Iwamaru, Y., Hashimoto, M., and Kitani, H. (2009). Modulation of the ATP-lnduced release and processing of IL-1beta in microglial cells. *Crit. Rev. Immunol.* 29 (4), 335–345. doi:10.1615/critrevimmunol.v29.i4.40

Terstappen, G. C., Meyer, A. H., Bell, R. D., and Zhang, W. (2021). Strategies for delivering therapeutics across the blood-brain barrier. *Nat. Rev. Drug Discov.* 20 (5), 362–383. doi:10.1038/s41573-021-00139-y

Torti, M., Vacca, L., and Stocchi, F. (2018). Istradefylline for the treatment of Parkinson's disease: Is it a promising strategy? *Expert Opin. Pharmacother.* 19 (16), 1821–1828. doi:10.1080/14656566.2018.1524876

Toth, P., Tarantini, S., Davila, A., Valcarcel-Ares, M. N., Tucsek, Z., Varamini, B., et al. (2015). Purinergic glio-endothelial coupling during neuronal activity: Role of P2Y1 receptors and eNOS in functional hyperemia in the mouse somatosensory cortex. *Am. J. Physiol. Heart Circ. Physiol.* 309 (11), H1837–H1845. doi:10.1152/ajpheart.00463.2015

Toulorge, D., Schapira, A. H., and Hajj, R. (2016). Molecular changes in the postmortem parkinsonian brain. *J. Neurochem.* 139, 27–58. doi:10.1111/jnc.13696

Tozaki-Saitoh, H., Tsuda, M., Miyata, H., Ueda, K., Kohsaka, S., and Inoue, K. (2008). P2Y12 receptors in spinal microglia are required for neuropathic pain after peripheral nerve injury. *J. Neurosci.* 28 (19), 4949–4956. doi:10.1523/JNEUROSCI.0323-08.2008

van Vliet, E. A., Ndode-Ekane, X. E., Lehto, L. J., Gorter, J. A., Andrade, P., Aronica, E., et al. (2020). Long-lasting blood-brain barrier dysfunction and neuroinflammation after traumatic brain injury. *Neurobiol. Dis.* 145, 105080. doi:10.1016/j.nbd.2020.105080

van Waarde, A., Dierckx, R., Zhou, X., Khanapur, S., Tsukada, H., Ishiwata, K., et al. (2018). Potential therapeutic applications of adenosine A2A receptor ligands and opportunities for A2A receptor imaging. *Med. Res. Rev.* 38 (1), 5–56. doi:10.1002/med.21432

Vazquez-Villoldo, N., Domercq, M., Martin, A., Llop, J., Gomez-Vallejo, V., and Matute, C. (2014). P2X4 receptors control the fate and survival of activated microglia. *Glia* 62 (2), 171–184. doi:10.1002/glia.22596

Verma, R., Cronin, C. G., Hudobenko, J., Venna, V. R., Mccullough, L. D., and Liang, B. T. (2017). Deletion of the P2X4 receptor is neuroprotective acutely, but induces a depressive phenotype during recovery from ischemic stroke. *Brain Behav. Immun.* 66, 302–312. doi:10.1016/j.bbi.2017.07.155

von Kugelgen, I. (2021). Molecular pharmacology of P2Y receptor subtypes. *Biochem. Pharmacol.* 187, 114361. doi:10.1016/j.bcp.2020.114361

Wang, H., Hong, L. J., Huang, J. Y., Jiang, Q., Tao, R. R., Tan, C., et al. (2015). P2RX7 sensitizes Mac-1/ICAM-1-dependent leukocyte-endothelial adhesion and promotes neurovascular injury during septic encephalopathy. *Cell Res.* 25 (6), 674–690. doi:10.1038/cr.2015.61

Wang, K., Sun, M., Juan, Z., Zhang, J., Sun, Y., Wang, G., et al. (2022). The improvement of sepsis-associated encephalopathy by P2X7R inhibitor through inhibiting the omi/HtrA2 apoptotic signaling pathway. *Behav. Neurol.* 2022, 3777351. doi:10.1155/2022/3777351

Wang, T. F., and Guidotti, G. (1998). Widespread expression of ecto-apyrase (CD39) in the central nervous system. *Brain Res.* 790 (1-2), 318–322. doi:10.1016/s0006-8993(97)01562-x

Wei, L., Syed, M. S., Yan, J., Zhang, L., Wang, L., Yin, Y., et al. (2018). ATP-activated P2X7 receptor in the pathophysiology of mood disorders and as an emerging target for the development of novel antidepressant therapeutics. *Neurosci. Biobehav Rev.* 87, 192–205. doi:10.1016/j.neubiorev.2018.02.005

Weisman, G. A., Camden, J. M., Peterson, T. S., Ajit, D., Woods, L. T., and Erb, L. (2012). P2 receptors for extracellular nucleotides in the central nervous system: Role of P2X7 and P2Y- receptor interactions in neuroinflammation. *Mol. Neurobiol.* 46 (1), 96–113. doi:10.1007/s12035-012-8263-z

Wilson, H. L., Varcoe, R. W., Stokes, L., Holland, K. L., Francis, S. E., Dower, S. K., et al. (2007). P2X receptor characterization and IL-1/IL-1Ra release from human endothelial cells. *Br. J. Pharmacol.* 151 (1), 115–127. doi:10.1038/sj.bjp.0707213

Wittendorp, M. C., Boddeke, H. W., and Biber, K. (2004). Adenosine A3 receptor-induced CCL2 synthesis in cultured mouse astrocytes. *Glia* 46 (4), 410–418. doi:10.1002/glia.20016

Wu, S. T., Han, J. R., Yao, N., Li, Y. L., Zhang, F., Shi, Y., et al. (2022). Activation of P2X4 receptor exacerbates acute brain injury after intracerebral hemorrhage. *CNS Neurosci. Ther.* 28 (7), 1008–1018. doi:10.1111/cns.13831

Yamamoto, M., Guo, D. H., Hernandez, C. M., and Stranahan, A. M. (2019). Endothelial Adora2a activation promotes blood-brain barrier breakdown and cognitive impairment in mice with diet-induced insulin resistance. *J. Neurosci.* 39 (21), 4179–4192. doi:10.1523/JNEUROSCI.2506-18.2019

Yang, F., Zhao, K., Zhang, X., Zhang, J., and Xu, B. (2016). ATP induces disruption of tight junction proteins via IL-1 beta-dependent MMP-9 activation of human blood-brain barrier *in vitro*. *Neural Plast.* 2016, 8928530. doi:10.1155/2016/8928530

Yang, Y., Kimura-Ohba, S., Thompson, J. F., Salayandia, V. M., Cosse, M., Raz, L., et al. (2018). Vascular tight junction disruption and angiogenesis in spontaneously hypertensive rat with neuroinflammatory white matter injury. *Neurobiol. Dis.* 114, 95–110. doi:10.1016/j.nbd.2018.02.012

Yegutkin, G. G. (2008). Nucleotide- and nucleoside-converting ectoenzymes: Important modulators of purinergic signalling cascade. *Biochim. Biophys. Acta* 1783 (5), 673–694. doi:10.1016/j.bbamcr.2008.01.024

Yu, F., Zhu, C., Xie, Q., and Wang, Y. (2020). Adenosine A(2A) receptor antagonists for cancer immunotherapy. *J. Med. Chem.* 63 (21), 12196–12212. doi:10.1021/acs.jmedchem.0c00237

Zerr, M., Hechler, B., Freund, M., Magnenat, S., Lanois, I., Cazenave, J. P., et al. (2011). Major contribution of the P2Y$_1$receptor in purinergic regulation of TNFα-induced vascular inflammation. *Circulation* 123 (21), 2404–2413. doi:10.1161/CIRCULATIONAHA.110.002139

Zhang, Y., Zhu, W., Yu, H., Yu, J., Zhang, M., Pan, X., et al. (2019). P2Y4/TSP-1/TGF-β1/pSmad2/3 pathway contributes to acute generalized seizures induced by kainic acid. *Brain Res. Bull.* 149, 106–119. doi:10.1016/j.brainresbull.2019.04.004

Zhao, H., Zhang, X., Dai, Z., Feng, Y., Li, Q., Zhang, J. H., et al. (2016). P2X7 receptor suppression preserves blood-brain barrier through inhibiting RhoA activation after experimental intracerebral hemorrhage in rats. *Sci. Rep.* 6, 23286. doi:10.1038/srep23286

Zhao, M., Jiang, X. F., Zhang, H. Q., Sun, J. H., Pei, H., Ma, L. N., et al. (2021). Interactions between glial cells and the blood-brain barrier and their role in Alzheimer's disease. *Ageing Res. Rev.* 72, 101483. doi:10.1016/j.arr.2021.101483

Zhao, Z., Nelson, A. R., Betsholtz, C., and Zlokovic, B. V. (2015). Establishment and dysfunction of the blood-brain barrier. *Cell* 163 (5), 1064–1078. doi:10.1016/j.cell.2015.10.067

Zhao, Z., Shang, X., Chen, Y., Zheng, Y., Huang, W., Jiang, H., et al. (2020). Bacteria elevate extracellular adenosine to exploit host signaling for blood-brain barrier disruption. *Virulence* 11 (1), 980–994. doi:10.1080/21505594.2020.1797352

Zhou, Y., Peng, Z., Seven, E. S., and Leblanc, R. M. (2018). Crossing the blood-brain barrier with nanoparticles. *J. Control. Release.* 270, 290–303. doi:10.1016/j.jconrel.2017.12.015

Zhou, Y., Wang, Y., Wang, J., Anne, S. R., and Yang, Q. W. (2014). Inflammation in intracerebral hemorrhage: From mechanisms to clinical translation. *Prog. Neurobiol.* 115, 25–44. doi:10.1016/j.pneurobio.2013.11.003

Zhou, Y., Zeng, X., Li, G., Yang, Q., Xu, J., Zhang, M., et al. (2019). Inactivation of endothelial adenosine A2A receptors protects mice from cerebral ischaemia-induced brain injury. *Br. J. Pharmacol.* 176 (13), 2250–2263. doi:10.1111/bph.14673

frontiers | Frontiers in Pharmacology

TYPE Original Research
PUBLISHED 14 February 2023
DOI 10.3389/fphar.2023.1117762



OPEN ACCESS

EDITED BY
Henning Ulrich,
University of São Paulo, Brazil

REVIEWED BY
Larissa G. Pinto,
King's College London, United Kingdom
Elsa Fabbretti,
Independent Researcher, Trieste, Italy

*CORRESPONDENCE
Alexei Verkhratsky,
alexej.verkhratsky@manchester.ac.uk
Hong Nie,
hongnie1970@163.com

SPECIALTY SECTION
This article was submitted to Experimental Pharmacology and Drug Discovery, a section of the journal Frontiers in Pharmacology

RECEIVED 06 December 2022
ACCEPTED 01 February 2023
PUBLISHED 14 February 2023

CITATION
Luo Z, Wang T, Zhang Z, Zeng H, Yi M, Li P, Pan J, Zhu C, Lin N, Liang S, Verkhratsky A and Nie H (2023), Polyphyllin VI screened from Chonglou by cell membrane immobilized chromatography relieves inflammatory pain by inhibiting inflammation and normalizing the expression of $P2X_3$ purinoceptor. *Front. Pharmacol.* 14:1117762. doi: 10.3389/fphar.2023.1117762



# Polyphyllin VI screened from Chonglou by cell membrane immobilized chromatography relieves inflammatory pain by inhibiting inflammation and normalizing the expression of $P2X_3$ purinoceptor

Zhenhui Luo[1,2], Tingting Wang[1,2], Zhenglang Zhang[1,2], Hekun Zeng[1,2], Mengqin Yi[1,2], Peiyang Li[1,2], Jiaqin Pan[1,2], Chunyan Zhu[3], Na Lin[3], Shangdong Liang[4], Alexei Verkhratsky[5]* and Hong Nie[1,2]*

[1]International Cooperative Laboratory of Traditional Chinese Medicine Modernization and Innovative Drug Development of Chinese Ministry of Education (MOE), College of Pharmacy, Jinan University, Guangzhou, China, [2]Guangdong Province Key Laboratory of Pharmacodynamic Constituents of TCM and New Drugs Research, College of Pharmacy, Jinan University, Guangzhou, China, [3]Institute of Chinese Materia Medica, China Academy of Chinese Medical Sciences, Beijing, China, [4]Neuropharmacology Laboratory of Physiology Department, Basic Medical School, Nanchang University, Nanchang, Jiangxi, China, [5]Faculty of Biology, Medicine, and Health, The University of Manchester, Manchester, United Kingdom

**Objective:** Inflammatory pain is one of the most common diseases in daily life and clinic. In this work, we analysed bioactive components of the traditional Chinese medicine Chonglou and studied mechanisms of their analgesic effects.

**Material and methods:** Molecular docking technology and U373 cells overexpressing P2X3 receptors combined with the cell membrane immobilized chromatography were used to screen possible CL bioactive molecules interacting with the P2X3 receptor. Moreover, we investigated the analgesic and anti-inflammatory effects of Polyphyllin VI (PPIV), in mice with chronic neuroinflammatory pain induced by CFA (complete Freund's adjuvant).

**Results:** The results of cell membrane immobilized chromatography and molecular docking showed that PPVI was one of the effective compounds of Chonglou. In mice with CFA-induced chronic neuroinflammatory pain, PPVI decreased the thermal paw withdrawal latency and mechanical paw withdrawal threshold and diminished foot edema. Additionally, in mice with CFA-induced chronic neuroinflammatory pain, PPIV reduced the expression of the pro-inflammatory factors IL-1, IL-6, TNF-α, and downregulated the expression of P2X3 receptors in the dorsal root ganglion and spinal cord.

**Conclusion:** Our work identifies PPVI as a potential analgesic component in the Chonglou extract. We demonstrated that PPVI reduces pain by inhibiting inflammation and normalizing P2X3 receptor expression in the dorsal root ganglion and spinal cord.

KEYWORDS

Chonglou, polyphyllin VI, chronic neuroinflammatory pain, P2X3 receptor, cell membrane immobilized chromatography

# 1 Introduction

Pain, and the inflammatory pain in particular, is common in daily life and clinical practice, (Taneja et al., 2017). (Ronchetti et al., 2017). Even after resolution of inflammation, chronic pain can develop and last for a long period (Demir et al., 2013; Raja et al., 2020; Finnerup et al., 2021). Over 7% of the world's population is estimated to have chronic pain with neuropathic symptoms, however, due to the challenges in categorization and the incomplete understanding of the underlying processes, this proportion may be understated (van Hecke et al., 2014; Bouhassira, 2019).

Neuroinflammation that can affect the peripheral or central nervous system is primarily defined by the infiltration of leukocytes, reactive gliosis, and the upregulation of inflammatory mediators (Escartin et al., 2021). It is generally believed that inflammation is crucial in the maintenance and management of chronic pain (Vergne-Salle and Bertin, 2021). Findings from fundamental studies utilizing chronic pain-prone animals demonstrated that chronic pain results from a pathologically altered neural circuits evoked by peripheral tissue inflammation and peripheral nerve damage (Malcangio, 2019). ATP promotes nociceptive processing by activating the ligand-gated ion channel family of P2X receptors, among which, the $P2X_3$ receptor, is highly expressed by primary afferent neurons. In sensory neurons, $P2X_3$ receptors function as homomeric ($P2X_3$) and heteromeric ($P2X_{2/3}$) channels (Jarvis, 2003). Exogenous application of ATP and related agonists excites the peripheral and central nervous system and increases sensitivity to noxious stimuli. Specific targeting of the $P2X_3$ receptor by genetic deletion and knockdown results in a hypoalgesic phenotype (Butler and Meegan, 2008). Studies have shown that the pharmacological blockade of $P2X_3$ receptors completely blocked specific types of chronic inflammatory and neuropathic pain (Kaan et al., 2010; Xu et al., 2012; Jorge et al., 2020). Peripheral nerve injury differentially alters the functional expression of $P2X_3$ receptors in small- and large-diameter primary afferent neurons (Inoue, 2021). As a result, $P2X_{2,3}$ purinoceptors can represent targets for pain therapy.

*Chonglou* (CL) is the dried rhizome of *Paris polyphylla* var. *yunnanensis* or *P. polyphylla ar. chinensis*. Steroidal saponins, flavonoids, sugars, volatile oils, amino acids, trace minerals, etc., are among CL's active constituents, mediating anti-tumor (Tian et al., 2020), anti-infection (Qiumin et al., 2017), organ-protecting (Man et al., 2014), and anti-inflammatory effects (Yan et al., 2021;

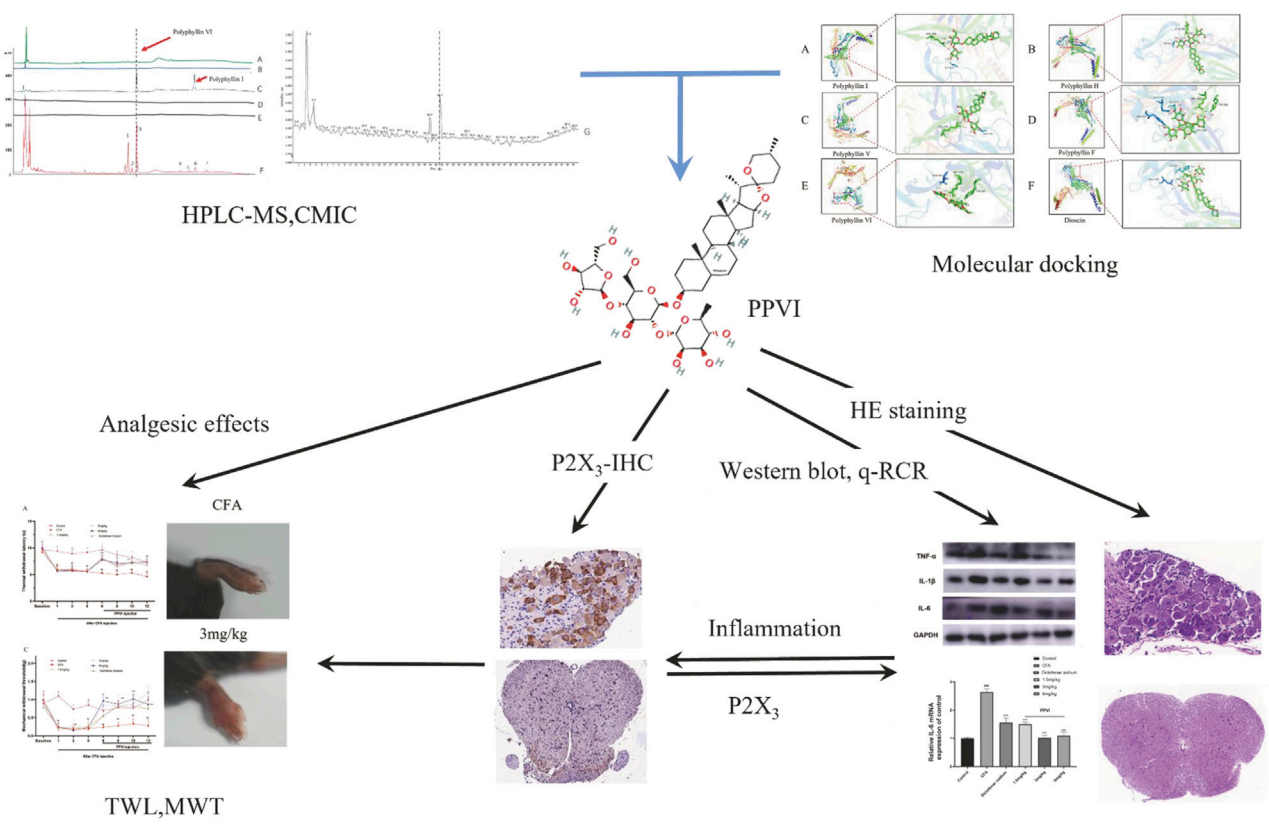


FIGURE 1
The flowchart the article. Polyphyllin VI was screened from CL by CMIC and relieved the chronic inflammatory pain *via* suppressing $P2X_3R$ in the following experiments.

**TABLE 1 Primer sequences for RT-qPCR.**

| Name | Sequence (5′–3′) |
|---|---|
| IL-1β (Forward sequence) | GCAACTGTTCCTGAACTCAACT |
| IL-1β (Reverse sequence) | ATCTTTTGGGGTCCGTCAACT |
| IL-6 (Forward sequence) | TAGTCCTTCCTACCCCAATTTCC |
| IL-6 (Reverse sequence) | TTGGTCCTTAGCCACTCCTTC |
| TNF-α (Forward sequence) | CCCTCACACTCAGATCATCTTCT |
| TNF-α (Reverse sequence) | GCTACGACGTGGGCTACAG |
| $P2X_3$ (Forward sequence) | AAAGCTGGACCATTGGGATCA |
| $P2X_3$ (Reverse sequence) | CGTGTCCCGCACTTGGTAG |
| β-Actin (Forward sequence) | GTGACGTTGACATCCGTAAAGA |
| β-Actin (Reverse sequence) | GCCGGACTCATCGTACTCC |

Zhou et al., 2021). Several active compounds of CL such as polyphyllin D, polyphyllin A, polyphyllin I, polyphyllin II, polyphyllin VI (PPVI), and polyphyllin VII were identified (Wang Q. et al., 2018; Pang et al., 2020; Teng et al., 2020; Ahmad et al., 2021; Kwon et al., 2021). Bioactive chemicals from CL for the treatment of inflammatory pain and the underlying mechanisms were not fully elucidated.

The development and use of traditional Chinese medicines (TCM) are significantly hampered by the difficulty in identifying active compounds among the hundreds of ingredients in medicinal formulae. A novel screening technique named Cell Membrane Immobilization Chromatography (CMIC), based on the biospecific affinity adsorption of biologically active substances to receptors or channels in cells was developed for isolating active compounds from the natural samples (Nie et al., 2008; Nie et al., 2011; Zhang et al., 2021). In this study, we used cell membrane immobilized chromatography (CMIC) to screen the active ingredients in CL that may interact with the $P2X_3$ receptor. We identified PPVI as the main active ingredient of the CL extract and investigated the analgesic potency and mechanism of PPVI by molecular docking combined with CMIC on U373 cells expressing P2X receptors. The flowchart in Figure 1 overviews technical procedures and experimental outcomes for assessing PPVI's impact and mechanisms of action.

# 2 Material and methods

## 2.1 Preparation and extraction of CL

CL was purchased from the First Affiliated Hospital of Jinan University and certified by Professor Nie Hong. The drugs were pulverized to a fine powder (30 mesh) by the grinder, 1.25 g of fine powder was dissolved in 50 mL of analytical methanol (99.9%), and sonicated for half an hour under ultrasonic conditions (60°C, 39.6 kHz) to obtain 25 mg/mL CL decoction liquid. The medicinal liquid of the decoction was filtered by double-circle quantitative filter paper and passed through a 0.22 μm microporous membrane to obtain the CL decoction liquid sample. Polyphyllin I (B21668, Polyphyllin II (B21669 and Polyphyllin VI (B21670) were purchased from Shanghaiyuanye Bio-Technology Co. Ltd.; the purity of each reference compound was greater than 98%, which was evaluated by analytical high-performance liquid chromatography combined with diode array detection and mass spectrometry (HPLC-DAD-MS).

## 2.2 HPLC with mass spectrometry

HPLC-DAD analysis using Agilent 1200 series was equipped with ChemStation software (Agilent Technologies, Valderbrunn, Germany). Chromatographic separation was performed on a ChromCoreTM 120 C18 column (laboratory technology NanoChrom, Jiangsu, China) with a diameter of 4.6 × 250 mm and a length of 5 μm. The mobile phase consisted of 0.1% aqueous ammonia (A) and acetonitrile (B). The following gradient elution procedure is used for separation: 0–40 min, 30%–60% B; 40–50 min, 60%–30% B; then balance for 10 min. The flow rate was 1 mL/min and the column temperature was maintained at 30°C. The DAD is set to scan from 190 to 400 nm. The separated compound was detected at 203 nm. Agilent 3500 TOF/MS (Agilent Technologies, Santa Clara, California, United States) equipped with electrospray ionization (ESI) interface for HPLC-DAD-TOF/MS analysis. ESI mass source spectrometers operate in negative and positive ion modes. Operating parameters are set as follows: dry gas temperature, 325°C; dry gas (N2) flow rate, 11.0 L/min; atomizer, 30 PSIG; Fragmentation voltage, 175 V; and capillary voltage, 3500 V. The range is set to 100–1000 m/z. Data acquisition and analysis were performed using Masshunter Workstation software (version B.02.00, Agilent Technologies, Inc., Waldbronn, Germany).

## 2.3 Cell membrane immobilized chromatography

U373 cells (College of Pharmacy, Jinan University) were cultured in Dulbecco's modified Eagle's media with 10% fetal bovine serum (v/v), 1% 100 U/mL penicillin, and 100 μg/mL streptomycin to perform CMIC. A 37°C humidified incubator with 5% carbon dioxide ($CO_2$) was used to keep U373 cells. U373 cells were plated in a cell culture flask (25 $cm^2$) cultivated until confluency was achieved. For 1 h, U373 cells were cultured in a humidified incubator with 5% $CO_2$ at 37°C and 2 mL of CL water extracts (5 g/L). To get rid of any potential non-selectively combining elements, the CL water extracts in the flask were removed. The flask was then rinsed five times with 1 mL of phosphate-buffered saline (PBS). Washing duration was tuned by analyzing CL in a separate washing eluate because full removal of components that are not particularly binding is essential. For analysis using HPLC-DAD-TOF/MS (HPLC-DAD-coupled with diode array detection and time of flight mass spectrometry), the eluate from the fifth washing was collected. The last phase involved denatured U373 cells and the dissociation of associated chemicals by co-incubation with 2 mL of methanol for 30 min. Using a Termovap sample concentrator, the attached ingredients solution was evaporated to 500 μL at room temperature. The material that had evaporated was analyzed using HPLC-DAD-TOF/MS. The CMIC was described in detail previously (Zhang et al., 2021).

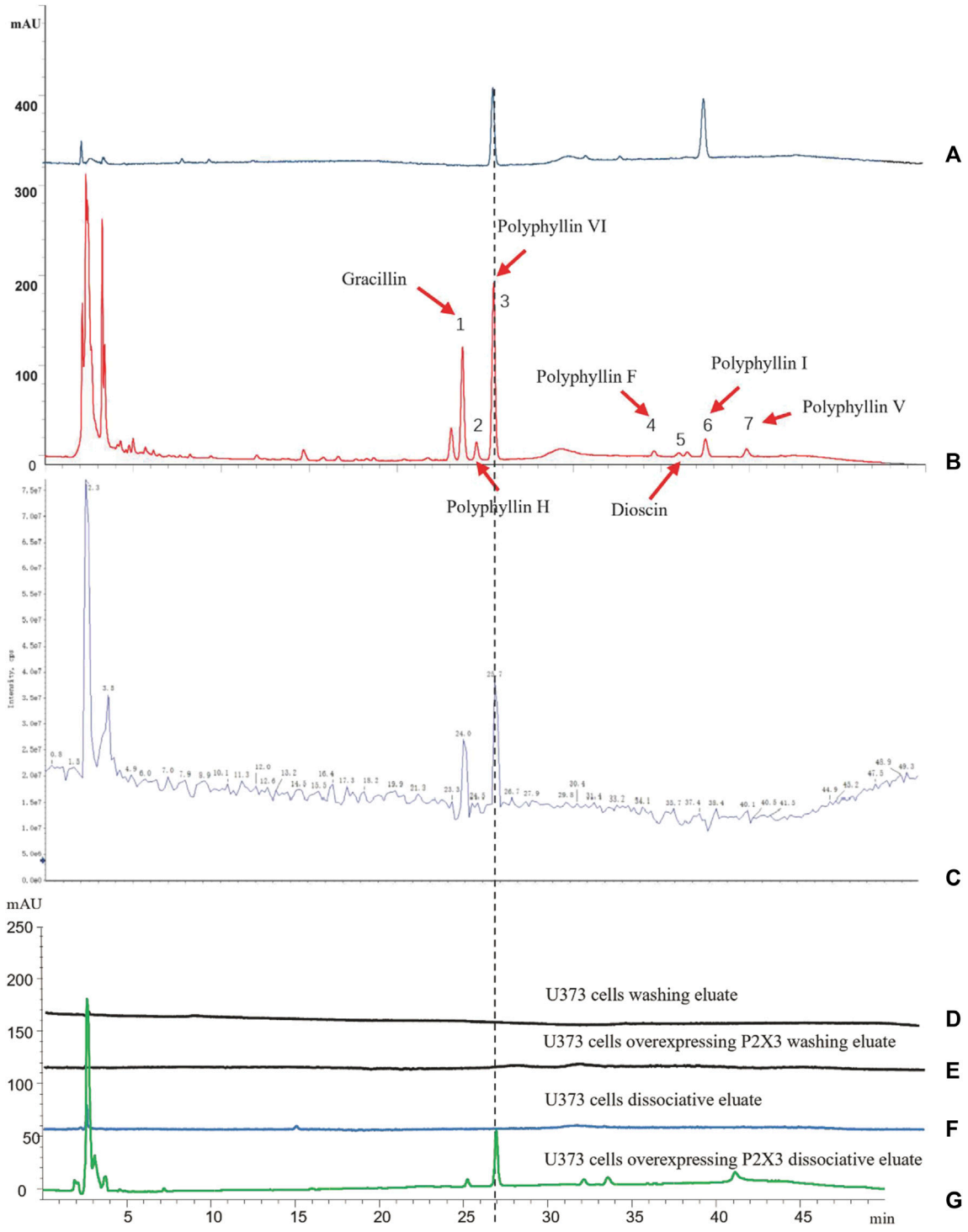


FIGURE 2
The CMIC of CL with U373 cells. **(A)** The HPLC chromatogram of the standard solution (Polyphyllin VI, Polyphyllin I). **(B,C)** THe HPLC-MS chromatogram of CL extract. **(D,E)** The HPLC chromatogram of the eluate of U373 cells and U373 cells expressing $P2X_3$. **(F,G)** The HPLC chromatogram of dissociation medium of U373 cells and U373 cells expressing $P2X_3$.

## 2.4 Molecular docking simulation

Using Open Babel 2.4.1, the molecular structure file of PPVI was downloaded and converted to PDBQT format after being obtained and downloaded from PubChem (https://pubchem.ncbi.nlm.nih.gov/). The crystal structure of the target protein was then retrieved and downloaded from the RCSB Protein Data Bank database (RCSBPDB, https://www.rcsb.org/). Using

**TABLE 2 HPLC-MS chromatogram of CL extract compounds identification.**

| NO. | Expected RT | Retention time | Retention time Delta (min) | Adduct/ Charge | Formula | Precursor mass | Found at mass | Mass error (ppm) | Component name |
|---|---|---|---|---|---|---|---|---|---|
| 1 | 24.9 | 24.9 | 0 | $[M-H]^-$ | $C_{45}H_{72}O_{17}$ | 883.47 | 883.4703 | 0.7 | Gracillin |
| 2 | 25.74 | 25.74 | 0 | $[M-H]^-$ | $C_{44}H_{70}O_{17}$ | 869.454 | 869.4521 | −2.2 | Polyphyllin H |
| 3 | 26.65 | 26.65 | 0 | $[M-H]^-$ | $C_{39}H_{62}O_{13}$ | 737.412 | 737.4112 | −0.8 | Polyphyllin VI |
| 4 | 35.61 | 35.69 | 0.08 | $[M-H]^-$ | $C_{51}H_{82}O_{20}$ | 1013.533 | 1013.5243 | −8.3 | Polyphyllin F |
| 5 | 37.07 | 37.1 | 0.03 | $[M-H]^-$ | $C_{45}H_{72}O_{16}$ | 867.475 | 867.4784 | 4.2 | Dioscin |
| 6 | 38.56 | 38.6 | 0.04 | $[M-H]^-$ | $C_{44}H_{70}O_{16}$ | 853.459 | 853.4587 | −0.4 | Polyphyllin I |
| 7 | 40.96 | 40.95 | 0.01 | $[M-H]^-$ | $C_{39}H_{62}O_{12}$ | 721.417 | 721.4157 | −1.6 | Polyphyllin V |

**TABLE 3 Affinities and amino acid sites of ligand-protein detected by molecular docking.**

| Protein | Ligand | Binding energy kcal/mol | Amino acid binding site |
|---|---|---|---|
| $P2X_3$ | Dioscin | −12.0 | ARG295/281, TYR285, TRP152, GLY129/130 |
| | Polyphyllin H | −11.7 | ARG295/529, GLN102, TRP152, GLU109 |
| | Polyphyllin I | −11.6 | TYR285, ARG295, GLN102, TRP152 |
| | Polyphyllin V | −11.2 | GLU109/156, GLY129/130, ARG295, TYR285 |
| | Polyphyllin VI | −10.8 | ARG295/281, TYR285, TRP152, GLY129/130 |
| | Polyphyllin F | −10.6 | ARG295/281, TYR285, TRP152, GLU109 |
| | Gracillin | −5.7 | ARG25, GLY314, ASP248 |

AutoDock Tools (Trott and Olson, 2010), the target protein's ligands and water were eliminated, yielding a new protein. It simultaneously determines the size and center of the docking box, calculates charge, inserts hydrogen atoms, outputs the PDBQT format file, and all of these things. Vina was used to dock the active ingredients with the target protein one at a time, choosing the conformation with the best docking score (Affinity). The outcomes were then examined using Pymol, which produced graphs.

## 2.5 Animals

6–9 weeks adult female C57BL/6 mice (20–25 g) were obtained from Guangdong Yaokang Biotechnology Co., Ltd. They were housed in Jinan University Laboratory Animal Center at a standard temperature of 24°C ± 1°C under a 12 h light-dark cycle (dark from 7:00 p.m. to 7:00 a.m.) with free access to food and water. All experiments were conducted by the National Institutes of Health Guide for the Care and Use of Laboratory animals in rigorous line with the International Association for the Study of Pain guidelines. Our research was approved by the Jinan University Animal Ethics Committee. The behavioral test was performed by experimenters who were blinded to the experimental group.

## 2.6 Construction of CFA model and drugs administration

The mechanical withdrawal threshold (MWT) and the thermal paw withdrawal latency (TWL) of C57BL/6 mice were measured after the mice were placed in the animal room for a week to adjust to the environment. Mice were then placed on a metal mesh, covered with plexiglass, and tested. Mice with no significant differences were selected according to MWT and TWL, and divided into six groups ($N$ = 10) using a random number table. The following experimental groups were set: Control group, CFA model group, and CFA model + different dosages of Polyphyllin by intraperitoneal injection (1.5, 3, and 6 mg/kg, respectively designated as PPVI-1.5, PPVI-3, and PPVI-6 groups); The CFA modeling approach including three steps were used. The mouse left hind foot was injected with 30 μL of CFA, the mice pain threshold was measured in Von-Frey nylon silk and hot plate protocols, and the mice ability to tolerate pain was assessed. Based on the mice ability to tolerate pain, the validity of the CFA model was judged. The diclofenac sodium (7.5 mg/kg) was administered by intraperitoneal injection following CFA modeling. Five days after the CFA model was established drugs were administered once per day for a total of 7 days. Carbon dioxide was utilized for euthanasia after the experiment.

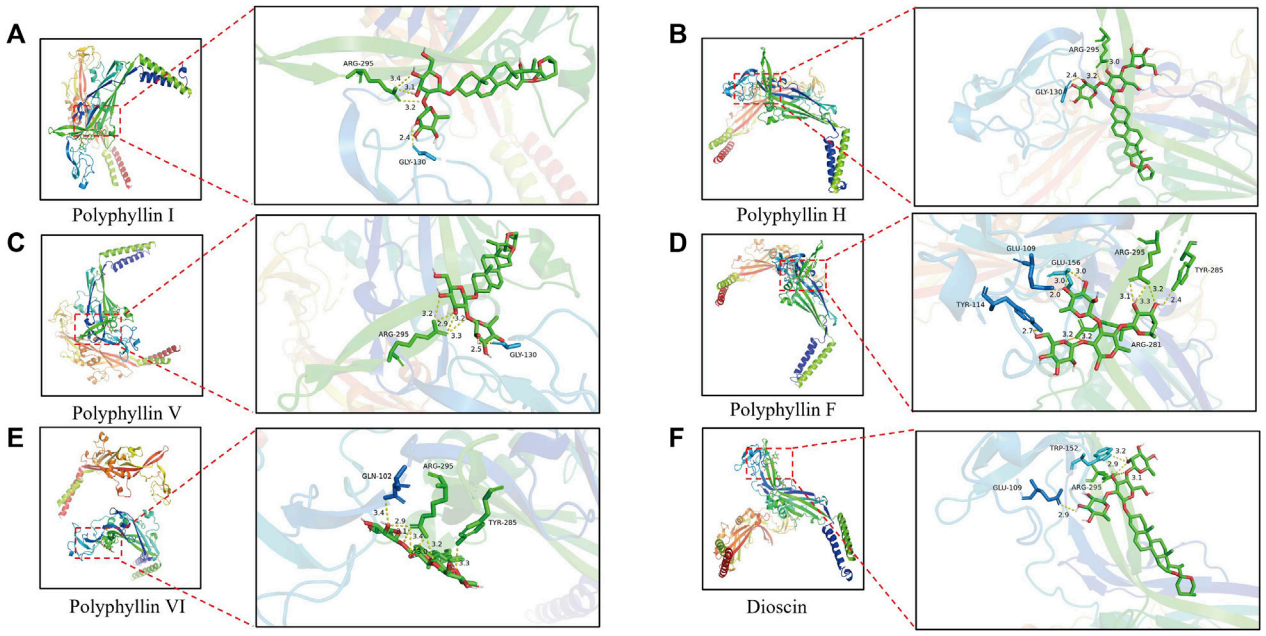


FIGURE 3
Molecular docking models of $P2X_3$ and Dioscin, Polyphyllin H, Polyphyllin I, Polyphyllin V, Polyphyllin VI, Polyphyllin F. **(A)** $P2X_3$ and Polyphyllin I docking mode and the interaction plane diagram. **(B)** $P2X_3$ and Polyphyllin H docking mode and the interaction plane diagram. **(C)** $P2X_3$ and Polyphyllin V docking mode and the interaction plane diagram. **(D)** $P2X_3$ and Polyphyllin F docking mode and the interaction plane diagram. **(E)** $P2X_3$ and Polyphyllin VI docking mode and the interaction plane diagram. **(F)** $P2X_3$ and Dioscin docking mode and the interaction plane diagram.

## 2.7 The von Frey test

After 30 min of acclimatization, mice were tested using von Frey hair (0.04 g, 0.07 g, 0.16 g, 0.40 g, 0.60 g, 1.00 g, 1.40 g, and 2.00 g), which was slightly bent to stimulate the lateral part of the mouse's left plantar. The mice were placed on an elevated mesh metal plate, covered with perforated transparent 10 cm × 6 cm × 6 cm plexiglass cages. Special emphasis was taken to separate pain-induced withdrawal behavior from the withdrawal response following physical exercise. If the stimulus is positive, it is recorded with an X; if it is negative, it is marked with an O. After changing the O to X or X to O, the above procedure is repeated for four rounds, with the pressure value indicated by the letter X (the last used fiber) being recorded after each round. If there is no response, the level of pressure is increased to the next level, the first mechanical stimulation is given with a force of 1.0 g, and so on. The formula for calculating the threshold value is as follows: Log 50%g threshold = $X_f$ + kδ ($X_f$ = value (in log units) of the final von Frey hair used; k = tabular valufor the pattern of positive/negative responses; and $\delta$ = mean difference (in log units) between stimuli (Chaplan et al., 1994).

## 2.8 The hot-plate test

Before the experiment, mice were prescreened by having their abdominal hair removed, and being placed one at a time on a (55.00.5) ˚C hot plate apparatus. The pain thresholds were recorded using hind feet licked or lifted as pain indicators. Mice with a pain threshold of 5–30 s were chosen for the experiment. The selected mice were placed one at a time on the hot plate device, and the mice pain threshold was measured three times, with 10-min intervals between each measurement. The average value was taken as the baseline pain threshold or the pre-administration, normal pain tolerance. The average time that mice spend licking their paws on a hot plate after taking PPVI, which correlates to the mice's response to heat stimulation after taking PPVI, is measured as the pain threshold. The pain thresholds before and after administration were determined and counted for the 60 s if the mice on the hot plate equipment still did not exhibit any signs of discomfort after the 60 s.

## 2.9 The measurement of foot swelling

Vernier calipers were used to measure each group of mice toe thickness before modeling, during modeling, and after drug treatment. The difference between the thickness of the left and right hind limbs was utilized to indicate the degree of inflammation and swelling. Each group's degree of swelling was calculated.

## 2.10 RT-qPCR

Using Trizol reagent (Thermo Fisher), total RNA was obtained from $L_3$-$L_5$ DRG and the spinal cord. The concentration and purity of extracted RNA were assessed using a spectrophotometer. For qPCR, RNA with an

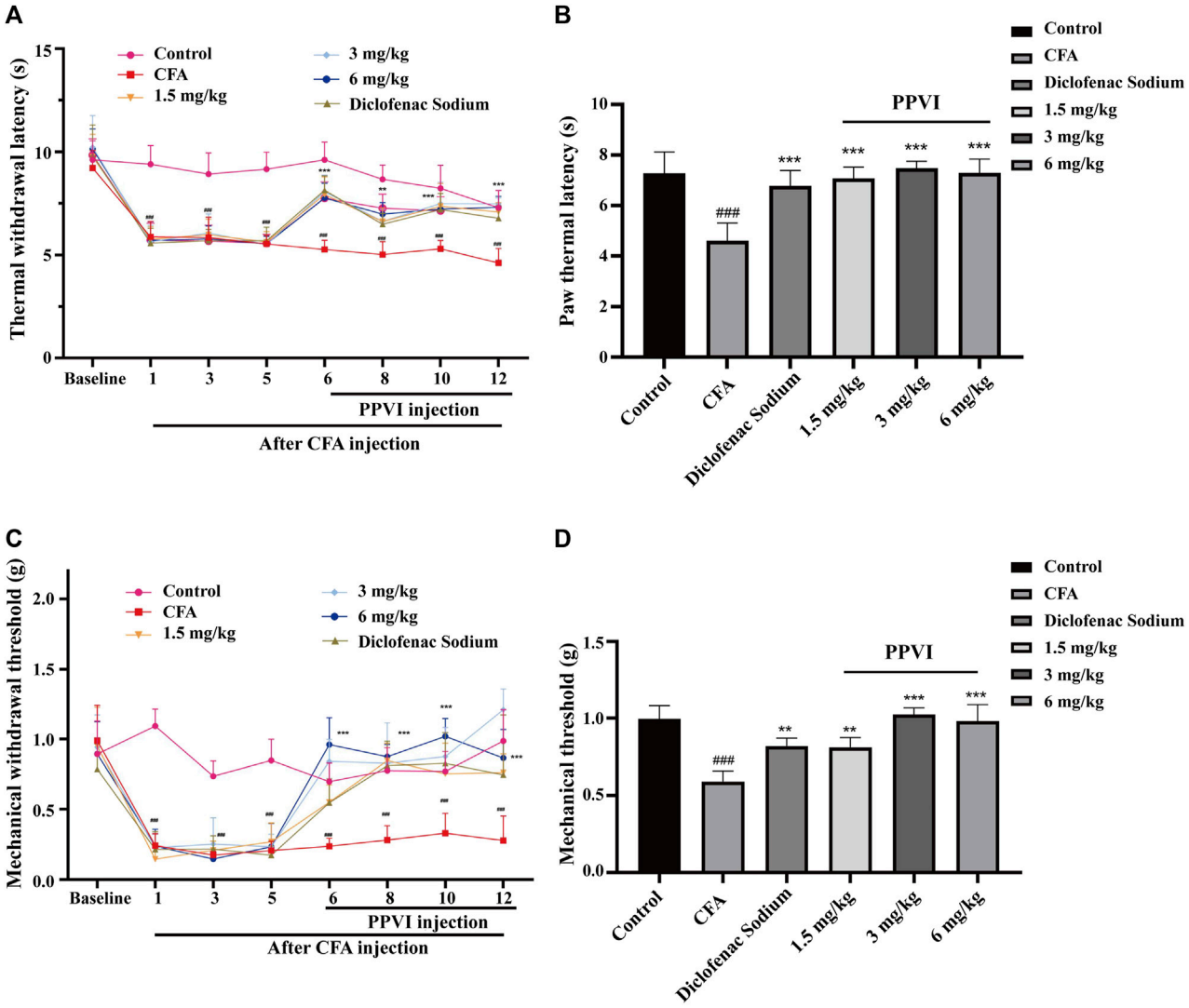


FIGURE 4
Effect of administration of PPVI on the TWL and MWT in CFA-induced chronic neuroinflammatory pain mice. **(A)** The TWL of mice in each group were detected on the day before CFA injection, 1, 3, 5 days after injection, and 1, 3, 5, and 7 days after PPVI admistration, $n = 10$ in each group. **(B)** THe TWL of mice in ache group were detected 12 days after CFA injection. **(C)** The MWT of mice in each group were detected on the day before CFA injection, 1, 3, 5 days after injection, and 1, 3, 5, and 7 days after PPVI administration. $n = 10$ in each group. **(D)** The MWT of mice in each group was detected 12 days after CFA injection. Data are presented as mean ± S.E.M, significant differences among different groups are indicated as ###$p < 0.001$, vs. control; **$p < 0.001$ vs. CFA group.

approximate absorbance ratio of 2.0 (OD260/OD280 nm) was selected, and RT Master Mix for qPCR II was used to transcribe the RNA into cDNA. Quantitative real-time PCR (RT-qPCR) was performed to measure the expression of the mRNA using a qPCR PreMix (SYBR Green) Kit. The test's primers are listed in Table 1. The relative expressions of the relevant genes were calculated using the $2^{-\Delta\Delta CT}$ method.

## 2.11 Western blot

Protein extraction was described by (Luo et al., 2021). Sodium dodecyl sulfate-polyacrylamide gel electrophoresis (SDS-PAGE) was used to separate 20 μg of proteins from each sample, which was then placed onto a polyvinylidene fluoride (PVDF) membrane. Before the primary antibody incubation at 4°C overnight, the membranes were blocked with 5% milk for 2 h. The following primary antibodies were then used: $P2X_3$ (Abcam, ab300493), IL-1 (Abcam, ab283818), GAPDH (Abcam, ab9485), TNF-α (Abcam, ab215188), and IL-6 (Abcam, ab290735). Horseradish peroxidase (HRP)-conjugated secondary antibody was applied to the blotted PVDF membrane following the primary antibody reaction (Boster Biological Technology Co. Ltd.). The ECL chemiluminescence western blot detection technique was carried out *via* the use of a gel imaging device and ImageJ.

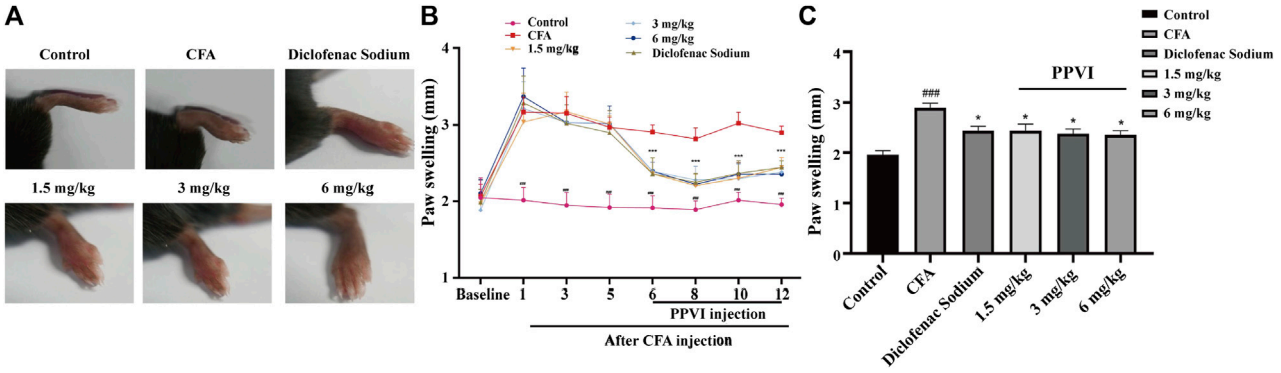


FIGURE 5
Effect of administration of PPVI on the foot swelling of CFA-induced chronic neuroinflammatory pain mice. **(A)** The foot swelling of mice in each group was detected on the 12 days after CFA injection. **(B)** The foot swelling of mice in each group was detected on the day before CFA injection, 1, 3, and 5 days after injection, and 1, 3, 5, and 7 days after PPVI administration, $n = 10$ in each group. **(C)** The foot swelling of mice in each group was detected 12 days after the CFA injection. Data are presented as mean ± S.E.M, significant differences among different groups are indicated as ###$p < 0.001$, vs. control; *$p < 0.05$ vs. CFA group.

## 2.12 Histology and immunohistochemistry

### 2.12.1 Hematoxylin-eosin staining

The DRG and spinal cord tissue of the $L_3$-$L_5$ segment of mice were fixed in 4% paraformaldehyde for 24 h, dehydrated in the order of 75%, 85%, and 95% alcohol for 2 h, dehydrated with absolute ethanol I, II for 30 min. Anhydrous ethanol-xylene and xylene were dehydrated for 10 min respectively, and then transferred to 58°C paraffin wax I, II, and III for 1 h. Tissues were embedded using a Leica embedding machine and then placed in a −20°C freezer until the paraffin solidified. The DRG and spinal cord were cut into 5 μm thick wax slices with a microtome, placed in a 60 oven for 20 min, and then soaked in xylene for 20 min to completely remove the remaining paraffin; The DRG and spinal cord slices were restored the tissue water in absolute ethanol, 95%, 85%, 75%, 50%, rinsed for 3 min and put in hematoxylin staining for 3 min, rinsed with tap water for 3 min, exposed to 1% alcohol hydrochloric acid to differentiate for 5 s, and waited for the tissue to turn red before rinsing in distilled water. Hematoxylin and eosin-stained sections of the DRG and spinal cord were observed under an optical microscope and scanned with a pathological slide scanner.

### 2.12.2 Immunohistochemistry

Mice underwent intra-cardiac perfusion with 4% paraformaldehyde for tissue fixation. $L_3$-$L_5$ segment DRGs and spinal cord were dissected and placed in 4% paraformaldehyde, fixed at room temperature for 6 h. Fixed DRG and spinal cord preparations were cut into 5um thick slices and dried in an incubator set to 50°C to 60°C for 20 min. The slices were subjected to a 5-min soak in absolute ethanol twice, followed by 2-min soaks in 95%, 80%, and 70% ethanol, and 5 min in distilled water. 3% $H_2O_2$ solution was added for 10 min. Subsequently, DRG and spinal cord slices were washed three times and rinsed with PBS for 5 min. Goat serum was added for blocking for 45 min. Slices were incubated with primary antibody against $P2X_3$ receptors (Abcam, ab300493) at 1: 200 dilutions overnight at 4°C, washed, incubated with HRP-conjugated secondary antibody (goat polyclonal; Abcam; 1: 200) for 40 min, washed, soaked in DAB solution for 3 min, mounted on neutral gum and observed under an optical microscope and scanned with a pathological slide scanner.

## 2.13 Statistical analysis

The means and standard error of means (SEM) for each outcome are shown. The GraphPad Prism 8.0 program was used for statistical analysis. Independent-sample t-tests were used to assess potential differences between any given pair of groups. Tukey's *post hoc* analysis was performed to examine differences between any two groups using a one-way analysis of variance (ANOVA). Two-way repeated ANOVA was used to compare different groups, and then Tukey's *post hoc* analysis was conducted. The $p < 0.05$ significance level was used for the whole experiment.

# 3 Results

## 3.1 Screening and identification of active compounds in PPVI using cell membrane immobilized chromatography

First, we identified the primary components of the CL extract by HPLC-MS. Seven primary peaks were discovered in the CL extract HPLC with two peaks matching the standard solution PPVI and PPI (Figures 2A, B). CL was further analyzed with HPLC-DAD-TOF/MS to reveal these substances in the CL extract (Figure 2C), identified by comparing the retention time (tR), UV absorption traits, and mass spectra with those in the literature and/or those of known reference compounds (Qin et al., 2018; Guan et al., 2021; Xie et al., 2021) to provide a preliminary compounds description (Table 2). These ingredients are Gracillin, Dioscin, Polyphyllin H, Polyphyllin I, Polyphyllin V, Polyphyllin VI, and Polyphyllin F. Second, we compared the components of U272 cells before and after overexpressing the $P2X_3$ receptor, and screened out the

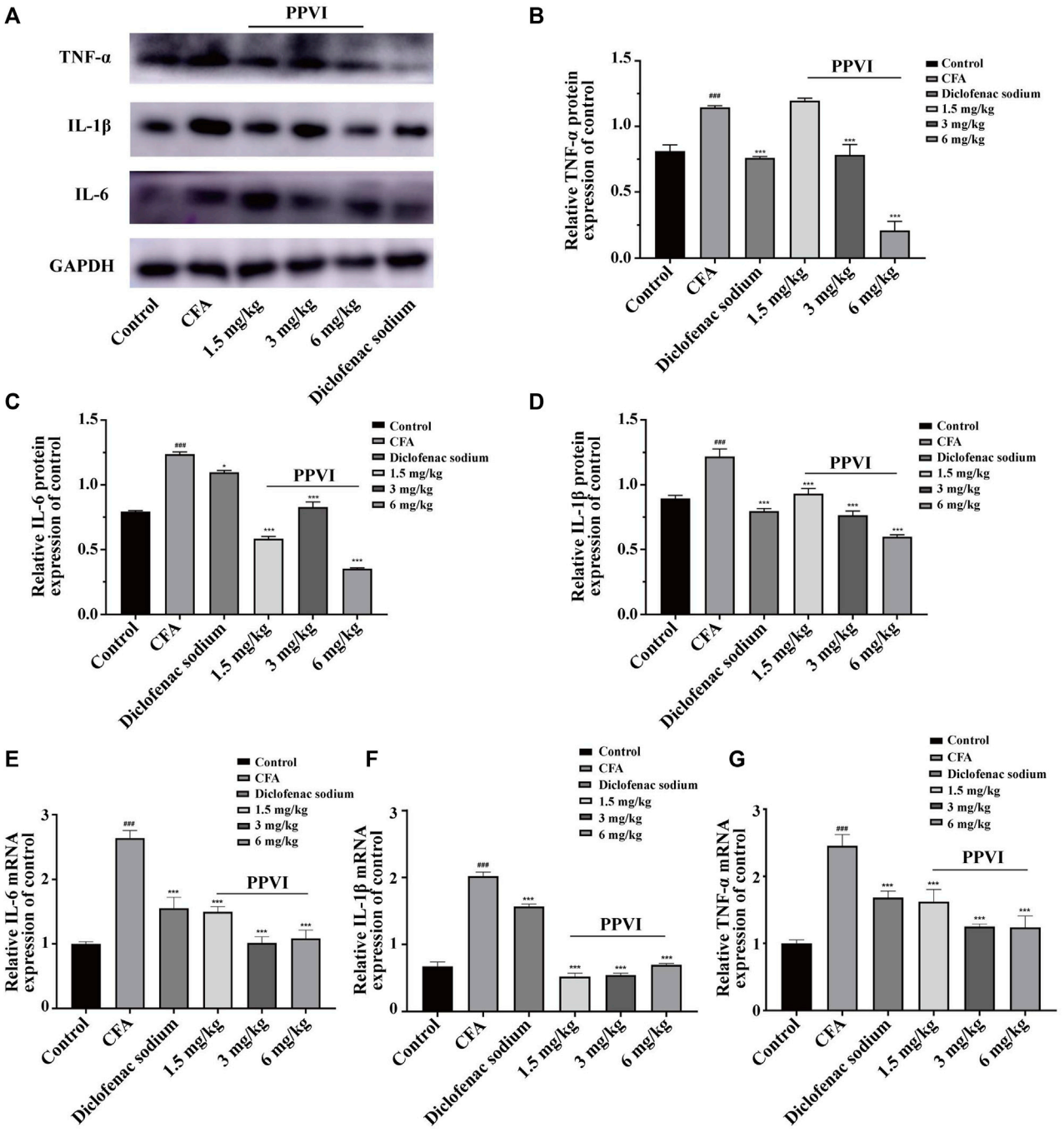


FIGURE 6
Effect of administration of PPVI on the expression of inflammatory factors IL−1β, IL-6, TNF-α in CFA-induced chronic neuroinflammatory pain mice. **(A–D)** The protein expression of inflammatory factors IL−1β, IL-6, and TNF-α in each group ($n$ = 10). **(E–G)** The mRNA expression of inflammatory factors IL−1β, IL-6, and TNF-α in each group ($n$ = 10). Data are presented as mean ± S.E.M, significant differences among different groups are indicated as ###$p$ < 0.001, vs. control; *$p$ < 0.05, **$p$ < 0.01, ***$p$ < 0.001 vs. CFA group.

components with the greatest difference. No peaks were seen in the eluate of the sixth washing (Figures 2D, E). However, in the dissociative eluate of the U373 cells overexpressing $P2X_3$, the PPVI response value in the HPLC was relatively increased compared with the control U373 cells (Figures 2F, G). These results indicated that PPVI could interact with $P2X_3$ receptors.

## 3.2 Molecular docking of PPVI and $P2X_3$ receptor

Molecular docking was applied to validate the binding of $P2X_3$ receptors to seven active compounds shown in Table 3. Dioscin, Polyphyllin H, Polyphyllin I, Polyphyllin V, Polyphyllin VI, and

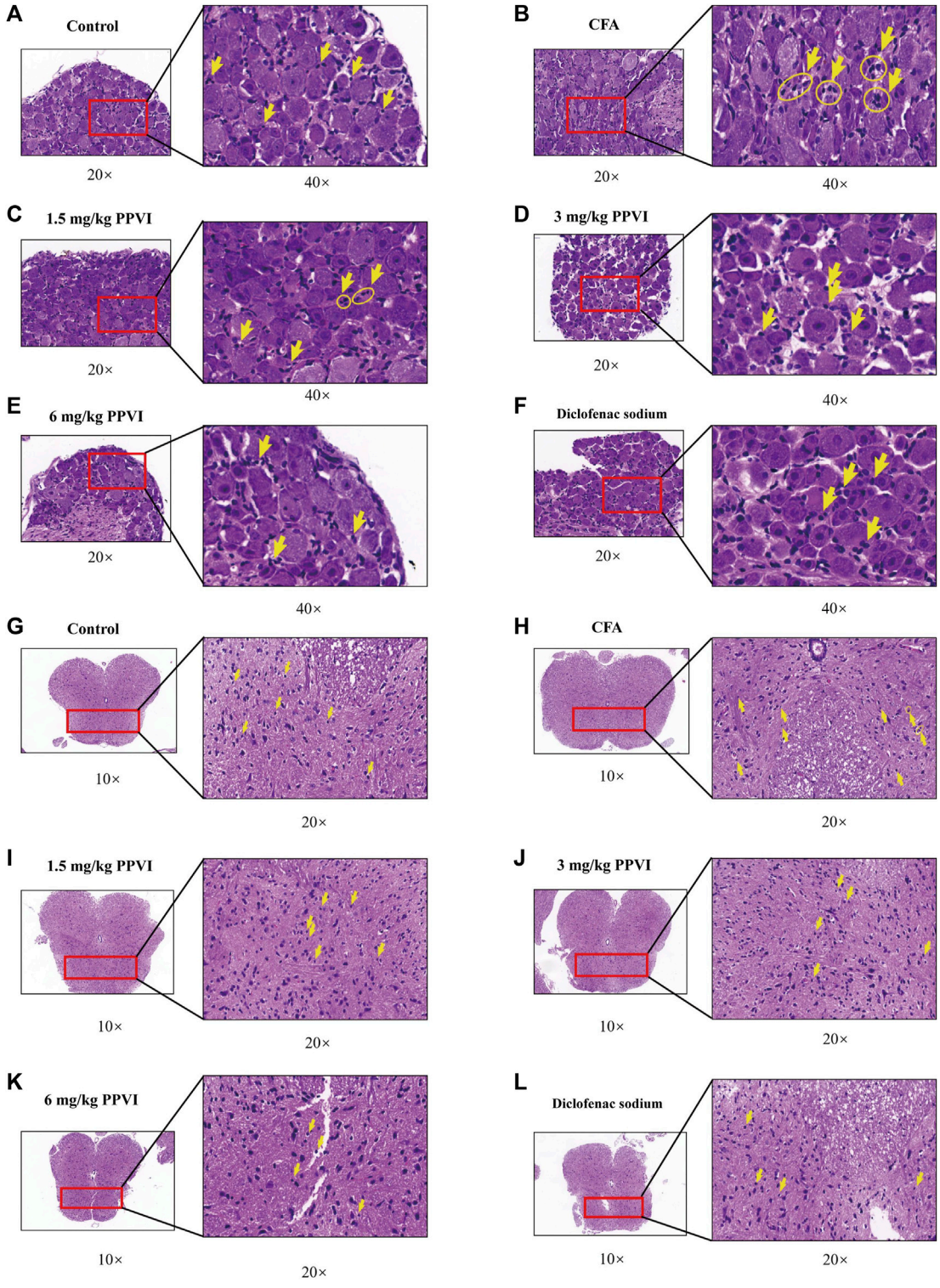


FIGURE 7
HE staining of DRG and spinal cord. **(A–F)** The HE staining of DRG in nerve cells in each group was detected by microscope (×200, ×400). **(G–L)** The HE staining of the spinal cord in nerve cells in each group was detected by microscope (×100, ×200).

Polyphyllin F are compatible with the structure of the $P2X_3$ receptor, had binding energies of −12.0, −11.7, −11.6, −11.2, −10.8, and −10.6 kcal/mol, respectively, showing good binding of the receptor to the ligand by considering the absolute affinity value with >6 kcal/mol as the selected standard, implying a possible modulatory role (Figures 3A–F).

### 3.3 Effects of the PPVI on thermal withdrawal latency and mechanical withdrawal threshold in CFA-induced pain mice

The results of TWL and MWT are shown in Figure 6 and the TWL (Figure 4A) and MWT (Figure 4C) were assessed in mice before modeling on days 1, 3, and 5 after the CFA injection. We found significant differences between the CFA group, the PPVI treatment group (1.5 mg/kg, 3 mg/kg, 6 mg/kg), and the diclofenac sodium group as compared to the control group, supporting the validity of the CFA paradigm. The TWL (Figure 4B) and MWT (Figure 4D) of mice in the PPVI administration group and the diclofenac sodium group were significantly higher than that of mice in the CFA group ($p < 0.001$). In the 1.5 mg/kg PPVI administration group analgesic effect was comparable to that of the diclofenac sodium group.

### 3.4 Effects of PPVI on foot swelling in CFA-induced chronic neuroinflammatory pain mice

The paw swelling was assessed in mice before pharmacological treatment on days 1, 3, and 5 following the CFA injection. The paws of the mice were swollen with significant differences (Figure 5) between the CFA, PPVI treatment group (1.5 mg/kg, 3 mg/kg, and 6 mg/kg), and diclofenac sodium group as compared to the control group, proving the validity of the CFA paradigm. Then, for 7 days, the PPVI group and the diclofenac sodium group received PPVI and diclofenac sodium injections, while the CFA and control groups received normal saline injections, while the left paw swelling was continuously monitored. The paw swelling of the mice in the PPVI groups (1.5 mg/kg, 3 mg/kg, and 6 mg/kg) and the diclofenac sodium group was significantly attenuated (Figures 5A–C).

### 3.5 Effects of PPVI on the expression of pro-inflammatory factors in CFA-induced chronic neuroinflammatory pain mice

To verify the anti-inflammatory effect of PPVI on DRGs and the spinal cord in CFA-induced mice, we performed assays using WB and qPCR. The results showed that the protein expression (Figures 6A–D) and mRNA expression (Figures 6E–G) of IL-1β, IL-6, and TNF-α of DRGs and spinal cord in CFA-induced mice were significantly increased compared with the control group. However, after 7 days of treatment with PPVI (1.5 mg/kg, 3 mg/kg, and 6 mg/kg), the expression of the IL-1β, and IL-6, TNF-α were normalized compared with the CFA-induced mice group.

### 3.6 Effects of PPVI on neural cells in DRG and spinal cord in CFA-induced inflammatory pain mice

HE-stained DRG and spinal cord sections are shown in Figure 7. Few inflammatory cells were observed in $L_3$-$L_5$ DRGs, while in the CFA group DRGs contained neutrophils, lymphocytes and macrophages gathered into small clusters (Figures 7A, B). After treatment with 1.5 mg/kg, 3 mg/kg, and 6 mg/kg PPVI, the presence of these inflammatory cells was significantly reduced in $L_3$-$L_5$ DRGs (Figures 7C–F). The distribution of glial cells is relatively uniform in the dorsal horn of the $L_3$-$L_5$ spinal cord of the control group. In contrast in the CFA group, aggregation of glial cells with pyknosis and vacuolization of neurons were observed in the dorsal horn of the $L_3$-$L_5$ spinal cord (Figures 7G, H indicated with an arrow). However, treatment with 1.5 mg/kg, 3 mg/kg, and 6 mg/kg PPVI reversed these changes (Figure 7I–L).

### 3.7 PPVI affects the expression of $P2X_3$ receptors in DRG of CFA pain mice

Immunohistochemistry showed that the expression of $P2X_3$ receptors in $L_3$-$L_5$ DRGs from CFA mice was significantly increased compared with the control group (Figures 8A, B). However, treatment with PPVI (1.5 mg/kg, 3 mg/kg, and 6 mg/kg) and diclofenac sodium restored the expression of $P2X_3$ receptors to control levels (Figures 8C–F) which is a significant difference compared with the CFA group. Further WB analysis showed that expression of $P2X_3$ in DRGs was significantly upregulated in CFA mice compared with the control group and treatment with PPVI (1.5 mg/kg, 3 mg/kg, and 6 mg/kg) and diclofenac sodium restored the expression of $P2X_3$ receptors in $L_3$-$L_5$ DRGs (Figures 8G–I).

### 3.8 PPVI normalized expression of $P2X_3$ receptors in the dorsal horn of the spinal cord in CFA-induced pain mice

We also analyzed the effect of PPVI on the expression of $P2X_3$ receptors in the $L_3$-$L_5$ spinal cord of CFA-induced pain mice. Compared with the control group, the expression of $P2X_3$ receptors in the dorsal horn of the spinal cord of CFA mice was significantly upregulated (Figures 9A,B). However, treatment with PPVI (1.5 mg/kg, 3 mg/kg, and 6 mg/kg) and diclofenac sodium restored the expression of $P2X_3$ receptors (Figures 9C–F). Further WB analysis showed increased protein expression of $P2X_3$ receptors in the dorsal horn of CFA mice compared with the control group. However, treatment with PPVI (1.5 mg/kg, 3 mg/kg, and 6 mg/kg) and diclofenac sodium restored the protein expression of $P2X_3$ receptors (Figures 9G–I).

## 4 Discussion

*Polyphylla* var. *yunnanensis* is widely used as an anti-tumor treatment in traditional Chinese medicine (He et al., 2015). A recent study found that Rhizoma Paridis saponins extract from *Polyphylla* var. *yunnanensis* demonstrates analgesic effects in a mouse model of chronic cancer pain (Wang G. et al., 2018), although underlying mechanisms and the active ingredients of *Polyphylla* var. *yunnanensis* remain unknown. In this study, the

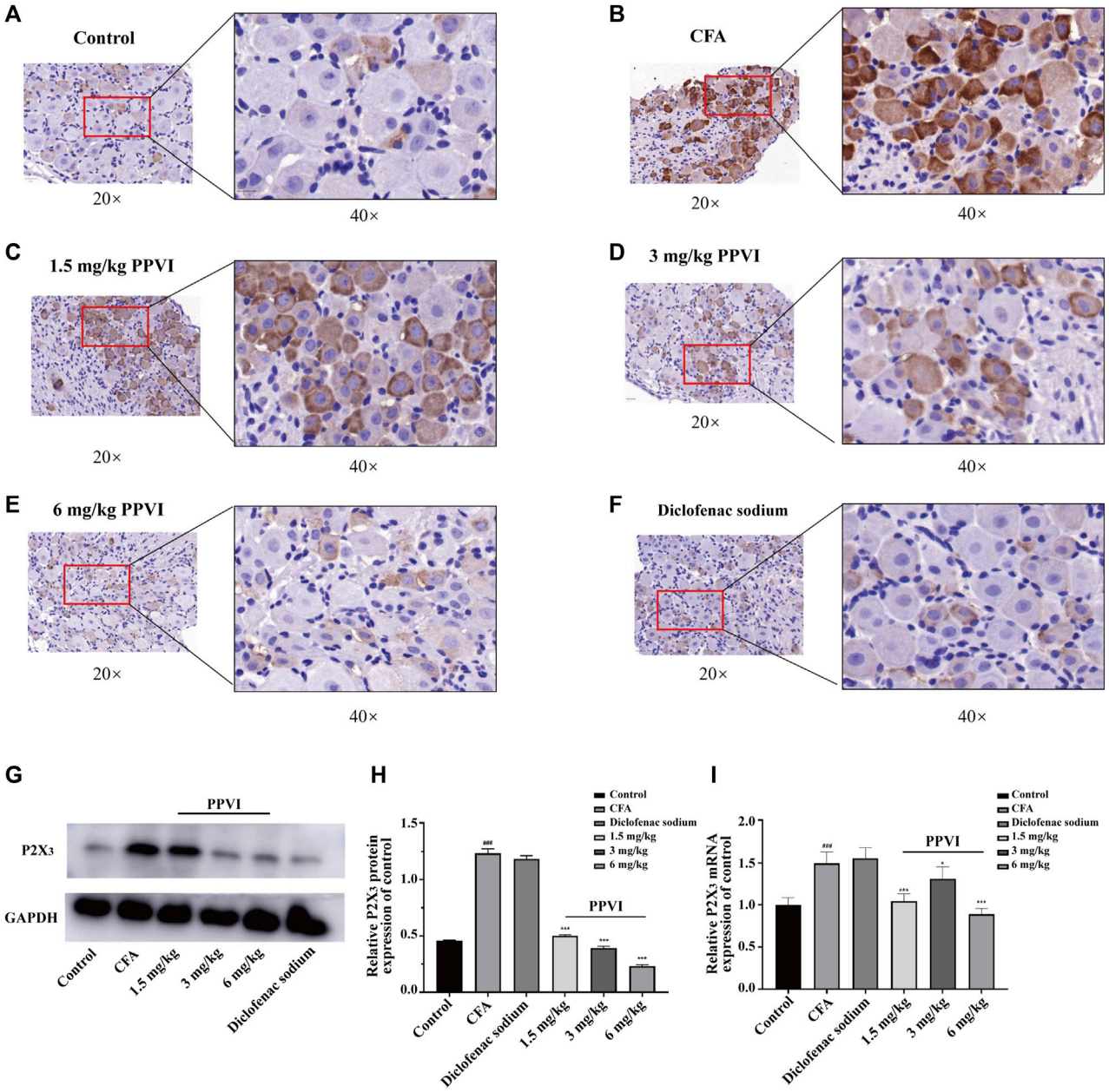


FIGURE 8
Effect of administration of PPVI on the expression of $P2X_3$ of DRG in CFA-induced chronic neuroinflammatory pain mice. **(A–F)** The expression of $P2X_3$ in nerve cells in each group was detected by immunohistochemistry ($n$ = 3). **(G–I)** The protein and mRNA expression of $P2X_3$ detected by western blot and qPCR in each group ($n$ = 10). Data are presented as mean ± S.E.M, significant differences among different groups are indicated as ###$p$ < 0.001, vs. control; *$p$ < 0.05, **$p$ < 0.001 vs. CFA group.

*Polyphylla* var. *yunnanensis* extract contained seven main active ingredients: Dioscin, Polyphyllin H, Polyphyllin I, Polyphyllin V, Polyphyllin VI, and Polyphyllin F. In glioblastoma or glial cells, little or no $P2X_3$ receptors were expressed since $P2X_3$ is specific for sensory neurons (Inoue and Tsuda, 2021). Therefore, we used the U373 cells overexpressing $P2X_3$ receptors to compare the differences between the U373 cells overexpressing $P2X_3$ and normal U373 cells to observe the dissociated fluid components caused by the increase of $P2X_3$ receptors. Combining the results of the docking of $P2X_3$ and active molecules, we initially screened the main active ingredient polyphyllin VI in the Chonglou extract that may have a regulatory effect on the $P2X_3$ receptor.

A suspension of whole or crushed, heat-inactivated mycobacteria is present in mineral oil that is used to make CFA (Stills, 2005). Stimulation of the immune response, which results in delayed hypersensitivity at the injection site, as well as significant inflammatory reactions and hyperalgesia induces chronic pain. (Sadler et al., 2022).

Changes in functional expression of $P2X_3$ receptors are closely related to inflammation, while CFA injections or

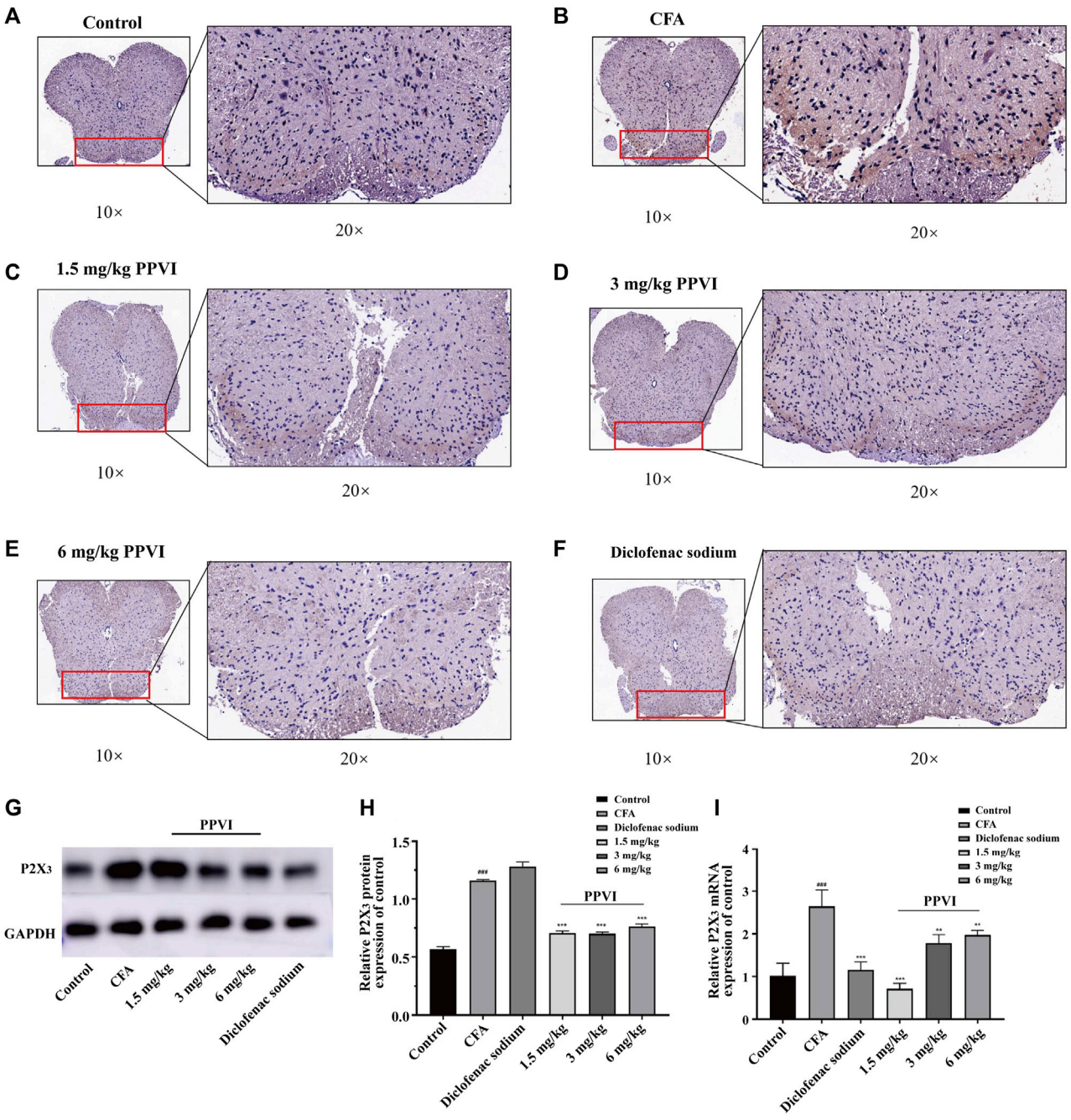


FIGURE 9
Effect of administration of PPVI on the expression of $P2X_3$ of the spinal cord in CFA-induced chronic neuroinflammatory pain mice. **(A–F)** The expression of $P2X_3$ in nerve cells in each group was detected by immunohistochemistry ($n$ = 3). **(G–I)** The protein and mRNA expression of $P2X_3$ detected by western blot and qPCR in each group ($n$ = 10). Data are presented as mean ± S.E.M, significant differences among different groups are indicated as ###$p$ < 0.001, vs. control; *$p$ < 0.05, **$p$ < 0.01, ***$p$ < 0.001 vs. CFA group.

chronic nerve compression and temporal mandibular joint disorders increase the expression of $P2X_3$ receptors (Xu and Huang, 2002; Ambalavanar et al., 2005; Shinoda et al., 2005). Intrathecal injection of $P2X_3$ receptor agonist α, $\beta$-meATP enhances pain behavior (Xiang et al., 2008), while intrathecal injection of $P2X_3$ receptor antagonist A-317491 or treatment with antisense $P2X_3$ receptor oligonucleotides significantly reduces formalin- or α,$\beta$-meATP injection-induced nociceptive behavior and nociceptive inflammatory response in DRG and spinal cord after partial sciatic nerve ligation, CFA adjuvant, formalin or α,$\beta$-meATP injection into the skin (Barclay et al., 2002; Hemmings-Mieszczak et al., 2003; McGaraughty et al., 2003; Pissanetzky, 2016). In addition, inflammatory cytokines IL-1, IL-6, and TNF-α also contribute to the pathophysiology of

chronic pain (del Rey et al., 2012; Li et al., 2017; Yang et al., 2020). Inflammatory cytokines have a role in peripheral inflammation, a key contributor to chronic pain. IL-1, IL-6, and TNF-α, that can trigger immunopathological reactions and intensify inflammatory signals, are particularly important (del Rey et al., 2012; Burnstock, 2016; Yang et al., 2020).

Several cell types in DRG and the spinal cord, including immune cells, neurons, and glial cells, produce IL-1 in response to peripheral nerve injury (Liddelow et al., 2017; Voet et al., 2019; Trapero and Martin-Satue, 2020). Increased expression of $P2X_3$ receptors may potentiate the production of IL-1, which intensifies the inflammatory response of microglia in the spinal cord (Shieh et al., 2006). Hypomethylation of the $P2X_3$ receptor gene promoter regions in rat tumor cells improves the binding of members of the NF-κB family of transcriptional regulators and increases pain sensitivity, which (Zhou et al., 2015). These studies suggest that inflammation can upregulate the expression of $P2X_3$ in sensory nerves, while the activation of $P2X_3$ can promote the secretion of inflammatory factors. This study found that PPVI reduced CFA mice paw edema and pain threshold, indicating a significant analgesic effect. Further experiments showed that PPVI reduced the number of inflammatory cells in DRG and downregulated the inflammatory factors TNF-α, IL-1β, and IL-6 expression in DRG and spinal cord of CFA mice. Subsequently, we demonstrated that PPVI inhibited $P2X_3$ expression in the DRG and spinal cord of CFA mice, indicating that the analgesic effect is linked to the decrease in $P2X_3$ receptors expression and the decrease in inflammatory cytokines. However, further research is still needed to investigate how PPVI regulates the signaling pathway between $P2X_3$ and inflammation in DRG and the spinal cord.

## 5 Conclusion

In summary, by using molecular docking technology and U373 cells overexpressing $P2X_3$ receptors combined with the cell membrane immobilized chromatography we identified PPVI as the main active component of CL. PPVI increases the mechanical and thermal withdrawal threshold of CFA-induced pain mice and relieves the pain and foot swelling. In addition, PPVI downregulates the expression of TNF-α, IL-1β, and IL-6 in DRG and spinal cord to alleviate the inflammation; PPVI also normalizes the expression of $P2X_3$ purinoceptors. Our work provides insight into the potential new targets of PPVI for the treatment of inflammatory pain.

## Data availability statement

The datasets presented in this study can be found in online repositories. The names of the repository/repositories and accession number(s) can be found in the article/supplementary material.

## Ethics statement

The animal study was reviewed and approved by Jinan University Animal Ethics Committee.

## Author contributions

Conceptualization, ZL, and TW; Funding acquisition, AV and HN; Investigation, HZ, TW, and ZZ; Methodology LL JP and TZ; Formal analysis ZL, ZZ, CZ, and TW; Supervision, AV, ZL, PL, SL, and HN; Writing—original draft, ZL, and TW; Writing—review and editing, ZL, NL, TW, and HN. All authors have read and agreed to the published version of the manuscript. ZL and TW contributed equally to this work.

## Funding

This study was supported by grants from the National Natural Science Foundation of China (No. 8181101216).

## Conflict of interest

The authors declare that the research was conducted in the absence of any commercial or financial relationships that could be construed as a potential conflict of interest.

## Publisher's note

All claims expressed in this article are solely those of the authors and do not necessarily represent those of their affiliated organizations, or those of the publisher, the editors and the reviewers. Any product that may be evaluated in this article, or claim that may be made by its manufacturer, is not guaranteed or endorsed by the publisher.

## References

Ahmad, B., Rehman, S. U., Azizullah, A., Khan, M. F., Din, S. R. U., Ahmad, M., et al. (2021). Molecular mechanisms of anticancer activities of polyphyllin VII. *Chem. Biol. Drug Des.* 97 (4), 914–929. doi:10.1111/cbdd.13818

Ambalavanar, R., Moritani, M., and Dessem, D. (2005). Trigeminal P2X3 receptor expression differs from dorsal root ganglion and is modulated by deep tissue inflammation. *Pain* 117 (3), 280–291. doi:10.1016/j.pain.2005.06.029

Barclay, J., Patel, S., Dorn, G., Wotherspoon, G., Moffatt, S., Eunson, L., et al. (2002). Functional downregulation of P2X3 receptor subunit in rat sensory neurons reveals a significant role in chronic neuropathic and inflammatory pain. *J. Neurosci.* 22 (18), 8139–8147. doi:10.1523/JNEUROSCI.22-18-08139.2002

Bouhassira, D. (2019). Neuropathic pain: Definition, assessment and epidemiology. *Rev. Neurol.* 175 (1-2), 16–25. doi:10.1016/j.neurol.2018.09.016

Burnstock, G. (2016). Purinergic mechanisms and pain. *Adv. Pharmacol.* 75, 91–137. doi:10.1016/bs.apha.2015.09.001

Butler, S. G., and Meegan, M. J. (2008). Recent developments in the design of anti-depressive therapies: Targeting the serotonin transporter. *Curr. Med. Chem.* 15 (17), 1737–1761. doi:10.2174/092986708784872357

Chaplan, S. R., Bach, F. W., Pogrel, J. W., Chung, J. M., and Yaksh, T. L. (1994).Quantitative assessment of tactile allodynia in the rat paw. *J. Neurosci. Methods* 53 (1), 55–63. doi:10.1016/0165-0270(94)90144-9

del Rey, A., Apkarian, A. V., Martina, M., and Besedovsky, H. O. (2012). Chronic neuropathic pain-like behavior and brain-borne IL-1β. *Ann. N. Y. Acad. Sci.* 1262 (1), 101–107. doi:10.1111/j.1749-6632.2012.06621.x

Demir, I. E., Schafer, K. H., Tieftrunk, E., Friess, H., and Ceyhan, G. O. (2013). Neural plasticity in the gastrointestinal tract: Chronic inflammation, neurotrophic signals, and hypersensitivity. *Acta Neuropathol.* 125 (4), 491–509. doi:10.1007/s00401-013-1099-4

Escartin, C., Galea, E., Lakatos, A., O'Callaghan, J. P., Petzold, G. C., Serrano-Pozo, A., et al. (2021). Reactive astrocyte nomenclature, definitions, and future directions. *Nat. Neurosci.* 24 (3), 312–325. doi:10.1038/s41593-020-00783-4

Finnerup, N. B., Kuner, R., and Jensen, T. S. (2021). Neuropathic pain: From mechanisms to treatment. *Physiol. Rev.* 101 (1), 259–301. doi:10.1152/physrev.00045.2019

Guan, L., Ju, B., Zhao, M., Zhu, H., Chen, L., Wang, R., et al. (2021). Influence of drying process on furostanoside and spirostanoside profiles of Paridis Rhizoma by combination of HPLC, UPLC and UPLC-QTOF-MS/MS analyses. *J. Pharm. Biomed. Anal.* 197, 113932. doi:10.1016/j.jpba.2021.113932

He, H., Sun, Y. P., Zheng, L., and Yue, Z. G. (2015). Steroidal saponins from Paris polyphylla induce apoptotic cell death and autophagy in A549 human lung cancer cells. *Asian Pac J. Cancer Prev.* 16 (3), 1169–1173. doi:10.7314/apjcp.2015.16.3.1169

Hemmings-Mieszczak, M., Dorn, G., Natt, F. J., Hall, J., and Wishart, W. L. (2003). Independent combinatorial effect of antisense oligonucleotides and RNAi-mediated specific inhibition of the recombinant rat P2X3 receptor. *Nucleic Acids Res.* 31 (8), 2117–2126. doi:10.1093/nar/gkg322

Inoue, K. (2021). Nociceptive signaling of P2X receptors in chronic pain states. *Purinergic Signal* 17 (1), 41–47. doi:10.1007/s11302-020-09743-w

Inoue, K., and Tsuda, M. (2021). Nociceptive signaling mediated by P2X3, P2X4 and P2X7 receptors. *Biochem. Pharmacol.* 187, 114309. doi:10.1016/j.bcp.2020.114309

Jarvis, M. F. (2003). Contributions of P2X3 homomeric and heteromeric channels to acute and chronic pain. *Expert Opin. Ther. Targets* 7 (4), 513–522. doi:10.1517/14728222.7.4.513

Jorge, C. O., de Azambuja, G., Gomes, B. B., Rodrigues, H. L., Luchessi, A. D., and de Oliveira-Fusaro, M. C. G. (2020). P2X3 receptors contribute to transition from acute to chronic muscle pain. *Purinergic Signal* 16 (3), 403–414. doi:10.1007/s11302-020-09718-x

Kaan, T. K., Yip, P. K., Patel, S., Davies, M., Marchand, F., Cockayne, D. A., et al. (2010). Systemic blockade of P2X3 and P2X2/3 receptors attenuates bone cancer pain behaviour in rats. *Brain* 133 (9), 2549–2564. doi:10.1093/brain/awq194

Kwon, S. J., Ahn, D., Yang, H. M., Kang, H. J., and Chung, S. J. (2021). Polyphyllin D shows anticancer effect through a selective inhibition of src homology region 2-containing protein tyrosine phosphatase-2 (SHP2). *Molecules* 26 (4), 848. doi:10.3390/molecules26040848

Li, Q. Y., Xu, H. Y., and Yang, H. J. (2017). Effect of proinflammatory factors TNF-α,IL-1β, IL-6 on neuropathic pain. *Zhongguo Zhong Yao Za Zhi* 42 (19), 3709–3712. doi:10.19540/j.cnki.cjcmm.20170907.004

Liddelow, S. A., Guttenplan, K. A., Clarke, L. E., Bennett, F. C., Bohlen, C. J., Schirmer, L., et al. (2017). Neurotoxic reactive astrocytes are induced by activated microglia. *Nature* 541 (7638), 481–487. doi:10.1038/nature21029

Luo, Z., Zeng, A., Chen, Y., He, S., He, S., Jin, X., et al. (2021). Ligustilide inhibited Angiotensin II induced A7r5 cell autophagy via Akt/mTOR signaling pathway. *Eur. J. Pharmacol.* 905, 174184. doi:10.1016/j.ejphar.2021.174184

Malcangio, M. (2019). Role of the immune system in neuropathic pain. *Scand. J. Pain* 20 (1), 33–37. doi:10.1515/sjpain-2019-0138

Man, S., Fan, W., Gao, W., Li, Y., Wang, Y., Liu, Z., et al. (2014). Anti-fibrosis and anti-cirrhosis effects of Rhizoma paridis saponins on diethylnitrosamine induced rats. *J. Ethnopharmacol.* 151 (1), 407–412. doi:10.1016/j.jep.2013.10.051

McGaraughty, S., Wismer, C. T., Zhu, C. Z., Mikusa, J., Honore, P., Chu, K. L., et al. (2003). Effects of A-317491, a novel and selective P2X3/P2X2/3 receptor antagonist, on neuropathic, inflammatory and chemogenic nociception following intrathecal and intraplantar administration. *Br. J. Pharmacol.* 140 (8), 1381–1388. doi:10.1038/sj.bjp.0705574

Nie, H., Meng, L.-z., Zhang, H., Zhang, J.-y., Yin, Z., and Huang, X.-s. (2008). Analysis of anti-platelet aggregation components of Rhizoma Zingiberis using chicken thrombocyte extract and high performance liquid chromatography. *Chin. Med. J.* 121 (13), 1226–1229. doi:10.1097/00029330-200807010-00015

Nie, H., Zhang, H., Zhang, X. Q., Luo, Y., Meng, L. Z., Yin, Z., et al. (2011). Relationship between HPLC fingerprints and *in vivo* pharmacological effects of a traditional Chinese medicine: Radix Angelicae Dahuricae. *Nat. Prod. Res.* 25 (1), 53–61. doi:10.1080/14786419.2010.490784

Pang, D., Yang, C., Li, C., Zou, Y., Feng, B., Li, L., et al. (2020). Polyphyllin II inhibits liver cancer cell proliferation, migration and invasion through downregulated cofilin activity and the AKT/NF-κB pathway. *Biol. Open* 9 (2), bio046854. doi:10.1242/bio.046854

Pissanetzky, S. (2016). On the future of information: Reunification, computability, adaptation, cybersecurity, semantics. *IEEE Access* 4, 1117–1140. doi:10.1109/access.2016.2524403

Qin, X. J., Ni, W., Chen, C. X., and Liu, H. Y. (2018). Seeing the light: Shifting from wild rhizomes to extraction of active ingredients from above-ground parts of Paris polyphylla var. yunnanensis. *J. Ethnopharmacol.* 224, 134–139. doi:10.1016/j.jep.2018.05.028

Qiumin, H., Biao, X., Weihong, W., Chongyun, B., and Shaowei, H. (2017). Inhibitory effect and underlying mechanism of total saponins from Paris polyphylla var. yunnanensis on the proliferation of salivary adenoid cystic carcinoma ACC-83 cells. *Hua Xi Kou Qiang Yi Xue Za Zhi* 35 (3), 317–321. doi:10.7518/hxkq.2017.03.016

Raja, S. N., Carr, D. B., Cohen, M., Finnerup, N. B., Flor, H., Gibson, S., et al. (2020). The revised international association for the study of pain definition of pain: Concepts, challenges, and compromises. *Pain* 161 (9), 1976–1982. doi:10.1097/j.pain.0000000000001939

Ronchetti, S., Migliorati, G., and Delfino, D. V. (2017). Association of inflammatory mediators with pain perception. *Biomed. Pharmacother.* 96, 1445–1452. doi:10.1016/j.biopha.2017.12.001

Sadler, K. E., Mogil, J. S., and Stucky, C. L. (2022). Innovations and advances in modelling and measuring pain in animals. *Nat. Rev. Neurosci.* 23 (2), 70–85. doi:10.1038/s41583-021-00536-7

Shieh, C. C., Jarvis, M. F., Lee, C. H., and Perner, R. J. (2006). P2X receptor ligands and pain. *Expert Opin. Ther. Pat.* 16 (8), 1113–1127. doi:10.1517/13543776.16.8.1113

Shinoda, M., Ozaki, N., Asai, H., Nagamine, K., and Sugiura, Y. (2005). Changes in P2X3 receptor expression in the trigeminal ganglion following monoarthritis of the temporomandibular joint in rats. *Pain* 116 (1-2), 42–51. doi:10.1016/j.pain.2005.03.042

Stills, H. F., Jr. (2005). Adjuvants and antibody production: Dispelling the myths associated with freund's complete and other adjuvants. *ILAR J.* 46 (3), 280–293. doi:10.1093/ilar.46.3.280

Taneja, A., Della Pasqua, O., and Danhof, M. (2017). Challenges in translational drug research in neuropathic and inflammatory pain: The prerequisites for a new paradigm. *Eur. J. Clin. Pharmacol.* 73 (10), 1219–1236. doi:10.1007/s00228-017-2301-8

Teng, J. F., Mei, Q. B., Zhou, X. G., Tang, Y., Xiong, R., Qiu, W. Q., et al. (2020). Polyphyllin VI induces caspase-1-mediated pyroptosis via the induction of ROS/NF-κB/NLRP3/GSDMD signal Axis in non-small cell lung cancer. *Cancers (Basel)* 12 (1), 193. doi:10.3390/cancers12010193

Tian, Y., Gong, G. Y., Ma, L. L., Wang, Z. Q., Song, D., and Fang, M. Y. (2020). Anti-cancer effects of Polyphyllin I: An update in 5 years. *Chem. Biol. Interact.* 316, 108936. doi:10.1016/j.cbi.2019.108936

Trapero, C., and Martin-Satue, M. (2020). Purinergic signaling in endometriosis-associated pain. *Int. J. Mol. Sci.* 21 (22), 8512. doi:10.3390/ijms21228512

Trott, O., and Olson, A. J. (2010). AutoDock vina: Improving the speed and accuracy of docking with a new scoring function, efficient optimization, and multithreading. *J. Comput. Chem.* 31 (2), 455–461. doi:10.1002/jcc.21334

van Hecke, O., Austin, S. K., Khan, R. A., Smith, B. H., and Torrance, N. (2014). Neuropathic pain in the general population: A systematic review of epidemiological studies. *Pain* 155 (4), 654–662. doi:10.1016/j.pain.2013.11.013

Vergne-Salle, P., and Bertin, P. (2021). Chronic pain and neuroinflammation. *Jt. Bone Spine* 88 (6), 105222. doi:10.1016/j.jbspin.2021.105222

Voet, S., Srinivasan, S., Lamkanfi, M., and van Loo, G. (2019). Inflammasomes in neuroinflammatory and neurodegenerative diseases. *EMBO Mol. Med.* 11 (6), e10248. doi:10.15252/emmm.201810248

Wang, G., Liu, Y., Wang, Y., and Gao, W. (2018a). Effect of Rhizoma Paridis saponin on the pain behavior in a mouse model of cancer pain. *RSC Adv.* 8 (31), 17060–17072. doi:10.1039/c8ra00797g

Wang, Q., Zhou, X., Zhao, Y., Xiao, J., Lu, Y., Shi, Q., et al. (2018b). Polyphyllin I ameliorates collagen-induced arthritis by suppressing the inflammation response in macrophages through the NF-κB pathway. *Front. Immunol.* 9, 2091. doi:10.3389/fimmu.2018.02091

Xiang, Z., Xiong, Y., Yan, N., Li, X., Mao, Y., Ni, X., et al. (2008). Functional up-regulation of P2X 3 receptors in the chronically compressed dorsal root ganglion. *Pain* 140 (1), 23–34. doi:10.1016/j.pain.2008.07.006

Xie, J., Wang, R. Y., Yong, L., Gong, Y. X., Ding, L. S., Xin, Y., et al. (2021). Determination of nine nucleosides in Rhizoma Paridis by quantitative analysis of multi-components via a single marker method. *J. Sep. Sci.* 44 (9), 1866–1874. doi:10.1002/jssc.202001086

Xu, G. Y., and Huang, L. Y. (2002). Peripheral inflammation sensitizes P2X receptor-mediated responses in rat dorsal root ganglion neurons. *J. Neurosci.* 22 (1), 93–102. doi:10.1523/JNEUROSCI.22-01-00093.2002

Xu, J., Chu, K. L., Brederson, J. D., Jarvis, M. F., and McGaraughty, S. (2012). Spontaneous firing and evoked responses of spinal nociceptive neurons are attenuated by blockade of P2X3 and P2X2/3 receptors in inflamed rats. *J. Neurosci. Res.* 90 (8), 1597–1606. doi:10.1002/jnr.23042

Yan, X. X., Pan, Q. D., Sun, H. Y., Gao, L., Yang, R., and Yang, L. X. (2021). Traditional use of Paris polyphylla and its active components. *Zhongguo Zhong Yao Za Zhi* 46 (24), 6343–6352. doi:10.19540/j.cnki.cjcmm.20210901.101

Yang, Q. Q., Li, H. N., Zhang, S. T., Yu, Y. L., Wei, W., Zhang, X., et al. (2020). Red nucleus IL-6 mediates the maintenance of neuropathic pain by inducing the productions of TNF-α and IL-1β through the JAK2/STAT3 and ERK signaling pathways. *Neuropathology* 40 (4), 347–357. doi:10.1111/neup.12653

Zhang, Z., Pan, J., Zhu, T., Malewicz, N., Ye, K., Rong, J., et al. (2021). Oxymatrine screened from Sophora flavescens by cell membrane immobilized chromatography relieves histamine-independent itch. *J. Pharm. Pharmacol.* 73 (12), 1617–1629. doi:10.1093/jpp/rgab145

Zhou, N., Xu, L., Park, S. M., Ma, M. G., Choi, S. E., and Si, C. (2021). Genetic diversity, chemical components, and property of biomass Paris polyphylla var. yunnanensis. *Front. Bioeng. Biotechnol.* 9, 713860. doi:10.3389/fbioe.2021.713860

Zhou, Y. L., Jiang, G. Q., Wei, J., Zhang, H. H., Chen, W., Zhu, H., et al. (2015). Enhanced binding capability of nuclear factor-κB with demethylated P2X3 receptor gene contributes to cancer pain in rats. *Pain* 156 (10), 1892–1905. doi:10.1097/j.pain.0000000000000248

frontiers | Frontiers in Pharmacology

TYPE Review
PUBLISHED 10 March 2023
DOI 10.3389/fphar.2023.1098976



OPEN ACCESS

EDITED BY
Yong Tang,
Chengdu University of Traditional Chinese Medicine, China

REVIEWED BY
Aleksandra Korac
Shangdong Liang,
Nanchang University, China

*CORRESPONDENCE
Wei-Min Qu,
quweimin@fudan.edu.cn
Yi-Qun Wang,
yiqunwang@fudan.edu.cn
Zhi-Li Huang,
huangzl@fudan.edu.cn

†These authors have contributed equally to this work

SPECIALTY SECTION
This article was submitted to Experimental Pharmacology and Drug Discovery, a section of the journal Frontiers in Pharmacology

RECEIVED 15 November 2022
ACCEPTED 27 February 2023
PUBLISHED 10 March 2023

CITATION
Ma W-X, Yuan P-C, Zhang H, Kong L-X, Lazarus M, Qu W-M, Wang Y-Q and Huang Z-L (2023), Adenosine and P1 receptors: Key targets in the regulation of sleep, torpor, and hibernation. *Front. Pharmacol.* 14:1098976. doi: 10.3389/fphar.2023.1098976



# Adenosine and P1 receptors: Key targets in the regulation of sleep, torpor, and hibernation

Wei-Xiang Ma[1†], Ping-Chuan Yuan[2†], Hui Zhang[2†], Ling-Xi Kong[1], Michael Lazarus[3], Wei-Min Qu[1*], Yi-Qun Wang[1*] and Zhi-Li Huang[1*]

[1]State Key Laboratory of Medical Neurobiology, MOE Frontiers Center for Brain Science, Department of Pharmacology, School of Basic Medical Sciences, Institutes of Brain Science, Fudan University, Shanghai, China, [2]Anhui Provincial Engineering Research Center for Polysaccharide Drugs, Provincial Engineering Laboratory for Screening and Re-evaluation of Active Compounds of Herbal Medicines in Southern Anhui, School of Pharmacy, Wannan Medical College, Wuhu, China, [3]International Institute for Integrative Sleep Medicine (WPI-IIIS) and Faculty of Medicine, University of Tsukuba, Tsukuba, Ibaraki, Japan

Sleep, torpor, and hibernation are three distinct hypometabolic states. However, they have some similar physiological features, such as decreased core body temperature and slowing heart rate. In addition, the accumulation of adenosine seems to be a common feature before entry into these three states, suggesting that adenosine and its receptors, also known as P1 receptors, may mediate the initiation and maintenance of these states. This review, therefore, summarizes the current research on the roles and possible neurobiological mechanisms of adenosine and P1 receptors in sleep, torpor, and hibernation. Understanding these aspects will give us better prospects in sleep disorders, therapeutic hypothermia, and aerospace medicine.

KEYWORDS

**adenosine, P1 receptors, hibernation, sleep, torpor**

## 1 Introduction

Sleep, torpor, and hibernation are three distinct states which can reduce energy expenditure. Sleep, which takes up nearly one-third lifetime of most mammals and birds, is divided into rapid eye movement (REM) sleep and non-REM (NREM) sleep. REM sleep is characterized by phasic changes in various autonomic functions and an elevation in metabolic rate. However, NREM sleep is characterized by the organism's active contact with the environment and by a decrease in metabolism, body temperature ($T_b$), and energy expenditure (Silvani and Dampney, 2013; Schmidt, 2014; Silvani et al., 2018). Torpor is an energy-saving strategy in most mammals and birds, sometimes lasting only for a few hours, that helps organisms cope with the stress of an adverse environment (Ruf and Geiser, 2015). Just like NREM sleep, torpor state occurs with a reduction in $T_b$ and metabolic rate (Ruf and Geiser, 2015). Hibernation, also called multi-day torpor, is a seasonal energy conservation strategy that reduces $T_b$, energy expenditure, and water loss (Geiser, 2013; Ruf and Geiser, 2015). Most hibernators generally remain in hibernation for a winter, which helps them effectively withstand the cold environment.

Adenosine is a ubiquitous endogenous cell signal transducer and regulator, which mainly acts by activating 4 G protein-coupled receptors (GPCRs), namely, adenosine $A_1$, $A_{2A}$, $A_{2B}$, and $A_3$ receptors, as known as P1 receptors (Kazemzadeh-Narbat et al., 2015). Activation of $A_1$ and $A_3$ receptors exert inhibitory effects, however $A_{2A}$ and $A_{2B}$ exert excitatory. The four P1 receptors can reduce and increase the intracellular cyclic adenosine-3, 5 monophosphate

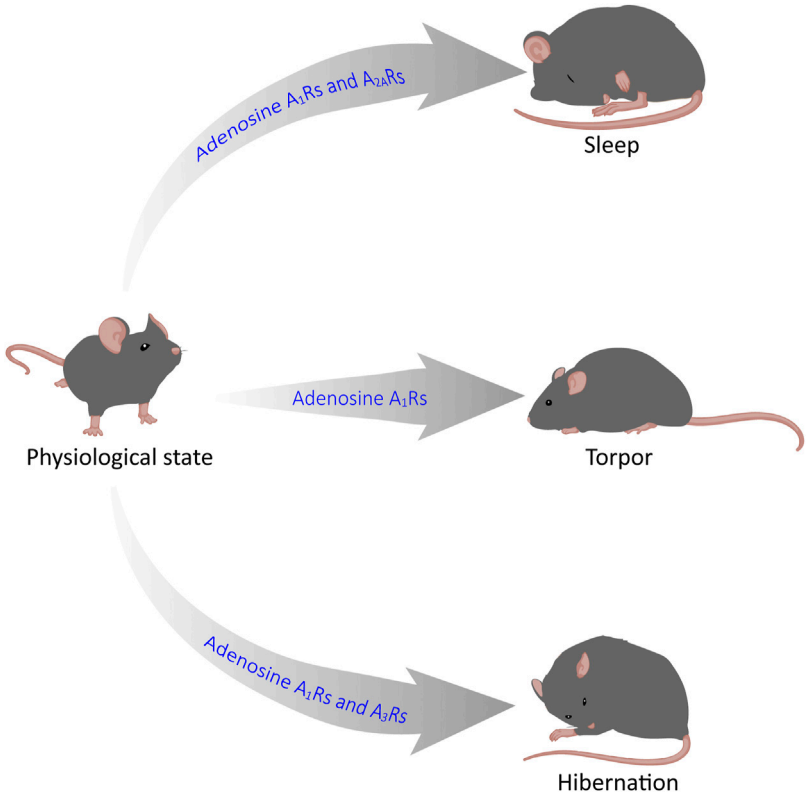


GRAPHICAL ABSTRACT
Adenosine mediates sleep, torpor and hibernation through P1 receptors. Recent reasearch has shown that P1 receptors play a vital role in the regulation of sleep-wake, torpor and hibernation-like states. In this review, we focus on the roles and neurobiological mechanisms of the CNS adenosine and P1 receptors in these three states. Among them, $A_1$ and $A_{2A}$ receptors are key targets for sleep-wake regulation, $A_1$Rs and $A_3$Rs are very important for torpor induction, and activation of $A_1$Rs is sufficient for hibernation-like state.

(cAMP) concentration *via* inhibiting or activating adenylate cyclase (AC), which makes adenosine and P1 receptors essential for the regulation of energy balance (Chiu and Freund, 2014).

Sleep, torpor, and hibernation are integral to energy balance. At the same time, adenosine which is a homeostatic bioenergetic network regulator appears to accumulate before entry into the three states, suggesting that adenosine and P1 receptors, may mediate sleep, torpor and hibernation (Drew and Jinka, 2013; Silvani et al., 2018). Much evidence suggests that activation or inhibition of the central nervous system (CNS) adenosine receptors by genetic or pharmacological means can alter the states of sleep, torpor, and hibernation. In this review, we focus on the role of adenosine in the CNS and summarize the current research on the roles and possible biological mechanisms of adenosine and P1 receptors in sleep, torpor, and hibernation. This may help us solve many problems in the future, such as treating sleep disorders and using artificial hibernation for medical applications and space exploration.

## 2 Physiological characteristics during sleep, torpor, and hibernation

Sleep, torpor, and hibernation appear shallow to deep states of diminished body temperature and metabolic rate. Sleep is a relatively rapid and reversible state. However, the animals in a torpor state are more difficult to awaken than sleepers. They may not respond immediately to stimuli, while hibernators typically take an hour or more from hibernation to awakening (Siegel, 2009). Animals control the duration of torpor based on the circadian system, typically remaining dormant for only part of the day and returning to a physiological state when $T_b$ rises to a consistently high level.

In contrast to torpor, hibernation lasts for days or weeks, and hibernators generally do not forage, relying mainly on early food storage or fat storage (Ruf and Geiser, 2015). Hibernation is not as common as daily sleep and torpor; only one-third of mammalian species are hibernators (Berger, 1984). Sleep, torpor, and hibernation are both energy-saving strategies for animals that share similar physiological characteristics and have their own characteristics (Table 1). An interesting commonality between sleep, torpor, and hibernation is the involvement of adenosine receptors. Adenosine is a purine nucleoside involved in many signaling pathways of energy homeostasis. One of the functions of sleep is to restore brain energy homeostasis, while the primary function of hibernation and torpor is to restore or protect body energy homeostasis (Drew and Jinka, 2013). According to many previous studies, adenosine $A_1$ receptors and $A_{2A}$ receptors ($A_1$Rs and $A_{2A}$Rs) play an essential role in inducing NREM, the activation of $A_1$R and $A_3$ receptors ($A_3$Rs) may induce torpor (Silvani et al.,

**TABLE 1 Physiological characteristics of sleep, daily torpor, and hibernation.**

| | Sleep | Torpor | Hibernation | References |
|---|---|---|---|---|
| Energy saving | 5%–15% | 60%–70% | >90% | Swoap et al. (2017), Mohr et al. (2020) |
| Metabolic rate | 70%–90% of BMR | ~35% of BMR | 6% of BMR | Ruf and Geiser (2015) |
| BP (relative decrease to normal value) | ~10% | 25%–30% | 40%–80% | Silvani and Dampney (2013), Ambler et al. (2021) |
| Body temperature (the decrease compared to 36°C–40°C) | <3°C | 5°C–20°C | 15°C–35°C | Berger (1984) |
| Respiration rate (% of active state) | 100%–80% | 5%–20% | 2%–3% | Mohr et al. (2020) |
| HR (% of active state) | 70%–90% | 10%–30% minimum HR (70 to 150 bpm) | 1%–4% minimum HR (5 to 10 bpm) | Swoap et al. (2017), Mohr et al. (2020) |
| EEG (NREM) | ↓ | ↓↓ | ↓↓↓ | Huang et al. (2021) |
| EMG (NREM) | ↓ | ↓↓ | ↓↓↓ | Huang et al. (2021) |
| HP | ↑ | ↑ | ↑ | Silvani and Dampney (2013) |

Note: ↓: decrease, ↑: increase.

2018), and the onset of hibernation may be due to the activation of $A_1$Rs (Jinka et al., 2011; Frare and Drew, 2021). In the following, we will briefly introduce the physiological characteristics of the three states and expand our review based on this.

## 2.1 Sleep

Most mammals and birds spend about one-third of their lives asleep, a quiet state in which humans or animals are less sensitive to their environment. Sleep is regulated by biological rhythms and neural loops and plays a vital role in the human body's functional recovery, learning and memory, and growth and development. It is characterized by loss of consciousness, decreased $T_b$, metabolism, and a decrease in heart rate (HR) and blood pressure (BP). According to the characteristic electroencephalographic (EEG) patterns, sleep can be divided into NREM and REM sleep.

NREM and REM sleep occur alternately throughout sleep time, with NREM accounting for the majority of the sleep time (Silvani and Dampney, 2013; Schmidt, 2014; Silvani et al., 2018). NREM sleep shows decreased systemic function, regular breathing, HR, reduced energy consumption, an EEG that consisted mainly of slow waves, reduced muscle tension, but still a definite posture, with no noticeable eye changes. NREM sleep is divided into four stages. Stages Ⅰ and Ⅱ are light sleep, and stages Ⅲ and Ⅳ are deep sleep. During deep sleep, cellular metabolism can be promoted throughout the body, immunity can be strengthened, and energy depleted during the wake period can be restored (Silvani et al., 2018). REM sleep is characterized by rapid eye movement, loss of thermoregulation, EEG activity similar to waking, marked decrease or disappearance of muscle tension, muscle relaxation, but active neurons in most brain regions, increased cerebral blood flow, irregular breathing, and increased HR. During REM sleep, humans or animals maintain a relatively high level of vigilance, which is essential for animals to survive in nature (Roth, 2004; Schmidt, 2014).

## 2.2 Torpor

Torpor, a behavior that saves energy by reducing metabolic rate (MR), is often identical to sleep, which occurs daily or lasts for days, transitions into sleep (also called daily torpor), and is regulated by circadian rhythms (Berger, 1984). A drastic reduction of MR associated with a decrease in $T_b$ results in the occurrence of torpor (Giroud et al., 2020). In addition, the autonomic nervous system is intimately involved in all stages of torpor. During an episode of torpor, the respiratory rate decreased, the HR related to ventilation increased periodically, and the decrease in ventilation was more significant than the MR, resulting in mild respiratory acidosis (Silvani et al., 2018).

A decrease in brain temperature usually accompanies the onset of torpor. If the brain temperature is above 25°C, EEG morphology and frequency during torpor are closest to the characteristics of NREM sleep. Then, both EEG amplitude and power decrease with decreasing $T_b$. When the brain temperature falls below 25°C, REM sleep gradually disappears, and when the temperature is between 10°C and 20°C, the animals alternate between long NREM sleep and short wakefulness. EEG becomes equipotential when the brain temperature is below 10°C, and it is impossible to determine alertness by electrophysiological methods (Ruf and Geiser, 2015; Ambler et al., 2021; Huang et al., 2021). When electromyography (EMG) was examined, EMG activity was found to decrease significantly with the inhibition of shivering thermogenesis, and a decrease of $T_b$ when entering the state of torpor was observed (Huang et al., 2021). Daily torpor appears independent of ambient temperature (Ta), season, and nutritional status, as it can last only a few hours and is frequently interrupted by activity and foraging. Torpor can occur throughout the year, although it is more frequent in winter. However, in some species that live in warm climates, summer torpor is more common than winter torpor. Compared with waking, the metabolic rate drops to an average of about 30% of the basal metabolic rate (BMR) during torpor. The energy consumption is usually reduced by 10% to 80%, depending on the time and depth of torpor (Geiser, 2013).

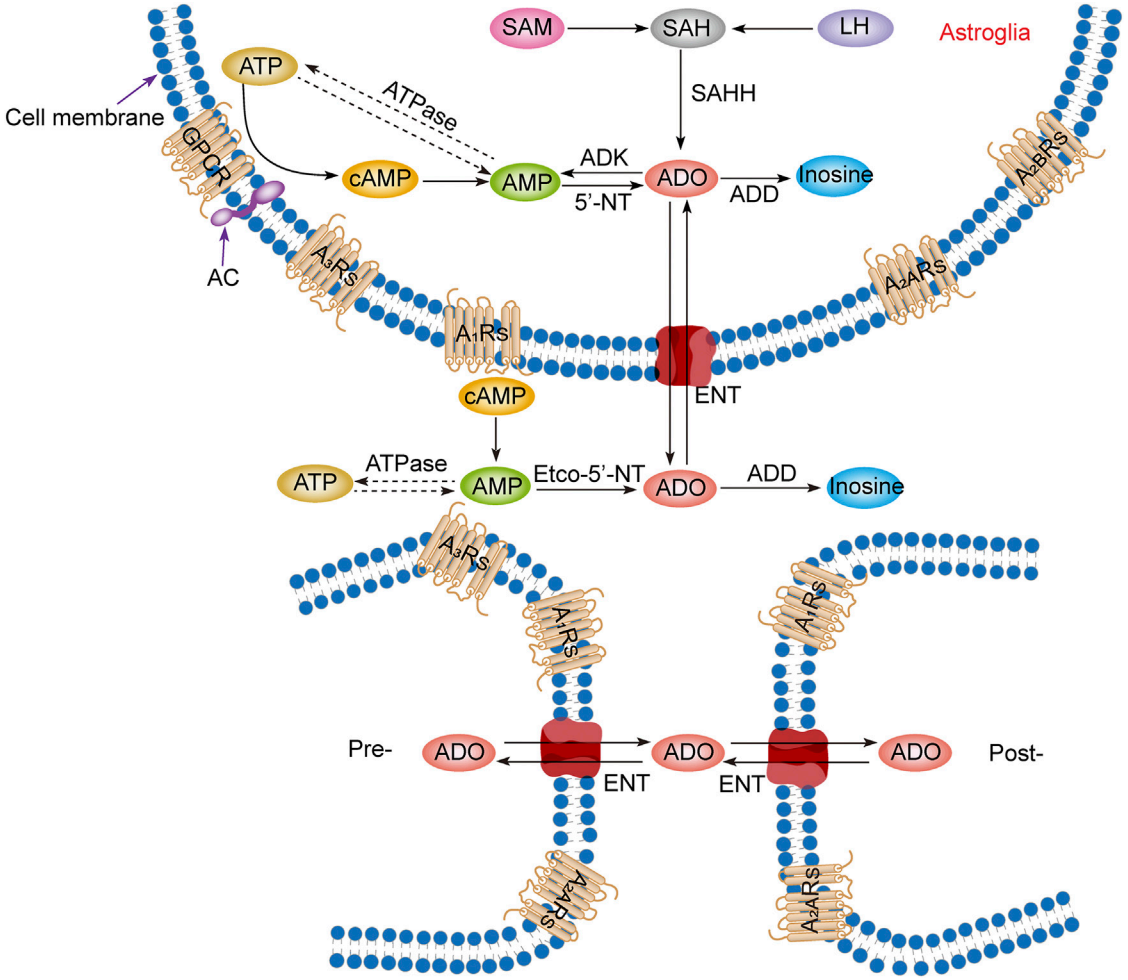


FIGURE 1
Adenosine metabolism and P1 receptors in the central nervous system. Adenosine metabolism occurs mainly in neuronal synapses and astrocytes. In cells, adenosine is formed from ATP, cAMP, or SAH. Extracellular adenosine is produced by ATP and cAMP metabolism but mainly by the balance of nucleoside transporters to regulate the concentration level inside and outside the membrane. SAM, S-adenosylmethionine; SAH, S-adenosyl homocysteine; LH, L-homocysteine; SAHH, S-adenosyl homocysteine hydrolase; ATP, adenosine triphosphate; ADP, adenosine diphosphate; AMP, adenosine monophosphate; cAMP, cyclic adenosine monophosphate; ADO, adenosine; ADD, adenosine deaminase; ADK, adenosine kinase; 5′-NT, 5′-nucleotidase; etco-5′-NT, etco-5′-nucleotidase; AC, adenylate cyclase; GPCR, G protein-coupled receptors; ENT, equilibrating nucleoside transporter; $A_1$Rs, adenosine $A_1$ receptors; $A_{2A}$Rs, adenosine $A_{2A}$ receptors; $A_{2B}$Rs, adenosine $A_{2B}$ receptors; $A_3$Rs, adenosine $A_3$ receptors; Pre-, presynaptic membrane; Post-, postsynaptic membrane.

## 2.3 Hibernation

Hibernation is a physiological adaptation that allows endothermic animals to cope with periodic limitations in their energy supply by lowering $T_b$ and metabolism and improve their freezing tolerance, which may enable them to survive seasonal changes in the food supply and temperature reduction (Geiser, 2013; Storey and Storey, 2013; Storey and Storey, 2017). When the metabolic rate decreases during hibernation, ventilation decreases, and prolonged apnea occurs (Milsom and Jackson, 2011). During deep hibernation, the $T_b$ of most mammals is near Ta. However, as $T_b$ approaches the freezing, MR rises sharply, preventing tissue damage from increased heat production (Milsom and Jackson, 2011; Geiser, 2013). Hibernating species include facultative hibernators (hamsters, bats) and obligatory hibernators (ground squirrels, bears, and lemurs). Facultative hibernators are animals that go into hibernation only when they sense cold, lack of food, or photoperiodic changes. Obligatory hibernators are animals that go into hibernation spontaneously and punctually at a specific time of year, regardless of food availability or temperature (Xu et al., 2013; Mohr et al., 2020).

Hibernation is not an uninterrupted process over several months. With the rise of Ta and the accumulation of metabolites, spontaneous periodic awakening may occur and interrupt dormancy. After a brief awakening, the animal returns to dormancy and repeats the cycle of dormancy-awakening until the end of hibernation. This periodic awakening consumes most of the energy during hibernation. The onset of hibernation is highly dependent on temperature. When Ta is between 20°C and 30°C, some species still hibernate, but the duration is usually only a few hours, similar to daily torpor (Geiser, 2013; Ruf and Geiser, 2015; Mohr et al., 2020; Ambler et al., 2021). Gene transcription and

translation are significantly inhibited during hibernation, and many other physiological parameters are significantly reduced and recover after awakening, such as HR, respiration, metabolic rate, and so on (Xu et al., 2013).

# 3 Sources and metabolic pathways of adenosine in the central nervous system

## 3.1 Source of adenosine

Intracellular adenosine is mainly produced through five pathways (Figure 1): 1) Adenosine triphosphate (ATP) loses two phosphate groups under the action of ATPase to become adenosine monophosphate (AMP), and AMP continues to lose the phosphate group under the action of an internal 5′-nucleotidase (5′-NT) to produce adenosine (Lopes et al., 2011). 2) Adenine reacts with 1-phosphate ribose to form adenosine (Hall and Frenguelli, 2018). 3) S-adenosylmethionine (SAM) and L-homocysteine produce S-adenosylhomocysteine (SAH) and further produce adenosine under the action of S-adenosylhomocysteine hydrolase (SAHH), but this pathway is not common in the CNS (Deussen et al., 1989; Latini and Pedata, 2001). 4) Extracellular adenosine is transported into the cell by the balanced nucleoside transporter in the cell membrane (Liu Y. J. et al., 2019). 5) cAMP is generated from ATP under the action of AC, which is regulated by GPCRs, and then converted through phosphodiesterases (PDEs) to AMP, which is eventually used to generate adenosine (Dos Santos-Rodrigues et al., 2015).

Production of extracellular adenosine occurs mainly by two pathways (Figure 1): 1) intracellular adenosine is transported to the extracellular space by the balanced nucleoside transporter located in the cell membrane (Sala-Newby et al., 1999). 2) Extracellular ATP and adenosine diphosphate (ADP) are converted to AMP by the enzyme ecto-nucleoside triphosphate diphosphohydrolase (E-NTPDase), also known as CD39. Subsequently, adenosine is generated by ecto-5′-nucleotidase (ecto-5′-NT), also known as CD73, which is mainly expressed on astrocytes, oligodendrocytes and microglia (Lazarus et al., 2019a).

In the equilibrium state, the intracellular adenosine level is 100 nM, and the extracellular adenosine level is 140–200 nM (Dunwiddie and Diao, 1994), but in the pathological state, such as ischemia and hypoxia, extracellular adenosine level increases three- to 10-fold (Andiné et al., 1990; Dux et al., 1990). It is worth noting that although adenosine can be produced from the synaptic terminals of neurons and enter the synaptic space, it is not secreted through vesicles but transported through nucleoside transporters, which has nothing to do with neural activities. Thus, adenosine is not a neurotransmitter but a regulatory factor (Huang et al., 2011; Lopes et al., 2011; Huang et al., 2014).

## 3.2 Adenosine metabolism

Adenosine has three main metabolic pathways (Figure 1): 1) It becomes inosine under the action of adenosine deaminase [8], and then generates hypoxanthine and hypoxanthine nucleotides by nucleoside phosphorylase, and finally becomes uric acid (Fredholm et al., 2005). 2) Adenosine is transported intracellular and extracellular domain through two-way balanced nucleoside transporter to regulate intracellular and extracellular adenosine levels (Liu Y. J. et al., 2019). 3) Adenosine kinase (ADK), which is mainly found in astrocytes, generates AMP and ADP by phosphorylating adenosine in the presence of ATP. This metabolic pathway can only occur in cells, so extracellular adenosine must enter cells to complete the cycle (Huang et al., 2011; Huang et al., 2014; Garcia-Gil et al., 2021).

# 4 Excitatory and inhibitory effects of various adenosine receptors

The physiological functions of adenosine is mediated by four purinergic type 1 receptors, known as $A_1$, $A_{2A}$, $A_{2B,}$ and $A_3$ receptors, which belong to GPCR family. $A_1$Rs and $A_3$Rs belong to the inhibitory adenylate cyclase G protein (Gi) family, whereas $A_{2A}$Rs and $A_{2B}$Rs belong to the stimulatory adenylate cyclase G protein (Gs) family (Wall and Dale, 2008; Lopes et al., 2011).

## 4.1 $A_1$ receptors

$A_1$Rs have the highest affinity for adenosine and can be activated when the concentration of adenosine is in the pM range. They are the most prominent adenosine receptor in the CNS, distributed mainly in the cerebral cortex, hippocampus, and thalamus. $A_1$Rs are located primarily in the excitatory nerve terminals (Kashfi et al., 2017). Activation of $A_1$Rs can inhibit the activity of adenylate cyclase (AC), decrease the cAMP content, and regulate the activity of cAMP-dependent protein kinase. $A_1$R activation can increase the release of intracellular $Ca^{2+}$, inhibit N-, Q- and P-type calcium channels, decrease the influx of extracellular $Ca^{2+}$, block the release of neurotransmitters, and reduce neuronal discharge to regulate neuronal activity (Wall and Dale, 2008). In the postsynaptic membrane, $A_1$Rs are activated to open $K^+$ channels and increase $K^+$ outflow, resulting in membrane hyperpolarization, which reduces excitability and protects neurons. When activated, A1Rs can also open the ATP-sensitive potassium channel (KATP) of substantia nigra neurons, increasing outward currents and decreasing membrane excitability (Stockwell et al., 2017).

## 4.2 $A_{2A}$ receptors

The affinity of $A_{2A}$Rs for adenosine is lower than that of $A_1$Rs, and the activation concentration of adenosine is in the nM range. $A_{2A}$Rs are mainly distributed in dopaminergic areas, such as striatum, nucleus accumbens (NAc), olfactory nodules and so on (Fang et al., 2017; Dong et al., 2022). When $A_{2A}$Rs are activated, they are coupled with Gs protein in the brain to increase the activity of AC and cAMP in striatal cells. In the hippocampus, $A_{2A}$Rs appear to be coupled with Gi/Go protein (Diógenes et al., 2004). $A_{2A}$Rs are mainly expressed in $D_2$ dopamine receptor cells and are particularly abundant in the plasma membrane of dendrites and dendritic spines, but less so in axons, axon terminals, and glial cells, and has an antagonistic effect with dopamine

$D_2$ receptors ($D_2$Rs) (Ferre et al., 1991; Strömberg et al., 2000). Presynaptic $A_{2A}$Rs can regulate the inhibition of $A_1$Rs. In contrast to $A_1$Rs, adenosine promotes the release of excitatory transmitters by activating $A_{2A}$Rs. In astrocytes, $A_{2A}$Rs are involved in the regulation of glutamate release and γ-aminobutyric acid (GABA) uptake (Cristóvão-Ferreira et al., 2009). The balance between $A_1$ and $A_{2A}$Rs is crucial to the adenosine response, and this close interaction between them can produce a response that is different from the sum of the two (Chiu and Freund, 2014).

### 4.3 $A_{2B}$ receptors

$A_{2B}$Rs have a low affinity for adenosine, and the activation concentration of adenosine should reach μM, suggesting that $A_{2B}$Rs mainly play a role under pathological conditions with increased extracellular adenosine concentration. $A_{2B}$Rs are primarily distributed in hippocampal neurons and glial cells, and a small amount is also found in the thalamus, lateral ventricle, and striatum. $A_{2B}$Rs can activate AC *via* Gs or phospholipase C (PLC) *via* Gq. Activation of $A_{2B}$Rs can increase intracellular cAMP, promote glycogen decomposition, and increase the energy supply of neurons to resist the pathological state of ischemia and hypoxia (van Calker et al., 1979; Hösli and Hösli, 1988; Dos Santos-Rodrigues et al., 2015).

### 4.4 $A_3$ receptors

$A_3$Rs have the lowest sensitivity compared to other adenosine receptors, but activation of $A_3$Rs has neuroprotective and neurotrophic effects. Although $A_3$Rs are distributed throughout the brain, their content varies greatly in different brain regions, especially in the hippocampus and cerebellum. $A_3$Rs act through Gi-mediated AC inhibition and Gq-mediated PLC activation. $A_3$Rs can regulate hippocampal synaptic plasticity and decrease adenylate cyclase activity. In short, $A_3$Rs activation is closely related to inflammation inhibition and cell protection (Lopes et al., 2003; Vlajkovic et al., 2007; Lopes et al., 2011).

## 5 The roles and neurobiological mechanisms of adenosine and P1 receptors in sleep, torpor, and hibernation

### 5.1 Increased levels of extracellular adenosine lead to drowsiness

Thanks to neurobiology and molecular biology advances, we are beginning to understand how sleep is initiated and maintained. Sustained wakefulness causes the body to produce and accumulate one or more endogenous somnogenic factors that induce sleep after reaching a certain threshold. The hypnotic effect of adenosine, an endogenous somnogenic factor, was discovered in 1954 (Feldberg and Sherwood, 1954). Typically, extracellular adenosine concentrations in the cerebral cortex and basal forebrain (BF) gradually increase during prolonged arousal, reaching a certain threshold that leads to drowsiness, while slowly decreasing during recovery sleep (Porkka-Heiskanen et al., 1997; Clasadonte et al., 2014; Huang et al., 2014; Tartar et al., 2021; Omond et al., 2022). Extracellular adenosine levels may be partially regulated by glutamatergic neurons (Peng et al., 2020; Sun and Tang, 2020). This is because activation of the glutamatergic BF neurons causes a large increase in extracellular adenosine, and specific ablation of glutamatergic BF neurons reduces the level of extracellular adenosine and significantly impairs sleep homeostasis regulation (Peng et al., 2020). Although adenosine is known to act on four evolutionarily conserved receptors, it is currently thought to regulate sleep-wake states by acting on the $A_1$Rs and $A_{2A}$Rs (Huang et al., 2014; Lazarus et al., 2019b).

### 5.2 Regulation of sleep homeostasis by $A_1$Rs is brain region-dependent

$A_1$Rs are required for normal sleep homeostasis because the conditional knockout of $A_1$Rs in the CNS during sleep restriction results in a reduced rebound slow-wave activity response (Bjorness et al., 2009). Mainstream research suggests that activation of $A_1$Rs promotes sleep, as $A_1$Rs agonists increase sleep (Radulovacki et al., 1984; Benington et al., 1995), whereas $A_1$Rs antagonists decrease sleep (Methippara et al., 2005; Thakkar et al., 2008). For example, when Oishi et al. (2008) injected the $A_1$Rs-selective agonist N6-cyclopentyladenosine (CPA) into the rat tuberomammillary nucleus (TMN), this significantly increased NREM sleep. $A_1$Rs may mediate sleep through three pathways (Lazarus et al., 2019b): 1) $A_1$Rs promote sleep by inhibiting wake-promoting neurons. $A_1$Rs are expressed in hypocretin/orexin neurons of the lateral hypothalamus (LH) and histaminergic neurons of the TMN, which are typical arousal centers. Activation of $A_1$Rs inhibits excitatory neurotransmission, including cholinergic arousal systems in the brainstem (Rainnie et al., 1994) and BF (Alam et al., 1999; Thakkar et al., 2003), the hypocretin/orexin neurons in the LH (Thakkar et al., 2002; Liu and Gao, 2007), and histaminergic systems in the TMN (Oishi et al., 2008). 2) $A_1$Rs promote sleep by disinhibiting sleep-active neurons in the ventrolateral preoptic nucleus (VLPO) and anterior hypothalamic area (Chamberlin et al., 2003; Morairty et al., 2004). 3) $A_1$Rs mediate homeostatic sleep pressure based on astrocytic gliotransmission (Halassa et al., 2009).

Moreover, A1Rs do not appear to fully promote sleep because $A_1$R knockout mice did not differ from wide-type mice in basal sleep amount and sleep-wake behavior after sleep deprivation (Stenberg et al., 2003). Infusion of CPA into the lateral ventricle of mice did not significantly alter NREM and REM sleep (Urade et al., 2003). However, microdialysis of the adenosine transporter inhibitor nitrobenzyl-thio-inosine (NBTIs) or $A_1$R agonists into the lateral preoptic area (LPO) increased the amount of wakefulness in rats (Methippara et al., 2005). Thus, $A_1$Rs may exert different sleep-wake effects by acting on different brain regions.

### 5.3 $A_{2A}$Rs are important receptors that mediate the sleep-promoting effect of adenosine

$A_{2A}$Rs are important targets in the regulation of sleep. $A_{2A}$Rs mediate the effects of many sleep-promoting substances, such as

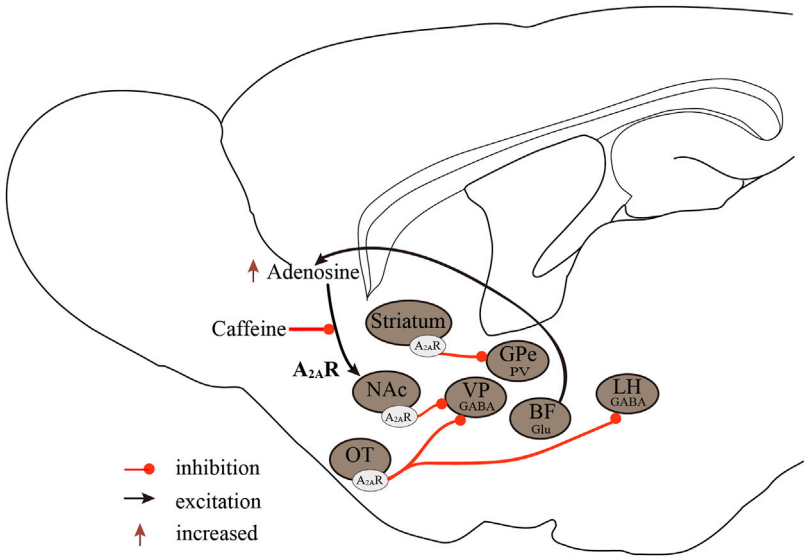


FIGURE 2
Neurobiological mechanisms of the $A_{2A}$Rs regulate sleep-wake states. $A_{2A}$Rs are important targets in sleep regulation, promoting sleep by inhibiting major arousal systems. Activation of $A_{2A}$R neurons in the NAc core, striatum, and OT promotes sleep, with $A_{2A}$Rs neurons in the NAc core projecting to the VP, striatal $A_{2A}$R neurons, and GPe PV neurons forming inhibitory circuits, and OT $A_{2A}$R neurons projecting to the VP and LH. Furthermore, BF glutamatergic neurons may regulate extracellular adenosine levels, and $A_{2A}$Rs rather than $A_1$Rs mediate the wake-promoting effects of caffeine. $A_{2A}$Rs, adenosine $A_{2A}$ receptors; $A_1$Rs, adenosine $A_1$ receptors; NAc, nucleus accumbens; VP, ventral pallidum; GPe, external globus pallidus; OT, olfactory tubercle; LH, lateral hypothalamus; Glu, glutamic acid; GABA, γ-aminobutyric acid.

ethanol and sake yeast (El Yacoubi et al., 2003; Nakamura et al., 2016; Fang et al., 2017; Nishimon et al., 2021). The selective $A_{2A}$R agonist CGS21680 injected into the subarachnoid space adjacent to the BF and LPO of rats or the lateral ventricle of mice significantly increased NREM and REM sleep (Satoh et al., 1998; Scammell et al., 2001; Urade et al., 2003; Methippara et al., 2005). Immediately after the cessation of CGS21680 perfusion, there is a strong rebound in wakefulness (Gerashchenko et al., 2000). However, the sleep-promoting effect induced by CGS21680 was abolished entirely in $A_{2A}$R knockout mice.

In addition, intraperitoneal administration of a positive $A_{2A}$R allosteric modulator {3, 4-difluoro-2-[(2-fluoro-4-iodophenyl) amino] benzoic acid} in WT mice but not $A_{2A}$R knockout mice enhanced $A_{2A}$R signaling and promoted NREM sleep in a dose-dependent manner (Korkutata et al., 2019). Several studies suggested that $A_{2A}$Rs mediated the sleep-regulating effects of prostaglandin D2 (PGD2). After administration of PGD2 or CGS21680 into the rostral BF, c-fos-positive cells were significantly increased in the VLPO, a sleep center, resulting in enhanced induction of NREM sleep, and in contrast, c-fos-positive neurons significantly decreased in the TMN of the posterior hypothalamus, a wake center (Satoh et al., 1999; Scammell et al., 2001). In *in-vivo* microdialysis experiments, infusion of CGS21680 into the BF dose-dependently decreased histamine release in the frontal cortex and medial preoptic area and increased GABA release in the TMN, but not in the frontal cortex (Hong et al., 2005). Furthermore, VLPO neurons have been divided into two types according to their different responses to serotonin and adenosine: Type-1 neurons were inhibited by serotonin, and type-2 neurons were excited. $A_{2A}$R agonists excited postsynaptic type-2 neurons in the VLPO but not type-1 neurons. Type-2 neurons were involved in sleep initiation, whereas type-1 neurons may contribute to sleep consolidation because type-1 neurons were activated only when the inhibitory effects of the arousal system were absent (Gallopin et al., 2005). In addition to the VLPO, injection of CGS21680 into the rostral BF also increased c-fos expression in the shell of the NAc and the medial portion of the olfactory tubercle (OT) (Satoh et al., 1999; Scammell et al., 2001). Microinjection of CGS21680 into the NAc shell also induced sleep-promoting effects (Satoh et al., 1999). $A_{2A}$Rs are highly expressed in the caudate putamen, NAc, and OT. Our recent series of studies have shown that activation of $A_{2A}$R neurons in these nuclei can strongly promote sleep (Oishi et al., 2017; Yuan et al., 2017; Li et al., 2020). Activation of the $A_{2A}$R neurons of the NAc core projecting to the ventral pallidum (VP) strongly induced NREM sleep. Conversely, inhibiting these neurons reduced sleep but did not affect the sleep homeostasis rebound (Oishi et al., 2017). Yuan et al. demonstrated the important role of the striatal $A_{2A}$R neurons projecting to the external globus pallidus (GPe) parvalbumin (PV) neurons in sleep control. Chemogenetic inhibition of striatal $A_{2A}$R neurons significantly decreased NREM sleep in the active period, which was mediated by the formation of inhibitory circuits between striatal $A_{2A}$R neurons and GPe PV neurons (Yuan et al., 2017). The OT $A_{2A}$R neurons project to the VP and LH *via* inhibitory innervations, and pharmacological or chemogenetic activation of OT $A_{2A}$R neurons resulted in increased NREM sleep in mice (Li et al., 2020). Moreover, $A_{2A}$Rs are co-localized with dopamine $D_2$Rs in these nuclei (Missale et al., 1998). Our studies demonstrated that $D_2$R-expressing neurons are essential for the induction and maintenance of wakefulness (Qu et al., 2008; Qiu et al., 2009; Qu et al., 2010; Liu Y. Y. et al., 2019; Yang et al., 2021). Thus, $A_{2A}$Rs and

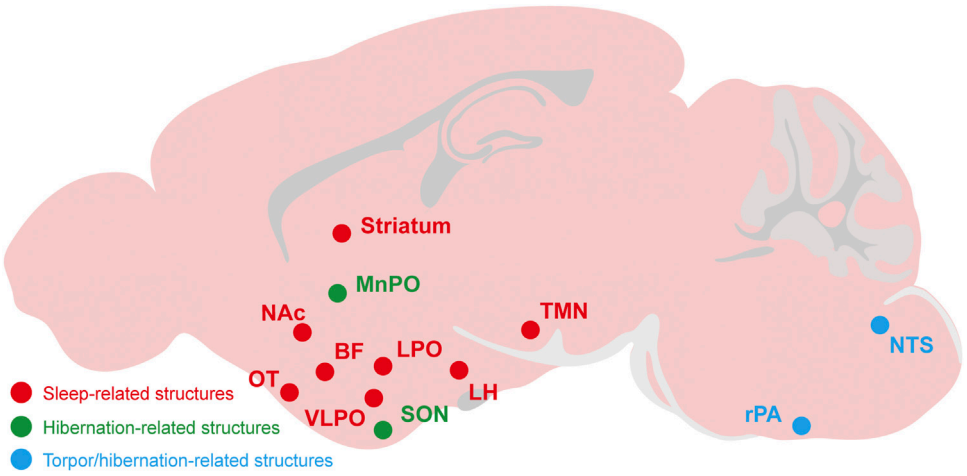


FIGURE 3
The relevant brain regions about adenosine and P1 receptors mediate sleep, torpor, and hibernation. The CNS adenosine and P1 receptors are important for the regulation of sleep-wake, torpor and hibernation. The roles and mechanisms of several brain regions and nuclei have been gradually revealed, such as the $A_{2A}$Rs-expressing neurons in the NAc, striatum, OT and other structures have a significant effect on sleep-wake regulation. The NTS and rPA may be the key brain regions of adenosine and P1 receptors mediating torpor and hibernation. NAc, nucleus accumbens; OT, olfactory tubercle; LH, lateral hypothalamus; BF, basal forebrainvlpo; VLPO, ventrolateral preoptic nucleus; LPO, lateral preoptic area; MnPO, median preoptic area; SON, supraoptic nucleus; TMN, tuberomammillary nucleus; rPA, raphe pallidus; NTS, nucleus tractus solitarius.

$D_2$Rs may jointly influence the sleep-wake cycle by balancing their activity.

Caffeine, unlike adenosine, is a wake-promoting substance abundant in refreshing beverages such as coffee and tea. Caffeine is an antagonist of $A_1$Rs and $A_{2A}$Rs, with similar affinity for both at low doses (Fredholm et al., 2001). Using $A_1$R knockout and $A_{2A}$R knockout mice, Huang et al. demonstrated that caffeine-induced wakefulness is dependent on $A_{2A}$Rs, as caffeine dose-dependently increased wakefulness in both wild-type and $A_1$R knockout but not $A_{2A}$R knockout mice (Huang et al., 2005). Similarly, selective silencing of $A_{2A}$Rs in the NAc shell inhibited caffeine-induced wakefulness (Lazarus et al., 2011).

In conclusion, the regulatory effect of $A_1$Rs on sleep-wake regulation is brain region-dependent. The excitation of $A_1$Rs in wake-promoting nuclei induces sleep and, conversely, causes arousal on sleep-promoting neurons. The $A_{2A}$Rs are the major sleep-regulating receptors that mediate the wake-promoting effects of caffeine, and activation of $A_{2A}$Rs promotes sleep by inhibiting major arousal systems (Figure 2).

## 5.4 Adenosine $A_1$Rs and $A_3$Rs play important roles in torpor

Adenosine may play a key role in torpor, as pyruvate induces torpor in obese mice based on adenosine signaling (Soto et al., 2018). In mice lacking all four adenosine receptors, adenosine does not cause hypothermia, bradycardia, or hypotension typical of the torpor state (Xiao et al., 2019). Peripheral or central infusion of adenosine or AMP results in a decrease in metabolic rate and body temperature similar to that observed in natural torpor, even in rats that do not naturally enter torpor (Swoap et al., 2007; Jinka et al., 2011; Iliff and Swoap, 2012; Olson et al., 2013; Tupone et al., 2013; Carlin et al., 2017; Vicent et al., 2017). Furthermore, the administration of $A_1$R or $A_3$R agonists to mice induces several features of daily torpor, including hypothermia (Anderson et al., 1994; Iliff and Swoap, 2012; Carlin et al., 2017; Swoap, 2017; Vicent et al., 2017), whereas $A_{2A}$Rs and $A_{2B}$Rs agonists do not (Anderson et al., 1994).

Currently, there are three ways to mimic the induction of torpor: 1) inhibition of the raphe pallidus (rPA) neurons in the brainstem (Cerri et al., 2021); 2) activation of $A_1$Rs or $A_3$Rs in the brain; 3) activation of glutamatergic Adcyap1+ neurons in the hypothalamus (Hrvatin et al., 2020). Here, we will discuss the induction of synthetic torpor by controlling $A_1$Rs and $A_3$Rs through pharmacological experiments. Although neither $A_1$Rs nor $A_{3A}$Rs are required for fasting-induced torpor (Carlin et al., 2017), administration of $A_1$R or $A_3$R agonists such as N6-cyclohexyladenosine (CHA) induces torpor-like states in some animals (Jinka et al., 2011; Olson et al., 2013; Tupone et al., 2013; Vicent et al., 2017; Frare et al., 2018), while antagonist administration prevents torpor or causes arousal from torpor during torpor phases (Jinka et al., 2011; Iliff and Swoap, 2012; Tamura et al., 2012). It is not yet certain whether adenosine action triggers the occurrence of natural torpor, but adenosine mediates at least some of the physiological features during torpor. For example, $A_3$R stimulation leads to hypothermia *via* peripheral mast cell degranulation, histamine release, and activation of central histamine $H_1$ receptors. However, $A_1$R agonist-induced hypothermia occurs *via* central sites, and the rPA, nucleus of the solitary tract (NTS) and the hypothalamic-pituitary-thyroid axis gate appear to play a pivotal role (Tupone et al., 2013; Carlin et al., 2017; Frare et al., 2018).

In the future, further efforts should be made to confirm the role of adenosine in torpor and its possible neurobiological and molecular mechanisms. First, microdialysis experiments,

**TABLE 2 Roles of adenosine receptors in sleep, torpor, and hibernation.**

| | Sleep | Torpor | Hibernation | References |
|---|---|---|---|---|
| Adenosine accumulation | Yes | Unknow | Unknow | Porkka-Heiskanen et al. (1997), Clasadonte et al. (2014), Huang et al. (2014), Tartar et al. (2021), Omond et al. (2022) |
| Key receptors | $A_1$Rs, $A_{2A}$Rs | $A_1$Rs, $A_3$Rs | $A_1$Rs | |
| Related brain regions | TMN, LH, Brain stem, BF, VLPO, LPO, NAc, OT, Striatum | NTS, rPA, hypothalamus | NTS, rPA, MnPO, SON, thalamus | Huang et al. (2014), Yuan et al. (2017), Oishi et al. (2017), Shimaoka et al. (2018), Silvani et al., 2018, Li et al., 2020 |
| Roles of adenosine receptors | $A_1$R-mediated sleep-wake effects are brain region-dependent; $A_{2A}$Rs promote sleep by inhibiting arousal systems | Activation of $A_1$Rs or $A_3$Rs mimic the induction of torpor | $A_1$Rs may mediate hibernation *via* regulating core body temperature | Huang et al. (2014), Drew et al. (2017), Silvani et al. (2018), Lazarus et al. (2019a) |

adenosine probes, and chemogenetic and optogenetic techniques should be used to confirm whether there is an accumulation and dynamic change of adenosine concentration during the initiation and maintenance of torpor and to reveal the possible mechanisms.

## 5.5 Central activation of $A_1$Rs is sufficient to induce and maintain a hibernation-like state

Seasonal changes in brain adenosine levels may contribute to an increase in A1R sensitivity leading to the onset of hibernation (Frare and Drew, 2021). Although the mechanisms controlling hibernation are currently unclear, activation of $A_1$Rs signaling in the CNS appears to be required for the onset of this phenomenon, as activation of the $A_1$Rs in the CNS can induce hibernation or some hibernation-like states in obligate, facultative, or non-hibernating animals (Drew et al., 2017; Shimaoka et al., 2018; Frare and Drew, 2021). In addition, Shimaoka et al. (2018) activated central $A_1$Rs in rats, a non-hibernating animal, which induced a hypothermia response similar to hibernation.

It is worth noting that activation of $A_1$Rs maintains core body temperature at a low level. In hibernators, core body temperature and metabolic rate reduction occur before hibernation, which may be the key to the $A_1$R-mediated hibernation (Barros et al., 2006). $A_1$Rs are highly expressed throughout the CNS, including the NTS. The NTS is the center that controls cardiovascular, respiratory, and metabolic functions, and the NTS neurons are responsible for the integration of central and peripheral signals related to energy expenditure-related (Barros et al., 2006). $A_1$Rs act as inhibitory receptors whose activation prevents the release of GABA to the NTS neurons that inhibit thermogenesis (Cao et al., 2010). Furthermore, the administration of CHA to the arctic ground squirrel increased c-fos expression in the NTS in both summer and winter (Frare et al., 2019). After the microinjection of CHA into the NTS, it inhibited brown adipose tissue (BAT) thermogenesis and shivering responses. In contrast, inhibition of $A_1$Rs counteracted BAT thermogenesis induced by intracerebroventricular injection of CHA (Tupone et al., 2013). In addition to inhibiting BAT thermogenesis, activation of $A_1$Rs in the NTS increases vasopressin secretion, which constricts blood vessels, including skin vessels, thereby increasing arterial blood pressure (McClure et al., 2005; McClure et al., 2011) and causing bradycardia, one of the initial physiological features of natural hibernation (Jinka, 2012). The rPA, the median preoptic area (MnPO) and the supraoptic nucleus (SON) also appear to mediate the effect of $A_1$Rs in BAT thermogenic, as the rPA and MnPO c-fos expression is lower in winter than in summer after CHA administration, and inhibition of rPA neurons produces hypothermia, however the SON is related to the seasonal increase in vasoconstriction (Cerri et al., 2013; Frare et al., 2019). Therefore, $A_1$Rs could mediate hypothermia similar to hibernation by inhibiting BAT thermogenesis *via* the NTS and rPA or by inhibiting cardiovascular function. In addition, as previously mentioned, in contrast to sleep, EEG amplitudes are significantly reduced during hibernation (Golanov and Reis, 2001; Magdaleno-Madrigal et al., 2010). Central activation of $A_1$Rs synchronized the EEG, whereas activation in the thalamus significantly reduced EEG amplitude (Saper et al., 2005). After central administration of CHA in rats, the EEG amplitude was greatly reduced, the delta wave amplitude was significantly reduced, and the theta wave almost disappeared (Tupone et al., 2013). Thus, the change in EEG amplitude may be another way $A_1$Rs mediate hibernation.

As with torpor, it is currently unclear whether adenosine accumulation is necessary for the initiation of hibernation, so further efforts are needed to address these scientific questions.

# 6 Conclusion and future perspective

In this review, we summarize the roles and neurobiological mechanisms of adenosine and its receptors in sleep-wake regulation, torpor, and hibernation (Table 2, Figure 3). The first step toward translating adenosine and P1 receptors into targets for medical applications is to understand their roles and mechanisms underlying these states of diminished metabolism and body temperature. We now know that $A_1$Rs and $A_{2A}$Rs jointly mediate sleep-wake regulation (Huang et al., 2014; Lazarus et al., 2019b), that activation of $A_1$Rs and $A_3$Rs is important for torpor (Carlin et al., 2017) and that hibernation requires $A_1$Rs rather than other adenosine receptors (Shimaoka et al., 2018; Frare and Drew, 2021).

It is worth noting that the adenosine system is also altered in various sleep disorders, for example, sleeping sickness and chronic insomnia disorder (Rijo-Ferreira et al., 2020; Ren et al., 2021). Some agonists, antagonists, or allosteric modulators targeting adenosine receptors have the potential to be used for treating sleep disorders (Jenner et al., 2020; Korkutata et al., 2022) or inducing synthetic torpor or hibernation for

therapeutic hypothermia, organ preservation, space exploration or longevity promotion (Jinka et al., 2015; Cerri, 2017; Sisa et al., 2017; Hadj-Moussa and Storey, 2019; Al-Attar and Storey, 2020; Cerri et al., 2021), showing that the pharmacological importance of targeting adenosine receptors in the future. However, much work remains to be done because small-molecule drugs targeting adenosine receptors have side effects (Korkutata et al., 2022) and can only mimic some physiological properties of torpor or hibernation by activating adenosine receptors, which is different from natural torpor or hibernation (Swoap, 2017; Vicent et al., 2017). Therefore, it is necessary to explore further the roles and mechanisms of adenosine and its receptors in sleep, torpor, and hibernation and gain more adenosine receptor modulators by structure- and function-based drug discovery. It is important to investigate the neural networks and molecular mechanisms that sleep torpor and hibernation have in common. The first step in conducting these studies is to confirm adenosine accumulation before torpor or hibernation and the dynamic changes in adenosine concentrations during torpor or hibernation using available technologies such as microdialysis, adenosine probes, and chemogenetic and optogenetic methods. Subsequently, several key technologies, from conditional knockout mice based on Cre/lox technology and RNA interference to modulation of neuronal activity with genetic or pharmacological techniques, can be used to confirm neuronal networks of sleep, torpor, and hibernation.

## Author contributions

W-XM, P-CY, and HZ wrote the manuscript. L-XK provided some advices and drew figures. Z-LH, W-MQ, Y-QW, and ML edited and revised the manuscript. All the authors have read and agreed to the content of the manuscript.

## Funding

This study was supported by the STI 2030-major project (2021ZD0203400 to Z-LH), the China National Key R&D Program; National Key Research and Development Program (2022YFA1604504 to Y-QW), the National Natural Science Foundation of China (82171479, 81871037 to Y-QW; 82020108014 and 32070984 to Z-LH), the Shanghai Science and Technology Innovation Action Plan Laboratory Animal Research Project (201409001800 to Z-LH), Program for Shanghai Outstanding Academic Leaders (to Z-LH), the Shanghai Municipal Science and Technology Major Project, and ZJ Lab, and Shanghai Center for Brain Science and Brain-inspired Technology (2018SHZDZX01 to Z-LH), Japan Society for the Promotion of Science [Grants-in-Aid for Scientific Research B (grant number 21H02802) and RECONNECT Initiative (grant number JP22K21351) to ML]; the Japan Science and Technology Agency [CREST (grant number JPMJCR1655) to ML]; Japan Agency for Medical Research and Development (AMED) [Moonshot Program (grant number JP21zf0127005) to ML]; the project "Social Application of Mobility Innovation and Future Social Engineering Research Phase IV (grant number CRI04006)," a joint research project between Toyota Motor Corporation and the University of Tsukuba to ML; and the World Premier International Research Center Initiative (WPI) from MEXT to ML.

## Conflict of interest

The authors declare that the research was conducted in the absence of any commercial or financial relationships that could be construed as a potential conflict of interest.

## Publisher's note



## References

Al-Attar, R., and Storey, K. B. (2020). Suspended in time: Molecular responses to hibernation also promote longevity. *Exp. Gerontol.* 134, 110889. doi:10.1016/j.exger.2020.110889

Alam, M. N., Szymusiak, R., Gong, H., King, J., and McGinty, D. (1999). Adenosinergic modulation of rat basal forebrain neurons during sleep and waking: Neuronal recording with microdialysis. *J. Physiol.* 521 Pt 3, 679–690. doi:10.1111/j.1469-7793.1999.00679.x

Ambler, M., Hitrec, T., and Pickering, A. (2021). Turn it off and on again: Characteristics and control of torpor. *Wellcome Open Res.* 6, 313. doi:10.12688/wellcomeopenres.17379.2

Anderson, R., Sheehan, M. J., and Strong, P. (1994). Characterization of the adenosine receptors mediating hypothermia in the conscious mouse. *Br. J. Pharmacol.* 113, 1386–1390. doi:10.1111/j.1476-5381.1994.tb17151.x

Andiné, P., Thordstein, M., Kjellmer, I., Nordborg, C., Thiringer, K., Wennberg, E., et al. (1990). Evaluation of brain damage in a rat model of neonatal hypoxic-ischemia. *J. Neurosci. Methods* 35, 253–260. doi:10.1016/0165-0270(90)90131-x

Barros, R. C., Branco, L. G., and Cárnio, E. C. (2006). Respiratory and body temperature modulation by adenosine A1 receptors in the anteroventral preoptic region during normoxia and hypoxia. *Respir. Physiol. Neurobiol.* 153, 115–125. doi:10.1016/j.resp.2005.09.013

Benington, J. H., Kodali, S. K., and Heller, H. C. (1995). Stimulation of A1 adenosine receptors mimics the electroencephalographic effects of sleep deprivation. *Brain Res.* 692, 79–85. doi:10.1016/0006-8993(95)00590-m

Berger, R. J. (1984). Slow wave sleep, shallow torpor and hibernation: Homologous states of diminished metabolism and body temperature. *Biol. Psychol.* 19, 305–326. doi:10.1016/0301-0511(84)90045-0

Bjorness, T. E., Kelly, C. L., Gao, T., Poffenberger, V., and Greene, R. W. (2009). Control and function of the homeostatic sleep response by adenosine A1 receptors. *J. Neurosci.* 29, 1267–1276. doi:10.1523/JNEUROSCI.2942-08.2009

Cao, W. H., Madden, C. J., and Morrison, S. F. (2010). Inhibition of Brown adipose tissue thermogenesis by neurons in the ventrolateral medulla and in the nucleus tractus solitarius. *Am. J. Physiol. Regul. Integr. Comp. Physiol.* 299, R277–R290. doi:10.1152/ajpregu.00039.2010

Carlin, J. L., Jain, S., Gizewski, E., Wan, T. C., Tosh, D. K., Xiao, C., et al. (2017). Hypothermia in mouse is caused by adenosine A(1) and A(3) receptor agonists and AMP via three distinct mechanisms. *Neuropharmacology* 114, 101–113. doi:10.1016/j.neuropharm.2016.11.026

Cerri, M. (2017). The central control of energy expenditure: Exploiting torpor for medical applications. *Annu. Rev. Physiol.* 79, 167–186. doi:10.1146/annurev-physiol-022516-034133

Cerri, M., Hitrec, T., Luppi, M., and Amici, R. (2021). Be cool to be far: Exploiting hibernation for space exploration. *Neurosci. Biobehav Rev.* 128, 218–232. doi:10.1016/j.neubiorev.2021.03.037

Cerri, M., Mastrotto, M., Tupone, D., Martelli, D., Luppi, M., Perez, E., et al. (2013). The inhibition of neurons in the central nervous pathways for thermoregulatory cold defense induces a suspended animation state in the rat. *J. Neurosci.* 33, 2984–2993. doi:10.1523/JNEUROSCI.3596-12.2013

Chamberlin, N. L., Arrigoni, E., Chou, T. C., Scammell, T. E., Greene, R. W., and Saper, C. B. (2003). Effects of adenosine on gabaergic synaptic inputs to identified ventrolateral preoptic neurons. *Neuroscience* 119, 913–918. doi:10.1016/s0306-4522(03)00246-x

Chiu, G. S., and Freund, G. G. (2014). Modulation of neuroimmunity by adenosine and its receptors: Metabolism to mental illness. *Metabolism* 63, 1491–1498. doi:10.1016/j.metabol.2014.09.003

Clasadonte, J., McIver, S. R., Schmitt, L. I., Halassa, M. M., and Haydon, P. G. (2014). Chronic sleep restriction disrupts sleep homeostasis and behavioral sensitivity to alcohol by reducing the extracellular accumulation of adenosine. *J. Neurosci.* 34, 1879–1891. doi:10.1523/JNEUROSCI.2870-12.2014

Cristóvão-Ferreira, S., Vaz, S. H., Ribeiro, J. A., and Sebastião, A. M. (2009). Adenosine A2A receptors enhance GABA transport into nerve terminals by restraining PKC inhibition of GAT-1. *J. Neurochem.* 109, 336–347. doi:10.1111/j.1471-4159.2009.05963.x

Deussen, A., Lloyd, H. G., and Schrader, J. (1989). Contribution of S-adenosylhomocysteine to cardiac adenosine formation. *J. Mol. Cell. Cardiol.* 21, 773–782. doi:10.1016/0022-2828(89)90716-5

Diógenes, M. J., Fernandes, C. C., Sebastião, A. M., and Ribeiro, J. A. (2004). Activation of adenosine A2A receptor facilitates brain-derived neurotrophic factor modulation of synaptic transmission in hippocampal slices. *J. Neurosci.* 24, 2905–2913. doi:10.1523/JNEUROSCI.4454-03.2004

Dong, H., Chen, Z. K., Guo, H., Yuan, X. S., Liu, C. W., Qu, W. M., et al. (2022). Striatal neurons expressing dopamine D(1) receptor promote wakefulness in mice. *Curr. Biol.* 32, 600–613.e4. doi:10.1016/j.cub.2021.12.026

Dos Santos-Rodrigues, A., Pereira, M. R., Brito, R., de Oliveira, N. A., and Paes-de-Carvalho, R. (2015). Adenosine transporters and receptors: Key elements for retinal function and neuroprotection. *Vitam. Horm.* 98, 487–523. doi:10.1016/bs.vh.2014.12.014

Drew, K. L., Frare, C., and Rice, S. A. (2017). Neural signaling metabolites may modulate energy use in hibernation. *Neurochem. Res.* 42, 141–150. doi:10.1007/s11064-016-2109-4

Drew, K. L., and Jinka, T. R. (2013). *The bioenergetic network of adenosine in hibernation, sleep, and thermoregulation, adenosine*. Berlin, Germany: Springer, 253–272.

Dunwiddie, T. V., and Diao, L. (1994). Extracellular adenosine concentrations in hippocampal brain slices and the tonic inhibitory modulation of evoked excitatory responses. *J. Pharmacol. Exp. Ther.* 268, 537–545.

Dux, E., Fastbom, J., Ungerstedt, U., Rudolphi, K., and Fredholm, B. B. (1990). Protective effect of adenosine and a novel xanthine derivative propentofylline on the cell damage after bilateral carotid occlusion in the gerbil hippocampus. *Brain Res.* 516, 248–256. doi:10.1016/0006-8993(90)90925-2

El Yacoubi, M., Ledent, C., Parmentier, M., Costentin, J., and Vaugeois, J. M. (2003). Caffeine reduces hypnotic effects of alcohol through adenosine A2A receptor blockade. *Neuropharmacology* 45, 977–985. doi:10.1016/s0028-3908(03)00254-5

Fang, T., Dong, H., Xu, X. H., Yuan, X. S., Chen, Z. K., Chen, J. F., et al. (2017). Adenosine A(2A) receptor mediates hypnotic effects of ethanol in mice. *Sci. Rep.* 7, 12678. doi:10.1038/s41598-017-12689-6

Feldberg, W., and Sherwood, S. L. (1954). Injections of drugs into the lateral ventricle of the cat. *J. Physiol.* 123, 148–167.

Ferre, S., von Euler, G., Johansson, B., Fredholm, B. B., and Fuxe, K. (1991). Stimulation of high-affinity adenosine A2 receptors decreases the affinity of dopamine D2 receptors in rat striatal membranes. *Proc. Natl. Acad. Sci. U. S. A.* 88, 7238–7241. doi:10.1073/pnas.88.16.7238

Frare, C., and Drew, K. L. (2021). Seasonal changes in adenosine kinase in tanycytes of the Arctic ground squirrel (Urocitellus parryii). *J. Chem. Neuroanat.* 113, 101920. doi:10.1016/j.jchemneu.2021.101920

Frare, C., Jenkins, M. E., Soldin, S. J., and Drew, K. L. (2018). The raphe pallidus and the hypothalamic-pituitary-thyroid Axis gate seasonal changes in thermoregulation in the hibernating arctic ground squirrel (urocitellus parryii). *Front. Physiol.* 9, 1747. doi:10.3389/fphys.2018.01747

Frare, C., Jenkins, M. E., McClure, K. M., and Drew, K. L. (2019). Seasonal decrease in thermogenesis and increase in vasoconstriction explain seasonal response to N(6)-cyclohexyladenosine-induced hibernation in the Arctic ground squirrel (Urocitellus parryii). *J. Neurochem.* 151, 316–335. doi:10.1111/jnc.14814

Fredholm, B. B., IJzerman, A. P. I. J., Jacobson, K. A., Klotz, K. N., and Linden, J. (2001). . *Pharmacol. Rev.* 53, 527–552.

Fredholm, B. B., Chen, J. F., Cunha, R. A., Svenningsson, P., and Vaugeois, J. M. (2005). Adenosine and brain function. *Int. Rev. Neurobiol.* 63, 191–270. doi:10.1016/S0074-7742(05)63007-3

Gallopin, T., Luppi, P. H., Cauli, B., Urade, Y., Rossier, J., Hayaishi, O., et al. (2005). The endogenous somnogen adenosine excites a subset of sleep-promoting neurons via A2A receptors in the ventrolateral preoptic nucleus. *Neuroscience* 134, 1377–1390. doi:10.1016/j.neuroscience.2005.05.045

Garcia-Gil, M., Camici, M., Allegrini, S., Pesi, R., and Tozzi, M. G. (2021). Metabolic aspects of adenosine functions in the brain. *Front. Pharmacol.* 12, 672182. doi:10.3389/fphar.2021.672182

Geiser, F. (2013). Hibernation. *Curr. Biol.* 23, R188–R193. doi:10.1016/j.cub.2013.01.062

Gerashchenko, D., Okano, Y., Urade, Y., Inoué, S., and Hayaishi, O. (2000). Strong rebound of wakefulness follows prostaglandin D2-or adenosine A2a receptor agonist-induced sleep. *J. Sleep. Res.* 9, 81–87. doi:10.1046/j.1365-2869.2000.00175.x

Giroud, S., Habold, C., Nespolo, R. F., Mejías, C., Terrien, J., Logan, S. M., et al. (2020). The torpid state: Recent advances in metabolic adaptations and protective mechanisms(†). *Front. Physiol.* 11, 623665. doi:10.3389/fphys.2020.623665

Golanov, E. V., and Reis, D. J. (2001). Neurons of nucleus of the solitary tract synchronize the EEG and elevate cerebral blood flow via a novel medullary area. *Brain Res.* 892, 1–12. doi:10.1016/s0006-8993(00)02949-8

Halassa, M. M., Florian, C., Fellin, T., Munoz, J. R., Lee, S. Y., Abel, T., et al. (2009). Astrocytic modulation of sleep homeostasis and cognitive consequences of sleep loss. *Neuron* 61, 213–219. doi:10.1016/j.neuron.2008.11.024

Hadj-Moussa, H., and Storey, K. B. (2019). Bringing nature back: Using hibernation to reboot organ preservation. *Febs J.* 286, 1094–1100. doi:10.1111/febs.14683

Hall, J., and Frenguelli, B. G. (2018). The combination of ribose and adenine promotes adenosine release and attenuates the intensity and frequency of epileptiform activity in hippocampal slices: Evidence for the rapid depletion of cellular ATP during electrographic seizures. *J. Neurochem.* 147, 178–189. doi:10.1111/jnc.14543

Hong, Z. Y., Huang, Z. L., Qu, W. M., Eguchi, N., Urade, Y., and Hayaishi, O. (2005). An adenosine A receptor agonist induces sleep by increasing GABA release in the tuberomammillary nucleus to inhibit histaminergic systems in rats. *J. Neurochem.* 92, 1542–1549. doi:10.1111/j.1471-4159.2004.02991.x

Hösli, E., and Hösli, L. (1988). Autoradiographic studies on the uptake of adenosine and on binding of adenosine analogues in neurons and astrocytes of cultured rat cerebellum and spinal cord. *Neuroscience* 24, 621–628. doi:10.1016/0306-4522(88)90355-7

Hrvatin, S., Sun, S., Wilcox, O. F., Yao, H., Lavin-Peter, A. J., Cicconet, M., et al. (2020). Neurons that regulate mouse torpor. *Nature* 583, 115–121. doi:10.1038/s41586-020-2387-5

Huang, Y. G., Flaherty, S. J., Pothecary, C. A., Foster, R. G., Peirson, S. N., and Vyazovskiy, V. V. (2021). The relationship between fasting-induced torpor, sleep, and wakefulness in laboratory mice. *Sleep* 44, zsab093. doi:10.1093/sleep/zsab093

Huang, Z. L., Qu, W. M., Eguchi, N., Chen, J. F., Schwarzschild, M. A., Fredholm, B. B., et al. (2005). Adenosine A2A, but not A1, receptors mediate the arousal effect of caffeine. *Nat. Neurosci.* 8, 858–859. doi:10.1038/nn1491

Huang, Z. L., Urade, Y., and Hayaishi, O. (2011). The role of adenosine in the regulation of sleep. *Curr. Top. Med. Chem.* 11, 1047–1057. doi:10.2174/156802611795347654

Huang, Z. L., Zhang, Z., and Qu, W. M. (2014). Roles of adenosine and its receptors in sleep-wake regulation. *Int. Rev. Neurobiol.* 119, 349–371. doi:10.1016/B978-0-12-801022-8.00014-3

Iliff, B. W., and Swoap, S. J. (2012). Central adenosine receptor signaling is necessary for daily torpor in mice. *Am. J. Physiol. Regul. Integr. Comp. Physiol.* 303, R477–R484. doi:10.1152/ajpregu.00081.2012

Jenner, P., Mori, A., and Kanda, T. (2020). Can adenosine A(2A) receptor antagonists be used to treat cognitive impairment, depression or excessive sleepiness in Parkinson's disease? *Park. Relat. Disord.* 80, S28–s36. doi:10.1016/j.parkreldis.2020.09.022

Jinka, T. R., Combs, V. M., and Drew, K. L. (2015). Translating drug-induced hibernation to therapeutic hypothermia. *ACS Chem. Neurosci.* 6, 899–904. doi:10.1021/acschemneuro.5b00056

Jinka, T. R. (2012). "Natural protection against cardiac arrhythmias during hibernation: Significance of adenosine," in *Cardiac Arrhythmias-New Considerations*, 151–166.

Jinka, T. R., Tøien, Ø., and Drew, K. L. (2011). Season primes the brain in an arctic hibernator to facilitate entrance into torpor mediated by adenosine A(1) receptors. *J. Neurosci.* 31, 10752–10758. doi:10.1523/JNEUROSCI.1240-11.2011

Kashfi, S., Ghaedi, K., Baharvand, H., Nasr-Esfahani, M. H., and Javan, M. (2017). A(1) adenosine receptor activation modulates central nervous system development and repair. *Mol. Neurobiol.* 54, 8128–8139. doi:10.1007/s12035-016-0292-6

Kazemzadeh-Narbat, M., Annabi, N., Tamayol, A., Oklu, R., Ghanem, A., and Khademhosseini, A. (2015). Adenosine-associated delivery systems. *J. Drug Target* 23, 580–596. doi:10.3109/1061186X.2015.1058803

Korkutata, M., Agrawal, L., and Lazarus, M. (2022). Allosteric modulation of adenosine A(2A) receptors as a new therapeutic avenue. *Int. J. Mol. Sci.* 23, 2101. doi:10.3390/ijms23042101

Korkutata, M., Saitoh, T., Cherasse, Y., Ioka, S., Duo, F., Qin, R., et al. (2019). Enhancing endogenous adenosine A(2A) receptor signaling induces slow-wave sleep without affecting body temperature and cardiovascular function. *Neuropharmacology* 144, 122–132. doi:10.1016/j.neuropharm.2018.10.022

Latini, S., and Pedata, F. (2001). Adenosine in the central nervous system: Release mechanisms and extracellular concentrations. *J. Neurochem.* 79, 463–484. doi:10.1046/j.1471-4159.2001.00607.x

Lazarus, M., Chen, J. F., Huang, Z. L., Urade, Y., and Fredholm, B. B. (2019a). Adenosine and sleep. *Handb. Exp. Pharmacol.* 253, 359–381. doi:10.1007/164_2017_36

Lazarus, M., Oishi, Y., Bjorness, T. E., and Greene, R. W. (2019b). Gating and the need for sleep: Dissociable effects of adenosine A(1) and A(2A) receptors. *Front. Neurosci.* 13, 740. doi:10.3389/fnins.2019.00740

Lazarus, M., Shen, H. Y., Cherasse, Y., Qu, W. M., Huang, Z. L., Bass, C. E., et al. (2011). Arousal effect of caffeine depends on adenosine A2A receptors in the shell of the nucleus accumbens. *J. Neurosci.* 31, 10067–10075. doi:10.1523/JNEUROSCI.6730-10.2011

Li, R., Wang, Y. Q., Liu, W. Y., Zhang, M. Q., Li, L., Cherasse, Y., et al. (2020). Activation of adenosine A(2A) receptors in the olfactory tubercle promotes sleep in rodents. *Neuropharmacology* 168, 107923. doi:10.1016/j.neuropharm.2019.107923

Liu, Y. J., Chen, J., Li, X., Zhou, X., Hu, Y. M., Chu, S. F., et al. (2019). Research progress on adenosine in central nervous system diseases. *CNS Neurosci. Ther.* 25, 899–910. doi:10.1111/cns.13190

Liu, Y. Y., Wang, T. X., Zhou, J. C., Qu, W. M., and Huang, Z. L. (2019). . *Psychopharmacol. Berl.* 236, 3169–3182. doi:10.1007/s00213-019-05275-3

Liu, Z. W., and Gao, X. B. (2007). Adenosine inhibits activity of hypocretin/orexin neurons by the A1 receptor in the lateral hypothalamus: A possible sleep-promoting effect. *J. Neurophysiol.* 97, 837–848. doi:10.1152/jn.00873.2006

Lopes, L. V., Rebola, N., Pinheiro, P. C., Richardson, P. J., Oliveira, C. R., and Cunha, R. A. (2003). Adenosine A3 receptors are located in neurons of the rat hippocampus. *Neuroreport* 14, 1645–1648. doi:10.1097/00001756-200308260-00021

Lopes, L. V., Sebastião, A. M., and Ribeiro, J. A. (2011). Adenosine and related drugs in brain diseases: Present and future in clinical trials. *Curr. Top. Med. Chem.* 11, 1087–1101. doi:10.2174/156802611795347591

Magdaleno-Madrigal, V. M., Martínez-Vargas, D., Valdés-Cruz, A., Almazán-Alvarado, S., and Fernández-Mas, R. (2010). Preemptive effect of nucleus of the solitary tract stimulation on amygdaloid kindling in freely moving cats. *Epilepsia* 51, 438–444. doi:10.1111/j.1528-1167.2009.02337.x

McClure, J. M., O'Leary, D. S., and Scislo, T. J. (2011). Neural and humoral control of regional vascular beds via A1 adenosine receptors located in the nucleus tractus solitarii. *Am. J. Physiol. Regul. Integr. Comp. Physiol.* 300, R744–R755. doi:10.1152/ajpregu.00565.2010

McClure, J. M., O'Leary, D. S., and Scislo, T. J. (2005). Stimulation of NTS A1 adenosine receptors evokes counteracting effects on hindlimb vasculature. *Am. J. Physiol. Heart Circ. Physiol.* 289, H2536–H2542. doi:10.1152/ajpheart.00723.2005

Methippara, M. M., Kumar, S., Alam, M. N., Szymusiak, R., and McGinty, D. (2005). Effects on sleep of microdialysis of adenosine A1 and A2a receptor analogs into the lateral preoptic area of rats. *Am. J. Physiol. Regul. Integr. Comp. Physiol.* 289, R1715–R1723. doi:10.1152/ajpregu.00247.2005

Milsom, W. K., and Jackson, D. C. (2011). Hibernation and gas exchange. *Compr. Physiol.* 1, 397–420. doi:10.1002/cphy.c090018

Missale, C., Nash, S. R., Robinson, S. W., Jaber, M., and Caron, M. G. (1998). Dopamine receptors: From structure to function. *Physiol. Rev.* 78, 189–225. doi:10.1152/physrev.1998.78.1.189

Mohr, S. M., Bagriantsev, S. N., and Gracheva, E. O. (2020). Cellular, molecular, and physiological adaptations of hibernation: The solution to environmental challenges. *Annu. Rev. Cell. Dev. Biol.* 36, 315–338. doi:10.1146/annurev-cellbio-012820-095945

Morairty, S., Rainnie, D., McCarley, R., and Greene, R. (2004). Disinhibition of ventrolateral preoptic area sleep-active neurons by adenosine: A new mechanism for sleep promotion. *Neuroscience* 123, 451–457. doi:10.1016/j.neuroscience.2003.08.066

Nakamura, Y., Midorikawa, T., Monoi, N., Kimura, E., Murata-Matsuno, A., Sano, T., et al. (2016). Oral administration of Japanese sake yeast (*Saccharomyces cerevisiae* sake) promotes non-rapid eye movement sleep in mice via adenosine A(2A) receptors. *J. Sleep. Res.* 25, 746–753. doi:10.1111/jsr.12434

Nishimon, S., Sakai, N., and Nishino, S. (2021). Sake yeast induces the sleep-promoting effects under the stress-induced acute insomnia in mice. *Sci. Rep.* 11, 20816. doi:10.1038/s41598-021-00271-0

Oishi, Y., Huang, Z. L., Fredholm, B. B., Urade, Y., and Hayaishi, O. (2008). Adenosine in the tuberomammillary nucleus inhibits the histaminergic system via A1 receptors and promotes non-rapid eye movement sleep. *Proc. Natl. Acad. Sci. U. S. A.* 105, 19992–19997. doi:10.1073/pnas.0810926105

Oishi, Y., Xu, Q., Wang, L., Zhang, B. J., Takahashi, K., Takata, Y., et al. (2017). Slow-wave sleep is controlled by a subset of nucleus accumbens core neurons in mice. *Nat. Commun.* 8, 734. doi:10.1038/s41467-017-00781-4

Olson, J. M., Jinka, T. R., Larson, L. K., Danielson, J. J., Moore, J. T., Carpluck, J., et al. (2013). Circannual rhythm in body temperature, torpor, and sensitivity to $A_1$ adenosine receptor agonist in arctic ground squirrels. *J. Biol. Rhythms* 28, 201–207. doi:10.1177/0748730413490667

Omond, S. E. T., Hale, M. W., and Lesku, J. A. (2022). Neurotransmitters of sleep and wakefulness in flatworms. *Sleep* 45 (5), zsac053. doi:10.1093/sleep/zsac053

Peng, W., Wu, Z., Song, K., Zhang, S., Li, Y., and Xu, M. (2020). Regulation of sleep homeostasis mediator adenosine by basal forebrain glutamatergic neurons. *Science* 369, eabb0556. doi:10.1126/science.abb0556

Porkka-Heiskanen, T., Strecker, R. E., Thakkar, M., Bjorkum, A. A., Greene, R. W., and McCarley, R. W. (1997). Adenosine: A mediator of the sleep-inducing effects of prolonged wakefulness. *Science* 276, 1265–1268. doi:10.1126/science.276.5316.1265

Qiu, M. H., Qu, W. M., Xu, X. H., Yan, M. M., Urade, Y., and Huang, Z. L. (2009). D(1)/D(2) receptor-targeting L-stepholidine, an active ingredient of the Chinese herb Stephonia, induces non-rapid eye movement sleep in mice. *Pharmacol. Biochem. Behav.* 94, 16–23. doi:10.1016/j.pbb.2009.06.018

Qu, W. M., Huang, Z. L., Xu, X. H., Matsumoto, N., and Urade, Y. (2008). Dopaminergic D1 and D2 receptors are essential for the arousal effect of modafinil. *J. Neurosci.* 28, 8462–8469. doi:10.1523/JNEUROSCI.1819-08.2008

Qu, W. M., Xu, X. H., Yan, M. M., Wang, Y. Q., Urade, Y., and Huang, Z. L. (2010). Essential role of dopamine D2 receptor in the maintenance of wakefulness, but not in homeostatic regulation of sleep, in mice. *J. Neurosci.* 30, 4382–4389. doi:10.1523/JNEUROSCI.4936-09.2010

Radulovacki, M., Virus, R. M., Djuricic-Nedelson, M., and Green, R. D. (1984). Adenosine analogs and sleep in rats. *J. Pharmacol. Exp. Ther.* 228, 268–274.

Rainnie, D. G., Grunze, H. C., McCarley, R. W., and Greene, R. W. (1994). Adenosine inhibition of mesopontine cholinergic neurons: Implications for EEG arousal. *Science* 263, 689–692. doi:10.1126/science.8303279

Ren, C. Y., Rao, J. X., Zhang, X. X., Zhang, M., Xia, L., and Chen, G. H. (2021). Changed signals of blood adenosine and cytokines are associated with parameters of sleep and/or cognition in the patients with chronic insomnia disorder. *Sleep. Med.* 81, 42–51. doi:10.1016/j.sleep.2021.02.005

Rijo-Ferreira, F., Bjorness, T. E., Cox, K. H., Sonneborn, A., Greene, R. W., and Takahashi, J. S. (2020). Sleeping sickness disrupts the sleep-regulating adenosine system. *J. Neurosci.* 40, 9306–9316. doi:10.1523/JNEUROSCI.1046-20.2020

Roth, T. (2004). Characteristics and determinants of normal sleep. *J. Clin. Psychiatry* 65, 8–11.

Ruf, T., and Geiser, F. (2015). Daily torpor and hibernation in birds and mammals. *Biol. Rev. Camb Philos. Soc.* 90, 891–926. doi:10.1111/brv.12137

Sala-Newby, G. B., Skladanowski, A. C., and Newby, A. C. (1999). The mechanism of adenosine formation in cells. Cloning of cytosolic 5'-nucleotidase-I. *J. Biol. Chem.* 274, 17789–17793. doi:10.1074/jbc.274.25.17789

Saper, C. B., Scammell, T. E., and Lu, J. (2005). Hypothalamic regulation of sleep and circadian rhythms. *Nature* 437, 1257–1263. doi:10.1038/nature04284

Satoh, S., Matsumura, H., and Hayaishi, O. (1998). Involvement of adenosine A2A receptor in sleep promotion. *Eur. J. Pharmacol.* 351, 155–162. doi:10.1016/s0014-2999(98)00302-1

Satoh, S., Matsumura, H., Koike, N., Tokunaga, Y., Maeda, T., and Hayaishi, O. (1999). Region-dependent difference in the sleep-promoting potency of an adenosine A2A receptor agonist. *Eur. J. Neurosci.* 11, 1587–1597. doi:10.1046/j.1460-9568.1999.00569.x

Scammell, T. E., Gerashchenko, D. Y., Mochizuki, T., McCarthy, M. T., Estabrooke, I. V., Sears, C. A., et al. (2001). An adenosine A2a agonist increases sleep and induces Fos in ventrolateral preoptic neurons. *Neuroscience* 107, 653–663. doi:10.1016/s0306-4522(01)00383-9

Schmidt, M. H. (2014). The energy allocation function of sleep: A unifying theory of sleep, torpor, and continuous wakefulness. *Neurosci. Biobehav Rev.* 47, 122–153. doi:10.1016/j.neubiorev.2014.08.001

Shimaoka, H., Kawaguchi, T., Morikawa, K., Sano, Y., Naitou, K., Nakamori, H., et al. (2018). Induction of hibernation-like hypothermia by central activation of the A1 adenosine receptor in a non-hibernator, the rat. *J. Physiol. Sci.* 68, 425–430. doi:10.1007/s12576-017-0543-y

Siegel, J. M. (2009). Sleep viewed as a state of adaptive inactivity. *Nat. Rev. Neurosci.* 10, 747–753. doi:10.1038/nrn2697

Silvani, A., Cerri, M., Zoccoli, G., and Swoap, S. J. (2018). Is adenosine action common ground for NREM sleep, torpor, and other hypometabolic states? *Physiol. (Bethesda)* 33, 182–196. doi:10.1152/physiol.00007.2018

Silvani, A., and Dampney, R. A. (2013). Central control of cardiovascular function during sleep. *Am. J. Physiol. Heart Circ. Physiol.* 305, H1683–H1692. doi:10.1152/ajpheart.00554.2013

Sisa, C., Turroni, S., Amici, R., Brigidi, P., Candela, M., and Cerri, M. (2017). Potential role of the gut microbiota in synthetic torpor and therapeutic hypothermia. *World J. Gastroenterol.* 23, 406–413. doi:10.3748/wjg.v23.i3.406

Soto, M., Orliaguet, L., Reyzer, M. L., Manier, M. L., Caprioli, R. M., and Kahn, C. R. (2018). Pyruvate induces torpor in obese mice. *Proc. Natl. Acad. Sci. U. S. A.* 115, 810–815. doi:10.1073/pnas.1717507115

Stenberg, D., Litonius, E., Halldner, L., Johansson, B., Fredholm, B. B., and Porkka-Heiskanen, T. (2003). Sleep and its homeostatic regulation in mice lacking the adenosine A1 receptor. *J. Sleep. Res.* 12, 283–290. doi:10.1046/j.0962-1105.2003.00367.x

Stockwell, J., Jakova, E., and Cayabyab, F. S. (2017). Adenosine A1 and A2A receptors in the brain: Current research and their role in neurodegeneration. *Molecules* 22, 676. doi:10.3390/molecules22040676

Storey, K. B., and Storey, J. M. (2013). Molecular biology of freezing tolerance. *Compr. Physiol.* 3, 1283–1308. doi:10.1002/cphy.c130007

Storey, K. B., and Storey, J. M. (2017). Molecular physiology of freeze tolerance in vertebrates. *Physiol. Rev.* 97, 623–665. doi:10.1152/physrev.00016.2016

Strömberg, I., Popoli, P., Müller, C. E., Ferré, S., and Fuxe, K. (2000). Electrophysiological and behavioural evidence for an antagonistic modulatory role of adenosine A2A receptors in dopamine D2 receptor regulation in the rat dopamine-denervated striatum. *Eur. J. Neurosci.* 12, 4033–4037. doi:10.1046/j.1460-9568.2000.00288.x

Sun, M. J., and Tang, Y. (2020). Extracellular levels of the sleep homeostasis mediator, adenosine, are regulated by glutamatergic neurons during wakefulness and sleep. *Purinergic Signal* 16, 475–476. doi:10.1007/s11302-020-09758-3

Swoap, S. J. (2017). Central adenosine and daily torpor in mice. *Temp. (Austin)* 4, 350–352. doi:10.1080/23328940.2017.1345713

Swoap, S. J., Körtner, G., and Geiser, F. (2017). Heart rate dynamics in a marsupial hibernator. *J. Exp. Biol.* 220, 2939–2946. doi:10.1242/jeb.155879

Swoap, S. J., Rathvon, M., and Gutilla, M. (2007). AMP does not induce torpor. *Am. J. Physiol. Regul. Integr. Comp. Physiol.* 293, R468–R473. doi:10.1152/ajpregu.00888.2006

Tamura, Y., Shintani, M., Inoue, H., Monden, M., and Shiomi, H. (2012). Regulatory mechanism of body temperature in the central nervous system during the maintenance phase of hibernation in Syrian hamsters: Involvement of β-endorphin. *Brain Res.* 1448, 63–70. doi:10.1016/j.brainres.2012.02.004

Tartar, J. L., Hiffernan, F. S., Freitas, K. E., Fins, A. I., and Banks, J. B. (2021). A functional adenosine deaminase polymorphism associates with evening melatonin levels and sleep quality. *J. Circadian Rhythms* 19, 5. doi:10.5334/jcr.209

Thakkar, M. M., Engemann, S. C., Walsh, K. M., and Sahota, P. K. (2008). Adenosine and the homeostatic control of sleep: Effects of A1 receptor blockade in the perifornical lateral hypothalamus on sleep-wakefulness. *Neuroscience* 153, 875–880. doi:10.1016/j.neuroscience.2008.01.017

Thakkar, M. M., Winston, S., and McCarley, R. W. (2003). A1 receptor and adenosinergic homeostatic regulation of sleep-wakefulness: Effects of antisense to the A1 receptor in the cholinergic basal forebrain. *J. Neurosci.* 23, 4278–4287. doi:10.1523/JNEUROSCI.23-10-04278.2003

Thakkar, M. M., Winston, S., and McCarley, R. W. (2002). Orexin neurons of the hypothalamus express adenosine A1 receptors. *Brain Res.* 944, 190–194. doi:10.1016/s0006-8993(02)02873-1

Tupone, D., Madden, C. J., and Morrison, S. F. (2013). Central activation of the A1 adenosine receptor (A1AR) induces a hypothermic, torpor-like state in the rat. *J. Neurosci.* 33, 14512–14525. doi:10.1523/JNEUROSCI.1980-13.2013

Urade, Y., Eguchi, N., Qu, W. M., Sakata, M., Huang, Z. L., Chen, J. F., et al. (2003). Sleep regulation in adenosine A2A receptor-deficient mice. *Neurology* 61, S94–S96. doi:10.1212/01.wnl.0000095222.41066.5e

van Calker, D., Müller, M., and Hamprecht, B. (1979). Adenosine regulates via two different types of receptors, the accumulation of cyclic AMP in cultured brain cells. *J. Neurochem.* 33, 999–1005.

Vicent, M. A., Borre, E. D., and Swoap, S. J. (2017). Central activation of the A(1) adenosine receptor in fed mice recapitulates only some of the attributes of daily torpor. *J. Comp. Physiol. B* 187, 835–845. doi:10.1007/s00360-017-1084-7

Vlajkovic, S. M., Abi, S., Wang, C. J., Housley, G. D., and Thorne, P. R. (2007). Differential distribution of adenosine receptors in rat cochlea. *Cell. Tissue Res.* 328, 461–471. doi:10.1007/s00441-006-0374-2

Wall, M., and Dale, N. (2008). Activity-dependent release of adenosine: A critical re-evaluation of mechanism. *Curr. Neuropharmacol.* 6, 329–337. doi:10.2174/157015908787386087

Xiao, C., Liu, N., Jacobson, K. A., Gavrilova, O., and Reitman, M. L. (2019). Physiology and effects of nucleosides in mice lacking all four adenosine receptors. *PLoS Biol.* 17, e3000161. doi:10.1371/journal.pbio.3000161

Xu, Y., Shao, C., Fedorov, V. B., Goropashnaya, A. V., Barnes, B. M., and Yan, J. (2013). Molecular signatures of mammalian hibernation: Comparisons with alternative phenotypes. *BMC Genomics* 14, 567. doi:10.1186/1471-2164-14-567

Yang, Y. F., Dong, H., Shen, Y., Li, L., Lazarus, M., Qu, W. M., et al. (2021). Mesencephalic dopamine neurons are essential for modafinil-induced arousal. *Br. J. Pharmacol.* 178, 4808–4825. doi:10.1111/bph.15660

Yuan, X. S., Wang, L., Dong, H., Qu, W. M., Yang, S. R., Cherasse, Y., et al. (2017). Striatal adenosine A(2A) receptor neurons control active-period sleep via parvalbumin neurons in external globus pallidus. *Elife* 6, e29055. doi:10.7554/eLife.29055

## Glossary

**$A_1$Rs** adenosine $A_1$ receptors
**$A_{2A}$Rs** adenosine $A_{2A}$ receptors
**$A_{2B}$Rs** adenosine $A_{2B}$ receptors
**$A_3$Rs** adenosine $A_3$ receptors
**AC** adenylate cyclase
**ADK** adenosine kinase
**ADP** adenosine diphosphate
**AMP** adenosine monophosphate
**ATP** adenosine triphosphate
**BAT** brown adipose tissue
**BF** basal forebrain
**BMR** basal metabolic rate
**BP** blood pressure
**cAMP** cyclic adenosine-3,5 monophosphate
**CHA** N6-cyclohexyladenosine
**CNS** central nervous system
**CPA** N6-cyclopentyladenosine
**EEG** electroencephalographic
**EMG** electromyography
**E-NTPDase** ecto-nucleoside triphosphate diphosphohydrolase
**Gi** inhibitory adenylate cyclase G protein
**GPCR** G protein coupled receptor
**GPe** external globus pallidus
**Gs** stimulating adenylate cyclase G protein
**HP** heart period
**HR** heart rate
**KATP** ATP sensitive potassium channel
**LH** lateral hypothalamus
**MR** metabolic rates
**NAc** nucleus accumbens
**NBTIs** nitrobenzyl-thio-inosine
**NREM** non-rapid eye movement
**NTS** nucleus tractus solitarius
**OT** olfactory tubercle
**PAM** positive allosteric modulator
**PLC** phospholipase C
**PV** parvalbumin
**REM** rapid eye movement
**rPA** raphe pallidus
**MnPO** median preoptic
**SON** supraoptic
**SAH** S-adenosylhomocysteine
**SAHH** S-adenosylhomocysteine hydrolase
**SAM** S-adenosylmethionine
**SWS** slow-wave sleep
**Ta** ambient temperature
**$T_b$** body temperature
**TMN** tuberomammillary nucleus
**VLPO** ventrolateral preoptic nucleus lateral preoptic area
**LPO** lateral preoptic
**VP** ventral pallidum γ-aminobutyric acid
**GABA** γ-aminobutyric acid
**5′-NT** 5′-nucleotidase

frontiers | Frontiers in Pharmacology

TYPE Original Research
PUBLISHED 16 March 2023
DOI 10.3389/fphar.2023.1120360



OPEN ACCESS

EDITED BY
Yong Tang,
Chengdu University of Traditional Chinese Medicine, China

REVIEWED BY
Thomas Grutter,
Université de Strasbourg, France
Stephan Kellenberger,
Université de Lausanne, Switzerland

*CORRESPONDENCE
Ralf Hausmann,
rhausmann@ukaachen.de

SPECIALTY SECTION
This article was submitted to Experimental Pharmacology and Drug Discovery, a section of the journal Frontiers in Pharmacology

RECEIVED 09 December 2022
ACCEPTED 24 February 2023
PUBLISHED 16 March 2023

CITATION
Grohs L, Cheng L, Cönen S, Haddad BG, Bülow A, Toklucu I, Ernst L, Körner J, Schmalzing G, Lampert A, Machtens J-P and Hausmann R (2023), Diclofenac and other non-steroidal anti-inflammatory drugs (NSAIDs) are competitive antagonists of the human P2X3 receptor. *Front. Pharmacol.* 14:1120360. doi: 10.3389/fphar.2023.1120360



# Diclofenac and other non-steroidal anti-inflammatory drugs (NSAIDs) are competitive antagonists of the human P2X3 receptor

Laura Grohs[1,2], Linhan Cheng[1], Saskia Cönen[1,3], Bassam G. Haddad[3], Astrid Bülow[1,4], Idil Toklucu[5], Lisa Ernst[6], Jannis Körner[5,7], Günther Schmalzing[1], Angelika Lampert[5], Jan-Philipp Machtens[1,3] and Ralf Hausmann[1]*

[1]Institute of Clinical Pharmacology, RWTH Aachen University, Aachen, Germany, [2]Department of Neurology, University Hospital, RWTH Aachen University, Aachen, Germany, [3]Molecular and Cellular Physiology (IBI-1), Institute of Biological Information Processing (IBI), Forschungszentrum Jülich, Jülich, Germany, [4]Department of Plastic Surgery, Hand Surgery—Burn Center, University Hospital, RWTH Aachen University, Aachen, Germany, [5]Institute of Physiology (Neurophysiology), RWTH Aachen University, Aachen, Germany, [6]Institute for Laboratory Animal Science and Experimental Surgery, RWTH Aachen University, Aachen, Germany, [7]Department of Anesthesiology, University Hospital, RWTH Aachen University, Aachen, Germany

**Introduction:** The P2X3 receptor (P2X3R), an ATP-gated non-selective cation channel of the P2X receptor family, is expressed in sensory neurons and involved in nociception. P2X3R inhibition was shown to reduce chronic and neuropathic pain. In a previous screening of 2000 approved drugs, natural products, and bioactive substances, various non-steroidal anti-inflammatory drugs (NSAIDs) were found to inhibit P2X3R-mediated currents.

**Methods:** To investigate whether the inhibition of P2X receptors contributes to the analgesic effect of NSAIDs, we characterized the potency and selectivity of various NSAIDs at P2X3R and other P2XR subtypes using two-electrode voltage clamp electrophysiology.

**Results:** We identified diclofenac as a hP2X3R and hP2X2/3R antagonist with micromolar potency (with $IC_{50}$ values of 138.2 and 76.7 μM, respectively). A weaker inhibition of hP2X1R, hP2X4R, and hP2X7R by diclofenac was determined. Flufenamic acid (FFA) inhibited hP2X3R, rP2X3R, and hP2X7R ($IC_{50}$ values of 221 μM, 264.1 μM, and ~900 μM, respectively), calling into question its use as a non-selective ion channel blocker, when P2XR-mediated currents are under study. Inhibition of hP2X3R or hP2X2/3R by diclofenac could be overcome by prolonged ATP application or increasing concentrations of the agonist α,β-meATP, respectively, indicating competition of diclofenac and the agonists. Molecular dynamics simulation showed that diclofenac largely overlaps with ATP bound to the open state of the hP2X3R. Our results suggest a competitive antagonism through which diclofenac, by interacting with residues of the ATP-binding site, left flipper, and dorsal fin domains, inhibits the gating of P2X3R by conformational fixation of the left flipper and dorsal fin domains. In summary, we demonstrate the inhibition of the human P2X3 receptor by various NSAIDs.

Diclofenac proved to be the most effective antagonist with a strong inhibition of hP2X3R and hP2X2/3R and a weaker inhibition of hP2X1R, hP2X4R, and hP2X7R.

**Discussion:** Considering their involvement in nociception, inhibition of hP2X3R and hP2X2/3R by micromolar concentrations of diclofenac, which are rarely reached in the therapeutic range, may play a minor role in analgesia compared to the high-potency cyclooxygenase inhibition but may explain the known side effect of taste disturbances caused by diclofenac.

KEYWORDS

**P2X3 receptor, nociception, chronic pain, non-steroidal anti-inflammatory drugs (NSAIDs), competitive antagonist, drug screening**

## 1 Introduction

P2X receptors (P2XR) constitute a family of non-selective cation channels gated by extracellular ATP (North and Barnard, 1997). Seven different subtypes (P2X1–7) can assemble into homo- or heterotrimers (Nicke et al., 1998; North, 2002).

The P2X3R, which is expressed in sensory neurons (Chen et al., 1995), plays a crucial role in nociception (Burnstock, 2016). P2X3-deficient mice exhibit an attenuated pain behavior after injection of ATP into the hind paw compared to wild-type mice (Cockayne et al., 2000), whereas the response to acute mechanical pain stimuli remains unchanged (Souslova et al., 2000). Accordingly, pharmacological inhibition of P2X3R has been shown to effectively reduce chronic or neuropathic pain in rodents (Jarvis et al., 2002). Recently, the modulator TMEM163, a 289-amino acid transmembrane protein, was shown to be required for the complete function of the neuronal P2X3R- and P2X4R- and pain-related ATP-evoked behavior in mice (Salm et al., 2020). In addition to P2X3R, involvement in nociception could also be assigned to heterotrimeric P2X2/3R, P2X4R, and P2X7R (Chessell et al., 2005; Cockayne et al., 2005; Tsuda et al., 2009). All of these seem to be more relevant for the development of neuropathic or inflammatory pain than for acute nociception (Chessell et al., 2005; Tsuda et al., 2009).

The significant role of P2X3R in nociception makes P2X3R a promising target for the development of new analgesics (North and Jarvis, 2013). However, until now, none of the developed antagonists has been approved for clinical use as an analgesic, even if gefapixant (formerly AF-219) is approved as an anti-cough agent in Japan (details are given as follows). One of the first potent and selective P2X3R (and P2X2/3R) antagonists was A-317491, which successfully reduced chronic pain in rodent models (Jarvis et al., 2002), but showed insufficient distribution in the central nervous system (Sharp et al., 2006). Several other P2X3R antagonists have been developed as clinical candidates, such as AF-219/gefapixant, BAY-1817080/eliapixant, BLU-5937, MK-3901, or S-600918/sivopixant (Spinaci et al., 2021; Niimi et al., 2022). The availability of the crystal structures of the human P2X3R (Mansoor et al., 2016), together with cryo-EM techniques, is ideally suited to facilitate structure-based drug design for P2X3Rs by revealing and characterizing novel ligand-binding sites (Oken et al., 2022).

The most advanced is the development of gefapixant, a P2X3R and P2X2/3R antagonist, which effectively reduced chronic cough caused by hypersensitivity of the cough reflex in phase 2 and 3 trials (Abdulqawi et al., 2015; Marucci et al., 2019). However, a disturbance in taste sensation was described as a side effect by all patients (Abdulqawi et al., 2015). Gefapixant is a first-in-class, non-narcotic selective P2X3 receptor antagonist and was recently approved for marketing in Japan as a treatment option for refractory or unexplained chronic cough (Markham, 2022). Another promising substance, BLU-5937, was able to effectively reduce chronic cough in animal models without altering taste sensation, possibly due to its considerably higher selectivity for P2X3R *versus* P2X2/3R (Garceau and Chauret, 2019). BLU-5937 is now part of a phase 2 study for the treatment of chronic cough (Marucci et al., 2019). Also, sivopixant was shown to reduce objective cough frequency and improved health-related quality of life, with a low incidence of taste disturbance, among patients with a refractory or unexplained chronic cough in a phase 2a trial (Niimi et al., 2022). Eliapixant showed favorable tolerability with no taste-related adverse events in its first-in-human study, and in a phase 1/2a study, eliapixant administration showed reduced cough frequency and severity and was well-tolerated with acceptable rates of taste-related events (Morice et al., 2014; Klein et al., 2022).

In light of the promising role of P2X3R antagonists for the treatment of pain and refractory cough, as well as the high likelihood of taste disturbances caused by not fully selective P2X3R antagonists (against heteromeric P2X2/3R), it appears interesting to investigate whether already approved drugs do affect the P2X3R-mediated responses. For this purpose, a screening of 2000 approved drugs, natural products, and bioactive substances was performed in a previous study of our group. In this screening, aurintricarboxylic acid (ATA) was identified as a potent P2X1R and P2X3R antagonist (Obrecht et al., 2019). An inhibitory effect could also be demonstrated for other drugs. These included various non-steroidal anti-inflammatory drugs (NSAIDs), and diclofenac showed the highest inhibitory effect of the screened NSAIDs. The analgesic, antipyretic, and anti-inflammatory effect of NSAIDs is generally described to result from the inhibition of prostaglandin synthesis by inhibiting cyclooxygenases COX-1 and COX-2 (Vane, 1971). Most NSAIDs constitute reversible, competitive blockers of the enzyme cyclooxygenase (COX), while acetylsalicylic acid (Aspirin®) can cause irreversible inactivation of COX through acetylation of serine 530 (Rome and Lands, 1975; DeWitt et al., 1990).

Considering the involvement of P2X3R in nociception, it is conceivable that inhibition of P2X3R by NSAIDs represents an additional mode of action besides COX inhibition. To investigate

whether the inhibition of P2XR contributes to the analgesic effect of NSAIDs, we determined the potency and selectivity of various NSAIDs at P2X3R and other P2XR subtypes using two-electrode voltage clamp (TEVC) electrophysiology. The investigated NSAIDs included diclofenac, ibuprofen, flunixin, meclofenamic acid, naproxen, and flufenamic acid (FFA). The latter was chosen because it additionally plays an important role in research as a non-selective ion channel blocker (Guinamard et al., 2013).

In the present study, we have for the first time shown that diclofenac is a hP2X3R and hP2X2/3R antagonist with micromolar potency. Our results strongly support a competitive antagonism through which diclofenac, by interacting with residues of the ATP-binding site, left flipper, and dorsal fin domains, inhibits the gating of P2X3R by conformational fixation of the left flipper and dorsal fin domains. In addition, a weaker inhibition of hP2X1R, hP2X4R, and hP2X7R was shown. Less potent inhibition of hP2X3R was observed for all other investigated NSAIDs. FFA was proven to significantly inhibit hP2X3R, rP2X3R, and hP2X7R.

# 2 Materials and methods

## 2.1 Chemicals

The investigated NSAIDs and most standard chemicals were purchased from Sigma–Aldrich/Merck (Taufkirchen, Germany), if not otherwise specified. ATP sodium salt and α,β-meATP were purchased from Roche Diagnostics (Mannheim, Germany) and Tocris Bioscience (Bristol, United Kingdom), respectively. Collagenase type 2 was purchased from Worthington Biochemical Corp (Lakewood, United States and distributed by CellSystems, Troisdorf, Germany).

## 2.2 Expression of P2X receptors in *X. laevis* oocytes

Oocyte expression plasmids encoding the wild-type (wt) and N-terminally His-tagged (His-) fusion constructs of the hP2X2R, hP2X3R, hP2X4R, and hP2X7R, and the mutant His-$^{20}$RMVL$^{23}$KVIV$^{23}$S$^{26}$N-hP2X1R, S$^{15}$V-rP2X3R, and His-S$^{15}$V-hP2X3R were the same as used in previous research (Hausmann et al., 2006; Wolf et al., 2011; Hausmann et al., 2014; Obrecht et al., 2019). In most cases, the N-terminal His-tagged variants of P2XRs were used here and in the previous studies to allow biochemical analyses on affinity-purified proteins using the same constructs. Although this was not required for the present study, it allows for better comparability with our previous studies. Capped cRNAs of different P2XRs were already available in the research group or were synthesized as previously described (Schmalzing et al., 1991; Stolz et al., 2015). cRNA was injected into collagenase-defolliculated *X. laevis* oocytes in aliquots of 41 nl or 23 nl (see Supplementary Table S1 for the amount of cRNA used for expression of the indicated P2XR) using a Nanoliter 2000 injector (World Precision Instruments, Sarasota, United States of America) as described previously (Hausmann et al., 2014; Stolz et al., 2015; Obrecht et al., 2019). To express the heteromeric hP2X2/3 receptor, cRNAs encoding His-hP2X2R and wt-hP2X3R were coinjected at a ratio (w/w) of 1:6. Oocytes were stored at 19°C in an oocyte ringer solution (ORi$^+$) containing 90 mM NaCl, 1 mM KCl, 1 mM $CaCl_2$, 1 mM $MgCl_2$, and 10 mM HEPES (Carl Roth, Karlsruhe, Germany) adjusted to pH 7.4 with NaOH and supplemented with 50 μg/ml gentamicin (AppliChem, Darmstadt, Germany). The procedures followed for the maintenance of and the surgical treatment for *X. laevis* adults were approved by the governmental animal care and use committee of the State Agency for Nature, Environment, and Consumer Protection (LANUV, Recklinghausen, Germany; reference no. 81-02.04.2019. A355), in compliance with Directive 2010/63/EU of the European Parliament and of the Council on the protection of animals used for scientific purpose.

## 2.3 Two-electrode voltage clamp electrophysiology

Ion currents mediated by P2X receptors were evoked by the indicated concentration of ATP or α,β-meATP and were recorded 1 or 2 days after cRNA injection at ambient temperature at a holding potential of −60 mV by two-electrode voltage clamp (TEVC) as previously described (Hausmann et al., 2006). Calcium-free ORi$^-$ solution (90 mM NaCl, 1 mM KCl, 2 mM $MgCl_2$, 10 mM HEPES, pH 7.4) was used to avoid bias due to calcium-activated chloride channels (CaCC) endogenously expressed in *X. laevis* oocytes (Miledi, 1982; Methfessel et al., 1986). For recordings of wt-hP2X7R, the composition of the ORi$^-$ solution was modified according to protocols described previously and contained 100 mM NaCl, 2.5 mM KCl, 1 mM $MgCl_2$, 5 mM HEPES, pH 7.4 (Klapperstück et al., 2000). The oocytes were continuously superfused with ORi$^-$ by gravity flow (5–10 ml/min). The agonists ATP or α,β-meATP and the investigated NSAIDs were diluted in ORi$^-$ on the day of the recording. The following agonist concentrations were used for the different P2X subtypes: 1 μM ATP (hP2X1R mutant, hP2X3R, rP2X3R, S$^{15}$V-hP2X3R, and S$^{15}$V-rP2X3R); 10 μM ATP (hP2X2R and hP2X4R); 300 μM free ATP$^{4-}$ (hP2X7R); and 1 μM α,β-meATP (hP2X2/3R). A peak current protocol (Supplementary Figure S1) was used to analyze fast- and intermediate desensitizing P2XR subtypes (P2X1R, P2X3R, and S$^{15}$V-P2X3R), and a steady-state protocol (Supplementary Figure S2) was used for slowly or partially desensitizing P2X subtypes (P2X2R, P2X2/3R, and P2X4R). For recordings of P2X7R, a modified steady-state protocol was used (Hausmann et al., 2006). The application of different bath solutions was controlled by computer-operated magnetic valves controlled by the CellWorks E 5.5.1 software (npi electronic, Tamm, Germany).

## 2.4 Pig dorsal root ganglia preparation

The dorsal root ganglia (DRG) of pigs were sampled according to the 3R criteria for reductions in animal use, as leftovers from previous independent animal studies (e.g., LANUV reference no. 81-02.04.2018. A051). For this purpose, pigs of the German Landrace breed, with an average age of 15 weeks (14.6 SD2.7) and weight of 47.3 kg (SD11.2), were euthanized using an overdose of pentobarbital 60 mg/kg body weight. Subsequently, the DRG were collected. The DRG of pigs were transferred on ice, and fine excision was performed in ice-cold DMEM F12 medium containing 10% FBS and treated with 1 mg/ml collagenase P, 1 mg/ml trypsin T1426, and 0.1 mg/ml DNAse for digestion. Then,

the DRG were cut into small pieces inside the digestion medium for surface enlargement and incubated at 37°C and 5% $CO_2$ for 120 ±30 min. After approximately 60 min in the digestion medium, the DRG were triturated using a glass pipette. After the full incubation time, they were triturated thrice using custom-pulled glass pipettes with decreasing tip diameters (from ~1.1–1.2 to ~0.3–0.4 mm). For further purification, the DRG were centrifuged at 500 G and 4°C twice for 4 minutes each, and the pellets were suspended in DMEM F12 with 10% FBS. They were subsequently separated from lighter cell fragments and myelin by centrifugation of a Percoll gradient containing a 60% Percoll and a 25% Percoll gradient for 20 min at 500 G. DRG neurons were plated on coverslips coated with poly-D-lysine (100 μg/ml), laminin (10 μg/ml), and fibronectin (10 μg/ml). Neurons were then cultured in neurobasal A medium supplemented with B27, penicillin, streptomycin, and L-glutamine and used for voltage-clamp recordings after 12–72 h in culture.

## 2.5 Whole-cell patch-clamp recordings of pig DRG neurons

Whole-cell voltage-clamp recordings of DRG neurons were performed using glass electrodes with micropipette tip resistances of 1.3–3.5 MΩ, pulled and fire-polished with a Zeitz DMZ-puller. The intracellular solution contained 10 mM NaCl, 140 mM CsF, 10 mM HEPES, 1 mM EGTA, 5 mM glucose, and 5 mM TEA-Cl (adjusted to pH 7.3 using CsOH). The extracellular bathing solution contained 140 mM NaCl, 3 mM KCl, 1 mM $MgCl_2$, 1 mM $CaCl_2$, 10 mM HEPES, and 20 mM glucose (adjusted to pH 7.4 using NaOH). The liquid junction potential was corrected by −7.8 mV. Membrane currents were measured at room temperature, with a holding potential of −77.8 mV, using a HEKA EPC-10 USB amplifier. α, β-methylene ATP (10 μM) and 100 μM diclofenac were applied using a gravity-driven perfusion system during the recordings. PatchMaster/FitMaster software (HEKA Electronics) and IGOR Pro (WaveMetrics) were used for data acquisition and analysis. Signals were digitized at a sampling rate of 5 kHz. The low-pass filter frequency was set to 10 kHz. Series resistance compensation was between 2.5 and 11.1 MΩ.

## 2.6 Data analysis

The recorded TEVC currents were analyzed using CellWorks Reader 6.2.2 (npi electronic, Tamm, Germany) and Microsoft Excel (Microsoft Corporation, Redmond, United States). The displayed current traces were generated using IGOR Pro 6.21 (WaveMetrics, Portland, United States) and edited with Microsoft PowerPoint (Microsoft Corporation, Redmond, United States). To generate concentration–response curves, non-linear regression analysis was performed using GraphPad Prism 5 (GraphPad Software, San Diego, United States).

Antagonist concentration–response data and $IC_{50}$ values were calculated by normalizing ATP-induced responses to the control responses (recorded in the presence and absence of the antagonist, respectively). The four-parameter Hill equation (Eq. 1) was iteratively fitted to data collected from a minimum of four independent repeat experiments to obtain antagonist concentration–response curves and $IC_{50}$ values.

$$\frac{I_{Ant}}{I_{max}} = \frac{top - bottom}{1 + \left(\frac{[Ant]}{IC_{50}}\right)^{nH}} + bottom \quad (1)$$

$I_{max}$ is the control response in the absence of the antagonist, $I_{Ant}$ is the response at the given antagonist concentration (Ant), and $IC_{50}$ is the antagonist concentration that causes 50% inhibition of the response elicited by a given agonist concentration. The ratio between the response in the presence of a certain antagonist concentration and the control response in the absence of the antagonist is indicated as "% control current".

In the case of fast-desensitizing P2XR subtypes (P2X1R and P2X3R), ATP is applied five times in repetition, and the ATP-induced current amplitude in the presence (after pre-incubation) of the antagonist (fourth application) is compared to the arithmetic mean of flanking control ATP-induced current amplitudes in the absence of the antagonist (third and fifth ATP application). Since some of the investigated NSAIDs showed an enduring, potentially irreversible inhibitory effect on the current amplitude, only the preceding (third) ATP-induced current amplitude was used to calculate the control current. The typical run-down of current amplitudes between consecutive, repetitive ATP applications was considered by applying a correction factor. The correction factor was calculated as the ratio of the fourth ATP-induced current amplitude to the third amplitude (Eq. 3) when the experiment was performed in the absence of the antagonist. When the experiment was performed in the presence of the antagonist, the ATP-induced current amplitude of the preceding current (third amplitude) was multiplied by this correction factor/quotient (Eq. 4) to obtain a control current corrected for the run-down effect. Since the magnitude of the run-down varies from day to day and batch to batch of oocytes, the correction factor was determined on each day of the experiments and was calculated as the arithmetic mean of several recordings (at least 3–5 and on average 5) on each day. Based on many years of experience with corresponding measurements, it was determined that the correction factor should be >0.4 and should scatter by a max of 10% around the mean value between the different measurements of a day for its calculation to include data from the experimental measurement day in the evaluation.

$$\text{correction factor} = \frac{\text{ATP-induced current amplitude 4 in absence of antagonist}}{\text{ATP-induced current amplitude 3 in absence of antagonist}} \quad (2)$$

$$\%\ \text{control current} = \frac{\text{ATP-induced current amplitude 4 in presence of antagonist}}{\text{ATP-induced current amplitude 3 in absence of antagonist} \times \text{correction factor}} \quad (3)$$

In the case of hP2X7R, the control current in the absence of the antagonist had to be extrapolated (Supplementary Figure S4 and Supplementary Figure S5) presuming a linear increase in permeability during continuous ATP application (North, 2002) since the permeability of the receptor is affected by the antagonist.

The $IC_{50}$ values are displayed as geometric means with 95% confidence intervals (95% CI). All other values (including % control current or % inhibition) are presented as arithmetic means ± SEM, if not otherwise stated. Values were compared using the *t*-test or one-/two-way analysis of variance and multiple comparison tests as indicated. Statistical significance was set at $p < .05$.

## 2.7 hP2X3R X-ray structure-based molecular-dynamics simulations and evaluation of diclofenac binding

The human ionotropic cation-selective ATP receptor P2X3 was modeled based on its structure in the apo-closed state (PDBID: 5SVJ) (Mansoor et al., 2016) and embedded in a 1-palmitoyl-2-oleoyl-phosphatidylcholine (POPC) bilayer using the *g_membed* functionality (Wolf et al., 2010) in GROMACS. Modeller was used to build the single-point mutant L191A of the P2X3 apo-closed state to make the supposed binding cavity of diclofenac easily accessible to simulate the binding event within the μs-time-scale of the simulations (Fiser and Sali, 2003). The standard protonation state at neutral pH was assigned to all residues. The system was simulated using GROMACS (Abraham et al., 2015) version 2021, with an integration time-step of 2 fs.

A pressure of 1 bar was applied semi-isotropically with a Berendsen barostat (Berendsen et al., 1984) using a time constant of 5 ps. A temperature of 310 K was maintained with a velocity-rescaling thermostat (Bussi et al., 2007). Van der Waals interactions were calculated with the Lennard–Jones potential and a cutoff radius of 1.2 nm, with forces smoothly switched to 0 in the range of 1.0–1.2 nm with no dispersion correction. The protein was described by the CHARMM36m (Huang et al., 2017) force field, lipids by the CHARMM36 force field (Klauda et al., 2010), and water by the TIP3P model (Jorgensen et al., 1983).

$Na^+$ and $Cl^-$ were added to provide a bulk concentration of approximately 50 mM NaCl. The crystal structure of hP2X3R in complex with the AF-219 negative allosteric modulator (PDB-ID: 5YVE) was aligned with apo-state hP2X3 (PDB-ID: 5SVJ); one diclofenac molecule per protomer was then fitted onto the AF-219 molecule using PyMOL and placed into the apo-state structure. Seven independent systems, each of the wildtype P2X3 apo-closed state and L191A apo-closed state, were simulated for more than 200 ns each, preceded by equilibration for about 200 ns: first with restraints on all heavy atoms and lipids in the *z*-direction, second on all heavy atoms, and third on backbone atoms only. All trajectories that showed a stable binding of diclofenac were selected and clustered with the GROMACS tool *gmx cluster* using the GROMOS algorithm; the cut-off for RMSD differences in a cluster was set to 0.35 nm.

Initial force-field parameters for diclofenac were generated according to the CHARMM generalized force field (CGenFF) (Vanommeslaeghe et al., 2010; Vanommeslaeghe et al., 2012; Vanommeslaeghe and MacKerell, 2012; Yu et al., 2012), using the CHARMM-GUI webserver (https://charmm-gui.org/). The initial molecular geometry and charge assignments were further optimized using the force-field toolkit (ffTK) (Mayne et al., 2013) version 2.1 plugin for the visual molecular dynamics (VMD) version 1.9.4a57 analysis suite (Humphrey et al., 1996). The ffTK program provides a workflow of quantum-mechanical calculations using ORCA (Neese et al., 2020) 5.0.3, followed by Newtonian optimizations using the nanoscale molecular dynamics (NAMD) (Phillips et al., 2020) engine. An initial parameter file is generated in ffTK by analogy using the protein structure file (psf) and protein coordinate file generated by CHARMM-GUI. The initial molecular geometry was optimized using ORCA at the MP2/6-31G* level of theory. After geometry optimization had converged, atomic partial charges were approximated using ORCA by calculating water-interaction energies at the HF/6-31G* level of theory. Aliphatic and aromatic hydrogens were assigned partial charges of .09 and .115, respectively; only hydroxyl hydrogens were optimized. To account for the positive charge associated with the dipole created by halogens known as alpha-holes, a lone-pair particle (LP) was added automatically *via* CHARMM-GUI (Pang et al., 2020). New bonded parameters for diclofenac only contained two dihedral terms, which are consistent with the CHARMM36 force field, used for diclofenac simulations; dihedral bonds were not further optimized due to having a bond energy penalty of less than 50 (unitless penalties as provided by the CGenFF program). Detailed instructions for using the most updated ffTK with support for the open-source quantum chemistry package, ORCA, can be found at the ffTK website (https://www.ks.uiuc.edu/Research/vmd/plugins/fftk) and the updated tutorial (https://www.ks.uiuc.edu/~mariano/fftk-tutorial.pdf).

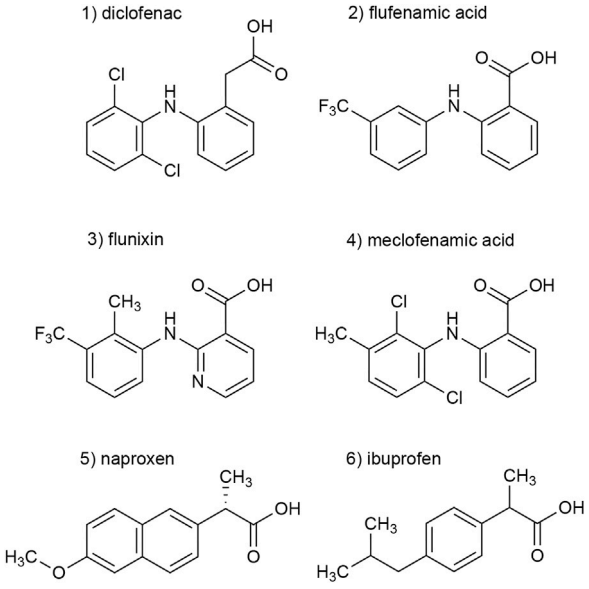


FIGURE 1
Chemical structures of the investigated NSAIDs (1–6).

# 3 Results

## 3.1 Validation of the inhibitory effect of various NSAIDs on P2X3R-mediated currents

In a previous screening of 2000 approved drugs, natural products, and bioactive substances, various NSAIDs were found to inhibit $S^{15}V$-rP2X3R-mediated currents (Obrecht et al., 2019). These included diclofenac, flunixin meglumine, meclofenamic acid, and niflumic acid, where diclofenac showed the greatest inhibitory effect (>80% inhibition) of the screened NSAIDs (Obrecht et al., 2019). Since pharmacological analyses of P2X3Rs are hampered by fast desensitization, preventing a binding equilibrium being reached between ATP and a simultaneously present antagonist, we used the $S^{15}V$-P2X3R mutant in the present study, which was shown to be

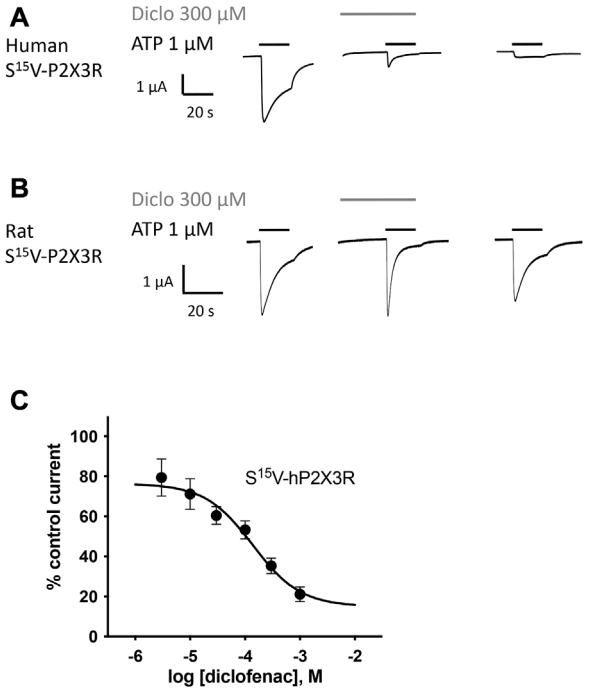


FIGURE 2
Diclofenac inhibition of ATP-induced currents of P2X3R is concentration-dependent. The effect of diclofenac on ATP-induced (1 µM) currents through S15V-hP2X3R **(A)** and S15V-rP2X3R **(B)** expressed in *X. laevis* oocytes was analyzed by TEVC electrophysiology. **(A,B)** Representative original current traces show the effects of 300 µM diclofenac on ATP-induced (black bars) currents of the indicated P2X3R. To ensure a binding equilibrium was reached, diclofenac was pre-incubated for 30 s before adding ATP (gray bar). **(C)** The resulting concentration–inhibition curve of diclofenac at hP2X3R exhibited an $IC_{50}$ of 138.2 µM (95% CI: 46.0–415.1 µM). Data points represent the means and SEM.

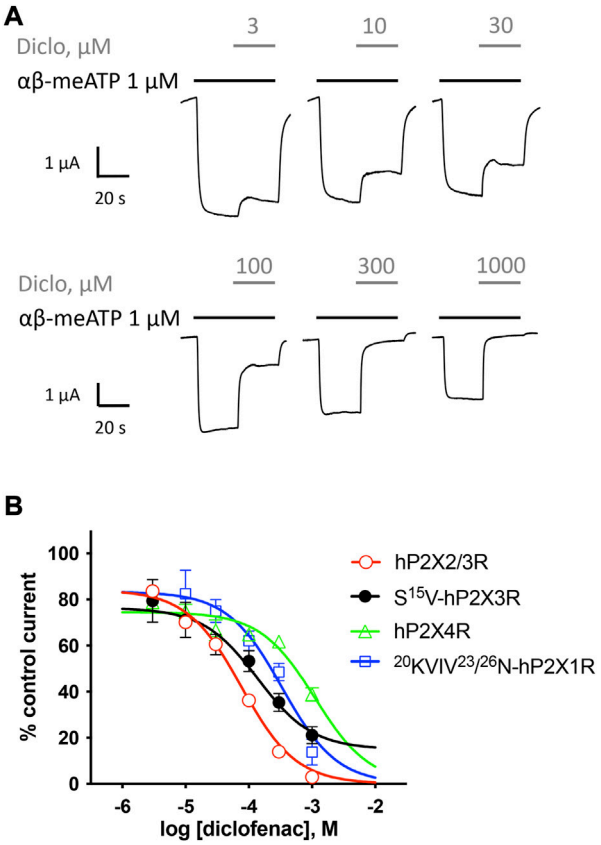


FIGURE 3
Effect of diclofenac at heteromeric hP2X2/3R and selectivity profiling. **(A)** Representative original current traces show the effects of 3–1000 µM diclofenac (gray bars) on α,β-meATP-induced (1 µM, black bars) currents through heteromeric hP2X2/3R expressed in *X. laevis* oocytes. **(B)** Concentration–inhibition curve of diclofenac at the indicated P2XR isoforms are shown as obtained from TEVC measurements using a peak current (P2X1R and P2X3R) or steady-state (P2X2/3R and P2X4R) protocol (c.f. Supplementary Figure S1/ Supplementary Figure S2). All $IC_{50}$ values are summarized in Table 2. Best-fit values of $logIC_{50}$ values of hP2X2/3R and S15V-hP2X3R are significantly different ($p$ = .0293). Best-fit values of $logIC_{50}$ of $^{20}KVIV^{23}/^{26}N$-hP2X1R are significantly different from hP2X2/3R ($p$ < .0001) but not from S15V-hP2X3R ($p$ = .2409). Best-fit values of $logIC_{50}$ of hP2X4R are significantly different from hP2X2/3R ($p$ < .0001) but not from S15V-hP2X3R ($p$ = .0917).

more suitable for automated fluorescence-based screening and also facilitated the pharmacological characterization of specific P2X3R ligands by TEVC (Hausmann et al., 2014; Obrecht et al., 2019). To validate the screening results, we characterized the potency of diclofenac, flunixin, and meclofenamic acid using TEVC on *X. laevis* oocytes heterologously expressing $S^{15}$V-rP2X3R and His-$S^{15}$V-hP2X3R. Instead of niflumic acid, we decided to investigate the structurally related flufenamic acid (FFA). Furthermore, we included the NSAIDs ibuprofen and naproxen in our investigations because these are used extensively in daily practice. The structural formulas of the NSAIDs investigated are shown in Figure 1 (Figure 1, compounds 1–6).

A peak current protocol including a 30-s preincubation of the antagonist was applied (Supplementary Figure S1) to determine the inhibitory effect of the NSAIDs at P2X3Rs. The current amplitude in the presence of the antagonist was compared to that of the preceding control current in the absence of the antagonist. The inhibitory effect of diclofenac, FFA, and flunixin was not reversible by the following washout, which was reflected in a reduced amplitude of the subsequent control current that could not be explained by the run-down alone (c.f. Figure 2A). Due to this potentially irreversible inhibitory effect, the subsequent amplitude in the absence of the antagonist did not provide a suitable reference and was not taken into account to calculate the control current.

All investigated NSAIDs were less effective at the rat P2X3R than at the human P2X3R (Figures 2A, B) or even had no effect at all on rat P2X3R; thus, we decided to focus our further investigation on human P2X receptors. Concentration–response analysis revealed that ATP-evoked hP2X3R-mediated responses were inhibited by various NSAIDs. Desensitizing P2X receptors showed increased error bars with lower diclofenac concentrations (see for instance $S^{15}$V-hP2X3 in Figure 2C/Figure 3B or the $^{20}KVIV^{23}/^{26}N$-hP2X1 in Figure 3B). This may be due to non-equilibrium during preincubation of low concentrations of diclofenac and/or the more error-prone evaluation of current amplitudes in the peak current protocol (Supplementary Figure S1) when using low diclofenac concentrations (likely due to the necessary estimation

**TABLE 1 Concentration–response analysis of NSAIDs at S15V-hP2X3R expressed in *X. laevis* oocytes. n.d., not determined. 1) Best-fit values of log$IC_{50}$ values of diclofenac and flufenamic acid are not significantly different ($p$ = .3071). 2) Best-fit values of log$IC_{50}$ values of diclofenac and flunixin are not significantly different ($p$ = .0775). 3) Best-fit values of log$IC_{50}$ values of flufenamic acid and flunixin are significantly different ($p$ = .001). 4) Mean values of diclofenac and flufenamic acid are not significantly different ($p$ = .1813). 5) Mean values of diclofenac and flunixin are significantly different ($p$ = .0017). 6) Mean values of flufenamic acid and flunixin are not significantly different ($p$ = .0537).**

| | $IC_{50}$, μM | 95% CI $IC_{50}$ | Max. inhibition at 1 mM | n |
|---|---|---|---|---|
| Diclofenac | 138.2[1,2] | 46.0–415.1 | 78.9% ± 3.7%[4,5] | 10 |
| Flufenamic acid | 221.7[1,3] | 98.9–496.8 | 69.8% ± 3.8%[4,6] | 10 |
| Flunixin | 32.4[2,3] | 11.6–90.2 | 53.7% ± 4.8%[5,6] | 8 |
| Ibuprofen | >300 | n.d | n.d | 8 |
| Meclofenamic acid | >300 | n.d | n.d | 9 |
| Naproxen | >300 | n.d | n.d | 9 |

of the control current at the time of the combined agonist/antagonist based on the previous ATP application and the necessary correction factor consideration). Thus, we have refrained from testing concentrations below 3 μM because the increasing errors may have resulted in unreliable values. Diclofenac proved to be the most effective antagonist, with an $IC_{50}$ value of 138.2 μM (95% CI: 46.0–415.1 μM; Figure 2C) and a maximum inhibition of ~80% at a concentration of 1 mM (Table 1). FFA proved to inhibit hP2X3R-mediated currents with a non-significant lower potency ($IC_{50}$ value of 221.7 μM; 95% CI: 98.9–496.8 μM; Table 1) in comparison to diclofenac. Flunixin, which is exclusively approved and used in veterinary medicine, had a significantly greater potency for the hP2X3 receptor than FFA ($IC_{50}$ value of 32.4 μM; 95% CI: 11.6–90.2 μM; Table 1), but a maximum inhibition of only 53% at a concentration of 1 mM was observed, indicating a significantly lower efficacy of flunixin than of diclofenac. By contrast, only weak inhibition of hP2X3R was observed for ibuprofen, meclofenamic acid, and naproxen. The current amplitude in the presence of 100 μM meclofenamic acid, naproxen, or ibuprofen was reduced by a maximum of 15%–18%, suggesting an estimated $IC_{50}$ value of >300 μM (Table 1). Due to their low inhibitory potency (ibuprofen, meclofenamic acid, and naproxen), low efficacy (flunixin) (c.f. Table 1), or their exclusive use in veterinary medicine (flunixin), these were not investigated further. Thus, only diclofenac—being the most effective antagonist—and FFA, due to its additional use in research, were further analyzed.

## 3.2 Characterization of the potency and selectivity of diclofenac at P2X receptors by TEVC

Selectivity profiling of diclofenac was performed at hP2X1R, hP2X2/3R, hP2X2R, hP2X4R, and hP2X7R (Figure 3B). To analyze the heteromeric hP2X2/3R, the ATP derivate α,β-meATP was used (Figure 3A) to evoke hP2X2/3R-mediated currents because it does not activate the homotrimeric hP2X2R. Currents mediated by the homotrimeric hP2X3R can be neglected due to its strong desensitization and run-down, when α,β-meATP is applied repetitively in short intervals (Bianchi et al., 1999; North, 2002). The desensitization kinetics of the heterotrimeric hP2X2/3 receptor resemble those of the homotrimeric hP2X2 receptor; therefore, the steady-state protocol was used (Figure 3A) (North, 2002). Diclofenac antagonized the heteromeric P2X2/3R with the highest potency of 76.7 μM (95% CI: 64.6–91.2 μM) and showed the following rank order of its potencies at P2XR subtypes: hP2X2/3R > hP2X3R > hP2X1R > hP2X4R. However, it should be noted that the differences in the $IC_{50}$ values were not significantly different between hP2X3R, hP2X1R, and hP2X4R. All $IC_{50}$ values are summarized in Table 2. By contrast, at the hP2X2R, diclofenac did not antagonize ATP-evoked P2X2R-mediated responses, but the presence of diclofenac exhibited a 1.7-fold increase in the P2X2R responses, and thus showed a potentiating effect at the P2X2R. Neither 100 μM diclofenac nor 300 μM FFA induced current at hP2X2R in the absence of ATP (Supplementary Figure 3 SA).

In summary, diclofenac was shown to be significantly more potent at hP2X2/3R ($IC_{50}$ 76.7 μM; 95% CI: 64.6–91.2 μM) than at hP2X3R ($IC_{50}$ 138.2 μM; 95% CI: 46.0–415.1 μM). However, it should be noted that the use of different agonists (α,β-meATP hP2X2/3R; ATP hP2X3R) complicates the assessment of a quantitative comparative analysis.

To assess the effect of diclofenac on the non-desensitizing hP2X7R, a modified steady-state protocol was used. For recordings of P2X7R, most scientists use divalent-free solutions such as ORi supplemented with 100 μM flufenamic acid (FFA) as an unselective ion channel blocker to inhibit non-specific chloride conductance in the absence of divalent ions (Weber et al., 1995; Hülsmann et al., 2003). However, since FFA is one of the investigated NSAIDs, this supplement was not reasonable. Therefore, the composition of the ORi-solution was modified as follows: 100 mM NaCl, 2.5 mM KCl, 1 mM $MgCl_2$, 5 mM HEPES, pH 7.4, and according to former protocols (Klapperstück et al., 2000), a free $ATP^{4-}$concentration of 300 μM was adjusted. About 300 μM of diclofenac reduced the $ATP^{4-}$-induced current amplitude by approximately 33% (Supplementary Figure S4), which suggested an estimated $IC_{50}$ value of >300 μM for diclofenac at hP2X7R. Since such high concentrations of diclofenac are clinically irrelevant, we refrained from performing a concentration–response analysis.

## 3.3 Mechanism of action of diclofenac

Although the $S^{15}V$ mutant of P2X3R desensitizes slowly (Hausmann et al., 2014), the desensitization may still prevent the

**TABLE 2** Concentration–response analysis of diclofenac at the indicated hP2XR subtypes expressed in *X. laevis* oocytes. *, no inhibition, but potentiation (c.f. Supplementary Figure S3); n.d., not determined. 1) Best-fit values of $logIC_{50}$ values of hP2X2/3R and S15V-hP2X3R are significantly different ($p = .0293$). 2) Best-fit value of $logIC_{50}$ of $^{20}KVIV^{23}/^{26}N$-hP2X1R is significantly different from hP2X2/3R ($p < .0001$). 3) Best-fit value of $logIC_{50}$ of $^{20}KVIV^{23}/^{26}N$-hP2X1R is not significantly different from that of $S^{15}V$-hP2X3R ($p = .2409$). 4) Best-fit value of $logIC_{50}$ of hP2X4R is significantly different from that of hP2X2/3R ($p < .0001$). 5) Best-fit value of $logIC_{50}$ of hP2X4R is not significantly different from that of S15V-hP2X3R ($p = .0917$). 6) Mean values of hP2X2/3R and $S^{15}V$-hP2X3R are significantly different ($p < .0001$). 7) Mean values of $^{20}KVIV^{23}/^{26}N$-hP2X1R and hP2X2/3R are significantly different ($p = .0376$). 8) Mean values of $^{20}KVIV^{23}/^{26}N$-hP2X1R and $S^{15}V$-hP2X3R are not significantly different ($p = .3381$). 9) Mean value of hP2X4 is significantly different from all other determined values ($p = < .0003$).

| | $IC_{50}$, μM | 95% CI $IC_{50}$ | Max. inhibition at 1 mM | n |
|---|---|---|---|---|
| $^{20}KVIV^{23}/^{26}N$-hP2X1R | 337.8[2,3] | 88.7–643.1 | 86.2% ± 4.9%[7,8] | 6 |
| hP2X2R | no inh.* | no inh.* | no inh.* | 10 |
| hP2X2/3R | 76.7[1,2,4] | 64.6–91.2 | 97.0% ± 0.9%[6,7] | 13 |
| S15V-hP2X3R | 138.2[1,3,5] | 46.0–415.1 | 78.9% ± 3.7%[6,8] | 10 |
| hP2X4R | 1,113[4,5] | 208.2–5,948 | 61.2% ± 2.8%[9] | 8 |
| hP2X7R | >> 300 | n.d | n.d | 9 |

reliable assessment of the mechanism of antagonism (Hausmann et al., 2014). Thus, the non-desensitizing heteromeric hP2X2/3R was used to assess the mechanism of action of diclofenac, which was also inhibited by diclofenac with the highest potency. To this end, the extent of inhibition of heteromeric hP2X2/3R by 30 μM diclofenac was determined using α,β-meATP concentrations of 1 or 30 μM as an agonist. We refrained from determining full agonist concentration–response curves at hP2X2/3R because simultaneous activation of homomeric hP2X2R occurs when hP2X2 and hP2X3 subunits are co-expressed and agonist concentration exceeds 30 μM α,β-meATP (Spelta et al., 2002). Approximately 30 μM diclofenac inhibited 1 or 30 μM α,β-meATP-induced current responses of the heteromeric hP2X2/3R by 44.8% ± 21.9% or 25.1% ± 10.1%, respectively (Figure 4A). Thus, inhibition by 30 μM diclofenac could be overcome by increasing concentrations of the agonist α,β-meATP, indicating competition of diclofenac and α,β-meATP at hP2X2/3R.

To further support the competitive nature of the inhibition and to exclude the possibility that diclofenac does bind in the negative allosteric site of hP2X3R as do other modulators (or negative allosteric antagonists) such as gefapixant (formerly AF-219) (Wang et al., 2018) or ATA (Obrecht et al., 2019), we examined mutations of amino acid residues in the allosteric site with respect to the effect of diclofenac. The allosteric site is formed by the lower body and dorsal fin domains of one subunit and the left flipper and lower body domains from the adjacent subunit and is thus located more closely to the transmembrane domains than the distinct ATP binding site (distance between the centers of the allosteric site and the ATP binding sites ~15 Å; minimal distance between both sites ~6 Å), which is formed by the head domain, upper body, and left flipper domains of one subunit and lower body and dorsal fin domains of the adjacent subunit (Mansoor et al., 2016; Wang et al., 2018). We have analyzed $N^{190}A$ and the $G^{189}R$ mutants [in the background of the $S^{15}V$-hP2X3R (Obrecht et al., 2019)] of the negative allosteric binding site described in previous studies (Wang et al., 2018; Obrecht et al., 2019). These were inhibited by 10 μM diclofenac to a similar extent as the $S^{15}V$-hP2X3R (Figure 4B), suggesting that the negative allosteric site of hP2X3R is not the binding site of diclofenac. In contrast to the findings for negative allosteric antagonists gefapixant/AF-219 (Wang et al., 2018) or ATA (Obrecht et al., 2019), the $L^{191}A/S^{15}V$-hP2X3R mutant was inhibited to a markedly greater extent by 10 μM diclofenac compared to the $S^{15}V$-hP2X3R (Figure 4B). However, whether the greater inhibition of the $L^{191}A/S^{15}V$-hP2X3R mutant by diclofenac may be due to either an energetically more favorable diclofenac binding environment (see below) or a lower agonist potency of ATP remains unknown. A competitive mechanism of action is also compatible with our findings of diclofenac inhibition as well as FFA inhibition of the $L^{191}A/S^{15}V$-hP2X3R mutant shown in Supplementary Figure S6, which illustrates representative original current traces of the $L^{191}A/S^{15}V$-hP2X3R, showing the effects of 10 μM diclofenac or 30 μM FFA on ATP-induced currents. The initial inhibition by diclofenac or FFA at the beginning of the co-application could be overcome by prolonged ATP co-application (arrow), suggesting the competitive binding of ATP and the antagonist to the ATP-binding site. However, we did not quantify these findings because the time course of solution exchange may have varied between experiments, which may affect the accuracy and thus precise quantification.

To investigate the binding mode of diclofenac and to shed light on a possible inhibition mechanism, we performed extensive all-atom molecular dynamics simulations of hP2X3R (Figure 5A) embedded in a lipid bilayer and surrounded by a physiological NaCl-based solution. Since the $L^{191}A$ mutation appears to facilitate diclofenac binding in our experiments, we initially assumed that diclofenac interacts with the receptor at a similar site like the allosteric inhibitor AF-219 (Wang et al., 2018), although $L^{191}A$ was shown to reduce binding of this compound. Therefore, we aligned the crystal structure of hP2X3R in complex with the negative allosteric modulator AF-219 (Wang et al., 2018) with the apo-state hP2X3, with one diclofenac molecule per protomer fitted onto the position of AF-219. We assessed the stability of the diclofenac-binding pose in our MD simulations and observed that diclofenac reoriented and moved toward the ATP-binding pocket on time scales of hundreds of nanoseconds.

In the seven independent simulation replicas, with three diclofenac molecules each, we observed 14 stable binding events for the hP2X3 wild-type and 14 for the L191A mutant, with some dissociation events (Supplementary Figure S7). We consistently observed diclofenac to alternatingly form salt–bridge interactions between its carboxyl groups and residues $K^{65}$, $K^{63}$, and $K^{176}$. Furthermore, diclofenac binding was stabilized by a hydrogen bond with $E^{270}$ and interactions between one of diclofenac's chlorine atoms at

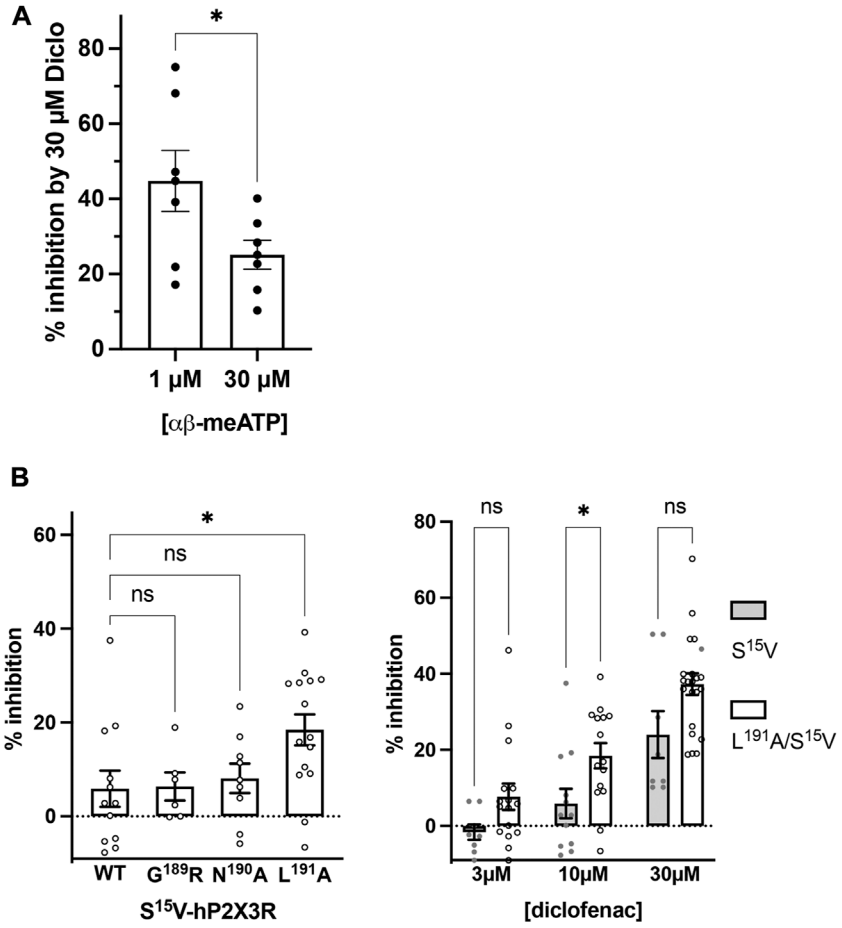


FIGURE 4
Diclofenac inhibition is modulated by the agonist concentration and the $L^{191}A$ mutant. **(A)** Bar graph showing the inhibition of the heteromeric hP2X2/3R by 30 µM diclofenac as determined with agonist concentrations of 1 µM or 30 µM α,β-meATP as indicated (% inhibition by 30 µM diclofenac ±SEM: 1 µM α,β-meATP, 44.8% ± 8.1%, $n$ = 7; 30 µM α,β-meATP, 25.1% ± 3.8%, $n$ = 7; $t$-test $p$ = .049). **(B)** Left panel: comparative analysis of diclofenac inhibition of 10 µM ATP-induced currents of $S^{15}V$-hP2X3R ("WT"), $G^{189}A/S^{15}V$-hP2X3R, $N^{190}A/S^{15}V$-hP2X3R, and $L^{191}A/S^{15}V$-hP2X3R. Bar graphs showing the inhibition of the indicated receptor by 10 µM diclofenac (% inhibition ±SEM: $S^{15}V$ (WT) −5.9% ± 3.9%, $n$ = 12; $G^{189}A/S^{15}V$ 6.4% ± 3.0%, $n$ = 6; $N^{190}A/S^{15}V$ 8.1% ± 3.1%, $n$ = 9; $L^{191}A/S^{15}V$ 18.4% ± 3.3%, $n$ = 15; ANOVA multiple comparison showed that only the $L^{191}A/S^{15}V$ was significantly different ($p$ = .0243 (*) from $S^{15}V$ (WT), while $G^{189}A/S^{15}V$ ($p$ = .9996 (ns)) or $N^{190}A/S^{15}V$ ($p$ = .9536 (ns)) were not. Right panel: comparative analysis of diclofenac inhibition of 10 µM ATP-induced currents of $S^{15}V$-hP2X3R and $L^{191}A/S^{15}V$-hP2X3R. Bar graphs showing the inhibition of the indicated receptor by 3, 10, or 30 µM diclofenac (% inhibition ±SEM: 3 µM diclofenac: $S^{15}V$ −1.6% ± 2.02%, $n$ = 8 and $L^{191}A/S^{15}V$ 7.7% ± 3.5%, $n$ = 16, ANOVA multiple comparison $p$ = .285 (ns); 10 µM diclofenac: $S^{15}V$ 5.9% ± 3.9%, $n$ = 12 and $L^{191}A/S^{15}V$ 18.4% ± 3.3%, $n$ = 15, ANOVA multiple comparison $p$ = .046 (*); 30 µM diclofenac: $S^{15}V$ 24.0% ± 6.2%, $n$ = 8 and $L^{191}A/S^{15}V$ 37.3% ± 2.8%, $n$ = 20, ANOVA multiple comparison $p$ = .053 (ns).

$K^{176}$ and $K^{201}$ (Figures 5B, C). A similar diclofenac binding pose was observed in simulations of $L^{191}A$-hP2X3R. We speculate that the removal of the bulky hydrophobic sidechain of $L^{191}$ may facilitate diclofenac binding by creating an energetically more favorable environment (Figure 5D). We then calculated the root-mean-squared fluctuations of the loop of the left flipper domain (residue stretch 265–277, hP2X3 numbering) and observed a reduction in flexibility upon diclofenac binding. Thus, it appears that diclofenac binding may partially rigidify this region and may thereby impair allosteric communication between the ATP-binding site and the lower body and transmembrane domains (Figure 5E). Summarizing, our simulations imply the binding pose of diclofenac, which is nearby but distinct from the binding pose of the allosteric inhibitor AF-219 and partially overlaps with ATP, suggesting a partially competitive inhibition mechanism (Figure 5F).

## 3.4 Effect of diclofenac at native P2XRs in DRG neurons

To examine whether diclofenac is capable of inhibiting native P2X3-subunit-containing receptors of nociceptive neurons with similar potency as oocyte-expressed recombinants hP2X2/3Rs and P2X3Rs, DRG neurons of pigs (3–4 months old) were analyzed. Currents elicited by 10 µM α,β-meATP were found in medium-sized (~35–60 µm diameter) porcine DRG neurons. 10 µM α,β-meATP was applied repeatedly every 3 min for 3 s duration onto cultured porcine DRG neurons (Figures 6A, B). Whole-cell currents elicited by α,β-meATP appeared as a slowly activating and non-desensitizing phenotype mediated by heteromeric P2X2/3Rs. These were inhibited by 100 µM diclofenac (pre-equilibrated for 20 s) by 70.5% ± 35.8% ($n$ =

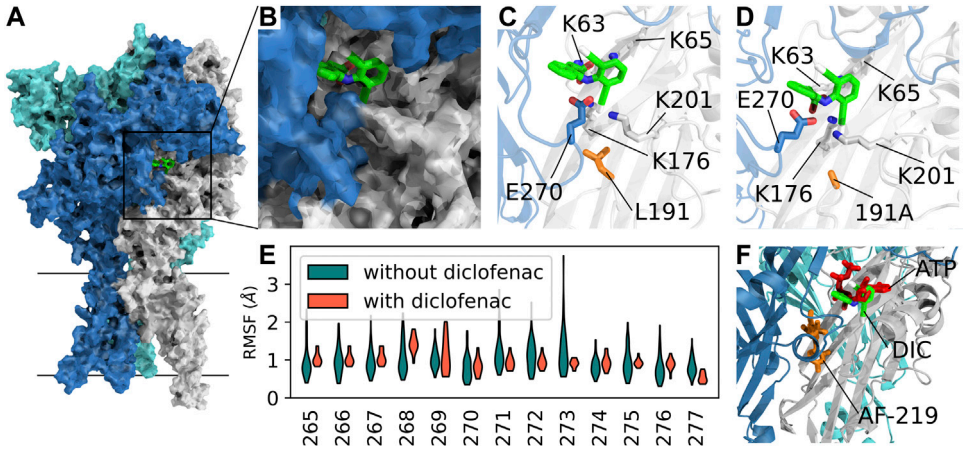


FIGURE 5
Competitive mechanism of action revealed by extensive all-atom molecular dynamics simulations. **(A)** Surface representation of apo-state P2X3 (PDB: 5SVJ) with bound diclofenac (obtained in our MD simulations) in the agonist-binding pocket between two adjacent subunits. **(B)** Close-up of the diclofenac-binding pocket as in **(A)**. **(C)** Average structure of the most frequently observed binding pose of diclofenac in P2X3 wildtype. Interacting residues within 4-Å distance are shown as sticks. **(D)** Same as C in the apo-state L191A mutant. The average structure of the first cluster of the independent simulations of the mutant shows a nearly identical binding pose. **(E)** RMSF (root-mean-squared fluctuation) of the left flipper domain for apo-state P2X3 wildtype with and without bound diclofenac to the agonist binding pocket. **(F)** Open-state P2X3R with bound ATP (PDB: 5SVK, ATP shown in red) with an overlay of AF-219 (shown in orange) and diclofenac (DIC, shown in green) shows the spatial position of the three molecules bound to hP2X3R. The position of AF-219 and diclofenac was obtained from an alignment of hP2X3R in complex with the AF-219-negative allosteric modulator (PDB-ID: 5YVE, AF-219 shown in orange) and the apo-state hP2X3R (PDB-ID: 5SVJ) with bound diclofenac and the ATP-bound open state PDB: 5SVK). An alignment of the open-state hP2X3R with bound ATP (5SVK) and hP2X3R in complex with the AF-219 negative allosteric modulator (5YVE) is shown in Supplementary Figure S8).

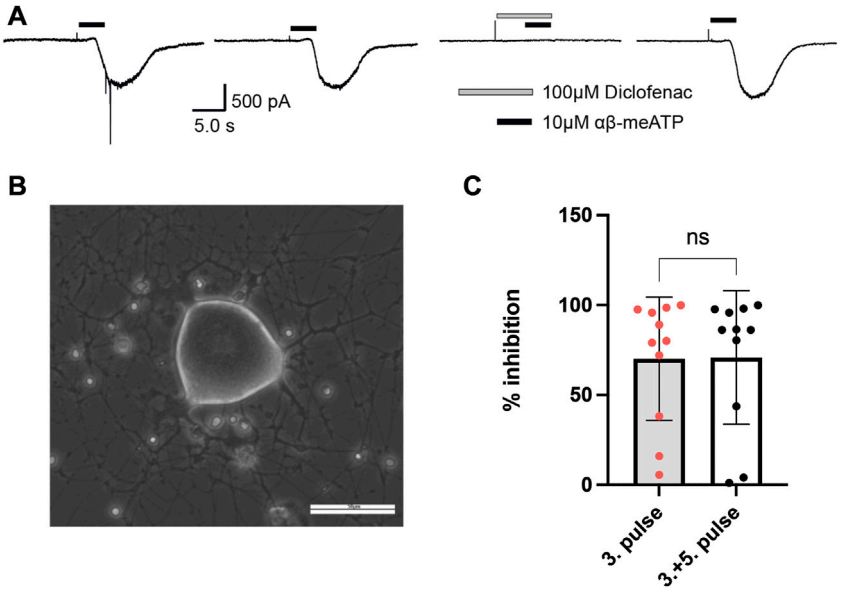


FIGURE 6
Diclofenac inhibition of P2X2/3R currents in dissociated porcine DRGs. **(A)** Representative original current traces of one porcine DRG neuron exposed four times for 3 s to 10 μM α,β-meATP in 3-min intervals. Please note that the neurons were exposed to five applications and that the first application is not shown here. Before the fourth application, 100 μM diclofenac was pre-incubated for 20 s before 10 μM α,β-meATP and 100 μM diclofenac were co-applied. **(B)** Representative picture of dissociated porcine DRGs at day 2 in culture. In the center a middle-sized DRG neuron is visible. Scale bar = 50 μm. **(C)** Bar graphs showing the relative diclofenac inhibition as calculated by the quotient of the max. α,β-meATP-induced peak current amplitude of the fourth application (in presence of diclofenac) vs. the preceding third ATP application (mean block ±SD = 70.2 ± 34.3%, $n$ = 11) (left bar) or vs. the mean of the preceding (third) and following (fifth) α,β-meATP application [mean Block ±SD = 70.9 ± 37.2%, $n$ = 11, $t$-test $p$ = .963 (ns)] (right bar).

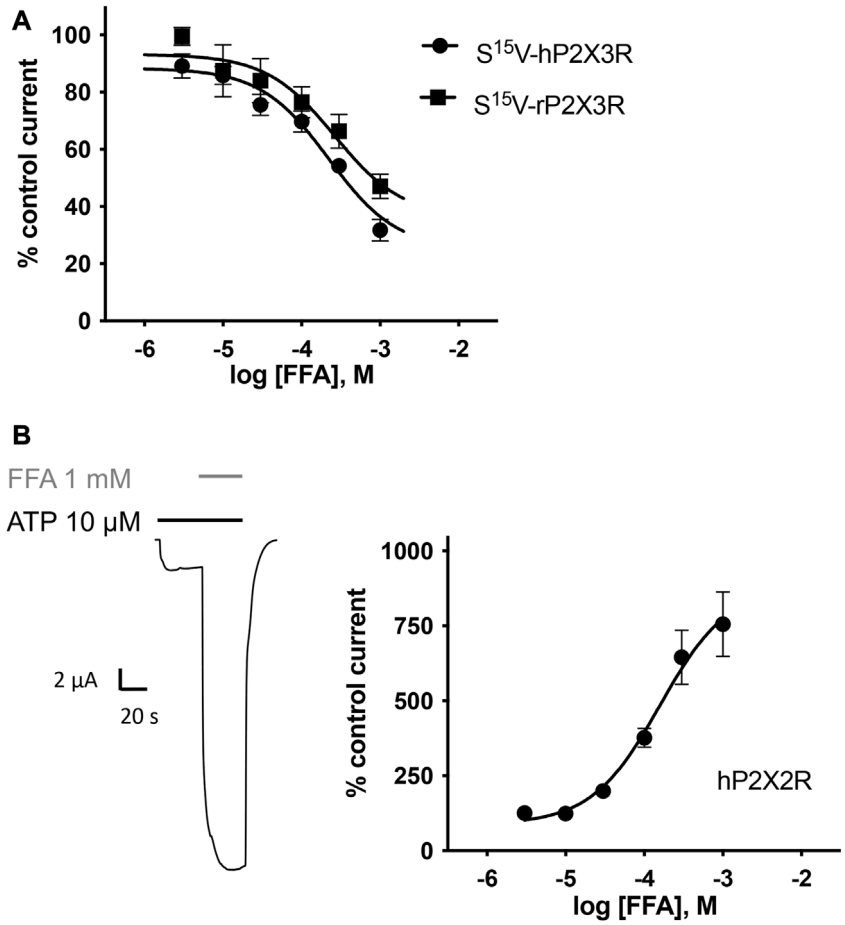


FIGURE 7
FFA inhibits P2X3R-mediated responses but potentiates hP2X2R-mediated responses. **(A)** Concentration–inhibition curve of FFA at human (●) and rat (■) $S^{15}$V-P2X3R exhibited $IC_{50}$ values of 221.7 µM (95% CI: 98.9–497 µM) and 264.1 µM (95% CI: 56.9–612 µM), respectively. $LogIC_{50}$ values are not significantly different ($p$ = .197). Data points represent the means and SEM **(B)** Left panel: Representative original current trace shows the effect of 1 mM FFA (gray bar) on the ATP-induced (10 µM, black bar) current mediated by hP2X2R expressed in *X. laevis* oocytes. Right panel: Concentration–response curve of FFA at hP2X2R (●) exhibited a half-maximal potentiation value of 158.4 µM (95% CI: 64.4–389.7 µM; $n$ = 8). Data points represent the means and SEM.

11) (Figure 6C). Thus, diclofenac inhibited native pig P2X2/3Rs expressed in medium-sized DRG neurons to a similar extent to hP2X2/3Rs heterologously expressed in *X. laevis* oocytes (c.f. Figure 3).

## 3.5 Characterization of the potency and selectivity of FFA at selected P2X receptors

Concentration–response analysis revealed a concentration-dependent inhibition of hP2X3R- and rP2X3R-mediated currents by micromolar concentrations of FFA. $IC_{50}$ values of 221.7 µM (95% CI: 98.9–497 µM) and 264.1 µM (95% CI: 56.9–612 µM) were determined at hP2X3R and rP2X3R, respectively (Figure 7A). In contrast to diclofenac, FFA did inhibit rP2X3R-mediated currents and was equipotent at hP2X3R and rP2X3R, ($IC_{50}$ value of 221.7 and 264.1 µM, respectively, not significantly different; Figure 7A). This indicates a weaker selectivity of FFA toward the human P2X3R in comparison to diclofenac. Importantly, a concentration of 100 µM FFA exerted a relevant inhibitory effect of 30% on hP2X3R and 25% on rP2X3R (Figure 7A).

In the case of FFA, selectivity profiling was performed at hP2X2R and hP2X7R. These two subtypes were chosen because they either were potentiated or are often analyzed in the presence of FFA, respectively. When ATP and FFA were co-applied at the hP2X2R, the current amplitude increased up to 8-fold compared to the steady-state current in the absence of FFA (Figure 7B). Thus, in comparison to diclofenac, FFA shows a markedly higher potentiating effect on hP2X2Rs. The effect of FFA on hP2X7R-mediated currents was assessed by applying concentrations of 100, 300, and 1000 µM. A concentration of 100 µM exerted a relevant inhibitory effect of ~39% (Supplementary Figure S5). A rough assessment of the $IC_{50}$ value, using the three tested concentrations, suggested a value of approximately 900 µM for hP2X7R inhibition.

# 4 Discussion

## 4.1 Inhibition of hP2X3R-mediated currents as an additional mode of action of NSAIDs

Our findings demonstrate the inhibition of the human P2X3R by various NSAIDs. Diclofenac proved to be the most effective antagonist with an $IC_{50}$ value of 138.2 μM. Among the investigated NSAIDs, diclofenac, FFA, and flunixin exerted an enduring, potentially irreversible inhibitory effect on the current amplitude, which could not be eliminated by the following washout period.

Considering the involvement of hP2X3R in nociception, it is conceivable that inhibition of hP2X3R contributes to the analgesic effect of NSAIDs and represents an additional mode of action besides COX inhibition. However, plasma levels and $IC_{50}$ values must be taken into consideration. In the case of diclofenac, low nanomolar plasma levels are reached during the transdermal application, whereas 10–20-fold higher concentrations can be observed in synovial tissues (Efe et al., 2014). When injected intramuscularly, significantly higher plasma levels of approximately 1.8 μg/ml (~6 μM) can be achieved (Drago et al., 2017). Similarly, maximum plasma levels of approximately 2.3–2.6 μg/ml (~7–8 μM) can be achieved with the oral application of 50–75 mg diclofenac (Kurowski et al., 1994; Kienzler et al., 2010). According to our experimental data, the current amplitude of hP2X2/3R and hP2X3R was reduced by approximately 20%–30% in the presence of 3–10 μM diclofenac. Therefore, it can be assumed that clinically relevant concentrations of diclofenac exert a significant inhibitory effect on hP2X3R-mediated currents. However, diclofenac shows a many-fold higher potency at COX1 ($IC_{50}$ value of .075 μM) and COX2 ($IC_{50}$ value of .038 μM) (Warner et al., 1999) than at hP2X3R ($IC_{50}$ value of 138.2 μM). The effect of diclofenac besides COX inhibition has also been studied by other groups, such as Gan (2010). For instance, in addition to COX inhibition, other effects such as the inhibition of acid-sensing ion channels (ASICs) were discovered (Voilley et al., 2001). However, the inhibition of P2X3R has not yet been described.

Similar to our findings for diclofenac, Hautaniemi et al. (2012) described the inhibition of P2X3R by the NSAID naproxen. According to our TEVC data, high micromolar to low millimolar concentrations of naproxen are necessary to inhibit hP2X3R, indicating a low potency of naproxen. These results are consistent with the results that Hautaniemi et al. (2012) obtained from calcium imaging of rat trigeminal neurons. Despite its lower potency in comparison to diclofenac, naproxen might as well exert a relevant inhibitory effect due to higher plasma levels. When administered orally, maximum plasma levels of approximately 70–80 μg/ml (~300–350 μM) are reached after about 2 h (Desager et al., 1976; Dresse et al., 1978).

## 4.2 Selectivity profiling of diclofenac at P2X receptors and related side effects

Selectivity profiling of diclofenac at different P2XR subtypes showed strong inhibition of hP2X3R and hP2X2/3R and weaker inhibition of hP2X1R, hP2X4R, and hP2X7R. The rank order of its potencies is as follows: hP2X2/3R > hP2X3R > hP2X1R > hP2X4R > hP2X7R.

Diclofenac had a similar maximum inhibitory effect and potency at hP2X1R and hP2X3R. In contrast to its potentially irreversible effect on hP2X3R, diclofenac seemed to exert a reversible inhibitory effect on hP2X1R. Inhibition of hP2X1R, which is involved in inflammatory responses (Lecut et al., 2009), might contribute to the anti-inflammatory effect of diclofenac. However, the difference in potency between hP2X1R ($IC_{50}$ 337.8 μM) and COX ($IC_{50}$ value of 0.075 μM or 0.038 μM of COX1 or COX2, respectively) should be kept in mind.

Considering its low potency at hP2X4R and hP2X7R, it is unlikely that inhibition of these P2X subtypes, which are involved in nociception (Chessell et al., 2005; Tsuda et al., 2009), contributes to the analgesic effect of diclofenac.

Remarkably, diclofenac had a weak potentiating effect on hP2X2R-mediated currents. Regarding its strong inhibitory effect on hP2X3R and its weak potentiating effect on hP2X2R, a predominantly inhibitory effect on the heterotrimeric hP2X2/3 receptor could have been expected. Surprisingly, diclofenac proved to be more potent at hP2X2/3R ($IC_{50}$ 76.7 μM) than at hP2X3R ($IC_{50}$ 138.2 μM). However, it should be kept in mind that the use of the correction factor in hP2X3R measurements and the use of different agonists at hP2X2/3 and hP2X3R imply a bias that may affect an accurate, direct quantitative comparison. Since the run-down varies between different recordings, the inhibitory effect of diclofenac on hP2X3R might be underestimated.

It is presumed that taste disorders, which have been observed in clinical trials of newly developed P2X3R antagonists, mainly result from the inhibition of heterotrimeric P2X2/3R (Garceau and Chauret, 2019; McGarvey et al., 2022). Therefore, the question arises whether diclofenac might cause taste disorders due to its inhibitory effect on hP2X2/3R. While taste disorders as a side effect are listed as "very rare" in the prescribing information, more than 110 suspected cases of ageusia, dysgeusia, or taste disorders have been reported in the European Union so far in EudraVigilance (up to 28/11/2022) due to diclofenac administration (http://www.adrreports.eu/de/). It must also be assumed that there are a high number of unreported cases. In a prospective, randomized clinical trial regarding the postoperative administration of diclofenac, 58% of patients reported an impaired taste sensation (Attri et al., 2015). Therefore, it seems likely that diclofenac affects taste sensation due to the inhibition of hP2X2/3R.

## 4.3 Mechanisms of action of diclofenac at P2X3R and functional implications for gating

We have found the following lines of experimental evidence for competitive inhibition of the P2X3-subunit containing receptors by diclofenac: 1) inhibition by 30 μM diclofenac of hP2X2/3R could be overcome by increasing concentrations of the agonist α,β-meATP; 2) at $L^{191}A/S^{15}V$-hP2X3R, the inhibition by diclofenac or FFA at the beginning of the co-application with ATP could be overcome by prolonged ATP co-application; 3) the $N^{190}A$ and the $G^{189}R$ mutants of the negative allosteric binding site (Wang et al., 2018; Obrecht et al., 2019), which markedly affected the extent of inhibition of hP2X3R by

the allosteric antagonists gefapixant/AF-219 or ATA, were inhibited by 100 μM diclofenac to a similar extent to hP2X3R.

In addition, our extensive all-atom molecular dynamics simulations have shown that the most common binding pose of diclofenac at hP2X3R largely overlaps with ATP bound to the open-state conformation of hP2X3R. Furthermore, we show by RMSF analysis that diclofenac when bound to hP2X3R alters the conformational flexibility of the left flipper and dorsal fin domains, crucially implicated in the ATP-induced gating of hP2X3R (Mansoor et al., 2016; Mansoor, 2022). Our simulation results also offer a mechanistic explanation for the inhibition of the ATP-induced gating of hP2X3R; the strong interactions of diclofenac with the residues K201 and E270 of the dorsal fin and left flipper domains, respectively, are likely to prevent the conformational rearrangements of the dorsal fin and left flipper domains. These are otherwise essential for channel gating or, mechanistically, for the transmission of ATP binding to the conformational rearrangement of the lower body domain, and eventually the opening of the ion channel pore.

According to our MD simulations, the strongest interactions of diclofenac and amino acid residues of the putative binding site were ionic interactions with lysines K63, K65, and K176 and hydrogen bonds with charged residues E270, K176, and K201. All of these amino acid residues are fully conserved between P2X subtypes and are essential for ATP binding, thus preventing targeted functional experiments for validating the diclofenac-binding pose. Therefore, we speculate that only non-conserved amino acid residues, dispensable for ATP binding or species-specific allosteric effects, may account for the differences in diclofenac-mediated effects between human and rat P2X3R. In summary, although awaiting further experimental confirmation, our results suggest that diclofenac acts *via* a similar mechanism of action to TNP-ATP (Mansoor et al., 2016).

### 4.4 Selectivity profiling of FFA at P2XRs questions its use in P2XR assays

FFA proved to inhibit human P2X3R-mediated currents with a similar potency ($IC_{50}$ value of 221.7 μM) to diclofenac ($IC_{50}$ 138.2 μM). In contrast to diclofenac, FFA did inhibit rat P2X3R-mediated currents ($IC_{50}$ value of 264,1 μM), indicating a weaker selectivity of FFA toward the human P2X3R. As FFA is usually applied transdermally, plasma levels do not exceed 180 nM even with repetitive application (Drago et al., 2017). Due to its low potency at hP2X3R and its low plasma levels, it must be assumed that P2X3R inhibition does not contribute to the analgesic effect of FFA in a relevant manner.

However, the inhibitory effect of FFA on P2X3R could be of importance for other scientists who perform functional recordings of P2XRs with solutions supplemented with FFA. Being a non-selective ion channel blocker, FFA is widely used in research to avoid bias resulting from the activation of various other ion channels (Guinamard et al., 2013). Our findings demonstrate that a commonly used concentration of 100 μM FFA exerts a relevant inhibitory effect of approximately 30% on hP2X3R and 25% on rP2X3R. However, especially for recordings of P2X7R, FFA is often used as a supplement to divalent-free ORi-solution (Hülsmann et al., 2003). While inhibition of the P2X3R by FFA has not yet been described by other groups, there are contradictory results regarding its effect on P2X7R. Suadicani et al. (2006) suggested a competitive antagonism of FFA at P2X7R, whereas Ma et al. (2009) did not find an inhibitory effect of FFA on P2X7R, but rather an inhibition of Pannexin-1 by FFA. According to our data, hP2X7R-mediated currents are reduced by approximately 40% in the presence of 100 μM FFA. Even when FFA is no longer applied, the permeability of the receptor remains affected as shown in Supplementary Figure S5 by comparing the slope of the linearly increasing current before and after FFA application, which may indicate a potentially irreversible effect of FFA on hP2X7R-mediated current responses.

Taken together, our results question the use of FFA as a non-selective ion channel blocker when P2XR-mediated currents are to be measured and add another target to the already known unspecific ion-channel modulation by FFA (Guinamard et al., 2013).

In comparison to diclofenac, FFA shows a significantly higher potentiating effect on hP2X2R with a 7–8-fold increase in current amplitudes. This potentiating effect of FFA on hP2X2R has already been described by other groups (Schmidt et al., 2018). However, Schmidt et al. (2018) did not attribute this effect to a direct interaction of FFA with the receptor, but to membrane alterations caused by the amphiphilic FFA. However, from our point of view, this theory seems questionable since it cannot explain the opposing effects of FFA on hP2X2R and hP2X3R.

## 5 Conclusion/summary

In a previous screening of 2000 approved drugs, natural products, and bioactive substances, various NSAIDs were found to inhibit S15V-rP2X3R-mediated currents (Obrecht et al., 2019). Using TEVC, we identified diclofenac as a hP2X3R and hP2X2/3R antagonist with micromolar potency (with $IC_{50}$ values of 138.2 and 76.72 μM, respectively), which was also shown to be effective in antagonizing native P2X2/3R-mediated responses in pig DRG neurons. Considering their involvement in nociception, the inhibition of hP2X3R and hP2X2/3R by micromolar concentrations of diclofenac may contribute to the analgesic effect of diclofenac and represent an additional, although less potent, mode of action besides the well-known COX inhibition. Our results support the presence of a competitive antagonism through which diclofenac, by interacting with residues of the ATP-binding site, left flipper, and dorsal fin domains, inhibits the gating of P2X3R by conformational fixation of the left flipper and dorsal fin domains. FFA proved to inhibit hP2X3R, rP2X3R, and hP2X7R, calling into question its use as a non-selective ion channel blocker, when P2XR-mediated responses are under study.

## Data availability statement

The raw data supporting the conclusion of this article will be made available by the authors, without undue reservation. The data

underlying the quantitative tables and figures are deposited at https://doi.org/10.6084/m9.figshare.22004789.v1.

## Ethics statement

The animal study was reviewed and approved by the governmental animal care and use committee of the State Agency for Nature, Environment, and Consumer Protection (LANUV, Recklinghausen, Germany.

## Author contributions

LG, AB, GS, J-PM, AL, and RH were involved in the study design. LG, LC, SC, BH, IT, JK, LE, J-PM, AL, and RH were involved in data collection and interpretation. LG wrote the first draft of the manuscript. All authors contributed to the revision of the manuscript, and read and approved the submitted version.

## Funding

This study was funded by grants from Deutsche Forschungsgemeinschaft (DFG), Germany (grant numbers HA 6095/1-1 and HA 6095/1-2) to RH and to J-PM (grant number MA 7525/2-1, as part of the Research Unit FOR 5046, project P2) and by a grant from the Interdisciplinary Centre for Clinical Research within the Faculty of Medicine at the RWTH Aachen University (IZKF TN1-1/IA 532001 and TN1-5/IA 532005).

## Acknowledgments

The authors gratefully acknowledge the computing time granted through JARA on the supercomputer JURECA at Forschungszentrum Jülich and the supercomputer CLAIX at RWTH Aachen University.

## Conflict of interest

The authors declare that the research was conducted in the absence of any commercial or financial relationships that could be construed as a potential conflict of interest.

## Publisher's note

All claims expressed in this article are solely those of the authors and do not necessarily represent those of their affiliated organizations, or those of the publisher, the editors, and the reviewers. Any product that may be evaluated in this article, or claim that may be made by its manufacturer, is not guaranteed or endorsed by the publisher.

## Supplementary material

The Supplementary Material for this article can be found online at: https://www.frontiersin.org/articles/10.3389/fphar.2023.1120360/full#supplementary-material

## References

Abdulqawi, R., Dockry, R., Holt, K., Layton, G., Mccarthy, B. G., Ford, A. P., et al. (2015). P2X3 receptor antagonist (AF-219) in refractory chronic cough: A randomised, double-blind, placebo-controlled phase 2 study. *Lancet* 385, 1198–1205. doi:10.1016/S0140-6736(14)61255-1

Abraham, M. J., Murtola, T., Schulz, R., Páll, S., Smith, J. C., Hess, B., et al. (2015). GROMACS: High performance molecular simulations through multi-level parallelism from laptops to supercomputers. *SoftwareX* 1-2, 19–25. doi:10.1016/j.softx.2015.06.001

Attri, J. P., Sandhu, G. K., Khichy, S., Singh, H., Singh, K., and Sharan, R. (2015). Comparative evaluation of oral flupirtine and oral diclofenac sodium for analgesia and adverse effects in elective abdominal surgeries. *Anesth. Essays Res.* 9, 72–78. doi:10.4103/0259-1162.150681

Berendsen, H. J. C., Postma, J. P. M., Van Gunsteren, W. F., Dinola, A., and Haak, J. R. (1984). Molecular dynamics with coupling to an external bath. *J. Chem. Phys.* 81, 3684–3690. doi:10.1063/1.448118

Bianchi, B. R., Lynch, K. J., Touma, E., Niforatos, W., Burgard, E. C., Alexander, K. M., et al. (1999). Pharmacological characterization of recombinant human and rat P2X receptor subtypes. *Eur. J. Pharmacol.* 376, 127–138. doi:10.1016/s0014-2999(99)00350-7

Burnstock, G. (2016). Purinergic mechanisms and pain. *Adv. Pharmacol.* 75, 91–137. doi:10.1016/bs.apha.2015.09.001

Bussi, G., Donadio, D., and Parrinello, M. (2007). Canonical sampling through velocity rescaling. *J. Chem. Phys.* 126, 014101. doi:10.1063/1.2408420

Chen, C. C., Akopian, A. N., Sivilotti, L., Colquhoun, D., Burnstock, G., and Wood, J. N. (1995). A P2X purinoceptor expressed by a subset of sensory neurons. *Nature* 377, 428–431. doi:10.1038/377428a0

Chessell, I. P., Hatcher, J. P., Bountra, C., Michel, A. D., Hughes, J. P., Green, P., et al. (2005). Disruption of the P2X7 purinoceptor gene abolishes chronic inflammatory and neuropathic pain. *Pain* 114, 386–396. doi:10.1016/j.pain.2005.01.002

Cockayne, D. A., Hamilton, S. G., Zhu, Q. M., Dunn, P. M., Zhong, Y., Novakovic, S., et al. (2000). Urinary bladder hyporeflexia and reduced pain-related behaviour in P2X3-deficient mice. *Nature* 407, 1011–1015. doi:10.1038/35039519

Cockayne, D. A., Dunn, P. M., Zhong, Y., Rong, W., Hamilton, S. G., Knight, G. E., et al. (2005). P2X2 knockout mice and P2X2/P2X3 double knockout mice reveal a role for the P2X2 receptor subunit in mediating multiple sensory effects of ATP. *J. Physiol.* 567, 621–639. doi:10.1113/jphysiol.2005.088435

Desager, J. P., Vanderbist, M., and Harvengt, C. (1976). Naproxen plasma levels in volunteers after single-dose administration by oral and rectal routes. *J. Clin. Pharmacol.* 16, 189–193. doi:10.1002/j.1552-4604.1976.tb01516.x

Dewitt, D. L., El-Harith, E. A., Kraemer, S. A., Andrews, M. J., Yao, E. F., Armstrong, R. L., et al. (1990). The aspirin and heme-binding sites of ovine and murine prostaglandin endoperoxide synthases. *J. Biol. Chem.* 265, 5192–5198. doi:10.1016/s0021-9258(19)34105-5

Drago, S., Imboden, R., Schlatter, P., Buylaert, M., Krahenbuhl, S., and Drewe, J. (2017). Pharmacokinetics of transdermal etofenamate and diclofenac in healthy volunteers. *Basic Clin. Pharmacol. Toxicol.* 121, 423–429. doi:10.1111/bcpt.12818

Dresse, A., Gerard, M. A., Quinaux, N., Fischer, P., and Gerardy, J. (1978). Effect of diflunisal on the human plasma levels and on the urinary excretion of naproxen. *Arch. Int. Pharmacodyn. Ther.* 236, 276–284.

Efe, T., Sagnak, E., Roessler, P. P., Getgood, A., Patzer, T., Fuchs-Winkelmann, S., et al. (2014). Penetration of topical diclofenac sodium 4 % spray gel into the synovial tissue and synovial fluid of the knee: A randomised clinical trial. *Knee Surg. Sports Traumatol. Arthrosc.* 22, 345–350. doi:10.1007/s00167-013-2408-0

Fiser, A., and Sali, A. (2003). Modeller: Generation and refinement of homology-based protein structure models. *Methods Enzymol.* 374, 461–491. doi:10.1016/S0076-6879(03)74020-8

Gan, T. J. (2010). Diclofenac: An update on its mechanism of action and safety profile. *Curr. Med. Res. Opin.* 26, 1715–1731. doi:10.1185/03007995.2010.486301

Garceau, D., and Chauret, N. (2019). BLU-5937: A selective P2X3 antagonist with potent anti-tussive effect and no taste alteration. *Pulm. Pharmacol. Ther.* 56, 56–62. doi:10.1016/j.pupt.2019.03.007

Guinamard, R., Simard, C., and Del Negro, C. (2013). Flufenamic acid as an ion channel modulator. *Pharmacol. Ther.* 138, 272–284. doi:10.1016/j.pharmthera.2013.01.012

Hausmann, R., Rettinger, J., Gerevich, Z., Meis, S., Kassack, M. U., Illes, P., et al. (2006). The suramin analog 4,4',4'',4'''-(carbonylbis(imino-5,1,3-benzenetriylbis (carbonylimino)))tetra-kis-benzenesulfonic acid (NF110) potently blocks P2X3 receptors: Subtype selectivity is determined by location of sulfonic acid groups. *Mol. Pharmacol.* 69, 2058–2067. doi:10.1124/mol.106.022665

Hausmann, R., Bahrenberg, G., Kuhlmann, D., Schumacher, M., Braam, U., Bieler, D., et al. (2014). A hydrophobic residue in position 15 of the rP2X3 receptor slows desensitization and reveals properties beneficial for pharmacological analysis and high-throughput screening. *Neuropharmacology* 79, 603–615. doi:10.1016/j.neuropharm.2014.01.010

Hautaniemi, T., Petrenko, N., Skorinkin, A., and Giniatullin, R. (2012). The inhibitory action of the antimigraine nonsteroidal anti-inflammatory drug naproxen on P2X3 receptor-mediated responses in rat trigeminal neurons. *Neuroscience* 209, 32–38. doi:10.1016/j.neuroscience.2012.02.023

Huang, J., Rauscher, S., Nawrocki, G., Ran, T., Feig, M., De Groot, B. L., et al. (2017). CHARMM36m: An improved force field for folded and intrinsically disordered proteins. *Nat. Methods* 14, 71–73. doi:10.1038/nmeth.4067

Hülsmann, M., Nickel, P., Kassack, M., Schmalzing, G., Lambrecht, G., and Markwardt, F. (2003). NF449, a novel picomolar potency antagonist at human P2X1 receptors. *Eur. J. Pharmacol.* 470, 1–7. doi:10.1016/s0014-2999(03)01761-8

Humphrey, W., Dalke, A., and Schulten, K. (1996). Vmd: Visual molecular dynamics. *J. Mol. Graph* 14 (33-8), 33–38. doi:10.1016/0263-7855(96)00018-5

Jarvis, M. F., Burgard, E. C., Mcgaraughty, S., Honore, P., Lynch, K., Brennan, T. J., et al. (2002). A-317491, a novel potent and selective non-nucleotide antagonist of P2X3 and P2X2/3 receptors, reduces chronic inflammatory and neuropathic pain in the rat. *Proc. Natl. Acad. Sci. U. S. A.* 99, 17179–17184. doi:10.1073/pnas.252537299

Jorgensen, W. L., Chandrasekhar, J., Madura, J. D., Impey, R. W., and Klein, M. L. (1983). Comparison of simple potential functions for simulating liquid water. *J. Chem. Phys.* 79, 926–935. doi:10.1063/1.445869

Kawate, T., Michel, J. C., Birdsong, W. T., and Gouaux, E. (2009). Crystal structure of the ATP-gated P2X(4) ion channel in the closed state. *Nature* 460, 592–598. doi:10.1038/nature08198

Kienzler, J. L., Gold, M., and Nollevaux, F. (2010). Systemic bioavailability of topical diclofenac sodium gel 1% versus oral diclofenac sodium in healthy volunteers. *J. Clin. Pharmacol.* 50, 50–61. doi:10.1177/0091270009336234

Klapperstück, M., Büttner, C., Böhm, T., Schmalzing, G., and Markwardt, F. (2000). Characteristics of P2X7 receptors from human B lymphocytes expressed in Xenopus oocytes. *Biochim. Biophys. Acta* 1467, 444–456. doi:10.1016/s0005-2736(00)00245-5

Klauda, J. B., Venable, R. M., Freites, J. A., O'connor, J. W., Tobias, D. J., Mondragon-Ramirez, C., et al. (2010). Update of the CHARMM all-atom additive force field for lipids: Validation on six lipid types. *J. Phys. Chem. B* 114, 7830–7843. doi:10.1021/jp101759q

Klein, S., Gashaw, I., Baumann, S., Chang, X., Hummel, T., Thuss, U., et al. (2022). First-in-human study of eliapixant (BAY 1817080), a highly selective P2X3 receptor antagonist: Tolerability, safety and pharmacokinetics. *Br. J. Clin. Pharmacol.* 88, 4552–4564. doi:10.1111/bcp.15358

Kurowski, M., Menninger, H., and Pauli, E. (1994). The efficacy and relative bioavailability of diclofenac resinate in rheumatoid arthritis patients. *Int. J. Clin. Pharmacol. Ther.* 32, 433–440.

Lecut, C., Frederix, K., Johnson, D. M., Deroanne, C., Thiry, M., Faccinetto, C., et al. (2009). P2X1 ion channels promote neutrophil chemotaxis through Rho kinase activation. *J. Immunol.* 183, 2801–2809. doi:10.4049/jimmunol.0804007

Ma, W., Hui, H., Pelegrin, P., and Surprenant, A. (2009). Pharmacological characterization of pannexin-1 currents expressed in mammalian cells. *J. Pharmacol. Exp. Ther.* 328, 409–418. doi:10.1124/jpet.108.146365

Mansoor, S. E., Lu, W., Oosterheert, W., Shekhar, M., Tajkhorshid, E., and Gouaux, E. (2016). X-ray structures define human P2X(3) receptor gating cycle and antagonist action. *Nature* 538, 66–71. doi:10.1038/nature19367

Mansoor, S. E. (2022). How structural biology has directly impacted our understanding of P2X receptor function and gating. *Methods Mol. Biol.* 2510, 1–29. doi:10.1007/978-1-0716-2384-8_1

Markham, A. (2022). Gefapixant: First approval. *Drugs* 82, 691–695. doi:10.1007/s40265-022-01700-8

Marucci, G., Dal Ben, D., Buccioni, M., Marti Navia, A., Spinaci, A., Volpini, R., et al. (2019). Update on novel purinergic P2X3 and P2X2/3 receptor antagonists and their potential therapeutic applications. *Expert Opin. Ther. Pat.* 29, 943–963. doi:10.1080/13543776.2019.1693542

Mayne, C. G., Saam, J., Schulten, K., Tajkhorshid, E., and Gumbart, J. C. (2013). Rapid parameterization of small molecules using the Force Field Toolkit. *J. Comput. Chem.* 34, 2757–2770. doi:10.1002/jcc.23422

Mcgarvey, L. P., Birring, S. S., Morice, A. H., Dicpinigaitis, P. V., Pavord, I. D., Schelfhout, J., et al. (2022). Efficacy and safety of gefapixant, a P2X(3) receptor antagonist, in refractory chronic cough and unexplained chronic cough (COUGH-1 and COUGH-2): Results from two double-blind, randomised, parallel-group, placebo-controlled, phase 3 trials. *Lancet* 399, 909–923. doi:10.1016/S0140-6736(21)02348-5

Methfessel, C., Witzemann, V., Takahashi, T., Mishina, M., Numa, S., and Sakmann, B. (1986). Patch clamp measurements on *Xenopus laevis* oocytes: Currents through endogenous channels and implanted acetylcholine receptor and sodium channels. *Pflugers Arch.* 407, 577–588. doi:10.1007/bf00582635

Miledi, R. (1982). A calcium-dependent transient outward current in *Xenopus laevis* oocytes. *Proc. R. Soc. Lond B Biol. Sci.* 215, 491–497. doi:10.1098/rspb.1982.0056

Morice, A. H., Millqvist, E., Belvisi, M. G., Bieksiene, K., Birring, S. S., Chung, K. F., et al. (2014). Expert opinion on the cough hypersensitivity syndrome in respiratory medicine. *Eur. Respir. J.* 44, 1132–1148. doi:10.1183/09031936.00218613

Neese, F., Wennmohs, F., Becker, U., and Riplinger, C. (2020). The ORCA quantum chemistry program package. *J. Chem. Phys.* 152, 224108. doi:10.1063/5.0004608

Nicke, A., Baumert, H. G., Rettinger, J., Eichele, A., Lambrecht, G., Mutschler, E., et al. (1998). P2X1 and P2X3 receptors form stable trimers: A novel structural motif of ligand-gated ion channels. *EMBO J.* 17, 3016–3028. doi:10.1093/emboj/17.11.3016

Niimi, A., Saito, J., Kamei, T., Shinkai, M., Ishihara, H., Machida, M., et al. (2022). Randomised trial of the P2X3 receptor antagonist sivopixant for refractory chronic cough. *Eur. Respir. J.* 59, 2100725. doi:10.1183/13993003.00725-2021

North, R. A., and Barnard, E. A. (1997). Nucleotide receptors. *Curr. Opin. Neurobiol.* 7, 346–357. doi:10.1016/s0959-4388(97)80062-1

North, R. A., and Jarvis, M. F. (2013). P2X receptors as drug targets. *Mol. Pharmacol.* 83, 759–769. doi:10.1124/mol.112.083758

North, R. A. (2002). Molecular physiology of P2X receptors. *Physiol. Rev.* 82, 1013–1067. doi:10.1152/physrev.00015.2002

Obrecht, A. S., Urban, N., Schaefer, M., Rose, A., Kless, A., Meents, J. E., et al. (2019). Identification of aurintricarboxylic acid as a potent allosteric antagonist of P2X1 and P2X3 receptors. *Neuropharmacology* 158, 107749. doi:10.1016/j.neuropharm.2019.107749

Oken, A. C., Krishnamurthy, I., Savage, J. C., Lisi, N. E., Godsey, M. H., and Mansoor, S. E. (2022). Molecular Pharmacology of P2X receptors: Exploring druggable domains revealed by structural biology. *Front. Pharmacol.* 13, 925880. doi:10.3389/fphar.2022.925880

Pang, Y. T., Pavlova, A., Tajkhorshid, E., and Gumbart, J. C. (2020). Parameterization of a drug molecule with a halogen sigma-hole particle using ffTK: Implementation, testing, and comparison. *J. Chem. Phys.* 153, 164104. doi:10.1063/5.0022802

Phillips, J. C., Hardy, D. J., Maia, J. D. C., Stone, J. E., Ribeiro, J. V., Bernardi, R. C., et al. (2020). Scalable molecular dynamics on CPU and GPU architectures with NAMD. *J. Chem. Phys.* 153, 044130. doi:10.1063/5.0014475

Rome, L. H., and Lands, W. E. (1975). Structural requirements for time-dependent inhibition of prostaglandin biosynthesis by anti-inflammatory drugs. *Proc. Natl. Acad. Sci. U. S. A.* 72, 4863–4865. doi:10.1073/pnas.72.12.4863

Salm, E. J., Dunn, P. J., Shan, L., Yamasaki, M., Malewicz, N. M., Miyazaki, T., et al. (2020). TMEM163 regulates ATP-gated P2X receptor and behavior. *Cell Rep.* 31, 107704. doi:10.1016/j.celrep.2020.107704

Schmalzing, G., Gloor, S., Omay, H., Kroner, S., Appelhans, H., and Schwarz, W. (1991). Up-regulation of sodium pump activity in *Xenopus laevis* oocytes by expression of heterologous beta 1 subunits of the sodium pump. *Biochem. J.* 279 (2), 329–336. doi:10.1042/bj2790329

Schmidt, A., Alsop, R. J., Rimal, R., Lenzig, P., Joussen, S., Gervasi, N. N., et al. (2018). Modulation of DEG/ENaCs by amphiphiles suggests sensitivity to membrane alterations. *Biophys. J.* 114, 1321–1335. doi:10.1016/j.bpj.2018.01.028

Sharp, C. J., Reeve, A. J., Collins, S. D., Martindale, J. C., Summerfield, S. G., Sargent, B. S., et al. (2006). Investigation into the role of P2X(3)/P2X(2/3) receptors in neuropathic pain following chronic constriction injury in the rat: An electrophysiological study. *Br. J. Pharmacol.* 148, 845–852. doi:10.1038/sj.bjp.0706790

Souslova, V., Cesare, P., Ding, Y., Akopian, A. N., Stanfa, L., Suzuki, R., et al. (2000). Warm-coding deficits and aberrant inflammatory pain in mice lacking P2X3 receptors. *Nature* 407, 1015–1017. doi:10.1038/35039526

Spelta, V., Jiang, L. H., Surprenant, A., and North, R. A. (2002). Kinetics of antagonist actions at rat P2X2/3 heteromeric receptors. *Br. J. Pharmacol.* 135, 1524–1530. doi:10.1038/sj.bjp.0704591

Spinaci, A., Buccioni, M., Dal Ben, D., Marucci, G., Volpini, R., and Lambertucci, C. (2021). P2X3 receptor ligands: Structural features and potential therapeutic applications. *Front. Pharmacol.* 12, 653561. doi:10.3389/fphar.2021.653561

Stolz, M., Klapperstuck, M., Kendzierski, T., Detro-Dassen, S., Panning, A., Schmalzing, G., et al. (2015). Homodimeric anoctamin-1, but not homodimeric anoctamin-6, is activated by calcium increases mediated by the P2Y1 and P2X7 receptors. *Pflugers Arch.* 467, 2121–2140. doi:10.1007/s00424-015-1687-3

Suadicani, S. O., Brosnan, C. F., and Scemes, E. (2006). P2X7 receptors mediate ATP release and amplification of astrocytic intercellular Ca2+ signaling. *J. Neurosci.* 26, 1378–1385. doi:10.1523/JNEUROSCI.3902-05.2006

Tsuda, M., Kuboyama, K., Inoue, T., Nagata, K., Tozaki-Saitoh, H., and Inoue, K. (2009). Behavioral phenotypes of mice lacking purinergic P2X4 receptors in acute and chronic pain assays. *Mol. Pain* 5, 28. doi:10.1186/1744-8069-5-28

Vane, J. R. (1971). Inhibition of prostaglandin synthesis as a mechanism of action for aspirin-like drugs. *Nat. New Biol.* 231, 232–235. doi:10.1038/newbio231232a0

Vanommeslaeghe, K., and Mackerell, A. D., Jr. (2012). Automation of the CHARMM general force field (CGenFF) I: Bond perception and atom typing. *J. Chem. Inf. Model* 52, 3144–3154. doi:10.1021/ci300363c

Vanommeslaeghe, K., Hatcher, E., Acharya, C., Kundu, S., Zhong, S., Shim, J., et al. (2010). CHARMM general force field: A force field for drug-like molecules compatible with the CHARMM all-atom additive biological force fields. *J. Comput. Chem.* 31, 671–690. doi:10.1002/jcc.21367

Vanommeslaeghe, K., Raman, E. P., and Mackerell, A. D., Jr. (2012). Automation of the CHARMM general force field (CGenFF) II: Assignment of bonded parameters and partial atomic charges. *J. Chem. Inf. Model* 52, 3155–3168. doi:10.1021/ci3003649

Voilley, N., De Weille, J., Mamet, J., and Lazdunski, M. (2001). Nonsteroid anti-inflammatory drugs inhibit both the activity and the inflammation-induced expression of acid-sensing ion channels in nociceptors. *J. Neurosci.* 21, 8026–8033. doi:10.1523/JNEUROSCI.21-20-08026.2001

Wang, J., Wang, Y., Cui, W. W., Huang, Y., Yang, Y., Liu, Y., et al. (2018). Druggable negative allosteric site of P2X3 receptors. *Proc. Natl. Acad. Sci. U. S. A.* 115, 4939–4944. doi:10.1073/pnas.1800907115

Warner, T. D., Giuliano, F., Vojnovic, I., Bukasa, A., Mitchell, J. A., and Vane, J. R. (1999). Nonsteroid drug selectivities for cyclo-oxygenase-1 rather than cyclo-oxygenase-2 are associated with human gastrointestinal toxicity: A full *in vitro* analysis. *Proc. Natl. Acad. Sci. U. S. A.* 96, 7563–7568. doi:10.1073/pnas.96.13.7563

Weber, W. M., Liebold, K. M., Reifarth, F. W., Uhr, U., and Clauss, W. (1995). Influence of extracellular Ca2+ on endogenous Cl-channels in Xenopus oocytes. *Pflugers Arch.* 429, 820–824. doi:10.1007/bf00374806

Wolf, M. G., Hoefling, M., Aponte-Santamaria, C., Grubmuller, H., and Groenhof, G. (2010). g_membed: Efficient insertion of a membrane protein into an equilibrated lipid bilayer with minimal perturbation. *J. Comput. Chem.* 31, 2169–2174. doi:10.1002/jcc.21507

Wolf, C., Rosefort, C., Fallah, G., Kassack, M. U., Hamacher, A., Bodnar, M., et al. (2011). Molecular determinants of potent P2X2 antagonism identified by functional analysis, mutagenesis, and homology docking. *Mol. Pharmacol.* 79, 649–661. doi:10.1124/mol.110.068700

Yu, W., He, X., Vanommeslaeghe, K., and Mackerell, A. D., Jr. (2012). Extension of the CHARMM General Force Field to sulfonyl-containing compounds and its utility in biomolecular simulations. *J. Comput. Chem.* 33, 2451–2468. doi:10.1002/jcc.23067

frontiers | Frontiers in Pharmacology

TYPE Original Research
PUBLISHED 29 March 2023
DOI 10.3389/fphar.2023.1152667



OPEN ACCESS

EDITED BY
Man Li,
Huazhong University of Science and Technology, China

REVIEWED BY
Shangdong Liang,
Nanchang University, China
Sheng-Feng Lu,
Nanjing University of Chinese Medicine, China

*CORRESPONDENCE
Xin Yang,
yangxin@cdutcm.edu.cn
Peter Illes,
Peter.Illes@medizin.uni-leipzig.de
Yong Tang,
tangyong@cdutcm.edu.cn

†These authors have contributed equally to this work

SPECIALTY SECTION
This article was submitted to Experimental Pharmacology and Drug Discovery, a section of the journal Frontiers in Pharmacology

RECEIVED 28 January 2023
ACCEPTED 14 March 2023
PUBLISHED 29 March 2023

CITATION
Shi N-R, Wang Q, Liu J, Zhang J-Z, Deng B-L, Hu X-M, Yang J, Wang X, Chen X, Zuo Y-Q, Liu T-T, Zheng J-L, Yang X, Illes P and Tang Y (2023), Association of the ADORA2A receptor and CD73 polymorphisms with epilepsy. *Front. Pharmacol.* 14:1152667. doi: 10.3389/fphar.2023.1152667



# Association of the ADORA2A receptor and CD73 polymorphisms with epilepsy

Nan-Rui Shi[1†], Qi Wang[2†], Jie Liu[2†], Ji-Zhou Zhang[1†], Bin-Lu Deng[2], Xiu-Min Hu[1], Jie Yang[2], Xin Wang[1], Xiang Chen[2], Yan-Qin Zuo[1], Ting-Ting Liu[2], Jia-Ling Zheng[3], Xin Yang[1*], Peter Illes[1,4*] and Yong Tang[1,5*]

[1]International Joint Research Centre on Purinergic Signalling, School of Acupuncture and Tuina/ School of Health and Rehabilitation, Chengdu University of Traditional Medicine, Chengdu, China, [2]Department of Neurology, Sichuan Provincial People's Hospital, University of Electronic Science and Technology of China, Chengdu, China, [3]School of Clinical Medicine, Chengdu University of Traditional Medicine, Chengdu, China, [4]Rudolf Boehm Institute for Pharmacology and Toxicology, University of Leipzig, Leipzig, Germany, [5]Acupuncture and Chronobiology Key Laboratory of Sichuan Province, Chengdu, China

Single-nucleotide polymorphisms are connected with the risk of epilepsy on occurrence, progress, and the individual response to drugs. Progress in genomic technology is exposing the complex genetic architecture of epilepsy. Compelling evidence has demonstrated that purines and adenosine are key mediators in the epileptic process. Our previous study found the interconnection of P2Y12 receptor single-nucleotide polymorphisms and epilepsy. However, little is known about the interaction between the purine nucleoside $A_{2A}$ receptor and rate-limiting enzyme ecto-5′-nucleotidase/CD73 and epilepsy from the genetic polymorphism aspect. The aim of the study is to evaluate the impact of $A_{2A}$R and CD73 polymorphisms on epilepsy cases. The study group encompassed 181 patients with epilepsy and 55 healthy volunteers. A significant correlation was confirmed between CD73 rs4431401 and epilepsy ($p < 0.001$), with TT genotype frequency being higher and C allele being lower among epilepsy patients in comparison with healthy individuals, indicating that the presence of the TT genotype is related to an increased risk of epilepsy (OR = 2.742, $p = 0.006$) while carriers of the C allele demonstrated a decreased risk of epilepsy (OR = 0.304, $p < 0.001$). According to analysis based on gender, the allele and genotype of rs4431401 in CD73 were associated with both male and female cases ($p < 0.0001$, $p = 0.026$, respectively). Of note, we found that A2AR genetic variants rs2267076 T>C ($p = 0.031$), rs2298383 C>T ($p = 0.045$), rs4822492 T>G ($p = 0.034$), and rs4822489 T>G ($p = 0.029$) were only associated with epilepsy in female subjects instead of male. It is evident that the TT genotype and T allele of rs4431401 in CD73 were genetic risk factors for epilepsy, whereas rs2267076, rs2298383, rs4822492, and rs4822489 polymorphisms of the $A_{2A}$R were mainly associated with female subjects.

KEYWORDS

**A2A receptor, CD73, single-nucleotide polymorphism, epilepsy, purinergic receptor**

## Introduction

Single-nucleotide polymorphisms (SNPs) are valuable for diagnosis and treatment guidance in epilepsy (Pal et al., 2010). As one of the prominent forms of gene variations in the human genome (Kim and Misra, 2007), SNPs are utilized to detect encoded proteins for prevention and treatment in epilepsy genetic studies. With progress in genomic technology, almost a thousand genes have been verified to relate to epilepsy etiology (Wang et al., 2017). Observational publications have reported that the GABA receptor and GABA transporter-1 SNPs are associated with the risk of epilepsy (Sesarini et al., 2015; Schijns et al., 2020). Several autophagy-related protein 5 gene polymorphisms show significant associations with the susceptibility to late-onset epilepsy and temporal lobe epilepsy (Zhang et al., 2021). Additionally, there is an increasing focus on the role of purinergic signaling receptors in various central nervous system diseases, including epilepsy (Scheffer et al., 2017; Nikolic et al., 2020; Beamer et al., 2021). We reported in our former study that the polymorphisms of the P2Y12 receptor are related to epilepsy susceptibility, and one of the polymorphisms may be specifically associated with seizure frequency (Wang et al., 2022). CD73 plays a key role in ATP metabolism, which generates the adenosine that activates the A2AR. The overfunction of A2AR is sufficient to trigger brain dysfunction and induce neuronal excitotoxicity (Cunha et al, 2016). In addition, genetic deletion of CD73 was found to attenuate neuron degeneration in mice (Augusto et al., 2021). However, the relationship between epilepsy and SNPs from the purinergic signaling facet, particularly adenosine $A_{2A}$ receptors ($A_{2A}R$) and 5′-nucleotidase (CD73), currently has only a limited number of investigations.

It has already been widely studied that $A_{2A}R$ and CD73 participate in the etiology of epilepsy, whether in experimental or observational studies (Xu et al., 2022; El Yacoubi et al., 2009; Augusto et al., 2021). $A_{2A}R$ exists in both synapses and neurons (Rebola et al., 2005; Borea et al., 2018), is associated with adenylyl cyclase activation, and is thought to have an excitatory effect on neurons upon activation (Corvol et al., 2001). In the hippocampus of both animal models and those of human brains, $A_{2A}R$ upregulation in synapses has been demonstrated to be one of the pathogenic characteristics of epilepsy (Canas et al., 2018; Crespo et al., 2018; Barros-Barbosa et al., 2016). Patients with mesial temporal lobe epilepsy have an elevated proportion of $A_{2A}R$ during epileptogenesis, and this enhanced astrocytic $A_{2A}R$ has more public involvement in disorders linked to neuroexcitotoxicity (Barros-Barbosa et al., 2016). Neuronal excitation in epilepsy may increase synaptic $A_{2A}$ activation, which aggravates synaptotoxicity and causes standard circuitry to deteriorate, resulting in epilepsy progression (Barros-Barbosa et al., 2016). In other words, $A_{2A}R$ overfunction plays an essential role in the cumulative aggravation of epilepsy rather than in the onset of seizure activity (Moreira-de-Sá et al., 2021). These studies support that $A_{2A}R$ may be involved in the pathophysiology of epilepsy by controlling the function of glial cells. Accordingly, the corresponding gene (ADORA2A) is studied as a promising candidate for epilepsy. ADORA2A is located on chromosome 22q 11.23 and has two coding exons spanning about 9 kb (MacCollin et al., 1994; Peterfreund et al., 1996). rs2298383 was proven to be associated with childhood epilepsy and a predisposition to childhood epilepsy (Fan et al., 2020). However, whether the association exists in a wider age range remains unclear. CD73 is an enzyme that catalyzes the last step in the extracellular metabolism of ATP to form adenosine (Alcedo et al., 2021) and is positioned ideally to promote $A_{2A}R$ activation after the conversion of released adenine nucleotides into adenosine (Cunha et al., 1996). A rodent study demonstrates that CD73 lost its activity along with the decreasing density of $A_{2A}R$ 48 h after hyperthermia-evoked convulsions. The amount and distribution of CD73 in the hippocampus of mesial temporal lobe epilepsy patients were higher and broader than that in control individuals, and hippocampal astrogliosis was observed in patients (Barros-Barbosa et al., 2016). Together, CD73 may be associated with epilepsy by promoting the $A_{2A}R$ activation after the conversion of released adenine nucleotides into adenosine. Furthermore, genetic variations in enzymes influencing extracellular adenosine homeostasis, including CD73, have been significantly associated with epilepsy. SNPs of CD73 have been significantly connected with epileptogenesis in the Caucasian race since variants may alter the function of CD73 to regulate the extracellular adenosine and seizure activity (Diamond et al., 2015), whereas the functions of ATP-related CD73 SNPs have not been completely illuminated in epileptic disease in the Asian race yet.

Given the substantiation that the adenosine $A_{2A}R$ and CD73 take part in the etiology of epilepsy in both clinical and rodent experiments, we designed this study to investigate changes between epilepsy cases and control individuals and from genetic variations aspects which are worth exploring as therapeutic targets for treatment development.

## Participants and methods

### Subjects

Between August 2020 and August 2021, 181 epilepsy cases (92 male and 89 female) were diagnosed according to the 2014 International League against Epilepsy criteria (Thijs et al., 2019), and there were 50 healthy participants (22 male and 28 female). The medians (ranges of the first quartile to the third quartile) of age for the cases and volunteers were 28 (23–47) and 26 (25–28), respectively. The subjects were recruited at the Sichuan Academy of Medical Science and Sichuan Provincial People's Hospital in China. Clinical data of patients were collected, including gender, age, disease diagnosis, seizure onset frequency, medical history, drug treatment, and imaging examination. Individuals with missing abovementioned clinical data were excluded from the study. Those with a history of pseudo-epileptic seizures, as well as with impaired hepatic and/or renal function, were excluded. Healthy controls were neurologically normal, with no personal or family history of epilepsy.

Following approval of the Sichuan Academy of Medical Science and Sichuan Provincial People's Hospital Ethics Committees, written informed consent was obtained from the individuals before participation in the study. Blood samples were taken with the consent of the individuals, and 2 ml blood from each participant was collected in EDTA tubes and kept at −20°C for extraction of DNA and genotyping. Samples were stored at −70°C until analysis.

## DNA extraction and genotyping

Genomic DNA was isolated from peripheral blood using a QIAGEN kit (QIAGEN, Hilden, Germany). Extracted DNA was quantified using a NanoDrop analyzer (ND-2000) spectrophotometer (NanoDrop Technologies Inc., Wilmington, DE, United States). Qualified DNA samples were stored at −80°C until further use.

We selected fourteen single-nucleotide polymorphisms from two genes involved in the adenosine cycle for analysis. Genotyping of CD73 rs4431401 T>C, rs2065114 A>G, rs2229523 A>G, rs4579322 T>A, rs9444348 G>A, rs9450282 A>G, rs6922 T>G, rs4373337 A>C, rs2267076 T>C, and $A_{2A}R$ rs3761422 T> rs2298383 C>T, rs4822492 C>G, rs2236624 T>C, and rs4822489 T>G polymorphisms was performed by the MassARRAY platform (Agena Bioscience, San Diego, CA, United States) at CapitalBio (Beijing, China). The primers for PCR amplification and extension were designed using the MassARRAY Assay Design v4.0 software. The PCR cycle program, as well as shrimp alkaline phosphatase digestion and extension, was performed according to the manufacturer's protocol. Extension products were desalted and detected using matrix-assisted laser desorption ionization time-of-fight. Finally, the data were processed with Typer v4.0 software (Agena Bioscience, San Diego, CA, United States).

## Statistical analysis

Statistical analysis was performed using the Statistical Package for the Social Sciences (SPSS), version 26.0 (IBM, Chicago, IL, United States). Categorical variables were expressed as numbers and percentages and compared by using the Pearson chi-squared test and Fisher's exact test. Numerical variables were expressed as medians with interquartile ranges and compared by the non-parametric independent-sample Wilcoxon signed-rank test. The $\chi^2$ test was used to assess the deviation from the Hardy–Weinberg equilibrium. The $\chi^2$ statistics or Fisher's exact test was used to compare the statistical differences in genotype distributions and allele frequencies between the cases and controls. The odds ratio (OR) was calculated with 95% confidence intervals (CIs). Statistical significance was defined as two-tailed $p < 0.05$.

# Results

Genotype frequencies of all investigated ADORA2A and CD73 SNPs conformed to the Hardy–Weinberg equilibrium in epilepsy and the healthy control samples.

## Clinical characteristics of the study participants

Demographic and clinical characteristics of the 231 enrolled participants are shown in Table 1.

The study included 181 patients (92 male and 89 female) and 50 volunteers (22 male and 28 female) with median ages of 28 years and 26 years, respectively. There were no statistically significant differences between epileptic patients and healthy controls in terms of gender or age.

## Genotypic and allelic distribution of the CD73 and $A_{2A}R$ SNPs

The frequency distributions of the CD73 and $A_{2A}R$ polymorphisms were compared between epilepsy patients and healthy controls. Of the fourteen investigated SNPs, a significant difference was observed in the CD73 SNP rs4431401. The genotype frequencies of CD73 rs4431401 T>C polymorphism CC, CT, and TT genotypes were found in 12.7%, 40.9%, and 46.4% of cases and 48%, 28%, and 24% of the control group, respectively. The allelic frequency was 33.1% for the C allele and 66.9% for the T allele in patients, while it was 62% for the C allele and 38% for the T allele in the volunteer group. The T allele and TT genotype were conspicuously higher among patients than in healthy controls (OR = 0.305, 95% CI = 0.193–0.483, $p = 0.0001$ for C vs. T; OR = 2.714, 95% CI = 1.333–5.529, $p = 0.006$ for TT vs. CT/CC), indicating that individuals with the T allele and TT genotype of rs4431401 T>C might have higher risks for epilepsy (Table 2). However, the risk of epilepsy did not differ in other CD73 and $A_{2A}R$ polymorphisms between the cases and the control group (Supplementary Tables S1, S2).

## Genotypic and allelic distribution of CD73 and $A_{2A}R$ SNPs in different genders

The CD73 and $A_{2A}R$ genotype and allele frequencies between the patients and controls of different genders are summarized in Table 3, Table 4, and Supplementary Tables S3 and S4. We found that the frequencies of the alleles and genotypes in CD73 rs4431401 between both male and female groups varied significantly ($p < 0.001$). With the T allele and TT genotype frequency being lower among the healthy in comparison with the epilepsy subjects, the presence of the T allele and TT genotype was connected with an increased risk of epilepsy (OR = 0.149, CI = 0.069–0.322, $p < 0.001$; OR = 5.092, CI = 1.408–18.407, $p = 0.013$, respectively) (Table 3). Females carrying the C allele/CC variant in CD73 rs4431401 had a lower risk of epilepsy in contrast with females who carried no copies (OR = 0.483, 95% CI = 0.263–0.890, $p = 0.026$ for C vs. T; OR = 3.039, 95% CI = 1.119–8.258, $p = 0.045$ for CT/TT vs. CC) (Table 3). No additional significant genotypic and allelic distribution between the female and male patients was observed in our study (Supplementary Table S3).

In the $A_{2A}R$ gene, there were no associations of the identified SNPs, rs3761422 and rs2236624, with analysis based on gender (Supplementary Table S4). Interestingly, we observed that SNPs for the $A_{2A}R$ gene differed between female cases and controls, including rs2267076 T>C ($p = 0.031$), rs2298383 C>T ($p = 0.045$), rs4822492 T>G ($p = 0.034$), and rs4822489 T>G ($p = 0.034$). The differences were mainly attributed to a greater proportion of heterozygotes and fewer homozygotes. They were observed in $A_{2A}R$ gene polymorphisms, where female cases with CT in

**TABLE 1 Demographic and clinical characteristics of the enrolled population.**

| Variables | Epileptic patients (n=181) | Healthy controls (n=50) | *p* value |
|---|---|---|---|
| Age(years) | 28 (23-47) | 26 (25-28) | 0.079 |
| Gender | | | |
| Male | 92 (50.5%) | 22 (44.0%) | 0.427 |
| Female | 89 (49.5%) | 28 (56.0%) | — |
| Drug treatment | | | |
| Monotherapy | 122 (67.4%) | — | — |
| Polytherapy | 57 (31.5%) | — | — |
| No | 2 (1.1%) | — | — |
| Neuroimaging | | | |
| Abnormal | 80 (44.2%) | — | — |
| Normal | 101 (55.8%) | — | — |
| Epileptic seizure frequencies | | | |
| < 2 times/year | 80 (44.2%) | — | — |
| ≥ 2 times/year | 101 (55.8%) | — | — |

**TABLE 2 Genotypic and allelic distribution of the CD73 gene between all patients and controls.**

| SNP ID | Genetic model | Genotype/allele | Cases | Controls | OR | 95% CI | *p value* |
|---|---|---|---|---|---|---|---|
| rs4431401 | Codominant | CC vs. CT vs. TT | 23 (12.7%)/74 (40.9%)/84 (46.4%) | 24 (48%)/14 (28%)/12 (24%) | – | – | 0.000* |
| | Allele contrast | C vs. T | 120 (33.1%)/242 (66.9%) | 62(62%)/38(38%) | 0.304 | 0.192–0.481 | 0.000* |
| | Dominant | TT vs. CT+CC | 84 (46.4%)/97 (53.6%) | 12 (24%)/38 (76%) | 2.742 | 1.346–5.587 | 0.006* |
| | Recessive | CT+TT vs. CC | 158 (87.3%)/23 (12.7%) | 26(52%)/24(48%) | 6.341 | 3.129–12.853 | 0.000* |
| | Overdominant | CC+TT vs. CT | 107 (59.1%)/74 (40.9%) | 36 (72%)/14 (28%) | 0.562 | 0.284–1.115 | 0.103 |

**TABLE 3 Genotypic and allelic distribution of the CD73 gene between all patients and controls in different genders.**

| SNP ID | Gender | Genetic model | Genotype/ allele | Cases | Controls | OR | 95% CI | *p* value |
|---|---|---|---|---|---|---|---|---|
| rs4431401 | Male | Codominant | CC vs. CT vs. TT | 11(12%)/40(43.5%)/ 41(44.6%) | 15(68.2%)/4(18.2%)/ 3(13.6%) | – | – | 0.000* |
| | | Allele contrast | C vs. T | 62(33.7%)/122(66.3%) | 34(77.3%)/10(22.7%) | 0.149 | 0.069–0.322 | 0.000* |
| | | Dominant | TT vs. CT+CC | 41(44.6%)/51(55.4%) | 3(13.6%)/19(86.4%) | 5.092 | 1.408–18.407 | 0.013* |
| | | Recessive | CT+TT vs. CC | 81(88%)/11(12%) | 7(31.8%)/15(68.2%) | 15.779 | 5.273–47.221 | 0.000* |
| | | Overdominant | CC+TT vs. CT | 52(56.5%)/40(43.5%) | 18(81.8%)/4(18.2%) | 0.289 | 0.091–0.921 | 0.049* |
| | Female | Codominant | CC vs. CT vs. TT | 12(13.5%)/34(38.2%)/ 43(48.3%) | 9(32.1%)/10(35.7%)/ 9(32.1%) | – | – | 0.067 |
| | | Allele contrast | C vs. T | 58(32.6%)/120(67.4%) | 28(50%)/28(50%) | 0.483 | 0.263–0.890 | 0.026* |
| | | Dominant | TT vs. CT+CC | 43(48.3%)/46(51.7%) | 9(32.1%)/19(67.9%) | 1.973 | 0.806–4.832 | 0.190 |
| | | Recessive | CT+TT vs. CC | 77(86.5%)/12(13.5%) | 19(67.9%)/9(32.1%) | 3.039 | 1.119–8.258 | 0.045* |
| | | Overdominant | CC+TT vs. CT | 55(61.8%)/34(38.2%) | 18(64.3%)/10(35.7%) | 0.899 | 0.371–2.174 | 0.828 |

rs2267076 (OR = 0.327, CI = 0.130–0.819, $p$ = 0.017), TC in rs2298383 (OR = 0.337, CI = 0.137–0.827, $p$ = 0.018), CG in rs4822492 (OR = 0.322, CI = 0.131–0.791, $p$ = 0.016), and GT in rs4822489 (OR = 0.322, CI = 0.131–0.791, $p$ = 0.016) had a higher proportion of heterozygotes than homozygotes (Table 4). Therefore, females who are heterozygous genotype carriers of rs2267076, rs229838, rs4822489, and rs4822492 polymorphisms have a higher risk of epilepsy.

**TABLE 4 Genotypic and allelic distribution of the A2AR gene between all patients and controls in different genders.**

| SNP ID | Gender | Genetic model | Genotype/ allele | Cases | Controls | OR | 95% CI | *p value* |
|---|---|---|---|---|---|---|---|---|
| rs2267076 | Female | Codominant | CC vs. TC vs. TT | 32(35%)/49(55.1%)/8(9%) | 14(50%)/8(28.6%)/6(21.4%) | – | – | 0.031* |
| | | Allele contrast | C vs. T | 113(63.5%)/65(36.5%) | 36(64.3%)/20(35.7%) | 0.966 | 0.516-1.806 | 1 |
| | | Dominant | TT vs. TC+CC | 8(9%)/81(91%) | 6(21.4%)/22(78.6%) | 0.362 | 0.114-1.154 | 0.097 |
| | | Recessive | TC+TT vs. CC | 57(64%)/32(36%) | 14(50%)/14(50%) | 1.781 | 0.755-4.201 | 0.267 |
| | | Overdominant | CC+TT vs. TC | 40(44.9%)/49(55.1%) | 20(71.4%)/8(28.6%) | 0.327 | 0.130-0.819 | 0.017* |
| | Male | Codominant | CC vs. TC vs. TT | 37(40.2%)/37(40.2%)/ 18(19.6%) | 7(31.8%)/10(45.5%)/ 5(22.7%) | – | – | 0.822 |
| | | Allele contrast | C vs. T | 111(60.3%)/73(39.7%) | 24(54.5%)/20(45.5%) | 1.267 | 0.653-2.459 | 0.499 |
| | | Dominant | TT vs. TC+CC | 18 (19.6%)/74(80.4%) | 5(22.7%)/17(77.3%) | 0.827 | 0.289-2.541 | 0.770 |
| | | Recessive | TC+TT vs. CC | 55(59.8%)/37(40.2%) | 15(68.2%)/7(31.8%) | 0.694 | 0.258-1.865 | 0.627 |
| | | Overdominant | CC+TT vs. TC | 55 (59.8%)/37(40.2%) | 12(54.5%)/10(45.5%) | 1.239 | 0.485-3.162 | 0.810 |
| rs2298383 | Female | Codominant | CC vs. CT vs. TT | 16(18%)/52(58.4%)/21(23.6%) | 7(25%)/9(32.1%)/12(42.9%) | – | – | 0.045* |
| | | Allele contrast | C vs. T | 84(47.2%)/94(52.8%) | 23(41.1%)/33(58.9%) | 1.282 | 0.689-2.356 | 0.446 |
| | | Dominant | TT vs. CT+CC | 21(23.6%)/68(76.4%) | 12(42.9%)/16(57.1%) | 0.412 | 0.168-1.007 | 0.057 |
| | | Recessive | CT+TT vs. CC | 73(82%)/16(18%) | 21(75%)/7(25%) | 1.521 | 0.553-4.185 | 0.587 |
| | | Overdominant | CC+TT vs. CT | 37(41.6%)/52(58.4%) | 19(67.9%)/9(32.1%) | 0.337 | 0.137-0.827 | 0.018* |
| | Male | Codominant | CC vs. CT vs. TT | 27(29.3%)/40(43.5%)/ 25(27.2%) | 5(22.7%)/10(45.5%)/ 7(31.8%) | – | – | 0.870 |
| | | Allele contrast | C vs. T | 94(51.1%)/90(48.9%) | 20(45.5%)/24(54.5%) | 1.253 | 0.648-2.425 | 0.615 |
| | | Dominant | TT vs. CT+CC | 25(27.2%)/67(72.8%) | 7(31.8%)/15(68.2%) | 0.800 | 0.292-2.191 | 0.792 |
| | | Recessive | CT+TT vs. CC | 65(70.7%)/27(29.3%) | 17(77.3%)/5(22.7%) | 0.708 | 0.237-2.113 | 0.608 |
| | | Overdominant | CC+TT vs. CT | 52(56.5%)/40(43.5%) | 12(54.5%)/10(45.5%) | 1.083 | 0.425-2.759 | 1 |
| rs4822492 | Female | Codominant | CC vs. CG vs. GG | 16(17%)/53(60.2%)/20(22.7%) | 7(25%)/9(32.1%)/12(42.9%) | – | – | 0.034* |
| | | Allele contrast | C vs. G | 85 (47.8%)/93(52.2%) | 23(41.1%)/33(58.9%) | 1.311 | 0.714-2.409 | 0.443 |
| | | Dominant | GG vs. CG+CC | 20(22.5%)/69(77.5%) | 12(42.9%)/16(57.1%) | 0.386 | 0.157-0.949 | 0.051 |
| | | Recessive | CG+GG vs. CC | 73(82%)/16(18%) | 21(75%)/7(25%) | 1.521 | 0.553-4.185 | 0.587 |
| | | Overdominant | CC+GG vs. CG | 36(40.4%)/53(59.6%) | 19(67.9%)/9(32.1%) | 0.322 | 0.131-0.791 | 0.016* |

(Continued on following page)

**TABLE 4 (*Continued*) Genotypic and allelic distribution of the A2AR gene between all patients and controls in different genders.**

| SNP ID | Gender | Genetic model | Genotype/ allele | Cases | Controls | OR | 95% CI | *p value* |
|---|---|---|---|---|---|---|---|---|
| | Male | Codominant | CC vs. CG vs. GG | 26(28.3%)/41(44.6%)/ 25(25.8%) | 5(22.7%)/10(45.5%)/ 7(31.8%) | – | – | 0.872 |
| | | Allele contrast | C vs. G | 93(50.5%)/91(49.5%) | 20(45.5%)/24(54.5%) | 1.226 | 0.634-2.373 | 0.616 |
| | | Dominant | GG vs. CG+CC | 25(27.2%)/67(72.8%) | 7(31.8%)/15(68.2%) | 0.800 | 0.292-2.191 | 0.792 |
| | | Recessive | CG+GG vs. CC | 66(71.7%)/26(28.3%) | 17(77.3%)/5(22.7%) | 0.747 | 0.250-2.233 | 0.791 |
| | | Overdominant | CC+GG vs. CG | 51(55.4%)/41(44.6%) | 12(54.5%)/10(45.5%) | 1.037 | 0.407-2.639 | 1 |
| rs4822489 | Female | Codominant | GG vs. GT vs. TT | 20(22.7%)/53(60.2%)/16(17%) | 12(27.6%)/9(53.4%)/7(19%) | – | – | 0.034* |
| | | Allele contrast | G vs. T | 93(52.2%)/85(47.8%) | 33(58.9%)/23(41.1%) | 0.763 | 0.415-1.401 | 0.443 |
| | | Dominant | TT vs. GT+GG | 16(18%)/73(82%) | 7(25%)/21(75%) | 0.658 | 0.239-1.809 | 0.587 |
| | | Recessive | GT+TT vs. GG | 69(77.5%)/20(22.5%) | 16(57.1%)/12(42.9%) | 2.588 | 1.053-6.357 | 0.051 |
| | | Overdominant | GG+TT vs. GT | 36(40.4%)/53(59.6%) | 19(67.9%)/9(32.1%) | 0.322 | 0.131-0.791 | 0.016* |
| | Male | Codominant | GG vs. GT vs. TT | 25(27.2%)/41(44.6%)/ 26(28.3%) | 7(31.8%)/10(45.5%)/ 5(22.7%) | – | – | 0.872 |
| | | Allele contrast | G vs. T | 91(49.5%)/93(50.5%) | 24(54.5%)/20(45.5%) | 0.815 | 0.421-1.578 | 0.616 |
| | | Dominant | TT vs. GT+GG | 26(28.3%)/66(71.7%) | 5(22.7%)/17(77.3%) | 1.339 | 0.448-4.006 | 0.791 |
| | | Recessive | GT+TT vs. GG | 67(72.8%)/25(27.2%) | 15(68.2%)/7(31.8%) | 1.251 | 0.456-3.427 | 0.792 |
| | | Overdominant | GG+TT vs. GT | 51(55.4%)/41(44.6%) | 12(54.5%)/10(45.5%) | 1.037 | 0.407-2.639 | 1 |

## Subgroup analysis of $A_{2A}R$ and CD73

We conducted sub-analyses to determine whether risk varied by subgroups differing in drug treatment, neuroimaging, or epileptic seizure frequencies. We did not find any significant connection between neuroimaging and seizure frequency subgroups but did find an association between genotypes and drug therapy among epilepsy cases (Supplementary Tables S5, S6). This relationship was evident only for single-nucleotide polymorphisms on the $A_{2A}R$ gene (Table 5). The frequency of the TT genotype (38.6% for polytherapy; 46.7% for monotherapy) and T allele (60.5% for polytherapy; 46.7% for monotherapy) for rs2298383 in the $A_{2A}R$ gene was higher among cases of polypharmacy than in single drug treatment groups, suggesting that patients that had the TT genotype and T allele (TT vs. CT/CC: OR = 0.390, CI = 0.194–0.781, $p$ = 0.010; C vs. T: OR = 1.749, CI = 1.113–2.478, $p$ = 0.017) had a higher potential of requiring two or more antiepileptic drugs. Similar to former results, in rs4822492, the GG genotype and G allele were associated with polytherapy (GG vs. CG/CC: OR = 0.370, CI = 0.184–0.744, $p$ = 0.006; C vs. G: OR = 1.844, CI = 1.172–2.902, $p$ = 0.009). In addition, we found that patients carrying the GG variant in $A_{2A}R$ rs4822489 were associated with polypharmacy (OR = 2.706, CI = 1.343–5.449, $p$ = 0.006).

# Discussion

We tested the hypothesis that adenosine-related SNPs are connected with the risk of epilepsy.

Our data showed that the T allele and TT genotype of SNP rs4431401 of CD73 was associated with a more pronounced predisposition to an increased risk of epilepsy, while $A_{2A}R$ gene rs2267076, rs2298383, rs4822492, and rs4822489 polymorphisms were more strongly linked with female epileptic patients. In contrast, there was no evidence for interactions of the identified SNPs: rs2065114, rs2229523, rs4579322, rs9444348, rs9450282, rs6922, and rs4373337 of CD73, rs3761422, and rs2236624 of $A_{2A}R$. Noteworthily, rs2298383, rs4822492, and rs4822489 on the $A_{2A}R$ gene were associated with medication administered among epilepsy cases. These findings provide insight into the genetic susceptibility of epileptic disease and assistance for clinical drug therapy.

**TABLE 5 Genotypic and allelic distribution of CD73 and A2AR genes between patients with monotherapy and polytherapy.**

| Gene | SNP ID | Genetic model | Genotype/ allele | Monotherapy | Polytherapy | OR | 95% CI | *p* value |
|---|---|---|---|---|---|---|---|---|
| CD73 | rs4431401 | Codominant | CC vs. CT vs. TT | 14 (11.5%)/51 (41.8%)/ 57 (46.7%) | 9 (15.8%)/22 (38.6%)/ 26 (45.6%) | – | – | 0.733 |
| | | Allele contrast | C vs. T | 79 (32.4%)/165 (67.6%) | 40 (35.1%)/74 (64.9%) | 0.886 | 0.554–1.416 | 0.631 |
| | | Dominant | TT vs. CT+CC | 57 (46.7%)/65 (53.3%) | 26 (45.6%)/31 (54.4%) | 1.046 | 0.556–1.965 | 1 |
| | | Recessive | CT+TT vs. CC | 108 (88.5%)/14 (11.5%) | 48 (84.2%)/9 (15.8%) | 1.446 | 0.586–3.571 | 0.474 |
| | | Overdominant | CC+TT vs. CT | 71 (58.2%)/51 (41.8%) | 35 (61.4%)/22 (38.6%) | 0.875 | 0.460–1.665 | 0.745 |
| A2AR | rs2267076 | Codominant | CC vs. TC vs. TT | 41 (33.6%)/63 (51.6%)/ 18 (14.8%) | 27 (47.4%)/23 (40.4%)/ 7 (12.3%) | – | – | 0.222 |
| | | Allele contrast | C vs. T | 145 (59.4%)/99 (40.6%) | 77 (67.5%)/37 (32.5%) | 0.704 | 0.441–1.124 | 0.161 |
| | | Dominant | TT vs. TC+CC | 18 (14.8%)/104 (85.2%) | 7 (12.3%)/50 (87.7%) | 1.236 | 0.485–3.152 | 0.818 |
| | | Recessive | TC+TT vs. CC | 81 (66.4%)/41 (33.6%) | 30 (52.6%)/27 (47.4%) | 1.778 | 0.936–3.377 | 0.098 |
| | | Overdominant | CC+TT vs. TC | 59 (48.4%)/63 (51.6%) | 34 (59.6%)/23 (40.4%) | 0.634 | 0.335–1.198 | 0.199 |
| A2AR | rs2298383 | Codominant | CC vs. CT vs. TT | 32 (26.2%)/66 (54.1%)/ 24 (19.7%) | 10 (17.5%)/25 (43.9%)/ 22 (38.6%) | – | – | 0.023* |
| | | Allele contrast | C vs. T | 130 (53.3%)/114 (46.7%) | 45 (39.5%)/69 (60.5%) | 1.749 | 1.113–2.748 | 0.017* |
| | | Dominant | TT vs. CT+CC | 24 (19.7%)/98 (80.3%) | 22(38.6%)/35(61.4%) | 0.390 | 0.194–0.781 | 0.010* |
| | | Recessive | CT+TT vs. CC | 90 (73.8%)/32 (26.2%) | 47 (82.5%)/10 (17.5%) | 0.598 | 0.271–1.322 | 0.257 |
| | | Overdominant | CC+TT vs. CT | 56 (45.9%)/66 (54.1%) | 32 (56.1%)/25 (43.9%) | 0.663 | 0.352–1.248 | 0.261 |
| A2AR | rs4822492 | Codominant | CC vs. CG vs. GG | 32 (26.2%)/67 (54.9%)/ 23 (18.9%) | 9 (15.8%)/26 (45.6%)/ 22 (38.6%) | – | – | 0.013* |
| | | Allele contrast | C vs. G | 131 (53.7%)/113 (46.3%) | 44 (38.6%)/70 (61.4%) | 1.844 | 1.172–2.902 | 0.009* |
| | | Dominant | GG vs. CG+CC | 23 (18.9%)/99 (81.1%) | 22 (38.6%)/35 (61.4%) | 0.370 | 0.184–0.744 | 0.006* |
| | | Recessive | CG+GG vs. CC | 90 (73.8%)/32 (26.2%) | 48 (84.2%)/9 (15.8%) | 0.527 | 0.233–1.195 | 0.132 |
| | | Overdominant | CC+GG vs. CG | 55 (45.1%)/67 (54.9%) | 31 (54.4%)/26 (45.6%) | 0.688 | 0.366–1.295 | 0.265 |
| A2AR | rs4822489 | Codominant | GG vs. GT vs. TT | 23 (18.9%) 67 (54.9%)/ 32 (26.2%) | 22 (38.6%)/26 (45.6%)/ 9 (15.8%) | – | – | 0.013* |
| | | Allele contrast | G vs. T | 113 (46.3%)/131 (53.7%) | 70(61.4%)/44(38.6%) | 0.542 | 0.345-0.853 | 0.009 |
| | | Dominant | TT vs. GT+GG | 32 (26.2%)/90 (73.8%) | 9 (15.8%)/48 (84.2%) | 1.896 | 0.837–4.298 | 0.132 |
| | | Recessive | GT + TT vs. GG | 99 (81.1%)/23 (18.9%) | 35 (61.4%)/22 (38.6%) | 2.706 | 1.343–5.449 | 0.006* |
| | | Overdominant | GG + TT vs. GT | 55 (45.1%)/67 (54.9%) | 31 (54.4%)/26 (45.6%) | 0.688 | 0.366–1.295 | 0.265 |

We found that carriers of rs4431401 in CD73, with a higher proportion of T allele and TT genotype, may have a higher predisposition for epilepsy. Observational studies focused on nephrotic syndrome (NS) (Yang et al., 2018; Zaorska et al., 2021) and uremia patients (Rothe et al., 2017) and found that rs4431401 (T>C) was significantly correlated with both differed NS risk and altered hormone sensitivity to NS. We also observed that both female and male subjects have a higher frequency of TT genotype compared to the controls. Since the risk factors of epilepsy are complex, such as family history, excessive sleep deprivation, and use of alcohol (Gavvala and Schuele, 2016), we speculate that one of the possible mechanisms is that gender difference influences the cognitive strategies on brain activation, such as women preferring the left hemisphere while men favoring the right hemisphere (Koepp, 2011). In addition, endogenous sex hormones may play a role. In an earlier cohort study, rs9444348 of CD73 was reported to have been significantly associated with a shorter time to first seizure and an increased seizure rate within 3 years of post-traumatic brain injury in Caucasian patients (Diamond et al., 2015). However, no difference was found in our present study. Race, the pathogenesis of epilepsy, and the statistical method were regarded to be the feasible reasons which are causing differences in results.

Females who carried a greater proportion of heterozygotes in rs2298383, rs2267076, rs4822492, and rs4822489 polymorphisms on the $A_{2A}R$ gene were identified to have an increased risk of epilepsy. On

the contrary, no significant difference was observed in male patients. Consistent with this, a rodent study showed that female rats were more susceptible to acquiring seizures than male rats (Dai et al., 2014). Since sex hormones are associated with neuronal development, neuronal excitability, and epileptic susceptibility (Patrone et al., 1999; Zupanc, 2006; Liu et al., 2012), the possible reason is the effect of endogenous sex hormones, such as androgen, estrogen, and progesterone, as well as their metabolites. In addition, a recent study based on southern Chinese children with epileptic diseases shows that the carriers of the rs2298383 TT genotype tended to have a lower chance of epilepsy (Fan et al., 2020). In addition, the haplotype C frequency at rs2298383 and rs4822492 polymorphisms was reported to be significantly higher than in controls in acute encephalopathy with biphasic seizures and late reduced diffusion in children from Japan (Shinohara et al., 2013). The fact that these results are incompatible with ours could be attributed to the differences in age and the regions from where the participants were enrolled. As for s2267076 and rs4822489, we found no directly comparable studies when we searched PubMed for studies published in English that investigated the association between them and the risk of epilepsy. We have, therefore, provided comparisons with broader literature. The current study indicates that a higher risk of rheumatoid arthritis was found in patients who consume more caffeine with a CT genotype of rs2267076 (Soukup et al., 2020). rs4822489 is associated with chronic heart failure and type 1 diabetes (Charles et al., 2011; Zhai et al., 2015). To our knowledge, the genetic polymorphisms rs2267076 and rs4822489 were first identified to be associated with epilepsy in the present study.

We also observed an increased risk of polypharmacy in individuals with the TT genotype and T allele of rs2298383. An earlier case-control study reported that rs2298383 polymorphisms associated with tear volume increase after caffeine intake (Arita et al., 2012). Caffeine has various pharmacologic effects on the human body, including stimulation of the central nervous system (van Dam et al., 2020). $A_{2A}R$, as one of the main target receptors of caffeine, has already been proven to play an important role in caffeine metabolism (Cappelletti et al., 2015). In addition, genetic factors are revealed to be associated with the direct effects of caffeine (Yang et al., 2010). In this way, an in-depth study needs to investigate whether rs2298383 is linked with polypharmacy of antiepileptic drugs and caffeine. In addition, though our results suggest that $A_{2A}R$ and CD73 gene polymorphisms do not correlate with the epileptic seizure frequency or abnormal/normal neuroimaging, they still require further investigation.

Some potential limitations should be considered. First, we only analyzed the population in southwestern China because representation from other regions of the country is lacking. Future studies should involve patients from the greater China region. Second, the SNPs of CD73 have been rarely reported in epilepsy. Hence, the discussion concerning the SNPs of CD73 is limited. Further validation and studies are necessary to confirm the relationship between CD73 and epilepsy. Finally, this study was confined to the association of SNPs with epilepsy and lacked specific epileptic sub-types due to the limited sample size. Therefore, more in-depth research is needed to improve our understanding of the association between CD73 and $A_{2A}$ receptors and the pathophysiology of epilepsy.

## Data availability statement

The original contributions presented in the study are included in the article/Supplementary Material; further inquiries can be directed to the corresponding authors.

## Ethics statement

The studies involving human participants were reviewed and approved by the Ethics Committee of the Sichuan Academy of Medical Science and Sichuan Provincial People's Hospital. The patients/participants provided their written informed consent to participate in this study.

## Author contributions

N-RS, QW, and JL performed the study, analyzed the data, and wrote the manuscript; J-ZZ, B-LD, X-MH, JY, XW, XC, Y-QZ, T-TL, and J-LZ, performed the study; and XY, PI, and YT designed the study and wrote the manuscript.

## Funding

This work was supported by grants from the Innovation Team and Talents Cultivation Program of National Administration of Traditional Chinese Medicine (ZYYCXTDD-202003) and the Science and Technology Program of Sichuan Province, China (2022YFH0006 and 23RCYJ0059).

## Conflict of interest

The authors declare that the research was conducted in the absence of any commercial or financial relationships that could be construed as a potential conflict of interest.

## Publisher's note

All claims expressed in this article are solely those of the authors and do not necessarily represent those of their affiliated organizations, or those of the publisher, the editors, and the reviewers. Any product that may be evaluated in this article, or claim that may be made by its manufacturer, is not guaranteed or endorsed by the publisher.

## Supplementary material

The Supplementary Material for this article can be found online at: https://www.frontiersin.org/articles/10.3389/fphar.2023.1152667/full#supplementary-material

# References


Alcedo, K. P., Bowser, J. L., and Snider, N. T. (2021). The elegant complexity of mammalian ecto-5'-nucleotidase (CD73). *Trends Cell. Biol.* 31 (10), 829–842. doi:10.1016/j.tcb.2021.05.008

Arita, R., Yanagi, Y., Honda, N., Maeda, S., Maeda, K., Kuchiba, A., et al. (2012). Caffeine increases tear volume depending on polymorphisms within the adenosine A2a receptor gene and cytochrome P450 1A2. *Ophthalmology* 119 (5), 972–978. doi:10.1016/j.ophtha.2011.11.033

Augusto, E., Gonçalves, F. Q., Real, J. E., Silva, H. B., Pochmann, D., Silva, T. S., et al. (2021). Increased ATP release and CD73-mediated adenosine A2A receptor activation mediate convulsion-associated neuronal damage and hippocampal dysfunction. *Neurobiol. Dis.* 157, 105441. doi:10.1016/j.nbd.2021.105441

Barros-Barbosa, A. R., Ferreirinha, F., Oliveira, Â., Mendes, M., Lobo, M. G., Santos, A., et al. (2016). Adenosine A2Areceptor, and ecto-5'-nucleotidase/CD73 are upregulated in hippocampal astrocytes of human patients with mesial temporal lobe epilepsy (MTLE). *Purinergic Signal* 12 (4), 719–734. doi:10.1007/s11302-016-9535-2

Beamer, E., Kuchukulla, M., Boison, D., and Engel, T. (2021). ATP and adenosine-Two players in the control of seizures and epilepsy development. *Prog. Neurobiol.* 204, 102105. doi:10.1016/j.pneurobio.2021.102105

Borea, P. A., Gessi, S., Merighi, S., Vincenzi, F., and Varani, K. (2018). Pharmacology of adenosine receptors: The state of the art. *Physiol. Rev.* 98 (3), 1591–1625. doi:10.1152/physrev.00049.2017

Canas, P. M., Porciúncula, L. O., Simões, A. P., Augusto, E., Silva, H. B., Machado, N. J., et al. (2018). Neuronal adenosine A2A receptors are critical mediators of neurodegeneration triggered by convulsions. *eNeuro* 5 (6), ENEURO.0385–18.2018. doi:10.1523/ENEURO.0385-18.2018

Cappelletti, S., Piacentino, D., Sani, G., and Aromatario, M. (2015). Caffeine: Cognitive and physical performance enhancer or psychoactive drug? *Curr. Neuropharmacol.* 13 (1), 71–88. doi:10.2174/1570159X13666141210215655

Charles, B. A., Conley, Y. P., Chen, G., Miller, R. G., Dorman, J. S., Gorin, M. B., et al. (2011). Variants of the adenosine A(2A) receptor gene are protective against proliferative diabetic retinopathy in patients with type 1 diabetes. *Ophthalmic Res.* 46 (1), 1–8. doi:10.1159/000317057

Corvol, J. C., Studler, J. M., Schonn, J. S., Girault, J. A., and Hervé, D. (2001). Galpha(olf) is necessary for coupling D1 and A2a receptors to adenylyl cyclase in the striatum. *J. Neurochem.* 76 (5), 1585–1588. doi:10.1046/j.1471-4159.2001.00201.x

Crespo, M., León-Navarro, D. A., and Martín, M. (2018). Early-life hyperthermic seizures upregulate adenosine A2A receptors in the cortex and promote depressive-like behavior in adult rats. *Epilepsy Behav.* 86, 173–178. doi:10.1016/j.yebeh.2018.06.048

Cunha, R. A., Correia-de-Sá, P., Sebastião, A. M., and Ribeiro, J. A. (1996). Preferential activation of excitatory adenosine receptors at rat hippocampal and neuromuscular synapses by adenosine formed from released adenine nucleotides. *Br. J. Pharmacol.* 119, 253–260. doi:10.1111/j.1476-5381.1996.tb15979.x

Cunha, R. A. (2016). How does adenosine control neuronal dysfunction and neurodegeneration? *J. Neurochem.* 139 (6), 1019–1055. doi:10.1111/jnc.13724

Dai, Y. J., Xu, Z. H., Feng, B., Xu, C. L., Zhao, H. W., and Wu, D. C. (2014). Gender difference in acquired seizure susceptibility in adult rats after early complex febrile seizures. *Neurosci. Bull.* 30(6), 913–922. doi:10.1007/s12264-014-1482-8

Diamond, M. L., Ritter, A. C., Jackson, E. K., Conley, Y. P., Kochanek, P. M., Boison, D., et al. (2015). Genetic variation in the adenosine regulatory cycle is associated with posttraumatic epilepsy development. *Epilepsia* 56 (8), 1198–1206. doi:10.1111/epi.13044

El Yacoubi, M., Ledent, C., Parmentier, M., Costentin, J., and Vaugeois, J. M. (2009). Adenosine A2A receptor deficient mice are partially resistant to limbic seizures. *Naunyn Schmiedeb. Arch. Pharmacol.* 380 (3), 223–232. doi:10.1007/s00210-009-0426-8

Fan, X., Chen, Y., Li, W., Xia, H., Liu, B., Guo, H., et al. (2020). Genetic polymorphism ofADORA2A is associated with the risk of epilepsy and predisposition to neurologic comorbidity in Chinese southern children. *Front. Neurosci.* 14, 590605. doi:10.3389/fnins.2020.590605

Gavvala, J. R., and Schuele, S. U. (2016). New-onset seizure in adults and adolescents: A review. *JAMA* 316 (24), 2657–2668. doi:10.1001/jama.2016.18625

Kim, S., and Misra, A. (2007). SNP genotyping: Technologies and biomedical applications. *Annu. Rev. Biomed. Eng.* 9, 289–320. doi:10.1146/annurev.bioeng.9.060906.152037

Koepp, M. J. (2011). Gender and drug effects on neuroimaging in epilepsy. *Epilepsia* 52 (4), 35–37. doi:10.1111/j.1528-1167.2011.03150.x

Liu, S. B., Zhang, N., Guo, Y. Y., Zhao, R., Shi, T. y., Feng, S. f., et al. (2012). G-protein-coupled receptor 30 mediates rapid neuroprotective effects of estrogen via depression of NR2B-containing NMDA receptors. *J. Neurosci.* 32 (14), 4887–4900. doi:10.1523/JNEUROSCI.5828-11.2012

MacCollin, M., Peterfreund, R., MacDonald, M., Fink, J. S., and Gusella, J. (1994). Mapping of a human A2a adenosine receptor (ADORA2) to chromosome 22. *Genomics* 20 (2), 332–333. doi:10.1006/geno.1994.1181

Moreira-de-Sá, A., Lourenço, V. S., Canas, P. M., and Cunha, R. A. (2021). Adenosine A2A receptors as biomarkers of brain diseases. *Front. Neurosci.* 15, 702581. doi:10.3389/fnins.2021.702581

Nikolic, L., Nobili, P., Shen, W., and Audinat, E. (2020). Role of astrocyte purinergic signaling in epilepsy. *Glia* 68 (9), 1677–1691. doi:10.1002/glia.23747

Pal, D. K., Pong, A. W., and Chung, W. K. (2010). Genetic evaluation and counseling for epilepsy. *Nat. Rev. Neurol.* 6 (8), 445–453. doi:10.1038/nrneurol.2010.92

Patrone, C., Andersson, S., Korhonen, L., and Lindholm, D. (1999). Estrogen receptor-dependent regulation of sensory neuron survival in developing dorsal root ganglion. *Proc. Natl. Acad. Sci. U. S. A.* 96 (19), 10905–10910. doi:10.1073/pnas.96.19.10905

Peterfreund, R. A., MacCollin, M., Gusella, J., and Fink, J. S. (1996). Characterization and expression of the human A2a adenosine receptor gene. *J. Neurochem.* 66 (1), 362–368. doi:10.1046/j.1471-4159.1996.66010362.x

Rebola, N., Canas, P. M., Oliveira, C. R., and Cunha, R. A. (2005). Different synaptic and subsynaptic localization of adenosine A2A receptors in the hippocampus and striatum of the rat. *Neuroscience* 132 (4), 893–903. doi:10.1016/j.neuroscience.2005.01.014

Rothe, H., Brandenburg, V., Haun, M., Kollerits, B., Kronenberg, F., Ketteler, M., et al. (2017). Ecto-5' -Nucleotidase CD73 (NT5E), vitamin D receptor and FGF23 gene polymorphisms may play a role in the development of calcific uremic arteriolopathy in dialysis patients - data from the German Calciphylaxis Registry. *PLoS One* 12 (2), e0172407. doi:10.1371/journal.pone.0172407

Scheffer, I. E., Berkovic, S., Capovilla, G., Connolly, M. B., French, J., Guilhoto, L., et al. (2017). ILAE classification of the epilepsies: Position paper of the ILAE commission for classification and terminology. *Epilepsia* 58 (4), 512–521. doi:10.1111/epi.13709

Schijns, O. E., Bisschop, J., Rijkers, K., Dings, J., Vanherle, S., Lindsey, P., et al. (2020). GAT-1 (rs2697153) and GAT-3 (rs2272400) polymorphisms are associated with febrile seizures and temporal lobe epilepsy. *Epileptic Disord.* 22 (2), 176–182. doi:10.1684/epd.2020.1154

Sesarini, C. V., Costa, L., Grañana, N., Coto, M. G., Pallia, R. C., and Argibay, P. F. (2015). Association between GABA(A) receptor subunit polymorphisms and autism spectrum disorder (ASD). *Psychiatry Res.* 229 (1-2), 580–582. doi:10.1016/j.psychres.2015.07.077

Shinohara, M., Saitoh, M., Nishizawa, D., Ikeda, K., Hirose, S., Takanashi, J. i., et al. (2013). ADORA2A polymorphism predisposes children to encephalopathy with febrile status epilepticus. *Neurology* 80 (17), 1571–1576. doi:10.1212/WNL.0b013e31828f18d8

Soukup, T., Hloch, K., Doseděl, M., Tebbens, J. D., Nekvindova, J., Šembera, Š., et al. (2020). The influence of coffee intake and genetics on adenosine pathway in rheumatoid arthritis. *Pharmacogenomics* 21 (11), 735–749. doi:10.2217/pgs-2020-0042

Thijs, R. D., Surges, R., O'Brien, T. J., and Sander, J. W. (2019). Epilepsy in adults. *Lancet.* 393 (10172), 689–701. doi:10.1016/S0140-6736(18)32596-0

van Dam, R. M., Hu, F. B., and Willett, W. C. (2020). Coffee, caffeine, and health. *N. Engl. J. Med.* 383 (4), 369–378. doi:10.1056/nejmra1816604

Wang, J., Lin, Z. J., Liu, L., Xu, H. Q., Shi, Y. W., Yi, Y. H., et al. (2017). Epilepsy-associated genes. *Seizure* 44, 11–20. doi:10.1016/j.seizure.2016.11.030

Wang, Q., Shi, N. R., Lv, P., Liu, J., Zhang, J. Z., Deng, B. L., et al. (2022). P2Y12 receptor gene polymorphisms are associated with epilepsy. *Purinergic Signal* 19, 155–162. doi:10.1007/s11302-022-09848-4

Xu, X., Beleza, R. O., Gonçalves, F. Q., Valbuena, S., Alçada-Morais, S., Gonçalves, N., et al. (2022). Adenosine A2A receptors control synaptic remodeling in the adult brain. *Sci. Rep.* 12 (1), 14690. doi:10.1038/s41598-022-18884-4

Yang, A., Palmer, A. A., and de Wit, H. (2010). Genetics of caffeine consumption and responses to caffeine. *Psychopharmacol. Berl.* 211 (3), 245–257. doi:10.1007/s00213-010-1900-1

Yang, R., Hong, H., Wang, M., and Ma, Z. (2018). Correlation between single-nucleotide polymorphisms within miR-30a and related target genes and risk or prognosis of nephrotic syndrome. *DNA Cell. Biol.* 37 (3), 233–243. doi:10.1089/dna.2017.4024

Zaorska, K., Zawierucha, P., Świerczewska, M., Ostalska-Nowicka, D., Zachwieja, J., and Nowicki, M. (2021). Prediction of steroid resistance and steroid dependence in nephrotic syndrome children. *J. Transl. Med.* 19 (1), 130. doi:10.1186/s12967-021-02790-w

Zhai, Y. J., Liu, P., He, H. R., Zheng, X. W., Wang, Y., Yang, Q. T., et al. (2015). The association of ADORA2A and ADORA2B polymorphisms with the risk and severity of chronic heart failure: A case-control study of a northern Chinese population. *Int. J. Mol. Sci.* 16 (2), 2732–2746. doi:10.3390/ijms16022732

Zhang, Y. X., Qiao, S., Cai, M. T., Lai, Q. L., Shen, C. H., and Ding, M. P. (2021). Association between autophagy-related protein 5 gene polymorphisms and epilepsy in Chinese patients. *Neurosci. Lett.* 753, 135870. doi:10.1016/j.neulet.2021.135870

Zupanc, M. L. (2006). Antiepileptic drugs and hormonal contraceptives in adolescent women with epilepsy. *Neurology* 66 (63), S37–S45. doi:10.1212/wnl.66.66_suppl_3.s37

frontiers | Frontiers in Pharmacology

TYPE Original Research
PUBLISHED 10 April 2023
DOI 10.3389/fphar.2023.1148190



OPEN ACCESS

EDITED BY
Henning Ulrich,
University of São Paulo, Brazil

REVIEWED BY
Sascha Kahlfuss,
Universitätsklinikum Magdeburg, Germany
Karina S. MacDowell,
Faculty of Medicine (UCM), Spain

*CORRESPONDENCE
Jan M. Deussing,
deussing@psych.mpg.de

SPECIALTY SECTION
This article was submitted o Experimental Pharmacology and Drug Discovery, a section of the journal Frontiers in Pharmacology

RECEIVED 19 January 2023
ACCEPTED 30 March 2023
PUBLISHED 10 April 2023

CITATION
von Mücke-Heim I-A, Martin J, Uhr M, Ries C and Deussing JM (2023), The human P2X7 receptor alters microglial morphology and cytokine secretion following immunomodulation. *Front. Pharmacol.* 14:1148190. doi: 10.3389/fphar.2023.1148190



# The human P2X7 receptor alters microglial morphology and cytokine secretion following immunomodulation

Iven-Alex von Mücke-Heim[1], Jana Martin[1], Manfred Uhr[2], Clemens Ries[1] and Jan M. Deussing[1]*

[1]Molecular Neurogenetics, Max Planck Institute of Psychiatry, Munich, Germany, [2]Core Unit Analytics and Mass Spectrometry, Max Planck Institute of Psychiatry, Munich, Germany

**Introduction:** In recent years, purinergic signaling via the P2X7 receptor (P2X7R) on microglia has repeatedly been implicated in depression genesis. However, it remains unclear which role the human P2X7R (hP2X7R) plays in regulating both microglia morphology and cytokine secretion upon different environmental and immune stimuli, respectively.

**Methods:** For this purpose, we used primary microglial cultures derived from a humanized microglia-specific conditional P2X7R knockout mouse line to emulate different gene-environment interactions between microglial hP2X7R and molecular proxies of psychosocial and pathogen-derived immune stimuli. Microglial cultures were subjected to treatments with the agonists 2′(3′)-O-(4-benzoylbenzoyl)-ATP (BzATP) and lipopolysaccharides (LPS) combined with specific P2X7R antagonists (JNJ-47965567, A-804598).

**Results:** Morphotyping revealed overall high baseline activation due to the in vitro conditions. Both BzATP and LPS + BzATP treatment increased round/ameboid microglia and decreased polarized and ramified morphotypes. This effect was stronger in hP2X7R-proficient (CTRL) compared to knockout (KO) microglia. Aptly, we found antagonism with JNJ-4796556 and A-804598 to reduce round/ameboid microglia and increase complex morphologies only in CTRL but not KO microglia. Single cell shape descriptor analysis confirmed the morphotyping results. Compared to KO microglia, hP2X7R-targeted stimulation in CTRLs led to a more pronounced increase in microglial roundness and circularity along with an overall higher decrease in aspect ratio and shape complexity. JNJ-4796556 and A-804598, on the other hand, led to opposite dynamics. In KO microglia, similar trends were observed, yet the magnitude of responses was much smaller. Parallel assessment of 10 cytokines demonstrated the proinflammatory properties of hP2X7R. Following LPS + BzATP stimulation, IL-1β, IL-6, and TNFα levels were found to be higher and IL-4 levels lower in CTRL than in KO cultures. Vice versa, hP2X7R antagonists reduced proinflammatory cytokine levels and increased IL-4 secretion.

**Discussion:** Taken together, our results help disentangle the complex function of microglial hP2X7R downstream of various immune stimuli. In addition, this is the first study in a humanized, microglia-specific *in vitro* model identifying a so far unknown potential link between microglial hP2X7R function and IL-27 levels.

KEYWORDS

P2X7 receptor (P2X7R), mouse model, cell culture, immunomodulation, knockout (KO) mice, microglia, cytokine secretion

# 1 Introduction

Major depression is a common and multifactorial mental disorder, which arises from complex gene-environment interactions (GBD-2017-Collaborators, 2018; Lopizzo et al., 2015). Alarmingly, current trend analyses report a significant and worldwide rise in depression incidence (Moreno-Agostino et al., 2021). Aside from the well characterized impact of genetic vulnerability and acute as well as chronic psychosocial stress (Lopizzo et al., 2015; Gonda et al., 2018), alterations in cellular and humoral immunity feeding into mild systemic inflammation have been identified as important factors in depression genesis (Miller and Raison, 2016; Wohleb et al., 2016; Medina-Rodriguez et al., 2018), at least in a subset of about 30% of patients (Raison and Miller, 2011; Nobis et al., 2020). The latter experience elevated blood levels of proinflammatory cytokines like tumor necrosis factor alpha (TNFα), C-reactive protein (CRP), or interleukin (IL)-6 (Felger and Lotrich, 2013; Miller and Raison, 2016; Mac Giollabhui et al., 2020), changes in immune cell composition and function (Miller, 2010; Miller and Raison, 2016; Drevets et al., 2022), which are often accompanied by altered metabolic parameters (de Kluiver et al., 2019; Lamers et al., 2020). Especially the monocyte-macrophage system including microglia, natural killer cells (NKs), and regulatory T cells ($T_{reg}$) along with different T helper cells (Th) display molecular and functional aberrations in depressed patients (Miller, 2010; Suzuki et al., 2017; Beurel et al., 2020; Cattaneo et al., 2020; Bauer and Teixeira, 2021). A recent study by Costi and colleagues, for instance, demonstrated a relation between elevated blood-derived immune cell reactivity in the form of cytokine release following *ex vivo* lipopolysaccharides (LPS) stimulation and anhedonia as well as reward anticipation in depression (Costi et al., 2021). This aligns with the existing literature on the relation between cytokine burden and symptom load (Rengasamy et al., 2021; Roohi et al., 2021; Sha et al., 2022), as well as with the beneficial effects of different anti-cytokine treatments for depressive symptoms in systemic inflammatory disorders (Köhler et al., 2014; Kappelmann et al., 2018; Wittenberg et al., 2020). This highlights the importance of immune mechanisms in psychiatric disorders and the need to improve our understanding of its complex interplay with depression genesis, clinical course, and symptom burden (Himmerich et al., 2019).

Among the different immune pathways potentially involved in depression genesis, purinergic signalling *via* the adenosine triphosphate (ATP) selective, membrane bound ionotropic P2X7 receptor (P2X7R) is considered a promising candidate (Di Virgilio et al., 2017; Deussing and Arzt, 2018; Drevets et al., 2022). Multiple studies have shown its involvement in stress-induced inflammation, depression, and depressive-like behaviours (von Mücke-Heim and Deussing, 2022; von Muecke-Heim et al., 2021). In the context of mood disorder genesis (Andrejew et al., 2020; Illes et al., 2020), both clinical and preclinical findings from mouse models emphasize the role of chronic psychosocial stress in causing ATP release in the central nervous system (CNS), leading to sterile inflammation *via* P2X7R-depedent purinergic pathways, which contribute to the development of depression (Franklin et al., 2018; Iwata et al., 2016; Ribeiro et al., 2019a; Velasquez and Rappaport, 2016; von Mücke-Heim and Deussing, 2022; Wohleb et al., 2016). On a functional level, binding of ATP or its synthetic agonist 2′(3′)-O-(4-benzoylbenzoyl)-ATP (BzATP) trigger rapid potassium efflux and sodium plus calcium influx, initiating proinflammatory intracellular pathways including, but not limited to, the NLR family pyrin domain containing 3 (NLRP3) inflammasome (Adinolfi et al., 2018). Downstream of these pathways, cells release proinflammatory cytokines like IL-1β, IL-6, and TNFα (Di Virgilio et al., 2017; Junger, 2011; von Muecke-Heim et al., 2021). Aptly, P2X7R is considered a major player in inflammation (Di Virgilio et al., 2017; Adinolfi et al., 2018). It is expressed on immune cells and is functionally particularly important for microglia and T cells (Junger, 2011; Jacobson and Müller, 2016; He et al., 2017; Burnstock, 2018; Rivas-Yáñez et al., 2020). In microglia and monocytes, P2X7R activation has differential effects on M1 and M2 states (de Torre-Minguela et al., 2016; Jiang et al., 2022). Still, it remains largely unknown which exact role the human P2X7R (hP2X7R) on microglia plays in regulating morphology and cytokine expression after P2X7R-targeted stimulation or inhibition.

The present study therefore aims to shed light on these mechanisms by use of primary microglia cultures of a humanized microglia-specific conditional knockout mouse line (hP2RX7-Cx3cr1) (Metzger et al., 2017). A cluster of pro- and anti-inflammatory cytokines along with microglial morphology were analysed at baseline as well as following both P2X7R agonistic and antagonistic stimuli. To the best of our knowledge, this is the first study to examine hP2X7R-expressing murine microglia beyond the well characterized IL-1β and TNFα release on a morphological as well as secretory level.

# 2 Materials and methods

## 2.1 Animals

Animals were housed in individually ventilated cages (Tecniplast, IVC Green Line-GM500) under standard laboratory conditions (21°C ± 2°C, 50% ± 5% humidity, 12:12 h light:dark cycle, lights on at 7:00 a.m.). Food and water were provided *ad libitum*. All experiments and protocols were performed in accordance with the European Communities' Council Directive 2010/63/EU and were approved by the committee for the Care and Use of Laboratory animals of the Government of Upper Bavaria, Germany.

Humanized mice expressing the human P2X7R (hP2X7R) instead of the murine variant had been established earlier ($P2rx7^{tm1.1(P2RX7)Jde}$). The humanized *P2rx7* allele is additionally equipped with *loxP* sites which allow for conditional disruption of hP2X7R expression (Metzger et al., 2017). Conditional knockout mice lacking hP2X7R in microglia were generated by breeding homozygous floxed hP2X7R mice ($hP2rx7^{P2RX7/P2RX7}$) to the microglia-specific tamoxifen-inducible driver line *Cx3cr1-CreERT2* ($Cx3cr1^{tm2.1(cre/ERT2)Litt}$; Parkhurst et al., 2013). Mice for primary cultures were obtained from breeding $hP2rx7^{P2RX7/P2RX7}$; $Cx3cr1^{+/+}$ females to $hP2rx7^{P2RX7/P2RX7}$; $Cx3cr1^{+/CreERT2}$ males. Control (CTRL; $hP2rx7^{P2RX7/P2RX7}$; $Cx3cr1^{+/+}$) and conditional knockout mice (KO; $hP2rx7^{P2RX7/P2RX7}$; $Cx3cr1^{+/CreERT2}$) were born in a 1:1 ratio. Genotyping was performed

by polymerase chain reaction (PCR) analysis of tail DNA using specific primers. *P2rx7:* hP2X7R-mIntron1-for 5′-AGA CTG TCA CCA GCA GCA GCT C-3′, hP2X7R-mIntron2-rev-a 5′-GCC AAG CAT TCT ACC AGT TGA-GC-3′, hP2X7R-hExon2 rev 5′-CAC GAA GAA AGA GTT CCC CTG C-3′, hP2X7R-KO-for 5′-GCA GTC TCT CTT TGC CTC GT-3′, hP2X7R-KO-rev 5′-CGT CGA CTG TCT TCT GGT CA-3′ (PCR products: wildtype = 417 bp; floxed = 298 bp; knockout = 222 bp). *Cx3cr1*: Cx3cr1-Cre-14278 5′-CTC CCC CTG AAC CTG AAA C-3′, Cx3Cr1-Cre-14277: 5′-CCC AGA CAC TCG TTG TCC TT-3′, Cx3Cr1-Cre-14276 5′-GTC TTC ACG TTC GGT CTG GT-3′ (PCR products: wildtype = 500 bp, Cre = 410 bp).

## 2.2 Primary microglia culture

Preparation of primary murine microglia cultures was performed as previously described (Lian et al., 2016). Standard T75 cell culture flasks (Sarstedt) were coated with 0.05 mg/mL poly-D-lysine (PDL, 70.000 mol wt, Sigma Aldrich) followed by three washing steps. Pups were decapitated at P1–P3 and the heads were immediately transferred to ice-cold dissection medium Dulbecco's Modified Eagle's Medium F-12 Nutrient Mixture (DMEM/F-12) with GlutaMax™ supplement (Gibco™, Sigma Aldrich) and 1% Penicillin/Streptomycin (P/S) (Fisher Scientific). Brains were extracted on a horizontal-laminar flow bench under sterile conditions. After the meninges, brainstem, cerebellum, and white matter were removed, the remaining cortical tissue was reduced to small pieces by use of microsurgical scissors, followed by glass Pasteur pipette dissociation. The suspension was centrifuged for 5 min at room temperature (RT) at 1,200 rpm. Supernatant was discarded and neuroglial cells were seeded in PDL coated flasks in dissection medium plus 10% heat-inactivated fetal bovine serum (Merck), 1% non-essential amino acids (Gibco™, Fisher Scientific), and 1% sodium pyruvate (Gibco™, Fisher Scientific). Individual neuroglia cultures were maintained for 14 days with two medium changes per week.

At day 15, microglia were extracted from neuroglia culture flasks by combined enzymatic and mechanic separation. In accordance with Saura et al. (2003) and Caldeira et al. (2014), flasks were first incubated for 30–60 min at 37°C with 0.25% Trypsin-EDTA (Gibco™, Fisher Scientific) diluted 1:2 with dissection medium (Saura et al., 2003; Caldeira et al., 2014). This mild trypsinization caused the detachment of a carpet-like layer of cells containing mainly astrocytes, leaving microglia attached to the flask bottom. In a second step and adapted from Woolf et al. (2021), pure 0.25% Trypsin-EDTA was added to the flask for 5 min (Woolf et al., 2021). In the meantime, flasks were shaken and tapped gently, resulting in an almost complete detachment of microglia. Trypsin-EDTA was then blocked by addition of serum-containing growth medium. Cells were centrifuged for 5 min at RT at 1,200 rpm and supernatant was discarded. Quantification of cells was performed by use of the Trypan Blue (Gibco™, Fisher Scientific) exclusion test using a Neubauer counting chamber. At least two 16-square quadrates were counted per flask (Strober, 2015). In the end, $5 \times 10^4$ cells were seeded per well in 0.5 mL growth medium in 24-well plates equipped with PDL-coated 5 mm cover slips.

Cre-mediated *hP2RX7* inactivation was induced by 4-hydroxytamoxifen (OH-TAM, Sigma Aldrich). OH-TAM was dissolved in methanol and added (final concentration 1 µM/well). OH-TAM treatment lasted 7 days and included two growth medium changes.

## 2.3 Treatments with LPS, BzATP, and selective P2X7R antagonists

To emulate different gene-environment interactions between microglial hP2X7R and molecular proxies pf psychosocial and pathogen-derived immune challenges, cell cultures wells were subjected to the following treatments at day 22 after the initial brain extraction: either 1) 30 min of 1 µM JNJ-47965567 (Sigma Aldrich), 2) 30 min of 10 µM A-804598 (Sigma Aldrich), 3) 60 min of 200 µM BzATP (Sigma Aldrich), or 4) priming for 24 h with 100 ng/mL LPS (Sigma Aldrich) plus 60 min of 200 µM BzATP. LPS and BzATP were dissolved in water and JNJ-47965567 along with A-804598 were solved in pure dimethyl sulfoxide (DMSO, Cell Signaling Technology). The added volume of all treatment substances per well was chosen as small as practically feasible (i.e., 0.49 µL of the JNJ-47965567 stock solution in 500 µL medium ≙ 0.1 %v/v; 3.2 µL of the A-804598 stock solution in 500 µL medium ≙ 0.6 %v/v) to avoid DMSO-related cytotoxicity. For each animal, two separate cell culture wells remained untreated as controls and were both used for analysis. Concentrations of stimulations and selective P2X7R antagonists were chosen based on previous studies to model a solitary stress-related (i.e., stimulation with BzATP) or double hit in the form of a bacterial plus stress-related stimulus (i.e., LPS + BzATP) *in vitro* (Bradley et al., 2011; de Torre-Minguela et al., 2016; He et al., 2017; He et al., 2021). In the end, cell culture supernatant was aliquoted in PE tubes and stored at −20°C for cytokine measurements. The two control wells per animal were pooled to minimize variability.

## 2.4 Cytokine measurements

To study the effects of different immunomodulatory stimuli on microglial hP2X7R-dependant cytokine release, the post-treatment cell culture supernatants were analyzed. The following cluster of pro- and anti-inflammatory cytokines was selected to, among other things, allow inferences for leucocytes, NK and T cells, and microglia with their proinflammatory M1 and anti-inflammatory M2 pole (Frade and Barde, 1998; Zhang and An, 2007; Zhu et al., 2010; Orihuela et al., 2016; Dubbelaar et al., 2018; Martinez-Sanchez et al., 2018; Himmerich et al., 2019; Jurga et al., 2020): TNFα, INF-γ, IL-1β, IL-2, IL-4, IL-6, IL-10, IL-12, IL-17/IL-17A, IL-27. To measure these factors *in vitro*, a custom-made high-sensitivity analyte kit for murine cytokines was purchased from R&D Systems (Luminex® Discovery Assay).

Before measurements were performed, the Luminex® 200 instrument (Invitrogen) was cleansed and calibrated according to its operating instructions. Sample preparation and measurements were performed strictly according to the kit manufacturer's specifications. In brief, the provided standards were reconstituted to establish two separate serial dilutions (i.e., 6 times 10 × dilution). Growth medium and calibrator

diluent were added to improve the signal-to-noise ration by correcting for fluorescent background noise caused by the different carrier substances. Samples were mixed 1:1 (=1: 2 dilution) with the calibrator diluent (75 µL each). Next, either 50 µL of samples and standard was transferred to the 96-well plate and 50 µL of fluorescent bead cocktail was added. The plate was covered with aluminum foil and incubated at RT on a horizontal shaker at 800 rpm for 2 h. Wells were cleansed 3x with wash buffer using a magnetic plate clipped to the 96-well plate bottom. Next, 50 µL of diluted biotin-antibody cocktail was added to each well and incubated in the dark at RT on a shaker at 800 rpm for 1 h. Wells were washed again 3x, followed by the addition of 50 µL of diluted Streptavidin-phycoerythrin and a 30 min incubation period at RT on a shaker at 800 rpm. Washing was performed another 3x and 100 µL of wash buffer was added to each well, followed by 2 min at RT on a shaker at 800 rpm. Finally, the 96-well plate was then transferred to the Luminex® 200 system and measurements were commenced. Doublet discriminator gates were set at 8,000 and 16,500, while reporter gain settings were left at default. For quality control, triplicate measurements were performed in two independent samples with different activation levels (i.e., LPS + BzATP in a Cre-negative sample; control sample of a Cre-positive animal). Results confirmed reliability of measures (Supplementary Figure S1). Standard curves were calculated by use of five parameters logistic regression and the provided six standards. Based on these, cytokine concentrations (pg/mL) were extracted and values were then doubled due to the 1: 2 dilution. Next, the background (i.e., mean cytokine concentration of the two untreated growth medium measurements) was subtracted. Since in some groups control wells yielded a concentration of 0 pg/mL, each treatment well's value was put into relation to the mean of the group's control wells (*x = individual value treatment/mean of group's control wells*). The controls contained the cell culture supernatant of the two control wells per animal in a 1:1 mixture.

## 2.5 Immunocytochemistry und fluorescence microscopy

Cover slips were fixed with 4% paraformaldehyde for 30 min, washed 3x with phosphate buffered saline (PBS) and then blocked with 5% normal goat serum (NGS, Thermo Fisher Scientific) in 0.2% Triton X-100 PBS for 30 min. Primary antibody incubation with rabbit anti-Iba1 (Synaptic Systems), rat anti-CD86 (Invitrogen), or mouse anti-cleaved-caspase 3 (Affinity) was performed over night with a 1:500 dilution under mild agitation at 4°C in the dark. The next morning, cover slips were washed 3x with PBS. Secondary antibody incubation was done using 1:500 goat anti-rabbit Alexa Fluor 488 (Invitrogen) or anti-rat Alexa Fluor 488 (Invitrogen) in 5% NGS in 0.2% Triton X-100 PBS at RT and under mild agitation in the dark for 2 h. Lastly, cover slips were washed thrice with PBS and mounted on standard glass slides with 20 µL of DAPI Fluoromount-G™ (Invitrogen).

Fluorescence images were acquired on an Olympus VS120 Slide Scanner. Per cover slip, two regions of interest (ROI, size: ~1 $mm^2$) were chosen at random in the DAPI channel to avoid bias based on microglia morphology to calculate cell numbers. The same ROIs were used for all image analyses and the respective statistics. Images were taken with a ×20 magnification, an exposure time of 515 ms (Iba-1/Alexa488 channel) and a Z-range of 18 µm (spacing: 6 µm, plane count: 3). Experimenters were blinded to genotype and treatments during image acquisition and analyses.

## 2.6 Image analysis: Cell numbers and microglia morphology

Images were analyzed using the Fiji software package (GNU General Public License, Release 2.9.0). Microglia number were calculated using a custom-designed macroinstruction (macro). Due to the purity of our cultures (Figure 1), a double discriminatory approach was unnecessary. Automated cell counting was therefore performed in the DAPI channel. The generated Fiji macro was validated, yielding no difference between the manual quantification of two blinded and independent experimenters and the automated macro results (Supplementary Figure S2).

Since microglia are highly reactive and dynamic cells, they respond to an array of stimuli by changes in their morphology. The latter can thus serve as a proxy of the underlying genetic, molecular, and functional changes as well as the environmental circumstances (Nimmerjahn et al., 2005; Dubbelaar et al., 2018; Fernández-Arjona et al., 2019; Jurga et al., 2020). Microglia morphology analysis was based both on morphotype categories and objective shape descriptors. Based on previous observations from our lab and in the style of a related study by He et al. (2021), microglia were classed by the respective experimenter according to three distinct morphotypes: 1) round or amoeboid (no processes), 2) polarized or rod-like (length-to-width ratio ≥ 3), and ramified (≥3 extensions/ramification). To obtain objective measures of cell shape, maximum intensity projections (MIP) containing both DAPI (blue) and Iba-1/Alexa488 (green) were generated and microglia were manually delineated. The following shape descriptors were extracted for each individual cell:

$$\textbf{Circularity} = 4\pi^{*}\left(\frac{Area}{Perimeter^{2}}\right) \quad \textbf{Aspect ratio} = \frac{Major\ axis}{Minar\ axis}$$

$$\textbf{Roundness} = 4^{*}\frac{Cell\ area}{(\pi^{*}major\ axis^{2})} \quad \textbf{Solidity} = \frac{Cell\ area}{Convex\ area}$$

Based on morphological assumptions (i.e., resting microglia have a small soma and many, thin, and long ramifications; activated microglia loose or reduce ramifications and their soma enlarges), we devised the following complexity index:

$$\textbf{Complexity index} = \frac{Perimeter}{Cell\ area}$$

For circularity and solidity, the interval of potential values is $x \in [0; 1]$. The interval for the aspect ratio and complexity index is $x \in [0; \infty]$. As an *in vitro* alternative to the often used skeletonization approach in immunohistochemistry (Morrison et al., 2017; Young and Morrison, 2018), we developed the aforementioned complexity index. It rests on the assumption, that microglia are closer to the *in vivo* resting state and that their shape complexity is higher, if the cell

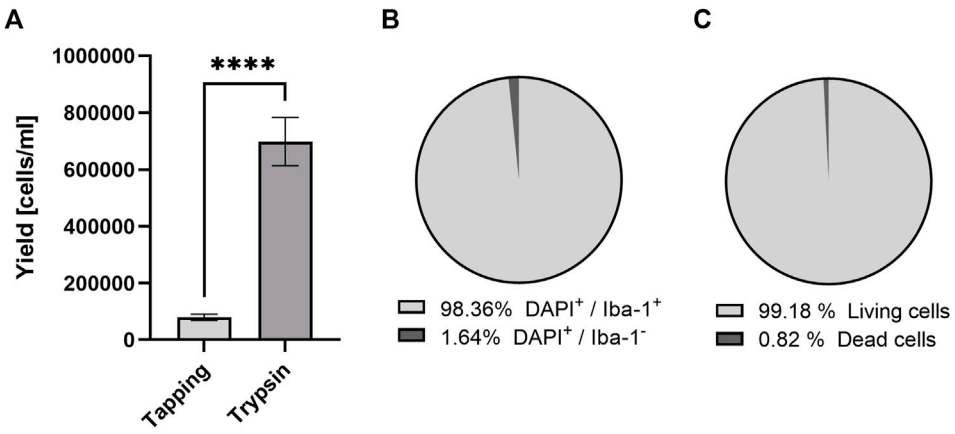


FIGURE 1
Purity and vitality of microglia based on two different isolation methods irrespective of genotype. Comparison of microglia yield from tapping and two-step mild trypsinization: **(A)** The total number of cells, **(B)** the proportion of microglia and **(C)** vital cells after 14 days of culturing after microglia enrichment. Data are expressed as mean ± S.E.M, T-test with Welch correction; tapping: $n$ = 33, mild trypsinization: $n$ = 25; $n$ = 10 ROIs.

perimeter is long and the surface area is comparatively small. This means, the higher the complexity index, the more complex the cell. Within this hypothesis frame, rod-like or polarized microglia are also labeled as more complex than round or ameboid cells. In addition to the shape descriptors and indices, the cell area and perimeter were extracted.

For qualitative intensity analyses, mean cellular gray values were extracted from Iba1+/DAPI+ cells (i.e., microglia) in the Iba1/GFP-channel of both ROIs.

## 2.7 Statistical analysis and Z scoring

Data are expressed as mean ± standard error of the mean (SEM) or percentage. Statistical analysis was performed using GraphPad Prism (Version 9.3.1). Statistical significance was defined as $p < 0.05$ and indexed as follows: $^{*}p < 0.05$, $^{**}p < 0.01$, $^{***}p < 0.001$, and $^{****}p < 0.0001$. Depending on the sample size and data structure, analyses were performed by a two-tailed T-test with Welch correction, a Chi$^2$ test, a one-Way ANOVA with Turkey's multiple comparisons test, or the Kruskall-Wallis test (KW) followed by Dunn's test for multiple comaprisons. To account for possible batch effects and experimental variability, cell numbers and shape descriptor data were put in relation to their two individual control wells [$x$ = *individual value treatment/mean of control wells* (n-fold) OR $x$ = *treatment value − mean of control wells* (delta)]. Morphological data were trimmed and outliers were calculated from raw values for each analysis type and excluded from group statistics if divergence was smaller than the first quartile ($Q_1$) − 1.7 * interquartile range (IQR) or larger than Q3 + 1.7 * IQR. During data collection and analysis, experimenters remained blinded.

To allow a comparison of cytokine clusters between groups, Z tests and scores were used as previously described (Guilloux et al., 2011; von Mücke-Heim et al., 2022):

$$\boldsymbol{Z\,test} = \frac{(X-\mu)}{\sigma} \quad \boldsymbol{Z\,score} = \frac{(Ztest1 + Ztest2 + Ztest3)}{Number\,of\,tests}$$

In brief, Z test calculations were performed for each cytokine and condition using hP2X7R KO sample values (X) and the CTRL groups mean (μ) and standard deviation (σ) of the same cytokine. Pro- and anti-inflammatory cytokine Z test results were then pooled in pro- and anti-inflammatory Z scores per animal and treatment condition.

To validate the cytokine Z score results, shape descriptor-based Z scores with similar directionality derived from roundness for pro-inflammatory and aspect ratio for anti-inflammatory clusters were added. As described above, hP2X7R KO sample values (X) and the CTRL groups mean (μ) and standard deviation (σ) of the respective shape descriptor were used to obtain shape descriptor Z scores. Lastly, the cytokine and shape descriptor Z scores were then summarized into a pro-inflammatory (ProIF) or anti-inflammatory (AntiIF) combined Z score per animal as follows:

$$\boldsymbol{ProIF\,Z\,score} = \frac{Z\,score\,(IL-1, IL-6, TNF) + Z\,score\,(roundness)}{2}$$

$$\boldsymbol{AntiIF\,Z\,score} = \frac{Z\,score\,(IL-4, IL-10) + Z\,score\,(aspect\,ratio)}{2}$$

# 3 Results

## 3.1 Mild trypsinization yields high-quality microglia cultures

We used the two-step mild trypsinization approach to isolate primary microglia (Saura et al., 2003; Woolf et al., 2021). In comparison to the shaking and tapping method (Lian et al., 2016), mild trypsinization yielded almost 9-fold more cells (Figure 1A). With the two-step trypsinization protocol we obtained cultures of high purity (≥98% of cells were microglia) and vitality (Figures 1B, C). Cultured microglia appeared healthy

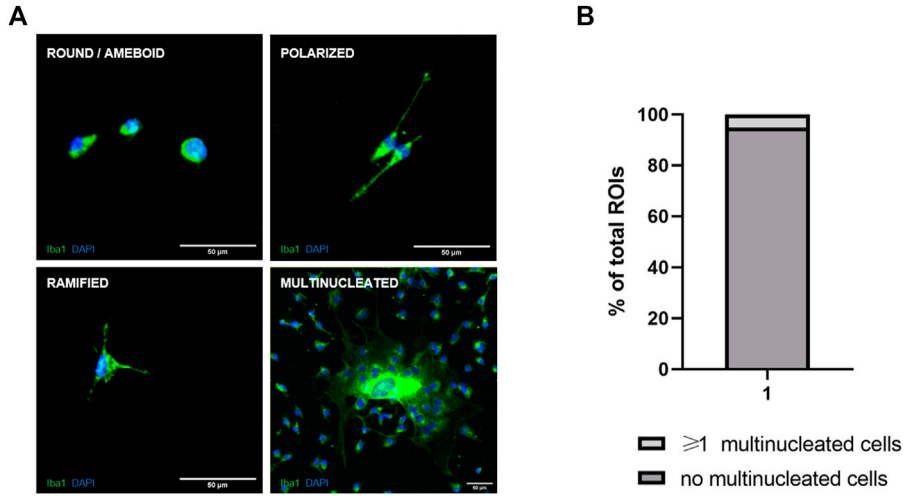


FIGURE 2
Morphotypes of microglia in primary cell cultures. **(A)** Representative images of the four main microglia morphotypes identified in primary cultures. **(B)** Percentage of ROIs with multinucleated Iba1-positive microglia in all samples irrespective of genotype.

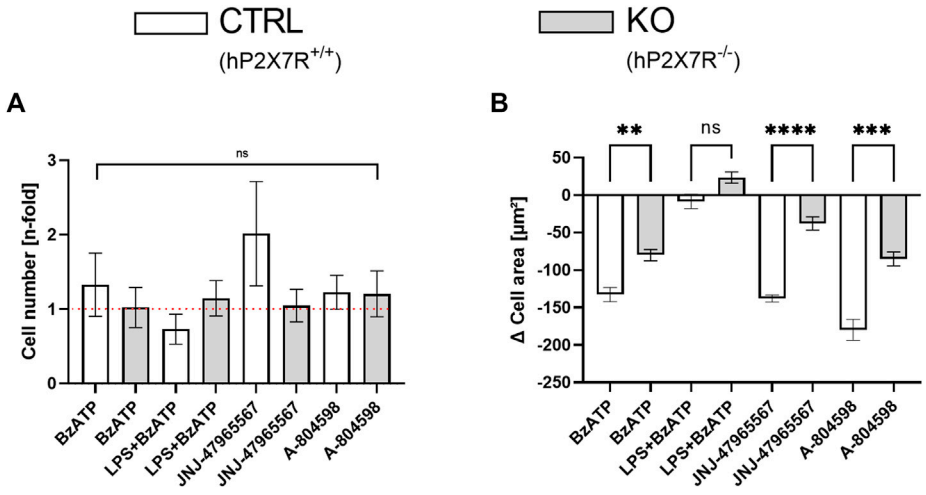


FIGURE 3
Cell count and area dynamics following hP2X7R-targeting treatments (i.e., BzATP, LPS + BzATP, JNJ-47965567, or A-804598). **(A)** Comparison of microglia cell number changes in relation to untreated genotype-matched control wells (visual red reference line: 1 = no difference) after treatment between CTRL and KO microglia. Cell counts were corrected per group by the respective untreated within-genotype controls. The hP2X7R-proficient group (CTRL) is displayed in white, the hP2X7R-knockout group (KO) is shown is grey. Data are expressed as mean + S.E.M, KW with Dunn's test, $n$ = 7–10 mice per group (A-804598 in hP2X7R wildtype animals $n$ = 4). **(B)** Between-genotype comparison of microglia cell area changes following pro- and anti-inflammatory treatments. Cell areas were corrected per group by the respective untreated within-genotype controls. The hP2X7R-proficient group (CTRL) is displayed in white, the hP2X7R-knockout group (KO) is shown is grey. Data are expressed as mean + S.E.M, KW with Dunn's test, $*p < 0.05$, $**p < 0.01$, $***p < 0.001$, and $****p < 0.0001$, $n$ = 8–11 mice with 813–1989 cells per group (except: A-804598 in CTRL group, $n$ = 5 mice and 654 cells).

and, as known from primary murine cultures with serum-containing medium, less ramified than in the *in vivo* situation. As previously described (He et al., 2021), we were also able to identify three distinct and different microglia morphotypes. In addition, we detected large and multinucleated cells (Figure 2A). However, since multinucleated cells were present only in about 5% of all ROIs, quantitative statistical analysis was not done (Figure 2B).

## 3.2 hP2X7R evokes changes of microglia numbers and morphology

At baseline, cell counts did not differ between microglial cultures isolated from hP2X7R proficient (CTRL) and P2X7R deficient (KO) animals, respectively (79 ± 61/µm² in CTRLs and 82 ± 57/µm²; $p > 0.05$ in T-test with Welch correction). Following stimulation with

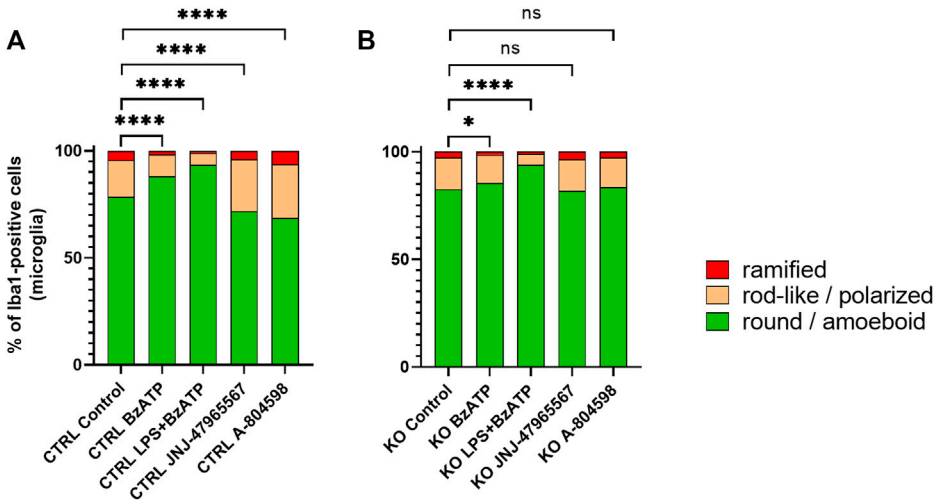


FIGURE 4
Manual morphotyping of microglial phenotype. Within-group comparison of **(A)** CTRL and **(B)** KO microglia morphology proportion changes between the baseline and after hP2X7R-targeting treatments (i.e., BzATP, LPS + BzATP, JNJ-47965567, A-804598). Data are expressed as % of total Iba1-positive cells per genotype and treatment condition including the untreated genotype controls. $Chi^2$ Test for the proportion of [round/ameboid] vs. [polarized + ramified microglia] between the CTRL or KO group's untreated control wells and the respective treatment conditions, $*p < 0.05$, $**p < 0.01$, $***p < 0.001$, and $****p < 0.0001$, $n$ = 8–11 mice with 952–3,428 cell per group (except: A-804598 in CTRL groups, $n$ = 5 mice and 933 cells).

BzATP, cell numbers increased by 33% in CTRL but not in KO cultures (Figure 3A). Whereas, the combined LPS + BzATP stimulation resulted in a 27% decline in CTRL and a minimal incline in KO cultures (Figure 3A). To uncover the reason for these observations, immunohistochemistry was performed: mean cellular intensity revealed higher values for cleaved caspase-3 and CD86 in LPS + BzATP treated CTRL compared to KO cultures (Supplementary Figure S3). This suggests more M1-polarization and apoptotic activity in double stimulated CTRL compared to KO cultures and a direct contribution of hP2X7R. The P2X7R antagonist-treated groups, on the other hand, showed higher cell counts in both genotypes. The difference was most prominent in JNJ-47965567-treated CTRL cells with a two-fold increment compared to controls. This increase, however, was mostly driven by one culture (5.3-fold gain), which also explains the high standard error in this group. Overall, changes in microglia numbers did not reach statistical significance (Figure 3A). The cell area, on the other hand, was significantly different in CTRL and KO animals in all treatment groups expect in the LPS + BzATP treated wells (Figures 3A, B). Mean indexed cell size decreased in the BzATP group as well as in the P2X7R antagonist conditions in both genotypes, but the extent of the decrease was more pronounced in CTRL cultures. This is interesting, since the absolute cell area mean was about 20% lower in CTRL microglia already at baseline (448 ± 210 μm$^2$ in CTRLs and 553 ± 243 μm$^2$).

Morphotyping revealed that most microglia were round or ameboid in all conditions and that polarized or ramified phenotypes were rare (at baseline % round/ameboid: CTRL = 78.6%, and KO = 82.6%) (Figures 4A, B). In both groups, stimulation with BzATP and even more stimulation with LPS + BzATP caused a significant increase of round or ameboid microglia and a subsequent decrease of the other two morphotypes. While the increase was similar for the LPS + BzATP condition in both groups, BzATP had a stronger effect in CTRL cells. Both P2X7R antagonists caused a significant reduction of round or ameboid microglia and a gain of polarized and ramified cells in CTRL cultures. Whereas, no relevant changes were found in this respect in the KO groups (Figures 4A, B).

At baseline, the mean cell perimeter was comparable in CTRL and KO microglia (100 ± 32 μm in CTRLs and 107 ± 37 μm in KOs). Shape descriptor analysis revealed a relative cell perimeter decrease in both genotype groups and in all conditions (Figure 5A). Based on the axiom that microglia activation generally leads to an overall reduction in ramification, this observation is in line with the trend found in the cell area analysis. However, is has to be noted, that the cell area and cell perimeter do not have a simple or linear relation, but very much depend on the experimental condition and the general microenvironment. In agreement with the trend seen in morphotyping, roundness and circularity increase in parallel following BzATP and LPS + BzATP, but decrease after JNJ-47965567 or A-804598 treatment in CTRL cultures. Similar yet less severe dynamics were found in KO cultures (Figures 5B, C). The reverse phenomenon was found with regard to the aspect ratio (Figure 5D). This is not surprising, since roundness and aspect ratio are mathematically related (roundness = 1/aspect ratio). While solidity increased in the CTRL BzATP and LPS + BzATP condition, it remained stable in the JNJ-47965567, and decreased in the A-804598 treated microglia. In KO cultures, on the other hand, the solidity increased in all conditions (Figure 5E). Lastly, the newly devised complexity index was attenuated in response to BzATP and LPS + BzATP in both groups. Surprisingly, the decremental effect of BzATP is decimal in CTRL compared to KO cultures. This difference is driven mainly by the data obtained from a single animal and well, respectively. If removed

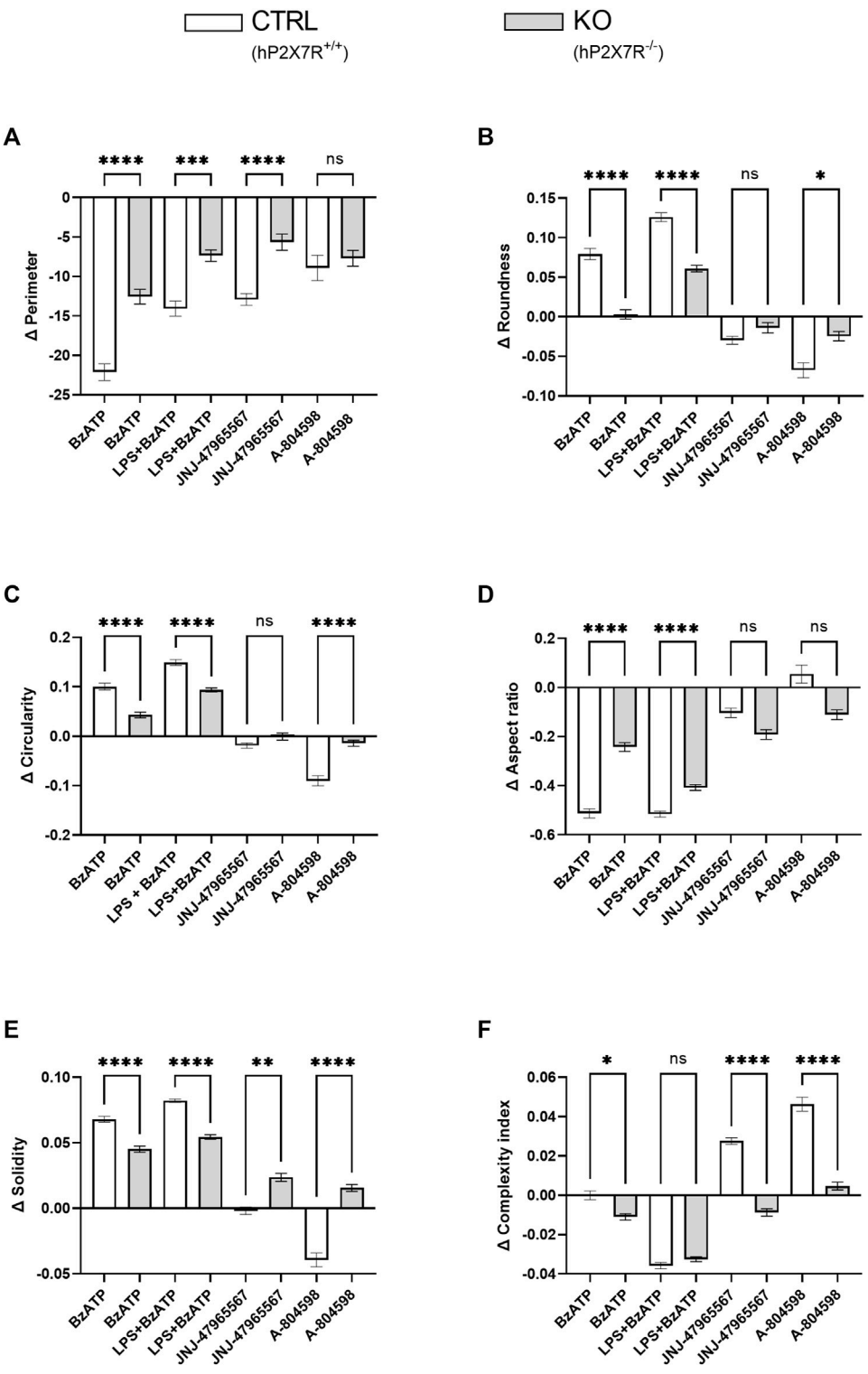


FIGURE 5
Microglia shape descriptors after hP2X7R-targeting treatments (i.e., BzATP, LPS + BzATP, JNJ-47965567, A-804598). Graphs show between-genotype and treatment comparisons of **(A)** cell perimeter, **(B,C)** roundness and circularity, **(D)** aspect ratio, **(E)** solidity, and **(F)** the complexity index. Shape descriptor values were corrected per group by the respective untreated within-genotype control well means. The hP2X7R-proficient group (CTRL) is displayed in white, the hP2X7R-knockout group (KO) is shown is grey. Data are expressed as mean + S.E.M, KW with Dunn's test, *$p < 0.05$, **$p < 0.01$, ***$p < 0.001$, and ****$p < 0.0001$, $n$ = 8–11 mice per group (except: A-804598 in CTRL group, $n$ = 5 mice). Cells per group (CTRL A-804598): perimeter = 831–2,131 (666); roundness = 815–2039 (645); circularity = 836–2,132 (666); aspect ratio = 785–1997 (616); solidity = 777–2072 (657); complexity = 800–2093 (651).

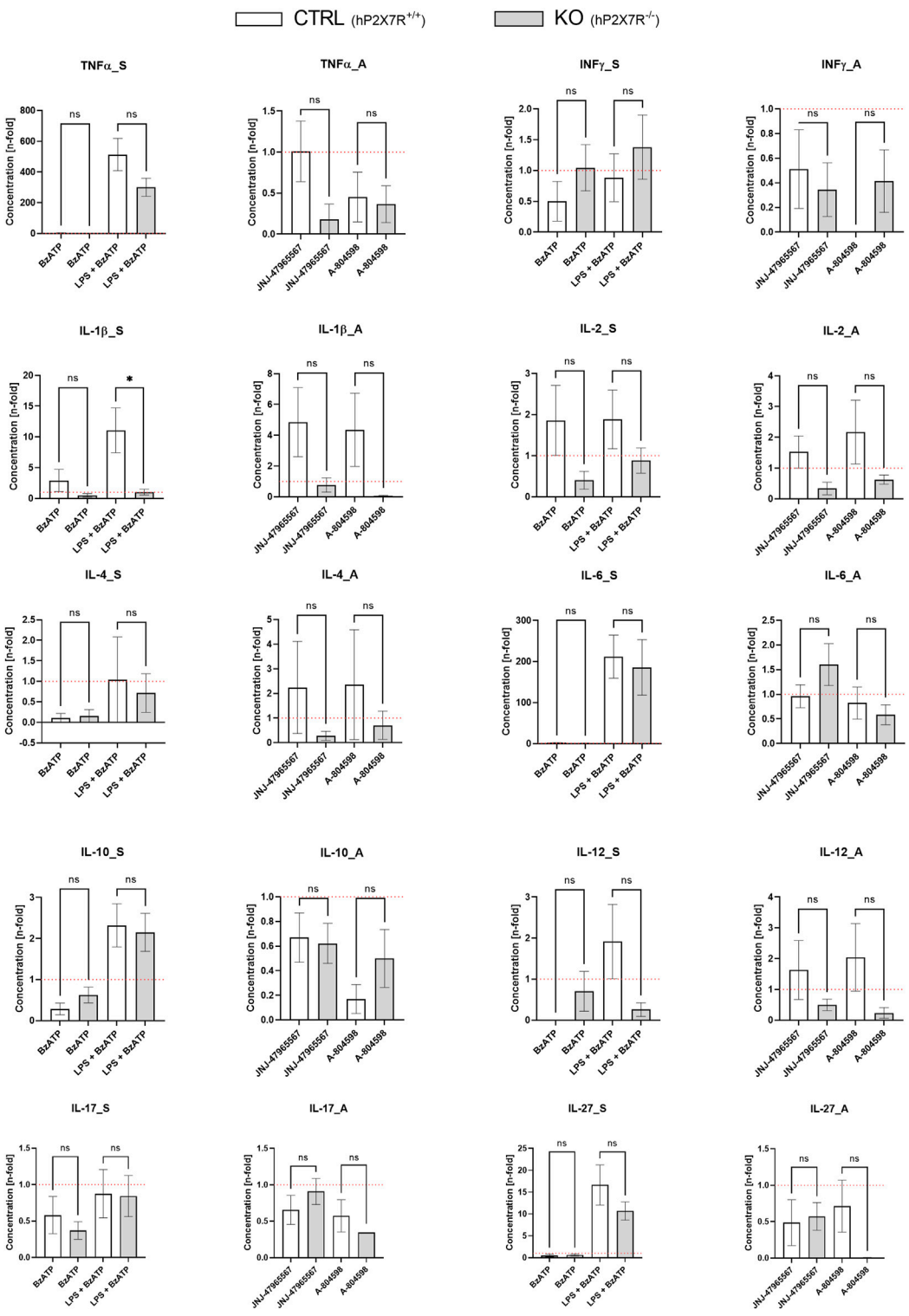


FIGURE 6
Cytokine secretion alterations following the different hP2X7R-targeting treatments (i.e., BzATP, LPS + BzATP, JNJ-47965567, A-804598). Graphs show the n-fold changes measured in cell culture supernatant of CTRL and KO microglia cultures side by side. For each of the ten cytokines (TNFα, INF-γ, IL-1β, IL-2, IL-4, IL-6, IL-10, IL-12, IL-17/IL-17A, IL-27), a stimulation (_S) and an antagonism (_A) graph is shown. All cytokine levels were first corrected by the untreated within-genotype control well means and n-fold changes were then calculated per group and treatment condition. The hP2X7R-proficient group (CTRL) is displayed in white the hP2X7R-knockout group (KO) is shown is grey. Comparisons were performed between the two genotypes for each of the treatments. Data are expressed as mean + S.E.M, T-test with Welch correction, *$p < 0.05$, **$p < 0.01$, ***$p < 0.001$, and ****$p < 0.0001$, $n$ = 5–7 mice per group.

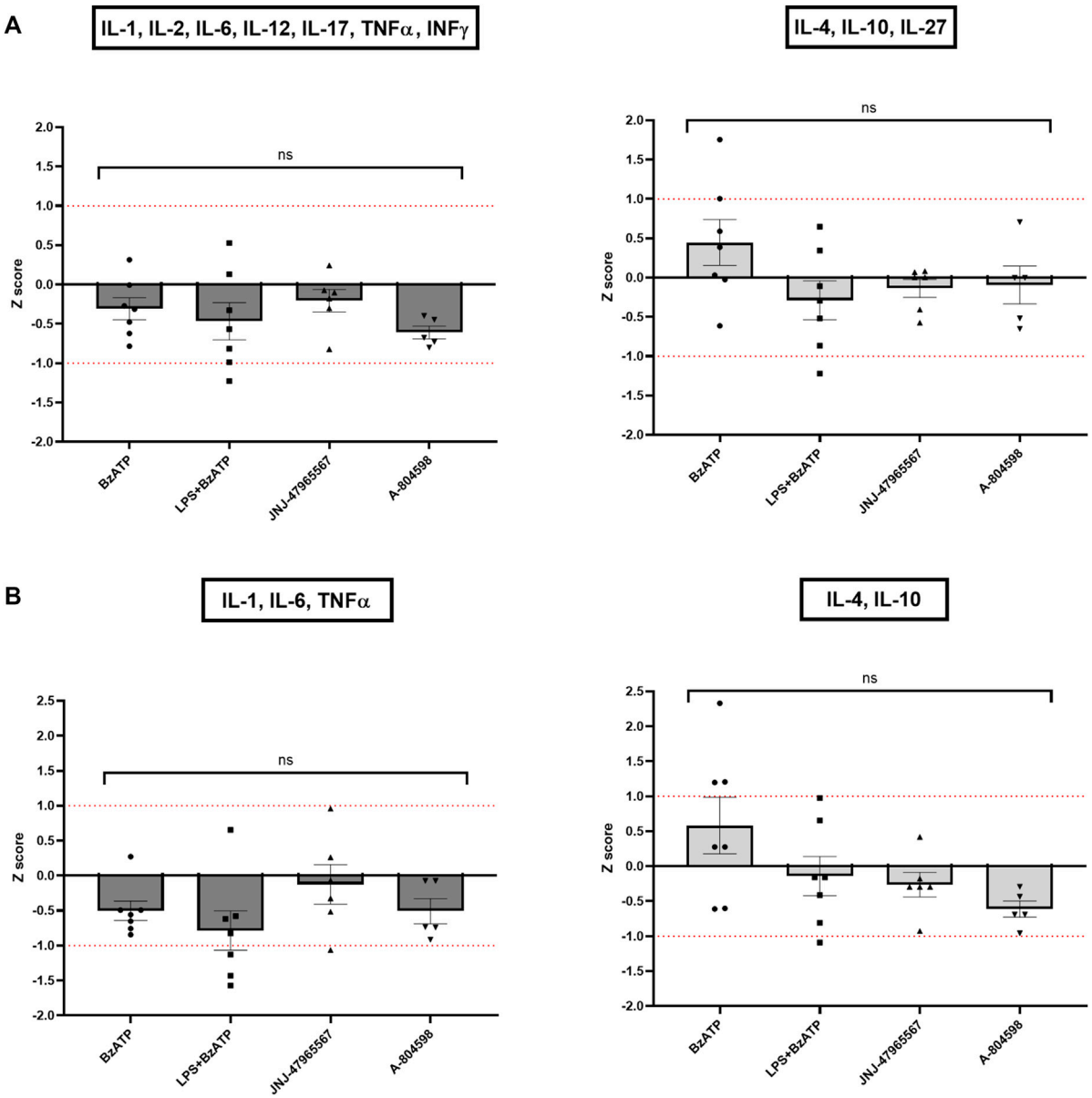


FIGURE 7
Z scores of pro- and anti-inflammatory cytokine clusters. Pro-inflammatory Z scores are coloured in dark grey, anti-inflammatory ones in light grey. **(A)** Z scores of all pro- or anti-inflammatory cytokines per KO animal and treatment condition in relation to the CTRL sample. **(B)** Z scores of only the core pro- or anti-inflammatory cytokines per KO well and treatment condition in relation to the CTRL sample. Data are expressed as mean + S.E.M, one-way ANOVA with Turkey's multiple comparisons test, *$p < 0.05$, **$p < 0.01$, ***$p < 0.001$, and ****$p < 0.0001$, $n = 5–7$ mice per group.

from the analysis, no difference can be found in the BzATP condition between CTRL and KO cultures. In the P2X7R antagonist treatment, complexity increases in CTRL but not in KO cultures (Figure 5F). In line with the between-genotype findings, within-genotype comparison confirmed hP2X7R-dependent dynamics (Supplementary Figure S4).

## 3.3 Cytokine levels are altered by hP2X7R-tageted stimulation and inhibition

To study the effects of different immunomodulatory stimuli on microglial hP2X7R-dependant cytokine release, we measured ten cytokines (TNFα, INF-γ, IL-1β, IL-2, IL-4, IL-6, IL-10, IL-12, IL-17/IL-17A, IL-27) in cell culture supernatant using the Luminex® technology (Figure 6). At baseline, cytokine levels between CTRL and KO cultures did not differ significantly. Following stimulation with BzATP, a minor and not statistically significant increase of IL-1β levels was seen in CTRL but not in KO cultures. BzATP also caused a decrease of IL-4 levels (9-fold decrease in CTRL; 6-fold in KO cultures). Changes, however, did not reach statistical significance. After 24 h of priming with 100 ng/mL LPS and 1 h of BzATP, considerable n-fold changes in cytokine levels were detected in both groups for TNFα, IL-6, and IL-27. In this respect, CTRL cultures showed consistently higher levels than KO cultures. The L-1β level increase was significantly different

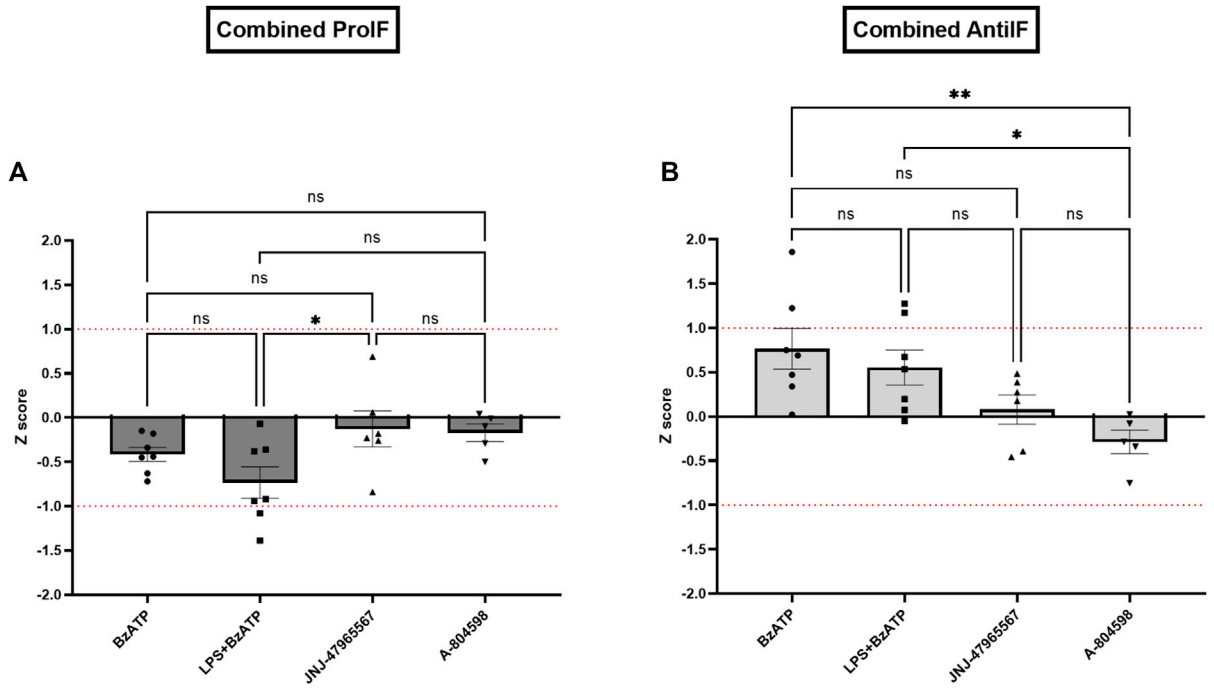


FIGURE 8
Combined Z scores of **(A)** three core pro-inflammatory cytokines IL-1β, IL-6, and TNFα and microglial roundness (displayed in dark grey) and **(B)** of two core anti-inflammatory cytokines IL-4 and IL-10 and the aspect ratio of microglia per KO animal and treatment condition in relation to the CTRL sample. Data are expressed as mean + S.E.M, one-way ANOVA with Turkey's multiple comparisons test, *$p < 0.05$, **$p < 0.01$, ***$p < 0.001$, and ****$p < 0.0001$, $n$ = 5–7 mice per group.

between CTRL and KO cultures ($p < 0.05$). In the P2X7R antagonist conditions, on the other hand, no statistically significant differences were found. Still, a slight trend was observed: in both genotypes treated with either one of the two P2X7R antagonists, the levels of TNFα, INF-γ, and partially IL-6—all highly proinflammatory cytokines–were found to have a mean coefficient of ≤ 1. This equals a drop below within-genotype untreated control well levels, which indicates anti-inflammatory properties of the inhibitors and khP2X7R knockout. Aptly, antagonist application increased IL-4 quantity in CTRL but not KO cultures by 2-fold.

In line with the single cytokine results comparing genotypes and treatments, Z score calculations referring to all (Figure 7A) or core (Figure 7B) proinflammatory and anti-inflammatory cytokines confirmed the differences between CTRL and KO cultures: except for the BzATP condition in the anti-inflammatory Z scores, hP2X7R-targeted stimulation led to a weaker increase of pro-inflammatory cytokine cluster in KO compared to CTRL microglia, while hP2X7R-targeting inhibition led to a stronger decrease of the same cytokines in KO compared to CTRL microglia. A corresponding trend was found for the anti-inflammatory Z scores. In the BzATP condition, however, the drop of anti-inflammatory cytokines IL-4, Il-10 ± IL-27 was overall half a standard deviation less in KO compared to CTRL cultures (Figures 7A, B—right). Though not statistically significant, this corroborates the stronger anti-inflammatory mechanisms and pathways in the absence of a functional hP2X7R. The augmented cytokine and shape descriptor Z scores confirmed these observations (Figure 8). For the combined ProIF Z score, a statistically significant difference between KO and CTRLs was found for comparing LPS + BzATP with the JNJ-47965567 condition ($p < 0.05$) (Figure 8A). Similarly, the AntiIF combined Z scores revealed a significant difference for the comparison of the BzATP and LPS + BzATP treatment with the A-804598 condition ($p < 0.01$ and $< 0.05$, respectively) (Figure 8B). These findings demonstrate the importance of hP2X7R in mediating the effects of both sterile (BzATP) and pathogen plus sterile (LPS + BzATP) stress. The synopsis of the single cytokines and related Z scores with the results of the combined ProIF and AntiIF Z scoring (Figures 6–8) confirms the modulatory role of microglial hP2X7R on a secretory, morphological, and combined level in the context of different immunomodulatory stimuli.

Lastly and on a more general note, measurements revealed low absolute cytokine concentrations in cell culture supernatants with no significant differences between CTRL and KO cultures at baseline (Supplementary Figure S5).

## 4 Discussion

To further characterize the role of microglial hP2X7R signaling in mediating the cellular and humoral response following stimulation or selective P2X7R antagonism, we have used fluorescence-based single cell morphotyping as well as cytokine measurements in primary murine microglia cultures. The novelty of our approach lies in the use of a genetically engineered mouse model possessing a humanized P2X7R together with detailed

morphological analyses and measurements of so far unchartered cytokines. This combinatory method allowed us to generate meaningful and new insight into hP2X7R properties and the consequences of its absence in different treatment conditions, which is vital for further *in vivo* and clinical studies. We were able to demonstrate that hP2X7R influences microglia morphology as well as cell count, area, perimeter, roundness, circularity, aspect ratio, solidity, and complexity following stimulation as well as selective antagonism. Cytokine quantification confirmed the effects of hP2X7R, primarily following stimulation *via* LPS and/or BzATP, in the form of TNFα, IL-1β, IL-6, and IL-27 level increase and IL-4 level decrease. To the best of our knowledge, this is the first detailed *in vitro* characterization of both morphological and cytokine changes in hP2X7R-expressing microglia after selective immune stimulation or inhibition.

In contrast to the *in vivo* situation (Kozlowski and Weimer, 2012; Leyh et al., 2021), we found microglial cell area to be increased in both genotypes. In addition, KO microglia were about 25% larger than WT cells at baseline. The mean microglial cell perimeter was, however, relatively low compared to the *in vivo* situation. Our findings are, though somewhat different from the *in vivo* condition, in line with previous publications evaluating microglial morphology in primary murine cell cultures (Caldeira et al., 2014). The observed combination of an increased cell area and a small perimeter together with the high proportion of round or ameboid microglia at baseline indicate that our *in vitro* microglia are somewhat activated compared to resting *in vivo* cells. Whether the observed morphological observation is exclusively indicative of a rather proinflammatory M1 polarization remains unclear. It has been shown that, compared to naive cells, a higher cell area is associated with a more M2-like phenotype, while a smaller cell area is commonly found in M1 polarized macrophages (Rostam et al., 2017). Whether this observation also transfers to murine microglia, especially in the *in vitro* situation, is not known. The classical ameboid morphology of microglia is however, at least *in vivo*, associated with an increased phagocytotic capacity, proinflammatory cytokine release, and therefore M1 polarization (Tam and Ma, 2014). Aptly, immunohistochemistry-based machine learning approaches have shown that ameboid microglia (i.e., activated morphotype) are associated with a small cell area and perimeter as well as an increased solidity in the murine cortex and hippocampus (Leyh et al., 2021). Since the employed procedure of microglia isolation from neonatal mice as well as the *in vitro* culturing is unphysiological and thus a strong contextual stimulus, observing morphologically activated microglia (i.e., round or ameboid) is not surprising and must be considered an inherent methodological drawback of primary cell cultures, especially in serum-containing growth medium (Montilla et al., 2020). In line with this argument and similar to our findings, previous studies that have made use of serum-containing medium have shown that microglia lose the majority of their ramifications *in vitro* (Caldeira et al., 2014; He et al., 2017; He et al., 2021; Hu et al., 2022). This phenomenon of "deramification" can be partially prevented with a serum-free growth medium, which contains TGF-β2, cholesterol, and macrophage colony-stimulating factor (TIC factors) to sustain microglia survival (Bohlen et al., 2017; Montilla et al., 2020). Some scholar have even argued that TIC medium is closer to the *in vivo* and thus physiological condition (i.e., the cerebrospinal fluid), since it contains only low protein and bioactive factor levels (Montilla et al., 2020). In opposition to this argument we reason, that both the serum-containing as well as TIC medium have inherent advantages and drawbacks. For instance, while serum-containing growth medium sustains and simultaneously activates cultured microglia, the serum-free TIC medium of Bohlen et al. (2017) artificially antagonizes the effects of the isolation procedure and culturing condition by forcing cells back into a more ramified and less activated state using TGF-β2. This TIC environment might bias experiments on inflammatory properties of microglia. Both methods are thus, by definition, non-physiological conditions and therefore skew observations in one or the other way (Montilla et al., 2020). However, if factoring in the methodological drawbacks into the experimental framework and data interpretation, both approaches can yield meaningful results. Since our primary study objective was to characterize the inflammatory effects of microglial hP2X7R under different conditions *in vitro*, an anti-inflammatory environment in the form of the TIC growth medium was deemed unsuitable. This decision was further corroborated by findings from *in vitro* experiments with serum-containing medium, which have shown that method-related inflammation drops significantly after 10 days *in vitro* (Caldeira et al., 2014).

As to be expected from prior studies, our morphotyping and shape descriptor analysis revealed that most microglia were rather large and round with little to no ramifications in both genotypes and all conditions. Irrespective of this clearly shifted morphological baseline, we were able to identify a distinct and, compared to CTRL cells, hP2X7R-potentiated increase in morphological and secretory activation towards a more M1 polarized phenotype (i.e., increase in round or ameboid cells, decrease in area and perimeter, increase in roundness/circularity and a decrease in aspect ratio, increase in solidity, reduction of complexity, increase of CD86 intensity in the LPS + BzATP condition, inflammatory cytokine release including IL-1β). This agrees with findings from earlier studies, which have found IL-1 β expression to be associated with a proinflammatory morphotype including a decrease in cell area and perimeter as well as an increase in circularity (Fernández-Arjona et al., 2019). Our findings further agree with the triangle TNFα, IL-1β, and IL-6, which is the typical secretory cluster seen in M1 polarization (Orihuela et al., 2016). This becomes even more evident when considering the cytokine dynamics beyond TNFα, IL-1β, and IL-6, namely, the decrease of the anti-inflammatory IL-4 and IL-10 following BzATP in both genotype groups as well as the increase following antagonist application in CTRL cells. IL-4 has a strong anti-inflammatory effect on microglia, triggers M2 polarization, and promotes neuronal stem cell survival and proliferation (Zuiderwijk-Sick et al., 2021; Jiang et al., 2022). This combination of P2X7R amplified humoral inflammation and morphological activation and, vice versa, P2X7R inhibition induced anti-inflammatory cytokine secretion and a trend towards a resting morphotype emphasizes the role of hP2X7R in inflammation regulation. This is highly important, since P2X7R has been hypothesized to mediate psychosocial stress induced neuroinflammation and ultimately depression and depressive-like behaviours, respectively (von Mücke-Heim and Deussing, 2022; von Muecke-Heim et al., 2021). Accordingly, clinical trials have demonstrated the effect of gain-of-function single nucleotide

polymorphisms (SNPs) on depression (Andrejew et al., 2020; Ribeiro et al., 2019a; Urbina-Treviño et al., 2022; von Mücke-Heim and Deussing, 2022), which fits the hypothesis of an increased immune activation along with defective inflammation resolution mechanisms in depression (Debnath et al., 2021). Our cytokine findings are furthermore in line with the well-known connection between toll-like receptor mediated LPS effects in pro-IL-1β production and P2X7R induced caspase-1 activation in amplifying mature IL-1β release (Ferrari et al., 2006; Mingam et al., 2008). Also, the shift towards ameboid morphology and elevated cytokines TNFα, IL-1β, IL-6 were found in related studies using LPS + BzATP (de Torre-Minguela et al., 2016; He et al., 2021). These findings are also conceptually in agreement with studies using BzATP and LPS as well as P2X7R antagonists *in vivo* and *in vitro* (Andrejew et al., 2020; Ribeiro et al., 2019a; Ribeiro et al., 2019b; von Muecke-Heim et al., 2021). Accordingly, and beyond these well-known proinflammatory effects, we were able to identify an increase of complex phenotypes (i.e., polarized and ramified microglia, reduction in roundness and circularity and solidity, increased complexity) as well as a tendential decrease in inflammatory cytokines after JNJ-4796556 and A-804598 application. Cluster findings in the form of cytokine and combined cytokine-morphology Z score analyses confirmed the findings from morphotyping, shape descriptor extraction, and single cytokine comparison. With regard to the observed microglia area and perimeter dynamics in CTRL microglia, we argue that stimulation caused the cells to be activated and to polarize towards a small and ameboid morphotype, while P2X7R antagonism resulted in a similar yet less pronounced trend without the increase of round or ameboid cells. Based on the evidence presented above and considering the shifted baseline and morphotyping results, respectively, the cell area and perimeter decrease in stimulation conditions likely equals a trend towards M1-like activation, while the P2X7R antagonism resembles a trend towards polarized or rod-like cells and thus more M2-like microglia. This aligns with findings from prior studies, which have shown that M2 microglia exhibit an elongated morphology (i.e., rod-like/polarized morphology) and even express typical M2 surface markers accompanied by a reduced secretion of inflammatory cytokines when forced in a polarized shape (McWhorter et al., 2013). And even though the concept of M1 and M2 polarization has been criticized for being a too simplistic approach towards microglia phenotypes (Ransohoff, 2016), it provides a useful framework of activation with two maxima. The latter is a helpful tool to dissect inflammation in an experimental setting (Orihuela et al., 2016; Jurga et al., 2020). Keeping this and all the observed morphological and secretory phenomena in mind, our data demonstrate the effect of hP2X7R on microglia on the continuum between ramified or resting, rod-like or polarized, and round or ameboid microglia (Tam and Ma, 2014; Jurga et al., 2020). It has, however, also been demonstrated that P2X7R is part of inflammation resolution *via* pathways other than NLRP3 and NFκB signaling in resting and M2 macrophages (de Torre-Minguela et al., 2016). This highlights the complexity of interpreting P2X7R-related dynamics in cell culture as well as in specific diseases and inflammatory stages (von Mücke-Heim and Deussing, 2022), which also relates to our findings. However, though we consider our findings overall conclusive, especially taking into account the detailed morphological analyses, our cytokine data have limitations with regards to the sample size and the multiplex analyte kit used for cytokine measurements. Therefore, we would suggest future studies to increase the sample size and to employ high-sensitivity ELISA-based assays for quantification of cytokines combined with intracellular pathway analyses (e.g., NFκB or PPAR δ) to best determine the role of hP2X7R in M1 and M2 polarization (Wang et al., 2014). Though it is established that antigen-presenting cells including microglia secret IL-27 (Kawanokuchi et al., 2013), this is, to the best of our knowledge, the first report of hP2X7R changed IL-27 secretion in the context of microglia and hP2X7R. Though IL-27 was initially classed as proinflammatory by promoting TNFα release and its relation with IL-6 signaling (Yoshida and Hunter, 2015), novel evidence has highlighted its function as a negative regulator of Th1, Th2, Th9, and Th17 function (Kawanokuchi et al., 2013; Yoshida and Hunter, 2015). Novel results even indicate a role of IL-27 in increasing $T_{reg}$ function (Yoshida and Hunter, 2015; Le et al., 2020), which suggests a role of IL-27 in inflammation resolution (Yoshida and Hunter, 2015; Lalive et al., 2017). This function of IL-27 is highly interesting in the context of the emerging evidence on immunometabolic subtypes and related phenomena in depression (Milaneschi et al., 2020; von Mücke-Heim and Deussing, 2022). Several studies have demonstrated altered T cell function in depression, particularly an increase in Th17 and a decrease in $T_{reg}$ cells (Miller, 2010; Suzuki et al., 2017; Ellul et al., 2018; Moschny et al., 2020). Surprisingly, IL-27 has not been extensively investigated in depression and does therefore not surface in large metanalyses on cytokine alterations in depression (Osimo et al., 2020). Ultimately, our findings underline the complex functions of microglial hP2X7R in inflammation downstream of sterile and combined immune stimuli and single out the potential connection between microglial hP2X7R and IL-27. The relevance of our findings remains to be determined. Thus, further trials are needed to investigate this potential role of P2X7R in altering microglia-derived IL-27 secretion patterns. The latter might be particularly relevant in the context of inflammation resolution of mood disorders like depression *via* treatments like electroconvulsive therapy, which is known to a cause short-term spike yet long-term attenuation of systemic and CNS inflammation (van Buel et al., 2015a; van Buel et al., 2015b; van Buel et al., 2017).

Taken together, we have demonstrated that microglial hP2X7R causes and potentiates morphological and secretory changes downstream of targeted immune stimulation as well as inhibition. In the future, additional *in vitro* and *in vivo* studies are necessary to further clarify the contribution of P2X7R-related purinergic signaling to mood disorder genesis and therapy. These studies should focus on immune changes downstream of differential gene-environment interactions (i.e., hP2X7R expression and function x psychosocial and/or pathogen-derived stressors), since the corresponding patterns, which are currently largely unchartered, likely contribute to state- and subtype-specific mood disorder immune pathology.

## Data availability statement

The original contributions presented in the study are included in the article/Supplementary Material, further inquiries can be directed to the corresponding author.

## Ethics statement

The animal study was reviewed and approved by Committee for the Care and Use of Laboratory animals of the Government of Upper Bavaria, Germany.

## Author contributions

I-AM-H designed the experiments, performed experiments, developed the used Fiji macro, conducted statistical analysis and data extraction, drafted figures, and wrote the manuscript. JM planned a subset of experiments, performed experiments, conducted statistical analysis, drafted figures, and subedited the manuscript. MU aided the planning of a subset of experiments and assisted in cytokine measurements, contributed statistical expertise and analysis improvement, and reviewed the manuscript. CR aided methodological expertise, data acquisition, and quality control, co-wrote the Fiji macro and subedited the manuscript. JD supervised all experiments and analyses, edited the manuscript and provided scientific advice, guidance, and support. All authors approved the submitted manuscript.

## Funding

I-AM-H receives funding from the Else Kroener-Fresenius Foundation. I-AM-H and CR receive funding from the International Max Planck Research School for Translational Psychiatry. CR receives a sponsorship from the Gunter Sachs Donation. JD receives funding from the German Federal Ministry of Education and Research (IMADAPT, FKZ: 01KU1901) and from the Marie Skłodowska-Curie innovative training network PurinesDX.

## Acknowledgments

We thank Stefanie Unkmeir and Sabrina Bauer for their assistance with genotyping and Annette Schubert for her help with the cytokine measurements.

## Conflict of interest

The authors declare that the research was conducted in the absence of any commercial or financial relationships that could be construed as a potential conflict of interest.

## Publisher's note



## Supplementary material

The Supplementary Material for this article can be found online at: https://www.frontiersin.org/articles/10.3389/fphar.2023.1148190/full#supplementary-material

## References

Adinolfi, E., Giuliani, A. L., De Marchi, E., Pegoraro, A., Orioli, E., and Di Virgilio, F. (2018). The P2X7 receptor: A main player in inflammation. *Biochem. Pharmacol.* 151, 234–244. doi:10.1016/j.bcp.2017.12.021

Andrejew, R., Oliveira-Giacomelli, Á., Ribeiro, D. E., Glaser, T., Arnaud-Sampaio, V. F., Lameu, C., et al. (2020). The P2X7 receptor: Central hub of brain diseases. *Front. Mol. Neurosci.* 13, 124. doi:10.3389/fnmol.2020.00124

Bauer, M. E., and Teixeira, A. L. (2021). Neuroinflammation in mood disorders: Role of regulatory immune cells. *Neuroimmunomodulation* 28 (3), 99–107. doi:10.1159/000515594

Beurel, E., Toups, M., and Nemeroff, C. B. (2020). The bidirectional relationship of depression and inflammation: Double trouble. *Neuron* 107 (2), 234–256. doi:10.1016/j.neuron.2020.06.002

Bohlen, C. J., Bennett, F. C., Tucker, A. F., Collins, H. Y., Mulinyawe, S. B., and Barres, B. A. (2017). Diverse requirements for microglial survival, specification, and function revealed by defined-medium cultures. *Neuron* 94 (4), 759–773.e8. doi:10.1016/j.neuron.2017.04.043

Bradley, H. J., Browne, L. E., Yang, W., and Jiang, L. H. (2011). Pharmacological properties of the rhesus macaque monkey P2X7 receptor. *Br. J. Pharmacol.* 164 (2), 743–754. doi:10.1111/j.1476-5381.2011.01399.x

Burnstock, G. (2018). Purine and purinergic receptors. *Brain Neurosci. Adv.* 2, 2398212818817494. doi:10.1177/2398212818817494

Caldeira, C., Oliveira, A. F., Cunha, C., Vaz, A. R., Falcão, A. S., Fernandes, A., et al. (2014). Microglia change from a reactive to an age-like phenotype with the time in culture. *Front. Cell. Neurosci.* 8, 152. doi:10.3389/fncel.2014.00152

Cattaneo, A., Ferrari, C., Turner, L., Mariani, N., Enache, D., Hastings, C., et al. (2020). Whole-blood expression of inflammasome- and glucocorticoid-related mRNAs correctly separates treatment-resistant depressed patients from drug-free and responsive patients in the BIODEP study. *Transl. Psychiatry* 10 (1), 232. doi:10.1038/s41398-020-00874-7

Costi, S., Morris, L. S., Collins, A., Fernandez, N. F., Patel, M., Xie, H., et al. (2021). Peripheral immune cell reactivity and neural response to reward in patients with depression and anhedonia. *Transl. Psychiatry* 11 (1), 565. doi:10.1038/s41398-021-01668-1

de Kluiver, H., Jansen, R., Milaneschi, Y., and Penninx, B. W. J. H. (2019). Involvement of inflammatory gene expression pathways in depressed patients with hyperphagia. *Transl. Psychiatry* 9 (1), 193. doi:10.1038/s41398-019-0528-0

de Torre-Minguela, C., Barberà-Cremades, M., Gómez, A. I., Martín-Sánchez, F., and Pelegrín, P. (2016). Macrophage activation and polarization modify P2X7 receptor secretome influencing the inflammatory process. *Sci. Rep.* 6 (1), 22586. doi:10.1038/srep22586

Debnath, M., Berk, M., and Maes, M. (2021). Translational evidence for the inflammatory response system (IRS)/Compensatory immune response system (CIRS) and neuroprogression theory of major depression. *Prog. Neuropsychopharmacol. Biol. Psychiatry* 111, 110343. doi:10.1016/j.pnpbp.2021.110343

Deussing, J. M., and Arzt, E. (2018). P2X7 receptor: A potential therapeutic target for depression? *Trends Mol. Med.* 24 (9), 736–747. doi:10.1016/j.molmed.2018.07.005

Di Virgilio, F., Dal Ben, D., Sarti, A. C., Giuliani, A. L., and Falzoni, S. (2017). The P2X7 receptor in infection and inflammation. *Immunity* 47 (1), 15–31. doi:10.1016/j.immuni.2017.06.020

Drevets, W. C., Wittenberg, G. M., Bullmore, E. T., and Manji, H. K. (2022). Immune targets for therapeutic development in depression: Towards precision medicine. *Nat. Rev. Drug Discov.* 21 (3), 224–244. doi:10.1038/s41573-021-00368-1

Dubbelaar, M. L., Kracht, L., Eggen, B. J. L., and Boddeke, E. W. G. M. (2018). The kaleidoscope of microglial phenotypes. *Front. Immunol.* 9, 1753. doi:10.3389/fimmu.2018.01753

Ellul, P., Mariotti-Ferrandiz, E., Leboyer, M., and Klatzmann, D. (2018). Regulatory T cells as supporters of psychoimmune resilience: Toward immunotherapy of major depressive disorder. *Front. neurology* 9, 167. doi:10.3389/fneur.2018.00167

Felger, J. C., and Lotrich, F. E. (2013). Inflammatory cytokines in depression: Neurobiological mechanisms and therapeutic implications. *Neuroscience* 246, 199–229. doi:10.1016/j.neuroscience.2013.04.060

Fernández-Arjona, M. d. M., Grondona, J. M., Fernández-Llebrez, P., and López-Ávalos, M. D. (2019). Microglial morphometric parameters correlate with the expression level of IL-1β, and allow identifying different activated morphotypes. *Front. Cell. Neurosci.* 13, 472. doi:10.3389/fncel.2019.00472

Ferrari, D., Pizzirani, C., Adinolfi, E., Lemoli, R. M., Curti, A., Idzko, M., et al. (2006). The $P2X_7$ receptor: A key player in IL-1 processing and release. *J. Immunol.* 176 (7), 3877–3883. doi:10.4049/jimmunol.176.7.3877

Frade, J. M., and Barde, Y. A. (1998). Microglia-derived nerve growth factor causes cell death in the developing retina. *Neuron* 20 (1), 35–41. doi:10.1016/s0896-6273(00)80432-8

Franklin, T. C., Xu, C., and Duman, R. S. (2018). Depression and sterile inflammation: Essential role of danger associated molecular patterns. *Brain, Behav. Immun.* 72, 2–13. doi:10.1016/j.bbi.2017.10.025

GBD-2017-Collaborators (2018). Global, regional, and national incidence, prevalence, and years lived with disability for 354 diseases and injuries for 195 countries and territories, 1990-2017: A systematic analysis for the global burden of disease study 2017. *Lancet* 392 (10159), 1789–1858. doi:10.1016/S0140-6736(18)32279-7

Gonda, X., Hullam, G., Antal, P., Eszlari, N., Petschner, P., Hökfelt, T. G., et al. (2018). Significance of risk polymorphisms for depression depends on stress exposure. *Sci. Rep.* 8 (1), 3946. doi:10.1038/s41598-018-22221-z

Guilloux, J. P., Seney, M., Edgar, N., and Sibille, E. (2011). Integrated behavioral z-scoring increases the sensitivity and reliability of behavioral phenotyping in mice: Relevance to emotionality and sex. *J. Neurosci. Methods* 197 (1), 21–31. doi:10.1016/j.jneumeth.2011.01.019

He, Y., Taylor, N., Fourgeaud, L., and Bhattacharya, A. (2017). The role of microglial P2X7: Modulation of cell death and cytokine release. *J. Neuroinflammation* 14 (1), 135. doi:10.1186/s12974-017-0904-8

He, Y., Taylor, N., Yao, X., and Bhattacharya, A. (2021). Mouse primary microglia respond differently to LPS and poly(I:C) *in vitro*. *Sci. Rep.* 11 (1), 10447. doi:10.1038/s41598-021-89777-1

Himmerich, H., Patsalos, O., Lichtblau, N., Ibrahim, M. A. A., and Dalton, B. (2019). Cytokine research in depression: Principles, challenges, and open questions. *Front. Psychiatry* 10, 30. doi:10.3389/fpsyt.2019.00030

Hu, J., Wang, P., Wang, Z., Xu, Y., Peng, W., Chen, X., et al. (2022). Fibroblast-conditioned media enhance the yield of microglia isolated from mixed glial cultures. *Cell. Mol. Neurobiol.* 43, 395–408. doi:10.1007/s10571-022-01193-9

Illes, P., Verkhratsky, A., and Tang, Y. (2020). Pathological ATPergic signaling in major depression and bipolar disorder. *Front. Mol. Neurosci.* 12 (331), 331. doi:10.3389/fnmol.2019.00331

Iwata, M., Ota, K. T., Li, X.-Y., Sakaue, F., Li, N., Dutheil, S., et al. (2016). Psychological stress activates the inflammasome via release of adenosine triphosphate and stimulation of the purinergic type 2X7 receptor. *Biol. Psychiatry* 80 (1), 12–22. doi:10.1016/j.biopsych.2015.11.026

Jacobson, K. A., and Müller, C. E. (2016). Medicinal chemistry of adenosine, P2Y and P2X receptors. *Neuropharmacology* 104, 31–49. doi:10.1016/j.neuropharm.2015.12.001

Jiang, X., Yi, S., Liu, Q., and Zhang, J. (2022). The secretome of microglia induced by IL-4 of IFN-γ differently regulate proliferation, differentiation and survival of adult neural stem/progenitor cell by targeting the PI3K-Akt pathway. *Cytotechnology* 74 (3), 407–420. doi:10.1007/s10616-022-00534-2

Junger, W. G. (2011). Immune cell regulation by autocrine purinergic signalling. *Nat. Rev. Immunol.* 11 (3), 201–212. doi:10.1038/nri2938

Jurga, A. M., Paleczna, M., and Kuter, K. Z. (2020). Overview of general and discriminating markers of differential microglia phenotypes. *Front. Cell. Neurosci.* 14, 198. doi:10.3389/fncel.2020.00198

Kappelmann, N., Lewis, G., Dantzer, R., Jones, P. B., and Khandaker, G. M. (2018). Antidepressant activity of anti-cytokine treatment: A systematic review and meta-analysis of clinical trials of chronic inflammatory conditions. *Mol. Psychiatry* 23 (2), 335–343. doi:10.1038/mp.2016.167

Kawanokuchi, J., Takeuchi, H., Sonobe, Y., Mizuno, T., and Suzumura, A. (2013). Interleukin-27 promotes inflammatory and neuroprotective responses in microglia. *Clin. Exp. Neuroimmunol.* 4 (1), 36–45. doi:10.1111/cen3.12005

Köhler, O., Benros, M. E., Nordentoft, M., Farkouh, M. E., Iyengar, R. L., Mors, O., et al. (2014). Effect of anti-inflammatory treatment on depression, depressive symptoms, and adverse effects: A systematic review and meta-analysis of randomized clinical trials. *JAMA Psychiatry* 71 (12), 1381–1391. doi:10.1001/jamapsychiatry.2014.1611

Kozlowski, C., and Weimer, R. M. (2012). An automated method to quantify microglia morphology and application to monitor activation state longitudinally *in vivo*. *PLOS ONE* 7 (2), e31814. doi:10.1371/journal.pone.0031814

Lalive, P. H., Kreutzfeldt, M., Devergne, O., Metz, I., Bruck, W., Merkler, D., et al. (2017). Increased interleukin-27 cytokine expression in the central nervous system of multiple sclerosis patients. *J. Neuroinflammation* 14 (1), 144. doi:10.1186/s12974-017-0919-1

Lamers, F., Milaneschi, Y., Vinkers, C. H., Schoevers, R. A., Giltay, E. J., and Penninx, B. (2020). Depression profilers and immuno-metabolic dysregulation: Longitudinal results from the NESDA study. *Brain Behav. Immun.* 88, 174–183. doi:10.1016/j.bbi.2020.04.002

Le, H. T., Keslar, K., Nguyen, Q. T., Blazar, B. R., Hamilton, B. K., and Min, B. (2020). Interleukin-27 enforces regulatory T cell functions to prevent graft-versus-host disease. *Front. Immunol.* 11, 181. doi:10.3389/fimmu.2020.00181

Leyh, J., Paeschke, S., Mages, B., Michalski, D., Nowicki, M., Bechmann, I., et al. (2021). Classification of microglial morphological phenotypes using machine learning. *Front. Cell. Neurosci.* 15, 701673. doi:10.3389/fncel.2021.701673

Lian, H., Roy, E., and Zheng, H. (2016). Protocol for primary microglial culture preparation. *Bio Protoc.* 6 (21), e1989. doi:10.21769/BioProtoc.1989

Lopizzo, N., Bocchio Chiavetto, L., Cattane, N., Plazzotta, G., Tarazi, F. I., Pariante, C. M., et al. (2015). Gene-environment interaction in major depression: Focus on experience-dependent biological systems. *Front. Psychiatry* 6, 68. doi:10.3389/fpsyt.2015.00068

Mac Giollabhui, N., Ng, T. H., Ellman, L. M., and Alloy, L. B. (2020). The longitudinal associations of inflammatory biomarkers and depression revisited: Systematic review, meta-analysis, and meta-regression. *Mol. Psychiatry* 26, 3302–3314. doi:10.1038/s41380-020-00867-4

Martinez-Sanchez, M. E., Huerta, L., Alvarez-Buylla, E. R., and Villarreal Luján, C. (2018). Role of cytokine combinations on CD4+ T cell differentiation, partial polarization, and plasticity: Continuous network modeling approach. *Front. Physiology* 9 (877), 877. doi:10.3389/fphys.2018.00877

McWhorter, F. Y., Wang, T., Nguyen, P., Chung, T., and Liu, W. F. (2013). Modulation of macrophage phenotype by cell shape. *Proc. Natl. Acad. Sci.* 110 (43), 17253–17258. doi:10.1073/pnas.1308887110

Medina-Rodriguez, E. M., Lowell, J. A., Worthen, R. J., Syed, S. A., and Beurel, E. (2018). Involvement of innate and adaptive immune systems alterations in the pathophysiology and treatment of depression. *Front. Neurosci.* 12, 547. doi:10.3389/fnins.2018.00547

Metzger, M., Walser, S., Aprile Garcia, F., Dedic, N., Chen, A., Holsboer, F., et al. (2017). Genetically dissecting P2rx7 expression within the central nervous system using conditional humanized mice. *Purinergic Signal.* 13, 153–170. doi:10.1007/s11302-016-9546-z

Milaneschi, Y., Lamers, F., Berk, M., and Penninx, B. (2020). Depression heterogeneity and its biological underpinnings: Toward immunometabolic depression. *Biol. Psychiatry* 88 (5), 369–380. doi:10.1016/j.biopsych.2020.01.014

Miller, A. (2010). Depression and immunity: A role for T cells? *Brain, Behav. Immun.* 24, 1–8. doi:10.1016/j.bbi.2009.09.009

Miller, A. H., and Raison, C. L. (2016). The role of inflammation in depression: From evolutionary imperative to modern treatment target. *Nat. Rev. Immunol.* 16 (1), 22–34. doi:10.1038/nri.2015.5

Mingam, R., De Smedt, V., Amédée, T., Bluthé, R. M., Kelley, K. W., Dantzer, R., et al. (2008). *In vitro* and *in vivo* evidence for a role of the P2X7 receptor in the release of IL-1 beta in the murine brain. *Brain Behav. Immun.* 22 (2), 234–244. doi:10.1016/j.bbi.2007.08.007

Montilla, A., Zabala, A., Matute, C., and Domercq, M. (2020). Functional and metabolic characterization of microglia culture in a defined medium. *Front. Cell. Neurosci.* 14, 22. doi:10.3389/fncel.2020.00022

Moreno-Agostino, D., Wu, Y.-T., Daskalopoulou, C., Hasan, M. T., Huisman, M., and Prina, M. (2021). Global trends in the prevalence and incidence of depression:a systematic review and meta-analysis. *J. Affect. Disord.* 281, 235–243. doi:10.1016/j.jad.2020.12.035

Morrison, H., Young, K., Qureshi, M., Rowe, R. K., and Lifshitz, J. (2017). Quantitative microglia analyses reveal diverse morphologic responses in the rat cortex after diffuse brain injury. *Sci. Rep.* 7 (1), 13211. doi:10.1038/s41598-017-13581-z

Moschny, N., Jahn, K., Maier, H. B., Khan, A. Q., Ballmaier, M., Liepach, K., et al. (2020). Electroconvulsive therapy, changes in immune cell ratios, and their association with seizure quality and clinical outcome in depressed patients. *Eur. Neuropsychopharmacol.* 36, 18–28. doi:10.1016/j.euroneuro.2020.03.019

Nimmerjahn, A., Kirchhoff, F., and Helmchen, F. (2005). Resting microglial cells are highly dynamic surveillants of brain parenchyma *in vivo*. *Science* 308 (5726), 1314–1318. doi:10.1126/science.1110647

Nobis, A., Zalewski, D., and Waszkiewicz, N. (2020). Peripheral markers of depression. *J. Clin. Med.* 9 (12), 3793. doi:10.3390/jcm9123793

Orihuela, R., McPherson, C. A., and Harry, G. J. (2016). Microglial M1/M2 polarization and metabolic states. *Br. J. Pharmacol.* 173 (4), 649–665. doi:10.1111/bph.13139

Osimo, E. F., Pillinger, T., Rodriguez, I. M., Khandaker, G. M., Pariante, C. M., and Howes, O. D. (2020). Inflammatory markers in depression: A meta-analysis of mean

differences and variability in 5,166 patients and 5,083 controls. *Brain, Behav. Immun.* 87, 901–909. doi:10.1016/j.bbi.2020.02.010

Parkhurst, C. N., Yang, G., Ninan, I., Savas, J. N., Yates, J. R., Lafaille, J. J., et al. (2013). Microglia Promote Learning-Dependent Synapse Formation through Brain-Derived Neurotrophic Factor. *Cell* 155 (7), 1596–1609. doi:10.1016/j.cell.2013.11.030

Raison, C. L., and Miller, A. H. (2011). Is depression an inflammatory disorder? *Curr. Psychiatry Rep.* 13 (6), 467–475. doi:10.1007/s11920-011-0232-0

Ransohoff, R. M. (2016). A polarizing question: Do M1 and M2 microglia exist? *Nat. Neurosci.* 19 (8), 987–991. doi:10.1038/nn.4338

Rengasamy, M., Marsland, A., McClain, L., Kovats, T., Walko, T., Pan, L., et al. (2021). Longitudinal relationships of cytokines, depression and anhedonia in depressed adolescents. *Brain, Behav. Immun.* 91, 74–80. doi:10.1016/j.bbi.2020.09.004

Ribeiro, D. E., Roncalho, A. L., Glaser, T., Ulrich, H., Wegener, G., and Joca, S. (2019a). P2X7 receptor signaling in stress and depression. *Int. J. Mol. Sci.* 20 (11), 2778. doi:10.3390/ijms20112778

Ribeiro, D. E., Stanquini, L. A., Biojone, C., Casarotto, P. C., Elfving, B., Müller, H. K., et al. (2019b). P2X7 receptors are involved in stress-related behaviours and antidepressant effect. *Eur. Neuropsychopharmacol.* 29, S213–S214. doi:10.1016/j.euroneuro.2018.11.350

Rivas-Yáñez, E., Barrera-Avalos, C., Parra-Tello, B., Briceño, P., Rosemblatt, M. V., Saavedra-Almarza, J., et al. (2020). P2X7 receptor at the crossroads of T cell fate. *Int. J. Mol. Sci.* 21 (14), 4937. doi:10.3390/ijms21144937

Roohi, E., Jaafari, N., and Hashemian, F. (2021). On inflammatory hypothesis of depression: What is the role of IL-6 in the middle of the chaos? *J. Neuroinflammation* 18 (1), 45. doi:10.1186/s12974-021-02100-7

Rostam, H. M., Reynolds, P. M., Alexander, M. R., Gadegaard, N., and Ghaemmaghami, A. M. (2017). Image based Machine Learning for identification of macrophage subsets. *Sci. Rep.* 7 (1), 3521. doi:10.1038/s41598-017-03780-z

Saura, J., Tusell, J. M., and Serratosa, J. (2003). High-yield isolation of murine microglia by mild trypsinization. *Glia* 44 (3), 183–189. doi:10.1002/glia.10274

Sha, Q., Madaj, Z., Keaton, S., Escobar Galvis, M. L., Smart, L., Krzyzanowski, S., et al. (2022). Cytokines and tryptophan metabolites can predict depressive symptoms in pregnancy. *Transl. Psychiatry* 12 (1), 35. doi:10.1038/s41398-022-01801-8

Strober, W. (2015). Trypan blue exclusion test of cell viability. *Curr. Protoc. Immunol.* 111. A3.B.3 A3.B.1-a3.B.3. doi:10.1002/0471142735.ima03bs111

Suzuki, H., Savitz, J., Kent Teague, T., Gandhapudi, S. K., Tan, C., Misaki, M., et al. (2017). Altered populations of natural killer cells, cytotoxic T lymphocytes, and regulatory T cells in major depressive disorder: Association with sleep disturbance. *Brain Behav. Immun.* 66, 193–200. doi:10.1016/j.bbi.2017.06.011

Tam, W. Y., and Ma, C. H. (2014). Bipolar/rod-shaped microglia are proliferating microglia with distinct M1/M2 phenotypes. *Sci. Rep.* 4, 7279. doi:10.1038/srep07279

Urbina-Treviño, L., von Mücke-Heim, I.-A., and Deussing, J. M. (2022). P2X7 receptor-related genetic mouse models – tools for translational research in Psychiatry. *Front. Neural Circuits* 16, 876304. doi:10.3389/fncir.2022.876304

van Buel, E. M., Bosker, F. J., van Drunen, J., Strijker, J., Douwenga, W., Klein, H. C., et al. (2015a). Electroconvulsive seizures (ECS) do not prevent LPS-induced behavioral alterations and microglial activation. *J. Neuroinflammation* 12, 232. doi:10.1186/s12974-015-0454-x

van Buel, E. M., Patas, K., Peters, M., Bosker, F. J., Eisel, U. L., and Klein, H. C. (2015b). Immune and neurotrophin stimulation by electroconvulsive therapy: Is some inflammation needed after all? *Transl. Psychiatry* 5 (7), e609. doi:10.1038/tp.2015.100

van Buel, E. M., Sigrist, H., Seifritz, E., Fikse, L., Bosker, F. J., Schoevers, R. A., et al. (2017). Mouse repeated electroconvulsive seizure (ECS) does not reverse social stress effects but does induce behavioral and hippocampal changes relevant to electroconvulsive therapy (ECT) side-effects in the treatment of depression. *PloS one* 12 (9), e0184603. doi:10.1371/journal.pone.0184603

Velasquez, S., and Rappaport, J. (2016). Inflammasome activation in major depressive disorder: A pivotal linkage between psychological stress, purinergic signaling, and the kynurenine pathway. *Biol. Psychiatry* 80 (1), 4–5. doi:10.1016/j.biopsych.2016.04.019

von Mücke-Heim, I.-A., and Deussing, J. M. (2022). The P2X7 receptor in mood disorders: Emerging target in immunopsychiatry, from bench to bedside. *Neuropharmacology*.

von Mücke-Heim, I.-A., Urbina-Treviño, L., Bordes, J., Ries, C., Schmidt, M. V., and Deussing, J. M. (2022). Introducing a depression-like syndrome for translational neuropsychiatry: A plea for taxonomical validity and improved comparability between humans and mice. *Mol. Psychiatry*.

von Muecke-Heim, I. A., Ries, C., Urbina, L., and Deussing, J. M. (2021). P2X7R antagonists in chronic stress-based depression models: A review. *Eur. Arch. Psychiatry Clin. Neurosci.* 271 (7), 1343–1358. doi:10.1007/s00406-021-01306-3

Wang, N., Liang, H., and Zen, K. (2014). Molecular mechanisms that influence the macrophage M1–M2 polarization balance. *Front. Immunol.* 5, 614. doi:10.3389/fimmu.2014.00614

Wittenberg, G. M., Stylianou, A., Zhang, Y., Sun, Y., Gupta, A., Jagannatha, P. S., et al. (2020). Effects of immunomodulatory drugs on depressive symptoms: A mega-analysis of randomized, placebo-controlled clinical trials in inflammatory disorders. *Mol. Psychiatry* 25 (6), 1275–1285. doi:10.1038/s41380-019-0471-8

Wohleb, E. S., Franklin, T., Iwata, M., and Duman, R. S. (2016). Integrating neuroimmune systems in the neurobiology of depression. *Nat. Rev. Neurosci.* 17 (8), 497–511. doi:10.1038/nrn.2016.69

Woolf, Z., Stevenson, T. J., Lee, K., Jung, Y., Park, T. I. H., Curtis, M. A., et al. (2021). Isolation of adult mouse microglia using their *in vitro* adherent properties. *Star. Protoc.* 2 (2), 100518. doi:10.1016/j.xpro.2021.100518

Yoshida, H., and Hunter, C. A. (2015). The immunobiology of interleukin-27. *Annu. Rev. Immunol.* 33 (1), 417–443. doi:10.1146/annurev-immunol-032414-112134

Young, K., and Morrison, H. (2018). Quantifying microglia morphology from photomicrographs of immunohistochemistry prepared tissue using ImageJ. *J. Vis. Exp.* 136, 57648. doi:10.3791/57648

Zhang, J. M., and An, J. (2007). Cytokines, inflammation, and pain. *Int. Anesthesiol. Clin.* 45 (2), 27–37. doi:10.1097/AIA.0b013e318034194e

Zhu, J., Yamane, H., and Paul, W. E. (2010). Differentiation of effector CD4 T cell populations (*). *Annu. Rev. Immunol.* 28, 445–489. doi:10.1146/annurev-immunol-030409-101212

Zuiderwijk-Sick, E. A., van der Putten, C., Timmerman, R., Veth, J., Pasini, E. M., van Straalen, L., et al. (2021). Exposure of microglia to interleukin-4 represses NF-κB-Dependent transcription of toll-like receptor-induced cytokines. *Front. Immunol.* 12, 771453. doi:10.3389/fimmu.2021.771453

frontiers | Frontiers in Pharmacology

TYPE Mini Review
PUBLISHED 10 May 2023
DOI 10.3389/fphar.2023.1179028



OPEN ACCESS

EDITED BY
Henning Ulrich,
University of São Paulo, Brazil

REVIEWED BY
Peter Illes,
Leipzig University, Germany

*CORRESPONDENCE
Jie Liu,
liujiesyy@126.com

†These authors contributed equally to this work and share first authorship

RECEIVED 03 March 2023
ACCEPTED 28 April 2023
PUBLISHED 10 May 2023

CITATION
Chen X, Wang Q, Yang J, Zhang L, Liu T-T, Liu J, Deng B-L and Liu J (2023), Diagnostic and therapeutic value of P2Y12R in epilepsy.
*Front. Pharmacol.* 14:1179028.
doi: 10.3389/fphar.2023.1179028



# Diagnostic and therapeutic value of P2Y12R in epilepsy

Xiang Chen[1†], Qi Wang[2†], Jie Yang[3], Li Zhang[4], Ting-Ting Liu[5], Jun Liu[6], Bin-Lu Deng[1] and Jie Liu[1,2,5*]

[1]Department of Neurology, School of Clinical Medicine, Southwest Medical University, Luzhou, China, [2]Department of Neurology, Sichuan Academy of Medical Sciences, Sichuan Provincial People's Hospital, Chengdu, China, [3]Zunyi Medical University, Zunyi, China, [4]Electrophysiology Unit, Department of Neurology, Chengdu Fourth People's Hospital, Chengdu, China, [5]Department of Neurology, Sichuan Provincial People's Hospital, University of Electronic Science and Technology of China, Chengdu, China, [6]Department of Geriatric Neurology, Qinglongchang Ward, Chengdu Sixth People's Hospital, Chengdu, China

There lacks biomarkers in current epilepsy diagnosis, and epilepsy is thus exposed to inadequate treatment, making it necessarily important to conduct search on new biomarkers and drug targets. The P2Y12 receptor is primarily expressed on microglia in the central nervous system, and acts as intrinsic immune cells in the central nervous system mediating neuroinflammation. In previous studies, P2Y12R in epilepsy has been found capable of controlling neuroinflammation and regulating neurogenesis as well as immature neuronal projections, and its expression is altered. P2Y12R is involved in microglia inhibition of neuronal activity and timely termination of seizures in acute seizures. In status epilepticus, the failure of P2Y12R in the process of "brake buffering" may not terminate the neuronal hyperexcitability timely. In chronic epilepsy, neuroinflammation causes seizures, which can in turn induce neuroinflammation, while on the other hand, neuroinflammation leads to neurogenesis, thereby causing abnormal neuronal discharges that give rise to seizures. In this case, targeting P2Y12R may be a novel strategy for the treatment of epilepsy. The detection of P2Y12R and its expression changes can contribute to the diagnosis of epilepsy. Meanwhile, the P2Y12R single-nucleotide polymorphism is associated with epilepsy susceptibility and endowed with the potential to individualize epilepsy diagnosis. To this end, functions of P2Y12R in the central nervous system were hereby reviewed, the effects of P2Y12R in epilepsy were explored, and the potential of P2Y12R in the diagnosis and treatment of epilepsy was further demonstrated.

KEYWORDS

**P2Y12 receptor, epilepsy, seizures, neuroinflammation, diagnosis, therapy**

## 1 Introduction

Epilepsy is one of the most common and disabling chronic neurological disorders, which affects over 70 million people globally and imposes considerable socio-economic burdens (Beghi, 2020; Hauser, 2019; Thijs et al., 2019). Besides, it is defined as a chronic disorder of spontaneous seizures caused by an imbalance between excitability and inhibition in the brain, and the neurobiological, cognitive, psychological and social consequences of the condition (Mo et al., 2019; Sarmast et al., 2020). Epilepsy can be caused by brain dysplasia, brain injury (infections, stroke, tumors, and traumatic brain injury (TBI)), also genetic abnormalities (e.g., genetic polymorphisms, copy number variants, or *de novo* mutations) (Rees, 2010; Pitkänen, A., and Lukasiuk, 2011; Pitkanen and Engel, 2014; Klein et al., 2018). The pathological process of epilepsy

includes synaptic reorganization, blood-brain barrier (BBB) disruption, alterations in neurotransmitter release, abnormal neurogenesis, neurodegeneration, and neuroinflammation (Jacobson and Boeynaems, 2010; Henshall and Kobow, 2015; Pitkanen et al., 2015; Guzman and Gerevich, 2016). At present, the diagnosis of epilepsy remains complex and clinically challenging. Video electroencephalography (EEG) monitoring is still the gold standard in hospitals, but this method is time-consuming, costly and low-yielding, and requires a high level of expertise (Engel and Pitkanen, 2020). The clinical manifestations of epilepsy are diversified, and some epilepsies (especially non-convulsive epilepsies) are easily confused with other disorders and may be misdiagnosed or missed, thus causing incorrect or unnecessary treatment. As a result, the diagnosis of epilepsy remains inadequate. Biomarkers have potential in the diagnosis of epilepsy (Engel and Pitkanen, 2020), which are useful in the diagnosis, differential diagnosis and prediction of seizures, and also have potential therapeutic uses, such as identifying persistent seizures and their mechanisms, predicting the effectiveness of antiepileptic drugs, assessing the likelihood of recurrence after stopping treatment, as well as assessing susceptibility to drug side effects (Sueri et al., 2018; Engel and Pitkanen, 2020; Perucca, 2021), making it necessarily important to search for biomarkers of epilepsy and further improve the diagnostic accuracy of epilepsy.

The current treatment choice for epilepsy is still antiepileptic drugs, with more than 30 antiseizure medications (ASMs) clinically available (Perucca, 2021). However, antiepileptic drugs control only 70% of patients with epilepsy, have no appreciable effect on disease process, and can cause serious side effects (such as fatigue, irritability, and dizziness) (Bialer and White, 2010; Thijs et al., 2019). Besides medication, additional treatments include neuromodulation devices and stimulators (such as vagus nerve stimulators (VNS)), reactive neuromodulation (RNS), Deep Brain Stimulator (DBS), resective epilepsy surgery and ketogenic diet (Rincon et al., 2021; Dyńka et al., 2022; Foutz and Wong, 2022; Hartnett et al., 2022; Imdad et al., 2022; Rho and Boison, 2022). In this case, it is still necessary to search for alternative therapeutic schemes with new mechanism to modify the disease progression and provide effective treatment for drug-resistant epilepsy (Alves et al., 2018). Therefore, different mechanisms of therapeutic regimens should be currently developed to suppress epilepsy and even to influence epilepsy progression.

For note, there is growing academic interest in the effect of neuroinflammation in epilepsy (Terrone et al., 2017). Microglia are intrinsic immune cells of the central nervous system that mediate neuroinflammation, on which, P2Y12 receptor (P2Y12R) is mainly expressed in the central nervous system (CNS); Thus, P2Y12R plays an influential pathophysiological role in the neuroinflammatory response to epilepsy and is potentially valuable for the diagnosis and treatment of epilepsy. This review will focus on the P2Y12 receptor, giving a brief overview of the structure and expression of P2Y12R, detailing the effects of P2Y12R in epilepsy, particularly neuroinflammation, and highlighting potential applications of P2Y12R in the diagnosis and treatment of epilepsy.

## 2 Potential therapeutic value of P2Y12R

P2Y12R is a member of the purinergic signaling family (Dahlquist and Diamant, 1974; Hynie, 1995; Burnstock, 2004; Burnstock, 2007). Purinergic signaling, which includes nucleotides (e.g., adenosine triphosphate (ATP)), their hydrolysis products (adenosine diphosphate (ADP), adenosine monophosphate (AMP)), nucleosides (e.g., adenosine), enzymes (CD39, CD73) and purinergic *p*) receptors, was proposed by Burnstock in 1972 and has been recognized as a new etiological factor or promising potential target for the treatment of central nervous system disorders (Huang et al., 2021; Li et al., 2022; Trinh et al., 2022; Iring et al., 2021; Ribeiro et al., 2022). The binding of extracellular nucleosides and nucleosides to purinergic receptors leads to the activation of intracellular signaling pathways, which in turn gives rise to changes in cell physiology (Zimmermann, 2006; Burnstock, 2008; Burnstock, 2018; Burnstock, 2020). ATP and its derivatives, diadenine nucleotides, act as partial agonists or antagonists of P2Y12R (Kauffenstein et al., 2004), where ADP is an endogenous agonist of P2Y12R (Bodor et al., 2003). P2Y12R, coupled with Gi protein, inhibits adenylate cyclase, thus reducing the production of cAMP and affecting intracellular calcium concentration (Cheffer et al., 2017). The crystal structure of P2Y12R is composed of seven hydrophobic transmembrane regions (TMs), which are connected by three extracellular loops (ELs) and three intracellular loops (Zhang K et al., 2014; Zhang et al., 2015). P2Y12R contains 342 amino acid residues and has two potential N-linked glycosylation sites at its extracellular amino terminus, which regulates its activity (Takasaki et al., 2001; Cattaneo, 2015). P2Y12R has four cysteine residues at the ELs (Cys 17, 97, 175, 270), which form two disulfide bonds that act accordingly upon stimulation/inhibition (Algaier et al., 2008; Ding et al., 2009; Hillmann et al., 2009; Gomez Morillas et al., 2021). Initially, the P2Y12 receptor was thought to be expressed only on platelets (Nie et al., 2017), and drugs that block P2Y12R (e.g., clopidogrel) were widely used as antiplatelet aggregation agents for the treatment of cardiovascular diseases (Raju et al., 2008). However, Hollopeter et al. found that P2Y12R was expressed in the brain (Hollopeter et al., 2001), and other studies further showed that it was also expressed on microglia, vascular smooth muscle cells, dendritic cells, lymphocytes, brown adipocytes, osteoblasts, osteoclasts, and primary cilia of bile duct cells (Wihlborg et al., 2004; Ben Addi et al., 2010; Diehl et al., 2010; Kronlage et al., 2010; Rauch et al., 2010; Gachet, 2012; Liverani et al., 2014; Jacobson et al., 2020; Mansour et al., 2020). It is currently believed that in the central nervous system (CNS), P2Y12R is primarily expressed in microglia and is stably expressed during the development of human brain (Butovsky et al., 2014; Zhang, Y et al., 2014; Lou et al., 2016; Cserép et al., 2020). Microglia are the first cells to respond to brain injury and neurodegeneration. Therefore, P2Y12R is considered as a marker to distinguish microglia cells from other brain cells and myeloid cells throughout human life (Moore et al., 2015; Mildner et al., 2017; Hammond et al., 2018; Cserép et al., 2020).

In the SE mouse model induced intra-amygdala KA and intraperitoneal pilocarpine, the transcription levels of uracil-sensitive P2Y receptors (P2Y2R, P2Y4R, and P2Y6R) in the hippocampus were increased, while those of adenine-sensitive P2Y receptors (P2Y1R, P2Y12R, and P2Y13R) were decreased. However, at the protein level, the expression of P2Y1, P2Y2, P2Y4 and P2Y6 was increased, while that of P2Y12 was decreased after SE, which might be attributed to the increased G protein coupling of the receptor to the P2Y receptor coupled to Gq,

as well as the downregulated or unchanged P2Y receptor coupled to Gi (Alves et al., 2017). Additionally, in chronic epilepsy, levels of P2Y1R, P2Y2R, and P2Y6R transcripts and P2Y1, P2Y2, and P2Y12 proteins were elevated, while those of other P2Y receptors were unchanged (Alves et al., 2017).

P2Y12R is essential for maintaining brain homeostasis. A recent study shows that P2Y12R deficiency disrupts neuronal precursor cell proliferation and leads to structural abnormalities in developmental and adult cortical cells (Cserép et al., 2022). Meanwhile, microglia affect neuronal proliferation in a P2Y12R-dependent manner and regulate neurogenesis and projections of immature neurons (Mo et al., 2019; Cserép et al., 2022). Besides, P2Y12R also promotes the proliferation of adult mouse subventricular zone (SVZ) cells (Suyama et al., 2012). Interestingly, the activation of P2Y1R and P2Y12R induces astrocyte proliferation *in vitro* (Quintas et al., 2011). Furthermore, in astrocyte and microglia co-cultures, microglia P2Y12R and P2Y13R are involved in blocking ADPβS-mediated astrocyte proliferation (Quintas et al., 2014). P2Y12R and P2Y13R are integrally linked, with the latter enhancing the chemotactic response of the former (Kyrargyri et al., 2020). Also, microglia P2Y12 is required for synaptic plasticity in the mouse visual cortex, and the destruction of P2Y12 reduces the branching of basal microglia processes under homeostasis, indicating a close correlation between microglia branching and P2Y12 expression (Haynes er al., 2006; Sipe et al., 2016). In addition, microglia-neuron interaction is known as microglial protuberance convergence (MPC) toward neuronal axons and dendrites (Eyo et al., 2018). Cserép et al. observed the unique nanostructure known as somatic purinergic connections of microglia-neuron connections in mouse and human brains, and claimed that somatic preferences in the adult brain promote the site formation of Kv2.1 clusters in neuronal cytosol, which are associated with neuronal mitochondrial activity, and are highly dynamic and P2Y12R-dependent (Cserép et al., 2020; Cserép et al., 2022). Microglia P2Y12Rs defines the somatic purinergic connection on doublecortin-positive (DCX+) developing neurons that enable microglia to monitor and shape neural development and facilitate neuronal integration within cortical networks (Cserép et al., 2022). In capillary injury, P2RY12-mediated activation of paravalvular microglia and microglia protrusions rapidly forms dense plexiform aggregate at the site of injury, which consists of membrane attachments expressing E-calmodulin, and acts as a physical barrier that temporarily closes the blood-brain barrier (Lou et al., 2016).

Microglia participate in neuroinflammation as resident immune cells in the brain. Under physiological conditions, microglia take a branching form, extending and retracting in all directions to survey the brain (Gomez Morillas et al., 2021). Purinergic signaling will be the primary system for triggering microglial cell extension (Koizumi et al., 2013), and microglia protrusions in P2Y12R-deficient mice do not extend, suggesting the involvement of P2Y12R in microglia protrusion extension and tropism (Haynes et al., 2006). Besides, ATP/ADP also inhibits the adenylyl cyclase pathway downstream of P2Y12R through the induced activated phospholipase C (PLC) and phosphatidylinositol 3-kinase (PI3K) pathways, and the activation of integrin-β1 and its accumulation at the end of extended protrusions are involved in the extension of microglia protrusions in brain tissues (Ohsawa et al., 2010; Ohsawa and Kohsaka, 2011). In addition, the activation of P2Y12R has been reported to enhance the activity of the twik-related halothane inhibitory K+ channel (THIK-1), which regulates microglia differentiation and brain monitoring functions under physiological conditions and maintains the "resting" potential of microglia (Madry et al., 2018; Gomez Morillas et al., 2021). In this case, P2Y12R is considered to mediate the monitoring role of microglia in the resting state.

## 2.1 Antiepileptic effect of P2Y12R works by controlling neuroinflammation

Neuroinflammation is an essential pathological process in epileptogenesis, which gives rise to the hyperexcitability of the brain (Engel et al., 2021). Currently, the potential applications of targeting inflammatory cytokines and purinergic receptors in epilepsy have been fully demonstrated (Burnstock, 2017; Alves et al., 2018; Rana and Musto, 2018). The Anne Schaefer team found that microglia inhibit neuronal activity in a negative feedbacking way similar to that of inhibitory neurons, acting as a "brake buffer" (Badimon et al., 2020), and matter considerably in the process of inhibiting neuronal activity in P2Y12R. Neuroinflammation overexcites neurons, and seizures result (Vezzani et al., 2010). During a seizure, ATP is released from the cell and metabolic ADP activates P2Y12R, which modulates the microglial phenotype after a seizure. ATP via P2Y12R attracts microglia, and the microglia ATP/ADP then hydrolyzes ectoenzyme CD39 into AMP. AMP is converted by CD73 into adenosine, which mediates the inhibition of neuronal activity via adenosine receptor A1R (Badimon et al., 2020), and finally acute epilepsy ceases. In status epilepticus, the failure of P2Y12R in the process of "brake buffering" may not terminate the neuronal hyperexcitability in time. Models of status epilepticus have been used in previous experiments, and the exacerbation of seizures in P2Y12R knockout mice again supports this idea (Eyo et al., 2014). In chronic epilepsy, neuroinflammation causes seizures on the one hand, which can in turn induce neuroinflammation, while on the other, neuroinflammation can lead to neurogenesis, which in turn causes abnormal neuronal discharges that lead to seizures. Recurrent seizures perpetuate chronic inflammation, which may be the cause of recurrent chronic epilepsy.

P2Y12R may be a drug target in epilepsy, where there is growing evidence proving its role in regulating neuroinflammation. Besides, an interaction exists between neuroinflammation and epilepsy. Previous studies have shown that neuroinflammation can cause epilepsy, seizures can also result from it, and neuroinflammation can promote neuronal hyperexcitability and lead to seizures (Vezzani et al., 2010). The mRNAs encoding P2Y12 and P2Y13 receptors are observed in the rat brainstem, where there are also cell bodies of catecholaminergic neurons innervating the hippocampus, and the activation of P2Y12R inhibits the release of norepinephrine in the hippocampus to affect neuronal excitability (Csölle et al., 2008). A variety of inflammatory mediators can be detected in brain tissue sections from epilepsy patients after surgical resection (Vezzani and Granata, 2005; Choi et al., 2009). Animal experiments have also indicated that extracellular ADP enhances microglia inflammation by acting on P2Y12R to activate nuclear factor-κ-gene binding (NF-κB) and NOD-like receptor thermal protein domain associated

protein 3(NLRP3) inflammatory vesicles and the release of IL-1β and IL-6, thereby increasing seizures (Cieślak et al., 2017; Suzuki et al., 2020). Besides, IL-1β induces seizures through the activation of the GluN2B subunit of the NMDA receptor, and increases the production of GluN2B mRNA and the upregulation of NMDA receptors on postsynaptic cells. In addition, 24 h after pentylenetetrazole (PTZ)-induced status epilepticus, it was observed in the rat hippocampal slices that GluN2B subunit expression is increased and LTP at hippocampal synapses is reduced, leading to impaired synaptic plasticity (Viviani et al., 2003; Postnikova et al., 2017). There are also alterations in the concentration of IL-1β in TLE that reduce GABA-mediated neurotransmission up to 30%, and lead to seizures due to neuronal hyperexcitability (Roseti et al., 2015). Both IL-1β and IL-6 reduce long-term potentiation (LTP), and microglia stimulation and elevated IL-1β levels will also result in the upregulation of IL-6 (Erta et al., 2012; Gruol, 2015; Rana and Musto, 2018). Upregulation of IL-6, an inflammatory cytokine, reduces LTP and hippocampal neurogenesis, while changes in hippocampal structure and morphology as well as the hyperexcitability of the hippocampal region lead to epileptogenesis (Samuelsson, 2005; Erta et al., 2012; Pineda et al., 2013; Levin and Godukhin, 2017). Lipopolysaccharide (LPS) that induces neuroinflammation may also lower the threshold for seizures (Sayyah et al., 2003; Heida and Pittman, 2005; Galic et al., 2008; Auvin et al., 2009; Auvin et al., 2010). Additionally, seizure activity itself can induce inflammation in the brain, and recurrent seizures can perpetuate chronic inflammation (Vezzani et al., 2010). These inflammatory factors can influence the severity and recurrence of seizures, thereby forming a vicious cycle (Vezzani et al., 2010). However, the role of P2Y12R in it is still not clear at present, and needs further explorations.

Under neuroinflammatory conditions, ATP is released extracellularly, activates both the P2Y12R receptor as ATP/ADP, and stimulates the adenosine receptor (AR) A3 as a metabolic receptor. P2Y12R activation acts as the first responder to microglial activation, and acts synergistically with A3. Meanwhile, high expression of both mediates the extension of microglial protrusions towards the injury site. Subsequently, upregulation of ARA2A and downregulation of P2Y12R induce microglia protrusion retraction. The microglia migratory activity is controlled by the interaction of P2Y12R and P2X4R. When the protrusions are fully retracted, microglia will transform into amoeboid morphology. Finally, P2Y6R and P2X4R activation induces phagocytosis and pinocytosis, respectively, while P2X4R and P2X7R are involved in secretory activity (Rivera et al., 2016; Fekete et al., 2018; Illes et al., 2020; Gomez Morillas et al., 2021). The activation of a number of other P1 and P2 receptors (Koizumi et al., 2013) regulates P2Y12 receptor-mediated responses, suggesting a close interaction between P2Y12R and other purinergic receptors that act together to get involved in neuroinflammation.

P2Y12 receptor-mediated greater response to the signals of "eat me" and "find me" renders activated microglia the ability to intervene more rapidly in damaged cells (Avignone et al., 2008). P2Y12R is involved in membrane fluffing, protrusion extension or retraction, and chemotactic motions of microglia. Activation of P2Y12R induces microglia reactivity and causes microglia protrusion growth, which also mediates microglia chemotaxis via phosphatidylinositol 3-kinase (PI3K)/phospholipase C (PLC) signaling. This matters considerably for the clearance of infected cells or cellular debris and tissue recovery (Ohsawa et al., 2007; Irino et al., 2008; Engel et al., 2021). Similar to synaptic extension, P2Y12 receptor-mediated migration of microglia also involves inhibition of the adenylate cyclase pathway and reduction of the cAMP levels and protein kinase A (Nasu-Tada et al., 2005). Charolidi et al. found that blocking microglia P2Y12 receptors with PSB0739 inhibits the release of chemokines (CCL2 and CXCL1), and microglia P2Y12R thus regulates the release of chemokines CCL2 and CXCL1 (Charolidi et al., 2015). All these processes depend on dual-pore domain-type potassium channels and are associated with alterations in mitochondrial membrane potential (Suzuki et al., 2020). Besides, microglia couple phagocytosis to apoptotic processes through P2Y12R signaling during development (Blume et al., 2020). The P2Y12R signaling pathway is involved in phagocytosis-mediated chemotaxis to the "find-me" signal ADP (Haynes et al., 2006), which is necessarily important for the rapid and efficient clearance of microglia-mediated apoptotic cells (Blume et al., 2020). Impaired microglial phagocytosis and reduced neurogenesis are observed in P2Y12 KO mice, and the involvement of microglia phagocytosis in a feedback loop that maintains homeostasis of adult hippocampal neurogenesis is also hereby revealed (Diaz-Aparicio et al., 2020).

Expression of P2Y12R on microglia depends on different activation patterns and CNS microenvironments (Colonna and Butovsky, 2017). Once activated, microglia are often categorized as the "classical" proinflammatory phenotype (M1) or the "alternative" anti-inflammatory type (M2) (Colonna and Butovsky, 2017). Under selective activation conditions (M2; IL-4 and IL-13), P2Y12 receptor expression increases, mediates microglia migration, and contributes to triggering an acute proinflammatory response to danger-related molecules released during central nervous system injury (Moore et al., 2015). However, under pro-inflammatory conditions, P2Y12R expression is reduced in rodent microglia, resulting in the failure to migrate up the ADP gradient (De Simone et al., 2010). In addition, P2RY12 expression is upregulated on the microglia of resting and non-inflammatory phenotype (M2), but downregulated during the M1/M2 transition of the post-activation inflammatory phenotype (Honda et al., 2001; Haynes et al., 2006). In this case, P2Y12R is considered a valuable sign that indicates the shift of the microglia functional pattern from chemotaxis to phagocytosis (Koizumi et al., 2013; Gomez Morillas et al., 2021), identifies non-pathological microglia, and differentiates activated microglia from stationary microglia (Mildner et al., 2017).

P2Y12R has been shown to regulate the microglia phenotype after seizures (Eyo et al., 2014; Eyo et al., 2017; Eyo et al., 2018). In the hippocampus of P2Y12 knockout (KO) mice intraperitoneally injected with kainic acid (KA) (18 mg/kg), the number of microglia primary protrusions is reduced, and seizures are worsened (Eyo et al., 2014). During seizures, neurons are highly active, and release glutamate from presynaptic terminals. Meanwhile, elevated glutamate levels activate neuronal NMDA receptors, thus causing an inward flow of extracellular calcium ions, while elevated intracellular calcium may lead to the release of ATP through ion channels such as pannexin 1 (PX1) or prepackaged vesicles. Besides, the released ATP diffuses into the extracellular space, forming a

**TABLE 1 Summary of the effects of P2Y12R in epilepsy.**

| type | | Seizure type | Methods/Models | Main results | References |
|---|---|---|---|---|---|
| Expression | | SE | IP KA (18–22 mg/kg) mice | Increased P2Y12R transcription in the hippocampus. | Avignone et al. (2008) |
| | | SE | intra-amygdala KA mice IP pilocarpine mice | Decreased P2Y12R transcription and protein expression after status epilepticus, and elevated levels of the P2Y12R protein in chronic epilepsy. | Alves et al. (2017) |
| Function | antiepileptic | SE | IP KA (18 mg/kg) P2Y12 KO mice | Increased seizure phenotype and reduced hippocampal microglial processes toard neurons in P2Y12-deficient mice. | Eyo et al. (2014) |
| | | MTLE | Hippocampal tissue section stained with fluorescent lectin from patients | Low-dose ADP inducing microglial proboscis elongation by blocking P2Y12, while high-dose ADP causing process retraction and membrane fluffing by joint activation of P2Y1/P2Y13 receptors. | Milior et al. (2020) |
| | epileptogenic | seizure | ICV KA (0.032 mg/mL) mice | Microglial P2Y12 receptors regulating seizure-induced neurogenesis and immature neuronal projections. | Mo et al. (2019) |
| SNPs | | epilepsy | patients with epilepsy | Possible correlation between the rs1491974 and rs6798347 polymorphisms of P2Y12R and epilepsy. | Wang et al. (2022) |

**Abbreviations:** IP, intraperitoneal; ICV, intracerebroventricular; KA, kainic acid; KO, knockout; MTLE, mesial temporal lobe epilepsy; SE, status epilepticus; and SNPs, single-nucleotide polymorphisms.

chemotactic gradient that activates P2Y12R in microglia, and inducing the extension of microglia protrusions toward neurons (Eyo et al., 2014). Acute seizures significantly alter the morphology and number of microglia in the hippocampal region, while glutamate treatment and prolongation of microglia protrusions during seizures play a neuroprotective role (Eyo et al., 2014). During seizures, P2Y12 receptors also regulate the microglial cell landscape through a cell shift mechanism (Eyo et al., 2018). In tissue slices from epileptic patients stained with fluorescent lectin, activation of the P2Y12 receptor initiates the extension of microglia protrusions (Haynes et al., 2006), which is similar to the situation in rodents, but the difference is that microglia retraction is triggered by the joint activation of P2Y1/P2Y13 receptors. Additionally, it was observed that low doses (1–10 μM for 15–30 min) of ADP induce the process extension for both initially amoeboid and ramified microglia, while high doses (1–2 mM for 30 min) of ADP cause process retraction and membrane ruffling (Milior et al., 2020). In summary, P2Y12R exerts a potential protective effect on epilepsy.

## 2.2 P2Y12R regulating neurogenesis and immature neuronal projections after seizures

Mo et al. ever claimed that P2Y12R regulates neurogenesis and immature neuronal projections after seizures in the intracerebroventricular kainic acid model, which composes some features of the epileptogenic environment (Danzer, 2018; Mo et al., 2019). Besides, it was hereby figured out that on the one hand, P2Y12R may promote the hyperactivity in epileptogenesis subsequent to the initial seizure, while on the other, as mentioned above, P2Y12R is involved in controlling neuroinflammation and microglia inhibiting neuronal activity and thus imposes an antiepileptic effect, so future work is needed to help further understand the detailed mechanism of the dual role of P2Y12R, epileptogenic and anti-epileptogenic (Mo et al., 2019). Interestingly, the removal of microglia exerts a more pronounced effect on seizure-induced neurogenesis than elimination of P2Y12R, suggesting that P2Y12R is not the only microglia protein that regulates seizure-induced neurogenesis (Mo et al., 2019). Therefore, other factors that regulate seizure-induced neurogenesis remain to be further investigated.

# 3 Potential diagnostic value of P2Y12R

## 3.1 P2Y12R expression during epilepsy

As described in the first study of expression in the P2YR family after seizures, increased P2Y12 Rtranscription in the hippocampus and increased P2Y12 activation-mediated microglial cell membrane currents 48 h after status epilepticus (SE) were observed in a mouse model of intraperitoneal kainic acid (KA)-induced SE (Avignone et al., 2008). The movement of microglia in the epileptic hippocampus toward P2Y12 receptor agonists was also found twice as rapid as in the normal hippocampus (Avignone et al., 2008). On the contrary, as stated before, in the SE mouse model induced intra-amygdala KA and intraperitoneal pilocarpine, P2Y12R transcription and protein expression were reduced after status epilepticus and P2Y12R protein levels were increased in chronic epilepsy (Alves et al., 2017). The expression of P2Y12R varied and diverged in different epilepsy models and at different stages of the disease. However, all indicated that P2Y12R expression was altered in epilepsy, which was endowed with the potential to assist in the diagnosis of epilepsy. The future application of positron emission tomography (PET) for the detection of P2Y12R itself in the brain needs further study.

### 3.2 Association between P2Y12R single-nucleotide polymorphism and epilepsy susceptibility

A study was reported on the association of single nucleotide polymorphisms (SNPs) in the P2Y12R gene with epilepsy, and it was found that carriers of the G allele of rs1491974 G>A or rs6798347 G>A may be associated with increased risk of epilepsy, with the rs1491974 G> A genotype and allele frequency differing significantly in females only, and individuals with this genotype may be exposed to more frequent seizures (Wang et al., 2022). However, a larger sample size and epilepsy classification are needed to further investigate the correlation between P2Y12R SNPs and epilepsy. P2Y12R SNPs currently have the potential to serve as a risk factor for epilepsy, with the potential for individualized diagnosis of epilepsy. There may be P2Y12R gene loci insensitive to P2Y12R-targeted drugs, and patients with insensitive loci can be removed by P2Y12R SNPs detection to achieve precision medicine in the future.

## 4 Conclusion and future perspectives

P2Y12R is closely associated with epilepsy and seizures (Table 1), and is thus endowed with potential application value in the diagnosis of epilepsy and seizures, which is also promising as an effective drug target. In acute seizures, P2Y12R is involved in the process of neuronal activity inhibition by microglia, terminating neuronal hyperexcitability and avoiding status epilepticus, while in chronic epilepsy, P2Y12R is a potential drug target by controlling neuroinflammation. Meanwhile, P2Y12R antagonists can inhibit neurogenesis and immature neuronal projections to prevent the next seizure, but the mechanism is still unclear and requires further exploration. The altered expression of P2Y12R in epilepsy and its own detection may support the diagnosis of epilepsy. In addition, P2Y12R SNPs can be a risk factor for epilepsy to inform the likelihood of epileptogenesis. In the future, it is expected that drugs targeting P2Y12R will act only on brain regions or cells where neurons are over-excited, terminate seizures, and delay seizure progression without affecting normal brain regions and cells. However, there are still considerable issues to be addressed before the application of P2Y12R to the diagnosis and treatment of epilepsy.

1) There are differences and divergences in the expression of P2Y12R in different epilepsy models and at different stages of pathogenesis. Changes in the expression and mechanism of P2Y12R across different seizure types, seizure severity and frequency, disease stages, animal models and epileptic patients should be additionally explored to provide new ideas for the diagnosis and treatment of epilepsy;
2) Changes in P2Y12 expression are not specific to epilepsy. A single change in purine signaling cannot be used as an independent diagnostic criterion, which, actually, needs to be combined with other measures for diagnostic evaluation in the clinical setting (Wong and Engel, 2022);
3) The association of P2Y12R SNPs with epilepsy requires a larger sample size of patients and different epilepsy types to verify the possibility of using P2Y12R as a genetic marker;
4) The current P2Y12R PET tracer for pro- and anti-inflammatory microglia has been validated in mouse models and human brain sections (Villa et al., 2018; Jackson et al., 2022; van der Wildt et al., 2022). Attempts should also be made to develop P2Y12R PET tracers and detect P2Y12R in animal models of epilepsy or in the human brain;
5) The dual mechanism of pro-epileptic and anti-epileptic action of P2Y12R in the whole process of epilepsy is still not completely understood, making it necessary to carry out further studies;
6) There is not yet a P2 receptor-based treatment that can entirely stop seizures, and P2 receptors are likely to be used for an adjunctive treatment (Engel et al., 2021). In early seizures, P2Y12R agonists inhibit neurohyperexcitability, control neuroinflammation, and assist in terminating seizures, while after seizures, P2Y12R antagonists inhibit neurogenesis and immature neuronal projections to prevent the next seizure. It is thus advisable for future research to combine P2Y12R with antiepileptic drugs to determine a more refined strategy for epilepsy treatment, particularly in refractory epilepsy.

In conclusion, much future research on the effect of P2Y12R in epilepsy should be carried out to further advance it into clinical practice.

## Author contributions

XC edited the manuscript and designed the table; QW and JY drafted the manuscript; LZ, T-TL, JL, and B-LD consulted the literatures; JiL revised the manuscript. All authors contributed to the article and approved the submitted version.

## Funding

This work was supported by the Science and Technology Program of Sichuan Province, China (22ZDYF0988).

## Conflict of interest

The authors declare that the research was conducted in the absence of any commercial or financial relationships that could be construed as a potential conflict of interest.

## Publisher's note

# References


Algaier, I., Jakubowski, J., Asai, F., and Von Kügelgen, I. (2008). Interaction of the active metabolite of prasugrel, R-138727, with cysteine 97 and cysteine 175 of the human P2Y12 receptor. *Thromb. Haemost.* 6, 1908–1914. doi:10.1111/j.1538-7836.2008.03136.x

Alves, M., Beamer, E., and Engel, T. (2018). The metabotropic purinergic P2Y receptor family as novel drug target in epilepsy. *Front. Pharmacol.* 9, 193. doi:10.3389/fphar.2018.00193

Alves, M., Gomez-Villafuertes, R., Delanty, N., Farrell, M. A., O'Brien, D. F., Miras-Portugal, M. T., et al. (2017). Expression and function of the metabotropic purinergic P2Y receptor family in experimental seizure models and patients with drug-refractory epilepsy. *Epilepsia* 58, 1603–1614. doi:10.1111/epi.13850

Auvin, S., Mazarati, A., Shin, D., and Sankar, R. (2010). Inflammation enhances epileptogenesis in the developing rat brain. *Neurobiol. Dis.* 40, 303–310. doi:10.1016/j.nbd.2010.06.004

Auvin, S., Porta, N., Nehlig, A., Lecointe, C., Vallée, L., and Bordet, R. (2009). Inflammation in rat pups subjected to short hyperthermic seizures enhances brain long-term excitability. *Epilepsy Res.* 86, 124–130. doi:10.1016/j.eplepsyres.2009.05.010

Avignone, E., Ulmann, L., Levavasseur, F., Rassendren, F., and Audinat, E. (2008). Status epilepticus induces a particular microglial activation state characterizedby enhanced purinergic signaling. *J. Neurosci.* 28, 9133–9144. doi:10.1523/JNEUROSCI.1820-08.2008

Badimon, A., Strasburger, H. J., Ayata, P., Chen, X., Nair, A., Ikegami, A., et al. (2020). Negative feedback control of neuronal activity by microglia. *Nature* 586, 417–423. doi:10.1038/s41586-020-2777-8

Beghi, E. (2020). The epidemiology of epilepsy. *Neuroepidemiology* 54, 185–191. doi:10.1159/000503831

Ben Addi, A., Cammarata, D., Conley, P. B., Boeynaems, J. M., and Robaye, B. (2010). Role of the P2Y12 receptor in the modulation of murine dendritic cell function by ADP. *J. Immunol.* 185 (10), 5900–5906. doi:10.4049/jimmunol.0901799

Bialer, M., and White, H. S. (2010). Key factors in the discovery and development of new antiepileptic drugs. *Nat. Rev. Drug Discov.* 9, 68–82. doi:10.1038/nrd2997

Blume, Z. I., Lambert, J. M., Lovel, A. G., and Mitchell, D. M. (2020). Microglia in the developing retina couple phagocytosis with the progression of apoptosis via P2RY12 signaling. *Dev. Dyn.* 249, 723–740. doi:10.1002/dvdy.163

Bodor, E. T., Waldo, G. L., Hooks, S. B., Corbitt, J., Boyer, J. L., and Harden, T. K. (2003). Purification and functional reconstitution of the human P2Y12 receptor. *Mol. Pharmacol.* 64, 1210–1216. doi:10.1124/mol.64.5.1210

Burnstock, G. (2018). Purine and purinergic receptors. *Brain Neurosci. Adv.* 2, 2398212818817494. doi:10.1177/2398212818817494

Burnstock, G. (2017). Purinergic signalling: Therapeutic developments. *Front. Pharmacol.* 8, 661. doi:10.3389/fphar.2017.00661

Burnstock, G. (2020). Introduction to purinergic signaling. *Methods Mol. Biol.* 2041, 1–15. doi:10.1007/978-1-4939-9717-6_1

Burnstock, G. (2004). Introduction: P2 receptors. *Curr. Top. Med. Chem.* 4, 793–803. doi:10.2174/1568026043451014

Burnstock, G. (2007). Physiology and pathophysiology of purinergic neurotransmission. *Physiol. Rev.* 87, 659–797. doi:10.1152/physrev.00043.2006

Burnstock, G. (2008). Purinergic signalling and disorders of the central nervous system. *Nat. Rev. Drug Discov.* 7, 575–590. doi:10.1038/nrd2605

Butovsky, O., Jedrychowski, M. P., Moore, C. S., Cialic, R., Lanser, A. J., Gabriely, G., et al. (2014). Identification of a unique TGF-β-dependent molecular and functional signature in microglia. *Nat. Neurosci.* 17, 131–143. doi:10.1038/nn.3599

Cattaneo, M. (2015). P2Y12 receptors: Structure and function. *J. Thromb. Haemost.* 13 (1), S10–S16. doi:10.1111/jth.12952

Charolidi, N., Schilling, T., and Eder, C. (2015). Microglial Kv1.3 channels and P2Y12 receptors differentially regulate cytokine and chemokine release from brain slices of young adult and aged mice. *PLoS One* 10 (5), e0128463. doi:10.1371/journal.pone.0128463

Cheffer, A., Castillo, A. R. G., Corrêa-Velloso, J., Gonçalves, M. C. B., Naaldijk, Y., Nascimento, I. C., et al. (2017). Purinergic system in psychiatric diseases. *Mol. Psychiatry* 23, 94–106. doi:10.1038/mp.2017.188

Choi, J., Nordli, D. R., Jr, Alden, T. D., DiPatri, A., Jr, Laux, L., Kelley, K., et al. (2009). Cellular injury and neuroinflammation in children with chronic intractable epilepsy. *J. Neuroinflammation* 6, 38. doi:10.1186/1742-2094-6-38

Cieślak, M., Wojtczak, A., and Komoszyński, M. (2017). Role of the purinergic signaling in epilepsy. *Pharmacol. Rep.* 69 (1), 130–138. doi:10.1016/j.pharep.2016.09.018

Colonna, M., and Butovsky, O. (2017). Microglia function in the central nervous system during health and neurodegeneration. *Annu. Rev. Immunol.* 35, 441–468. doi:10.1146/annurev-immunol-051116-052358

Cserép, C., Pósfai, B., Lénárt, N., Zsolt, L., Istva´n, K., A´da´m, D., et al. (2020). Microglia monitor and protect neuronal function through specialized somatic purinergic junctions. *Science* 40, 528–537. doi:10.1126/science.aax6752

Cserép, C., Schwarcz, A. D., Pósfai, B., László, Z., Kellermayer, A., Környei, Z., et al. (2022). Microglial control of neuronal development via somatic purinergic junctions. *Cell Rep.* 40, 111369. doi:10.1016/j.celrep.2022.111369

Csölle, C., Heinrich, A., Kittel, A., and Sperlágh, B. (2008). P2Y receptor mediated inhibitory modulation of noradrenaline release in response to electrical field stimulation and ischemic conditions in superfused rat hippocampus slices. *J. Neurochem.* 106, 347–360. doi:10.1111/j.1471-4159.2008.05391.x

Dahlquist, R., and Diamant, B. (1974). Interaction of ATP and calcium on the rat mast cell: Effect on histamine release. *ActaPharmacol Toxicol.* 34, 368–384. doi:10.1111/j.1600-0773.1974.tb03533.x

Danzer, S. C. (2018). Contributions of adult-generated granule cells to hippocampal pathology in temporal lobe epilepsy: A neuronal bestiary. *Brain Plast.* 3, 169–181. doi:10.3233/BPL-170056

De Simone, R., Niturad, C. E., De Nuccio, C., AjmoneCat, M. A., Visentin, S., and Minghetti, L. (2010). TGF-beta and LPS modulate ADP-induced migration of microglial cells through P2Y1 and P2Y12 receptor expression. *J. Neurochem.* 115, 450–459. doi:10.1111/j.1471-4159.2010.06937.x

Diaz-Aparicio, I., Paris, I., Sierra-Torre, V., Plaza-Zabala, A., Rodrı´guez-Iglesias, N., rquez-Ropero, Ma´, et al. (2020). Microglia actively remodel adult hippocampal neurogenesis through the phagocytosis secretome. *J. Neurosci.* 40, 1453–1482. doi:10.1523/JNEUROSCI.0993-19.2019

Diehl, P., Olivier, C., Halscheid, C., Helbing, T., Bode, C., and Moser, M. (2010). Clopidogrel affects leukocyte dependent platelet aggregation by P2Y12 expressing leukocytes. *Basic Res. Cardiol.* 105, 379–387. doi:10.1007/s00395-009-0073-8

Ding, Z., Bynagari, Y. S., Mada, S. R., Jakubowski, J. A., and Kunapuli, S. P. (2009). Studies on the role of the extracellular cysteines and oligomeric structures of the P2Y12 receptor when interacting with antagonists. *J. Thromb. Haemost.* 7, 232–234. doi:10.1111/j.1538-7836.2008.03202.x

Dyńka, D., Kowalcze, K., and Paziewska, A. (2022). The role of ketogenic diet in the treatment of neurological diseases. *Nutrients* 14, 5003. doi:10.3390/nu14235003

Engel, J., Jr., and Pitkanen, A. (2020). Biomarkers for epileptogenesis and its treatment. *Neuropharmacology* 167, 107735. doi:10.1016/j.neuropharm.2019.107735

Engel, T., Smith, J., and Alves, M. (2021). Targeting neuroinflammation via purinergic P2 receptors for disease modification in drug-refractory epilepsy. *J. Inflamm. Res.* 14, 3367–3392. doi:10.2147/JIR.S287740

Erta, M., Quintana, A., and Hidalgo, J. (2012). Interleukin-6, a major cytokine in the central nervous system. *Int. J. Biol. Sci.* 8, 1254–1266. doi:10.7150/ijbs.4679

Eyo, U. B., Mo, M., Yi, M. H., Murugan, M., Liu, J., Yarlagadda, R., et al. (2018). P2Y12R- dependent translocation mechanisms gate the changing microglial landscape. *Cell Rep.*23, 959–966. doi:10.1016/j.celrep.2018.04.001

Eyo, U. B., Peng, J., Murugan, M., Mo, M., and Lalani, A. (2017). Regulation of physical microglia-neuron interactions by fractalkine signaling after status epilepticus. *ENEURO* 3, 0209–0216. doi:10.1523/ENEURO.0209-16.2016

Eyo, U. B., Peng, J., Swiatkowski, P., Mukherjee, A., Bispo, A., and Wu, L. J. (2014). Neuronal hyperactivity recruits microglial processes via neuronal NMDA receptors and microglial P2Y12 receptors after status epilepticus. *J. Neurosci.* 34, 10528–10540. doi:10.1523/JNEUROSCI.0416-14.2014

Fekete, R., Cserép, C., Lénárt, N., Tóth, K., Orsolits, B., Martinecz, B., et al. (2018). Microglia control the spread of neurotropic virus infection via P2Y12 signalling and recruit monocytes through P2Y12-independent mechanisms. *Acta Neuropathol.* 136, 461–482. doi:10.1007/s00401-018-1885-0

Foutz, T. J., and Wong, M. (2022). Brain stimulation treatments in epilepsy: Basic mechanisms and clinical advances. *Biomed. J.* 45, 27–37. doi:10.1016/j.bj.2021.08.010

Gachet, C. (2012). P2Y(12) receptors in platelets and other hematopoietic and non-hematopoietic cells. *Purinergic Signal* 8, 609–619. doi:10.1007/s11302-012-9303-x

Galic, M. A., Riazi, K., Heida, J. G., Mouihate, A., Fournier, N. M., Spencer, S. J., et al. (2008). Postnatal inflammation increases seizure susceptibility in adult rats. *J. Neurosci.* 28, 6904–6913. doi:10.1523/JNEUROSCI.1901-08.2008

Gomez Morillas, A., Besson, V. C., and Lerouet, D. (2021). Microglia and neuroinflammation: What place for P2RY12? *Int. J. Mol. Sci.* 22, 1636. doi:10.3390/ijms22041636

Gruol, D. L. (2015). IL-6 regulation of synaptic function in the CNS. *Neuropharmacology* 96, 42–54. doi:10.1016/j.neuropharm.2014.10.023

Guzman, S. J., and Gerevich, Z. (2016). P2Y receptors in synaptic transmission and plasticity: Therapeutic potential in cognitive dysfunction. *Neural Plast.* 2016, 1207393. doi:10.1155/2016/1207393

Hammond, T. R., Dufort, C., Dissing-Olesen, L., Giera, S., Young, A., Wysoker, A., et al. (2018). Single-cell RNA sequencing of microglia throughout the mouse lifespan and in the injured brain reveals complex cell-state changes. *Immunity* 50, 253–271. doi:10.1016/j.immuni.2018.11.004

Hartnett, S. M., Greiner, H. M., Arya, R., Tenney, J., Aungaroon, G., Holland, K., et al. (2022). Responsive neurostimulation device therapy in pediatric patients with complex medically refractory epilepsy. *J. Neurosurg. Pediatr.* 30, 499–506. doi:10.3171/2022.7.PEDS2281

Hauser, W. A. (2019). An unparalleled assessment of the global burden of epilepsy. *Lancet Neurol.* 18, 322–324. doi:10.1016/S1474-4422(19)30042-0

Haynes, S. E., Hollopeter, G., Yang, G., Kurpius, D., Dailey, M. E., Gan, W. B., et al. (2006). The P2Y12 receptor regulates microglial activation by extracellular nucleotides. *Nat. Neurosci.* 9, 1512–1519. doi:10.1038/nn1805

Heida, J. G., and Pittman, Q. J. (2005). Causal links between brain cytokines and experimental febrile convulsions in the rat. *Epilepsia* 46, 1906–1913. doi:10.1111/j.1528-1167.2005.00294.x

Henshall, D. C., and Kobow, K. (2015). Epigenetics and epilepsy. *Cold Spring Harb. Perspect. Med.* 5 (12), a022731. doi:10.1101/cshperspect.a022731

Hillmann, P., Ko, G. -Y., Spinrath, A., Raulf, A., Kügelgen, I. V., Wolff, S. C., et al. (2009). Key determinants of nucleotide-activated G protein-coupled P2Y2 receptor function revealed by chemical and pharmacological experiments, mutagenesis and homology modeling. *J. Med. Chem.* 52, 2762–2775. doi:10.1021/jm801442p

Hollopeter, G., Jantzen, H. M., Vincent, D., Li, G., England, L., Ramakrishnan, V., et al. (2001). Identification of the platelet ADP receptor targeted by antithrombotic drugs. *Nature* 409, 202–207. doi:10.1038/35051599

Honda, S., Sasaki, Y., Ohsawa, K., Imai, Y., Nakamura, Y., Inoue, K., et al. (2001). Extracellular ATP or ADP induce chemotaxis of cultured microglia through Gi/o-coupled P2Y receptors. *J. Neurosci.* 21, 1975–1982. doi:10.1523/JNEUROSCI.21-06-01975.2001

Huang, Z., Xie, N., Illes, P., Di Virgilio, F., Ulrich, H., Tang, Y., et al. (2021). From purines to purinergic signalling: Molecular functions and human diseases. *Signal Transduct. Target Ther.* 6 (1), 162. doi:10.1038/s41392-021-00553-z

Hynie, S. (1995). Purinergic receptors—Nomenclature and classification of types and subtypes. *Cesk Fysiol.* 44, 139–144.

Illes, P., Rubini, P., Ulrich, H., Zhao, Y., and Tang, Y. (2020). Regulation of microglial functions by purinergic mechanisms in the healthy and diseased CNS. *Cells* 9 (5), 1108. doi:10.3390/cells9051108

Imdad, K., Abualait, T., Kanwal, A., AlGhannam, Z. T., Bashir, S., Farrukh, A., et al. (2022). The metabolic role of ketogenic diets in treating epilepsy. *Nutrients* 14, 5074. doi:10.3390/nu14235074

Iring, A., Tóth, A., Baranyi, M., Otrokocsi, L., Módis, L. V., Sperlágh, B., et al. (2021). The dualistic role of the purinergic P2Y12-receptor in an *in vivo* model of Parkinson's disease: Signalling pathway and novel therapeutic targets. *Pharmacol. Res. Feb* 176, 106045. Epub 2021 Dec 28. doi:10.1016/j.phrs.2021.106045

IrinoNakamuraInoue, Y. Y. K., Kohsaka, S., and Ohsawa, K. (2008). Akt activation is involved in P2Y12 receptor-mediated chemotaxis of microglia. *J. Neurosci. Res.* 86, 1511–1519. doi:10.1002/jnr.21610

Jackson, I. M., Buccino, P. J., Azevedo, E. C., Carlson, M. L., Luo, A. S. Z., Deal, E. M., et al. (2022). Radiosynthesis and initial preclinical evaluation of [11C]AZD1283 as a potential P2Y12R PET radiotracer. *Nucl. Med. Biol.* S0969-8051, 143–150. doi:10.1016/j.nucmedbio.2022.05.001

Jacobson, K. A., and Boeynaems, J. M. (2010). P2Y nucleotide receptors: Promise of therapeutic applications. *Drug Discov. Today* 15, 570–578. doi:10.1016/j.drudis.2010.05.011

Jacobson, K. A., Delicado, E. G., Gachet, C., Kennedy, C., von Kügelgen, I., Li, B., et al. (2020). Update of P2Y receptor pharmacology: Iuphar review 27. *Br. J. Pharmacol.* 177, 2413–2433. doi:10.1111/bph.15005

Kauffenstein, G., Hechler, B., Cazenave, J. P., and Gachet, C. (2004). Adenine triphosphate nucleotides are antagonists at the P2Y12 receptor. *J. Thromb. Haemost.* 2, 1980–1988. doi:10.1111/j.1538-7836.2004.00926.x

Klein, P., Dingledine, R., Aronica, E., Bernard, C., Blumcke, I., Boison, D., et al. (2018). Commonalities in epileptogenic processes from different acute brain insults: Do they translate? *Epilepsia* 59, 37–66. doi:10.1111/epi.13965

Koizumi, S., Ohsawa, K., Inoue, K., and Kohsaka, S. (2013). Purinergic receptors in microglia: Functional modal shifts of microglia mediated by P2 and P1 receptors. *Glia* 61, 47–54. doi:10.1002/glia.22358

Kronlage, M., Song, J., Sorokin, L., Isfort, K., Schwerdtle, T., Leipziger, J., et al. (2010). Autocrine purinergic receptor signaling is essential for macrophage chemotaxis. *Sci. Signal* 3 (132), ra55. doi:10.1126/scisignal.2000588

KyrargyriMadry, V. C., Rifat, A., Arancibia-Carcamo, I. L., Jones, S. P., and Chan, V. T. T. (2020). P2Y13 receptors regulate microglial morphology, surveillance, and resting levels of interleukin 1β release. *Glia* 68, 328–344. doi:10.1002/glia.23719

Levin, S., and Godukhin, O. (2017). Modulating effect of cytokines on mechanisms of synaptic plasticity in the brain. *Biochem. Mosc* 82, 264–274. doi:10.1134/S000629791703004X

Li, J., Rubini, P., Tang, Y., and Illes, P. (2022). Astrocyte-derived ATP: A new etiological factor for autism spectrum disorder. *Neurosci. Bull. Jan.* 38 (1), 104–106. Epub 2021 Nov 8. doi:10.1007/s12264-021-00788-4

Liverani, E., Kilpatrick, L. E., Tsygankov, A. Y., and Kunapuli, S. P. (2014). The role of P2Y$_{12}$ receptor and activated platelets during inflammation. *Curr. Drug T Argets.* 15, 720–728. doi:10.2174/1389450115666140519162133

Lou, N., Takano, T., Pei, Y., Xavier, A. L., Goldman, S. A., and Nedergaard, M. (2016). Purinergic receptor P2RY12-dependent microglial closure of the injured blood-brain barrier. *Proc. Natl. Acad. Sci. U. S. A.* 113, 1074–1079. doi:10.1073/pnas.1520398113

Madry, C., Kyrargyri, V., Arancibia-Cárcamo, I. L., Jolivet, R., Kohsaka, S., Bryan, R. M., et al. (2018). Microglial ramification,surveillance, and interleukin-1β release are regulated by the two-pore domain K+ channel THIK-1. *Neuron* 97, 299–312. doi:10.1016/j.neuron.2017.12.002

Mansour, A., Bachelot-Loza, C., Nesseler, N., Gaussem, P., and Gouin-Thibault, I. (2020). P2Y12 inhibition beyond thrombosis: Effects on inflammation. *Int. J. Mol. Sci.* 21, 1391. doi:10.3390/ijms21041391

Mildner, A., Huang, H., Radke, J., Stenzel, W., and Priller, J. (2017). P2Y12 receptor is expressed on human microglia under physiological conditions throughout development and is sensitive to neuroinflammatory diseases. *Glia* 65, 375–387. doi:10.1002/glia.23097

Milior, G., Morin-Brureau, M., Chali, F., Duigou, C. L., Savary, E., Huberfeldet, G., et al. (2020). Distinct P2Y receptors mediate extension and retraction of microglial processes in epileptic and peritumoral human tissue. *J. Neurosci.* 40, 1373–1388. doi:10.1523/JNEUROSCI.0218-19.2019

Mo, M., Eyo, U. B., Xie, M., Peng, J., Bosco, D. B., Umpierre, A. D., et al. (2019). Microglial P2Y12 receptor regulates seizure-induced neurogenesis and immature neuronal projections. *J. Neurosci.* 39, 9453–9464. doi:10.1523/JNEUROSCI.0487-19.2019

Moore, C. S., Ase, A. R., Kinsara, A., Rao, V. T., Michell-Robinson, M., Leong, S. Y., et al. (2015). P2Y12 expression and function in alternatively activated human microglia. *Neurol. Neuroimmunol. Neuroinflamm* 2, e80. doi:10.1212/NXI.0000000000000080

Nasu-Tada, K., Koizumi, S., and Inoue, K. (2005). Involvement of beta1 integrin in microglial chemotaxis and proliferation on fibronectin: Different regulations by ADP through PKA. *Glia* 52 (2), 98–107. doi:10.1002/glia.20224

Nie, X. Y., Li, J. L., Zhang, Y., Xu, Y., Yang, X. L., Fu, Y., et al. (2017). Haplotype of platelet receptor P2RY12 gene is associated with residual clopidogrel on-treatment platelet reactivity. *J. Zhejiang Univ. Sci. B* 18, 37–47. doi:10.1631/jzus.B1600333

Ohsawa, K., Irino, Y., Sanagi, T., Nakamura, Y., Suzuki, E., Inoue, K., et al. (2010). P2Y12 receptor-mediated integrin-beta1 activation regulates microglial process extension induced by ATP. *Glia* 58, 790–801. doi:10.1002/glia.20963

Ohsawa, K., IrinoNakamuraAkazawa, Y. Y. C., Inoue, K., and Kohsaka, S. (2007). Involvement of P2X4 and P2Y12 receptors in ATP-induced microglial chemotaxis. *Glia* 55, 604–616. doi:10.1002/glia.20489

Ohsawa, K., and Kohsaka, S. (2011). Dynamic motility of microglia: Purinergic modulation of microglial movement in the normal and pathological brain. *Glia* 59, 1793–1799. doi:10.1002/glia.21238

Perucca, E. J. (2021). The pharmacological treatment of epilepsy:recent advances and future perspectives. *Perucca Acta Epileptol.* 3, 22. doi:10.1186/s42494-021-00055-z

Pineda, E., Shin, D., You, S. J., Auvin, S., Sankar, R., and Mazarati, A. (2013). Maternal immune activation promotes hippocampal kindling epileptogenesis in mice. *Ann. Neurol.* 74, 11–19. doi:10.1002/ana.23898

Pitkanen, A., Lukasiuk, K., Dudek, F. E., and Staley, K. J. (2015). Epileptogenesis. *Cold Spring Harb. Perspect. Med.* 5, a022822. doi:10.1101/cshperspect.a022822

Pitkanen, A., and Engel, J., Jr. (2014). Past and present definitions of epileptogenesis and its biomarkers. *Neurotherapeutics* 11, 231–241. doi:10.1007/s13311-014-0257-2

Pitkänen, A., and Lukasiuk, K. (2011). Mechanisms of epileptogenesis and potential treatment targets. *Lancet Neurol.* 10, 173–186. doi:10.1016/S1474-4422(10)70310-0

Postnikova, T., Zubareva, O., Kovalenko, A., Kim, K., Magazanik, L., and Zaitsev, A. (2017). Status epilepticus impairs synaptic plasticity in rat hippocampus and is followed by changes in expression of NMDA receptors. *Biochem. Mosc* 82, 282–290. doi:10.1134/S0006297917030063

Quintas, C., Fraga, S., Goncalves, J., and Queiroz, G. (2011). Opposite modulation of astroglial proliferation by adenosine 5′-O-(2-thio)-diphosphate and 2-methylthioadenosine-5′-diphosphate: Mechanisms involved. *Neuroscience* 182, 32–42. doi:10.1016/j.neuroscience.2011.03.009

Quintas, C., Pinho, D., Pereira, C., Saraiva, L., Goncalves, J., and Queiroz, G. (2014). Microglia P2Y$_6$ receptors mediate nitric oxide release and astrocyte apoptosis. *J. Neuroinflammation* 11, 141. doi:10.1186/s12974-014-0141-3

Raju, N. C., Eikelboom, J. W., and Hirsh, J. (2008). Platelet ADP-receptor antagonists for cardiovascular disease: Past, present and future. *Nat. Clin. Pract. Cardiovasc Med.* 5, 766–780. doi:10.1038/ncpcardio1372

Rana, A., and Musto, A. E. (2018). The role of inflammation in the development of epilepsy. *J. Neuroinflammation* 15, 144. doi:10.1186/s12974-018-1192-7

Rauch, B. H., Rosenkranz, A. C., Ermler, S., Böhm, A., Driessen, J., Fischer, J. W., et al. (2010). Regulation of functionally active P2Y12 ADP receptors by thrombin in human smooth muscle cells and the presence of P2Y12 in carotid artery lesions. *Arterioscler. Thromb. Vasc. Biol.* 30, 2434–2442. doi:10.1161/ATVBAHA.110.213702

Rees, M. I. (2010). The genetics of epilepsy–the past, the present and future. *Seizure* 19, 680–683. doi:10.1016/j.seizure.2010.10.029

Rho, J. M., and Boison, D. (2022). The metabolic basis of epilepsy. *Nat. Rev. Neurol.* 18, 333–347. doi:10.1038/s41582-022-00651-8

Ribeiro, D. E., Petiz, L. L., Glaser, T., Tang, Y., Resende, R. R., Ulrich, H., et al. (2022). Purinergic signaling in cognitive impairment and neuropsychiatric symptoms of Alzheimer's disease. *Neuropharmacology* 226, 109371. Epub 2022 Dec 9. doi:10.1016/j.neuropharm.2022.109371

Rincon, N., Barr, D., and Velez-Ruiz, N. (2021). Neuromodulation in drug resistant epilepsy. *Aging Dis.* 12, 1070–1080. doi:10.14336/AD.2021.0211

Rivera, A., Vanzulli, I., and Butt, A. M. (2016). A central role for ATP signalling in glial interactions in the CNS. *Curr. Drug T Argets.* 17, 1829–1833. doi:10.2174/1389450117666160711154529

Roseti, C., van Vliet, E., Cifelli, P., Ruffolo, G., Baayen, J. C., Di Castro, M. A., et al. (2015). GABAA currents are decreased by IL-1βin epileptogenic tissue of patients with temporal lobe epilepsy: Implications for ictogenesis. *Neurobiol. Dis.* 82, 311–320. doi:10.1016/j.nbd.2015.07.003

Samuelsson, A., Jennische, E., Hansson, H. A., and Holmäng, A. (2005). Prenatal exposure to interleukin-6 results in inflammatory neurodegeneration in hippocampus with NMDA/GABAA dysregulation and impaired spatial learning. *AJP* 290, R1345–R1356. doi:10.1152/ajpregu.00268.2005

Sarmast, S. T., Abdullahi, A. M., and Jahan, N. (2020). Current classification of seizures and epilepsies: Scope, limitations and recommendations for future action. *Cureus* 12, e10549. doi:10.7759/cureus.10549

Sayyah, M., Javad-Pour, M., and Ghazi-Khansari, M. (2003). The bacterial endotoxin lipopolysaccharide enhances seizure susceptibility in mice: Involvement of proinflammatory factors: Nitric oxide and prostaglandins. *Neuroscience* 122, 1073–1080. doi:10.1016/j.neuroscience.2003.08.043

Sipe, G. O., Lowery, R. L., Tremblay, M. È., Kelly, E. A., Lamantia, C. E., and Majewska, A. K. (2016). Microglial P2Y12 is necessary for synaptic plasticity in mouse visual cortex. *Nat. Commun.* 7, 10905. doi:10.1038/ncomms10905

Sueri, C., Gasparini, S., Balestrini, S., Labate, A., Gambardella, A., Russo, E., et al. (2018). Diagnostic biomarkers of epilepsy. *Curr. Pharm. Biotechnol.* 19 (6), 440–450. doi:10.2174/1389201019666180713095251

Suyama, S., Sunabori, T., Kanki, H., Sawamoto, K., Gachet, C., Koizumi, S., et al. (2012). Purinergic signaling promotes proliferation of adult mouse subventricular zone cells. *J. Neurosci.* 32, 9238–9247. doi:10.1523/JNEUROSCI.4001-11.2012

Suzuki, T., Kohyama, K., Moriyama, K., Ozaki, M., Hasegawa, S., Ueno, T., et al. (2020). Extracellular ADP augments microglial inflammasome and NF-κB activation via the P2Y12 receptor. *Eur. J. Immunol.* 50 (2), 205–219. doi:10.1002/eji.201848013

Takasaki, J., Kamohara, M., Saito, T., Matsumoto, M., Matsumoto, S., Ohishi, T., et al. (2001). Molecular cloning of the platelet P2T(AC) ADP receptor: Pharmacological comparison with another ADP receptor, the P2Y(1) receptor. *Mol. Pharmacol.* 60, 432–439.

Terrone, G., Salamone, A., and Vezzani, A. (2017). Inflammation and Epilepsy: preclinical findings and potential clinical translation. *Curr. Pharm. Des.* 23, 5569–5576. doi:10.2174/1381612823666170926113754

Thijs, R. D., Surges, R., O'Brien, T. J., and Sander, J. W. (2019). Epilepsy in adults. *Lancet* 393, 689–701. doi:10.1016/S0140-6736(18)32596-0

Trinh, P. N. H., Baltos, J. A., Hellyer, S. D., May, L. T., and Gregory, K. J. (2022). Adenosine receptor signalling in Alzheimer's disease. *Purinergic Signal. Sep.* 18 (3), 359–381. Epub 2022 Jul 23. doi:10.1007/s11302-022-09883-1

van der Wildt, B., Janssen, B., Pekošak, A., Stéen, E. J. L., Schuit, R. C., Kooijman, E. J. M., et al. (2022). Novel thienopyrimidine-based PET tracers for P2Y12 receptor imaging in the brain. *ACS Chem. Neurosci.* 12, 4465–4474. doi:10.1021/acschemneuro.1c00641

Vezzani, A., French, J., Bartfai, T., and Baram, T. Z. (2010). The role of inflammation in epilepsy. *Nat. Rev. Neurol.* 7, 31–40. doi:10.1038/nrneurol.2010.178

Vezzani, A., and Granata, T. (2005). Brain inflammation in epilepsy: Experimental and clinical evidence. *Epilepsia* 46 (11), 1724–1743. doi:10.1111/j.1528-1167.2005.00298.x

Villa, A., Klein, B., Janssen, B., Pedragosa, J., Pepe, G., Zinnhardt, B., et al. (2018). Identification of new molecular targets for PET imaging of the microglial anti-inflammatory activation state. *Theranostics* 8, 5400–5418. doi:10.7150/thno.25572

Viviani, B., Bartesaghi, S., Gardoni, F., Vezzani, A., Behrens, M. M., Bartfai, T., et al. (2003). Interleukin-1beta enhances NMDA receptor-mediated intracellular calcium increase through activation of the Src family of kinases. *J. Neurosci.* 23, 8692–8700. doi:10.1523/JNEUROSCI.23-25-08692.2003

Wang, Q., Shi, N. R., Lv, P., Liu, J., Zhang, J. Z., Liu, J., et al. (2022). P2Y12 receptor gene polymorphisms are associated with epilepsy. *Purinergic Signal* 19, 155–162. doi:10.1007/s11302-022-09848-4

Wihlborg, A. K., Wang, L., Braun, O. O., Eyjolfsson, A., Gustafsson, R., Gudbjartsson, T., et al. (2004). ADP receptor P2Y12 is expressed in vascular smooth muscle cells and stimulates contraction in human blood vessels. *Arterioscler. Thromb. Vasc. Biol.* 24, 1810–1815. doi:10.1161/01.ATV.0000142376.30582.ed

Wong, Z. W., and Engel, T. (2022). More than a drug target: Purinergic signalling as a source for diagnostic tools in epilepsy. *Neuropharmacology* 222, 109303. doi:10.1016/j.neuropharm.2022.109303

Zhang K, K., Zhang, J., Gao, Z. -G., König, R., Quint, S., Kohlmann, J., et al. (2014). Structure of the human P2Y 12 receptor in complex with an antithrombotic drug. *Nature* 509, 115–118. doi:10.1038/nature13083

Zhang, Y., Peti-Peterdi, J., Müller, C. E., Carlson, N. G., Baqi, Y., Strasburg, D. L., et al. (2015). P2Y12 receptor localizes in the renal collecting duct and its blockade augments arginine vasopressin action and alleviates nephrogenic diabetes insipidus. *J. Am. Soc. Nephrol.* 26, 2978–2987. doi:10.1681/ASN.2014010118

Zhang Y, Y., Chen, K., Sloan, S. A., Bennett, M. L., Scholze, A. R., O'Keeffe, S., et al. (2014). An RNA-sequencing transcriptome and splicing database of glia, neurons, and vascular cells of the cerebral cortex. *J. Neurosci.* 34, 11929–11947. doi:10.1523/JNEUROSCI.1860-14.2014

Zimmermann, H. (2006). Ectonucleotidases in the nervous system. *Novartis Found. Symp.* 276, 113–128. discussion 128-30, 233-7, 275-81.

frontiers | Frontiers in Pharmacology

TYPE Original Research
PUBLISHED 16 October 2023
DOI 10.3389/fphar.2023.1241406



OPEN ACCESS

EDITED BY
Elena Adinolfi,
University of Ferrara, Italy

REVIEWED BY
Peter Illes,
Leipzig University, Germany
Bernadeta Szewczyk,
Polish Academy of Sciences, Poland

*CORRESPONDENCE
Beáta Sperlágh,
sperlagh@koki.hu

RECEIVED 16 June 2023
ACCEPTED 28 September 2023
PUBLISHED 16 October 2023

CITATION
Iring-Varga B, Baranyi M, Gölöncsér F, Tod P and Sperlágh B (2023), The antidepressant effect of short- and long-term zinc exposition is partly mediated by P2X7 receptors in male mice. *Front. Pharmacol.* 14:1241406. doi: 10.3389/fphar.2023.1241406



# The antidepressant effect of short- and long-term zinc exposition is partly mediated by P2X7 receptors in male mice

Bernadett Iring-Varga[1,2], Mária Baranyi[1], Flóra Gölöncsér[1], Pál Tod[1] and Beáta Sperlágh[1,2]*

[1]Laboratory of Molecular Pharmacology, Institute of Experimental Medicine, Budapest, Hungary, [2]János Szentágothai Doctoral School, Semmelweis University, Budapest, Hungary

**Background:** As a member of the purinergic receptor family, divalent cation-regulated ionotropic P2X7 (P2rx7) plays a role in the pathophysiology of psychiatric disorders. This study aimed to investigate whether the effects of acute zinc administration and long-term zinc deprivation on depression-like behaviors in mice are mediated by P2X7 receptors.

**Methods:** The antidepressant-like effect of elevated zinc level was studied using a single acute intraperitoneal injection in C57BL6/J wild-type and P2rx7 gene-deficient (P2rx7 −/−) young adult and elderly animals in the tail suspension test (TST) and the forced swim test (FST). In the long-term experiments, depression-like behavior caused by zinc deficiency was investigated with the continuous administration of zinc-reduced and control diets for 8 weeks, followed by the same behavioral tests. The actual change in zinc levels owing to the treatments was examined by assaying serum zinc levels. Changes in monoamine and brain-derived neurotrophic factor (BDNF) levels were measured from the hippocampus and prefrontal cortex brain areas by enzyme-linked immunosorbent assay and high-performance liquid chromatography, respectively.

**Results:** A single acute zinc treatment increased the serum zinc level evoked antidepressant-like effect in both genotypes and age groups, except TST in elderly P2rx7 −/− animals, where no significant effect was detected. Likewise, the pro-depressant effect of zinc deprivation was observed in young adult mice in the FST and TST, which was alleviated in the case of the TST in the absence of functional P2X7 receptors. Among elderly mice, no pro-depressant effect was observed in P2rx7 −/− mice in either tests. Treatment and genotype changes in monoamine and BDNF levels were also detected in the hippocampi.

**Conclusion:** Changes in zinc intake were associated with age-related changes in behavior in the TST and FST. The antidepressant-like effect of zinc is partially mediated by the P2X7 receptor.

KEYWORDS

**purinergic receptor, P2X7, depression, zinc, behavior**

# 1 Introduction

Major depressive disorder (MDD) is the most common psychiatric disorder, affecting 300 million people worldwide, regardless of age or sex, and causes an extremely high social and economic burden (Trivedi, 2020). A diagnosis of this mental condition requires a substantial mood change lasting at least 2 weeks, such as sadness or irritability, accompanied by a variety of psychophysiological changes, such as decreased sleep or sexual desire, lack of appetite, lethargy, and at its most extreme, suicidal thoughts (Belmaker and Agam, 2008). However, with the development of our knowledge about its pathophysiology and the expanding range of antidepressants, still 29%–46% of patients refuse to take the drugs prescribed by the physician for an inadequate response or at delayed effect (Fava and Davidson, 1996; Schroder et al., 2022). Most antidepressants target the inhibition of transporters responsible for the reuptake of monoamines (Artigas et al., 2002) or stimulation of monoaminergic transmission by other mechanisms (Maes, 1999; Schumacher et al., 2005). In addition, promising research supports the use of the N-methyl-D-aspartate (NMDA) receptor antagonist ketamine in the treatment of MDD and posttraumatic stress disorder (Ates-Alagoz and Adejare, 2013; Sachdeva et al., 2023).

As a complex disease, both genetic and environmental factors play key roles in its development. Several chromosomal regions may be involved in the development of mood disorders (Caspi et al., 2003; Roceri et al., 2004), such as purinergic receptor family member P2X7 (P2rx7) gain-of-function polymorphism (Czamara et al., 2018; Wingo et al., 2021), the role of which in the development of major depression remains controversial (Viikki et al., 2011; Feng et al., 2014). This structure is a non-selective cation channel that belongs to the P2X receptor family, which is sensitive to high ATP concentrations (Sperlagh et al., 2006). It is expressed on many cells of the human body, such as hematopoietic and immune cells, glial cells of the central and peripheral nervous system, central neurons, and hippocampal–cortical pyramidal cells and interneurons. The expression of the P2X7 receptor by neurons remains a subject of longstanding debate (Illes et al., 2017; Miras-Portugal et al., 2017). It modulates neurotransmitter release (Sperlagh et al., 2006; Sperlagh and Illes, 2007), and its activity is attributed to the influx of $Ca^{2+}$ and an increase in the release of glutamate and gamma amino-butyric acid (GABA) from nerve endings (Alloisio et al., 2008) and different areas of the brain (Sperlagh et al., 2002). P2X receptor-mediated currents are modulated by divalent cations, including $Zn^{2+}$ (Acuna-Castillo et al., 2007; Drevets et al., 2022). The receptor-mediated ion current is inhibited through the direct binding site of the extracellular loop (Kasuya et al., 2016) owing to allosteric modulation by agonist binding (Virginio et al., 1997). In terms of the inhibitory effect of divalent metal cations, zinc ranks first in terms of P2rx7 activation. The amino acids involved in this process are histidine and aspartic acid. According to previous measurements, the median inhibition concentration of $Zn^{2+}$ upon activation of mP2X7R is 183 ± 22 μM (Fujiwara et al., 2017).

Several animal experiments on rodents, have demonstrated the involvement of P2rx7 in the pathophysiology of depression. Inhibition of this receptor prevents depression-like behavior in mice (Kongsui et al., 2014; Iwata et al., 2016; Otrokocsi et al., 2017; Ribeiro et al., 2019a; Huang and Tan, 2021), and deletion of the receptor itself results in antidepressant-like behavior (Csolle et al., 2013a). The development of antidepressants that inhibit the P2X7 receptor is currently in the clinical phase (Bhattacharya and Jones, 2018; Drevets et al., 2022) for the treatment of therapy-resistant depression.

Zinc (Zn) is one of the most important essential trace element in the human body and is concentrated in glutamatergic synaptic vesicles. Changes in the extracellular and intracellular concentrations can lead to compromised homeostasis, which can cause or exacerbate psychiatric disorders (Ranjbar et al., 2013; Szewczyk et al., 2018). The hippocampus is the most zinc-rich region of the brain, where high concentrations of zinc are found in the mossy fiber terminals of the CA3 region, which use glutamate as a transmitter (Williams and Undieh, 2010). Zn is released into the extracellular space during neural activity and modulates ion channels (e.g., NMDA and AMPA) that are associated with abnormalities in depression tests. Short-term zinc deficiency causes depression-like behavior as observed in the tail suspension test (TST) and forced swim test (FST) in animals (Whittle et al., 2009; Mlyniec et al., 2012; Mlyniec and Nowak, 2012). Long-term zinc deprivation, lasting 2 weeks, also results in depression-like behavior; however, in this case, measurable differences can be observed in the hippocampal monoamine and zinc content in animals (Tamano et al., 2009), as well as in their serum corticosterone levels (Watanabe et al., 2010). Increased zinc levels as a result of various treatments induce antidepressant-like behavioral patterns in animals, and the immobility time decreases in these tests (Nowak et al., 2003; Szewczyk et al., 2019). Research to measure depression was also carried out in connection with the importance of the age of the animals (Shoji and Miyakawa, 2019), where the FST results may reflect a stronger panic-like response to a sudden aversive stimulus in aged animals, which showed greater immobility than younger mice. In contrast, aged mice showed less immobility than young mice in the TST, suggesting a reduction in depression-related behavior in aged mice. In human studies, serum zinc concentration has been proposed as a potential biomarker for the detection of MDD (Styczen et al., 2017). The concentration of zinc in the serum of patients with MDD was <0.12 μg/mL, whereas that of the control group was 0.66–1.10 μg/mL (Wang et al., 2018). This value fluctuated over a 24-h period; its change reached 20% depending on the food consumed (Roohani et al., 2013).

In this study, we investigated whether the acute administration of zinc in its active form of zinc ion ($Zn^{2+}$) as a $ZnCl_2$ solution induces antidepressant-like behavior in the presence or absence of P2X7 receptors. To examine the long-term effect of Zn, mice were fed different Zn-containing controlled diets for 8 weeks. As a result of aging, mice react more sensitively to changes in Zn homeostasis in behavioral experiments. To understand the molecular pathways, we measured monoamine content and brain-derived neurotrophic factor (BDNF) levels in the hippocampus (HC) and prefrontal cortex (PFC). However, zinc-induced antidepressant-like behaviors and changes in behaviors elicited by zinc deprivation in the diet were not consistently eliminated in P2rx7 gene-deficient animals, indicating that the effect of the micronutrient is partially mediated by the receptor.

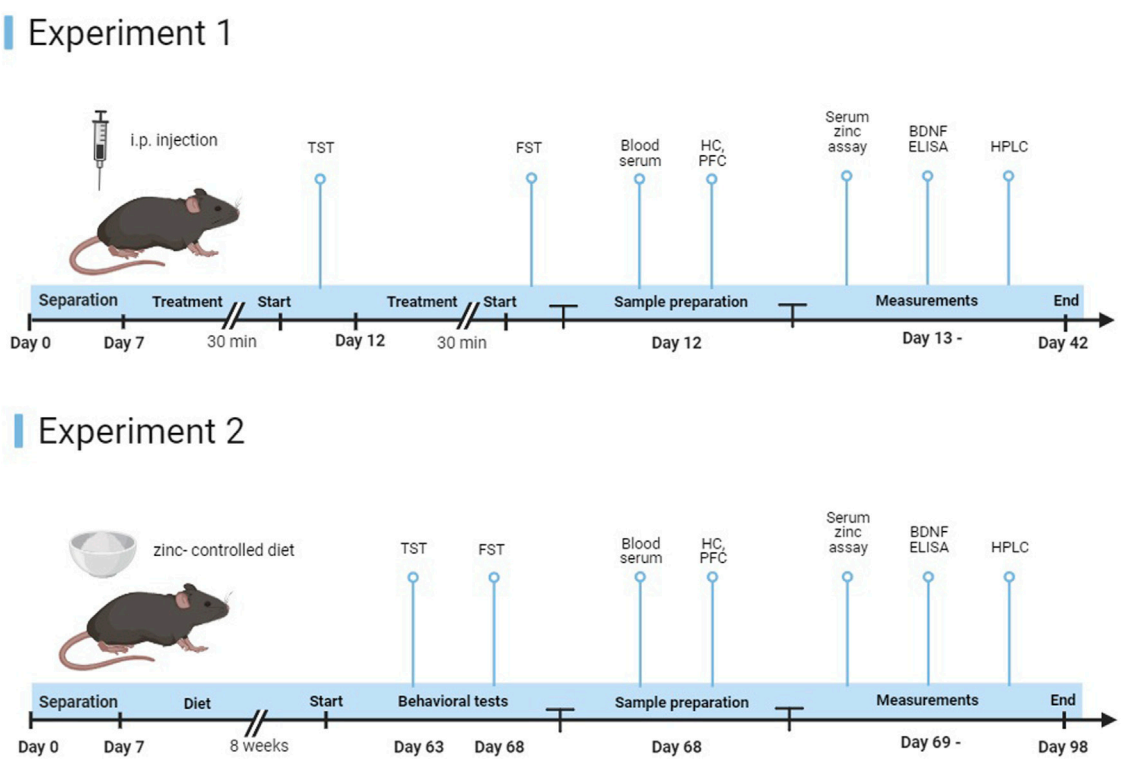


FIGURE 1
Representation of the study timeline. In experiment 1, young and elderly animals received a single intraperitoneal injection of $ZnCl_2$ (1 mg/kg) solution or saline, 30 min before the start of the experiments. After behavioral tests, mice were euthanized ($n$ = 8–11 animals/group). In experiment 2, after the 8-week protocol, we started behavioral experiments, followed by euthanasia of the mice ($n$ = 8–11 animals/group).

# 2 Materials and methods

## 2.1 Animals

In this study, behavioral tests and subsequent measurements were performed on 2–3-month "young" (average weight: 30 g) and 16–18-month "elderly" (average weight: 40 g), wild-type P2rx7 +/+ and knockout P2rx7 −/− C57Bl/6J male mice. Preliminary experiments were performed on young 2–3-month-old wild-type and knockout male and female (average weight: 22 g) C57Bl/6J animals. The original breeding pairs of P2rx 7-/- mice were kindly supplied by Christopher Gabel (Pfizer Inc., Groton CT, United States). The breeding and genotyping strategy protocol is described in details in our previous study (Csolle et al., 2013b). All mice in the experiment were housed on a 12 h-on/12 h-off light cycle at controlled temperature (23°C ± 2°C) and humidity (60% ± 10%) in individual plastic cages with *ad libitum* access to food and water. Rodents, such as mice, strongly compete to establish dominance hierarchies in their natural and artificial laboratory environments (Poshivalov, 1980; Capanna et al., 1984). The animals were individually housed to exclude possible confounding effects caused by competition. Preliminary validation experiments indicated that the pre-experiment separation of the animals, although it might have its own effect on behavior, is necessary to reveal consistent antidepressant effects in behavioral tests under our experimental conditions. Experiments and treatments were performed between 9:00 and 13:00 during the light phase (7:00–19:00). All efforts were made to minimize suffering and reduce the number of animals used. All experimental procedures were approved by the local Animal Care Committee of the Institute of Experimental Medicine (Budapest, Hungary, ref. no. PEI/EA/900-7/2020) in accordance with the Institutional Ethical Codex and Hungarian Act of Animal Care and Experimentation guidelines (40/2013, II.14). To use the appropriate number of animals, G*Power 3.1.9.7 software was used to calculate the sample size. For the calculation, we used the main experimental set-up as a basis, thus comparing two groups, WT SAL + WT 1 mg/kg $ZnCl_2$, with the following parameters: ANOVA fixed effects, 2-way: *a priori*: compute required sample size; α error probability: 0.05; power: 0.9; effect size: 1.987. Based on these settings, the use of an average of seven animals per group was recommended.

## 2.2 Treatment protocols

Two different experimental designs were used (Figure 1).

### 2.2.1 Acute treatment

The first experimental protocol tested the antidepressant effects of a zinc solution. Mice were fed a standard laboratory diet (18 mg M Zn/kg, equivalent to 50 mg/kg zinc sulfate monohydrate, S8189-S095, Ssniff). Prior to each experiment, the animals were treated with an acute intraperitoneal (i.p.) 1 mg/kg $ZnCl_2$ (Sigma-Aldrich,

United States) solution (0.48 mg M Zn/kg). As a control, physiological saline (0.9% NaCl) was added as previously described. Behavioral experiments (TST and FST) were started 30 min after treatments. The animals were euthanized immediately after the completion of the behavioral tests.

### 2.2.2 Long-term zinc-controlled diets

To study the long-term effect of zinc on mood-related behavior, in the second experimental protocol, P2rx7 +/+ and −/− mice were fed a higher (23 mg M Zn/kg, which is equivalent to 35 mg/kg zinc-carbonate D10012M, Research Diets) and lower zinc-supplemented and zinc-deficient (4 mg M Zn/kg, did not contain an added source of zinc, D19041002, Research Diets) diet for 8 weeks. Behavioral experiments began after the 2-month period.

## 2.3 Behavioral tests

### 2.3.1 Tail suspension test

To assess depression-like behavior (Cryan, Mombereau, and Vassout, 2005), experiments were performed using an automated instrument (BIO-TST2, Bioseb, France). The device was connected to a computer that recorded the movement of the animals in real-time. In each trial, three animals were suspended using an adhesive tape placed 1–2 centimeters from the end of their tails. Each chamber was activated 5 s after the last mouse was placed, and the measurements lasted for 6 min. The immobility time during the test was measured in seconds. In some cases, the animals (0%–16%) showed an abnormal movement pattern for the experiment, e.g., climbing on the hook and clinging to the wall of the device. These animals were excluded from the calculations in the *post hoc* analysis.

### 2.3.2 Forced swim test

The FST series of experiments can be used to detect depression-like phenotypes (Porsolt et al., 1977). The behavioral tests were performed one after the other 5 days apart. Similar to the previous behavioral experiment, the acutely treated animals received an i.p. injection 30 min before the start of the test. The immobility of mice is authoritative when they stop swimming, making movements only to keep their heads above the water surface. The animals were placed in a 2-L (height: 25 cm; diameter: 10 cm) clear glass cylinder (water temperature: 20° ± 2°C) filled to the same water level. The experiment lasted for 6 min for each case. In one study, four animals were simultaneously tested, the water was changed to fresh water, and the rollers were wiped clean before starting a new series of experiments. To prevent the animals from cooling, wipes were placed into their cages to soak up excess water. The results were evaluated using Noldus Observer XT software (Wageningen, Netherlands). The swimming time of the mice was expressed in seconds, and the final value was obtained as a percentage (%) of floating time/experimental time.

## 2.4 Biochemical analyses

### 2.4.1 Sample preparation

Immediately after the last behavioral experiment, the animals were anesthetized by isoflurane inhalation for blood collection from the inferior vena cava in 2-mL untreated collection tubes. Blood samples were allowed to stand at room temperature (20°C–25°C) for 1 h. Then, they were centrifuged for 15 min at 1,500 x g at 4°C (Megafuge 1.0 R, Heraeus, Germany), and the serum was used for zinc level determination. The samples were stored at −20°C before the assay. After serum collection, the mice were quickly decapitated to remove the HC and PFC. The brain areas were quickly stabilized with liquid nitrogen prior to high-performance liquid chromatography (HPLC) measurements. To measure BDNF protein levels, the prepared brain areas were placed on dry ice and stored at −20°C until homogenization. All samples were used for measurements within 1 month of the euthanization of the experimental animals.

### 2.4.2 Serum zinc concentration

The frozen samples were thawed at room temperature prior to use. A sensitive fluorometric kit (ab176725, Abcam, United States) was used for quantitative assays. Then, 50 µL of the thawed samples and standard zinc solution was pipetted into a 96-well plate. A detection solution was added to each sample to achieve a final concentration of 100 µL/well. The zinc in the sample bound with high specificity to the zinc detector in the solution, and the zinc probe exhibited a large and greatly increased fluorescence upon exposure to $Zn^{2+}$. We determined the fluorescence increase using a multi-mode plate reader at Ex/Em = 485/525 nm (Cytation™5 Cell Imaging Multi-Mode Reader, BioTek, United States). Zn concentrations (ng/mL) were calculated using GraphPad (GraphPad Software Inc., United States).

### 2.4.3 Determination of tissue monoamine content

Catechol and indole amines in the tissue extracts were measured by HPLC. The brain tissue homogenate concentration in C57BL/6 and P2X7 receptor-deficient mice was 100 mg/mL. The extract was prepared from hippocampus and prefrontal cortex brain area samples in an ultrasonic homogenizer with 0.1 M perchloric acid (PCA) solution containing theophylline (as an internal standard) at 10 µM concentration and 0.5 mM sodium metabisulphite (antioxidant for biogenic amines). The tissue extract was centrifuged at 3,510 *g* for 10 min at 4°C, and the pellet was saved for protein measurement according to Lowry et al. (1951). Perchloric anions in the supernatant were precipitated using 4 M dipotassium phosphate and removed by centrifugation. Samples were stored at −20°C until analysis, and 10 µL was used for separation. Quantification of the monoamines, noradrenaline (NA), dopamine (DA), and serotonin (5-HT), was performed using an online column switching liquid chromatographic technique. The solid phase extraction was carried out on an HALO Phenyl-Hexyl (75 × 2.1 mm I.D., 5 µm) column, and for separation, it was coupled to an ACE UltraCore SuperC18 (150 × 2.1 mm I.D., 5 µm) analytical column. The flow rate of the mobile phases ["A" 10 mM potassium phosphate, 0.25 mM EDTA "B" with 0.45 mM octane sulphonyl acid sodium salt, 8% acetonitrile (v/v), and 2% methanol (v/v), pH 5.2] was 250 µL/min in a step gradient application (Baranyi et al., 2006). A Shimadzu LC-20 AD HPLC system was used. The signs of the sample components were collected using an Agilent UV (1100 series variable wavelength detector) and a (BAS CC-4) amperometer. Monoamines were electrochemically detected at an oxidation potential of 0.73 V, whereas the internal

standard was indicated by UV at 253 nm. Concentrations were calculated using a two-point calibration curve internal standard method: $(A_i \times f \times B)/(C \times D_i \times E)$ ($A_i$: area of the biogenic amine component; B: sample volume; C: injection volume; $D_i$: response factor of the 1 pmol biogenic amine standard; E: protein content of the sample; f: recovery factor of the internal Standard [IS area in calibration/IS area in actual].

### 2.4.4 BDNF protein assay

At the beginning of the measurement, the samples were removed from the freezer and weighed. The specimens were processed using a tissue tearor (Model 985370, BioSpec, United States). For homogenization, 250 µL 1-amino-9,10-dihydro-9,10-dioxo-4-[[4-(phenylamino)-3-sulfophenyl]amino]-2-anthracenesulfonic acid sodium salt (PSB) solution and 250 µL lysis buffer (pH = 7.4, 50 mM Tris HCL, 150 mM NaCl, 5 mM $CaCl_2$, 0.02% $NaN_2$, and 1% Triton X-100 with 0.1% protease inhibitor) were added to each sample. HC and PFC were sonicated at power level 2 using pulses at 1-s intervals for 10–15 s. Subsequently, the samples were centrifuged at 5,000 *g* for 5 min at 4°C. The supernatants were collected and used for the measurements. For the BDNF assays, we used a human/mouse BDNF DuoSet enzyme-linked immunosorbent assay (ELISA) kit (DY248, R&D Systems, United States) and a Pierce™ BCA Protein Assay Kit (23227, Thermo Fisher Scientific, United States). The optical density of the samples (OD) was determined at 450 nm (Cytation™5 Cell Imaging Multi-Mode Reader, BioTek, United States), and the level of BDNF expression (pg/mL) of each sample was calculated against the seven-point standard curve plotted with GraphPad (GraphPad Software Inc, United States). The assay detection limit was 20–1,500 pg/mL. To measure the total protein levels in the samples, absorbance was measured at 560 nm, and values were expressed in pg/mg protein.

## 2.5 Statistics

Statistical analyses were performed using GraphPad Prism software v.8.0.2. (GraphPad Software Inc., United States). All data were presented as the mean ± SEM of "n" determinations. In behavioral experiments, animals with incorrect movements were excluded from the analysis. Other possible outlier values were detected by the ROUT method (q = 1%) (Motulsky and Brown, 2006). Data from behavioral tests and biochemistry analyses were analyzed by two- and three-way ANOVA, followed by Tukey's *post hoc* test. For determination of monoamine content, data were expressed as the mean ± standard error of mean at pmol/mg protein concentration. Data processing, calculations, and graphical representation were performed using Microsoft Office Excel 2010, and the TIBCO Data Science Workbench was used for statistical analysis. The Kolmogorov–Smirnov test was used to examine the normality of all continuous variables in the measurement. Where the measured variables met the normality assumption, factorial analysis of variance (FR-ANOVA) was used. We determined group differences in HC and PFC monoamine variance caused by acute i.p. zinc administration and long-term feeding with zinc-supplemented and -deficient diets in young and elderly, wild-type and P2X7 receptor-deficient mice. The threshold for statistical significance was set at $p < 0.05$. For detailed statistical tests of all experiments, the n and *p*-values are given in Supplementary Table S1.

# 3 Results

## 3.1 The antidepressant effect of a single intraperitoneal $ZnCl_2$ treatment is not associated with the P2X7 receptor

In the acute animal studies, we hypothesized that a single intraperitoneal $ZnCl_2$ treatment would exert antidepressant effects. Preliminary experiments (30, 10, 3, 1, and 0.5 mg/kg $ZnCl_2$, converted: 14.39, 4.8, 1.44, and 0.24 mg M Zn/kg) were performed to determine the dose (Supplementary Figures S1A–E). Higher doses caused more toxic effects; therefore, 1 mg/kg was selected for subsequent experiments (Supplementary Figures S1. F). To assess whether acute inhibition of P2rx7 with zinc can modify locomotor behavior, we performed an open field test (OFT) (Supplementary Material S1) on young, acutely treated male mice. $ZnCl_2$ treatment did not affect the activity of wild-type and P2X7 KO mice compared to saline-treated groups, and there was no significant difference in the locomotion of WT and P2X7 KO mice after i.p. administration (Supplementary Figure S2).

Confirming the results described in previous studies (Basso et al., 2009; Csolle et al., 2013a), P2rx7 deficiency elicited an antidepressant-like effect in male mice (Figure 2A). As a result of 1 mg/kg zinc solution, both the immobility and floating time of the mice in TST and FST, respectively, were substantially reduced in P2rx7 +/+ young adult animals. These effects were replicated in P2rx7 −/− mice, suggesting that the antidepressant-like effect of acute zinc treatment was negligibly mediated by P2X7 receptors (Figure 2A). We tested the antidepressant-like effects of zinc in young adult female mice. No differences were observed between the saline-treated wild-type and P2rx7-deficient animals. Moreover, 1 mg/kg zinc administration substantially increased the immobility time of wild-type animals in the TST, but not in the FST. No effects of acute zinc treatment were observed in female P2rx7-deficient mice (Supplementary Figure S3).

Identical experiments were performed using elderly male mice. No significant differences were observed among the genotypes of these animals (Figure 2B). In the TST, zinc treatment caused a decrease in the immobility time in wild-type animals; however, in P2rx7-deficient animals, zinc did not have a significant effect. In the FST, zinc treatment substantially decreased the immobility of both P2rx7 +/+ and P2rx7 −/− mice, with an overall genotype effect, but without a significant interaction. Because the effect of the treatment was also observed in knockout animals, it can be concluded that besides the TST in elderly animals, the effect of a single $ZnCl_2$ injection is not mediated by the P2X7 receptor.

To verify the effect of acute zinc injection, we measured serum zinc concentrations in the blood after the injections, which displayed substantial elevations in both young adults and elderly mice of both genotypes (Figures 3A, B).

## 3.2 The zinc-deficient diet caused depression-like behavior in young and elderly animals, which was partly mediated by the P2X7 receptor

Next, we compared the effect of a zinc-containing diet over a 2-month period on the behavior of male mice with no zinc

10.3389/fphar.2023.1241406

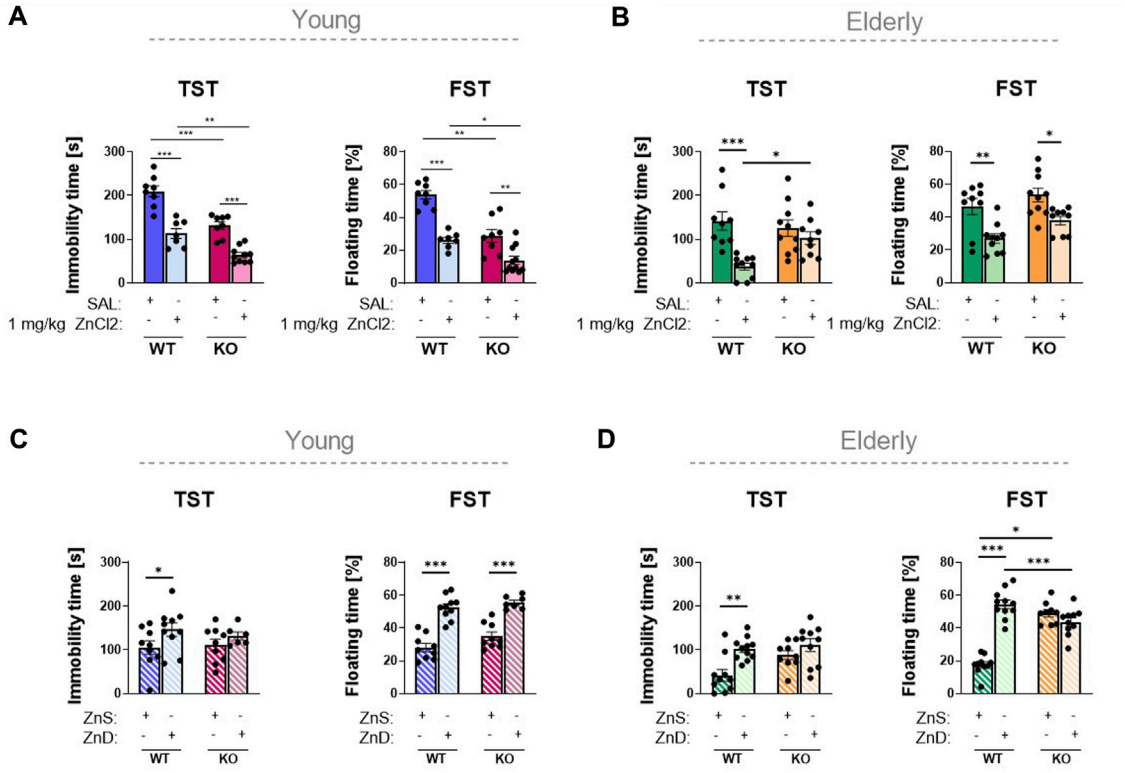


FIGURE 2
Investigation of the association between zinc content and depression in animal experiments **(A–D)**. P2rx7 +/+ control or P2rx7 −/− mice were treated with a single intraperitoneal injection of 1 mg/kg $ZnCl_2$ or saline in young ($n$ = 7–11) **(A)** and elderly ($n$ = 9–10) **(B)** animals. In the long-term experiments, wild-type or P2rx7-KO young ($n$ = 6–10) **(C)** and elderly ($n$ = 9–11) **(D)** animals were fed with a Zn-controlled diet. TST and FST behavior experiments were performed, the immobility or floating time is shown in the bar diagrams. Data are expressed as mean ± S.E.M. Data were analyzed by two-way ANOVA, followed by Tukey's test. *$p < 0.05$; **$p < 0.01$; ***$p < 0.001$. TST: tail suspension test; FST: forced swim test; WT: wild-type; KO: knockout; ZnS: zinc-supplemented diet; ZnD: zinc-deficient diet.

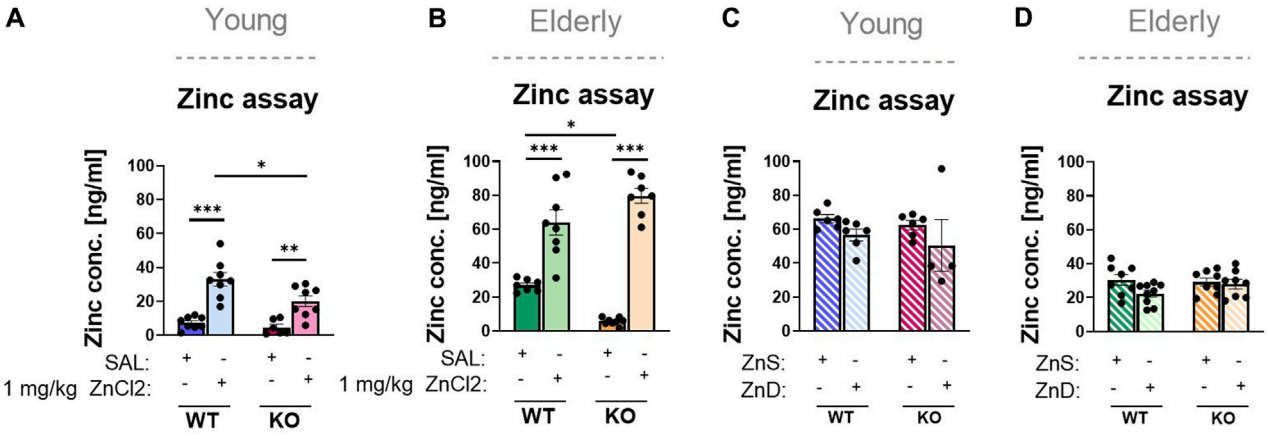


FIGURE 3
Results of zinc content in blood serum **(A–D)**. Wild-type and knock out, young ($n$ = 6–8) **(A)** and elderly ($n$ = 7–8) **(B)** mice were injected with an acute treatment of $ZnCl_2$ (1 mg/kg) or saline. P2rx7 +/+ and −/−, young ($n$ = 4–6) **(C)** and elderly (n = 8–9) **(D)** mice were fed a Zn-controlled diet. Data are expressed as mean ± S.E.M. Data were analyzed by two-way ANOVA, followed by Tukey's test. *$p < 0.05$; **$p < 0.01$; ***$p < 0.001$. WT: wild-type; KO: knockout; ZnS: zinc-supplemented diet; ZnD: zinc-deficient diet.

supplementation. As a result of the long-term experiments, relative zinc deficiency induced depression-like behavior in young mice, as reflected in longer immobility time in both TST and FST (Figure 2C). In contrast, no significant difference was detected in knockout animals that received either zinc-enriched or zinc-deprived diets in the TST, but not in the FST, indicating that the

10.3389/fphar.2023.1241406

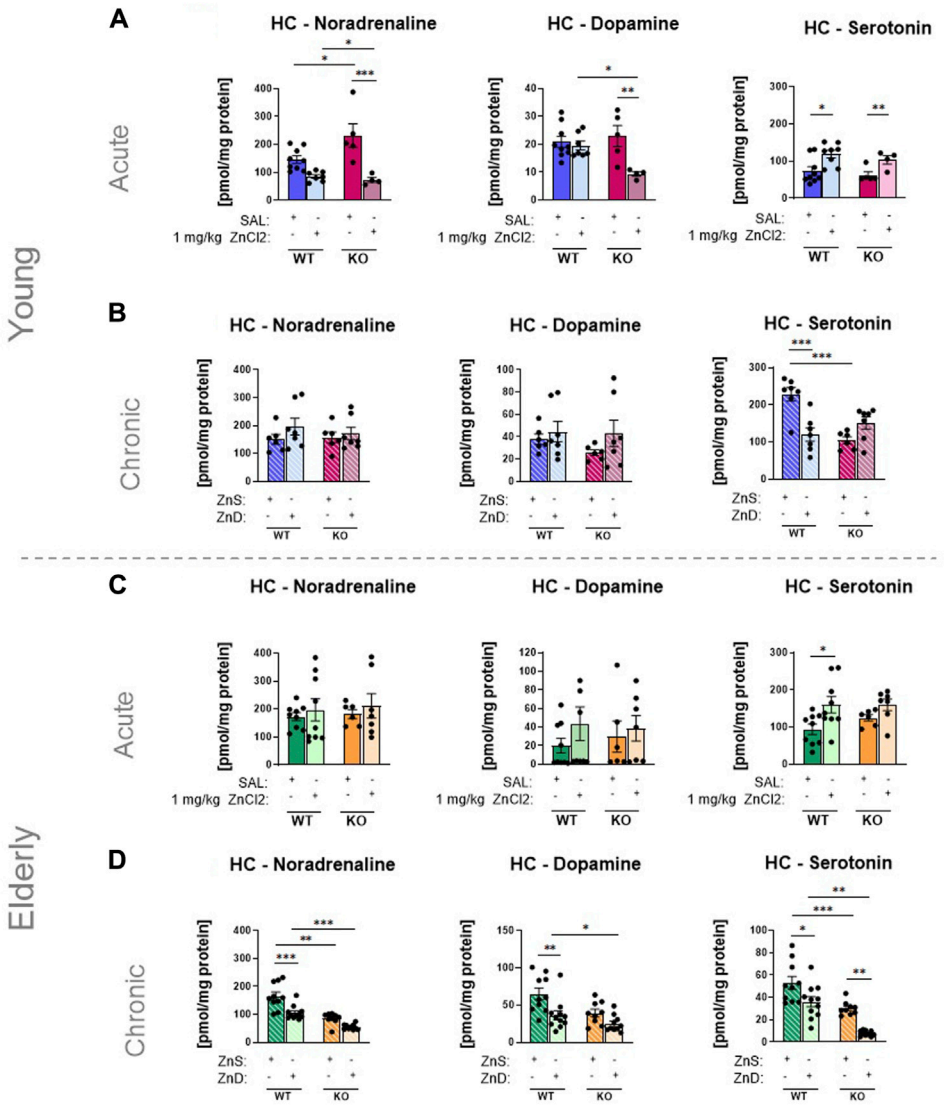


FIGURE 4
Zinc intake affects the monoamine contents of the hippocampus **(A–D)** using HPLC technique. Noradrenaline, dopamine and serotonin levels in P2rx7 +/+ and P2rx7 −/− mice were plotted in the acute ($n$ = 5–9) **(A)** and long-term fed with zinc-controlled diets young ($n$ = 6–7) **(B)** animals. Monoamine contents were also measured in elderly animals, that received similar acute treatment (n = 6–9) **(C)** or a zinc-controlled diet ($n$ = 9–11) **(D)**. Data are expressed as mean ± S.E.M. Data were analyzed by two-way ANOVA followed by Tukey's test. *$p$ < 0.05; **$p$ < 0.01; ***$p$ < 0.001. HC: Hippocampus; WT: wild-type; KO: knock out; ZnS: zinc-supplemented diet; ZnD: zinc-deficient diet.

relative depression-like effect of the zinc-deficient diet might be partly mediated by P2X7 receptors. Similar results were observed in the elderly group that received different zinc-containing diets ($n$ = 9–11 animals/group) (Figure 2D). In the wild-type groups receiving the zinc-deficient diet, substantially higher values of immobility were measured in both the TST and FST. We did not observe any significant difference in the weights of the animals during the 8-week experiment (Supplementary Figure S4). Just like in young adult mice, the depression-like effect of zinc deficiency was eliminated in the absence of the P2X7 receptor in the elderly groups.

Despite the different $Zn^{2+}$ content of the diet, serum $Zn^{2+}$ levels were uniformly increased when compared to those of the animals kept on a standard laboratory diet, probably because of the difference between the two diets in overall $Zn^{2+}$ content (Figures 3C, D). This was true for both young adult and elderly animals, although the serum zinc levels were considerably lower in the latter group (Figure 3D). In summary, we observed that in the case of the TST in young adult and in elderly mice, the antidepressant-like effect of long-term zinc enrichment was partially P2X7 receptor-dependent.

## 3.3 Excess zinc intake increased the serotonin content of the hippocampus

After the behavioral experiments, we examined how our results could be explained by two accepted theories of depression development: the monoamine and BDNF hypotheses. Using

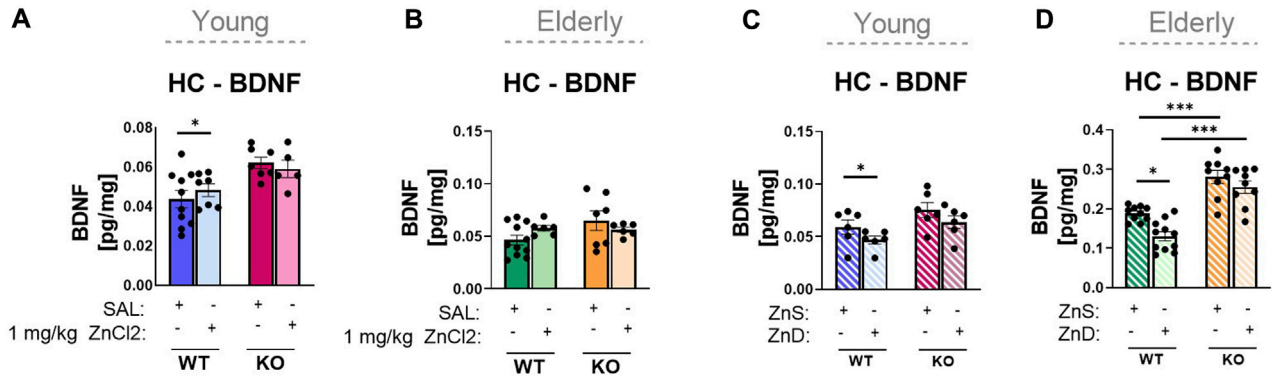


FIGURE 5
Examination of hippocampus BDNF protein content by ELISA **(A–D)**. Wild-type and knockout young ($n$ = 5–11) **(A)** and elderly ($n$ = 6–11) **(B)** mice were injected intraperitoneally with an acute treatment of saline or $ZnCl_2$ (1 mg/kg). P2rx7 +/+ and −/− young ($n$ = 6) **(C)** or elderly mice were fed a Zn-controlled diet ($n$ = 9–11) **(D)**. Data are expressed as mean ± S.E.M. Data were analyzed by two-way ANOVA, followed by Tukey's test. *$p$ < 0.05; **$p$ < 0.01; *** $p$ < 0.001. HC: hippocampus; WT: wild-type; KO: knockout; ZnS: zinc-supplemented diet; ZnD: zinc-deficient diet.

HPLC, concentrations of monoamines, such as NA, DA, and 5-HT, were measured in the HC, a brain area relevant to the behaviors measured in the FST and TST (Hao et al., 2019). Following a single injection of $ZnCl_2$ solution, 5-HT levels in the HC of young mice were increased in both wild-type and knockout animals (Figure 4A), whereas no treatment-induced changes were observed in DA and NA levels (Figures 4A–D). Likewise, a long-term zinc-deficient diet decreased serotonin levels in the HC (Figure 4B), but only in wild-type mice, which was consistent with the behavioral results found in the TST (Figure 2C). In the elderly group, a substantial increase in 5-HT levels was observed in P2rx7 +/+ mice, but not in KO mice, which was consistent with the results of the behavioral experiment (Figures 2B, 4C). In contrast, the zinc-deficient diet reduced the levels of all three monoamines in elderly wild-type mice (Figure 4D), which might be associated with lower basal serum zinc levels in these animals (Figure 3D). In the PFC, we detected treatment-related changes in monoamine levels only in the elderly animals (Supplementary Figures S5A, B). The 5-HT content increased in the wild-type group, but not in the P2rx7 −/− animals acutely treated with $ZnCl_2$ ($n$ = 6–7 animals/group) (Supplementary Figure S5A). In the elderly group, long-term feeding of zinc-deprived diet animals ($n$ = 9–11 animals/group), NA and 5-HT levels were reduced in a P2X7-dependent way in the PFC (Supplementary Figure S5B).

Another important neurochemical readout of an antidepressant action is the change in hippocampal BDNF levels. Corresponding to the effects detected in behavioral studies, in young adult animals, acute $ZnCl_2$ treatment increased, where Zn deprivation reduced hippocampal BDNF levels, with an overall genotype effect in the former group, but without interaction (Figures 5A, C). In the elderly group, acute $ZnCl_2$ treatment did not affect the BDNF level in the hippocampus of wild-type animals (Figure 5B), whereas zinc-controlled diet and Zn deprivation decreased it (Figure 5D). In P2rx7-deficient animals, neither acute $ZnCl_2$ treatment nor zinc deprivation had any effect on hippocampal BDNF levels in either age groups (Figures 5A–D). Similar data were obtained during the PFC examination (Supplementary Figure S6). Acute zinc treatment caused an increase in BDNF levels only in young P2X7 +/+ animals (Supplementary Figure S6A). The long-term diets showed changes between genotypes in the elderly group, and both diets increased the BDNF levels in the knockout males (Supplementary Figure S6D).

## 4 Discussion

The antidepressant action of P2rx7 inhibition (Csolle et al., 2013b; Wang et al., 2016; Ribeiro et al., 2019b) and $Zn^{2+}$ (Mlyniec et al., 2012; Mlyniec et al., 2014; Wang et al., 2018) has been well-established in animal studies, and the inhibitory action of $Zn^{2+}$ on P2X7 receptors has also been documented (Moore and Mackenzie, 2008; Kovacs et al., 2018; Martinez-Cuesta et al., 2020). $Zn^{2+}$ and other divalent cations inhibit P2rx7-mediated ion currents via direct binding to the extracellular loop (Liu et al., 2008; Kasuya et al., 2016). Zn is a micronutrient essential for the functioning of the human body and predominantly accumulates in specific regions of the brain, such as the cortex, hippocampus, and amygdala. The largest amount is bound to metalloproteins; the rest is stored in presynaptic vesicles, and the neurons containing them are called zinc-enriched neurons (ZENs) (Takeda, 2000). In the cortex and hippocampus, these ZEN terminals are associated with glutamatergic neurotransmission (Westbrook and Mayer, 1987), whereas in the cerebellum, they are associated with GABA neurotransmission (Wang et al., 2002). By inhibiting glutamate and GABA receptors, zinc plays an important role in synaptic plasticity (Wolf et al., 2018) and can modify the excitability of neurons (Sperlagh et al., 2002; Acuna-Castillo et al., 2007). Zn also inhibits P2X7-mediated functional responses in the hippocampus, such as increased glutamate release in acute slices (Sperlagh et al., 2002) and propidium uptake by hippocampal astrocytes (Kovacs et al., 2018).

Based on these data, our primary goal was to investigate whether P2rx7 plays a role in the mechanism of action of zinc in modulating depression-like behavior in mice in the TST and FST. Simple behavioral tests are widely used for screening potential antidepressant effects; however, they have some drawbacks. Certain drugs and antidepressants increase motor

activity, thus yielding false positive results in the aforementioned behavioral experiments (Borsini and Meli, 1988). To achieve this goal, we examined the effects of acute systemic $ZnCl_2$ treatment and a special diet enriched or deprived of zinc. To examine these two effects, we used diets with different zinc contents for the acute and long-term zinc-regulated series of experiments. In the acute protocol, we investigated the antidepressant effects of a single excess dose of Zn. In this case, the diet of the mice did not change compared with the previously used standard laboratory diet, and we measured the changes caused by the injected zinc solution. In the 8-week zinc-controlled diet series of experiments, we examined depression-like behavior caused by zinc deficiency, where we built our own protocol based on literature data (Mlyniec et al., 2012). To validate the effect of the aforementioned treatments, zinc concentrations were measured in the serum following these interventions as based on a previous study, where serum and brain zinc levels were inferred from each other (Wang et al., 2010). In accordance with the available literature (Rafalo-Ulinska et al., 2022), the serum zinc concentration in wild-type mice was substantially increased by acute zinc treatment. Rafało-Ulińska et al. administered 40 mg zinc hydroaspartate/kg or 0.9% NaCl solution orally to their male mice, 1 h before decapitation. Based on their measurements, compared to the serum zinc concentration of the control animals (0.4 ± 0.04 μg/mL), the zinc content of the blood serum of the treated animals was 15 times higher, 6.0 ± 0.85 μg/mL. In our experiments, the 1 mg/kg $ZnCl_2$ solution with the shorter duration of action (30 min), compared to the 0.9% NaCl i.p., compared to treated control mice (7.29 ± 1.27 ng/mL), resulted in a nearly 5-fold higher serum zinc concentration (33.05 ± 4.02 ng/mL). A similar change was observed in the P2rx7 −/− animals; compared to the serum zinc concentration of 4.69 ± 1.77 ng/mL in the controls, we measured a value of 20.03 ± 3.17 ng/mL in the treated mice. Accordingly, acute zinc intake in young and elderly animals reduced the floating time for both genotypes in the behavioral experiments, except for the TST of old animals, where no significant difference was found in the immobility time of the KO animals. This is an antidepressant-like effect, which cannot be explained by the action on locomotor activity, as we could not find either a treatment- or genotype-related difference between the groups in the open field arena within the timeframe of the FST and TST (Supplementary Figure S2). We also replicate previous literature data showing that P2rx7 deficiency by itself exhibited an antidepressant effect, and regarding the movement of the control, that of WT mice was identical to the results of previous experiments (Kroczka et al., 2000; Szewczyk et al., 2002; Nowak et al., 2003; Rosa et al., 2003; Csolle et al., 2013a). However, we were not able to replicate these results in young female mice. One possible explanation for these findings is that the estrous cycle influences the responsiveness of female animals to these tests. The estrous cycle may have an effect on female mouse behavior in anxiety- and fear-related tests compared to male mice (Lovick and Zangrossi, 2021). We also failed to observe an antidepressant-like effect of zinc in female mice, which is noteworthy, as previous studies on the association between zinc and depression were also performed in male animals (Mlyniec et al., 2012; Mlyniec and Nowak, 2012). Therefore, because the prevalence of depression is higher in female animals, the effects of excess zinc and zinc deprivation on depression-like behaviors in female mice require further investigation. Our results in male mice imply that the antidepressant-like effect of acute systemic $ZnCl_2$ treatment is largely independent of the genotype and is mediated by other signaling pathways, such as glutamatergic or GABAergic transmission, or a direct or indirect impact on BDNF levels, as confirmed in the present study (Figure 5A). When animals were fed a long-term, Zn-controlled diet, serum zinc levels were higher than those in the animals fed a standard laboratory diet irrespective of the genotype, in young adults but not in elderly animals. The exact reason for this discrepancy is unknown; however, the most likely reason is the different actual zinc content of the standard laboratory diet (18 mg M Zn/kg) and the Zn-controlled diet (23 mg M Zn/kg). Zinc deprivation in the controlled diet group did not affect serum zinc concentrations. This is consistent with the findings of Wong et al. (2009) and might be explained by the fact that, in contrast to the acute, high-dose treatment, fewer micronutrients were administered to the mice for a longer period, so the serum levels could be saturated.

We have also found differences in basal immobility values between the experiments assessing the effect of acute Zn treatment and the effects of the zinc-controlled diet. The difference in the results obtained by the control groups in the behavioral tests can be explained by the different experimental designs. The mice in the zinc-controlled diet experiment did not receive an injection of saline solution before the behavioral test, which itself is a stressful stimulus. This assumption is supported by the fact that the basal immobility time of wild-type mice is uniformly lower in long-term zinc-regulated diet experiments with naïve mice in both the young adult and elderly groups than in their acutely saline-treated counterparts.

Nevertheless, in our experiments, we showed that a long-term zinc-deprived diet increased immobility in both the FST and TST, and the effect in the TST was attenuated in P2rx7-deficient mice. The same effects were observed in elderly animals, that is, the pro-depressant effect of zinc deprivation was also lost in the absence of P2X7Rs. These results indicate that, in the case of an acute $Zn^{2+}$ treatment, the divalent cation has a multiplicity of molecular targets, especially ion channels that might mediate its effect on depressive-like behavior. These include NMDA, α-amino-3-hydroxy-5-methyl-4-isoxazolepropionic acid (AMPA), GABA receptors, Zn transporters, and G protein-coupled receptor 39 (GPR39) (Costa et al., 2023). The immobility time of wild-type control animals of the same age, but participating in different experiments, varied more than that of P2X7 KO mice (Figures 2A, B). Further experiments are required to determine the specific explanation; however, according to our observations and those of others (Smith et al., 2020), in general, P2X7 KO animals are calmer than their peers and adapt more easily to changing conditions. This is supported by the attenuated adrenocorticotropic hormone and corticosterone responses to acute stress (Csolle et al., 2013b; von Muecke-Heim et al., 2021). In addition, P2X7 receptors might participate in the effect of the TST in old animals; however, this partial involvement argues against the major contribution of the

P2X7 receptor to the antidepressant effect of an acute, systemic Zn load. In contrast, in the case of more subtle, long-term changes in Zn concentrations in the local brain microenvironment caused by dietary changes, the inhibitory effect of Zn on P2X7 receptor channels might be more substantial as a mediator of $Zn^{2+}$-related actions on behavior, as observed in the TST in both young adult and elderly animals and in the corresponding neurochemical alterations.

While searching for potential mechanisms of action, we examined brain monoamine and BDNF levels, which are consistent with the underlying hypotheses of depression-like behaviors. According to the monoamine hypothesis, the pathophysiological basis of depression is a deficit in monoaminergic transmission in the central nervous system (Delgado, 2000; Hirschfeld, 2000), whereas the BDNF theory emphasizes that depression is owing to dysfunctional neurogenesis in brain regions responsible for emotions and cognition (Duman and Monteggia, 2006); that is, the expression of neuronal growth factors decreases when we perceive a stress effect (Kim et al., 2020). In our experiments, as a result of acute Zn injection, the concentration of 5-HT in the HC was increased in both young and old mice, all of which validated the results of the behavioral experiments. Moreover, long-term Zn deprivation reduced monoamine levels in both age groups, indicating that the hippocampal NA, DA, and 5-HT levels of elderly animals are more sensitive to treatment. In this group, changes in PFC monoamine levels were also consistent with depression-like behavior caused by the zinc-deprived diet, especially in the case of NA and 5-HT, which are key pharmacological targets in mood disorders. As for BDNF measurements, our data partially support the results found in the literature, demonstrating increased hippocampal BDNF levels in young adult wild-type animals in response to the acute Zn treatment and a decrease in response to Zn deprivation (Williams and Undieh, 2010; Csolle et al., 2013a; Starowicz et al., 2019; Rafalo-Ulinska et al., 2020). The effect of acute Zn treatment to stimulate BDNF production in young adult wild-type mice is also demonstrated in the PFC. However, in old animals, only zinc deprivation, but not acute treatment, affected BDNF levels and only in wild-type animals.

In conclusion, our data demonstrate that the antidepressant-like effect of extracellular zinc is partially mediated by P2rx7 in a male mouse model, which is supported by changes observed in behavioral experiments. The extent of its contribution probably also depends on the age of the animal and the initial zinc saturation in the serum and brain.

## Data availability statement

The original contributions presented in the study are included in the article/Supplementary Material; further inquiries can be directed to the corresponding author.

## Ethics statement

The animal study was approved by the Animal Care Committee of the Institute of Experimental Medicine, Budapest, Hungary, ref. no. PEI/EA/900-7/2020. The study was conducted in accordance with the local legislation and institutional requirements.

## Author contributions

BI-V and BS designed the research; BI-V, FG, and PT performed the experiments; MB conducted the HPLC analyses; BI-V and MB analyzed the data; and BI-V and BS wrote the manuscript. All authors contributed to the article and approved the submitted version.

## Funding

This work was supported by the Hungarian Research and Development Fund (grant number 131629 to BS), Hungarian Brain Research Program (grant number NAP2022-I-1/2022 to BS), Recovery and Resilience Facility of the European Union within the framework of Programme Széchenyi Plan Plus (grant number RRF-2.3.1-21-2022-00011, National Laboratory of Translational Neuroscience and grant number RRF-2.3.1-21-2022-00015, National Laboratory of Drug Research and Development to BS). This article is based upon work from COST Action CA21130, supported by COST (European Cooperation in Science and Technology).

## Acknowledgments

The authors thank Ferenc Erdélyi at the Medical Gene Technology Unit for providing technical support and assistance in the behavioral experiments and acknowledge the support of the Cell Biology Center (Cell Imaging Multi-Mode Reader).

## Conflict of interest

The authors declare that the research was conducted in the absence of any commercial or financial relationships that could be construed as a potential conflict of interest.

## Publisher's note



## Supplementary material

The Supplementary Material for this article can be found online at: https://www.frontiersin.org/articles/10.3389/fphar.2023.1241406/full#supplementary-material

# References


Acuna-Castillo, C., Coddou, C., Bull, P., Brito, J., and Huidobro-Toro, J. P. (2007). 'Differential role of extracellular histidines in copper, zinc, magnesium and proton modulation of the P2X7 purinergic receptor. *J. Neurochem.* 101, 17–26. doi:10.1111/j.1471-4159.2006.04343.x

Alloisio, S., Cervetto, C., Passalacqua, M., Barbieri, R., Maura, G., Nobile, M., et al. (2008). 'Functional evidence for presynaptic P2X7 receptors in adult rat cerebrocortical nerve terminals. *FEBS Lett.* 582, 3948–3953. doi:10.1016/j.febslet.2008.10.041

Artigas, F., Nutt, D. J., and Shelton, R. (2002). 'Mechanism of action of antidepressants. *Psychopharmacol. Bull.* 36 (2), 123–132.

Ates-Alagoz, Z., and Adejare, A. (2013). 'NMDA Receptor Antagonists for Treatment of Depression. *Pharm. (Basel)* 6, 480–499. doi:10.3390/ph6040480

Baranyi, M., Milusheva, E., Vizi, E. S., and Sperlagh, B. (2006). 'Chromatographic analysis of dopamine metabolism in a Parkinsonian model. *J. Chromatogr. A* 1120, 13–20. doi:10.1016/j.chroma.2006.03.018

Basso, A. M., Bratcher, N. A., Harris, R. R., Jarvis, M. F., Decker, M. W., and Rueter, L. E. (2009). 'Behavioral profile of P2X7 receptor knockout mice in animal models of depression and anxiety: relevance for neuropsychiatric disorders. *Behav. Brain Res.* 198, 83–90. doi:10.1016/j.bbr.2008.10.018

Belmaker, R. H., and Agam, G. (2008). 'Major depressive disorder. *N. Engl. J. Med.* 358, 55–68. doi:10.1056/NEJMra073096

Bhattacharya, A., and Jones, D. N. C. (2018). 'Emerging role of the P2X7-NLRP3-IL1β pathway in mood disorders. *Psychoneuroendocrinology* 98, 95–100. doi:10.1016/j.psyneuen.2018.08.015

Borsini, F., and Meli, A. (1988). Is the forced swimming test a suitable model for revealing antidepressant activity? *Psychopharmacol. Berl.* 94, 147–160. doi:10.1007/BF00176837

Capanna, E., Corti, M., Mainardi, D., Parmigiani, S., and Brain, P. F. (1984). 'Karyotype and intermale aggression in wild house mice: ecology and speciation. *Behav. Genet.* 14, 195–208. doi:10.1007/BF01065541

Caspi, A., Sugden, K., Moffitt, T. E., Taylor, A., Craig, I. W., Harrington, H., et al. (2003). 'Influence of life stress on depression: moderation by a polymorphism in the 5-HTT gene. *Science* 301, 386–389. doi:10.1126/science.1083968

Costa, I., Barbosa, D. J., Silva, V., Benfeito, S., Borges, F., Remiao, F., et al. (2023). 'Research Models to Study Ferroptosis's Impact in Neurodegenerative Diseases'. *Pharmaceutics* 15, 1369. doi:10.3390/pharmaceutics15051369

Cryan, J. F., Mombereau, C., and Vassout, A. (2005). 'The tail suspension test as a model for assessing antidepressant activity: review of pharmacological and genetic studies in mice. *Neurosci. Biobehav Rev.* 29, 571–625. doi:10.1016/j.neubiorev.2005.03.009

Csolle, C., Ando, R. D., Kittel, A., Goloncser, F., Baranyi, M., Soproni, K., et al. (2013a). 'The absence of P2X7 receptors (P2rx7) on non-haematopoietic cells leads to selective alteration in mood-related behaviour with dysregulated gene expression and stress reactivity in mice. *Int. J. Neuropsychopharmacol.* 16, 213–233. doi:10.1017/S1461145711001933

Csolle, C., Baranyi, M., Zsilla, G., Kittel, A., Goloncser, F., Illes, P., et al. (2013b). 'Neurochemical Changes in the Mouse Hippocampus Underlying the Antidepressant Effect of Genetic Deletion of P2X7 Receptors. *PLoS One* 8, e66547. doi:10.1371/journal.pone.0066547

Czamara, D., Muller-Myhsok, B., and Lucae, S. (2018). 'The P2RX7 polymorphism rs2230912 is associated with depression: A meta-analysis. *Prog. Neuropsychopharmacol. Biol. Psychiatry* 82, 272–277. doi:10.1016/j.pnpbp.2017.11.003

Delgado, P. L. (2000). 'Depression: the case for a monoamine deficiency. *J. Clin. Psychiatry* 61 (6), 7–11.

Drevets, W. C., Wittenberg, G. M., Bullmore, E. T., and Manji, H. K. (2022). 'Immune targets for therapeutic development in depression: towards precision medicine. *Nat. Rev. Drug Discov.* 21, 224–244. doi:10.1038/s41573-021-00368-1

Duman, R. S., and Monteggia, L. M. (2006). 'A neurotrophic model for stress-related mood disorders. *Biol. Psychiatry* 59, 1116–1127. doi:10.1016/j.biopsych.2006.02.013

Fava, M., and Davidson, K. G. (1996). 'Definition and epidemiology of treatment-resistant depression. *Psychiatr. Clin. North Am.* 19, 179–200. doi:10.1016/s0193-953x(05)70283-5

Feng, W. P., Zhang, B., Li, W., and Liu, J. (2014). 'Lack of association of P2RX7 gene rs2230912 polymorphism with mood disorders: a meta-analysis. *PLoS One* 9, e88575. doi:10.1371/journal.pone.0088575

Fujiwara, M., Ohbori, K., Ohishi, A., Nishida, K., Uozumi, Y., and Nagasawa, K. (2017). 'Species Difference in Sensitivity of Human and Mouse P2X7 Receptors to Inhibitory Effects of Divalent Metal Cations. *Biol. Pharm. Bull.* 40, 375–380. doi:10.1248/bpb.b16-00887

Hao, Y., Ge, H., Sun, M., and Gao, Y. (2019). 'Selecting an Appropriate Animal Model of Depression. *Int. J. Mol. Sci.* 20, 4827. doi:10.3390/ijms20194827

Hirschfeld, R. M. (2000). 'History and evolution of the monoamine hypothesis of depression. *J. Clin. Psychiatry* 61 (6), 4–6.

Huang, Z., and Tan, S. (2021). 'P2X7 Receptor as a Potential Target for Major Depressive Disorder. *Curr. Drug Targets* 22, 1108–1120. doi:10.2174/1389450122666210120141908

Illes, P., Khan, T. M., and Rubini, P. (2017). Neuronal P2X7 Receptors Revisited: Do They Really Exist? *J. Neurosci.* 37, 7049–7062. doi:10.1523/JNEUROSCI.3103-16.2017

Iwata, M., Ota, K. T., Li, X. Y., Sakaue, F., Li, N., Dutheil, S., et al. (2016). 'Psychological Stress Activates the Inflammasome via Release of Adenosine Triphosphate and Stimulation of the Purinergic Type 2X7 Receptor. *Biol. Psychiatry* 80, 12–22. doi:10.1016/j.biopsych.2015.11.026

Kasuya, G., Fujiwara, Y., Takemoto, M., Dohmae, N., Nakada-Nakura, Y., Ishitani, R., et al. (2016). 'Structural Insights into Divalent Cation Modulations of ATP-Gated P2X Receptor Channels. *Cell Rep.* 14, 932–944. doi:10.1016/j.celrep.2015.12.087

Kim, Y. K., Kim, O. Y., and Song, J. (2020). 'Alleviation of Depression by Glucagon-Like Peptide 1 Through the Regulation of Neuroinflammation, Neurotransmitters, Neurogenesis, and Synaptic Function. *Front. Pharmacol.* 11, 1270. doi:10.3389/fphar.2020.01270

Kongsui, R., Beynon, S. B., Johnson, S. J., Mayhew, J., Kuter, P., Nilsson, M., et al. (2014). 'Chronic stress induces prolonged suppression of the P2X7 receptor within multiple regions of the hippocampus: a cumulative threshold spectra analysis. *Brain Behav. Immun.* 42, 69–80. doi:10.1016/j.bbi.2014.05.017

Kovacs, G., Kornyei, Z., Toth, K., Baranyi, M., Brunner, J., Neubrandt, M., et al. (2018). 'Modulation of P2X7 purinergic receptor activity by extracellular Zn(2+) in cultured mouse hippocampal astroglia. *Cell Calcium* 75, 1–13. doi:10.1016/j.ceca.2018.07.010

Kroczka, B., Zieba, A., Dudek, D., Pilc, A., and Nowak, G. (2000). 'Zinc exhibits an antidepressant-like effect in the forced swimming test in mice. *Pol. J. Pharmacol.* 52, 403–406.

Liu, X., Surprenant, A., Mao, H. J., Roger, S., Xia, R., Bradley, H., et al. (2008). 'Identification of key residues coordinating functional inhibition of P2X7 receptors by zinc and copper. *Mol. Pharmacol.* 73, 252–259. doi:10.1124/mol.107.039651

Lovick, T. A., and Zangrossi, H., Jr. (2021). 'Effect of Estrous Cycle on Behavior of Females in Rodent Tests of Anxiety. *Front. Psychiatry* 12, 711065. doi:10.3389/fpsyt.2021.711065

Lowry, O. H., Rosebrough, N. J., Farr, A. L., and Randall, R. J. (1951). 'Protein measurement with the Folin phenol reagent. *J. Biol. Chem.* 193, 265–275. doi:10.1016/s0021-9258(19)52451-6

Maes, M. (1999). 'Major depression and activation of the inflammatory response system. *Adv. Exp. Med. Biol.* 461, 25–46. doi:10.1007/978-0-585-37970-8_2

Martinez-Cuesta, M. A., Blanch-Ruiz, M. A., Ortega-Luna, R., Sanchez-Lopez, A., and Alvarez, A. (2020). 'Structural and Functional Basis for Understanding the Biological Significance of P2X7 Receptor. *Int. J. Mol. Sci.* 21, 8454. doi:10.3390/ijms21228454

Miras-Portugal, M. T., Sebastian-Serrano, A., de Diego Garcia, L., and Diaz-Hernandez, M. (2017). 'Neuronal P2X7 Receptor: Involvement in Neuronal Physiology and Pathology. *J. Neurosci.* 37, 7063–7072. doi:10.1523/JNEUROSCI.3104-16.2017

Mlyniec, K., Davies, C. L., Budziszewska, B., Opoka, W., Reczynski, W., Sowa-Kucma, M., et al. (2012). 'Time course of zinc deprivation-induced alterations of mice behavior in the forced swim test. *Pharmacol. Rep.* 64, 567–575. doi:10.1016/s1734-1140(12)70852-6

Mlyniec, K., and Nowak, G. (2012). 'Zinc deficiency induces behavioral alterations in the tail suspension test in mice. Effect of antidepressants'. *Pharmacol. Rep.* 64, 249–255. doi:10.1016/s1734-1140(12)70762-4

Mlyniec, K., Ostachowicz, B., Krakowska, A., Reczynski, W., Opoka, W., and Nowak, G. (2014). 'Chronic but not acute antidepresant treatment alters serum zinc/copper ratio under pathological/zinc-deficient conditions in mice. *J. Physiol. Pharmacol.* 65, 673–678.

Moore, S. F., and Mackenzie, A. B. (2008). 'Species and agonist dependent zinc modulation of endogenous and recombinant ATP-gated P2X7 receptors. *Biochem. Pharmacol.* 76, 1740–1747. doi:10.1016/j.bcp.2008.09.015

Motulsky, H. J., and Brown, R. E. (2006). 'Detecting outliers when fitting data with nonlinear regression - a new method based on robust nonlinear regression and the false discovery rate. *BMC Bioinforma.* 7, 123. doi:10.1186/1471-2105-7-123

Nowak, G., Szewczyk, B., Wieronska, J. M., Branski, P., Palucha, A., Pilc, A., et al. (2003). 'Antidepressant-like effects of acute and chronic treatment with zinc in forced swim test and olfactory bulbectomy model in rats. *Brain Res. Bull.* 61, 159–164. doi:10.1016/s0361-9230(03)00104-7

Otrokocsi, L., Kittel, Á., and Sperlágh, B. (2017). 'P2X7 Receptors Drive Spine Synapse Plasticity in the Learned Helplessness Model of Depression. *Int. J. Neuropsychopharmacol.* 20, 813–822. doi:10.1093/ijnp/pyx046

Porsolt, R. D., Bertin, A., and Jalfre, M. (1977). 'Behavioral despair in mice: a primary screening test for antidepressants. *Arch. Int. Pharmacodyn. Ther.* 229, 327–336.

Poshivalov, V. P. (1980). 'The integrity of the social hierarchy in mice following administration of psychotropic drugs. *Br. J. Pharmacol.* 70, 367–373. doi:10.1111/j.1476-5381.1980.tb08712.x

Rafalo-Ulinska, A., Pochwat, B., Misztak, P., Bugno, R., Kryczyk-Poprawa, A., Opoka, W., et al. (2022). 'Zinc Deficiency Blunts the Effectiveness of Antidepressants in the Olfactory Bulbectomy Model of Depression in Rats. *Nutrients* 14, 2746. doi:10.3390/nu14132746

Rafalo-Ulinska, A., Poleszak, E., Szopa, A., Serefko, A., Rogowska, M., Sowa, I., et al. (2020). 'Imipramine Influences Body Distribution of Supplemental Zinc Which May Enhance Antidepressant Action'. *Nutrients* 12, 2529. doi:10.3390/nu12092529

Ranjbar, E., Kasaei, M. S., Mohammad-Shirazi, M., Nasrollahzadeh, J., Rashidkhani, B., Shams, J., et al. (2013). 'Effects of zinc supplementation in patients with major depression: a randomized clinical trial. *Iran. J. Psychiatry* 8, 73–79.

Ribeiro, D. E., Casarotto, P. C., Staquini, L., Pinto E Silva, M. A., Biojone, C., Wegener, G., et al. (2019a). 'Reduced P2X receptor levels are associated with antidepressant effect in the learned helplessness model. *PeerJ* 7, e7834. doi:10.7717/peerj.7834

Ribeiro, D. E., Muller, H. K., Elfving, B., Eskelund, A., Joca, S. R., and Wegener, G. (2019b). 'Antidepressant-like effect induced by P2X7 receptor blockade in FSL rats is associated with BDNF signalling activation. *J. Psychopharmacol.* 33, 1436–1446. doi:10.1177/0269881119872173

Roceri, M., Cirulli, F., Pessina, C., Peretto, P., Racagni, G., and Riva, M. A. (2004). 'Postnatal repeated maternal deprivation produces age-dependent changes of brain-derived neurotrophic factor expression in selected rat brain regions. *Biol. Psychiatry* 55, 708–714. doi:10.1016/j.biopsych.2003.12.011

Roohani, N., Hurrell, R., Kelishadi, R., and Schulin, R. (2013). 'Zinc and its importance for human health: An integrative review. *J. Res. Med. Sci.* 18, 144–157.

Rosa, A. O., Lin, J., Calixto, J. B., Santos, A. R., and Rodrigues, A. L. (2003). 'Involvement of NMDA receptors and L-arginine-nitric oxide pathway in the antidepressant-like effects of zinc in mice. *Behav. Brain Res.* 144, 87–93. doi:10.1016/s0166-4328(03)00069-x

Sachdeva, B., Sachdeva, P., Ghosh, S., Ahmad, F., and Sinha, J. (2023). 'Ketamine as a therapeutic agent in major depressive disorder and posttraumatic stress disorder: Potential medicinal and deleterious effects'. *Ibrain* 9, 90–101. doi:10.1002/ibra.12094

Schroder, H. S., Patterson, E. H., and Hirshbein, L. (2022). 'Treatment-resistant depression reconsidered'. *SSM - Ment. Health* 100081, 7. doi:10.1016/j.ssmmh.2022.100081

Schumacher, J., Jamra, R. A., Becker, T., Ohlraun, S., Klopp, N., Binder, E. B., et al. (2005). 'Evidence for a relationship between genetic variants at the brain-derived neurotrophic factor (BDNF) locus and major depression. *Biol. Psychiatry* 58, 307–314. doi:10.1016/j.biopsych.2005.04.006

Shoji, H., and Miyakawa, T. (2019). 'Age-related behavioral changes from young to old age in male mice of a C57BL/6J strain maintained under a genetic stability program. *Neuropsychopharmacol. Rep.* 39, 100–118. doi:10.1002/npr2.12052

Smith, K. L., Todd, S. M., Boucher, A., Bennett, M. R., and Arnold, J. C. (2020). 'P2X(7) receptor knockout mice display less aggressive biting behaviour correlating with increased brain activation in the piriform cortex. *Neurosci. Lett.* 714, 134575. doi:10.1016/j.neulet.2019.134575

Sperlagh, B., and Illes, P. (2007). Purinergic modulation of microglial cell activation. *Purinergic Signal* 3, 117–127. doi:10.1007/s11302-006-9043-x

Sperlagh, B., Kofalvi, A., Deuchars, J., Atkinson, L., Milligan, C. J., Buckley, N. J., et al. (2002). 'Involvement of P2X7 receptors in the regulation of neurotransmitter release in the rat hippocampus. *J. Neurochem.* 81, 1196–1211. doi:10.1046/j.1471-4159.2002.00920.x

Sperlagh, B., Vizi, E. S., Wirkner, K., and Illes, P. (2006). 'P2X7 receptors in the nervous system. *Prog. Neurobiol.* 78, 327–346. doi:10.1016/j.pneurobio.2006.03.007

Starowicz, G., Jarosz, M., Frackiewicz, E., Grzechnik, N., Ostachowicz, B., Nowak, G., et al. (2019). Long-lasting antidepressant-like activity of the GPR39 zinc receptor agonist TC-G 1008. *J. Affect Disord.* 245, 325–334. doi:10.1016/j.jad.2018.11.003

Styczen, K., Sowa-Kucma, M., Siwek, M., Dudek, D., Reczynski, W., Szewczyk, B., et al. (2017). The serum zinc concentration as a potential biological marker in patients with major depressive disorder. *Metab. Brain Dis.* 32, 97–103. doi:10.1007/s11011-016-9888-9

Szewczyk, B., Branski, P., Wieronska, J. M., Palucha, A., Pilc, A., and Nowak, G. (2002). 'Interaction of zinc with antidepressants in the forced swimming test in mice. *Pol. J. Pharmacol.* 54, 681–685.

Szewczyk, B., Pochwat, B., Muszyńska, B., Opoka, W., Krakowska, A., Rafało-Ulińska, A., et al. (2019). Antidepressant-like activity of hyperforin and changes in BDNF and zinc levels in mice exposed to chronic unpredictable mild stress. *Behav. Brain Res.* 372, 112045. doi:10.1016/j.bbr.2019.112045

Szewczyk, B., Szopa, A., Serefko, A., Poleszak, E., and Nowak, G. (2018). The role of magnesium and zinc in depression: similarities and differences. *Magnes. Res.* 31, 78–89. doi:10.1684/mrh.2018.0442

Takeda, A. (2000). 'Movement of zinc and its functional significance in the brain. *Brain Res. Brain Res. Rev.* 34, 137–148. doi:10.1016/s0165-0173(00)00044-8

Tamano, H., Kan, F., Kawamura, M., Oku, N., and Takeda, A. (2009). 'Behavior in the forced swim test and neurochemical changes in the hippocampus in young rats after 2-week zinc deprivation. *Neurochem. Int.* 55, 536–541. doi:10.1016/j.neuint.2009.05.011

Trivedi, M. H. (2020). 'Major Depressive Disorder in Primary Care: Strategies for Identification. *J. Clin. Psychiatry* 81. doi:10.4088/JCP.UT17042BR1C

Viikki, M., Kampman, O., Anttila, S., Illi, A., Setala-Soikkeli, E., Huuhka, M., et al. (2011). 'P2RX7 polymorphisms Gln460Arg and His155Tyr are not associated with major depressive disorder or remission after SSRI or ECT. *Neurosci. Lett.* 493, 127–130. doi:10.1016/j.neulet.2011.02.023

Virginio, C., Church, D., North, R. A., and Surprenant, A. (1997). 'Effects of divalent cations, protons and calmidazolium at the rat P2X7 receptor. *Neuropharmacology* 36, 1285–1294. doi:10.1016/s0028-3908(97)00141-x

von Muecke-Heim, I. A., Ries, C., Urbina, L., and Deussing, J. M. (2021). 'P2X7R antagonists in chronic stress-based depression models: a review. *Eur. Arch. Psychiatry Clin. Neurosci.* 271, 1343–1358. doi:10.1007/s00406-021-01306-3

Wang, C. Y., Wang, T., Zheng, W., Zhao, B. L., Danscher, G., Chen, Y. H., et al. (2010). Zinc overload enhances APP cleavage and Aβ deposition in the Alzheimer mouse brain. *PLoS One* 5, e15349. doi:10.1371/journal.pone.0015349

Wang, J., Um, P., Dickerman, B. A., and Liu, J. (2018). 'Zinc, Magnesium, Selenium and Depression: A Review of the Evidence, Potential Mechanisms and Implications'. *Nutrients* 10, 584. doi:10.3390/nu10050584

Wang, W., Xiang, Z. H., Jiang, C. L., Liu, W. Z., and Shang, Z. L. (2016). 'Effects of antidepressants on P2X7 receptors. *Psychiatry Res.* 242, 281–287. doi:10.1016/j.psychres.2016.06.001

Wang, Z., Danscher, G., Kim, Y. K., Dahlstrom, A., and Mook Jo, S. (2002). 'Inhibitory zinc-enriched terminals in the mouse cerebellum: double-immunohistochemistry for zinc transporter 3 and glutamate decarboxylase. *Neurosci. Lett.* 321, 37–40. doi:10.1016/s0304-3940(01)02560-5

Watanabe, M., Tamano, H., Kikuchi, T., and Takeda, A. (2010). 'Susceptibility to stress in young rats after 2-week zinc deprivation. *Neurochem. Int.* 56, 410–416. doi:10.1016/j.neuint.2009.11.014

Westbrook, G. L., and Mayer, M. L. (1987). 'Micromolar concentrations of Zn2+ antagonize NMDA and GABA responses of hippocampal neurons. *Nature* 328, 640–643. doi:10.1038/328640a0

Whittle, N., Lubec, G., and Singewald, N. (2009). 'Zinc deficiency induces enhanced depression-like behaviour and altered limbic activation reversed by antidepressant treatment in mice. *Amino Acids* 36, 147–158. doi:10.1007/s00726-008-0195-6

Williams, S. N., and Undieh, A. S. (2010). 'Brain-derived neurotrophic factor signaling modulates cocaine induction of reward-associated ultrasonic vocalization in rats. *J. Pharmacol. Exp. Ther.* 332, 463–468. doi:10.1124/jpet.109.158535

Wingo, T. S., Liu, Y., Gerasimov, E. S., Gockley, J., Logsdon, B. A., Duong, D. M., et al. (2021). 'Brain proteome-wide association study implicates novel proteins in depression pathogenesis. *Nat. Neurosci.* 24, 810–817. doi:10.1038/s41593-021-00832-6

Wolf, C., Weth, A., Walcher, S., Lax, C., and Baumgartner, W. (2018). 'Modeling of Zinc Dynamics in the Synaptic Cleft: Implications for Cadherin Mediated Adhesion and Synaptic Plasticity. *Front. Mol. Neurosci.* 11, 306. doi:10.3389/fnmol.2018.00306

Wong, C. P., Song, Y., Elias, V. D., Magnusson, K. R., and Ho, E. (2009). 'Zinc supplementation increases zinc status and thymopoiesis in aged mice. *J. Nutr.* 139, 1393–1397. doi:10.3945/jn.109.106021

# Frontiers in Pharmacology

**Explores the interactions between chemicals and living beings**

The most cited journal in its field, which advances access to pharmacological discoveries to prevent and treat human disease.

---

## Discover the latest Research Topics

See more →


**Frontiers**

Avenue du Tribunal-Fédéral 34
1005 Lausanne, Switzerland
frontiersin.org

**Contact us**

+41 (0)21 510 17 00
frontiersin.org/about/contact